



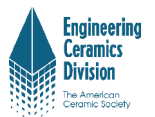
# Abstracts

## 36<sup>TH</sup> INTERNATIONAL CONFERENCE AND EXPOSITION ON ADVANCED CERAMICS AND COMPOSITES

January 22-27, 2012

Hilton Daytona Beach Resort and Ocean Center  
Daytona Beach Florida, USA

[www.ceramics.org/daytona2012](http://www.ceramics.org/daytona2012)



Organized by The American Ceramic Society and The American Ceramic Society's Engineering Ceramics Division

**The American Ceramic Society**  
**36th International Conference & Exposition**  
**on Advanced Ceramics and Composites**

**ABSTRACT BOOK**

**January 22-27, 2012**  
**Daytona Beach, Florida**

# Introduction

---

This volume contains abstracts for more than 900 presentations during the 36th International Conference & Exposition on Advanced Ceramics and Composites in Daytona Beach, Florida. The abstracts are reproduced as submitted by authors, a format that provides for longer, more detailed descriptions of papers. The American Ceramic Society accepts no responsibility for the content or quality of the abstract content. Abstracts are arranged by day, then by symposium and session title. An Author Index appears at the back of this book. The Meeting Guide contains locations of sessions with times, titles and authors of papers, but not presentation abstracts.

## How to Use the Abstract Book

---

Refer to the Table of Contents to determine page numbers on which specific session abstracts begin. At the beginning of each session are headings that list session title, location and session chair. Starting times for presentations and paper numbers precede each paper title. The Author Index lists each author and the page number on which their abstract can be found.

Copyright © 2012 The American Ceramic Society ([www.ceramics.org](http://www.ceramics.org)). All rights reserved.

### MEETING REGULATIONS

The American Ceramic Society is a nonprofit scientific organization that facilitates the exchange of knowledge meetings and publication of papers for future reference. The Society owns and retains full right to control its publications and its meetings. The Society has an obligation to protect its members and meetings from intrusion by others who may wish to use the meetings for their own private promotion purpose. Literature found not to be in agreement with the Society's goals, in competition with Society services or of an offensive nature will not be displayed anywhere in the vicinity of the meeting. Promotional literature of any kind may not be displayed without the Society's permission and unless the Society provides tables for this purpose. Literature not conforming to this policy or displayed in other than designated areas will be disposed. The Society will not permit unauthorized scheduling of activities during its meeting by any person or group when those activities are conducted at its meeting place in interference with its programs and scheduled activities. The Society does not object to appropriate activities by others during its meetings if it is consulted with regard to time, place, and suitability. Any person or group wishing to conduct any activity at the time and location of the Society meeting must obtain permission from the Executive Director or Director of Meetings, giving full details regarding desired time, place and nature of activity.

During oral sessions conducted during Society meetings, unauthorized photography, videotaping and audio recording is prohibited. Failure to comply may result in the removal of the offender from the session or from the remainder of the meeting.

*Registration Requirements:* Attendance at any meeting of the Society shall be limited to duly registered persons.

*Disclaimer:* Statements of fact and opinion are the responsibility of the authors alone and do not imply an opinion on the part of the officers, staff or members of The American Ceramic Society. The American Ceramic Society assumes no responsibility for the statements and opinions advanced by the contributors to its publications or by the speakers at its programs; nor does The American Ceramic Society assume any liability for losses or injuries suffered by attendees at its meetings. Registered names and trademarks, etc. used in its publications, even without specific indications thereof, are not to be considered unprotected by the law. Mention of trade names of commercial products does not constitute endorsement or recommendations for use by the publishers, editors or authors.

Final determination of the suitability of any information, procedure or products for use contemplated by any user, and the manner of that use, is the sole responsibility of the user. Expert advice should be obtained at all times when implementation is being considered, particularly where hazardous materials or processes are encountered.

# Table of Contents

---

Plenary Session .....	1
<b>European Union - USA Engineering Ceramics Summit</b>	
EU/USA Summit I .....	1
EU/USA Summit II .....	2
<b>S1: Mechanical Behavior and Performance of Ceramics &amp; Composites</b>	
Fracture, Mechanical Properties I .....	3
<b>S4: Armor Ceramics</b>	
Impact, Penetration and Material Modeling .....	4
<b>S7: 6th International Symposium on Nanostructured Materials and Nano-Composites</b>	
Nanomaterials for Photocatalysis, Solar Hydrogen and Thermoelectrics I .....	7
Nanomaterials for Photocatalysis, Solar Hydrogen and Thermoelectrics II .....	7
<b>S8: 6th International Symposium on Advanced Processing and Manufacturing Technologies for Structural and Multifunctional Materials and Systems (APMT) in honor of Professor R. Judd Diefendorf</b>	
In Honor of Professor R. Judd Diefendorf .....	8
<b>S9: Porous Ceramics: Novel Developments and Applications</b>	
Processing Methods for Porous Ceramics I .....	10
Processing Methods for Porous Ceramics II .....	10
<b>S14: Advanced Materials and Technologies for Rechargeable Batteries</b>	
Advanced Materials and Designs for Lithium Batteries .....	12
<b>FS2: Computational Design, Modeling, and Simulation of Ceramics and Composites</b>	
Simulation of Structure and Properties of Advanced Ceramics .....	14
<b>FS3: Next Generation Technologies for Innovative Surface Coatings</b>	
Technology for Innovative Surface Engineering .....	16

## **European Union - USA Engineering Ceramics Summit**

EU/USA Summit III .....	18
EU/USA Summit IV .....	18

## **S1: Mechanical Behavior and Performance of Ceramics & Composites**

Fracture, Mechanical Properties II .....	19
--	----

## **S4: Armor Ceramics**

Dynamic Behavior .....	21
------------------------	----

## **S7: 6th International Symposium on Nanostructured Materials and Nano-Composites**

Nanodevices and Industrial Application .....	22
Synthesis and Industrial Development of Nanoparticles .....	23

## **S8: 6th International Symposium on Advanced Processing and Manufacturing Technologies for Structural and Multifunctional Materials and Systems (APMT) in honor of Professor R. Judd Diefendorf**

Advanced Forming and Powder Technology .....	24
--	----

## **S9: Porous Ceramics: Novel Developments and Applications**

Membranes and High SSA Ceramics .....	26
Structure and Properties of Porous Ceramics I .....	27

## **S14: Advanced Materials and Technologies for Rechargeable Batteries**

Materials Characterization and Diagnostics For Lithium Batteries .....	28
--	----

## **FS2: Computational Design, Modeling, and Simulation of Ceramics and Composites**

Characterization and Modeling of Surfaces, Interfaces and Grain Boundaries at Multiple Scales	29
---	----

## **FS3: Next Generation Technologies for Innovative Surface Coatings**

Next Generation Production Methods for Surface Engineering .....	31
--	----

## **FS4: Advanced (Ceramic) Materials and Processing for Photonics and Energy**

Multifunctional Materials for Biological Applications .....	32
---	----

Optical Properties of Nanomaterials .....	33
<b>European Union - USA Engineering Ceramics Summit</b>	
EU/USA Summit V .....	34
EU/USA Summit VI .....	34
<b>S1: Mechanical Behavior and Performance of Ceramics &amp; Composites</b>	
Ceramic Fiber Reinforced Composites .....	35
<b>S4: Armor Ceramics</b>	
Transparent Materials I .....	37
<b>S7: 6th International Symposium on Nanostructured Materials and Nano-Composites</b>	
Industrial Application of Nanomaterials and One Dimensional Structures .....	39
Nanostructured Membranes, Functional Coatings and Nanocomposites .....	40
<b>S8: 6th International Symposium on Advanced Processing and Manufacturing Technologies for Structural and Multifunctional Materials and Systems (APMT) in honor of Professor R. Judd Diefendorf</b>	
Advanced Composite Manufacturing .....	41
SPS and Micro-Wave Assisted Technology .....	42
<b>S9: Porous Ceramics: Novel Developments and Applications</b>	
Structure and Properties of Porous Ceramics II .....	43
Mechanical Properties of Porous Ceramics .....	44
<b>S14: Advanced Materials and Technologies for Rechargeable Batteries</b>	
Ceramics for Electric Energy Generation, Storage, and Distribution .....	45
<b>FS2: Computational Design, Modeling, and Simulation of Ceramics and Composites</b>	
Novel Simulation Method and Virtual Material Design .....	46
<b>FS3: Next Generation Technologies for Innovative Surface Coatings</b>	
Longer Life Solution, Technological Problems and Solutions, and Mass Production .....	48

<b>FS4: Advanced (Ceramic) Materials and Processing for Photonics and Energy</b>	
Advanced Materials for Environmental Applications I .....	50
Solid State Ionics .....	50
<b>S1: Mechanical Behavior and Performance of Ceramics &amp; Composites</b>	
Symposium 1:Poster Session .....	51
<b>S4: Armor Ceramics</b>	
Symposium 4:Poster Session .....	55
<b>S9: Porous Ceramics: Novel Developments and Applications</b>	
Symposium 9:Poster Session .....	58
<b>S14: Advanced Materials and Technologies for Rechargeable Batteries</b>	
Symposium 14:Poster Session .....	59
<b>FS2: Computational Design, Modeling, and Simulation of Ceramics and Composites</b>	
Focused Session 2:Poster Session .....	60
<b>FS3: Next Generation Technologies for Innovative Surface Coatings</b>	
Focused Session 3:Poster Session .....	62
<b>FS4: Advanced (Ceramic) Materials and Processing for Photonics and Energy</b>	
Focused Session 4:Poster Session .....	64
<b>S1: Mechanical Behavior and Performance of Ceramics &amp; Composites</b>	
In-Situ Evaluations Using X-rays/Neutrons and NDE .....	64
<b>S2: Advanced Ceramic Coatings for Structural, Environmental, and Functional Applications</b>	
Thermal Barrier Coatings I .....	67
<b>S4: Armor Ceramics</b>	
Transparent Materials II .....	69
Opaque Materials I .....	69

<b>S7: 6th International Symposium on Nanostructured Materials and Nano-Composites</b>	
Nanotubes, Nanowires and Other One-dimensional Structures .....	70
Nanostructured Materials and their Application .....	71
<b>S8: 6th International Symposium on Advanced Processing and Manufacturing Technologies for Structural and Multifunctional Materials and Systems (APMT) in honor of Professor R. Judd Diefendorf</b>	
Green Manufacturing .....	72
Joining and Integration .....	73
<b>S9: Porous Ceramics: Novel Developments and Applications</b>	
Applications of Porous Ceramics .....	74
<b>S5: Next Generation Bioceramics</b>	
Porous Bioceramics - Joint Session with Symposium 9 on Porous Ceramics .....	75
<b>S12: Materials for Extreme Environments: Ultrahigh Temperature Ceramics (UHTCs) and Nanolaminated Ternary Carbides and Nitrides (MAX Phases)</b>	
Structural Stability under Extreme Environments I .....	76
Structural Stability under Extreme Environments II and Novel Processing Methods I .....	77
<b>S14: Advanced Materials and Technologies for Rechargeable Batteries</b>	
Lithium Metal Air Batteries and Beyond Lithium Batteries .....	78
<b>FS3: Next Generation Technologies for Innovative Surface Coatings</b>	
Low Friction Coating .....	80
<b>FS4: Advanced (Ceramic) Materials and Processing for Photonics and Energy</b>	
Photoelectrochemical Systems .....	82
Photovoltaics .....	83
<b>S1: Mechanical Behavior and Performance of Ceramics &amp; Composites</b>	
Environmental Effects of Ceramics and Composites .....	84
Reliability .....	84



<b>S2: Advanced Ceramic Coatings for Structural, Environmental, and Functional Applications</b>	
Thermal Barrier Coatings II .....	.85
<b>S3: 9th International Symposium on Solid Oxide Fuel Cells (SOFC): Materials, Science and Technology</b>	
SOFC Applications and Technology Overview .....	.87
SOFC Applications and IC Development .....	.87
<b>S4: Armor Ceramics</b>	
Opaque Materials II .....	.89
<b>S5: Next Generation Bioceramics</b>	
Advanced Processing of Bioceramics I .....	.90
Advanced Processing of Bioceramics II .....	.91
<b>S7: 6th International Symposium on Nanostructured Materials and Nano-Composites</b>	
Bio-active Nanomaterials and Nanostructured Materials for Bio-medical Applications .....	.92
Synthesis and Characterization Techniques for Nanostructures .....	.93
<b>S8: 6th International Symposium on Advanced Processing and Manufacturing Technologies for Structural and Multifunctional Materials and Systems (APMT) in honor of Professor R. Judd Diefendorf</b>	
Novel Processing .....	.94
<b>S12: Materials for Extreme Environments: Ultrahigh Temperature Ceramics (UHTCs) and Nanolaminated Ternary Carbides and Nitrides (MAX Phases)</b>	
New Methods for Joining .....	.96
Novel Processing Methods II .....	.97
<b>Global Young Investigators Forum</b>	
Frontiers in Ceramic Sensors I .....	.99
Frontiers in Ceramic Sensors II .....	.99

<b>FS4: Advanced (Ceramic) Materials and Processing for Photonics and Energy</b>	
Multiferroics for Photovoltaics .....	100
Advanced Materials for Environmental Applications II .....	101
<b>S2: Advanced Ceramic Coatings for Structural, Environmental, and Functional Applications</b>	
Symposium 2: Poster Session .....	102
<b>S3: 9th International Symposium on Solid Oxide Fuel Cells (SOFC): Materials, Science and Technology</b>	
Symposium 3: Poster Session .....	103
<b>S5: Next Generation Bioceramics</b>	
Symposium 5: Poster Session .....	105
<b>S7: 6th International Symposium on Nanostructured Materials and Nano-Composites</b>	
Symposium 7: Poster Session .....	106
<b>S8: 6th International Symposium on Advanced Processing and Manufacturing Technologies for Structural and Multifunctional Materials and Systems (APMT) in honor of Professor R. Judd Diefendorf</b>	
Symposium 8: Poster Session .....	110
<b>S10: Thermal Management Materials and Technologies</b>	
Symposium 10: Poster Session .....	112
<b>S11: Nanomaterials for Sensing Applications: From Fundamentals to Device Integration</b>	
Symposium 11: Poster Session .....	112
<b>S12: Materials for Extreme Environments: Ultrahigh Temperature Ceramics (UHTCs) and Nanolaminated Ternary Carbides and Nitrides (MAX Phases)</b>	
Symposium 12: Poster Session .....	113
<b>S13: Advanced Ceramics and Composites for Nuclear Applications</b>	
Symposium 13: Poster Session .....	115

## **Global Young Investigators Forum**

GYIF Poster Session .....115

## **FS1: Geopolymers, Inorganic Polymers, Hybrid Organic-Inorganic Polymer Materials**

Focused Session 1:Poster Session .....116

## **S1: Mechanical Behavior and Performance of Ceramics & Composites**

Processing-Microstructures-Properties Correlations I .....117

## **S2: Advanced Ceramic Coatings for Structural, Environmental, and Functional Applications**

Environmental Barrier Coatings and Protective Coating-Component Systems for Extreme Environments .....119

## **S3: 9th International Symposium on Solid Oxide Fuel Cells (SOFC): Materials, Science and Technology**

Electrode Materials and Microstructural Engineering I .....121

Electrode Materials and Microstructural Engineering II .....122

## **S5: Next Generation Bioceramics**

Bioinspired, Biomimetic, and Biologically-derived Ceramics I .....123

Bioinspired, Biomimetic, and Biologically-derived Ceramics II .....124

## **S7: 6th International Symposium on Nanostructured Materials and Nano-Composites**

Synthesis, Functionalization, Processing and Self-assembly of Nanoparticles I .....124

Synthesis, Functionalization, Processing and Self-assembly of Nanoparticles II .....125

## **S8: 6th International Symposium on Advanced Processing and Manufacturing Technologies for Structural and Multifunctional Materials and Systems (APMT) in honor of Professor R. Judd Diefendorf**

Processing, Structure and Properties .....126

## **S11: Nanomaterials for Sensing Applications: From Fundamentals to Device Integration**

Sensing Devices I .....128

<b>S12: Materials for Extreme Environments: Ultrahigh Temperature Ceramics (UHTCs) and Nanolaminated Ternary Carbides and Nitrides (MAX Phases)</b>	
Processing, Structure and Property Relationships .....	130
Novel Characterization Methods .....	131
<b>S13: Advanced Ceramics and Composites for Nuclear Applications</b>	
Ceramics for Nuclear Reactors and Fuels .....	132
<b>Global Young Investigators Forum</b>	
Frontiers in Ceramic Hybrid Materials and Composites for Biomedical Applications .....	133
Frontiers in Ceramic Chemistry and Biomedical Applications .....	134
<b>S1: Mechanical Behavior and Performance of Ceramics &amp; Composites</b>	
Processing-Microstructure-Properties Correlations II .....	136
<b>S2: Advanced Ceramic Coatings for Structural, Environmental, and Functional Applications</b>	
Coatings to Resist Wear, Erosion and Extreme Environments .....	138
<b>S3: 9th International Symposium on Solid Oxide Fuel Cells (SOFC): Materials, Science and Technology</b>	
Mechanical and Thermal Properties .....	140
SOFC Electrolyte and Seal .....	141
<b>S5: Next Generation Bioceramics</b>	
Advanced Processing of Bioceramics III .....	142
Advanced Processing of Bioceramics IV .....	143
<b>S10: Thermal Management Materials and Technologies</b>	
Characterization of Thermal Management Materials .....	144
Processing and Integration Strategies for Thermal Management Materials .....	145
<b>S11: Nanomaterials for Sensing Applications: From Fundamentals to Device Integration</b>	
Sensing Devices II .....	146

<b>S12: Materials for Extreme Environments: Ultrahigh Temperature Ceramics (UHTCs) and Nanolaminated Ternary Carbides and Nitrides (MAX Phases)</b>	
Design of New Compositions/Composites with Fascinating Properties .....	147
Fundamental Understanding and Novel Processing Methods .....	148
<b>S13: Advanced Ceramics and Composites for Nuclear Applications</b>	
Advanced Non-oxide Ceramics: Fabrication, Characterization, and Radiation Damage Tolerance .....	149
<b>Global Young Investigators Forum</b>	
Frontiers in Ceramic Energy Generation and Storage .....	152
Frontiers in Ceramic Characterization and Catalytical Properties .....	153
<b>FS1: Geopolymers, Inorganic Polymers, Hybrid Organic-Inorganic Polymer Materials</b>	
Chemistry, Processing and Microstructure .....	154
<b>S1: Mechanical Behavior and Performance of Ceramics &amp; Composites</b>	
Tribological Applications .....	156
Characterization .....	157
<b>S2: Advanced Ceramic Coatings for Structural, Environmental, and Functional Applications</b>	
Advanced Processing and Protective Coating Systems for Extreme Environments .....	158
<b>S3: 9th International Symposium on Solid Oxide Fuel Cells (SOFC): Materials, Science and Technology</b>	
Novel Processing Approaches for Cell and Stack Materials .....	159
Cell Component, Cell Design and Reliability .....	160
<b>S5: Next Generation Bioceramics</b>	
Medical and Dental Applications of Bioceramics I .....	161
Medical and Dental Applications of Bioceramics II .....	162

<b>S12: Materials for Extreme Environments: Ultrahigh Temperature Ceramics (UHTCs) and Nanolaminated Ternary Carbides and Nitrides (MAX Phases)</b>	
Methods for Improving Mechanical, Oxidation and Thermal Shock Resistance .....	163
Fundamental Understanding of the Structure-Property Relationships .....	164
<b>S13: Advanced Ceramics and Composites for Nuclear Applications</b>	
Ceramics and Glass for Waste Immobilization .....	165
Joining and Coating .....	166
<b>Global Young Investigators Forum</b>	
Frontiers in Hybrid Materials and Composites .....	167
Frontiers in Precursor and Ceramic Chemistry .....	168
<b>FS1: Geopolymers, Inorganic Polymers, Hybrid Organic-Inorganic Polymer Materials</b>	
Fiber-reinforced Geopolymer Composites .....	169
Bioapplications, Inorganic-organic Hybrids, and Phosphate-based Inorganic Polymers ....	169

## Monday, January 23, 2012

### Plenary Session

Room: Coquina Salon D

#### 9:00 AM

#### (ICACC-PL-001-2012) Ceramic Composites for High Temperature Aerospace Structures and Propulsion Systems (Invited)

D. Marshall\*, Teledyne Scientific, USA

The optimization of fiber architecture in ceramic composites has provided new opportunities for the design of aerospace structures and propulsion systems that require lightweight, strong, high temperature materials. The development of textile based composites for application in hypersonics, turbine engines, and rocket nozzles will be discussed. The most extreme applications use active cooling, enabled by the use of thin textile-based hot skins that are able to tolerate extreme thermal gradients. They can also be formed into structures that enable other functionality, including transpiration and film cooling, mitigation of thermal stresses, and shape-morphing structures with potential use in combustion flow paths of hypersonic vehicles. The major challenges and strategies for realizing the potential of these textile-based CMC structures will be discussed.

#### 9:40 AM

#### (ICACC-PL-002-2012) Ceramics for innovative energy and storage systems (Invited)

A. Michaelis\*, Fraunhofer Institute for Ceramic Technologies and Systems IKTS, Germany

The joint application of structural and functional ceramic process technologies such as "ceramic thick film deposition" allows for unique combination of electronic, ionic (electrochemical) and mechanical materials properties enabling for development of new, highly integrated systems. With this approach significant progress for meeting the performance and cost targets of advanced energy conversion and storage systems can be achieved. We present examples for Solar Cell, Fuel Cell and Li-Ion battery development.

#### 10:40 AM

#### (ICACC-PL-003-2012) Advanced Battery Materials and Technologies for Next Generation Automobiles: Beyond Li-ion Batteries (Invited)

Y. Ukyo\*, TOYOTA Central Research & Development Laboratories Inc., Japan

In my talk, I will present the important role of ceramic materials in batteries, especially in Li-ion battery, for hybrid vehicles (plug-in hybrid vehicles) and all electric vehicles. As it is well known, battery is one of chemical reactors in which all components are under very severe environments, such as high oxidation/ reduction condition and large volumetric changes. I will discuss the various material degradation issues during high temperature cycling of Li-ion batteries. Possible solutions to mitigate the battery degradation, based on materials perspective, will be presented. Further, I will touch upon the possibility of new battery concepts, beyond the Li-ion battery, for next generation automobiles.

#### 11:20 AM

#### (ICACC-PL-004-2012) Overview of Brazilian Ceramics R&D Activities and Challenges in Design and Processing of Multifunctional Ceramic Materials and Systems (Invited)

J. Varela\*, M. A. Ramirez, E. Longo, Universidade Estadual Paulista, Brazil

There has been a long term and sustained effort in advanced ceramics research in Brazil over last few decades. These efforts are focussed on developing ceramic materials and technologies for energy, environmental, industrial, and biological applications. In this presentation, an overview of recent research and development activities in the area of advanced structural and multifunctional ceramics will be presented. In the area of multifunctional ceramics, various challenges in

design and processing of different materials and systems will be discussed in detail. The stability of non-ohmic properties of some semi-conducting oxides will be discussed. The effect of electric field stresses on the stability of ZnO and SnO<sub>2</sub> based varistor is discussed in terms of chemical defects at depletion layers and secondary phases. Moreover the non-ohmic and dielectric properties of CaCu<sub>3</sub>Ti<sub>4</sub>O<sub>12</sub> (CCTO) are influenced by its chemical composition. Models for grain boundary barriers and intra-grain defects will be critically discussed to explain the electrical properties of these systems. A nano barrier layer capacitor model is proposed to explain the giant dielectric constant in CCTO in both, single crystal and polycrystalline, systems.

## European Union - USA Engineering Ceramics Summit

### EU/USA Summit I

Room: Coquina Salon F

Session Chair: Sanjay Mathur, University of Cologne

#### 1:30 PM

#### (ICACC-EUUSA-001-2012) Porous Wall, Hollow Glass Microspheres (Invited)

G. Wicks\*, Savannah River National Lab, USA

The Savannah River National Laboratory (SRNL) has developed a new class of materials called "Porous Wall, Hollow Glass Microspheres" or PWHGMs. These glass microballoons are about 1/3 the diameter of a human hair, range in size from 2 to 100 microns, and have wall thicknesses or shells of only 1-2 micron. What makes these materials one-of-a-kind, is that the team found a way to induce and control 'thorough-wall porosity' on a scale of 100 to 3,000 angstroms. This unique porosity has been used to fill the microballoons with absorbents as well as other materials, including solids, liquids and gases, and provides for the encapsulated materials a contained environment, even for reactive species. Micrographs of filled PWHGMs have appeared on the cover of several magazines, with one caption stating "Porous Glass Microspheres..... SRNL's breakthrough opens new realms for Energy, Environment, Medicine and Security". These materials have resulted in about a dozen new research programs in a variety of areas. The technology has been patented, one license issued so far, and recently, has also received the R&D 100 Award signifying it as "...one of the 100 most technically significant products to enter the marketplace in 2011". These exciting new materials will be discussed.

#### 2:00 PM

#### (ICACC-EUUSA-002-2012) New ceramic membranes for energy- and environmental applications (Invited)

A. Michaelis\*, I. Voigt, Fraunhofer Institute for Ceramic Technologies and Systems IKTS, Germany

Ceramic membranes are well established for micro-, ultra- or nano-filtration applications such as waste water purification. Further innovations require an improved control and reduction of pore size. This allows for new applications in gas separation and pervaporation systems. For this, pores sizes below 1 nm have to be generated using specific structural features of selected materials. Several new methods for preparation of such membranes are presented. In a first example we use the well know crystallographic cage structure of zeolites. Employing a new hydrothermal route allows for synthesis of dense zeolite films on porous substrates. It is shown that these membranes can be used for dewatering of bioethanol. In a further example we use carbon layers with well defined lattice distances of 0.35 nm as a membrane for separation of hydrogen from gas mixtures. By further chemical modification of these carbon layers a well designed adsorption selective behaviour can be achieved as is demonstrated with membranes for purification of biogas. As a last example we present perovskite materials showing mixed conducting behaviour. Due to an oxygen vacancy structure in the crystal lattice these materials can be used to generate

oxygen which in turn can be used to improve the efficiency of combustion processes. Besides an improved energy balance in the combustion process this leads to reduction of CO<sub>2</sub> emissions.

**2:30 PM**

**(ICACC-EUUSA-003-2012) Next Generation Microturbine with Ceramic Hot-Section (Invited)**

J. Kesseli\*, T. Wolf, J. Nash, Brayton Energy, USA

A 350kW gas turbine engine is under development for vehicular and stationary power applications. The high firing temperature afforded by the silicon nitride turbine rotor, and advanced intercooled-recuperated cycle, yields exceptionally high projected shaft efficiency of 44% LHV. This engine is well suited for direct-drive vehicle applications by virtue of excellent part-load efficiency, and favorable torque characteristics stemming from a free-power-turbine architecture. Design challenges in the stationary hot section are met through novel application of ceramic elements and high-temperature metals. This paper focuses on design issues for the ceramic turbine, covering projections of rotor life and performance findings from an ongoing engine test program.

**EU/USA Summit II**

Room: Coquina Salon F

Session Chair: Mrityunjay Singh, OAI/NASA GRC

**3:20 PM**

**(ICACC-EUUSA-004-2012) Advances in Ceramic Membranes for H<sub>2</sub>/Syngas Production and Clean Energy Applications (Invited)**

J. C. Chen\*, D. M. Taylor, M. F. Carolan, Ceramatec, Inc., USA; D. W. Studer, Air Products and Chemicals, Inc., USA

An overview of advances in Ion Transport Membranes (ITMs) for H<sub>2</sub>/syngas production and clean energy applications will be presented. The ITM Syngas process is a breakthrough technology that combines air separation and high-temperature synthesis gas generation processes into a single ceramic membrane reactor, with potential for significant savings in the capital cost of Syngas production. ITM technology based on different mixed-conducting oxides will be reviewed using concepts from electrochemistry and solid state chemistry. Emphasis is on the defect chemistry, the mechanism of oxygen transport through mixed conductors and the associated surface exchange kinetics, providing some basic background knowledge for development of ITM technology. Progress in fabrication of ceramic wafer with thin dense membrane supported on multi-channel structure will be presented. Manufacturing techniques are being developed from lab-scale wafer to pilot reactor scale module. Testing of the ITM module progressed from lab-scale to pilot reactor scale will be also presented. Technical challenges of ceramic materials, wafer/module fabrication, process control and reactor engineering for ITM technology will be discussed. Results to date confirm ITM technology can achieve step-change improvement for H<sub>2</sub>/syngas production and other clean energy applications.

**3:50 PM**

**(ICACC-EUUSA-005-2012) Polymer-Derived-Ceramics Research and Development in Europe (Invited)**

P. Colombo\*, University of Padova, Italy

Pre-ceramic polymers were proposed about 40 years ago as precursors for the fabrication of mainly Si-based advanced ceramics (polymer-derived ceramics or PDCs). This approach led to significant technological developments, such as the fabrication of ceramic fibers and the discovery of amorphous ceramic materials capable of operating at very high temperatures (up to 2000°C). Functional properties have been now discovered in several PDC systems, such as piezo-resistivity, semi-conductivity and luminescence, and have been linked to the particular structure of these materials at the nanoscale. This paper will review the current state of the art for the field, and illustrate the research efforts currently taking place in Europe, leading to the devel-

opment of novel compositions and components suitable for a wide range of engineering applications.

**4:20 PM**

**(ICACC-EUUSA-006-2012) Innovations in bioactive ceramics and glasses for tissue engineering, drug delivery and regenerative medicine (Invited)**

A. Boccaccini\*, University of Erlangen-Nuremberg, Germany

Beyond the well established and expanding applications of bioceramics in medicine, e.g. as permanent implants and bioactive coatings, there is increasing interest in developing bioactive ceramics and glasses and their composites with biodegradable polymers, for applications in the fields of tissue engineering and drug delivery. Specific innovations involving the design and fabrication of multifunctional scaffolds that combine a variety of biodegradable polymers, signalling molecules, therapeutic drugs and bioactive ceramics will be presented. In this context, significant efforts are being devoted to investigating the effect of the dissolution products of bioactive glasses, both silicate and phosphate glasses, on cellular response, which includes understanding the effect of specific metallic ions (bioinorganics) on osteogenesis and angiogenesis during bone formation, both in vitro and in vivo. In addition, gaining further understanding of the antibacterial effect of specific ions released from bioactive glasses for combating infections more effectively is of particular interest. Specific research areas attracting large research efforts will be presented and promising avenues for future research activities will be discussed, highlighting the current needs and challenges for improving the overall performance of bioactive ceramics in tissue engineering and drug delivery.

**4:50 PM**

**(ICACC-EUUSA-007-2012) Silica Mesoporous Particles in Nanomedicine: State of the Art (Invited)**

A. Garcia-Bennett\*, Uppsala University, Sweden

Mesoporous silica based nanoparticles are of potential interest for the development of novel targeted drug delivery vehicles due to their high surface areas (above 1000 m<sup>2</sup>/g) and large internal pore volumes. Their uses in pharmaceuticals to improve drug formulation, drug bioavailability, to mitigate drug toxicity, to act as adjuvants in immunoregulation and in cellular targeting through controlled drug delivery strategies has been shown. This work aims to review some of the groundbreaking work being conducted at the interface between nanomaterials and pharmaceutical sciences using mesoporous particles as drug delivery vehicles and drawing particular attention towards their use as vehicles for targeted delivery in cancer treatment. Folic acid and folate derivatives are important biomolecules due to their involvement in nucleotide and DNA synthesis, as 5-methyltetrahydrofolate monoglutamate. They are hence essential molecules in the reproduction and survival of cells and tissue. The toxicology of mesoporous materials appears thus far to be closely related to conventional amorphous silica, and in vivo murine models suggest that high doses of mesoporous silica are well tolerated in oral and intravenous administration routes. Other state of the art studies are being performed in complex areas such as theranostics, and regenerative medicine attesting to the promising potential of mesoporous particles.

**5:20 PM**

**(ICACC-EUUSA-008-2012) Nonhydrolytic Sol-Gel Reactions for the Synthesis of Oxide Materials (Invited)**

J. Pinkas\*, Masaryk University, Czech Republic

Nonhydrolytic sol-gel processes are promising new routes for the preparation of new oxide, silicate and phosphate materials. These reactions are based on aprotic polycondensations with the elimination of small organic molecules (ethers, esters, alkylhalides, etc.) in the absence of hydroxyl groups. One of our goals was the synthesis of new precursors - aluminum chloride-alkoxides - and their nonhydrolytic



transformation to alumina by alkylhalide elimination. The second area of interest was improving the synthesis of phosphosilicate gels. We prepared phosphosilicate gels by the elimination of acetic acid esters in heteropolycondensation reactions between silicon(IV) acetate and tris(trimethylsilyl) ester of phosphoric acid. The nonhydrolytic ester elimination provides clear amorphous hybrid phosphosilicate gels at room temperature. Finally, a novel non-hydrolytic synthesis of a  $\text{SiO}_2 \cdot \text{TiO}_2$  mixed oxide system by the polycondensation of silicon(IV) acetate with titanium(IV) dimethylamide, diethylamide, and isopropoxide was studied. The materials were tested in the epoxidation of cyclohexene by cumyl hydroperoxide and showed a high selectivity but a mediocre activity. Catalytic properties were significantly improved by combining non-hydrolytic and hydrolytic methods yielding mesoporous and homogeneously mixed silica-titania dioxide.

## S1: Mechanical Behavior and Performance of Ceramics & Composites

### Fracture, Mechanical Properties I

Room: Coquina Salon D

Session Chairs: Jon Salem, NASA Glenn Research; Joaquin Ramirez-Rico, Universidad de Sevilla - CSIC

#### 1:30 PM

##### (ICACC-S1-001-2012) Meeting the Challenges in Thermomechanical Characterization of CMCs (Invited)

F. Zok\*, University Of California, Santa Barbara, USA

The presentation will highlight recent developments in design and execution of information-rich experiments for thermomechanical characterization of CMCs and their role in failure prediction of CMC components in propulsion systems. Effects of multi-axial stresses as well as temperature and stress gradients will be emphasized. Models of material behavior under these conditions will also be described and assessed.

#### 2:00 PM

##### (ICACC-S1-002-2012) Modeling of Delamination and Damage Processes in CMC Components

R. S. Kumar\*, United Technologies Research Center, USA

Design of gas turbine engine components made of ceramic matrix composite (CMC) materials requires: 1) detailed understanding of damage processes at multiple length scales; 2) nonlinear constitutive models that capture essential damage mechanisms; and 3) efficient, validated computational tools that can predict the initiation, propagation, and ultimate failure of complex-shaped parts under multiaxial stress states. This paper presents the results of a modeling framework that considers both intra-laminar ply damage (matrix cracking and fiber failure) and interlaminar damage (delamination) processes in complex-shaped CMC sub-elements. The ply damage mechanisms are modeled using micromechanics-based nonlinear constitutive equations with matrix cracking, longitudinal splitting, and fiber failure modes represented via internal damage variables. The initiation and propagation of delaminations between the plies are modeled explicitly using a cohesive zone finite element approach. The model is used to predict the behavior of various test coupons and sub-elements made from a 2D woven fabric CMC and the results are compared against experimental data. In addition, a parametric study is conducted to explore the effects of variations in material properties on the overall damage response of the sub-elements.

#### 2:20 PM

##### (ICACC-S1-003-2012) High-Temperature Interlaminar Tension Test Method Development for Ceramic Matrix Composites

T. Engel\*, Hyper-Therm HTC, Inc., USA

Ceramic Matrix Composite (CMC) materials are an attractive design option for various high-temperature structural applications. How-

ever, 2D fabric-laminated CMCs typically exhibit low interlaminar tensile (ILT) strengths, and interply delamination is a concern for some targeted applications. Currently, standard test methods only address the characterization of interlaminar tensile strengths at ambient temperatures, which is problematic given that nearly all CMCs are slated for service in elevated temperature applications. This work addresses the development of a new test technique for the high-temperature measurement of CMC interlaminar tensile properties.

#### 2:40 PM

##### (ICACC-S1-004-2012) Electrical Resistivity of a Variety of SiC/SiC Composites

G. Morscher\*, J. Dainovic, The University of Akron, USA; C. Smith, Ohio Aerospace Institute, USA

Electrical resistivity is a potential NDE/damage-detection technique for SiC/SiC composites. A variety of composites with melt-infiltrated matrices and different fiber types were tested at room temperature while monitoring electrical resistivity (ER) and acoustic emission (AE) during the test. AE was used to determine stress-dependent matrix cracking. The change in resistivity during the test and for the different composites was modeled based on the constituent content and fiber-architecture, the resistivities of the composite constituents, the number of matrix cracks, and the increased resistance associated with each crack.

#### 3:20 PM

##### (ICACC-S1-005-2012) Laser Heat Flux Testing and Characterization of Composite Materials using Digital Image Correlation

M. D. Novak\*, F. W. Zok, University of California Santa Barbara, USA

High-temperature digital image correlation offers an experimental route to measure strain at temperatures up to 1500°C, with spatial resolution at the tow level of composite materials. Supplementing strain maps with imaging pyrometry provides an information-rich approach for thermomechanical characterization. Such an approach can be used in conjunction with laser heating to assess material response under a wide range of conditions, such as extreme thermal gradients and applied loads. The testing and analysis of C/SiC and SiC/SiC materials are described, demonstrating the unique capabilities of laser heat flux testing with digital image correlation.

#### 3:40 PM

##### (ICACC-S1-006-2012) Evaluating the Effect of Embedded Sensors on CMC Mechanical Properties

C. Smith\*, Ohio Aerospace Institute, USA; J. Kiser, R. Okojie, L. Evans, NASA GRC, USA; A. Calomino, NASA LARC, USA

A NASA-led interdisciplinary team with members from several NASA centers and Industry has been developing SITPS (structurally integrated thermal protection system) for use on hypersonic vehicles. In support of that effort, a task was established to develop fully-functional embedded wireless sensors for use in SITPS. The goal is for those sensors to be capable of receiving and transmitting information within a CMC (ceramic matrix composite) article operating at temperatures above 2000°F. One of the initial steps in this task has been to investigate CMC specimens which are representative of SITPS surface/outer mold line material. During processing, some of the specimens were embedded with SiC chips (disks) that are representative of the substrates that the future wireless sensors will be assembled on. Non-destructive evaluation, such as CT, thermography and X-radiography were used to evaluate the bonding between the SiNC matrix and the dummy sensors and to determine the location of the chips. Mechanical tests were then conducted at both room temperature and elevated temperature to develop an understanding of the interaction between the SiC chips and the composite. Matrix cracking was monitored via Acoustic Emission. Fracture surfaces and polished sections were examined to characterize the damage and the effect of the SiC chips.

4:00 PM

### (ICACC-S1-007-2012) Thermal Shock, Microstructure, Ionic Conductivity, and OOF2 Modeling of 8YSZ Composites

J. P. Angle\*, M. M. Chan, M. L. Mecartney, University of California, Irvine, USA

Zirconia-based oxygen sensors operate at 900°C and thermal shock is one of the major causes of failure. This project investigates the thermal shock behavior of 8 mol% yttria-stabilized zirconia (8YSZ) with added second phases such as silica, alumina and mullite. Theoretical calculations indicate the thermal shock resistance (TSR) should increase with the addition of these second phases. Quenching experiments and three-point bending were used to determine the critical temperature difference and flexural strength for compositions with up to 20 vol.% second phase. Increased TSR was observed with an increase in the volume of second phase, with the most significant improvement when the percolation limit of the second phase was reached. Grain size analysis by scanning electron microscopy found that additions of nanocrystalline second phases led to a smaller grain size and increased TSR. While a fine grain size is advantageous for TSR, an increase in grain boundaries can decrease the ionic conductivity. Object Oriented Finite Element Analysis Version 2 (OOF2) developed by NIST was used to determine how microstructures with varying grain sizes and compositions affect both thermal and mechanical properties of 8YSZ composites. Results from electrochemical impedance spectroscopy will be used to analyze the effect of grain size reduction and presence of second phases on ionic conductivity.

4:20 PM

### (ICACC-S1-008-2012) Measurement of Temperature Dependence of Thermal Stress in Polycrystalline Oxide Ceramics

Y. Dong\*, H. Kakisawa, Y. Kagawa, The University of Tokyo, Japan

An effective way of measuring damage evolution and crack growth in polycrystalline alumina with different grain sizes is established. The micro damage evolution and crack growth behaviors in polycrystalline alumina have been observed from room temperature to elevated temperatures. Initial damage is introduced using Vickers indentation or Rockwell indentation. The variations of damages and cracks are continuously monitored by CCD camera with UV lens under UV illumination as a function of temperature. When the temperature reaches about 800°C, a bandpass filter is necessary to cut black-body radiation of high-temperature objects on the intensity of captured images. The measured images are converted to two- or three-dimensional strain distributions utilizing a digital image correlation system. The change of strain distribution with temperature is discussed with local and global thermal/residual strain of a polycrystalline alumina.

4:40 PM

### (ICACC-S1-009-2012) Tensile fracture mechanism of silicon impregnated C/C composite

A. Ohtani\*, K. Goto, Japan Aerospace Exploration Agency, Japan

Carbon/carbon composite (C/C) has been widely used for structural material such as space vehicles, nuclear reactors, aircraft brake, and racing car brake, because of its light weight, high strength and toughness at very high temperature. However, interlaminar strength and interlaminar shear strength are very poor, and C/C composite have low gas-barrier properties. In order to improve their problems, Si infiltrated C/C composite (C/C-Si) have been developed. C/C-Si has better interlaminar strength and interlaminar shear strength, in addition the high wear-resistant characteristics, thus C/C-Si is now started to use as a heat resist. However, C/C-Si has also the problem of less than 1/3 of tensile strength compared to the C/C composite. The possible reasons of lower strength are because of the degradation of carbon fiber by Si, the stress concentration at the tip of initial transverse crack, and enlargement of adhesive properties between fiber and matrix. But the fracture mechanism of C/C-Si composite has not been investigated in the previous study. A lower tensile strength of C/C-Si might be improved by the clarification of the fracture mechanism. In this study, tensile tests and in-situ observation for C/C-Si were car-

ried out. In order to clarify the reason for the lower tensile strength of C/C-Si, the micro-fracture mechanism in C/C-Si under tensile loading was investigated.

5:00 PM

### (ICACC-S1-010-2012) Effects of Target Support on Foreign Object Damage in an Oxide/Oxide CMC

D. C. Faucett\*, M. Ayre, J. M. Wright, S. R. Choi, NAVAIR, USA

Foreign object damage (FOD) phenomenon of an oxide/oxide ceramic matrix composite (CMC) were assessed using spherical steel ball projectiles in an impact velocity range of 100 to 350 m/s. CMC test coupons were ballistically impacted at a normal incidence angle while supported in three different configurations of full support, partial support, or cantilever support. Surface and subsurface impact damages, typically in the forms of craters, fiber breakage, delamination, and cone cracks, were characterized with respect to the mode of target supports. Effects of the target supports were also determined via post-impact residual strength measurements in order to better assess the severity of impact damage. The results will be compared with those of an MI SiC/SiC CMC determined previously. Some analytical considerations of impact force with respect to the support mode will be also discussed in conjunction with the impact history recorded during impact events.

5:20 PM

### (ICACC-S1-011-2012) Machinability Studies of Al/SiC/B4C Metal Matrix Hybrid Composites using PCD 1600 grade insert

A. Maheshwari\*, A. Erode Natarajan, A. S. Teja, Sri Venkateswara College Of Engineering, India

Hybrid Metal Matrix Composites (MMC) (Al-SiC/B4C) are widely used in aeronautical and automobile industries due to their excellent mechanical and physical properties. Due to the above properties these composites will slowly replace the conventional material application in Aeronautical and automotive industries. Machining these composites is difficult because of the harder reinforcement of SiC and B4C particles. Tools wear out more quickly and this in turn reduces the life of conventional and coated tool materials with in a short period of time. This paper presents the experimental investigation on turning A356 matrix metal reinforced with 10% by weight of Silicon carbide (SiCp) particles and 5% by weight of Boron carbide particles, the particle size of the silicon carbide and boron carbide ranges from 20 microns to 50 microns, fabricated in house by stir casting method. Fabricated samples are turned on medium duty lathe of 2kW spindle power with Poly crystalline Diamond (PCD) inserts of 1600 grade at various cutting conditions. Parameters such as power consumed by main spindle, machined surface roughness and tool wear and tear are studied. Scanning Electron Microscope (SEM) images support the result. It is evident that surface finish and power consumed are good for 1600 grade at higher cutting speed and tool wear is strongly dependent on abrasive of hard reinforcement particles.

## S4: Armor Ceramics

### Impact, Penetration and Material Modeling

Room: Coquina Salon E

Session Chair: Brian Leavy, Army Research Lab

1:30 PM

### (ICACC-S4-001-2012) Mesoscale Modeling of the Dynamic Response of Armor Ceramics (Invited)

T. H. Antoun\*, O. Vorobiev, E. Herbold, I. Lomov, Lawrence Livermore National Laboratory, USA

Continuum mechanics based constitutive models are widely used in simulations of the macroscopic response of armor ceramics. These models rely on fitting parameters to phenomenologically describe inelastic processes that occur when the material is loaded beyond its elastic limit. As a result, there is no direct correlation between model

parameters and the microstructural properties of the material. For this reason, phenomenological constitutive models tend to produce good results within the domain for which they are calibrated, but they often lack the predictive capability required to extrapolate outside that domain. The predictive capability of phenomenological models can be improved by directly linking the macroscopic material response predicted by the models to the underlying microstructural deformation mechanisms. Recent advances in modeling capabilities coupled with modern high performance computing platforms enable physics-based simulations of heterogeneous media with unprecedented details, offering a prospect for significant advances in the state of the art. This presentation provides an overview of some of these modern computational approaches, discusses their advantages and limitations, and presents simulation results that elucidate several aspects of the complex behavior of armor ceramics and similar heterogeneous materials in extreme dynamic loading environments.

**2:00 PM**

**(ICACC-S4-002-2012) Mechanism-Based Modeling of the Failure of Brittle Materials under Dynamic Multiaxial Loading**

G. Hu\*, K. Ramesh, Johns Hopkins University, USA

A dynamically interacting microcrack damage model is developed to capture the dynamic failure of brittle materials under multiaxial loading conditions. The micromechanics is that of a wing-crack mechanism, assuming a defect density and flaw distributions in both orientation and size. Interactions among cracks are modeled by means of a crack-matrix-effective-medium approach. The material damage, defined as a tensorial parameter incorporating the anisotropic effects, is calculated based upon the crack length and orientation development under local stress fields. The model also accounts for plasticity at high pressures. At low confining stresses, the wing-cracking mechanism dominates, leading to the degradation of the modulus and peak strength of the material, whereas at high enough confining stresses, the crack mechanism is completely shut-down and the dislocation mechanism (validated by shock loaded experiments) is activated. The effects of Poisson's ratio, flaw distribution, confining stress, etc., are explored through parametric studies. The model can be used to capture the dynamic failure of brittle solids under complex multiaxial loading conditions.

**2:20 PM**

**(ICACC-S4-003-2012) Impact Performance of Ceramic-Metal Composites**

B. G. Compton\*, E. A. Gamble, F. W. Zok, University of California, Santa Barbara, USA

This study investigates the performance potential of ceramic-metal composites (cermets) in multi-component armor systems. Cermets are high hardness, high toughness, high strength materials with a degree of tunability not found in traditional armor ceramics. To assess ballistic performance, a series of through-penetration and fully supported impact tests were conducted on titanium carbide-based cermet tiles. Performance was compared to a commercial armor grade alumina under similar loading conditions. Post-impact analysis reveals that cermets are significantly less susceptible to microcrack damage and radial cracking than alumina. In through-penetration tests cermets are found to perform better than alumina on a thickness basis and comparable to alumina on a mass basis. In contrast to alumina, dynamic shear bands are identified as a new performance-limiting failure mechanism in this class of materials. Efforts to incorporate the underlying failure mechanisms into a model will be discussed along with the implications to armor material design.

**2:40 PM**

**(ICACC-S4-004-2012) Specimen Size Effects on the Dynamic Failure Strength of Brittle Materials**

N. Daphalapurkar\*, G. Hu, K. T. Ramesh, Johns Hopkins University, USA

The dynamic failure strength of brittle materials is sensitive to flaw-size distributions (e.g. processing-related flaws in ceramics).

These flaw-size distributions lead to variability in the failure strength of the material. Models available in the literature have considered the following phenomena: (a) for a constant specimen size, the dynamic failure strength increases with increasing strain rate through a power-law relation and is attributed to the inertia of the growing microcracks. (b) sampling of the flaw-size distribution (e.g. due to decreasing specimen sizes) leads to an increase in both the mean of the failure strength and the variation in the failure strength. However, understanding the effect of specimen size as the limiting size for the growth of microcracks that might influence the dynamic failure strength has been a challenge. In this study, failure processes are explicitly simulated to study the effect of varying specimen sizes on the dynamic failure strength. We use the finite element method along with the cohesive zone model to perform simulations incorporating pre-existing flaw-size distributions. Our simulation results are compared with the trends observed from Kolsky bar experiments to reflect on the role of specimen size and flaw-size distribution in damage evolution and failure of brittle materials.

**3:20 PM**

**(ICACC-S4-005-2012) Brittle Model for Porous Materials under Impact: Calibration and Uses for Material Comparison**

C. Z. Katcoff\*, L. Graham-Brady, K. T. Ramesh, Johns Hopkins University, USA

Following the model created by Paliwal and Ramesh (2008) for rectilinear flaws, a model for impact of brittle materials has been created for ceramics with circular flaws. The porous material model has been compared to experimental impact data to calibrate model fit parameters. The current porous material model accounts for a single method of material failure and, therefore, we expect and observe that the model over-predicts experimental results. A combined model with both rectilinear and circular flaws is also compared to experiments. Although the current model is not able to match experimental material strength values, the model does work well to compare the strength of materials subjected to high-strain-rate loading for materials with generally known flaw size and shape information.

**3:40 PM**

**(ICACC-S4-006-2012) Compression Tests of Boron Carbide and Silicon Carbide under Moderate Confinement**

S. Chocron\*, C. E. Anderson, K. A. Dannemann, A. E. Nicholls, N. L. King, Southwest Research Institute, USA

This paper summarizes the characterization work performed on intact and predamaged boron carbide and silicon carbide tested in compression under confinement in a pressure vessel or using a thick steel confining sleeve. The focus is on the effect of pressure (up to 2 GPa hydrostatic pressure) on the strength of both materials. The techniques used for characterization are described. The failure curves obtained are presented and written as Drucker-Prager and Mohr-Coulomb failure criteria. Optical and stereomicroscopy were used to evaluate and document the damage. Finally the results are discussed and compared to the literature. It is shown that data obtained with very different techniques (confined compression, plate impact and divergent plate impact) overlap increasing the confidence in the results.

**4:00 PM**

**(ICACC-S4-007-2012) Confined plate impact experiment of ceramics to study source of inelasticity**

S. Satapathy\*, US Army Research Laboratory, USA

Complex stress states that accompany an impact and penetration event often lead to cracking and comminution in ceramics. However, most computational models are based on simple 1D stress or 1D strain experiments. Very few, if any, experiments exist that can measure the strength under well-defined combined loading states. Even with such limited quantification of constitutive behavior, ceramics

are often modeled with modified “plasticity” type theory with decoupled hydrostatic and deviatoric behavior for convenience. The deviation of the Hugoniot from the hydrostat that indicates plastic flow in metals can manifest in brittle materials through crack evolution, not plasticity necessarily. While in the plasticity theory such deviation depends on the flow strength, in the brittle theory it depends on tensile strength and the principal stresses. Therefore, by applying a lateral confinement to the sample in a plate impact experiment, one would be able to produce distinct combined stress states that can help scrutinize the origin of inelasticity. The experimental result and analysis of such a confined plate impact experiment will be presented in this paper for a ceramic material.

**4:20 PM**

**(ICACC-S4-008-2012) A Novel Class of Equations of State for Hydrocode**

S. Bilyk, M. Greenfield\*, US Army Research Laboratory, USA

A novel class of Equations of State (EoS) for hydrocode is analyzed. It includes two functions  $\Delta(V)$  and  $\chi(E)$ , where  $V$  is a specific volume and  $E$  is a specific internal energy density. Both functions should be determined by comparison with experimental data. By appropriate choice of those functions various physical phenomena can be reliably reproduced and further studied. It is widely recognized now that the search of an absolutely universal EOS hardly exists or too complex for implementation. In other words, various domains of the parameter space require quite different EOS. In different domains of the parameter space the most important (reference) phenomena can be different. For instance, for the compression the reference phenomenon is the appearance of a shock wave. For extension one of the most important phenomenon is a spall. By choosing different functions  $\Delta(V)$  and  $\chi(E)$  in different domains of the parameter space both reference phenomena can be taken into account. We demonstrate how the approach can be applied to ceramic substances.

**4:40 PM**

**(ICACC-S4-009-2012) Influence of a conical projectile tip on the transition from interface defeat to penetration**

P. Lundberg\*, R. Renström, FOI, Swedish Defence Research Agency, Sweden

A large number of interface defeat experiments have been published by various researchers. Unconfined as well as confined and pre-stressed targets in various test scales have been used. An observation is that confinement and pre-stress seems to become less important as the impact test scale becomes smaller. A small scale unconfined target can show similar response as a heavily confined large scale target. This behaviour seems to be related to the formation of a cone shaped crack close to the impact zone. Since the crack resistance of the ceramic material increases with decreasing scale, in contrast to the otherwise scale-invariant elastic stress field, the extension of the cone crack to a critical size will occur at higher impact velocities as the scale decreases. The relatively strong influence of scale on the transition velocity will have an interesting effect on projectiles with a pointed tip, e.g. small arms munitions. The variation in tip diameter as the projectile erodes corresponds to a variation in scale, and thus the ceramic material will show a variation in fracture strength as the projectile tip erodes. The influence of a conical tip on the transition velocity has been studied in an earlier paper and the results from a series of impact experiments using conical tungsten projectiles is here interpreted in relation to the possible influence of scale.

**5:00 PM**

**(ICACC-S4-010-2012) Numerical Convergence of Ballistic Impacts with Ceramic Targets**

S. R. Beissel\*, T. J. Holmquist, Southwest Research Institute, USA

\*\*\*Approval for Public Release Pending\*\*\* The purpose of this study is to investigate the numerical demands of computations of ballistic impacts with ceramic targets. Accurate computations re-

quire a level of refinement that limits differences from the converged solution to an acceptable tolerance. Since ceramics are apt to abruptly lose strength and localize strains, an appropriate level of refinement is expected to exceed that for metallic targets. Finite-element computations are performed of a 7.62-mm ogive-nosed bullet impacting a layer of silicon carbide over an aluminum substrate using six levels of mesh refinement. The cracking patterns in the SiC are compared for all levels of refinement, and convergence plots of absorbed energies and damage in the SiC are presented. Results indicate a lack of convergence for the levels of refinement considered. In contrast, convergence is demonstrated for the same levels of refinement when the SiC is replaced by steel without strain softening and the bullet nose is blunted. Additional computations with SiC targets demonstrate the growth of minute variations to significant differences in the cracking patterns and absorbed energies. In conclusion, the convergence of computations of bullets impacting ceramic targets is precluded at moderate levels of refinement by both the unstable (softening) material response and the sharp projectile tip.

**5:20 PM**

**(ICACC-S4-011-2012) Constitutive Characterization and Simulations of Penetration into Thick Glass Targets**

C. E. Anderson\*, Southwest Research Inst, USA; S. Chocron, R. Bigger, Southwest Research Institute, USA

The strengths as a function of confining pressure for a soda-lime glass and a borosilicate glass were determined. The characterization data were interpreted in terms of a Drucker-Prager constitutive model. The two glasses have similar pressure-dependent slopes, but the borosilicate glass has a larger cap than the soda-lime glass. Simulations were then conducted of penetration experiments into thick glass targets. It is demonstrated that using the constitutive parameters determined from the characterization experiments result in the simulations replicating the experiments. Parametric simulations show the sensitivity of the numerical simulations to changes in the constitutive parameters.

**5:40 PM**

**(ICACC-S4-012-2012) Numerical Study of the Effect of Small Size Surface Flaws on the Ballistic Behavior of Transparent Laminated Targets**

C. G. Fountzoulas\*, P. J. Patel, Army Research Laboratory, USA

Glasses and glass-ceramics are the primary striking ply materials used in transparent armor due to availability, cost, and existing mature manufacturing. Glass is manufactured on a very large scale and there is considerable handling of the glass prior to the lamination process. It has been established that the strength of glass is the highest for a pristine surface. Existing surface flaws, including scratches, reduce the strength of the glass and may deteriorate its effectiveness in an armor configuration. The objective of this study is to understand initially the role of an individual surface flaw on the ballistic performance of the glass, which later will include more surface flaws. The initial approach is to replicate by modeling and simulation the experimental results in order to produce generic strength material model not only for glass but for other transparent ceramics as well. The rapid advancement of the computational power and the recent advances in the numerical techniques and materials models have resulted in improved simulation tools for ballistic impact into single and multi-layer armor configurations. The parameters varied in this computational study are the flaw length and depth using ANSYS/AUTODYN commercial software. The paper will describe the computational results and compare and contrast them to available experimental data.

## S7: 6th International Symposium on Nanostructured Materials and Nano-Composites

### Nanomaterials for Photocatalysis, Solar Hydrogen and Thermoelectrics I

Room: Coquina Salon B

Session Chairs: Palani Balaya, National University of Singapore; Gongxuan Lu, Lanzhou Institute of Chemical Physics, CAS

1:30 PM

#### (ICACC-S7-001-2012) Mesoporous Titanium Oxide Spheres for High Efficiency Dye Sensitized Solar Cells (Invited)

Y. Cheng\*, F. Huang, Monash University, Australia; D. Chen, The University of Melbourne, Australia; Y. Chen, Monash University, Australia; L. Cao, The University of Melbourne, Australia; X. Zhang, Monash University, Australia; R. Caruso, The University of Melbourne, Australia

Dye sensitized solar cell (DSC) is constructed with a semiconductor working electrode, a dye, an electrolyte and a counter electrode. The role of the mesoporous working electrode, usually made of nano titanium oxide (TiO<sub>2</sub>) particles, is to extract and transport electrons from photo-excited dyes to the external circuit. Monodisperse mesoporous TiO<sub>2</sub> beads with submicron-sized diameters have been synthesised through a combined sol-gel and solvothermal process, in which the TiO<sub>2</sub> crystallite size, specific surface area, pore size distribution and the diameter of the beads can be controlled. The mesoporous TiO<sub>2</sub> beads show high surface areas and excellent interparticle connection and provide an idea nano structure for DSC applications. Working electrodes constructed with the mesoporous beads have demonstrated both higher dye loading and stronger light scattering effects, as well as longer electron diffusion lengths and extended electron lifetimes over nano particle TiO<sub>2</sub> electrodes due to the well interconnected, densely packed nanocrystalline TiO<sub>2</sub> particles inside the beads. All of these have resulted in DSC devices showing significant improvements in the conversion efficiency. In addition, the mesoporous beads can be pre-treated before construction of the electrode films, thus offering unique characteristics for making flexible DSCs on plastic substrates.

2:00 PM

#### (ICACC-S7-002-2012) Engineered metal oxide photoanodes for highly efficient excitonic solar cells (Invited)

A. Vomiero\*, I. Concina, CNR IDASC, Italy; A. Braga, V. Galstyan, Brescia University, Italy; N. Memarian, CNR IDASC, Italy; G. Faglia, G. Sberveglieri, Brescia University, Italy

Nano-engineered metal oxides are key components to enhance photoconversion efficiency in excitonic solar cells. A series of strategies can be applied for improving charge photogeneration, injection and collection, including light trapping mechanisms and fast electron transport. Here we review our recent achievements on photoanodes based on quasi one-dimensional nanostructures and nano-networks. Specifically, we will illustrate application of single crystalline ZnO nanowires, ZnO hierarchically assembled aggregates, TiO<sub>2</sub> nanotubes and ZnO-TiO<sub>2</sub> networks. The influence of the geometrical features, of the crystalline assembly and of the optical properties of the layers on photovoltaic performances will be discussed.

2:30 PM

#### (ICACC-S7-003-2012) Nanostructure and Nanoheterojunction for High-Efficiency Photocatalytic and Photoelectrochemical Water Splitting (Invited)

L. Guo\*, S. Shen, Xi'an Jiaotong University, China

The development of the necessary semiconductor photocatalysts has undergone considerable research. Although there are a large number of photocatalyst has been developed, the number of high-efficiency photocatalysts is still limited. As previously reported, nanostructure

and nanoheterojunction design has been generally adopted as one of the most effective approaches to enhance charge separation, opening new potential for the development of high-efficiency photocatalysts for water splitting to produce hydrogen. For example, different kinds of nanostructured and nano-heterogeneous semiconducting materials with excellent activity for photocatalytic and photoelectrochemical hydrogen generation under visible light, have been developed in our lab. Especially, nano-twin CdS-ZnS solid solutions showed a relatively high quantum yield ~43% at 420 nm for photocatalytic hydrogen production. This presentation will describe the primary approaches for efficient photogenerated charge separation in photocatalytic water splitting by fabrication of nanostructured and nano-heterogeneous semiconducting materials, with a focus on the recent progress of our own research. Acknowledgement. The authors acknowledge the support by the National Basic Research Program of China (No. 2009CB220000), Natural Science Foundation of China (No. 50821064 and No. 90610022)

### Nanomaterials for Photocatalysis, Solar Hydrogen and Thermoelectrics II

Room: Coquina Salon B

Session Chairs: Alberto Vomiero, CNR IDASC; Yi-Bing Cheng, Monash University

3:20 PM

#### (ICACC-S7-004-2012) Nanostructural Control in Conjugated Polymer/Metal Oxide Nanohybrid Solar Cells (Invited)

Y. Tachibana\*, A. Azarifar, S. Makuta, RMIT University, Australia; J. Terao, Kyoto University, Japan; S. Seki, Osaka University, Japan

Inorganic metal oxide/conjugated polymer hybrid materials have a wide variety of attractive potentialities to introduce novel structural design in material sciences and to derive novel functions for device applications. In particular, a hybrid structure based on a conducting polymer/metal oxide semiconductor is one of the most advantageous combinations for photo-electronic devices such as LEDs and photovoltaics. The functions of the photovoltaic devices based on the hybrid nanomaterials are controlled by photo-induced charge separation and recombination efficiencies. Modification of the hybrid interface is therefore vital to control these efficiencies. However, studies in this interfacial control are relatively limited, compared to the material developments. In this presentation, influence of the interfacial nanostructural control on the charge transfer dynamics will be addressed. The relationship with the device performance will also be discussed. This work was financially supported by JST PRESTO program, Japan, and TEPCO Research Foundation, Japan. The Venture Business Laboratory, Osaka University is also acknowledged for the financial support.

3:50 PM

#### (ICACC-S7-005-2012) Energy Conversion using Nano-structured Solar Cells (Invited)

S. R. Gajjala, W. Hai, K. Ananthanarayanan, P. Balaya\*, National University of Singapore, Singapore

Nano-structured solar cells have the potential towards low cost fabrication and also it can be processed easily. Currently there is a considerable focus in such devices as an alternative to conventional silicon based photovoltaic devices. In this talk, we will present our recent results on (a) dye-sensitized solar cells and (b) organic solar cells, with a special attention on the role of ceramics such as TiO<sub>2</sub> and NiO in optimizing the power conversion efficiency of such devices. Dye-sensitized solar cells using sub-micron sized mesoporous TiO<sub>2</sub> aggregates as photoanode exhibit a high power conversion efficiency of 9.00% at 1 Sun and up to 10.80 % at 0.16 Sun illumination. The factors contributing to such high efficiency are analyzed by surface area measurements, diffuse reflectance and intensity modulated photocurrent/voltage spectroscopy and electrochemical impedance spectroscopy measurements. For the organic photovoltaics, sol-gel NiO

thin films are used as the anode interfacial layer in P3HT:PCBM based organic solar cells, replacing the conventional poly-(3,4-ethylenedioxythiophene):poly-(styrenesulfonate) (PEDOT:PSS) interfacial layer. Device stability has been further studied by intensity modulated photocurrent spectroscopy, which suggests that the enhanced stability is related to the suppression of trap-induced space-charge effects, caused by oxygen and moisture ingress.

**4:10 PM**

**(ICACC-S7-006-2012) High Efficient Visible Light Hydrogen Evolution over Dye-sensitized Reduced Graphene Oxide Photocatalyst (Invited)**

G. Lu\*, Lanzhou Institute of Chemical Physics, CAS, China

Based on its higher redox potential, graphene may also exhibit excellent electron-accepting and transporting properties that facilitates the reduction of proton to hydrogen. However, whether graphene or its derivatives indeed can be used as an efficient electron mediator for hydrogen evolution from water in a dye-sensitized photocatalytic system under visible light irradiation is still needed to be verified. In this paper, we report a highly efficient and visible light driven photocatalytic hydrogen evolution system with a readily available Eosin Y as a photosensitizer, reduced graphene oxide (RGO) sheets as an electron relay mediator for efficiently accepting and transporting electrons, and Pt nanoparticles as catalyst, which were dispersed on the surface of RGO sheets. The apparent quantum yield of 9.3% for hydrogen evolution has been achieved at 520 nm. In EY-Pt system, the initial rate for H<sub>2</sub> evolution is also low (ca. 1.37  $\mu\text{mol h}^{-1}$ ). The photocatalytic H<sub>2</sub> evolution occurs steadily without noticeable degradation; the rate of H<sub>2</sub> evolution is about 10.17  $\mu\text{mol h}^{-1}$ .

**4:40 PM**

**(ICACC-S7-007-2012) Surface doping of W<sub>6+</sub> for enhanced photoelectrochemical water splitting over  $\alpha$ -Fe<sub>2</sub>O<sub>3</sub> nanorod photoanodes (Invited)**

S. Shen\*, J. Jiang, Xi'an Jiaotong University, China; C. X. Kronawitter, S. S. Mao, Lawrence Berkeley National Laboratory, USA; L. Guo, Xi'an Jiaotong University, China

Recently, there is growing interest in nanostructured metal oxides for photoelectrodes, especially one-dimensional nanostructures such as nanorods, nanotubes, and nanowires, mainly due to their short lateral diffusion length favoring charge fast transport to the semiconductor/electrolyte interface for photochemical reaction. Taking  $\alpha$ -Fe<sub>2</sub>O<sub>3</sub> film as an example,  $\alpha$ -Fe<sub>2</sub>O<sub>3</sub> nanotube arrays showed efficient PEC properties owing to its good charge carrier transfer ability.  $\alpha$ -Fe<sub>2</sub>O<sub>3</sub> nanorod film was observed to possess higher PEC efficiency than nanoparticulate  $\alpha$ -Fe<sub>2</sub>O<sub>3</sub> film, mainly because the size of nanorod-diameters tend to match the short hole diffusion length, facilitating hole transport. Therefore, in this study,  $\alpha$ -Fe<sub>2</sub>O<sub>3</sub> nanorod films were fabricated and targeted for W<sub>6+</sub> doping. W<sub>6+</sub> could be controllably doped into the surface of  $\alpha$ -Fe<sub>2</sub>O<sub>3</sub> nanorod films. The effects of W<sub>6+</sub> doping on charge transfer properties and PEC activities were investigated in detail.

**5:00 PM**

**(ICACC-S7-008-2012) In-situ Boron Nitride Nanotubes Growth on Commercial Silicon Carbide Fiber Tows**

J. B. Hurst\*, C. Hung, NASA GRC, USA

SiC/SiC composites have been considered for a variety of high temperature structural applications such as turbomachinery. In this work, the concept of "fuzzy" fibers, previously demonstrated by growing carbon nanotubes on the surface of carbon fibers, is examined for BNNT grown on SiC fibers. It has been found that this concept improved interlaminar shear strength properties by 69% for a CNT-thermoset resin system. Similar results for ceramic composites would enable laminate or 2D weaves rather resorting to expensive and difficult 3D weaves, justifying the expense of BNNT. BNNT is

grown in a radial direction on the surface of Hi-Nicalon<sup>TM</sup>, Hi-Nicalon-STM fibers, and Sylramic<sup>TM</sup> fibers. The impact of growing BNNT on SiC fiber tows on the mechanical properties of those coated SiC fibers relative to pristine fiber surfaces is investigated.

**5:20 PM**

**(ICACC-S7-009-2012) Perovskite Nanosheets Produced by Chemical Exfoliation**

J. Liu, J. Shi, V. Knox, S. Misture\*, Alfred University, USA

Aurivillius phase Bi<sub>2</sub>CaNaNb<sub>3</sub>O<sub>12</sub> was chemically exfoliated into two dimensional perovskite nanosheets (BCNN-NS) in water. The thickness of individual nanosheets corresponded to the perovskite block in the parent layered compound. The crystal structure of ion-exchanged Bi<sub>2</sub>CaNaNb<sub>3</sub>O<sub>12</sub> and the perovskite-like nanosheets was analyzed using TEM, X-ray diffraction and neutron diffraction. We present structure models for partially and fully exfoliated phases extracted from neutron pair distribution function analysis, IR spectroscopy and thermogravimetry. The photodecomposition rate of methylene blue by the TiO<sub>2</sub>-BCNN-NS was measured. The highly dispersed nanosheets were self-organized on TiO<sub>2</sub> particles, result an enhanced photocatalytic activity, and demonstrated the potential to serve as a photo catalyst for various applications.

**5:40 PM**

**(ICACC-S7-010-2012) Preparation of CdS sensitized TiO<sub>2</sub> mesoporous submicrotubes and enhanced photocatalytic properties for hydrogen production**

Y. Chen\*, J. Shi, L. Guo, State Key Laboratory of Multiphase Flow in Power Engineering, Xi'an Jiaotong University, China

Photocatalytic hydrogen production using nanomaterials, as a promising route for energy conversion, has received increasing attention. Combining narrow-bandgap semiconductor with TiO<sub>2</sub> to form composite photocatalysts was proved to be an efficient way to achieve high photocatalytic activities. The morphology of TiO<sub>2</sub> and the architecture of composite photocatalysts have great effects on the photocatalytic activities. In this work, TiO<sub>2</sub> mesoporous submicrotubes were firstly synthesized via a simple solvothermal method. CdS nanoparticles were then decorated on TiO<sub>2</sub> tubes by a precipitation method to form CdS/TiO<sub>2</sub> composites. SEM and TEM results revealed that the spiny mesoporous titania tubes were obtained, forming mesoporous structure in the tube walls. CdS nanoparticles with good crystallinity were decorated on the external and inner surfaces of TiO<sub>2</sub>. The hydrogen production rates of composite photocatalysts were influenced by the Cd/Ti molar ratio, and CdS/TiO<sub>2</sub> displayed enhanced hydrogen production compared to the single component. The improved properties can be ascribed to three factors. The hierarchical structure of TiO<sub>2</sub> tubes provided the enhanced light absorption; the heterojunction between CdS and TiO<sub>2</sub> contributed to the much efficient charge separation; the large specific areas of TiO<sub>2</sub> tubes afforded more active sites for hydrogen production.

## **S8: 6th International Symposium on Advanced Processing and Manufacturing Technologies for Structural and Multifunctional Materials and Systems (APMT) in honor of Professor R. Judd Diefendorf**

### **In Honor of Professor R. Judd Diefendorf**

Room: Coquina Salon A

Session Chairs: Mrityunjay Singh, OAI/NASA GRC; Tatsuki Ohji, AIST

**1:30 PM**

**(ICACC-S8-001-2012) Aerospace Materials Development (Invited)**

R. J. Diefendorf\*, Clemson U., USA

The demands of rockets and aerospace generated a parallel development of high temperature, and high specific stiffness and strength

materials. Reentry and rocket nozzle requirements led to the development of pyrolytic graphite, but the beneficial anisotropy in thermal conductivity was overbalanced by the anisotropy in CTE. The infiltration of a carbon fiber preform with a pyrolytic carbon matrix provided an alternate. Composites also overcame the unacceptable brittle failure of monolithic ceramics. The applications of polymeric and carbon matrix composites and later ceramic matrix composites were dependent on the development and understanding of high performance fibers, such as carbon, boron and silicon carbide. Finally reliable composite fabrication processes were developed, allowing composite usage in aerospace technology. While some of these advances are no longer relevant, there has been fallout: coated nuclear fuel particles, heart valves, aircraft brakes, highly oriented pyrolytic graphite, graphene, non-stick molds for aspheric glass lenses.

**2:00 PM**

**(ICACC-S8-002-2012) Assessment of Ceramic Matrix Composites for Targeted Applications (Invited)**

R. Shinavski\*, Hyper-Therm High-Temperature Composites, Inc, USA

A large number of permutations exist for potential ceramic matrix composite systems in terms of fiber, fiber coating, and matrix combinations. This palette of materials must be downselected intelligently based upon application specific requirements such that the best suited composite system is selected for the application with regards to processing methods, properties and cost. It is advantageous to make this downselection as early in the application development cycle as to conserve time and money during the development process. An initial downselection can be made based upon inspection, but frequently additional testing is required to vet the material for the application. Dr. Shinavski will discuss utilization of methods learned from studying under Professor Judd Diefendorf that allow an initial assessment to determine if a selected material is suited for the application's requirements. Several case studies will be examined for SiC matrix composites, where preliminary material property evaluations provide an indication of suitability for the intended application. Applications discussed will range from aerospace to nuclear applications of SiC matrix composites.

**2:30 PM**

**(ICACC-S8-008-2012) Carbon Fiber Reinforced Composites Manufactured by Reactive Melt Infiltration Processes (Invited)**

W. Krenkel\*, R. Voigt, F. Lenz, University of Bayreuth, Germany

The reinforcement of ceramics with chopped or continuous fibers is the most promising way to overcome the inherent brittleness of these materials. With respect to costs, reinforcements of carbon fibers and matrices formed by the carbide reaction of molten metals (reactive melt infiltration process) show the biggest potential for the manufacture of structural materials, in particular of large and complex shaped components. Fibers, carbonaceous binder systems and optionally passive fillers are used to manufacture a fiber preform in a first step. During the subsequent heat treatment in an inert atmosphere the binder system is pyrolyzed to amorphous carbon resulting in a micro-cracked and porous matrix. The most commonly used material system is C/SiC as a result of the infiltration of pure silicon or silicon alloys into carbon/carbon fiber preforms. Based on these experiences, hafnium carbide containing matrices have been developed by using hafnium alloys as a reactive melt. Also, ternary carbides (so-called MAX phases) were formed by the reaction of liquid silicon with a matrix consisting of titanium carbide and carbon. In this case, residual silicon, Ti<sub>3</sub>SiC<sub>2</sub> and TiSi<sub>2</sub> are the coexisting phases after a thermal treatment at 1350 °C.

**3:20 PM**

**(ICACC-S8-004-2012) From carbon fiber to ceramic matrix composite (Invited)**

F. Teyssandier\*, R. Pailler, University of Bordeaux 1, France

Laboratory for Thermostructural Composites (LCTS) has been working in several fields in which the outstanding contribution of

Professor R. Judd Diefendorf is honored in this symposium. Three main topics will be illustrated. The control of pyrocarbon chemical vapor infiltration is a key issue in the processing of high-performance C/C composites. The gas-phase chemistry plays a key role in the various nanotextural transitions. Using the full scale modeling of reactor, the relation between nanotexture and processing conditions can be explained. Mechanical as well as thermal properties of high modulus carbon fibers are of prime importance for their applications. Using an original fiber testing apparatus, the tensile behavior of carbon fibers can be investigated up to 2400 °C. The apparatus allows determining strength and Young's modulus. The thermal expansion can as well be determined: axial thermal expansion that can be easily obtained but also transverse thermal expansion which can be calculated and measured. A classical way to achieve damage-tolerance in CMCs is to engineer the fiber/matrix interface in order that a crack initiated in the brittle matrix does not propagate in a catastrophic manner through the reinforcing fibers. This property can be enhanced by use of multi-layered interphases that improves the toughness of the composite and furthermore increases the oxidation resistance and thus life time of the whole composite.

**3:50 PM**

**(ICACC-S8-005-2012) Multiscale Damage Evolution Behaviors of Carbon Fiber-Dispersed Si/SiC Matrix Triple Phase Composites (Invited)**

Y. Kagawa\*, The University of Tokyo, Japan

Short carbon fiber-dispersed Si/SiC triple phase composites (CF/Si/SiC) have been developed for recent advanced applications in aerospace, high-speed train and automotive applications. In the applications, understanding of damage evolution behavior in the CF/Si/SiC is important to keep safety applications. In the present study, local and global damage evolution behaviors in the CF/Si/SiC composites are observed under uniaxial monotonic and repeated loading/unloading compressive loading conditions. Both local damage and global damage parameters are obtained from the experimental results. The evolution of global damage is modeled into "MOSAIC COMPOSITE MODEL." Using the model, local damage evolution behavior is successfully incorporated into global damage model. The global damage parameter is well correlated with the analysis based on the model. Application of the model for optimum property design is discussed.

**4:20 PM**

**(ICACC-S8-006-2012) UBE's precursor polymers and the derived functional ceramics (Invited)**

T. Ishikawa\*, Ube Industries, Ltd., Japan

We have developed functional ceramics by precursor methods using polymetalocarbosilanes containing metal-atoms (Ti, Zr, or Al). Polycarbosilane, which is obtained by thermal rearrangement reaction of polydimethylsilane, has high ceramic yields, and so the polycarbosilane is available for preceramic polymer. The polycarbosilane has some cross-linking points and ring structures, which are composed of Si-Si or Si-CH<sub>2</sub>-Si bonds. Polymetalocarbosilane, which is produced by condensation reaction of the polycarbosilane with organometallic compounds, has much higher ceramic yield than the polycarbosilane because the polymetalocarbosilane has several cross-linking point composed of Si-O-(metal)-O-Si bonds and/or Si-(metal)-Si bonds. The polymetalocarbosilane shows good melt-spinability. After melt-spinning the polymetalocarbosilane, the spun fiber was cured in air and fired in inert gas atmosphere, and then amorphous Si-Ti-C-O fiber, Si-Zr-C-O fiber, and Si-Al-C-O fiber are produced. Moreover, SiC polycrystalline fiber (Tyranno SA) was produced by sintering the amorphous Si-Al-C-O fiber in Ar atmosphere. Furthermore, making the best use of the abovementioned fiber technology, a unique photocatalytic fiber, which is composed of silica-based core and surface gradient composition of titania nano-crystals, was developed. In this

paper, the characteristics and applications of these precursors and ceramic fibers will be discussed.

**4:50 PM**

### **(ICACC-S8-007-2012) Industrial Aspects of PyC- and SiC-CVD Processes (Invited)**

R. Weiss\*, K. Brennfleck, D. Kehr, Schunk Kohlenstofftechnik GmbH, Germany

In semiconductor industry above all in the field of solar cell production the demand of large parts, e. g. PyC-coated crucibles or SiC-coated heating elements is permanently increasing. There is a tendency to replace more and more graphite components by CFC, resulting in a strongly improved lifetime of the components and a reduction of contaminations of the semiconductor processes. In addition to the optimisation of the gas flow pattern and the deposition rate in large coating vessels, a lot of efforts have yet to be made with respect to the mismatch of the thermal expansion coefficients of substrate and coating in the case of CFC in order to avoid delaminations, a problem which is getting more difficult with increasing sizes.

## **S9: Porous Ceramics: Novel Developments and Applications**

### **Processing Methods for Porous Ceramics I**

Room: Coquina Salon C

Session Chair: Paolo Colombo, University of Padova

**1:30 PM**

### **(ICACC-S9-001-2012) Multifunctional carbon bonded filters for metal melt filtration (Invited)**

C. G. Aneziris\*, M. Emmel, V. Rongos, Institute of Ceramics, Glass and Construction Materials, Germany

There exists an increasing pressure on the metal-making and metal-using industry to remove solid and liquid inclusions such as deoxidation products, sulfides, nitrides carbides etc. and thereby improve metal cleanliness. It is well known that size, type and distribution of non-metallic inclusions in metal exert considerable effects on the mechanical properties of the cast products. Ceramic foam filters are since 40 years unique assisting products for the foundries for metal products with superior properties. In terms of this contribution intelligent filter materials as well as smart filter systems with a functionalized filter surface based on carbon bonded compositions will be demonstrated. Active as well as reactive surface coatings can lead to less primary and secondary inclusions as well as contribute to less inclusions generation below the liquidus temperature of the metal melt. Repairing coatings can lead to more flexible structures with less friability at room temperature and the addition of nanometer additions based on carbon nanotubes and alumina nanosheets can reinforce the carbon bonded material in cellular macro structures greater than 200 mm in diameter for filtration of large castings.

**2:00 PM**

### **(ICACC-S9-002-2012) Fabrication and Properties of Highly Porous Ceramic Monolith by Gelation Freezing Route**

M. Fukushima, T. Ohji\*, Y. Yoshizawa, National Institute of Advanced Industrial Science and Technology (AIST), Japan

The novel gelation freezing (GF) route was developed to prepare highly porous silicon carbide, alumina and cordierite with more than 90% porosity and uni-directionally oriented micrometer-sized cylindrical cells. Depending on the process conditions such as freezing temperature, additives and solid load in the slurry, varied microstructures of cell shape, cell size, number of cell and cell thickness was obtained. Then, the addition of anti-freezing protein could lead to the uniform cell size distribution, which greatly inhibited growth of ice crystals in the radial direction. These porous materials gave high compressive strength (the maximum: 17MPa for 87% porosity) as

well as high air permeability (range of 10-10 to 10-11m<sup>2</sup>; close to the ideal value), which are substantially higher than those of other porous ceramics reported so far.

**2:20 PM**

### **(ICACC-S9-003-2012) Effect of Freezing Gradient on Pore Size and Orientation for Freeze-Cast Alumina**

S. Miller\*, K. Faber, Northwestern University, USA

Freeze casting is a unique method of fabricating porous ceramics that offers the ability to tailor pore and pore network characteristics to specific applications through control of processing parameters like solids loading, freezing temperature and sintering temperature. To freeze cast porous ceramics with directional pores, ceramic powders are added to a dispersion medium to make a slurry which is then frozen from the bottom up. Crystals nucleate and grow, either engulfing or expelling the ceramic powders depending on the solidification front velocity. When expelled from the solidifying liquid, the ceramic powders are compacted between the crystals, which are subsequently sublimed, leaving a porous ceramic green-body. Sintering can be performed without a binder burnout step and the resulting ceramic consists of an interconnected pore network. The purpose of this study is to investigate the effect of freezing temperature and temperature gradients induced by directional freezing slurries on pore size and orientation. Water-based and camphene-based dispersions are compared. Mercury porosimetry, scanning electron and optical microscopies are employed to assess pore size, and using microscopy, orientation.

**2:40 PM**

### **(ICACC-S9-004-2012) Porous Coatings for Complex 3D-Structures Formed by Self-Assemblage**

M. Woiton\*, M. Heyder, Bavarian Center for Applied Energy Research, Germany; A. Laskowsky, University of Magdeburg, Germany; E. Stern, Bavarian Center for Applied Energy Research, Germany; M. Scheffler, C. J. Brabec, University of Magdeburg, Germany

Net-like ceramic layers were produced by dip coating with a polymer solution containing two immiscible preceramic polymers, a solvent, and a non-solvent. The process of net formation starts right after the coating process when the solvent and the non-solvent evaporate. Pore size has been shown to be adjustable in the range of 1 to 60  $\mu\text{m}$  by layer thickness, polymer/polymer ratio, particle size of the fillers, nature of the substrate, and viscosity of the slurry. After drying and crosslinking at elevated temperatures the layers were converted into ceramic layers under shape retention. In filler-free systems a polymer/polymer demixing process was identified as the structure formation process. However, in filler loaded systems the structure formation is more complex and influenced by the parameters given above. After thermal conversion a significant increase in specific surface area was detected. Thus, the structured ceramic surfaces are potential candidates for applications where supply of active-components is an important issue, e. g. in energy storage and conversion, in catalytic processes, or as medical implants. Additionally these self-assembled coatings are of particular interest for facile fabrication of defined micro structured surfaces on complex 3D-structures. The process of ceramic net-like structure generation by demixing mechanisms is the only process which provides such structures to ceramic layers.

### **Processing Methods for Porous Ceramics II**

Room: Coquina Salon C

Session Chair: Yuji Iwamoto, Nagoya Institute of Technology

**3:20 PM**

### **(ICACC-S9-005-2012) Processing, Microstructure and Properties of Reticulated Carbon Foam (Invited)**

R. A. Olson\*, D. P. Haack, Porvair-SELEE Corporation, USA

Reticulated carbon foam manufactured via the sponge replication technique has a much more homogeneous, more open structure relative to traditional ceramic foam manufactured by similar method. To



characterize this difference, the flow properties of various carbon foam samples having different pore sizes and densities were measured and compared to those for conventional ceramic foam. The part-to-part variation for carbon foam proved to be much lower than that for ceramic, and equivalent pressure drops were achieved in carbon foam at much smaller pore sizes. These and other aspects of the processing, microstructure, properties and performance of carbon foam will be discussed.

### 3:50 PM

#### (ICACC-S9-006-2012) Porous ceramics with tailorable properties

P. Karandikar\*, G. Evans, M. Aghajanian, M Cubed Technologies, Inc., USA

SiC and B4C materials have been used successfully for a variety of applications such as armor, wear components, nuclear waste containment, thermal management, precision components, and refractories. Typically, SiC and B4C are used in the fully-dense or nearly fully-dense form. However, there are many applications that require these materials in a porous form. In this work, processing methods have been developed to produce SiC and B4C with a wide range of porosity. In addition to the porosity, other characteristics such as permeability, pore size, pore-size distribution, purity, grain size, and strength can also be tailored. The porous materials produced are subjected to microstructural (optical, SEM), chemical, physical, elastic, and mechanical characterization. The resultant microstructure-property relationships will be presented in this paper.

### 4:10 PM

#### (ICACC-S9-007-2012) The effect of setting mechanism on the properties of ceramic foams produced by O/W emulsions

F. S. Ortega\*, FEI, Brazil

A new route for the production of ceramic foams is presented: the emulsification of a nonpolar liquid into an aqueous ceramic suspension. The resulting system consists of an aqueous ceramic suspension containing small droplets of a nonpolar liquid, which work as a sacrificial template. The setting of the ceramic emulsion is a required step to obtain crack-free bodies. Two approaches were assessed to set the ceramic emulsion: the hydration of an inorganic binder (Alphabond 500) and the gelcasting process. SEM of the cellular structure revealed isolated pores for samples with low porosity, changing to an interconnected network of pores as the porosity increased. Pore diameters were between 5 to 20  $\mu\text{m}$ . For emulsions set by the gelcasting process it was possible to emulsify up to 60 vol.% of nonpolar liquid (kerosene), resulting in samples with diametrical strength between 2.0 and 48 MPa, as the porosity varied between 20 and 64 vol.%. On the other hand, for emulsions set by the hydration of Alphabond 500, the strength of the samples varied between 13,1 MPa, for apparent porosity of 71,7% and 77,2 MPa, for apparent porosity of 48,6%. The use of a hydraulic binder resulted in higher strength values and higher porosities. On the other hand, it is restricted to products where its presence is allowed.

### 4:30 PM

#### (ICACC-S9-008-2012) Additive manufacturing of macro-cellular ceramic structures (Invited)

N. Travitzky\*, T. Schlordt, L. Schlier, University of Erlangen-Nuremberg, Germany; J. Cypris, M. Weclas, University of Applied Sciences Nuremberg, Germany; T. Fey, P. Greil, University of Erlangen-Nuremberg, Germany

Additive manufacturing techniques such as robotic controlled deposition (robocasting) and three-dimensional printing (3D-printing) were examined for fabrication of macro-cellular Al<sub>2</sub>O<sub>3</sub> and SiC-based structures. A macro-cellular alumina structures were fabricated by robocasting using an aqueous colloidal gel. The gels retained the shape to cast line morphology with a diameter of approximately 0.3 mm. Cellular Al<sub>2</sub>O<sub>3</sub> grid structures with a total porosity of ~53% were fabricated with a deposition speed of 30 mm<sup>2</sup>s<sup>-1</sup>. The grids were sintered in air at 1600 °C resulting in failure-free cellular structures

with a fractional strut density of ~95 %. A macro-cellular SiC-based structures with a high porosity > 80 % and with axial and radial cylindrical struts having a diameter in the range of ~1 mm and a length of 2 to 8 mm were fabricated by 3D-printing. Printed and infiltrated with a liquid silicone resin macro-cellular SiC-based parts were successfully pyrolysed with linear shrinkage of 2% only, which makes near-net-shape manufacturing of these structures possible. The composites revealed a SiC content of approximately 50 vol. % balanced by Si show a dense, homogeneous microstructure. Compressive strength of 618 MPa for the single struts was evaluated. Cellular SiC ceramics offer a high potential for applications in air-fuel mixture formation and for non-stationary lean-burn under piston engine-like conditions.

### 5:00 PM

#### (ICACC-S9-009-2012) Wollastonite and cordierite foams from silicones filled with micro-particles and novel processing

E. Bernardo\*, G. Parcianello, P. Colombo, University of Padova, Italy; S. Matthews, SCF Processing Ltd, Ireland

Wollastonite and cordierite are important engineering ceramics, with applications especially in the form of highly porous components. Both phases have been recently developed by the thermal treatment of silicone resins filled with reactive powders. In both cases, the reaction between silica resulting from the oxidation of the polymer and the fillers leads to the formation of almost phase pure and fine grained engineering ceramics. In this paper we discuss novel processing approaches, that could enable industrial applications. Wollastonite was obtained from a silicone containing CaCO<sub>3</sub> micro-powders, by means of conventional polymer extrusion supported by super-critical carbon dioxide. The novel mixture was so effective that its wollastonite yield is comparable to that achieved with much more reactive nano-sized fillers. Silicone/CaCO<sub>3</sub> mixtures were converted into highly porous foams (porosity of about 80%) by a secondary low temperature treatment, before final ceramization at 900°C. Cordierite, on the other hand, was produced by adding to the silicone resin, besides Al<sub>2</sub>O<sub>3</sub>, Mg(OH)<sub>2</sub> micro-powders, which undergo thermal decomposition into MgO and water, thus providing both a reactive oxide component and a foaming agent, since the release of water occurs at a temperature low enough to exploit the viscous flow of the polymer, before ceramization.

### 5:20 PM

#### (ICACC-S9-010-2012) Preparation of porous $\beta$ -Si<sub>3</sub>N<sub>4</sub> ceramics in an air atmosphere furnace

A. K. Gandhi, K. P. Plucknett\*, Dalhousie University, Canada

Silicon nitride (Si<sub>3</sub>N<sub>4</sub>) ceramics are used in a wide range of engineering applications, due to their high strength and toughness, elevated temperature stability, and excellent wear and corrosion resistance. Conventionally,  $\beta$ -Si<sub>3</sub>N<sub>4</sub> ceramics are sintered in a controlled nitrogen atmosphere, to prevent excessive oxidation or decomposition. However, it has recently been demonstrated that  $\beta$ -Si<sub>3</sub>N<sub>4</sub> can be prepared in an air atmosphere furnace, even in a porous form, when using an  $\alpha$ -Si<sub>3</sub>N<sub>4</sub> powder bed (which oxidises to form a protective SiO<sub>2</sub> surface coating). The effects of sintering additive selection upon the preparation of porous  $\beta$ -Si<sub>3</sub>N<sub>4</sub>, utilising a variety of rare earth oxides, are discussed. In addition, the influence of fugitive filler additions has been investigated, to vary the final porosity level. The effects of these various processing parameters upon the microstructure development (using SEM, XRD, etc.) will be reported. Initial mechanical and thermal property evaluation will also be discussed.

### 5:40 PM

#### (ICACC-S9-011-2012) Porous Silicon Oxycarbide Glasses from Polyhydridomethylsiloxane Using a Templating Approach

G. D. Soraru, University of Trento, Italy; Y. Blum\*, SRI International, USA; P. Aravind, University of Trento, Italy

Porous silicon oxycarbide glasses have been obtained using different approaches: from hybrid aerogels, from preceramic foams, and from

periodic mesoporous organosilicas. We hereby report the synthesis of mesoporous SiCOs using a templating approach. A linear polyhydridomethylsiloxane, PHMS, is crosslinked with a templating polydimethylsiloxane, (PDMS) vinyl terminated via hydrosilylation reaction using a Pt catalyst. SiCOs have been obtained by pyrolysis in inert atmosphere of the starting precursors. Mesoporosity is formed by the decomposition of the PDMS chains. The specific surface area, total porosity and pore size can be easily tuned by changing the MW of the templating PDMS. At 800°C surface area up to 450 m<sup>2</sup>/g, pore volume up to 0.6 cc/g and pore size up to 12 nm have been recorded. Standard techniques were employed for characterizing the materials.

**6:00 PM**

**(ICACC-S9-012-2012) Preparation of Porous Alumina Ceramic with Ultra-high Porosity by Freeze Casting**

D. Li\*, M. Li, Institute of Metal Research, CAS, China

Porous alumina ceramic was prepared by freeze casting method using tert-butyl alcohol (TBA) as the solvent. The as-prepared porous alumina ceramic possessed long straight porous structure. The non-dendrite pore feature was quite distinguished from that prepared based on common solvents such as water and camphene. The porosity of the ceramic could be regulated through the solid loading. When the solid loading in the slurry was 20 vol.%, the porosity of the alumina ceramic was 65%. With decreasing the solid loading, the porosity of the alumina ceramic increased linearly. The relationship between the total porosity (P) and initial solid loading (X) has been established. The ultra-high porosity of 82% could be achieved when the solid loading was 10 vol.%. Moreover, the density of the porous alumina ceramic with the porosity of 82% was even lower than water's. The compressive strength of the porous alumina ceramic with the porosity of 63% and 82% was determined to be 37.0 MPa and 2.6 MPa, respectively.

## S14: Advanced Materials and Technologies for Rechargeable Batteries

### Advanced Materials and Designs for Lithium Batteries

Room: Coquina Salon H

Session Chairs: Ilias Belharouak, Argonne National Laboratory; Kristina Edstrom, Uppsala University

**1:30 PM**

**(ICACC-S14-001-2012) The capacity of 3D-structured electrode materials for Li-ion batteries (Invited)**

K. Edstrom\*, D. Brandell, T. Gustafsson, Uppsala University, Sweden

More and more complex geometries are tested as either direct electrode materials for Li-ion batteries or as support structures for electrochemically active materials. The goal is to enhance both energy- and power density and at the same time obtain more efficient use of the volume in the battery. Some examples of structures are; nano-wires, foams, nano-pillars, trenches etc. In this presentation some examples of 3D-structurisation will be presented: interdigitated structures, 3D nano-pillars and trench structures covered with different active electrode materials. The role and success of different deposition methods such as ALD, electrophoretic- and electrodeposition will be discussed. The 3D systems will be compared to conventional 2D systems with respect to cycling stability and efficiency. Some examples of materials are model studies of Cu<sub>2</sub>Sb as the negative and TiO<sub>2</sub> as the positive electrode material. New thin solvent-free polymer electrolytes have also been tested in this context. To build a whole functioning battery based on 3D structures is still a challenge but there are many activities in this area and progress could soon be anticipated.

**2:00 PM**

**(ICACC-S14-002-2012) ALD of Al<sub>2</sub>O<sub>3</sub> for Highly Improved Performance in Li-ion Batteries (Invited)**

A. C. Dillon\*, Y. Jung, L. Riley, C. Ban, National Renewable Energy Laboratory, USA; A. Cavanagh, S. George, S. Lee, University of Colorado, USA; S. Harris, P. Lu, General Motors, USA

We have demonstrated atomic layer deposition (ALD) as a promising method to enable superior cycling performance for a vast variety of battery electrodes. For example, an Al<sub>2</sub>O<sub>3</sub> ALD coating with a thickness of ~ 8 Å was able to stabilize the cycling of unexplored MoO<sub>3</sub> nanoparticle anodes with a high volume expansion. The ALD coating enabled stable cycling at C/2 with a capacity of ~ 900 mAh/g. For uncoated electrodes it was only possible to observe stable cycling at C/10. Also, we recently reported that a thin ALD Al<sub>2</sub>O<sub>3</sub> coating with a thickness of ~5 Å can enable natural graphite (NG) electrodes to exhibit remarkably durable cycling at 50C. The ALD-coated NG electrodes displayed a 98% capacity retention after 200 charge-discharge cycles. In contrast, bare NG showed a rapid decay. Additionally, Al<sub>2</sub>O<sub>3</sub> ALD films with a thickness of 2 to 4 Å have been shown to allow LiCoO<sub>2</sub> to exhibit 89% capacity retention after 120 charge-discharge cycles performed up to 4.5 V vs Li/Li+. In contrast, bare LiCoO<sub>2</sub> rapidly deteriorated in the first few cycles. Finally, we have recently fabricated full cells of NG and LiCoO<sub>2</sub> where we coated both electrodes, one or the other electrode as well as neither electrode. In creating these full cells, we observed some surprising results that lead us to obtain a greater understanding of the ALD coatings. These results will be presented in detail.

**2:30 PM**

**(ICACC-S14-003-2012) Sodium or Lithium intercalation in some original FeII phosphates structures: Lamellar Na<sub>3</sub>Fe<sub>3</sub>(PO<sub>4</sub>)<sub>4</sub>, Alluaudites Li<sub>y</sub>Na<sub>1-y</sub>MnFe<sub>2</sub>(PO<sub>4</sub>)<sub>3</sub> (y = 0, 0.5, 0.75) and Tavorite LiFePO<sub>4</sub>.OH / FePO<sub>4</sub>.H<sub>2</sub>O (Invited)**

D. Carlier\*, K. Trad, N. Marx, L. Croguennec, A. Wattiaux, ICMCB-CNRS, France; F. Le Cras, CEA, France; M. Ben Amara, Faculté des sciences de Monastir, Tunisia; C. Delmas, ICMCB-CNRS, France

Since the discovery of the LiFePO<sub>4</sub> behaviour as positive electrode in lithium batteries, the search for other polyanionic compounds is intense. In this context, we were interested in three systems: the Na<sub>3</sub>Fe<sub>3</sub>(PO<sub>4</sub>)<sub>4</sub> lamellar phase, the Li<sub>y</sub>Na<sub>1-y</sub>MnFe<sub>2</sub>(PO<sub>4</sub>)<sub>3</sub> alluaudite type phases and the tavorite LiFePO<sub>4</sub>.OH and analogous FePO<sub>4</sub>.H<sub>2</sub>O phases. The Na<sub>3</sub>Fe<sub>3</sub>(PO<sub>4</sub>)<sub>4</sub> structure is 2D and a 3D ionic diffusion is expected. The Alluaudite and tavorite structures, both exhibit 1D chains of MO<sub>6</sub> octahedra connected through PO<sub>4</sub> tetrahedra thus forming 1D channels that can allow the alkaline ions diffusion. The synthesis and structural characterization (XRD, neutrons, NMR and Mössbauer) of these phases are reported. All phases were tested as positive electrode in sodium and/or lithium cells. Ex situ and in situ X-ray diffraction data and Mössbauer spectroscopy measurements were performed in order to study the intercalation/ deintercalation process of Na<sup>+</sup> and Li<sup>+</sup>. Attempt to optimize the electrochemical performances by decreasing the particle size was performed and will also be discussed.

**3:20 PM**

**(ICACC-S14-004-2012) Nanocomposite Materials for Energy Storage Application (Invited)**

D. Wang\*, Z. Song, T. Xu, M. Gordin, Penn State University, USA

The role of nanostructure in addressing the challenges in energy has attracted wide attention. Many promising results of nanostructured materials in energy storage have demonstrated the importance of optimum dimension and architecture and controlled crystallographic orientation of the nanostructured materials to optimize transport of electrons, ion and other species and therefore improve device performance. Our research has been directed at synthesizing composites comprising active and inactive phases controlled at nanoscale by ex-

ploiting novel low-cost approaches. This talk will present synthesis of graphene-based nanocomposite materials (e.g. metal oxide, polymer or intermetallic alloy as active materials) via combining self-assembly and controlled nucleation and growth with controlled active phase and spatial arrangement. The nanocomposites have been studied as electrodes in Li battery showing superior capacity retention and high rate performance during lithiation/delithiation. Understanding the roles of nanostructure in these applications may provide insights into the design of advanced Li batteries and other approaches for energy storage. Opportunities and challenges of these nanostructured materials for next generation Li-ion batteries will be presented and discussed.

### 3:50 PM

#### (ICACC-S14-005-2012) Synthesis, structure and electrochemical Li insertion properties of $A_2Ti_6O_{13}$ ( $A=Na, Li, H$ ) (Invited)

A. Kuhn\*, J. Pérez-Flores, F. García-Alvarado, San Pablo-CEU University, Spain; C. Baecht, Helmholtz-Zentrum Dresden-Rossendorf, Germany; M. Hoelzel, University of Technology Munich, Germany; I. Sobrados, J. Sanz, Institut of Materials Science, Spain

In this work the soft-chemistry synthesis of  $Li_2Ti_6O_{13}$  and  $H_2Ti_6O_{13}$  using facile ion exchange reactions starting from  $Na_2Ti_6O_{13}$  is reported. Crystal structures of the titanates have been determined using X-ray and neutron diffraction. The comparison of structural characteristics shows that all analyzed phases display monoclinic symmetry, space group  $C2/m$ , with similar unit cell parameters. The Rietveld analysis of diffraction patterns reveals small structural modifications of the  $(Ti_6O_{13})_2$ -framework upon Na/Li/H exchange, in which the monovalent Na, Li and H cations occupy different sites. Cation site coordination and polyhedra distortion have been further analyzed by  $^{23}Na$ ,  $^7Li$  and  $^1H$  MAS-NMR. However, these subtle structural changes produce pronounced differences in the electrochemical Li insertion properties, and a quite different reaction mechanism is evidenced for Li insertion in  $Li_2Ti_6O_{13}$  and  $H_2Ti_6O_{13}$  than for  $Na_2Ti_6O_{13}$ . Suitability of the herein studied titanates as anode materials in Li-ion rechargeable batteries is assessed.

### 4:20 PM

#### (ICACC-S14-006-2012) Three-Dimensional Lithium-ion Rechargeable Batteries (Invited)

A. Prieto\*, Colorado State University, USA

A critical challenge in the fabrication of high power density batteries is that the diffusion length for Li-ions be reduced. We are approaching this challenge in two ways. First, we are synthesizing nanostructured materials, whereby the solid-state diffusion length for Li-ions is reduced in each electrode. Second, the anode and the cathode in our proposed 3D battery are interpenetrating. The diffusion length between the anode and cathode, via the solid electrolyte, is on the order of a few hundred nanometers. Electrodeposition is the main synthetic tool for the fabrication of the proposed 3D architecture. We will present battery cycling studies and electron microscopy of the battery materials before and after cycling.

### 4:50 PM

#### (ICACC-S14-007-2012) Electrospun Nanofiber Networks as Electrode Materials for Li-ion Batteries

S. Mathur, R. von Hagen\*, A. Lepcha, M. Büyükyazi, University of Cologne, Germany; K. Möller, H. Lorrmann, H. Andersen, Fraunhofer ISC, Germany

New ways of low cost production, structuring and simple integration of nanostructured electrode materials into batteries are of current interest. The electrospinning method offers a great potential in the 1-D nanofiber design and production of anode/cathode materials with complex structure and composition with reliable control over morphology and no need of further work-up steps. By the judicious choice of precursor solutions in sol-gel type electrospinning and the calcination of the fiber networks under inert atmosphere, we were

able to produce self-supporting electrodes of  $LiFe_{1-y}MnyPO_4/C$  and  $\alpha-Li_3V_2(PO_4)_3/C$  which showed superior electrochemical performance in terms of rate and stability. The electrochemical performance in regard to the materials composition ( $y$  in  $LiFe_{1-y}MnyPO_4$ ) and nanostructure was analyzed by cyclic voltammetry, constant current measurement and impedance spectroscopy. The free standing 1D-3D interconnected composite (active material/carbon) nanofiber networks could directly be used as electrode material without the need of further additives. The nanofibers further were characterized by SEM, BET, HR-TEM and XRD before and after the electrochemical cycling.

### 5:10 PM

#### (ICACC-S14-008-2012) Lithium diffusion pathways and possible reaction mechanisms in $FeF_3/FeF_2$ cathode predicted by variable charge molecular dynamics simulations

Y. Ma\*, G. Lockwood, S. Garofalini, Rutgers University, USA

The increasing demand for high capacity power sources has stimulated much research in lithium ion batteries (LIBs). Recently, an alternative to the intercalation reaction, known as the conversion reaction, has been proposed where multiple valence states of the metal cation can be accessed during the redox cycle, thus leading to a higher energy density. Unfortunately, the precise molecular mechanisms and pathways for the reactions are not known, allowing for the need for computational techniques to address this problem. In this work, a transferable variable charge potential enabling the study of conversion materials  $FeF_3$  and  $FeF_2$  was developed and tested. This potential was then applied to study the Li diffusion pathways in both  $FeF_3$  and  $FeF_2$ . Molecular dynamics simulations showed that the [001] diffusion channel in  $FeF_2$  has the lowest diffusion barrier, which was also confirmed by first principles computations. Barriers along other channels and the corresponding surface energies were also obtained. Based on these results, possible mechanisms of the conversion reaction were proposed and discussed, which would be helpful in designing LIBs with enhanced performance.

### 5:30 PM

#### (ICACC-S14-009-2012) Synthesis and Electrochemical Analysis of $SiCN-MoS_2$ Nanosheet Composite for Lithium Ion Battery Anodes

R. Bhandavat\*, L. David, U. Banera, G. Singh, Kansas State University, USA

We have demonstrated a novel synthesis method for  $SiCN$  functionalized  $MoS_2$  nanosheet composite and compared its electrochemical performance with exfoliated  $MoS_2$ . The electrochemical tests were performed on assembled coin cells with the sample material coated on anode current collector. The structure and morphology of the synthesized material were characterized using X-ray diffraction, X-ray photoelectron spectroscopy, UV-visible spectroscopy and transmission electron microscopy which revealed a sidewall functionalization of  $MoS_2$  by amorphous  $SiCN$ . Electrochemical performance of  $SiCN-MoS_2$  nanosheets exhibits a substantial decrease in the first cycle loss (~44%) and cycle hysteresis (~6%) with a marginal improvement in the reversible capacity without compromising the cycle capacity at current extraction rate of 100mA/g. As the  $SiCN$  functionalization of  $MoS_2$  tends to inhibit the solid electrolyte interphase film formation, reversible capacity increases due to ease of lithium ion deintercalation during charging cycle. Improvement in overall performance parameters are attributed to (a) increase in the binding sites for the lithium ion intercalation and ion transfer and (b) better structural stability of the composite due to  $SiCN$  functionalization.

### 5:50 PM

#### (ICACC-S14-010-2012) Li Insertion in $SiCO$ Ceramics – Ab-Initio Simulations

P. Kroll\*, UT Arlington, USA

We present combined modeling and simulation studies of Li insertion in amorphous  $SiCO$  ceramics to understand the high capacity of these novel anode materials. Atomistic models of amorphous  $SiCO$  in

various forms, as glass with and without so-called “free” carbon or nano-clustered Si, have been crafted using a network modeling approach. Subsequently, all models have been optimized and computed within density functional theory. Random insertion of Li atoms tests for sites with high and favorable insertion energy. We find that Li prefers bonding to O as cationic Li<sup>+</sup>, while the surplus electron is promoted to unoccupied state. The enthalpy of insertion, then, depends strongly on the energy of such unfilled electronic states available in the SiCO host matrix, which in turn is determined by amount and structure of embedded graphite or nano-clustered Si. Strong and irreversible bonding of Li into SiCO is provided, if bonding of Li outweighs the promotion energy for the electron. An fortuitous balance between Li-O bonding and electron promotion exists for aromatic carbon embedded in SiCO. Inserting multiple Li atoms into SiCO reveals a strong correlation between the amount of inserted Li and the number of C atoms in graphitic segregations, which matches experimental observation. Thus, our computational studies explain the high Li capacity of SiCO compounds and provide basic understanding for developing new batteries.

## FS2: Computational Design, Modeling, and Simulation of Ceramics and Composites

### Simulation of Structure and Properties of Advanced Ceramics

Room: Ponce de Leon

Session Chairs: Hans Seifert, Karlsruhe Institute of Technology

**1:30 PM**

#### (ICACC-FS2-001-2012) Modeling of radiation damage in nanocrystalline silicon carbide (Invited)

I. Szlufarska\*, D. Morgan, N. Swaminathan, M. Zheng, University of Wisconsin, USA

Silicon carbide is a promising structural material for next generation nuclear reactors. Refining grain diameter of SiC leads to dramatic improvements in mechanical properties, but the effects on radiation resistance are poorly understood. In this talk we will discuss the current state of knowledge on radiation effects in nanocrystalline silicon carbide, including the results of our multi-scale simulations. Using molecular dynamics we have shown that primary defect production in SiC is not affected by the grain refinement, but that grain boundaries can be affected by radiation. We constructed ab initio rate-theory model for SiC's long-term point defect evolution and predicted how amorphization couples to temperature and grain size. We demonstrated that in addition to migration barriers, recombination barriers for defects can play an important role in the resistance of SiC to radiation-induced amorphization. Despite their importance, contradictory reports regarding these barriers have been published in the literature. Our ab initio molecular dynamics simulations have resolved these discrepancies by providing a detailed energy landscape for interstitial-vacancy pairs migrating toward each other from large distances and recombining. Comparison of predicted trends to preliminary experimental data obtained by collaborators at the University of Wisconsin will also be discussed.

**2:00 PM**

#### (ICACC-FS2-002-2012) Thermal Conductivity of Amorphous Ceramics from Ab-Initio Molecular Dynamics Simulations (Invited)

P. Kroll\*, B. Kouchmeshky, UT Arlington, USA

Modeling and simulation of amorphous ceramics and glasses provide insight and understanding of structure and related phenomena of such complex materials. Density functional calculations are especially useful, since the approach does not depend on availability and accuracy of a phenomenological force field. In this paper we present results we obtained from ab-initio molecular dynamic simulations at

elevated temperature for a variety of amorphous material, ranging from silica glass over SiCO to HfSiCNO. We employ kinetic theory to calculate the life-time of phonons and to derive the thermal conductivity. In many systems we support the trend of increasing conductivity with increasing temperature. However, we also observe a limit of this behavior at very high temperatures. Complex systems such as SiCO do not always follow a “rule of mixture”, but do exhibit very low thermal conductivity due to a particular microstructure. Our results are important to further simulate thermal transport in glasses and melts in ceramics pertaining to ultra-high temperature applications.

**2:20 PM**

#### (ICACC-FS2-003-2012) Transferable variable charge potential for the study of energy conversion materials in Lithium ion batteries

Y. Ma\*, G. Lockwood, S. Garofalini, Rutgers University, USA

The capability of increasing the capacity of Li-ion batteries (LIB) rests in the ability to access multiple valence states of the metal cation in the cathode, which is the key feature of energy conversion materials such as FeF<sub>3</sub> and FeF<sub>2</sub>. However, such a change in the valence states brings challenge to molecular simulations since a proper description of multiple phases and multiple charge states is required. In this work, a transferable variable charge potential is developed and the ability of this potential to address the above challenge is tested. This potential is based on the electronegativity equalization principle and is implemented through the iterative fluctuation charge method. Using molecular dynamics simulations, the structural and elastic properties of FeF<sub>3</sub>, FeF<sub>2</sub> and LiF, which are observed in a conversion reaction, were correctly reproduced. The charge distribution in these compounds was in excellent agreement with first principles Bader charges. The surface energetics and relaxations were also calculated and the results agree well with first principles data. The above results suggest the applicability of this potential in addressing the complex reaction mechanisms at atomistic level.

**2:40 PM**

#### (ICACC-FS2-004-2012) Phase stability of Al<sub>3</sub>BC<sub>3</sub>: first-principles calculation and in situ Raman experiments (Invited)

J. Wang\*, H. Xiang, Institute of Metal Research, China; Y. Zhou, Aerospace Research Institute of Materials and Processing Technology, China

The phase stability of Al<sub>3</sub>BC<sub>3</sub> under mechanical perturbations was investigated by first-principles calculation. We predict that Al<sub>3</sub>BC<sub>3</sub> shows high specific elastic stiffness but extremely low shear deformation resistance; and it may undergo a hexagonal-to-tetragonal structural transformation at high hydrostatic pressure. A homogeneous orthorhombic shear strain transition path is proposed and the transformation enthalpy barrier yields a low value, which ensures that the transition can readily occur around the predicted pressure. The theoretical Raman active modes are analyzed based on lattice dynamics phonon calculations and are used to completely assign the experimental phonon modes. The in situ Raman spectra were measured under different pressures. The experiment shows that Al<sub>3</sub>BC<sub>3</sub> remains good structural stability up to 27 GPa. Interestingly, abnormal mode softening is identified when we further increase the applied pressure. The phenomenon is explained by changes of the coordination number and bonding between Al and C atoms along the basal plane according to the theory prediction.

**3:20 PM**

#### (ICACC-FS2-005-2012) First Principles Calculations of Temperature and Pressure Dependent Physical Properties of MAX Phase Materials (Invited)

L. Ouyang\*, Tennessee State University, USA

MAX phase materials have layered atomic structure and often possess unusual physical properties such as metal-like thermal and electrical conductivity and ceramic-like mechanical properties and chemical inertness. To search for a suitable MAX phase mate-

rial as thermal barrier coating for high temperature alloys, we systematically studied a series of MAX phase compounds for their thermodynamic properties and mechanic properties. The calculations employ Vienna ab initio package based on density functional theory and G(P,T) package for automating physical properties calculations including optical and dielectric property, Gibbs free energy, temperature pressure-dependent thermal expansion and elastic constant, etc. The computed physical properties were collected in a searchable database and data mining tools can be used to identify suitable MAX phase materials that meet the material design requirements.

**3:40 PM**

**(ICACC-FS2-006-2012) Understanding the Behavior of Native Point Defects in ZrC by First-Principles Calculation**

Y. Zhang\*, J. Wang, Institute of Metal Research, China; Y. Zhou, Aerospace Research Institute of Materials and Processing Technology, China

Zirconium Carbide is a candidate material for coating of TRistructural-ISotropic (TRISO) nuclear fuel, to replace SiC or serve as an oxygen getter. Understanding the behavior of native point defects is of great significance to explain the tolerance to displacive irradiation damage and changes of properties of defective ZrC. Furthermore, point defects make great impacts on its neighboring chemical bonding, which are important to determine material properties, such as mechanical property, electron and thermal conductivity and high temperature stability. We will present the defect formation energies at different chemical potentials for all possible native point defects in ZrC by first-principles investigation. Then we analyze the effects of different point defects on the bonding strengths of neighboring Zr-C bonds. At last, the preferred diffusion paths and the migration energy barriers of carbon vacancies and carbon interstitials are discussed.

**4:00 PM**

**(ICACC-FS2-007-2012) Mechanical properties of apatite crystals using multi-axial tensile experiment and construction of failure envelope (Invited)**

W. Ching\*, S. Aryal, A. Misra, University of Missouri-Kansas City, USA

A method to characterize the strength of a material by constructing a three-dimensional failure envelope in the stress space using data generated from multi-axial tensile experiment is presented. The "experiments" are performed on supercells by applying successive tensile strain in small steps until the stress reaches the failure point when the stress reaches a maximum. The stress data  $\sigma_{ij}$  corresponding to the applied strain is extracted. The "experiment" is carried out with strains ( $\epsilon_{xx}$ ,  $\epsilon_{yy}$ ,  $\epsilon_{zz}$ ) applied in as many directions as feasible. The final set of stress data  $\sigma = (\sigma_{xx}, \sigma_{yy}, \sigma_{zz})$  at the failure points are collected to construct a failure envelope which represents a single parameter to describe the strength of a material. The envelope is rendered in a color-scale to depict the specific locations of the weak and strong parts in the first quadrant of the stress space. This technique is applied to bioceramics crystals hydroxyapatite and fluoroapatite and the differences in their mechanical properties demonstrated.

**4:30 PM**

**(ICACC-FS2-008-2012) Modeling hardness of materials and its application to the search for superhard materials from first-principles calculations (Invited)**

X. Chen\*, H. Niu, D. Li, Y. Li, Institute of Metal Research, Chinese Academy of Sciences, China

Though extensively studied, hardness, defined as the resistance of a material to deformation, still remains a challenging issue for a formal theoretical description due to its inherent mechanical complexity. Here, we demonstrate that the intrinsic correlation between hardness and elasticity of materials correctly reproduces the

Vickers hardness for a wide variety of crystalline materials as well as bulk metallic glasses (BMGs). Our results suggest that, if a material is intrinsically brittle (such as BMGs that fail in the elastic regime), its Vickers hardness linearly correlates with the shear modulus ( $H_v = 0.151G$ ). This correlation also provides the robust theoretical evidence on the famous empirical correlation observed by Teter in 1998. In addition to this, our results show that the hardness of polycrystalline materials can be correlated with the product of the squared Pugh's modulus ratio ( $k = G/B$ ) and the shear modulus ( $H_v = 2.0(k^2G)^{0.585-3}$ ). Motivated by the interest to find new hard materials we have applied our proposed model to CrB<sub>4</sub>, a compound known for over half a century and characterized by a three-dimensional framework based on B<sub>4</sub> units, similar to the superhard C<sub>4</sub> allotrope of carbon. Our predictions suggest that CrB<sub>4</sub> hold promise to have a remarkably high hardness. Its high-strength physical original will be discussed in details.

**4:50 PM**

**(ICACC-FS2-009-2012) Multiscale modeling of ultra high temperature ceramics (UHTC) ZrB<sub>2</sub> and HfB<sub>2</sub>: application to lattice thermal conductivity (Invited)**

J. W. Lawson\*, NASA Ames Research Center, USA; M. S. Daw, Clemson University, USA; T. H. Squire, C. W. Bauschlicher, NASA Ames Research Center, USA

We are developing a multiscale framework in computational modeling for the ultra high temperature ceramics (UHTC) ZrB<sub>2</sub> and HfB<sub>2</sub>. These materials are characterized by high melting point, good strength, and reasonable oxidation resistance. They are candidate materials for a number of applications in extreme environments including sharp leading edges of hypersonic aircraft. In particular, we used a combination of ab initio methods, atomistic simulations and continuum computations to obtain insights into fundamental properties of these materials. Ab initio methods were used to compute basic structural, mechanical and thermal properties. From these results, a database was constructed to fit a Tersoff style interatomic potential suitable for atomistic simulations. These potentials were used to evaluate the lattice thermal conductivity of single crystals and the thermal resistance of simple grain boundaries. Finite element method (FEM) computations using atomistic results as inputs were performed with meshes constructed on SEM images thereby modeling the realistic microstructure. These continuum computations showed the reduction in thermal conductivity due to the grain boundary network.

**5:20 PM**

**(ICACC-FS2-010-2012) Atomistic reconstruction of pyrocarbons: from imaging to property computation (Invited)**

J. Leyssale, CNRS, France; J. Da Costa, University Bordeaux, France; B. Farbos, CNRS, France; C. Germain, University Bordeaux, France; G. L. Vignoles\*, University Bordeaux 1, France

We present an original approach for the construction of atomic scale models for nanotextured materials such as pyrocarbons based on HRTEM lattice fringe imaging. Starting from an HRTEM LF micrograph with high- and low-frequency filtering, a set of 2D image statistical descriptors is collected. This set is imposed as a constraint to a random 3D image generator with a transverse isotropy hypothesis. The generated 3D images are then used as an attractive potential field superimposed to the usual intermolecular potentials in Molecular Dynamics simulations of liquid carbon quenching. The obtained sets of up to 20,000 carbon and hydrogen atoms may be used for the evaluation of several properties. First, structural properties like simulated HRTEM LF images and pair distribution functions are compared to experimental data, with an excellent agreement. Second, a virtual mechanical testing of the structure is presented and discussed.

### FS3: Next Generation Technologies for Innovative Surface Coatings

#### Technology for Innovative Surface Engineering

Room: Coquina Salon G

Session Chairs: Taejin Hwang, Korea Institute of Industrial Technology; Tsuyoshi Honma, Nagaoka University of Technology

1:30 PM

#### (ICACC-FS3-002-2012) Multifunctional thin film resistors prepared by ALD for high-efficiency inkjet printheads

S. Kwon\*, Y. Shin, W. Kwack, Pusan National University, Republic of Korea; S. Shin, K. Moon, Korea Institute of Industrial Technology, Republic of Korea

In past decades, the thermal inkjet (TIJ) printer has been widely used as one of the most well-known digital printing technology due to its low cost, and high printing quality. Since the printing speed of TIJ printers are much slower than that of laser printers, however, there has been intensive efforts to raise the printing speed of TIJ printers. One of the most plausible methods to raise the printing speed of TIJ printers is to adopt a page-wide array TIJ printhead. To accomplish this goal, the high efficiency inkjet heating resistor films should be developed to settle the high power consumption problem of a page-wide array TIJ printhead. In this study, we investigated noble metal based multicomponent thin film resistor films prepared by atomic layer deposition (ALD) for a high efficiency inkjet printhead. Design concept, preparation, material properties of noble metal based multicomponent thin films will be discussed in terms of multifunctionality.

1:50 PM

#### (ICACC-FS3-003-2012) HfInZnO-based thin film transistors: the effects of the Hf ratio on the film properties and the bias stability

M. Moon, H. Jeon, S. Na, D. Jung, H. Kim, H. Lee\*, Sungkyunkwan University, Republic of Korea

Transparent amorphous oxides are promising materials for the active layer of thin film transistors (TFTs). Among them, InGaZnO-based oxide semiconductors are actively studied owing to their excellent properties including a high mobility. Nevertheless, the remaining impediment to commercialization is a stability issue under surrounding environments, in particular, on-current bias stress (BS). Here, in an effort to improve instability under bias stress, we investigated the film properties of HfInZnO with various Hf ratios (from 0 to 0.95) and the device performance (including the stability under bias stress) of their TFTs. The microstructure of the films was investigated using transmission electron microscopy and the electrical properties were examined using Hall measurements. We also used X-ray photoelectron spectroscopy (XPS) to examine the oxygen binding state of the films. We compared the transistor characteristics of the devices, confirming an intimate relationship between the oxygen vacancy concentration and the transistor characteristics including the bias stability.

2:10 PM

#### (ICACC-FS3-004-2012) Thermal anisotropy of epoxy resin-based nano hybrid film with oriented boron nitride nanosheets under rotation magnetic field

H. Cho\*, M. Mitsuhashi, T. Nakayama, T. Suzuki, S. Tanaka, W. Jiang, H. Suematsu, K. Niihara, Nagaoka University of Technology, Japan

Fabrication of epoxy resin-based nano hybrid materials with oriented boron nitride (BN) nanosheets was fabricated under rotation magnetic field. BN is a well known electrical insulator with wide band gap and displays remarkable chemical inertness and thermal conductivity. Its nanoscale structures are of potential use for electronic devices and nanostructured ceramic materials. Nevertheless, significant difficulties exist in the fabrication of BN nanosheets with controlled orientation and alignment by chemical medication or electrical methods due to its poor wetting property and wide band gap (5.5~6.4 eV). In this research, we demonstrate the well controlled orientation of unmodified BN nanosheets using rotation magnetic field. BN

nanosheets in the hybrid mixtures were located either parallel or perpendicular to the direction of the rotation magnetic field of 60 rpm at 10 T. The analysis revealed that the unmodified BN nanosheets were successfully oriented in the epoxy resin-based nano hybrid material. They showed reversed thermal anisotropy depending on anisotropy of BN nanosheets. Furthermore, the nano hybrid material noticeably improved thermal conductivity. The mechanisms for the orientation of BN nanosheets under magnetic fields and the enhancement of thermal conductivity will be discussed.

2:30 PM

#### (ICACC-FS3-005-2012) Fabrication of freestanding TiO<sub>2</sub> and TiO<sub>2</sub>-based multicomponent nanotube arrays using ALD and BCP templates

Y. Shin\*, S. Kwon, Pusan National University, Republic of Korea; S. Ku, G. Jo, J. Kim, KAIST, Republic of Korea

One dimensional nanomaterials such as nanowires, nanotubes, nanorods, and nanobelts, have attracted special attention because they possess unique structural one dimensionality and possible quantum confinement effects in two dimensions. As a result, they are expected to play an important role as building blocks in future nanoscale devices. The potential applications for these materials has been expanded through the efforts of several researchers. Among them, well ordered and vertically aligned titanium oxide (TiO<sub>2</sub>) nanotube arrays on substrates hold great potential for various applications, such as photovoltaics, sensors, and photocatalysis, primarily due to their directionality, high surface-to-volume ratios, and the ability to control their properties by varying nanotube dimensions. And, TiO<sub>2</sub> based multicomponent nanotubes such as doped or nanolaminated nanotubes are also extensively studied to tune TiO<sub>2</sub> nanotubes' properties. Herein, we fabricated freestanding TiO<sub>2</sub> and TiO<sub>2</sub> based multicomponent nanotube arrays by combining ALD and block-copolymer (BCP) templates. Microstructural properties and electrical properties will be discussed in this presentation.

2:50 PM

#### (ICACC-FS3-006-2012) Synthesis and electrochromic characterization of polyaniline-silica nanoparticles using surface modified colloidal silica with aminosilane

H. Lee\*, J. Park, G. Kim, Korea Institute of Industrial Technology (KITECH), Republic of Korea; M. Lee, Yonsei University, Republic of Korea

Polyaniline (PANI) has attracted much interest due to its outstanding electrical, optical and electro-optical properties. A key problem concerned to its successful application is its poor processability. Preparation of colloidal dispersions of PANI-silica nanocomposites produced by the polymerization of aniline in the presence of silica nanoparticles as steric stabilizers is one of the ways to solve the problem. In this work, we report the effect of surface modification of colloidal silica using aminosilane on the morphology of composite nanoparticle and electrochromic properties of the films which were prepared with PANI-silica nanoparticles. The morphology of the PANI-silica core-shell nanoparticles were confirmed by TEM and EDS analysis, and the nanoparticles were nearly monodispersed. The electrochromic characterization results showed that the surface modification of colloidal silica with aminosilane enhanced the optical contrast of PANI-silica films. The amino group may serve as an active site on the silica surface to bind aniline molecules so that the electrochromic active PANI contents of composites were increased.

3:30 PM

#### (ICACC-FS3-007-2012) Fabrication of crystal patterns on glass substrates by scanning laser irradiation (Invited)

T. Honma\*, Nagaoka University of Technology, Japan

Laser-induced structural modification to construct micro-architectures in materials has attracted much attention. Laser micro-fabrication in materials is a simple process compared with photolitho-

graphic techniques requiring multiple processing steps and an important technique for high technology devices. We proposed the spatially and orientation controlled crystallization in glass by laser irradiation. We developed laser irradiation technique to fabricate two-dimensional planar LiNbO<sub>3</sub> crystal architectures on the surface of Li<sub>2</sub>O-Nb<sub>2</sub>O<sub>5</sub>-SiO<sub>2</sub> glass by continuous wave ytterbium fiber laser irradiations. Lasers are scanned continuously with narrow steps (0.3 and 0.5 μm) and thus with overlaps of laser irradiated parts. For the planar LiNbO<sub>3</sub> crystals (50 μm × 100 μm) patterned by laser scanning with a power of 0.9 W and a speed of 7 μm/s, it is demonstrated from polarized micro-Raman scattering spectra and azimuthal dependence of second harmonic intensities that the c-axis orientation of LN crystals is established along the laser scanning direction. The laser irradiation technique gives us uniform crystal films on the glass surface.

4:00 PM

**(ICACC-FS3-008-2012) Fabrication of nanocrystalline InGaZnO films: the microstructure and the device performance of their thin film transistors**

H. Jeon\*, H. Choi, M. Moon, S. Na, D. Jung, H. Kim, H. Lee, Sungkyunkwan University, Republic of Korea

In recent years, transparent oxide semiconductors (TAOS) have captivated researchers by offering a combination of several technologically important features high electron mobility, high transparency, the capability for low temperature processing, etc. which makes them an excellent candidate for the active layer of thin film transistors (TFTs) for display applications. Among this class of materials, amorphous InGaZnO<sub>4</sub> (IGZO) has been the focus of many research and development efforts after its first demonstration as the active layer of TFTs. Here, we fabricated nanocrystalline IGZO films by co-sputtering from InGaO and ZnO targets with a high Zn ratio at an elevated temperature. By combining high resolution transmission electron microscopy and X-ray diffraction (XRD) analysis, we unraveled that the nanocrystalline structure sensitively changed depending on the process conditions (substrate temperature and Zn ratio). Furthermore, measurement of the electrical characteristics of the transistors fabricated from the films disclosed that the microstructure changes induced by substrate heating profoundly influenced the overall device performance.

4:20 PM

**(ICACC-FS3-009-2012) Corrosion protection for Mg by a sol-gel chemical method**

H. Kim, T. Hwang\*, Korea Institute of Industrial Technology, Republic of Korea

Mg is a light-weight metallic material. It is attracting vigorous attention from the industry, because of its high specific strength and abundance. However, it has a critical weakness such as fast corrosion by water. The main purpose of this work was developing an effective surface protection coating on a mass production basis. We employed the inorganic-organic hybrid material synthesized by a sol-gel chemical method. A special composition was tested, which can facilitate the low temperature curable films. With a consideration that the inherent hydroxide layer is playing an important role, we modified the bare surface of Mg in a series of pretreatment solutions. The corrosion protection properties of the films were compared by potentiodynamic polarization scan, electrochemical impedance analysis, and salt spray test. The low temperature cured hybrid films improved a lot the corrosion resistance. The films on the properly surface modified Mg noticeably reduced the corrosion current. Microstructure and impedance analysis disclosed that high resistive dense oxide layer was successfully formed by the surface modification, and it enhanced the corrosion protectability. The experimental observation in this study told us that the sol-gel prepared hybrid films could greatly improve the corrosion resistance of Mg, and the improvement could be greatly affected by the pretreatment on the Mg substrate.

4:40 PM

**(ICACC-FS3-010-2012) Gas sensing properties of noble metal decorated nano-grain TiO<sub>2</sub> thick films with controlled porosity**

J. Park\*, G. Kim, H. Lee, Korea Institute of Industrial Technology (KITECH), Republic of Korea

It is known that the sensing properties of thick film gas sensors are influenced by the film structure, such as the particles size, defects, and necking between particles. It is very important that the microstructures of polycrystalline metal oxides determined the number of junctions and the nature of inter-granular barriers. It is widely accepted that barriers formed among grains have a Schottky nature. Thus, the understanding of the Schottky barrier formation mechanisms is crucial in the development of better gas sensor devices. Furthermore, noble metal nanoparticles have received great interest from both technological and scientific point of view for improving catalytic activity. In this work, nanoparticles of noble metals including Au and Pt were synthesized on the surface of TiO<sub>2</sub> film with different porosity. To tune the porosity of TiO<sub>2</sub> film, TiO<sub>2</sub> sol was changed various parameters such as Ti-precursor molar weight, the amount of DI water for the hydrolysis and solvent. Their response properties were investigated as a function of the controlled porosity and noble metal nanoparticles at concentrations of toxic gases and operating temperature. We discuss the effect of the porosity of TiO<sub>2</sub> film and noble metal nanoparticles on TiO<sub>2</sub> film using AC and DC measuring in chemical sensors.

5:00 PM

**(ICACC-FS3-011-2012) High Velocity Suspension Flame Sprayed (HVSFS) coatings for automotive applications**

R. Gadow\*, A. Killinger, A. Manzat, University of Stuttgart, Germany

HVSFS processing is a promising method to produce structural and functional coatings by the direct injection of nano and micro ceramic suspensions in a supersonic flame spray system. New technologies for processing and application of nanoscale materials for improved tribofunctional coatings for cylinder liners in high performance passenger car and truck engines will be shown. The HVSFS flame spray process represents a novel process for the direct processing of aqueous and non-aqueous nano-powder suspensions which opens new application fields even for established materials since nanoscale coating structures can improve properties and performance compared to the respective standard coatings. Especially in the application field of thermally sprayed tribofunctional coatings, nano-materials show enhanced characteristics regarding coating microstructure, porosity and surface topography as well as wear and corrosion resistance. The potential of direct use of nanoscale suspension feedstocks in advanced thermal spray processing will be demonstrated in various industrial applications, e.g. internal combustion engines, industrial facilities and special tools.

5:20 PM

**(ICACC-FS3-012-2012) Synthesis and Characterization of Superhydrophobic Silica Layers via Electrospray (Invited)**

E. Kim, C. Lee, S. Kim\*, Inha University, Republic of Korea

We present the preparation of superhydrophobic silica layers through a combination of nanoscale surface roughness and fluorination. Electro spraying SiO<sub>2</sub> precursor solutions that were prepared by a sol-gel route and included trichloro(1H,1H,2H,2H-perfluorooctyl)silane as a fluorination source produced highly rough, fluorinated silica layers. In sharp contrast to the fluorinated flat silica layer, the fluorinated rough silica layer showed much enhanced repellency toward liquid droplets of different surface tensions. The surface fraction and the work of adhesion of superhydrophobic silica layers were determined, respectively, based on Cassie-Baxter equation and Young-Dupre equation. The satisfactory durability in water for 30 days, the ultraviolet resistance and the thermal stability up to 400 °C of the superhydrophobic silica layers prepared in this work confirm a promising practical application.

Tuesday, January 24, 2012

### European Union - USA Engineering Ceramics Summit

#### EU/USA Summit III

Room: Coquina Salon F

Session Chair: Mrityunjay Singh, OAI/NASA GRC

**8:00 AM**

#### (ICACC-EUUSA-009-2012) Ceramic Matrix Composite Turbine Vane for Rotorcraft Engines (Invited)

M. C. Halbig\*, NASA Glenn Research Center, USA

Ceramic matrix composite (CMC) components are being developed for turbine engine applications. Compared to metallic components, the CMC components offer benefits of higher temperature capability, less cooling requirements, and lower density which correlate to reduced fuel burn, reduced emissions, and lighter weight. This presentation discusses a technology development effort for overcoming challenges in fabricating a cooled CMC vane for the high pressure turbine for rotorcraft engines. An overview of various areas of technology development including design and analysis of concept components, small component fabrication, ceramic joining and integration, and material and component testing and characterization will be presented.

**8:30 AM**

#### (ICACC-EUUSA-010-2012) Status of Carbon/Ceramic Brakes: Properties, Production and Perspectives (Invited)

W. Krenkel\*, University of Bayreuth, Germany; R. Renz, Porsche AG, Germany

In the last ten years carbon fiber reinforced SiC (C/SiC), manufactured via the Liquid Silicon Infiltration (LSI) process, have demonstrated their superior tribological and thermo-mechanical behaviour in comparison to cast iron, resulting in different applications of lightweight brake disks and pads. As the frictional requirements differ widely for these different applications, the microstructures and properties of the composites also show big differences in terms of fiber length, carbon/silicon carbide ratio, coefficient of friction and wear rate. In general, the microstructure design of C/SiC composites is a compromise between an adequate level of fracture toughness (i.e. high amounts of carbon fibers) and a high wear stability (i.e. high amounts of SiC). The current design of ceramic brake disks comprises internally ventilated, thick-walled disks with geometries and designs similar to metallic brake disks. New applications in lightweight transportation systems offer new degrees of freedom in the design and fabrication of C/SiC disks. Considering the complete manufacture process, comprising all steps of fabrication like green body fabrication, pyrolysis of the matrix, siliconizing, machining, quality assurance, etc. new technology approaches promise a considerable reduction of the current high production costs, a prerequisite for a future mass production.

**9:00 AM**

#### (ICACC-EUUSA-011-2012) Recent developments in joining issues and ceramic matrix composites (Invited)

M. Ferraris\*, Politecnico di Torino, Italy

Recent development in joining issues and ceramic matrix composites (CMC) in EU will be briefly discussed. EU and national projects on these subjects, industrial involvements and research groups working in these areas will be presented, with the aim of strengthening and optimizing EU-USA cooperation. This talk will address the current needs and future challenges in the field of ceramic matrix composites.

#### EU/USA Summit IV

Room: Coquina Salon F

Session Chair: Sanjay Mathur, University of Cologne

**9:50 AM**

#### (ICACC-EUUSA-012-2012) Synthesis of silicon-carbon nanoceramics in high temperature aerosol reactor (Invited)

A. Lahde\*, University of Eastern Finland, Finland

Powders consisting of metallic nanoparticles and nanoceramics with small grain size, narrow size distribution and high purity are needed for full exploitation of nano-sized material for novel industrial applications. The particle preparation with the gas phase processes (e.g. chemical vapour synthesis) enable good control over these properties. However, the selection of the precursor material and its reaction kinetics are important parameters in the process optimization. We have prepared silicon-carbon nanoceramics with the atmospheric pressure chemical vapour synthesis (APCVS). APCVS is based on the vaporization of the metal-organic precursor (hexamethyldisilane, HMDS) and the subsequent decomposition in high temperature ( $T = 800 - 1400$  °C) vertical tube flow reactor. The geometric mean diameter of particle agglomerates ranged from 160 to 200 nm ( $T = 800 - 1200$  °C). At the reactor temperature of 800 °C, the synthesized particles were amorphous preceramics containing mostly SiC<sub>4</sub>, Si-CH<sub>2</sub>-Si and Si-H units. These particles had a high specific surface area and pronounced oxidation tendency compared to the particles produced at higher temperatures. The composition of the particles turned towards nanocrystalline 3C-SiC with crystallite size around 2 nm and 5 nm as the reaction temperature increased to 1200 °C and 1400 °C, respectively.

**10:20 AM**

#### (ICACC-EUUSA-013-2012) The State of Ceramics Research at Corning (Invited)

C. Heckle\*, Corning Incorporated, USA

Corning is well known as a Specialty Glass and Ceramics company and our current products include flat glass for large displays, chemically strengthened glass for mobile applications and cellular ceramics for catalytic converter substrates and diesel filters. Corning also has a rich research portfolio in a diverse set of materials beyond these current product lines. Global megatrends drive our research portfolio to include work on CO<sub>2</sub> capture, materials to support lithium batteries, and thermoelectric materials, among others. Corning is investing in broadening our ceramic product offering base and some of those investments will be discussed.

**10:50 AM**

#### (ICACC-EUUSA-014-2012) Inorganic Nanofibers via Electrospinning – on the Road to Industrial Application (Invited)

K. Schierle-Arndt\*, F. Major, E. Klimov, M. Gärtner, BASF SE, Germany

The number of publications dealing with inorganic nanofibers has increased in the last 10 years significantly. Therefore also industry is interested in this area and puts effort in nanofiber development. Possible applications are gas sensors, filters, catalysts, fuel cells batteries or thermoelectric modules. One method for the production of nanofibers is electrospinning. A precursor solution containing metal salts, a polymer and a solvent, is spun to a green fiber, which contains the metal salts in a polymer matrix. In the final calcination step the inorganic nanofiber is built either as an oxide (e.g. ZnO, Al<sub>2</sub>O<sub>3</sub>, TiO<sub>2</sub>, SiO<sub>2</sub>) or as a metal (e.g. Ag, Cu) depending on the calcination conditions. The talk shall give an overview about inorganic nanofibers and their properties depending on process parameters. Special focus will be on the scale up into miniplant and pilot scale including necessary adaptations with each step on the example of aluminum doped zinc oxide nanofibers.



11:20 AM

**(ICACC-EUUSA-015-2012) Strategic Initiative Materials (SIM): Joint materials research between Flemish research institutes and industry (Invited)**

M. K. Van Bael\*, A. Hardy, Hasselt University, Belgium

Together with 10 major materials producing and materials processing companies and with the support of the Flemish Government, the Belgian employers organization Agoria Vlaanderen, the collective centre of the Belgian technological industry SIRRIS and the 5 Flemish universities founded the Strategic Initiative Materials 'SIM'. SIM is a platform to finance and direct joint strategic research by universities and companies in order to strengthen their position on the medium to long term. Research programs and projects are set-up based on open calls for proposals in the areas of "materials for energy & light", "durable & sustainable structural materials" and "tailored nanomaterials in their environment". The SoPPoM program is one of the currently three approved research programs within the SIM initiative. In the SoPPoM program, 6 complementary projects are run by 5 research institutes and various industrial partners. The program aims to create in Flanders a breakthrough in the issue of cost reduction versus efficiency for the production of CIGS and OPV thin film photovoltaic systems by developing a fundamental understanding about solution based manufacturing of thin film PV cells and modules.

**S1: Mechanical Behavior and Performance of Ceramics & Composites****Fracture, Mechanical Properties II**

Room: Coquina Salon D

Session Chairs: Dileep Singh, Argonne National Lab; Rajan Tandon, Sandia National Lab

8:00 AM

**(ICACC-S1-012-2012) An experimentally-verified and adjustable-parameter-free equation for indentation toughness in the presence of lateral and radial cracking**

R. I. Todd\*, University of Oxford, United Kingdom; X. Huang, Harbin Institute of Technology, China; S. Guo, University of Oxford, United Kingdom

Despite extensive and justified criticism, the indentation crack method continues to be widely used for measuring the toughness of ceramics. It is therefore important for the ceramics community that progress is made towards addressing the problems with the technique. Some of the most serious problems concern the assumed loading of the cracks by the residual stresses in and around the indentation. These include: (i) a lack of experimental verification of the assumed stress field, (ii) the presence of empirical parameters in the equations used that are adjusted to give the "right" answer and (iii) the frequent presence of subsurface lateral cracking, invalidating the assumptions that underpin the method. This presentation addresses all three of these problems by developing an equation that gives an absolute prediction (i.e. no adjustable parameters) for the stresses around a Vickers indentation in the presence of lateral and radial cracking. The predicted stress at the surface is experimentally validated for indentations in alumina. The equation is then used to derive the fracture toughness as a function of the indentation size and radial crack length. Toughness measurements using the new equations are made on alumina and other ceramics and are shown to compare favourably with the results of existing techniques.

8:20 AM

**(ICACC-S1-013-2012) Using the Hertzian Ring Crack Initiation Approach to Measure Surface Flaw Size Densities**

R. Tandon\*, Sandia National Lab, USA

The surface crack size distribution (csd) in brittle materials is an important descriptor of surface quality, and maybe a good predictor of

crack initiation loads at local stress concentrators. Here the Hertzian indentation approach is used to measure csd on a glass surface. Using analytical and finite-element approaches, we show that frictional tractions significantly alter the contact stresses for dissimilar elastic contacts. Experimental data comparing crack initiation loads and cracking location for WC on glass, and glass on glass contacts support the predictions of the analysis. The data also indicate that control of humidity in test environment is critical to obtaining the actual csd's on a surface. An approximate analysis for determining the crack size from crack initiation loads is described. The crack sizes obtained on a glass surface using the Hertzian approach are significantly lower than ones obtained using a conventional strength test. The "searched area" concept is applied to report the flaw density on surfaces. Sandia is a multi-program laboratory operated by Sandia Corporation, a Lockheed Martin Company, for the United States Department of Energy's National Nuclear Security Administration under Contract-DE-AC04-94AL85000.

8:40 AM

**(ICACC-S1-014-2012) SPM observation of crack propagation behavior of  $\text{Si}_3\text{N}_4$  ceramics**

J. Tatami\*, M. Ohnishi, T. Wakihara, K. Komeya, T. Meguro, Yokohama National University, Japan

In-situ observation of fracture behavior of ceramics provides useful information to improve their mechanical properties. Scanning probe microscope (SPM) has atomic or nanoscale resolution and SPM is able to provide three-dimensional and quantitative information. We have observed the fracture surface and the crack induced by Vickers indentation of several kinds of ceramics by using SPM in nanoscale. In this study, crack propagation behavior was directly observed using a one-sided Chevron notched specimen by SPM.  $\text{Si}_3\text{N}_4$  ceramics used in this study was fabricated using  $\text{Y}_2\text{O}_3$  and  $\text{Al}_2\text{O}_3$  as sintering aids. The sample was loaded by three-point bending apparatus. As a result, it was observed that a crack in the  $\text{Si}_3\text{N}_4$  ceramics stably propagated. The crack in the  $\text{Si}_3\text{N}_4$  ceramics did not always propagate continuously from the tip of the crack. It was also observed that some of the micro cracks discontinuously formed and they connected. Grain boundary fracture occurred at the interface between glass phase and a  $\text{Si}_3\text{N}_4$  grain.

9:00 AM

**(ICACC-S1-015-2012) Mixed-Mode Fracture in an R-Curve Material**

K. Gopalakrishnan\*, J. J. Mecholsky, Jr., University of Florida, USA

Ceramics which exhibit increasing resistance with crack growth (R-curve behavior) has wide applications that involve combined tensile and shear loading. In this study, mixed-mode fracture is analyzed for a mica glass ceramic, a representative R-curve material. Indentation cracks of different sizes were introduced at the center of the tensile surface of mica glass ceramic bars which were fractured in flexure. Mode mixity was introduced by orienting the crack in different directions with respect to the principal tensile stress. Crack and fracture mirror sizes were measured using quantitative fractography. The ratio of the crack size to the mirror radius was found to be a function of the crack size and the degree of mode mixity in the R-curve material. The mixed-mode stress intensity factors were evaluated and were found to be a function of the crack size. Four mixed-mode fracture theories, based on the singular stress terms, were evaluated. The minimum strain energy density theory was the most effective in describing mixed-mode fracture from surface cracks in the mica glass ceramic in flexure. The role of the non-singular stress terms in mixed-mode fracture of ceramics in flexure will be discussed.

9:20 AM

**(ICACC-S1-016-2012) Strength Properties of Aged Poled Lead Zirconate Titanate Subjected to Electromechanical Loadings**

K. Zhang, H. Wang, H. Lin\*, Oak Ridge National Lab, USA

Commercially available PZT PSI-5A4E is considered to be an excellent candidate for use in fuel injection systems. Aging, mechanical

loading, and electric field all affect the strength and integrity of PZT. The previous study on aged 5A4E, using ball-on-ring (BOR) biaxial flexure strength testing showed the application of 3 times coercive field in the negative direction greatly increased the failure stress of 5A4E. In the present work, aged 5A4E specimens were examined through BOR under electric field range of  $-3E_c$  to  $+3E_c$  with a controlled electric loading path. Weibull strength distribution plots were used to interpret the mechanical strength of 5A4E. It was found that regardless the field direction, application of electric field with preloaded electric field from 0 to  $-3E_c$  increased the failure stress of 5A4E. The results showed that effects of electric field on the failure stress were different with and without a preloaded electric field from 0 to  $-3E_c$ . Additionally, the higher the electric field strength the higher the mechanical strength of 5A4E is. Surface located flaws were identified to be responsible for the failure of 5A4E. Research sponsored by the U.S. Department of Energy, Assistant Secretary for Energy Efficiency and Renewable Energy, Office of Vehicle Technologies, as part of the Propulsion Materials Program, under contract DE-AC05-00OR22725 with UT-Battelle, LLC.

### 10:00 AM

#### (ICACC-S1-017-2012) Glass Cracking Near Edges and Interfaces

R. Tandon\*, Sandia National Lab, USA; D. Shahin, Missouri University of Science and Technology, USA

Understanding and mitigating cracking near free or constrained edges of glass is a technologically important problem. Vickers indentation is an extremely useful tool to study the behavior of glasses, and has been used to estimate toughness, residual stresses and gain insight into materials behavior. When used to probe the behavior of cracks near edges, indentation cracks are subjected to an additional loading: that due to the elastic mismatch between the glass and the free/constrained edge. Here, we use a fracture mechanics solution that treats indentation cracks as point-loaded 2-d cracks to understand the cracking behavior of soda-lime silicate glass at free edges and at glass-epoxy interface. Crack lengths are measured as the crack progressively nears the interface, and the results are reasonably close to the predictions based on the mechanics model. The curvature of the crack path is correlated to the mixed-modity of the loading, and the effect of compressive stresses parallel to the crack path on its "curving" behavior is examined. The mechanics model may be useful in studying crack behavior along other material interfaces and different edge conditions. Sandia is a multi-program laboratory operated by Sandia Corporation, a Lockheed Martin Company, for the United States Department of Energy's National Nuclear Security Administration under Contract-DE-AC04-94AL85000.

### 10:20 AM

#### (ICACC-S1-018-2012) Edge Chip Fracture Resistance of Dental Materials

G. Quinn\*, American dental association foundation, USA; K. Hoffman, American dental association foundation, USA; J. Quinn, American dental association foundation, USA

The edge chipping test was used to measure the fracture resistance of several dental restoration ceramics and compared to other dental materials. Materials tested included a feldspathic porcelain, a 3Y-TZP, a filled resin-matrix composite, a resin denture material, and human dentin. The effects of varying the testing machine and indenter type are discussed.

### 10:40 AM

#### (ICACC-S1-019-2012) Fretting fatigue failure of engineering ceramics

C. Woerner\*, K. Lang, Insitut fuer Angewandte Materialien - Werkstoffkunde, Germany

Rollers made of ceramic are very well suitable for hot rolling of high-strength steels. During the shaping process the ceramic rollers are highly loaded. The appearing complex loading is caused by a cyclic

loading from the rotation of the rollers and high Hertzian stresses connected with friction, caused by the contact between the rollers and the rolling stock during the shaping process. To investigate the lifetime behaviour of potential roller materials fretting fatigue tests are carried out in a modified four-point-bending unit, where a fretting pad is pressed on to the tensile side of the bending bar and oscillated. In the test series, the loading types of the fretting pad were varied. The tested material is the model material silicon-nitride (SL200BG). Silicon-nitride is damaged by fretting load, caused by crack initiation and/or activation, which leads to lower residual strengths. Also with an additional cyclic four point bending loading, the lifetime gets significant lower. The strong tensile field in the specimen caused by the oscillating fretting pad leads to an activation of the surface defects, but doesn't influence the R-Curve of the material. With the additional cyclic loading comes a strong degradation of the reinforcing elements, which leads to a more lowered R-Curve, then expected from the pure four point bending. The variation of the fretting loading helps to separate and understand the damage mechanisms.

### 11:00 AM

#### (ICACC-S1-020-2012) Mechanical stability limits of $Ba_{0.5}Sr_{0.5}Co_{0.8}Fe_{0.2}O_{3-\delta}$ ceramic membrane material

J. Malzbender\*, G. Pecanac, Forschungszentrum Jülich, Germany

The high oxygen permeation of mixed ionic electronic conducting ceramic materials renders them a promising option for the application as gas separation membranes. However, in addition to the permeation and chemical stability also the mechanical reliability has to be warranted. Focusing on  $Ba_{0.5}Sr_{0.5}Co_{0.8}Fe_{0.2}O_{3-\delta}$  the mechanical stability limits at room temperature and elevated temperatures are derived. Hence, in addition to elastic and fracture properties also lifetime aspects at room and typical operation temperatures are considered. The analysis is based on an assessment of the slow crack growth sensitivity using the loading rate sensitivity of the characteristic strength at room temperature and creep rupture tests in a three point bending arrangement at high temperature.

### 11:20 AM

#### (ICACC-S1-021-2012) Controlled Crack Propagation Tests in Novel Alumina-Based Refractories

E. Skiera\*, R. W. Steinbrech, J. Malzbender, Forschungszentrum Juelich, Germany; C. G. Aneziris, S. Dudczig, Technical University Bergakademie Freiberg, Germany

Novel, innovative, carbon-reduced and carbon-free refractory materials are currently under development within the framework of the national priority program "Fire". The influence of microstructure on crack propagation was studied in fracture tests with two refractory materials processed at TU Freiberg. Both, the almost pure alumina (99%  $Al_2O_3$ ) and the alumina variant with titania and zirconia additives (AZT: 95%  $Al_2O_3$ , 2,5%  $TiO_2$ , 2,5%  $ZrO_2$ ) were sintered at 1600°C and had a maximum grain size of about 1 mm. Wedge Splitting Tests (WST) and, for comparison, Compact Tension Tests (CT) were carried out at room temperature monitoring simultaneously the crack growth by optical (LM) or electron microscopy (SEM) on polished side faces of the specimens. Image correlation tools were developed to visualize in-situ and after the tests the crack advance and to gain information about the crack path. The AZT refractory exhibited much more pronounced deflection, branching and bridging of the cracks. Also fracture strength and stiffness were significantly lower than in the alumina material. Implications for the thermal shock behavior of both refractory variants are discussed in terms of the Hasselman parameter  $R^{**}$ .

### 11:40 AM

#### (ICACC-S1-022-2012) Nanoscratch Induced Deformation in Sapphire

L. Huang\*, C. Bonifacio, K. van Benthem, A. K. Mukherjee, J. M. Schoenung, UC Davis, USA

Mechanical behavior and plasticity at micro- or nano-scale of alumina ceramics can be improved when the grain size is reduced to the

ultrafine regime. Based on the crystal structure of alumina ceramics, the initiation of plasticity in terms of slip or twinning in nanoscratch tests strongly depends on the orientation of grains, which is not easily detectable in polycrystalline samples. Therefore, investigating the nanoscratch induced deformation in sapphire wafers with various orientations can provide a better way to further reveal the corresponding deformation mechanisms, particularly the initiation of plasticity, depending on crystallography, in the process. In this research, the nanoscratch induced deformation and microstructure evolution in sapphire wafers, with predetermined (10-10), (1-210) and (0001) surface orientations have been investigated. Scratch groove morphologies have been observed using scanning electron microscopy (SEM), atomic force microscopy (AFM) and transmission electron microscopy (TEM). The focused ion beam (FIB) technique has been applied to prepare a site-specific cross-sectional TEM sample, enabling visualization of subsurface deformation features. The resulting microstructural features are further rationalized by means of elastic and residual stress field calculations.

## S4: Armor Ceramics

### Dynamic Behavior

Room: Coquina Salon E

Session Chair: Jerry LaSalvia, U.S. Army Research Laboratory

8:00 AM

#### (ICACC-S4-013-2012) Ceramic Armour Development (Invited)

B. James\*, Dstl, United Kingdom

Research and development of ceramic armour has been undertaken at the UK MOD's Defence Science and Technology Laboratory over many years. The prime motivation for this work has been to provide lighter, more robust ceramic armour for UK platforms. Whilst the final aim is for fully developed armour systems, the route followed has included fundamental research into the structure of ceramics, the interaction of stresses with the intrinsic ceramic structure and the geometrical structure of armour systems, the understanding and management of stress waves within ceramic composite systems and the development of material models for ceramic materials. This talk will describe some of the more important findings from this research giving some of the significant results. One of the inferences from previous work is that defect structure is very important in the failure behaviour of ceramic materials. Initial results will be shown of the development of characterisation techniques to identify and monitor the behaviour of ceramic defects that might affect the performance in ballistic impact.

8:30 AM

#### (ICACC-S4-014-2012) From Mechanisms to Materials: Armor Ceramics (Invited)

K. T. Ramesh\*, Johns Hopkins University, USA

The design of improved armor ceramics is predicated on the understanding of the deformation and failure mechanisms that occur within these materials during the impact event. Observation of these mechanisms requires a combination of advanced experimental techniques with high temporal resolution and advanced characterization techniques with high spatial resolution. We demonstrate, using dynamic visualization techniques, that the failure mechanisms active during the impact event are often not those that would be suggested by observations of slowly loaded ceramics. In particular, the microstructural characteristics of these materials result in the development of length scales and time scales that interact with the loading scales. We present a fundamental physics-based approach to modeling these mechanisms, and use this approach to suggest avenues for the design of improved materials for such applications.

9:00 AM

#### (ICACC-S4-015-2012) High Speed Electrical Monitoring of Crack Propagation in Layered Ballistic Protection Systems

E. K. Oberg\*, C. S. Dunleavy, T. W. Clyne, University of Cambridge, United Kingdom; P. Bourke, Tencate Advanced Armour, United Kingdom

A small gas gun has been used to measure energy absorption during ballistic impact of bi-layered specimens comprising an alumina front plate and a (woven) carbon fibre composite laminate back plate. Spherical projectiles of 8mm diameter were used and the impact velocities ranged between 220 and 300 m s<sup>-1</sup>. An electrical technique has been developed to monitor crack advance characteristics during ballistic impact, allowing the velocities of radial cracks to be measured as well as the nature of the crack pattern development. This was done by means of a grid of thin layer gold electrical circuit elements on front or back surfaces of the alumina plate. These elements were then incorporated into an electrical circuit and high speed data acquisition was carried out during impact. It was confirmed that these velocities typically range up to about 50% of the speed of sound in the medium, both for alumina (speed about 2-3 km s<sup>-1</sup>) and for Perspex. The figures obtained were in good agreement with values obtained using high speed photography, which tends to be a more cumbersome methodology. The fracture patterns have also been correlated with the presence of the composite layer and variations in the interfacial bond strength. It is shown that the interfacial adhesion can have an effect on the fracture pattern development and on the energy absorbed by the bi-layer specimens during ballistic impact.

9:20 AM

#### (ICACC-S4-016-2012) Dislocation Mechanisms in Aluminum Nitride Under Shock Loading

G. Hu\*, Johns Hopkins University, USA; C. Williams, Army Research Laboratory, USA; C. Chen, K. Ramesh, Johns Hopkins University, USA; J. McCauley, Army Research Laboratory, USA

Ceramic materials in dynamic impact applications are subjected to not only high strains and stress rates, but also multiaxial stress states. Using a shock recovery technique, aluminum nitride (AlN) specimens were shock loaded and recovered for microstructural analysis. TEM and HRTEM were used to characterize the deformation mechanisms involved in the AlN material. At high pressures the deformation mechanisms are observed to be dislocation dominated, as can be predicted through newly developed micromechanical models.

10:00 AM

#### (ICACC-S4-017-2012) Quantitative measurement of flaw population and cracking resistance on surfaces of armour silicon carbide ceramics

S. Ghosh\*, H. Wu, Loughborough University, United Kingdom

Flaw population and resistance of cracking initiation and propagation are essential measurements that are the key inputs for modelling dynamic damage of ceramics with continuum mechanics. In this paper, we conducted Hertzian indentation on the surface of armour silicon carbide ceramics, and the flaw population and fracture toughness were quantified using Hertzian cracking load and the size of Hertzian cracks on the surface. Surfaces finished under different conditions, e.g. as-sintered, as-polished and as-ground, were included for comparative study. Different sizes of spherical indenter were used to probe information from different depths on the surfaces. Fracture toughness measured with Vickers indentation and nanoindentation on the same surfaces will also be presented for discussion on the resistance of cracking initiation and propagation in silicon carbide ceramics.

10:20 AM

#### (ICACC-S4-018-2012) Split Hopkinson Pressure Bar Testing of Alumina and Alumina-Based Composite Materials

C. J. Dancer\*, S. Falco, N. Petrinic, R. Todd, University of Oxford, United Kingdom

Split Hopkinson Pressure Bar (SHPB) testing enables the dynamic compressive strength of ceramic materials to be measured. However

there are several widely acknowledged difficulties with obtaining accurate results using this technique. SHPB tests were used to measure the compressive strength of high purity alumina samples in different specimen geometries, measuring the strain directly from the sample using digital image correlation. By comparing the results, the effect of specimen geometry on the stress distribution in the material and therefore on the measured compressive fracture stress was determined. These findings were compared to numerical models. Once the most suitable specimen geometry was established, this method was used to measure the dynamic compressive strength of an alumina silicon-carbide composite. The results are compared to those for pure alumina and pure silicon carbide to assess the suitability of the composite material for armour applications.

**10:40 AM**

**(ICACC-S4-019-2012) Dynamic Response of Granular Tungsten Carbide under Pressure-Shear Loading**

S. Alexander\*, T. Thornhill, W. Reinhart, T. Vogler, Sandia National Laboratories, USA

The dynamic response of granular tungsten carbide (WC) under combined pressure-shear loading was investigated to determine its deviatoric response (strength), an important aspect for modeling the granular material as well as the consolidated ceramic. Pressure-shear loading was obtained via oblique impact using a 4" bore compressed gas gun with a slotted barrel to prevent projectile rotation. The WC powder was placed between two elastic anvils and impacted at 20 deg. obliquity. Velocity interferometry was used to measure both longitudinal and transverse particle velocities. Samples were longitudinally compressed up to about 2 GPa and subsequently sheared. Results indicate flow strength similar to, but less than those observed for sand and alumina powders however differences in particle size and compressibility of the powders makes direct comparison difficult. Additionally, pressure and shear induced changes to the particle morphology were studied via post-shock recovery and SEM analysis of the powder. Results indicate little change in the WC particles following normal impact in contrast with greatly reduced particle sizes following shear loading illustrating the important role of shear waves in the fracture mechanics of granular powders. Sandia is a multi-program lab operated by Sandia Corp., a wholly owned subsidiary of Lockheed Martin, for the U.S. DOE's NNSA under contract DE-AC04-94AL85000.

**11:00 AM**

**(ICACC-S4-020-2012) Analysis of crack patterns in non-oxide ceramics after ballistic test**

C. Roberson\*, Advanced Defence Materials Limited, United Kingdom; P. J. Hazell, Cranfield University, United Kingdom; D. Liaptis, N. P. Ludford, TWI Limited, United Kingdom

Sets of boron carbide and silicon carbide tile samples have been fabricated by commercial manufacturers. Two conditions have been explored; one with excellent commercial tile quality and the other containing intentionally placed multiple gross defects. The locations of the defects have been mapped using C-Scan ultrasound and the tiles made up into identical ballistic targets, preserving the location of the defects within each tile. The sets of targets have been ballistic tested to determine the  $V_{50}$  values for each condition deriving a measure of the effect on ballistic performance of the inclusion of gross defects in the ceramic structure. Subsequently the ballistic targets have been subjected to digital X-ray imaging and the crack patterns in the ceramic have been analysed using image analysis software. The effect of the coupling of the stress waves with the gross defects on the crack patterns within the ceramic can be seen. Reference to past literature and the use of a physics based model has been used to help understand the influence on the development of crack patterns during ballistic impact of gross defects within the ceramic microstructure. Results of the ballistic testing suggests that the presence of gross defects has a

lower than expected effect on the ballistic performance of the two materials.

**11:20 AM**

**(ICACC-S4-021-2012) Dynamic Electro-mechanical Damage Behavior of Piezoelectric Ceramics**

L. E. Lamberson\*, K. T. Ramesh, Johns Hopkins University, USA

Piezoelectric ceramics are conventionally used to generate an electrical signal from an external mechanical load (or vice versa) in the linear elastic regime. Some ceramics used in armor applications, such as aluminum nitride and silicon carbide, are also piezoelectric. However, little is understood regarding the potential to exploit the coupled electro-mechanical response under dynamic loading to the point of failure. This talk focuses on high strain rate Kolsky bar experiments (10E3) on single crystal silicon carbide, aluminum nitride and quartz, in order to establish the dynamic polarization process as a function of damage. Our initial results suggest a slight increase in the piezoelectric stress coefficient from loading to unloading. These results are explained utilizing damage micromechanics and Eshelby inclusion theory.

**11:40 AM**

**(ICACC-S4-022-2012) High Strain Rate Response and Dynamic Failure of Alumina**

J. Yuan\*, G. Tan, J. Ma, Nanyang Technological University, Singapore

Dynamic behavior of an advanced alumina ( $Al_2O_3$ ) at high strain rate is investigated using a Split Hopkinson Pressure Bar (SHPB) tester. With the available conditions of specimen dimensions and SHPB settings, the maximum strain rate in SHPB tests, that are able to provide valid test data in terms of specimen stress equilibrium and constant strain rate, is formulated and applied in testing. Pulse shaping technique is applied to adjust the test strain rate in SHPB tests. Influence of wave dispersion on test data is considered. SHPB test data at strain rate beyond the valid maximum strain rate is also obtained to identify the effects of specimen stress equilibrium and constant strain rate as well as wave dispersion on the dynamic response and failure of the alumina. In addition, quasi-static compressive tests are carried out on a universal testing machine to reveal the strain rate effect on deformation and failure mechanism of the alumina.

## **S7: 6th International Symposium on Nanostructured Materials and Nano-Composites**

### **Nanodevices and Industrial Application**

Room: Coquina Salon B

Session Chairs: Anna Lahde, University of Eastern Finland; Erica Corral, University of Arizona

**8:00 AM**

**(ICACC-S7-011-2012) Toughening in Graphene Ceramic Composites (Invited)**

L. S. Walker, V. R. Marotto, University of Arizona, USA; M. A. Rafiee, N. Koratkar, Rensselaer Polytechnic Institute, USA; E. L. Corral\*, University of Arizona, USA

Graphene is a promising reinforcement material for use in composite systems due its two exceptional properties and two-dimensional structure. Conventional ceramic matrix composites use one-dimensional reinforcements in order to enhance toughness. However, we find that using graphene to enhance the toughness of bulk silicon nitride ceramics we are able to significantly enhance toughness of our ceramics. Our approach uses graphene platelets (GPL) that are homogeneously dispersed with silicon nitride particles and densified using spark plasma sintering at a densification temperature that enables the GPL to survive the harsh processing environment, as confirmed by Raman spectroscopy. We find that the 100 % alpha-silicon

nitride fracture toughness increases by up to ~235% (from ~2.8 to ~6.6 MPa-m<sup>1/2</sup>) at ~1.5% GPL volume fraction. Most interestingly novel toughening mechanisms were observed that show GPL wrapping and anchoring themselves around individual ceramic grains to resist sheet-pullout. The resulting cage-like graphene structures that encapsulate the individual grains were observed to deflect propagating cracks in not just two- but three-dimensions.

**8:30 AM**

**(ICACC-S7-012-2012) Lateral Growth of ZnO Nanorods in Solution and Their Application for High Performance Field Effect Transistors (Invited)**

Y. Hahn\*, Y. Park, H. Choi, J. Kim, Chonbuk National University, Republic of Korea

We have exploited a method for the lateral growth of multiple ZnO nanorods between electrodes in solution without the use of metal catalyst to fabricate high performance field-effect transistors (FETs). This method enables to directly align overlapped or overlap-free nanowires between electrodes with eliminating the vertical growth components and complex structural networks. The overlap-free ZnO nanorods FETs showed better performance with mobility of ~8.5 cm<sup>2</sup>/V/s and on/off ratio of ~4x10<sup>5</sup> than the overlapped ZnO nanorods FETs having mobility of ~5.3 cm<sup>2</sup>/V/s and on/off ratio of ~3x10<sup>4</sup>. All the FETs fabricated in this work showed much better performance than the previously reported solution-based ZnO FETs.

**9:00 AM**

**(ICACC-S7-013-2012) Effects of the pulsation reactor process on the material properties of nanoscaled ZrO<sub>2</sub>**

L. Leidolph\*, IBU-tec advanced materials AG, Germany

A pulsation reactor is applied to produce a new generation of ceramic materials like partly stabilized zirconia (PSZ) nanoparticles with novel properties and a tailor-made kind and content of stabilizer. One development is another type of ZrO<sub>2</sub> for high performance ceramics what combines unique mechanical, thermal and biological/chemical properties to allow innovative solutions for many applications. The exclusive pulsation reactor technology enables a large scale production of nano-sized powders with very high homogeneity, which is necessary particularly for doped materials. The advanced sintering behavior based on the fact that the powder particles do not build hard aggregates through sinter effects during the thermal production process. Different precursors are used to produce these types of fine powders. Physic-chemical characteristics of the produced powders such as powder morphology, specific surface area, thermal behavior, phase identification were studied. The results show that the particle morphology and particle size have a great effect on the sintering behavior of the created zirconia powders. A transfer of the nanoparticles into a granulate is necessary to enable a suitable pressing and a sufficiently dense form after sintering. The correlation between the properties of the granulate, the specific press, sintering conditions and the structure of the ceramics will be discussed.

**9:20 AM**

**(ICACC-S7-014-2012) Properties of organic semiconductor-metal oxide nanowire composite transistors**

C. Sun\*, Nanyang Technological University, Singapore; N. Mathews, Nanyang Technological University, Singapore; L. H. Wong, Nanyang Technological University, Singapore; S. G. Mhaisalkar, Nanyang Technological University, Singapore

Transistors fabricated from solution processable organic semiconductors have reached impressive performance, yet suffers from drawbacks like unipolar charge transport behavior. Poly(3-hexylthiophene) (P3HT) represent a class of conjugated polymers that is widely used as the hole-transporting material in organic field-effect transistors (OFETs). Ambipolar transistors which combine P3HT with n-type metal oxide nanowire networks are introduced in this

work. Highly oriented tin oxide (SnO<sub>2</sub>) nanowire network (nanonets) were firstly fabricated through contact printing approach. These nanowire networks are studied at submillimeter scales for their utilization as the active material in n-type thin film transistors. A layer of P3HT which was drop-casted over SnO<sub>2</sub> transistor allows the operation of the transistor in two regimes. For further optimization, the morphology of the organic semiconducting was improved by thermal annealing. Light illumination on the devices enabled the electron-hole pair generation at the nanowire-polymer interface which increased the current and carrier mobility. An interlayer between the n-type semiconductor and p-type semiconductor was also applied to prevent recombination of the charge carriers which enhanced the performance. This study provided the basic idea of nanowire network ambipolar transistors and the interaction between metal-oxide nanowires and organic polymers.

**Synthesis and Industrial Development of Nanoparticles**

Room: Coquina Salon B

Session Chairs: Erica Corral, University of Arizona; Yoon-Bong Hahn, Chonbuk National University

**10:00 AM**

**(ICACC-S7-015-2012) Synthesis of silicon-carbon nanoceramics with high temperature aerosol reactor (Invited)**

A. Lähde\*, M. Miettinen, University of Eastern Finland, Finland; M. Johansson, University of Åbo, Finland; S. Suvanto, J. Riikonen, University of Eastern Finland, Finland; U. Tapper, Technical Research Center of Finland, Finland; T. T. Pakkanen, V. Lehto, J. Jokiniemi, University of Eastern Finland, Finland

Powders consisting of metallic nanoparticles and nanoceramics with small grain size, narrow size distribution and high purity are needed for full exploitation of nano-sized material for industrial applications. The particle preparation with the gas phase processes enable good control over these properties. However, the selection of the precursor material and its reaction kinetics are important parameters in the process optimization. We have prepared Si-C based nanoceramics with the atmospheric pressure chemical vapour synthesis (APCVS). APCVS is based on the vaporization of the metal-organic precursor (hexamethyldisilane, HMDS) and the subsequent decomposition in high temperature (T=800–1400 C) vertical tube flow reactor. The decomposition of HMDS is a radical chain reaction producing silicon based nanoceramics with a narrow size distribution. The geometric mean diameter of particle agglomerates ranged from 160 to 200 nm (T=800-1200 C). At the reactor temperature of 800 C, the synthesized particles were amorphous preceramics containing mostly SiC<sub>4</sub>, Si-CH<sub>2</sub>-Si and Si-H units. These particles had a high specific surface area and pronounced oxidation tendency compared to the particles produced at higher temperatures. The composition of the particles turned towards nanocrystalline 3C-SiC with crystallite size around 2 nm and 5 nm as the reaction temperature increased to 1200 C and 1400 C, respectively.

**10:30 AM**

**(ICACC-S7-016-2012) Highly Specific Nanoparticles from gas phase synthesis – An Economic Route towards Sustainable Energy Technology (Invited)**

T. P. Huelsner, H. Wiggers\*, C. Schulz, Institute of Energy and Environmental Technology, Germany

The growing demand for energy and the limited fossil resources require advanced and green technologies for energy generation and energy saving. As conversion of energy is very often based on interface-related transfer processes, nanoscale materials are promising candidates to enhance energy-related applications. Gas phase synthesis is a widely used technique for the production of nanoparticles achieving annual production capacities of many thousand tons. However, the quality and diversity of the resulting

materials is often limited and usually agglomerates with a broad particle size distribution are formed. To enable and develop sophisticated methods for the production of nanoparticles with highly specific properties, we designed a unique pilot-plant-scale particle synthesis plant for the synthesis of up to a few kg nanoparticles/h. It consists of three different synthesis concepts based on a hot-wall reactor, a flame reactor and a microwave plasma reactor. Due to very high flexibility in time-temperature profile, residence time and pressure, we are able to synthesize materials with tuned morphology, size and size distribution covering spherical, non-agglomerated freestanding particles as well as 3-dimensional fractal aggregates. Some examples will be shown for synthesis and utilization of specifically synthesized nanoparticles for thermoelectrics and batteries.

### 11:00 AM

#### **(ICACC-S7-017-2012) Phase evolution studies and ferroelectric properties of Lead Zirconate Titanate (PZT) nanopowder and films thereof (Invited)**

R. P. Tandon\*, University of Delhi, India

Synthesis of PZT nanopowder having composition close to MBP has been carried out using conventional sol-gel process. The phase evolution of PZT nanopowder has been monitored by the techniques XPS, XRD, DTA/TGA, FTIR and TEM. These studies yielded excellent correlation with each other and led to the same conclusion that the pure perovskite phase of PZT nanopowder is obtained at 800 °C. It is observed that the crystallization of gel powder takes place above 500 °C and organic residue remains in the gel powder heat treated below 460 °C. The nanopowder heat treated at 550 °C and 650 °C consists of mixture of pyrochlore and perovskite phase and the amount of pyrochlore phase decreases with increasing temperature. The crystallite size for pure perovskite phase as estimated from TEM image is consistent with that calculated from XRD analysis. The composition calculated from XPS analysis is close to the targeted value. The pure nanopowder was used to make thick films (25 µm) of PZT using modified sol-gel technique. This serves a unique means of making thick films for MEMs application. The film exhibited Curie temperature at 382 °C and high piezoelectric coefficient ( $d_{33}$ ) close to 275 pC/N. Other ferroelectric properties have also been reported.

### 11:30 AM

#### **(ICACC-S7-018-2012) Nanostructured Oxides from Natural Minerals for Industrial applications (Invited)**

V. Rajendran\*, P. Manivasakan, P. R. Rauta, N. R. Dhineshbabu, K S Rangasamy College of Technology, India

Nanostructured metal oxides play a vital role in many areas of chemistry, physics, and materials science. The cost effective method has been developed for mass production of nano metal oxides such as  $\text{TiO}_2$ ,  $\text{Al}_2\text{O}_3$  and  $\text{ZrO}_2$  from natural minerals respectively Ilmenite, Bauxite and Zircon Sand. The present work has been focusing on nano effects in biomedical, textiles, refractories and productive coatings. The effect of incorporation of nano particles on refractories such as silica and meg-chrome brick have been explored in terms of refractory properties such as bulk density (BD), apparent porosity (AP), cold crushing strength (CCS), refractoriness under load (RUL) and reversible thermal expansion (RTE). The observed results reveal that the incorporation of nano particles increases the strength and compactness of refractory. Similarly, nano zirconia and titania particles were coated on the cotton fabrics employing dip coating method. The antibacterial effects of nano  $\text{ZrO}_2$  and  $\text{TiO}_2$  coated and uncoated cotton fabrics were studied to explore the biomedical applications.  $\text{TiO}_2$  nanoparticles coated cotton fabrics shows good UV protection efficiency and better antibacterial activity. Nano  $\text{ZrO}_2$  and  $\text{Al}_2\text{O}_3$  used for anticorrosive coatings on stainless steel in acid media. Nanostructured coatings on stainless steel show better productive efficiency than conventional coatings.

## **S8: 6th International Symposium on Advanced Processing and Manufacturing Technologies for Structural and Multifunctional Materials and Systems (APMT) in honor of Professor R. Judd Diefendorf**

### **Advanced Forming and Powder Technology**

Room: Coquina Salon A

Session Chairs: Nahum Travitzky, University of Erlangen-Nuremberg; Eugene Medvedovski, Umicore Thin Film Products

### 8:10 AM

#### **(ICACC-S8-009-2012) Additive Manufacturing of complex-shaped ceramic structures (Invited)**

N. Travitzky\*, P. Greil, University of Erlangen-Nuremberg, Germany

Design and development of advanced ceramic materials for medical and high performance applications ranging from automotive to aerospace and bringing these materials into use is one of the most challenging tasks of modern materials engineering. Owing to the inability of current technology related methods to produce complex-shaped ceramic parts with the desired microstructures and properties, novel techniques, so-called Additive Manufacturing (AM) techniques are becoming increasingly important processing techniques. The mechanical properties of the materials fabricated by Additive Manufacturing techniques in many cases are similar to the corresponding properties for commercially available ceramic-based materials fabricated by other methods. AM technologies can create parts using advanced materials superior to traditional ones. Layer-wise fabrication of the parts by AM techniques, however, can lead to unsatisfactory surface roughness. Therefore, different methods are suggested for surface finish improvement. Dense ceramic/glass, porous ceramics and ceramic/metal composites with complex geometry have been fabricated via different AM processing routes. Microstructure and mechanical properties of the fabricated composites have been investigated.

### 8:40 AM

#### **(ICACC-S8-010-2012) Fabrication of Complex-Shaped Ceramic Components by Injection Molding of Ceramic Suspension Gels at Room Temperature**

V. L. Wiesner\*, J. P. Youngblood, R. W. Trice, Purdue University, USA

Room temperature injection molding of ceramic suspension gels (CeraSGels) is proposed as a novel, low-cost and energy efficient processing method capable of forming dense ceramic components with complex geometries. CeraSGels are highly loaded with ceramic (>50 vol.%) and have a low amount of polymer carrier (<5 vol.%). Rheological studies using parallel plate rheometry of alumina CeraSGels showed that suspensions containing PVP as a viscosity modifier behaved like yield-pseudoplastic fluids at room temperature. Alumina samples have been fabricated with high green body strength despite low polymer content. After binder burnout and sintering, bulk density of sintered samples using the Archimedes technique was found to reach >98% theoretical density with linear shrinkage of <16%. SEM revealed minimal pore formation within sintered samples. Strength of the formed parts will be measured using the ASTM-C1323-96 C-ring test.

### 9:00 AM

#### **(ICACC-S8-011-2012) Ceramic Injection Moulding Using a Partially Water-Soluble Binder System: Effect of Back-Bone Polymers on the Process**

O. Weber\*, T. Hanemann, Karlsruhe Institute of Technology, Germany

With the technique powder injection moulding (PIM) it is possible to manufacture near-net-shape complex micro geometries cost effec-

tively and multiplicatively. Quality and stability of each process step as well as properties of final parts strongly depend on the choice of a suited combination of binder polymers. On this reason the represented research work deals with the study concerning to the process stability if different raw materials of poly-(methyl-methacrylate) (PMMA) are applied as a back-bone polymer. Feedstocks based on zirconia powder were observed, polyethylene glycol was used as basic polymer. To provide a uniform distribution of powder particles in the binder matrix stearic acid was added as a surfactant. Three kinds of commercially available PMMA and one of own production were compared whereby all four feature a similar molar mass distribution and differ in their apparent condition only: granular, pearly and edged shaped. The results of this study showed which essential influence this outward properties of PMMA have on compounding of homogeneous feedstocks, separation occurs between powder and binder components, dimensional stability of injection moulded and sintered parts as well as achieved densities of final micro products.

9:20 AM

**(ICACC-S8-012-2012) Low Pressure Injection Molding of Advanced Ceramic Components with Complex Shapes for Mass Production**

E. Medvedovski\*, Umicore Thin Film Products, USA; M. Peltsman, Peltsman Corp., USA

This presentation reviews the technology of low pressure injection molding that is successfully used for manufacturing of advanced ceramics with different compositions, particularly for the components with custom-designed complex shapes when the production is achieved hundreds pieces/ day or week or higher. The major principles of this technology are reviewed based on the extensive processing experience. Semi-automated equipment for low pressure injection molding technology is described.

10:00 AM

**(ICACC-S8-013-2012) Shaping of Large-Sized Sputtering Targets**

A. Kaiser\*, LAEIS GmbH, Luxembourg

Sputtering targets are used in PVD coating plants (PVD = physical vapor deposition) as a source for the coating material. Materials to be used can be indium tin oxide (ITO), alumina doped zinc oxide (AZO) and others. Large plates of various sputtering materials with an area of up to more than 0.5 m<sup>2</sup> and a thickness of < 10 mm up to approx. 40 mm are produced using uniaxial hydraulic presses. Despite their high aspect ratio the plates show good green strength and can be handled without problems. The uniaxial pressing is used either as the only shaping method for a subsequent pressureless sintering or as pre-densification for a second compaction step in an isostatic press. The advantage there is reduction of scrap to a minimum and to increase the throughput capacity of the isostatic press.

10:20 AM

**(ICACC-S8-014-2012) Pressure slip casting of calcium containing coarse grain oxide ceramics**

S. Schaffoener\*, C. G. Aneziris, TU Bergakademie Freiberg, Germany

This contribution investigates the possibility of pressure slip casting of calcium containing coarse grain oxide ceramics with an organic binder solution only. Pressure slip casting of ceramics is a way to produce complicated near net shape geometries. Further advantages are the possibility of automation, faster production, higher densities and lower quality variations of the body. However, until recently there has been only little attention paid to the possibility of forming ceramics with coarse grain by pressure slip casting. Calcium containing minerals like perovskite (CaTiO<sub>3</sub>) and calcium zirconate (CaZrO<sub>3</sub>) exhibit a remarkable thermodynamic stability and are therefore very interesting because of their potential use in vacuum metallurgy. To start with the raw materials are synthesized by solid state reactions and subsequently crushed and milled. In a second step a stable and pumpable

slip composition with fine and coarse particle fractions is formulated and casted in a compression permeability filtration (CPF) cell as well as in a commercial slip casting machine. This study presents major factors of the pressure slip casting process of coarse grain ceramics and the reached strength of the body. The influence of the slip rheology and possible anisotropy of the body were investigated by a new developed falling sphere viscometer and computer tomography.

10:40 AM

**(ICACC-S8-015-2012) Characterization of Ceramic Powders during Compaction Using Electrical Measurements**

T. Pruynt\*, R. Gerhardt, Georgia Institute of Technology, USA

The percolation threshold of an added filler, which improves the composite's electrical conductivity, in a ceramic composite is highly dependent on the processing conditions in powder-metallurgy. A non destructive method to test for this threshold in the ceramic composite still in its green state would allow for quality control that is typically only possible during the final state. In this study we evaluated the electrical response of ceramic compacts during dry pressing as a function of applied pressure. Semiconductive SiC and insulating Al<sub>2</sub>O<sub>3</sub> powders were used for the experiments along with combinations of the two. In order to determine the influence of porosity in the ceramic powder compacts, a custom made die with an insulating outer sleeve was used to carry out dc and ac measurements. Measurements were performed as a function of loading and unloading compaction pressure. Dc measurements can only detect the combined response from the powders and the porosity. However, from the impedance spectroscopy data, at least two semicircles were observed in the complex impedance plot that allows separation of the two processes. One of these semicircles represents the bulk material property, while the other is likely due to the void space and interfaces. The admittance, modulus and permittivity were also examined and showed behavior highly dependent on these two processes.

11:00 AM

**(ICACC-S8-016-2012) Highly particle-oriented alumina powder compact prepared from non-aqueous dispersed slurry**

S. Tanaka\*, R. Furushima, K. Uematsu, Nagaoka University of Technology, Japan

A highly textured alumina green compact was obtained from well dispersed non-aqueous slurry in a high magnetic field. Compatibility of poly(vinyl butyral)PVB to mixed organic solvents of xylene and isopropyl alcohol was studied in alumina slurry system. The intrinsic viscosity of a PVB molecule in a mixed organic solvent was higher than that in the plain solvent. The high intrinsic viscosity indicated the expanded conformation of the PVB molecule in the solvents. The viscosity of slurry showed that the expanded conformation of the PVB molecule in the solvents was effective for dispersion of alumina particles. Dispersed alumina particles in a mixed organic solvent could be observed by the optical microscopy. Well dispersed slurry based upon good compatibility of PVB and organic solvent led to a highly particle-oriented green compact and the homogeneous green sheets.

11:20 AM

**(ICACC-S8-017-2012) Mechanical Milling and Densification of High Purity Si-C Powder with Low Contamination**

S. Lee\*, B. An, H. Kim, KIMS, Republic of Korea

The suppression of contamination from the ball and jar during the mechanical milling of SiC and/or Si + C powder is important in order to produce high purity sintered SiC. We solved the problem by using high purity reaction bonded silicon carbide (RBSC) ball and jar for planetary milling. The weight gain of Si + C powder mixture caused by the contaminants was 0.7wt% and 9.5wt% after milling at 400r.p.m. for 72h when using ball to powder ratio of 5 : 1 and 10 : 1, respectively. The ball to powder ratio had very strong effect on the wear of the ball and jar. The powder mixture had amorphous structure after the milling. The weight gain of nano-SiC powder was 8wt%

after the milling at 400r.p.m. for 72h using ball to powder ratio of 10 : 1. The metallic contaminants of the milled SiC or Si + C powder could be effectively reduced due to the low metallic impurity content of the RBSC ball and jar (4N grade). Rather dense SiC (R. D. >95%) was obtained after spark plasma sintering of the milled Si + C powder at 2000oC for 1 h under 120 MPa pressure.

### 11:40 AM

#### (ICACC-S8-018-2012) The Role of Milling Liquids in Processing Metal-Ceramic-Precursor Powders

N. Holstein\*, University of Applied Science Koblenz, Germany; K. Wiegandt, J. Kriegesmann, Hamburg University of Technology, Germany; R. Janssen, University of Applied Science Koblenz, Germany

The combination of metals and ceramics either homogenously distributed (metal-ceramic composites) offer an encouraging concept to develop advanced composites exhibiting specific properties. The focus is on precursors suitable for conventional powder metallurgical processing techniques, exemplified by Cr-Al<sub>2</sub>O<sub>3</sub> composites. Additionally, metal ceramic precursor can be used as well to form advanced oxide ceramics like the Reaction-Bonded-Aluminum-Oxide (RBAO). For both variants, a fine grained, homogenous precursor is the essential prerequisite – particularly, if the reactive synthesis routes are aimed for complete densification by pressureless sintering. The precursor powders have been wet grinded in an attrition mill. Organic milling liquids with different properties were under examination. The characterization is based on stability investigations of the milling suspensions. In addition, the influence of the powder characteristics on the respective reaction bonding or reaction sintering mechanism is examined. Central theme is to demonstrate and understand the process of mechanical alloying between ceramic and metal phases during the milling process. Thereby, the effect of polarity, chemical group affiliation of the solvent and water content will be presented as well. In the final discussion, special emphasis will be given to fundamental aspects of interactions between particles and the non-aqueous media.

## S9: Porous Ceramics: Novel Developments and Applications

### Membranes and High SSA Ceramics

Room: Coquina Salon C

Session Chair: Irene Peterson, Corning Incorporated

### 8:00 AM

#### (ICACC-S9-013-2012) Ordered-microporous membranes-preparation, properties and prospects (Invited)

M. Matsukata\*, Waseda University, Japan

Membrane separation using ordered-microporous inorganic materials will offer us great opportunities to reduce energy demands in chemical and petroleum industries. In this presentation, principles for preparing microporous inorganic membranes will be introduced. FAU type zeolite membrane is one of the candidates for dehydration of isopropyl alcohol. We have tried to optimize preparation procedure and conditions of FAU-membrane. Zeolite membranes are often prepared by using the secondary growth method including dip-coating of seeds and hydrothermal growth of seeds on porous supports. We focused on the interaction between seed particles, and between seed particles and porous alumina support surface, in order to control both the amount of seed loaded on the support and distribution of seed particles on the support surface and inside of surface. The control of pH determined average size of seed particles in slurry. Capillary force during dip-coating procedure also governed the amount of zeolite seeds loaded on support, leading to the control of membrane thickness and compactness. The resultant FAU membrane highly separated water from IPA with a high water permeance, while the separation factor of water/IPA mixtures was substantially affected by the seeding conditions. Membranes

prepared under optimized conditions show promising properties for industrial use.

### 8:30 AM

#### (ICACC-S9-014-2012) Synthesis and characterization of carbon dioxide-permselective organoamino group-functionalized amorphous silica membranes

A. Kawai, Nagoya Institute of Technology, Japan; K. Miyajima, Noritake Co., Limited, Japan; K. Sekimoto, S. Honda, Y. Iwamoto\*, Nagoya Institute of Technology, Japan

Amorphous silica-based membranes containing organoamino groups have been designed and synthesized. This is expected to be essential to enhance the CO<sub>2</sub> permselectivity of the amorphous silica-based membranes by the CO<sub>2</sub> facilitated transport mechanism. The organoamino groups containing amorphous silica-based inorganic-organic hybrid materials were synthesized through polymer precursor route. Commercial perhydropoyasilazane (PHPS) in xylene solution was modified with an aminosilane-coupling agent, R-Si(OCH<sub>3</sub>)<sub>3</sub> {R=(CH<sub>2</sub>)<sub>2</sub>-[NH-(CH<sub>2</sub>)<sub>2</sub>]-NH<sub>2</sub>} below 373 K in Ar. The chemically modified PHPS could be converted into organoamino group-functionalized amorphous silica by air-oxidation at room temperature. Crack-free thin film with a thickness of approximately 1 micrometer was also successfully fabricated on a tubular porous Al<sub>2</sub>O<sub>3</sub> ceramic support. CO<sub>2</sub> permeance at room temperature of the synthesized membrane was 1.3 x 10<sup>-6</sup> mol Pa-1m-2s-1, and found to be apparently higher than those of other gas molecules such as N<sub>2</sub> and He. Further study of the membrane performance is in progress, and the results will be discussed at the conference.

### 8:50 AM

#### (ICACC-S9-015-2012) Gas Permiability and Fracture Properties of Porous Alumina with Various Pore Structures for Support Substrates of Ceramic Membranes

S. Honda\*, N. Nishihara, S. Hashimoto, Nagoya Institute of Technology, Japan; T. Eda, H. Watanabe, K. Miyajima, Noritake Co., Limited, Japan; Y. Iwamoto, Nagoya Institute of Technology, Japan

The gas permiability and fracture properties of alumina porous structures, the support substrates for permselective microporous ceramic membranes were studied. To study the influence of porosity and pore sizes on the various properties systematically, porous alumina with different porous structure were fabricated. The mechanical and thermal properties related to the thermal shock resistance were also measured and the influence of porosity on the properties was carefully examined. Gas permiability of porous alumina were increased with increase in porosity and pore size. The fracture strength, Young's modulus values and thermal conductivity were decreased with increase in porosity of the samples with same pore size. However, the sample with well-growing necking of alumina grain was higher properties in spite of the large pore size. Thermal expansion coefficient was not affected to the pore structure. Porous structure was clarified that combined with high gas permeability and excellent fracture properties.

### 9:10 AM

#### (ICACC-S9-016-2012) Porous membranes derived from Polysiloxanes for electrochemical applications

M. Wilhelm\*, M. Adam, G. Grathwohl, University of Bremen, Germany

This work presents the development of porous membranes derived from different polysiloxane/filler combinations. As filler activated carbon and SiC particles were used to obtain sufficient electro conductivity and to alter the porosity. After a heat treatment using temperatures in the range of 500 to 1400°C the microstructure (XRD), porosity (N<sub>2</sub> adsorption, Hg intrusion), permeability, chemical durability, electro conductivity and hydrophilicity/hy-



drophobicity of the membrane were investigated. While high specific surface areas are observed for materials derived at lower pyrolysis temperatures, membranes prepared at 1400°C show a mainly macroporous structure. The permeability of these thin membranes (500µm) for gases and their conductivity make them suitable for use as gas diffusion layer (GDL). The chemical durability against bases increases with rising pyrolysis temperature. However, durability is only satisfying for membranes pyrolysed at a temperature of 1400 °C, what can be attributed to an enhanced formation of SiC at high temperatures. Moreover these membranes show an increasing hydrophilicity with increasing pyrolysis temperature. Cathode materials for battery application were prepared by coating the GDL with a catalytic layer. The electrochemical performance of these new cathode materials was investigated in first electrochemical tests.

9:30 AM

**(ICACC-S9-017-2012) Synthesis of Novel Polysiloxane and Polycarbosilane Aerogels from Si-H and Si-Vy Bearing Precursors**

G. D. Soraru\*, P. Camostrini, P. Aravind, A. Gaston, University of Trento, Italy; Y. Blum, SRI International, USA

Aerogels are unique solid materials having extremely low densities (up to 95% of their volume is air), large open pores, low thermal conductivity and high surface areas. The pore sizes of aerogels lie within the scale length of 1-100 nm, showing micro to macroporosity. We hereby report the synthesis of novel polysiloxane and polycarbosilane aerogels through hydrosilylation reaction between the Si-H and the vinyl groups of the precursors in presence of a Pt catalyst and acetone or toluene as solvent. The dilution of the reagents has been varied increasing the volume % of the solvent in the initial solution from 70 vol% up to 97 vol%. The synthesis is carried out at using a reaction bomb up to 200°C for 2 hrs. The wet porous networks have been supercritically dried using CO<sub>2</sub>. Accordingly highly porous aerogels made of polysiloxane and polycarbosilane, have been obtained. Porous siloxane aerogels with pore diameter in the range 3-10 nm, porosity up to 1.90 cc/g and specific surface area up to ca 600 m<sup>2</sup>/g have been accordingly obtained. The aerogels were then pyrolysed in argon atmosphere to obtain porous, monolithic silicon oxycarbide glasses.

**Structure and Properties of Porous Ceramics I**

Room: Coquina Salon C

Session Chair: Alek Pyzik, Dow Chemical Company

10:10 AM

**(ICACC-S9-018-2012) Aluminum titanate-based composites for diesel particulate filter application (Invited)**

M. Backhaus-Ricoult\*, Corning Incorporated, USA

“detail to follow per approval of S-9 symposium organizer”

10:40 AM

**(ICACC-S9-019-2012) Effect of Pore Size Distribution and Cell Geometry on Filtration Efficiency and Pressure Drop (Invited)**

I. Peterson\*, G. Merkel, J. Wang, M. Fischer, A. Ozturk, C. Warren, Corning Incorporated, USA; M. Moreno, Corning Incorporated, France; M. Wallen, J. Heine, Corning Incorporated, USA

Using two different model (non-commercial) compositions, a series of filters was fabricated with median pore sizes ranging from 8 to 25 microns, in a variety of square cellular geometries. The effects of median pore size and cell wall thickness and cell density on filtration efficiency and clean and soot-loaded pressure drop were measured. A computational model was developed to predict the effect of cell wall thickness and cell density on filtration efficiency and backpressure.

11:10 AM

**(ICACC-S9-020-2012) SiC foams decorated with ceramic nanowires: permeation and aerosol filtration behavior**

M. Innocentini, R. Caldato, Universidade de Ribeirão Preto, Brazil; E. Tanabe, J. Coury, Universidade Federal de São Carlos, Brazil; M. Fukushima, AIST, Japan; P. Colombo\*, University of Padova, Italy

Commercially available open-cell SiC foams were used as the main components in a high-efficiency air filter. Ceramic nanowires (NWs) were grown on the surface of the cellular scaffold by depositing a polysilsesquioxane preceramic polymer coating with a catalyst (cobalt or copper-based) and a carbon-based additive, and by heating in N<sub>2</sub> at a temperature of 1450°C. Through a process of catalyst assisted pyrolysis, Si<sub>2</sub>N<sub>2</sub>O and Si<sub>3</sub>N<sub>4</sub> NWs formed on the surface of the ceramic struts. Permeation behaviour was investigated with air flow at room temperature. Samples were tested for collection of dust particles in the nanometric range. The influences of air velocity and filtration time on collection efficiency were also investigated and results were compared to those obtained with HEPA filters. The presence of NWs greatly improved the collection of particles, but gave an increase in pressure drop. This increase, however, was within the acceptable values for filtration purposes. The results showed that particle removal efficiency was similar to that of HEPA filters, with comparatively less resistance to air flow.

11:30 AM

**(ICACC-S9-021-2012) A novel method for pore size and porosity analysis of meso- and macroporous solids using electroacoustics**

A. Dukhin, Dispersion Technology Inc, USA; M. Thommes\*, Quantachrome Instruments, USA

We present a new method of determining pore size and porosity of meso- and macroporous materials/ceramics by transmitting ultrasound pulses of a single or multiple frequencies through the porous material. In our contribution we will discuss a novel, fast experimental technique (experiments can often be completed in less than 10 minutes) for pore size characterization based on measurement of the seismic current. We demonstrate the applicability of this novel method for various systems covering a wide range of pore sizes covering a wide pore size range from ca. nanometers to micrometers (e.g. porous glasses, porous titania materials/ceramics, geological cores etc.). We also show that the porosity can be obtained in a simple way by measuring the experimentally determined ratio of the electrical conductivity of the porous material to the equilibrium conductivity of the media (supernate); using this data the porosity can be calculated by applying the well-known Maxwell-Wagner theory.

11:50 AM

**(ICACC-S9-022-2012) Effect of h-BN content on thermal shock resistance and dielectric properties of porous h-BN/Si<sub>3</sub>N<sub>4</sub> composite ceramics prepared by gel casting**

S. Wang, D. Jia\*, Z. Yang, X. Duan, Y. Zhou, Harbin Institute of Technology, China

Porous h-BN/Si<sub>3</sub>N<sub>4</sub> composite ceramics with different h-BN contents (5vol%, 10vol% and 15vol%) have been fabricated by gel casting. Sintering was carried out at 1750°C for 1h under a 0.1MPa nitrogen atmosphere. The h-BN content has strong influence on the rheological behaviors of the suspensions, and the slurry has a suitable viscosity when h-BN content is lower than 10vol%. Effects of h-BN content on the microstructure, mechanical properties, dielectric properties and thermal shock resistance of h-BN/Si<sub>3</sub>N<sub>4</sub> composite ceramics were investigated. X-ray diffraction (XRD) and scanning electron microscopy (SEM) studies showed that h-BN particles homogeneously scattered in the β-Si<sub>3</sub>N<sub>4</sub> matrix, and the porous composite ceramics show an excellent comprehensive performance. For the 10vol%h-BN/Si<sub>3</sub>N<sub>4</sub> composite ceramics with a porosity of 49.4%, the flexural strength of 106.6MPa, dielectric constant of about 3.8 and a tangent loss of (3~7)×10<sup>-3</sup> indicating that it could be one of the most ideal candidates for wave-transparent applications.

### S14: Advanced Materials and Technologies for Rechargeable Batteries

#### Materials Characterization and Diagnostics For

##### Lithium Batteries

Room: Coquina Salon H

Session Chairs: Dany Carlier, CNRS; Anne Dillon, National Renewable Energy Laboratory

8:00 AM

##### (ICACC-S14-011-2012) Multiscale electronic transport mechanism and true conductivities in amorphous carbon-LiFePO<sub>4</sub> nanocomposites (Invited)

K. Seid, Université de Nantes, CNRS, France; J. Badot, Chimie ParisTech (ENSCP), CNRS, UPMC Univ Paris 06, France; O. Dubrunfaut, Laboratoire de Génie Electrique de Paris, France; D. Guyomard, Université de Nantes, CNRS, France; S. Levasseur, UMICORE Cobalt & Specialty Materials, Belgium; B. Lestriez\*, Université de Nantes, CNRS, France

Composite and nanostructured materials have hierarchical architecture with different levels: a) macroscopic (substructure of porous clusters); b) mesostructural (particles constituting the clusters); c) microscopic and nanometric (coatings, bulk of the particles). The identification of the key parameters that play on the electronic transport across all observed size scales is required, but is not possible using conventional dc-conductivity measurements. In this paper, the powerful broadband dielectric spectroscopy (BDS) from low-frequencies (few Hz) to microwaves (few GHz) is applied to one of the most important composite material for lithium batteries. LiFePO<sub>4</sub> is wrapped by a carbon coating whose electrical properties, although critical for battery performance, have never been measured due to its nanometer-size and the powdery nature of such material. We achieve the description of the electronic transport mechanism from the nanoscale (crystallites of sp<sup>2</sup>-coordinated carbon atoms) up to the sample macroscopic scale for this material. Moreover, the absolute conductivities and their respective drop when going from one scale to another are given, for the very first time, in the case of a composite powdery material for lithium batteries.

8:30 AM

##### (ICACC-S14-012-2012) In-situ high-energy synchrotron x-ray study of Li-Air and Li-ion rechargeable batteries (Invited)

Y. Ren\*, C. Lin, N. Karan, L. Trahey, M. Balasubramanian, Z. Chen, Argonne National Laboratory, USA

The increasing demand in safer and higher performance rechargeable batteries for broad applications has led to global efforts to develop advanced battery materials. There is a critical need in understanding key material issues in batteries under realistic conditions and in real time. High flux high-energy synchrotron x-rays provide a powerful tool for in-situ probing materials in working conditions. Here we will present our recent results from in-situ synchrotron high-energy x-ray diffraction studies of advanced materials in Li-air and Li-ion rechargeable batteries. We will show how the  $\alpha$ -MnO<sub>2</sub>-based electrocatalysts behave during charging/discharging processes and their role as catalysts in Li-air batteries. We will also present the real-time structural evolution of high energy composite cathode materials and its close correlation with the electrochemical performance in Li-ion batteries. The failure mechanism of Li-ion batteries during thermal runaway was also studied by in-situ high-energy x-rays and will be presented. Furthermore, we will demonstrate non-destructive in-situ material characterization of commercial 18650 cells. (Use of the Advanced Photon Source was supported by the U. S. Department of Energy, Office of Science, Office of Basic Energy Sciences, under Contract No. DE-AC02-06CH11357.)

9:00 AM

##### (ICACC-S14-013-2012) Synthesis of Li-La-Ba-Ta-O electrolyte by RF magnetron sputtering for micro battery

S. Jee\*, S. Lee, Y. Yoon, Yonsei Univ, Republic of Korea

Thin film lithium ion rechargeable batteries have been researched for their application in miniaturized ionic power devices such as electronic paper, smart cards, and RFID-Tag. Besides, development of an advanced solid electrolyte is greatly needed. Especially, Ultra-thin electrolyte is being required for the microelectronic devices. In this study, the feasibility of applying lithium lanthanum Barium Tantalum (Li-La-Ba-Ta-O) thin films as solid-state electrolytes in solid-state ionic energy systems such as thin film batteries was evaluated. The Li-La-Ba-Ta-O thin film electrolyte with garnet structure was prepared by radio frequency (RF) magnetron sputtering under atmosphere of argon (Ar) gas. We propose that the sandwich structure makes it possible to use a Li-La-M-O thin film as a thin film solid electrolyte without potential short circuiting of the Li-La-Ba-Ta-O thin film. For the final cell structure of SUS / Li-La-Ba-Ta-O / SUS / SiO<sub>2</sub> / Si, impedance measurements conducted at room temperature revealed ionic conductivities in the range of 10<sup>-6</sup> ~ 10<sup>-7</sup> S/cm for the various RF power conditions of the Li-La-Ba-Ta-O thin films. This result suggests that the Li-La-Ba-Ta-O ultra-thin film electrolyte has potential as a solid oxide thin film electrolyte in micro thin film battery.

9:20 AM

##### (ICACC-S14-014-2012) Lithium Intercalation in Low Dimensional Materials as Anodes for Li-ion Batteries (Invited)

R. Shahbazian Yassar\*, H. Ghassemi, Q. Gao, Michigan Technological University, USA; M. Au, Savannah River National Laboratory, USA; P. Heiden, N. Chen, Michigan Technological University, USA

Silicon nanowires and TiO<sub>2</sub> nanotubes are promising materials for Lithium-ion batteries. This report focuses on the in-situ observation of lithiation and delithiation in Si nanorods and TiO<sub>2</sub> nanotubes. The intercalation of Li ions in Si nanorods was monitored during charging and the fracture of nanorods was quantified in terms of size. The electrochemical testing of these low dimensional structures were conducted inside a transmission electron microscope equipped with a novel in-situ electrical probing holder. In addition, the intercalation of crystalline anatase and amorphous TiO<sub>2</sub> was studied and their fracture events were monitored in real time.

10:10 AM

##### (ICACC-S14-015-2012) Electrode/Electrolyte Interphase Studies in Lithium Batteries Using High Field Multinuclear NMR (Invited)

M. Cuisinier\*, N. Dupré, J. Martin, Z. Wang, Institut des Matériaux Jean Rouxel - Université de Nantes - CNRS, France; K. Suzuki, M. Hirayama, R. Kanno, Tokyo Institute of Technology, Japan; D. Guyomard, Institut des Matériaux Jean Rouxel - Université de Nantes - CNRS, France

The solid electrolyte interphase (SEI) between the negative electrode and the electrolyte of a Li-ion battery is known to factor into the overall battery behavior in terms of irreversible capacity loss, charge transfer kinetics, and storage properties. Interfacial reactions and the growth of a passivation layer at the electrode surface upon cycling have been also highlighted for different positive electrode materials and have proven of paramount importance as they can lead to performance degradation of the battery upon aging and cycling. This work gives an overview of the NMR approach developed to extract and interpret information on the electrode/electrolyte interphase in Li battery materials. The use of quantitative <sup>7</sup>Li, <sup>19</sup>F and <sup>31</sup>P MAS NMR is combined with XPS and EELS to study the interphase chemistry and to unravel its inhomogeneous architecture. Examples dealing with LiNi<sub>0.5</sub>Mn<sub>0.5</sub>O<sub>2</sub>, Li<sub>1.2</sub>Ni<sub>0.4</sub>Mn<sub>0.4</sub>O<sub>2</sub>, LiNi<sub>0.4</sub>Mn<sub>1.6</sub>O<sub>4</sub> and LiFePO<sub>4</sub> cathode materials, playing with formulation, additives and/or coatings, illustrate the technique capabilities as a diagnosis tool to probe evolution of electrochemical behavior and/or failure

mechanisms along electrochemical cycling of Li-ion batteries. Among presented results, it will be shown that the electrochemical behavior of  $\text{LiFePO}_4$  is strongly driven by its surface chemistry via parameters such as aging, coating or even crystalline orientation.

**10:40 AM**

**(ICACC-S14-016-2012) Electrolytes for Rechargeable Lithium batteries (Invited)**

Y. Abu-Lebdeh\*, National Research Council Of Canada, Canada

Rechargeable lithium batteries are successfully used in consumer electronic devices and strongly considered for applications with much higher energy-demand such as transportation and the electrical grid. This can be achieved by developing new materials or enhancing the functionality of currently used ones for the active and inactive components of the battery. In this presentation, thermally and electrochemically more stable electrolytes will be discussed along with their interfaces (SEI, CEI) with the two battery electrodes. The role of the type of additives or binders on the battery performance of new electrode materials will also be discussed.

**11:10 AM**

**(ICACC-S14-017-2012) Surface and Subsurface Damage Characterization of Graphite Anodes Electrochemically Cycled in Lithium-ion Cells**

S. Bhattacharya\*, A. Riahi, A. Alpas, University of Windsor, Canada

While volume change (12%) of graphite anodes used in lithium-ion batteries is not severe during electrochemical cycling, they exhibit drastic capacity drop accompanied by exfoliation and removal of particulates from the surface. Microstructural aspects of damage in cycled graphite are identified in this work to understand the surface and subsurface degradation mechanisms. To study the effect of applied voltage on graphite damage, in-situ optical microscopy was performed during cyclic voltammetry tests and severity of surface damage in the form of particle removal was quantified. FIB-milled cross-sectional microstructures of graphite electrodes exhibited partial delamination of graphite layers adjacent to the solid electrolyte (SEI)/graphite interface by formation of interlayer cracks. Deposition of  $\text{LiC}_6$ ,  $\text{Li}_2\text{CO}_3$  and  $\text{Li}_2\text{O}$  near the tips of these cracks caused partial closure of graphite cracks and thus reduced the crack growth rate during subsequent electrochemical cycling. Interconnecting graphite fibres bridged crack faces and retarded crack propagation. HR-TEM techniques revealed coexistence of crystalline (~ 5-20 nm) and amorphous regions within SEI. Fractured graphite particles comminuted to nano-size fragments were mixed with the decomposition products of SEI forming a protective layer, and prevented further damage to electrode surface during subsequent cycling.

**FS2: Computational Design, Modeling, and Simulation of Ceramics and Composites**

**Characterization and Modeling of Surfaces, Interfaces and Grain Boundaries at Multiple Scales**

Room: Ponce de Leon

Session Chairs: Jingyang Wang, Institute of Metal Research; Wai-Yim Ching, University of Missouri-Kansas City

**8:00 AM**

**(ICACC-FS2-011-2012) Combining X-ray Diffraction Contrast Tomography and Mesoscale Grain Growth Simulations in STO: an integrated approach for the investigation of microstructure evolution (Invited)**

M. Syha\*, W. Rheinheimer, M. Baeurer, Karlsruhe Institute of Technology, Germany; W. Ludwig, European Synchrotron Radiation Facility, France; E. M. Lauridsen, Risø National Laboratory, Denmark; D. Weygand, P. Gumbsch, Karlsruhe Institute of Technology, Germany

Using strontium titanate as model system for perovskite ceramics, 3D x-ray diffraction contrast tomography (DCT) and mesoscale grain

growth simulations are combined in order to correlate grain morphology, orientation dependent grain boundary properties and growth behavior in these highly anisotropic materials. The shrinkage of pores and the grain growth of STO microstructures is monitored by DCT. Exposing bulk STO samples alternately to ex-situ annealing and high energy X-ray DCT measurements, fully three dimensional microstructures are reconstructed and complemented by crystallographic orientations resulting from diffraction information. The results are used to characterize the connection between grain morphology and orientation dependent interface properties. These reconstructed microstructures serve as realistic reference structures for a 3D vertex dynamics model, rendering systematic parameter studies on the inclination dependent interface properties possible. 3D evolving microstructures obtained from reconstruction and simulation respectively are presented in combination with detailed topological and crystallographical characterizations. The results are discussed in the context of reconstruction accuracy, comparison to other modeling approaches and applicability to other ceramic materials.

**8:20 AM**

**(ICACC-FS2-012-2012) Growth Stress in SiO<sub>2</sub> during Oxidation of SiC Fibers**

R. Hay\*, Air Force Research Laboratory, USA

A method to calculate the three principal growth stresses in SiO<sub>2</sub> scales formed during SiC fiber oxidation has been developed. The method assumes that during oxidation the initial volume expansion at the SiC-SiO<sub>2</sub> interface is three-dimensional and equal in all directions, and that subsequent SiO<sub>2</sub> shear stress relaxation is described by the stress-dependent Eyring viscosity model. Large compressive stresses of ~10 GPa in SiO<sub>2</sub> adjacent to the SiC-SiO<sub>2</sub> interface are relaxed to much lower levels at all temperatures. At 1200° - 1300°C viscous flow of amorphous SiO<sub>2</sub> further relaxes stress to negligible levels. At 700° - 900°C, axial and hoop stress at the GPa level persist. Radial stresses only reach values greater than 100 MPa at 700° - 900°C for scales thicker than ~0.1 fiber radii. Radial expansion of the scale eventually causes hoop stress and later axial stress to become tensile in the outer scale. Differences in stress-states developed for crystallized and uncrystallized scales are considered. Some tentative calculations for crystalline SiO<sub>2</sub> scales are compared with experimental evidence for stress in the crystalline SiO<sub>2</sub> scales of Hi-NicalonTM-S SiC fibers. Assumptions and limitations of the method are discussed, along with implications for fiber strength and oxidation kinetics.

**8:40 AM**

**(ICACC-FS2-013-2012) A Density-Functional Theory Investigation of Oxidative Corrosion of the UO<sub>2</sub>(111)Surface (Invited)**

A. Chaka\*, G. Oxford, NIST, USA

Uranium dioxide is a key ceramic material for the nuclear power industry, as it constitutes the most common component of nuclear fuel rods. Corrosion can destroy the integrity of fuel rods in a reactor or in nuclear waste storage facilities, as the volume of oxidized UO<sub>2</sub> can expand by as much as 38 %. How the oxidation proceeds, however, is not well understood. In this work, density-functional theory and ab initio thermodynamics are used to delineate the initial stages of surface and subsurface oxidation of UO<sub>2</sub> at the (111) surface as a function of temperature and oxygen pressure. Initially, chemisorption of oxygen on the clean stoichiometric surface results in formation of highly stable triple-bonded uranyl groups and oxidation of the top-most uranium atoms to U<sup>6+</sup> at a minimal p(O<sub>2</sub>) near 0 K. Once the surface is saturated with uranyl groups and the oxygen chemical potential increases above -1.0 eV, subsurface oxidation becomes thermodynamically favored. The degree of oxidation of the subsurface uranium atoms is determined by quantifying the transfer of electrons from the localized U 5f bands to those dominated by the delocalized O 2p bands as oxygen atoms occupy octahedral interstitial sites in the UO<sub>2</sub> lattice.

**9:00 AM**

**(ICACC-FS2-014-2012) Effect of Absorbates and Surface Defects on Work Function of ZnO Based on First Principles DFT Calculations**

J. Du\*, Y. Li, University of North Texas, USA

ZnO is a wide band gap semiconductor that also finds applications as a transparent conductor in solar cells and flexible electronics. The work function of ZnO depends on the type and morphology of the surfaces. Fine tuning the work function and understanding the effect of absorbates and defects on work function is critical in these applications. In this paper, we present Density Functional Theory (DFT) based calculations of polar and non-polar ZnO surfaces. Surface energy and atomic structure of these surfaces were obtained after full geometry optimization. Based on the relaxed surface models, work functions were calculated and effect of surface coverage of absorbates and introduction of defects was studied. It was found that increasing the coverage of surface absorbates and defect concentration decreased the work function. The mechanism behind these changes was investigated by studying the electron density and surface dipole moments. These results will help to understand the mechanism of surface dipole moment change and to find methods to optimize work function for different applications.

**9:20 AM**

**(ICACC-FS2-015-2012) Sintering of multi-phase Mo-Si-B and the effects of doping**

J. Jung\*, J. Luo, Clemson University, USA

Mo-Si-B based multi-phase alloys are considered as a promising oxidation-resist high-temperature materials. In this study, Mo-Si-B samples are prepared by reactive sintering. Sintering experiments have been conducted for one-phase, two-phase and three-phase Mo-Si-B of different bulk compositions to probe the mechanisms of reactive sintering. Furthermore, the effects of adding a small amount of various dopants (sintering aids, such as Ni, Co and Fe) on the densification of the Mo-Si-B system are systematically investigated. A long-term goal is to establish the high-temperature interfacial thermodynamics for grain boundaries in multicomponent alloys via extending earlier studies for simpler binary refractory alloys [Phys. Rev. B 84, 014105 (2011)] to guide the selection of sintering aids and the design of sintering protocols for multicomponent materials.

**10:00 AM**

**(ICACC-FS2-016-2012) Modeling of Oxide Interfaces (Invited)**

C. Fisher\*, A. Kuwabara, H. Moriwake, Japan Fine Ceramics Center, Japan; H. Oki, Toyota Motor Corporation, Japan; Y. Ikuhara, University of Tokyo, Japan

Using a combination of density functional theory and empirical potential models, we have examined the structures and properties of a number of different interfaces, both homophase and heterophase, in oxide systems at the atomic level. One of the main systems that will be discussed in this talk is Li-ion battery cathode material LiCoO<sub>2</sub>. In particular, we report results for a number of high-symmetry twist boundaries observed in LiCoO<sub>2</sub> thin films by scanning transmission electron microscopy. Insights gained from examination of antiphase domain boundaries, in which rows of Li ions are aligned with rows of Co ions across the interface, that form within the thin films will also be presented. Multi-oxide systems such as LiCoO<sub>2</sub>/Al<sub>2</sub>O<sub>3</sub>, NiO/ZrO<sub>2</sub> and MgO/BaZrO<sub>3</sub> can also form relatively coherent heterogeneous interfaces for certain favorable crystal alignments, making them amenable to detailed characterization using atomistic computational methods. We present our methodology for probing the structures and properties of these more complex systems, with particular emphasis on their electronic, ionic-conduction and defect properties. The effects of lattice mismatch at interfaces will also be discussed.

**10:30 AM**

**(ICACC-FS2-017-2012) Modeling Grain Boundary Phase Behaviors (Invited)**

J. Luo\*, Clemson Univ, USA

HRTEM studies revealed the widespread existence of impurity-based, nanometer-thick, intergranular films (IGFs) [Luo, Crit. Rev. Solid State Mater. Sci. 32, 67 (2007)], which can be considered as a class of equilibrium or metastable "grain boundary (GB) phases". Studies also revealed the existence of a series of discrete grain boundary phases (i.e., clean/intrinsic GB, monolayer, bilayer, trilayer, equilibrium nano-IGF, and complete wetting), which are named "complexions" [Harmer, J. Am. Ceram. Soc. 93, 301 (2010); Science 332, 182 (2011)]. Recent studies to develop a preliminary type of GB "phase" diagrams (lambda diagrams) are reviewed [Shi & Luo, PRB 84, 014105 (2011)], where the model predications are systematically validated by experiments. Current efforts are placed on extending the models and methods from binary to ternary alloys. Studies to develop thermodynamic models for discrete GB phases (complexions) will also be discussed.

**11:00 AM**

**(ICACC-FS2-018-2012) Atomistic simulations and TEM measurements of Si<sub>3</sub>N<sub>4</sub>-amorphous SiO<sub>2</sub> interface with La and Lu**

I. G. Batyrev\*, J. Snownczynski, N. S. Weingarten, B. M. Rice, J. Andzelm, J. J. Swab, US Army Research Laboratory, USA; J. C. Idrobo, ORNL, USA

A model of Si<sub>3</sub>N<sub>4</sub> interface with amorphous SiO<sub>2</sub> was created by molecular dynamics (MD) quenching of a melt of SiO<sub>2</sub> in contact with N terminated solid  $\beta$ -Si<sub>3</sub>N<sub>4</sub>. The MD simulations of the annealing of SiO<sub>2</sub> from 5000 K and constrained atoms of Si<sub>3</sub>N<sub>4</sub> were performed using large-scale atomic/molecular massively parallel simulator. The obtained interface then was used in total energy first-principles calculations, based in density function theory, in order to understand the nonuniform interatomic mixing of oxygen and nitrogen at different atomic sites. The theoretical interfaces were compared with recent experimental observations obtained in aberration-corrected scanning transmission electron microscopy via atomically resolved imaging and electron energy-loss spectroscopy. A PBE approximation and HSE06 hybrid functional were used with 30 percent of mixing and 10 Å of screening range. Energy trends in ordering of Si, N and O atoms in silica near the interface were also examined. We also elucidated the details of segregation of La and Lu to the interface with nonuniform distribution of N and O around the interface. The results of simulations of the experimentally found nonuniform mixing have important implications for understanding Si<sub>3</sub>N<sub>4</sub> interfaces with amorphous intergranular films.

**11:20 AM**

**(ICACC-FS2-019-2012) Molecular Dynamics Simulations of La Doped Intergranular Films in Silicon Nitride: Effect of Structure on Properties**

Y. Jiang\*, S. H. Garofalini, Rutgers University, USA

Intergranular films (IGFs) play an important role in the properties of high temperature structural ceramics. Molecular dynamics computer simulations have been used to evaluate the structure, energy and fracture behavior of silicon oxynitride intergranular films (IGFs) containing rare-earth ions (La) between silicon nitride crystals as a function of IGF thickness, composition, and crystal orientations (prism, basal, and high index). La adsorption at specific sites on the prism surface is observed as an effect of composition and thickness in our simulations, at locations precisely consistent with HAADF-STEM results. IGFs with low nitrogen content show almost all La segregating to the interface, leaving little La within the glassy IGF, while other IGFs may show more La remaining in the glassy IGF. This is consistent with the change in binding energy of the La ions in the IGF interior in comparison to that at the interfaces, reducing the driving force for segregation and potentially affecting strength and fracture behavior. Preferential adsorption of La onto the prism surface poisons the

surface, inhibiting growth along its surface normal, whereas, as a function of composition, growth along the basal surface normal is observed, providing an atomistic mechanism for the experimentally observed anisotropic grain growth of silicon nitride.

## FS3: Next Generation Technologies for Innovative Surface Coatings

### Next Generation Production Methods for Surface Engineering

Room: Coquina Salon G

Session Chairs: Toshiyuki Matsui, Osaka Prefecture University; DaeYong Jeong, Inha University

#### 8:20 AM

#### (ICACC-FS3-013-2012) Synthesis and novel application of nano- or mezzo-scale porous 3C-SiC coatings by Si carbonization technique (Invited)

T. Matsui\*, H. Tsuda, H. Mabuchi, Osaka Prefecture University, Japan; A. Kakitsuji, Technology Research Institute of Osaka Prefecture, Japan

Silicon carbonization technique has been intensively studied to produce nano- or mezzo-scale porous silicon carbide (SiC) from elemental Si bulk and powders. This near-net-shaping porous SiC production process is absolutely simple and low-cost. The starting material of Si is put into graphite cases filled with pure graphite powder. Then, the cases are heated up to around 1650 K in vacuum and kept at this temperature for a certain time under atmospheric pressure of the purged argon gas. During the process, CO and CO<sub>2</sub> gases are generated in the furnace from the graphite and the residual oxygen under argon atmosphere, which simultaneously produce 3C-SiC and SiO gas from Si by a solid-gas reaction. As a result, the porous silicon carbide with beta-modification (3C-SiC) can be synthesized. If the Si wafers are used for starting material, the porous 3C-SiC coating layers can be obtained. The thickness of the layers and the size of the porosities can be arbitrary determined by selecting the process parameter. We will also talk about the possible novel applications of such material: a support for heterogeneous catalysts owing to its higher surface area, and high-temperature thermoelectric material due to its low thermal conductivity etc.

#### 8:50 AM

#### (ICACC-FS3-014-2012) Superconducting MgB<sub>2</sub> Thick Films Prepared by Aerosol Deposition

S. Hirose\*, AIST, Japan

A superconducting film would be attractive for fabricating the superconducting coils, Josephson devices, etc. Aerosol deposition (AD) method is the room temperature coating method of various metal and ceramic materials based on direct impact solidification effect. This AD process would open a new possibility for realizing these superconducting devices. In this presentation, we show the formation of MgB<sub>2</sub> deposited by AD method, and investigate the physical properties of AD films for realizing superconducting devices. MgB<sub>2</sub> films were deposited by AD method at room temperature. Over 50 μm thickness was obtained, which was independent of the substrate materials. SEM, XRD and TEM measurements reveal that the poly-crystal MgB<sub>2</sub> thick film with nm size grains was obtained by AD method. Also, AD-MgB<sub>2</sub> films were well packed and a amount of porosity in the film was very small. From the dc magnetization measurement, the T<sub>c</sub> 39 K was achieved from temperature dependence of dc susceptibility of a MgB<sub>2</sub> AD film. This T<sub>c</sub> value of AD film is coincident with that of MgB<sub>2</sub> bulk as reported. In addition, by considering the fact of the room temperature preparation method of AD, it is encouraged us to achieve ecological energy-saving preparation process.

#### 9:10 AM

#### (ICACC-FS3-015-2012) Next generation surface technologies for the exterior parts of mobile devices

T. Yim\*, Korea Institute of Industrial Technology, Republic of Korea

The exterior parts industry for mobile devices is ever expanding business as its forward industry grows in a furious speed. Since the industry is one of the most powerful cash cows of Korean economy, the mobile devices' exterior parts industry is also regarded as one of the lucrative businesses. Generally, the technologies used for the exterior parts production could well be categorized into one of the followings; Forming, coloring or decoration, and protective coating. The case forming includes plastic extrusion and metal pressing. The coloring, decoration and protective coating would be done by painting, physicochemical deposition, or electroplating. For example, almost all the mobile phone cases subsequently undergo the above-mentioned processes for a production. The mobile phone industrial trend shift would directly lay an influence on the exterior parts industry, and consequently, influence the technological development effort in the fields of surface industry. Conversely, this effort of development would also trigger a significant advance in the mobile devices industry itself. The protections for the mobile devices cases include physical and chemical protection functions, while the decoration holds color and touch of noble materials. In this presentation, the future development of the next-generation surface technology for the mobile devices would be discussed.

#### 9:30 AM

#### (ICACC-FS3-016-2012) Control of the oxygen content with oxygen gas introduction of Cr(N,O) thin films prepared by pulsed laser deposition

K. Suzuki\*, T. Endo, T. Fukushima, A. Sato, T. Suzuki, T. Nakayama, H. Suematsu, K. Niihara, Nagaoka University of Technology, Japan

Hard coatings, such as CrN, have been used for cutting tools. By partial replacement of N in CrN with O, Cr(N,O) thin film with B1 (NaCl type) structure can be produced. Furthermore, hardness of the thin film is increased with increasing the oxygen content. In our previous work, thin films were prepared by depositing Cr vapor in N<sub>2</sub> or NH<sub>3</sub> ambient gas with residual oxygen so that precise oxygen content control was difficult. In this work, O<sub>2</sub> gas was introduced for precise oxygen content control of Cr(N,O) thin films prepared by pulsed laser deposition. Cr(N,O) thin films were prepared by irradiation third harmonic of a Nd: yttrium aluminum garnet pulse laser onto a Cr target. After the chamber was evacuated to a pressure of 1.0×10<sup>-5</sup> Pa, O<sub>2</sub> gas was introduced and then nitrogen plasma from RF radical source was supplied. The thin films were prepared under a fixed total pressure. The prepared thin films were characterized by X-ray diffraction, infrared spectroscopy and electron energy loss spectroscopy. According to these results, it was found that composition ratio of oxygen and nitrogen (O/N) of the thin films was changed from 0 to 8.6 with increasing the oxygen partial pressure (P<sub>O<sub>2</sub></sub>). The thin films with only B1-Cr(N,O) phase were prepared under P<sub>O<sub>2</sub></sub> < 7.5×10<sup>-5</sup> Pa. The oxygen content of Cr(N,O) thin film was successfully controlled by P<sub>O<sub>2</sub></sub>.

#### 10:10 AM

#### (ICACC-FS3-017-2012) Synthesis and thermal conductivity of thick AlN-YAG coating by plasma spraying

K. Baik\*, W. Soh, D. Noh, Chungnam National University, Republic of Korea

In this study, AlN-YAG composite coatings were manufactured by atmospheric plasma spraying from two different powders: spray-dried and plasma-treated. The mixture of both AlN and YAG was first mechanically alloyed and then spray-dried to obtain an agglomerated powder. The spray-dried powder was primarily spherical in shape and composed of an agglomerate of primary particles. The decomposition of AlN was pronounced at elevated temperatures due to the porous nature of spray-dried powder, and was completely eliminated in nitrogen environment. A highly spherical, dense AlN-YAG composite

powder was synthesized by plasma alloying and spheroidization (PAS) in an inert gas environment. The AlN-YAG coatings consisted of irregular-shaped, crystalline AlN particles embedded in amorphous YAG phase, indicating solid deposition of AlN and liquid deposition of YAG. The PAS-processed powder produced a lower-porosity and higher-hardness AlN-YAG coating due to a greater degree of melting in the plasma jet, compared to the spray-dried powder. The amorphization of YAG matrix was evidence of complete melting of feedstock powder in flight because a fully molten YAG droplet formed an amorphous phase during splat quenching. The AlN-YAG coating had a thermal conductivity of  $\sim 11 \text{ Wm}^{-1}\text{K}^{-1}$  which was several times higher than that of conventional Al<sub>2</sub>O<sub>3</sub> coating.

**10:30 AM**

**(ICACC-FS3-018-2012) Carbon nanomaterials for energy storage and conversion (Invited)**

W. Choi\*, Florida International University, USA

Graphene is a newly discovered 2D material that exhibits high carrier mobility, good mechanical properties, high transparency and excellent thermal stability. To date, considerable works have been demonstrated in applications of graphene including transistors, supercapacitors, solar cells etc. In particular, application in solar cells with the enhanced efficiency is of great interest, since graphene has exhibited remarkable transparency in the entire solar spectrum including infrared (IR) region. That is an added advantage of its application in high efficiency solar cell for harvesting more light photons from the solar spectrum. In addition to this, graphene has shown ability to be transferred on any flexible substrates using scalable methods. This versatile transformation property remains a promising opportunity for developing light-weighted flexible electrodes for flexible electronics. This talk will focus on engineering carbon nanomaterials, graphene and carbon nanotubes (CNTs) for high efficiency flexible battery and dye sensitized solar cells. Particularly, engineering the interfaces of graphene-polymer, graphene-substrate and graphene-CNTs will be discussed towards higher efficiency energy applications. Our recent results of a novel binder-free multi-wall carbon nanotube structure as a flexible battery, and a large graphene film for a field emission device and dye sensitized solar cells will be presented.

**11:00 AM**

**(ICACC-FS3-019-2012) Enhancement of materials properties with the induced stress in aerosol deposition**

D. Jeong\*, Inha University, Republic of Korea; G. Han, J. Ryu, D. Park, Korea Institute of Materials Science (KIMS), Republic of Korea

The aerosol-deposition (AD) process is well known as a deposition technique for making dense nano-crystalline thick films at room temperature (RT). Solid particles with the desired crystalline phase were synthesized first and thick films are formed by collision of particles on to a substrate at RT. It is well known that the AD process was promising for the thick film fabrication of process sensitive materials, such as BiFeO<sub>3</sub> and Pb(ZrTi)O<sub>3</sub>. In addition to the easy and process insensitive characteristics of AD process, AD process could induce the additional stress between the film and substrate owing to the strong collision of particles resulting in modulation of the materials properties. In this research, we will introduce the enhancement of the materials properties in thick films, which were fabricated by AD process.

**11:20 AM**

**(ICACC-FS3-020-2012) Optical and Mechanical Properties of Infrared Transmitting Coatings Prepared by Aerosol Deposition**

H. Tsuda\*, J. Akedo, S. Hirose, AIST, Japan; K. Ohashi, NEC, Japan

Aerosol deposition (AD) is a coating technology based on consolidation by impact of powder particles onto a substrate, and has excellent features such as a high deposition rate and low process temperature. For these advantageous features, the AD method is applied for a wide range of device development and various uses with ceramic

materials. By the AD method, fine dense and transparent ceramic coatings can be deposited at room temperature. Fluoride materials such as barium fluoride and calcium fluoride are widely used in infrared systems because of the broad transmission band from visible to infrared spectral region and low dispersion. However, the mechanical properties of the fluoride materials are not necessarily strong in practical applications. In this work, infrared transmitting ceramic coatings were fabricated on fluoride substrates by AD. The optical and mechanical properties of the coatings on the fluoride substrates were investigated. The infrared optical and mechanical properties of the coatings were characterized by optical transmittance in the infrared wavelength range and surface hardness measurement respectively. The experimental results will be shown in the conference.

**11:40 AM**

**(ICACC-FS3-021-2012) The use of Aerosol Deposition Technique in all-solid-state Li-ion fabrication**

D. Popovici\*, AIST, Japan; H. Nagai, S. Fujishima, Toyota Motor Co., Japan; J. Akedo, AIST, Japan

Aerosol deposition (AD) is a decade-old deposition technique that allows fabrication of thick ceramic and metal layers at room temperature on various substrates using the material in powder form. This technique is based on room temperature impact consolidation (RTIC) phenomena in which the initial powder particle is accelerated towards a target where, by fracture and a plastic-like deformation, will become part of the deposited layer. The layers are of high density, density that can reach 95% of the theoretical value. An AD-fabricated film is retaining the crystalline structure of the powder used for fabrication and this means that there is no need of thermal treatments after film formation to generate crystalline structure. Moreover, the adhesion between the AD-formed layer and the substrate is very good due the formation of an anchoring layer at the interface. Considering these aspects, it is easy to understand why this technique is a good candidate in applications that require deposition of ceramic layers on substrates where complex circuits are already present, or in applications that involves fabrication of multiple crystalline layers with different chemical compositions in a multi-layer (stacked) structure.

## FS4: Advanced (Ceramic) Materials and Processing for Photonics and Energy

### Multifunctional Materials for Biological Applications

Room: Oceanview

Session Chair: Marco Rolandi, University of Washington

**8:00 AM**

**(ICACC-FS4-001-2012) Nanomaterials for optical and biological applications (Invited)**

F. Stellacci\*, EPFL, Switzerland

A bird eye view of any folded protein shows a complex surface composed of hydrophobic and hydrophilic patches closely packed. To date little is known on the fundamental properties that such packing determines. In this talk I will present my group's endeavor into the synthesis, characterization, and understanding of a family of nanomaterials (mixed monolayer protected nanoparticles) that possess a surface coexistence of patches of opposite hydrophilicity resembling that present on folded protein. I will show that these materials are ideal model compound to uncover the basic properties that such coexistence determines at the solid liquid interface, and will conclude with example of application of these nanoparticles when used as mimic of biological entities (e.g. as cell penetrating peptides, as nanoenzymes, etc.).

8:30 AM

**(ICACC-FS4-002-2012) Lanthanide-Doped Nanoparticles: Towards Multi-Functional Bioprobes (Invited)**

F. Vetrone\*, Université du Québec, Canada

Multi-photon excited luminescent nanomaterials are emerging as useful tools in diagnostic medicine and therapeutics. These nanomaterials are excited with near-infrared (NIR) light, which is silent to tissues thus minimizing autofluorescence, possesses greater tissue penetration capabilities and does not cause damage to the sample. Moreover, these nanomaterials require femtosecond (fs) excitation light to induce the multi-photon excited luminescence, which results in increased spatial resolution. An alternative to multi-photon excited nanomaterials is lanthanide ( $\text{Ln}^{3+}$ )-doped upconverting nanoparticles, which have the ability to (up)convert NIR light to higher energies spanning the UV to the NIR. This occurs via the process of upconversion resulting from the multitude of  $\text{Ln}^{3+}$  electronic energy states, many of which are equally spaced leading to the sequential absorption of multiple NIR photons. These energy states are long-lived eliminating the need for fs laser excitation and thus, upconversion can be observed following excitation with low energy cw NIR diode lasers. In contrast, other multi-photon excited nanomaterials require the simultaneous absorption of photons from ultrafast fs lasers. Here, we present the synthesis of upconverting  $\text{Ln}^{3+}$ -doped fluoride nanoparticles and show how these nanoparticles could be used as multi-functional bioprobes for imaging and nanothermometry of malignant cancer cells.

9:00 AM

**(ICACC-FS4-003-2012) pH-dependant transformations of Bioglass®: implications for bone regeneration and composite scaffold synthesis (Invited)**

M. G. Cerruti\*, S. Abdollahi, McGill University, Canada

Bioglass® (BG) is a silicate-based glass that when in contact with body fluids, dissolves and releases silicate, phosphate, calcium and sodium ions. Calcium and phosphate ions reprecipitate and form a layer of hydroxycarbonate apatite (HCA) on the BG surface, which is similar to the inorganic component of bone. The HCA layer then integrates with surrounding tissue fibrillar collagen, the organic component of bone, to form a matrix that attracts osteoblasts, stimulating bone tissue regrowth. BG is commercially available and is used for both tooth and bone regeneration, either by itself or in composite scaffolds including a polymeric phase as the main matrix. In this presentation we will show that the transformations of BG are strongly dependent on the pH of the solution in which it reacts, and that the optimal pH for BG to generate a layer of HCA on its surface is the physiological one. This has important implications on the transformations of BG incorporated in composite poly-ester scaffolds: if the scaffolds are prepared with the solvent casting and particulate leaching technique, which includes a leaching step in water, the BG particles start transforming already during the scaffold processing phase, before immersion in body fluids.

9:30 AM

**(ICACC-FS4-004-2012) In-vitro and in-vivo Investigation of Near-Infrared Emitting, Paramagnetic  $\text{Gd}_2\text{O}_3:\text{Er}^{3+}, \text{Yb}^{3+}$  Nanostructures for Bioimaging Applications**

E. Hemmer\*, T. Yamano, H. Takeshita, T. Fujiki, H. Kishimoto, Tokyo University of Science, Japan; M. A. Boss, R. B. Goldfarb, National Institute of Standards and Technology (NIST), USA; K. Soga, Tokyo University of Science, Japan

Organic dyes used as fluorescent markers in bioimaging suffer from color fading, phototoxicity and scattering when ultraviolet light is used as the excitation source. Lanthanide containing inorganic compounds are promising candidates to overcome those problems. Besides their optical properties, their magnetic characteristics make them interesting for application as opto-magnetic biomarkers. In

particular, near-infrared (NIR) absorbing and emitting materials are attractive because NIR light reduces phototoxicity and scattering. Multifunctional  $\text{Gd}_2\text{O}_3:\text{Er}^{3+}, \text{Yb}^{3+}$  nanoparticles and nanorods for opto-magnetic bioimaging were synthesized by hydrothermal and precipitation methods. In order to provide good chemical durability, to avoid agglomeration, and to control the cellular uptake, the nanostructures were modified with PEG-*b*-PAAC. *In-vitro* investigations of the modified structures showed good biocompatibility towards macrophages. The biodistribution in mouse organs was investigated by use of an over-1000-nm NIR *in-vivo* fluorescence bioimaging system, which revealed an accumulation in clearance organs like the liver and spleen as well as in the lung. Measurements of magnetization, magnetic susceptibility, and nuclear magnetic resonance (NMR) relaxivity will be presented.

**Optical Properties of Nanomaterials**

Room: Oceanview

Session Chair: Giuliano Gregori, Max Planck Institute for Solid State Research

10:10 AM

**(ICACC-FS4-005-2012) Nanostructured photoanodes and colloidal quantum dots for improved light harvesting in excitonic solar cells (Invited)**

G. Sberveglieri\*, A. Vomiero, I. Concina, A. Braga, G. Faglia, V. Galstyan, University of Brescia, Italy

Photoelectrochemical solar cells, which use quantum dots (QDs) as active media for light harvesting, are a specific type of the general class of the excitonic solar cells. They have the potential to induce a revolution in the field of photoconversion and electric current generation thanks to their peculiar characteristics: low cost, low environmental impact, improved photoconversion efficiency, while maintaining good long term stability. Recent theoretical investigations indicate that it should be possible to obtain photoconversion efficiency up to 45%, thanks to two main principal photogeneration processes, namely, multiple exciton generation (MEG) and the presence of intra-gap energy bands. A further possibility for increasing the photoconversion efficiency is based on the improvement of the charge transport mechanism inside the photoanode, which can be gained by applying nano-engineered photoanodes based on either single crystalline nanowires or cylindrical nanotubes. These structures have been demonstrated to enhance charge collection and inhibiting the recombination processes at the photoanode. The effect on the overall photoconversion efficiency of different types of QDs composed of one single metal (CdS, CdSe, CdTe, PbS, PbSe, PbTe, ZnS, ZnSe, ZnTe) as well as composite systems (e.g. CdS-PbS) will be considered and discussed.

10:40 AM

**(ICACC-FS4-006-2012) Photo-induced electron transfer reactions at semiconductor quantum dot interfaces (Invited)**

Y. Tachibana\*, RMIT University, Australia

Semiconductor quantum dots (QDs) have recently received significant interests for their photovoltaic applications. One of their most attractive properties is known as "quantum size effect", where the band gap energy becomes larger by reducing QD size. By employing this concept, the potential energy levels of QD conduction and valence bands can be adjusted with the QD size, and thus an appropriate size can be tuned to optimize efficient photoinduced charge separation and retard charge recombination at the QD interfaces, thereby improving performance of solar cells. In addition, QDs exhibit large absorption coefficients ( $>10^5 \text{ M}^{-1} \text{ cm}^{-1}$ ), and absorb light when the energy is higher than the band gap energy, allowing QDs to be used as light absorbers. In contrast, fundamental understanding for the factors controlling the interfacial reactions is still limited. In this presentation, we attempt to elucidate relationship of the interfacial nanostructures with the electron transfer rates, and their applications to

solar energy conversion devices will be presented. This work was financially supported by JST PRESTO program, Japan, and TEPCO Research Foundation, Japan. The Venture Business Laboratory, Osaka University is also acknowledged for the financial support.

**11:10 AM**

**(ICACC-FS4-007-2012) Frontiers of Nanostructured Materials and Nanotechnology (Invited)**

J. Narayan\*, NC State University, USA

Nanoscience through nanotechnology is envisioned to impact profoundly our quality of life, provided it can be transitioned successfully to manufacturing of useful and improved products. Dramatic improvements in properties and performance of solid state materials can be achieved through manipulation of defects and interfaces in nanostructured materials. Nanostructured materials containing nanodots and nanolayers can be fabricated in a controlled way to obtain novel materials and structures with significantly improved properties. This talk reviews some key developments in nano structural materials, nanomagnetic materials, nanooptical materials and "Nano-Pocket" light emitting diodes (LEDs).

**11:40 AM**

**(ICACC-FS4-008-2012) Si, Ge, and SiGe nanostructure direct-write using scanning probes and conducting stamps (Invited)**

M. Rolandi\*, University of Washington, USA

The high-speed fabrication of Si, Ge, and SiGe heterostructures with nanoscale accuracy is a challenging pursuit essential for novel advances in electronics, photonics, and energy. We have recently developed a novel approach for the direct-write of Si, Ge, and SiGe nanostructures in which the biased tip of an atomic force microscope (AFM) locally reacts an organometallic liquid precursor (diphenylsilane and diphenylgermane). Here, we present recent efforts in improving the throughput by using conducting stamps that mimic multiple AFM tips working in parallel. Microscale and nanoscale features on gold-coated PDMS stamps are used to locally react diphenylsilane and diphenylgermane when a bias is applied. In this fashion, high quality and carbon-free (SIMS, x-ray PEEM, TEM) Si, Ge, and SiGe heterostructures with deterministic placement, size, and composition control are produced on extended areas of the substrate. Strategies for wafer scale fabrication for back-contacted silicon based PV will be discussed.

## European Union - USA Engineering Ceramics Summit

### EU/USA Summit V

Room: Coquina Salon F

Session Chair: Alexander Michaelis, Fraunhofer Institute for Ceramic Technologies and Systems IKTS

**1:30 PM**

**(ICACC-EUUSA-016-2012) Solar Hydrogen Production with Disorder-Engineered Titania (Invited)**

S. Mao\*, EETD Advanced Energy Technologies, USA

This presentation will provide an overview of recent progress in the development of disorder-engineered titanium dioxide nanocrystals as applied to solar-driven water splitting. Starting with a brief introduction of the literature on titanium dioxide modification aimed to increase solar absorption, the concept of disorder engineering will be introduced along with the electronic band structure resulted from disorder incorporation. The approach of making disorder-engineered titanium dioxide nanocrystals will be presented, followed by measurements of their structural, electronic, and optical properties. Photocatalysis experiments based on solar-driven hydrogen production using disorder-engineered titanium dioxide nanocrystals, that can absorb solar energy in both visible and infrared wavelength regions, will be discussed.

**2:00 PM**

**(ICACC-EUUSA-017-2012) Challenges for Ceramic Materials in Breakthrough Energy Applications (Invited)**

K. Joachim\*, Deutsche Gesellschaft für Materialkunde e.V. (DGM), Germany

This talk will present an overview of research and development activities in the field of ceramics for energy application from German and European viewpoints. In addition, the role of the German Federation of Materials Science (DGM) will be elaborated in bundling these efforts at the national and international levels.

**2:30 PM**

**(ICACC-EUUSA-018-2012) New approaches for silicon in three valuable energy management applications (Invited)**

J. Carberry\*, Mossey Creek Energy, USA

Many applications for finely divided silicon have been limited or even uninvestigated because of the inherent dangers of milling fine silicon and its historical unavailability of clean finely divided silicon. Silicon's high thermal conductivity, very low coefficient of expansion (CTE), its ability to be tailored for specific semiconductor and electrical and thermoelectric properties at low cost otherwise make it very attractive. The lack of use of silicon is largely because it has always been very difficult and even dangerous to produce silicon that is free of oxidation, processed such that it is safe and economical, and yet can be produced with a wide range of desired particle sizes and distributions. A MCE-patented invention for a unique, safe, low cost process for milling silicon into a wide variety of particle sizes and distributions, as small as a few hundred nanometers, has provided the platform from which the authors have investigated and are developing three new approaches valuable to more efficient exploitation of energy. We believe these offer highly valuable solutions in these energy applications: photovoltaic; thermal transfer materials for improved protection of semiconductors, capacitors, inverters, and motors; and a previously unconsidered yet attractive thermoelectric material.

### EU/USA Summit VI

Room: Coquina Salon F

Session Chair: Walter Krenkel, University of Bayreuth

**3:20 PM**

**(ICACC-EUUSA-019-2012) Status of PVD Technology in Poland (Invited)**

W. Gulbinski\*, Koszalin University of Technology, Poland

Modern thin film technologies based on physical vapour deposition (PVD) are nowadays widely used in numerous branches of industry. Also in Poland the scope of their applications is growing year by year. The presentation will contain a short overview of activities of Polish research centers involved in development of PVD based technologies. Emphasis will be placed on high rate magnetron sputtering and hard coatings for tool industry. From industry side, the production profile of the main Polish companies, including PVD technology end-users and equipment suppliers will be presented.

**3:50 PM**

**(ICACC-EUUSA-020-2012) Miniaturized Surface Ionization Gas Sensors (Invited)**

G. Mueller\*, A. Hackner, S. Beer, EADS Innovation Works, Germany; F. Ramirez-Hernandez, Institut de Recerca en Energia de Catalunya (IREC), Spain; J. Prades, Universitat de Barcelona, Spain; J. R. Morante, Institut de Recerca en Energia de Catalunya (IREC), Spain; S. Mathur, University of Cologne, Germany

We report on novel kinds of miniaturized gas sensors whose operation is based on the principle of surface ionization (SI). In SI gas sensing adsorbed analyte species are ionized at a heated solid surface and the formed ions are extracted towards an oppositely charged collector electrode positioned a short distance above the emitting surface. We show that SI sensors allow for a fast, sensitive and selective detection



of hazardous compounds in the presence of large concentrations of less reactive background species. Highest performance is obtained with devices based on single metal oxide nanowires. Applications with regard to the detection of security threats (illicit drugs and explosives) will be demonstrated.

**4:20 PM**

**(ICACC-EUUSA-021-2012) Plasma technologies for energetics and sensing: towards the metal oxide highway via the nano-road (Invited)**

D. Barreca\*, Padova University, Italy

Plasma technologies, such as Plasma Enhanced-Chemical Vapor Deposition (PE-CVD) and Radio Frequency- (RF) Sputtering, candidate themselves as unique strategies for the fabrication of advanced nanomaterials, thanks to the activation of unique process pathways under mild non-equilibrium conditions. In this presentation, the potential of plasma-assisted fabrication in advanced nanosystem development is discussed. The key issues to be addressed in material morphological design and tailoring are highlighted in relation to the following case studies: • Ag/TiO<sub>2</sub> nanosystems obtained by a hybrid plasma-liquid phase approach, of great interest in view of pollutant degradation by visible light; • highly oriented ZnO nanorod arrays, that show unprecedented performances in gas detection and in light-activated functional applications for self-cleaning devices; • Ag/ZnO nanocomposites, employed for the first time in the photocatalytic production of hydrogen, one of the most significant energy vectors of the future; • pure and fluorine-doped Co<sub>3</sub>O<sub>4</sub> nanostructures, a cutting-edge platform for hydrogen production and sensing. Key results obtained by an extensive chemical and physical system characterization will be presented and discussed, in an attempt to answer the questions "what's going on?" and "what's next?" for further advancements in these fields.

**4:50 PM**

**(ICACC-EUUSA-022-2012) Importance of Precursor Chemistry in Atomic Layer Deposition (Invited)**

M. Leskela\*, University of Helsinki, Finland

In Atomic Layer Deposition (ALD) the gaseous precursors are introduced one at the time into the reactor and substrate surface. Besides the normal requirements of chemical vapor deposition (CVD) precursors (volatile, non-toxic, non-corrosive, cheap) the ALD precursors have to fulfill two contradictory requirements: thermal stability and reactivity. The precursors have to adsorb on the surface and form stable surface species and not decompose. The surface species have to react fast with the other incoming precursor to form the desired film material. Good combination of ALD precursors is that which can not be used in CVD due to fast reaction in gas phase if the precursors are simultaneously in reactor. The ALD metal precursors can be grouped in elements, inorganic, complex and metalorganic compounds. Only a few elements are volatile and reactive enough to be used in ALD. Metal complexes used in ALD are quite many: alkoxides,  $\beta$ -diketonates, keto-iminates, alkyl amides (imides), amidinates, phosphines and silyl compounds. Metalorganic compounds are limited to alkyl and cyclopentadienyl compounds. The non-metal precursors are usually hydrides like water, hydrogen peroxide, ammonia, hydrogen sulfide but compounds like alcohols, hydrazines, silanes have also been used. The advantages and drawbacks of different precursors will be presented and the trends in ALD precursor chemistry will be discussed.

**5:20 PM**

**(ICACC-EUUSA-023-2012) Bio-inspired Ceramic Composites for Engineering Applications (Invited)**

J. Martinez-Fernandez\*, J. Ramirez-Rico, F. M. Varela-Feria, C. Vera-García, A. Gutierrez-Pardo, University of Seville-CSIC, Spain; M. Singh, Ohio Aerospace Institute, NASA Glenn Research Center, USA

Biomorphic SiC ceramics are a new class of materials produced with natural, renewable resources. This technology provides a low-cost

and eco-friendly route to advanced ceramic materials, with near-net shape potential and amenable to rapid prototyping. BioSiC materials have tailorable microstructure and properties, and behave like ceramic materials manufactured by conventional approaches. If the residual Si phase is removed, a porous SiC ceramic closely resembling the original precursor is obtained. These anisotropic porous materials have a microstructure not easily attainable with conventional porous ceramic processing techniques. Additionally, the resulting SiC scaffold can be reinfiltred with a variety of metal alloys or second phases to create composites and cermets. Several applications have been proposed for these materials, owing to their good thermomechanical properties and characteristic microstructure, such as structural elements, high-temperature heat exchangers, thermal management devices, high-temperature filtration systems, catalyst supports or electrical resistances. Additionally, due to their microstructure that closely resembles that of bone, porous bioSiC materials are considered for their application as cortical bone substitute. An overview of the material science research at regional and national level will be also presented in the framework of the EU-USA Ceramic Engineering Forum.

## **S1: Mechanical Behavior and Performance of Ceramics & Composites**

### **Ceramic Fiber Reinforced Composites**

Room: Coquina Salon D

Session Chairs: Walter Krenkel, University of Bayreuth; Randall Hay, Air Force Research Laboratory

**1:30 PM**

**(ICACC-S1-023-2012) Ceramic components based on non-oxide fibre composite materials for advanced systems in the high-temperature energy technology**

K. Schoenfeld\*, TU, Germany; H. Klemm, A. Michaelis, FhG IKTS, Germany

There is an increasing need for high temperature components in the energy technology which can't be covered with conventional solutions based on metallic materials. For safety reasons, these components have to ensure both functionality in the temperature range of 1000 °C and a high stability up to 1600 °C in case of failure. Caused by the unique requirements during operation a maximal strength level with a high damage tolerance is required. Non-oxide ceramic fibre composites were developed with filament winding technology and polymer impregnation and pyrolyse process (PIP). Main focus was placed on the development of materials with application-oriented properties under corrosive conditions up to temperatures of 1600 °C and the implementation of these advanced materials into components and functional prototypes for energy technology (e.g. heat pipes). Based on SiC Fibres CMC with SiCN matrix were manufactured which are stable on air until 1400°C. Additional these components offer strength until 200 MPa. Due to additional interface coating damage tolerance fracture behaviour is reached. As a result new applications in energy technology and other industrial should be made accessible with the development of innovative high temperature ceramic matrix composites and their prototypes and components fabricated.

**1:50 PM**

**(ICACC-S1-024-2012) Determination of the true statistical flaw strength parameters for SiC Nicalon fibres**

J. L. Lamon\*, M. R'Mili, N. Godin, CNRS, France

The present paper investigates large sets of SiC fiber failure strengths (500 to 1000 data) produced using tensile tests on tows that contained either 500 or 1000 filaments. The probability density function was determined through acoustic emission monitoring which allowed detection and counting of fiber fractures. The statistical distribution of filament strengths was then, described using the normal distribution. The Weibull equation was then fitted to this normal distribution for estimation of the statistical parameters. A perfect agreement between

both distributions was obtained, and a quite negligible scatter in statistical parameters was observed, as opposed to the wide variability that is reported in the literature. Thus it was concluded that the fiber flaw strengths are distributed normally and that the Weibull parameters that were obtained are the true parameters. In a second step, the conventional method of estimation of Weibull parameters was applied, to the large sets of data, and then, to subsets selected randomly. The influence of other factors involved in the conventional method of determination of statistical parameters is discussed. It is demonstrated that selection of specimens and sample size are preponderant factors in Weibull statistical parameters variability.

### 2:10 PM

#### (ICACC-S1-025-2012) Kinetics of Passive Oxidation of Hi-Nicalon-S SiC Fibers in Wet Air: Relationships between SiO<sub>2</sub> Scale Thickness, Crystallization, and Fiber Strength

R. Hay\*, G. Fair, Air Force Research Laboratory, USA; A. Hart, University of Cincinnati, USA; R. Bouffieux, New Mexico Tech., USA

Relationships between Hi-Nicalon-S SiC fiber strength, the thickness and crystallinity of the SiO<sub>2</sub> scale, and the oxidation temperature and time in wet air were characterized. Hi-Nicalon-S SiC fiber was oxidized in wet air at temperatures from 700° to 1300°C. Passive oxidation kinetics were determined by measurement of the SiO<sub>2</sub> scale thicknesses from TEM micrographs of oxidized fiber cross-sections, and modeled using Deal-Grove kinetics. Avrami kinetics were used to model scale crystallization. The tensile strength distributions of fibers were measured using 30 single filament tensile tests. Residual stress and growth stress in the oxide scales were calculated from the volume expansion during oxidation and the CTE mismatch between SiO<sub>2</sub> and SiC. The oxidation and crystallization kinetics are compared to those for dry air.

### 2:30 PM

#### (ICACC-S1-026-2012) Optimizing Strength and Toughness of CMCs reinforced with Wavy, Finite-length Carbon Nanotubes

F. Pavia\*, W. A. Curtin, Brown University, USA

Strengthening and toughening of a ceramic matrix through the introduction of carbon nanotubes (CNTs) is promising yet challenging. Theories for micron-scale fibers are applicable if the CNTs are aligned, straight, and infinite in length. CNTs being used in current generations of materials are, however, wavy and of finite length. Here, we develop a shear-lag model for predicting the “single matrix crack” strength and work of fracture for a CMC containing wavy, finite-length CNTs having a statistical distribution of strengths, as a function of all the material parameters including morphology and constant plus Coulombic interfacial friction. For CNTs of finite length  $L$ , radius of curvature  $R$ , and Coulomb friction coefficient  $\mu$ , we find the strength and toughness depend only on characteristic strength  $\sigma_c$ , characteristic length  $\delta_c$ , and two new dimensionless parameters  $\mu\delta_c/R$  and  $L/\delta_c$ . Parametric results for a typical CNT-CMC show that there is an optimal region of morphology ( $L$  and  $R$ ) that maximizes composite strength and toughness, exceeding the properties of composites with straight ( $R=\infty$ ) and long ( $L=\infty$ ) reinforcements. Therefore, while factors such as the CNT strength distribution and CNT/matrix interface sliding resistance may not be easily controlled, the tuning, via processing, of purely geometrical properties of the CNTs ( $L$  and  $R$ ) alone can aid in maximizing composite properties.

### 2:50 PM

#### (ICACC-S1-027-2012) The growth of carbon nanotubes in three-dimensional carbon felt and the hybrid enhancement to Cf/SiC composites

H. Jianbao\*, D. Shaoming, Z. Xiangyu, H. Zhihui, Y. Jinshan, L. Qinggang, W. Bin, L. Bo, Shanghai Institute of Ceramics, China

Multi-walled carbon nanotubes (MWCNTs) were grown by chemical vapor infiltration in carbon fibers felt with PyC/SiC interfaces which commonly used as interfaces in ceramic matrix composites (CMC). Systematically study, by varying the reaction temperatures, growth

time, gas flow rates (the resident time), was carried out in relation to morphology and yield of the products. Dense and uniform MWCNTs were drafted on the carbon fiber surface throughout the felt. The morphology of CNTs was examined by canning and transmission electron microscopy. Carbon fiber/carbon nanotubes hybrids are promising to realize multifunctional Enhancements to CMCs. Three-dimensional(3D) Cf/SiC composites reinforced with Carbon fiber/carbon nanotubes hybrids were fabricated, and the thermal conductivity(TC), mechanical properties were examined. The mechanics of enhancement were also discussed.

### 3:30 PM

#### (ICACC-S1-028-2012) Investigation of critical fiber length in phenol matrix based short fiber CFRP

D. Heim\*, S. Zaremba, K. Drechsler, Technical University of Munich, Germany

For short fiber CFRP based on a phenol matrix the influence of fiber length in terms of tensile strength is investigated. The effect of fiber length within a representative phenol matrix structure (high porosity) is studied by a double lap joint principle. Therefore, a laminate with three layers is manufactured in such a way that each layer exhibits a cut. The two outer layers have the joint at the same position; the middle layer's joint has an offset which is adequate to the overlap length. Specimens with an overlap length ranging from 4 mm to 36 mm are mechanically tested. The CFRP show a nonlinear increase in tensile strength for short overlaps. As the overlap length increases, tensile strength reaches an upper limit asymptotically. This overlap length behavior is already known from adhesive double lap joints. The transition point between the rise and the asymptotic region is useful to determine the optimal overlap length. Due to contrary effects in short fiber composites (e.g. heterogeneity with increasing fiber length), the optimum length for the overlap is not the same as for the fiber. If the model system is appropriate for short fiber composites, the optimal overlap length corresponds to an upper limit fiber length. The double lap joint principle could be an effective way of determining a maximum fiber length for a specific fiber matrix combination with a realistic matrix structure.

### 3:50 PM

#### (ICACC-S1-029-2012) Processing and Testing of $\gamma$ -RE<sub>2</sub>Si<sub>2</sub>O<sub>7</sub> Matrix Composites

E. E. Boakye\*, K. A. Keller, P. Mogilevsky, T. Parthasarathy, UES Inc., USA; M. K. Cinibulk, R. S. Hay, AFRL, USA; M. Ahrens, Wright State University, USA

The  $\gamma$ -polymorph of the rare-earth disilicates (RE<sub>2</sub>Si<sub>2</sub>O<sub>7</sub>) is a potential oxidation-resistant alternative to carbon or BN for CMC fiber-matrix interphases.  $\gamma$ -RE<sub>2</sub>Si<sub>2</sub>O<sub>7</sub> is a “quasi-ductile” ceramic in the sense that it is soft (Vickers hardness ~6 GPa) and machinable. Prior TEM results of indented samples showed both extensive dislocation slip and fracture similar to observations made for monazite. Preliminary fiber pushout results of SCS-0 fibers in dense Ho<sub>2</sub>Si<sub>2</sub>O<sub>7</sub> and Y<sub>2</sub>Si<sub>2</sub>O<sub>7</sub> matrices showed fiber debonding and push-out, with sliding stresses of 30-60 MPa, which is within the range reported for C, BN, and LaPO<sub>4</sub> coatings. Nicalon/ $\gamma$ -Y<sub>2</sub>Si<sub>2</sub>O<sub>7</sub> and Hi-Nicalon S/ $\gamma$ -Y<sub>2</sub>Si<sub>2</sub>O<sub>7</sub> composites were made by filament winding; the  $\gamma$ -Re<sub>2</sub>Si<sub>2</sub>O<sub>7</sub> powder was produced as previously reported at 1400C. The resultant composite properties, including room temperature tensile strength, microstructural uniformity and fiber distribution, will be reported.

### 4:10 PM

#### (ICACC-S1-030-2012) Ultra High Toughness Ceramic Composites: Optimising Metal Fibre Reinforced Ceramic Matrix Composites (MFCs)

S. R. Pemberton\*, University of Cambridge, United Kingdom; L. Marston, Fiberstone Products Ltd, United Kingdom; T. W. Clyne, University of Cambridge, United Kingdom

A commercially available metal fibre reinforced ceramic matrix composite (MFC), going by the tradename Fiberstone™ and

comprising ~ 11 vol. % stainless steel fibres in a modified alumina matrix, has been studied via single fibre tensile testing, fibre pull-out testing and Izod testing to investigate its fracture behaviour. A simple analytical model has been produced and shown to successfully predict trends in the composite's fracture energy. Use of this model has allowed optimisation of the MFC's toughness and an ultra high toughness ceramic matrix composite has been developed, with measured fracture energies of up to 80 kJ m<sup>-2</sup>, values comparable to those for ductile metals. It will be shown that such high toughness is achievable through maximising the plastic deformation of the steel fibre reinforcements, and the effect of changing fibre ductility on the composite's overall toughness will be examined. Additional effects such as fibre size and shape will also be discussed. Finally, results will be presented from an investigation into the effect of improved fibre anchorage in the ceramic matrix in an attempt to eliminate fibre pull-out, forcing fibres crossing the crack plane to undergo plastic deformation and rupture. This study confirmed the powerful potential for toughening via such plastic deformation, provided the fibres are relatively strong and ductile.

**4:30 PM**

**(ICACC-S1-031-2012) Interfacial Studies of Microfibrillated Cellulose Filled CF/Epoxy Composites**

M. H. Gabr\*, K. Okubo, T. Fujii, Doshisha University, Japan

Fiber reinforced composites (FRCs) are increasingly replacing metals in many engineering and medical applications. Composite materials formed by natural fibers and polymeric matrices constitute a current area of interest in composites research. Cellulose, the most abundant natural homopolymer, is considered to be one of the most promising renewable resources and an environmentally friendly alternative to products derived from the petrochemical industry. In previous work; we propose an effective technique in fabrication of probe disk for semiconductor testing device using cellulose as an alternative material of ceramics. In this study, Microfibrillated cellulose (MFC) was introduced as filler in order to improve the interfacial strength between the epoxy as a matrix and carbon fiber as reinforcement. Interfacial shear strength (IFSS) was measured by a single fiber pull-out test. CTBN as liquid rubber was used as modifier to investigate its effect on the mechanical properties of epoxy/MFC composites. The composite was characterized by different techniques, namely, tensile, bending, dynamic mechanical analysis (DMA), and scanning electron microscope (SEM). The results reveal that at a fiber content 0.5% of MFC and 10% CTBN, IFSS increased two times as compared to unfilled epoxy which could be attributed to strong adhesion between filled epoxy, CF, and rubber.

**4:50 PM**

**(ICACC-S1-032-2012) The study on the strength prediction of comeld composites joints**

H. Zhang\*, W. Wen, H. Cui, Nanjing University of Aeronautics and Astronautics, China

It is well known that the joint is one of the weakness points. Comeld is a novel technology which can be applied in connecting composites and metals. However, there are no papers or reports about the study on its mechanical properties. As the directions of the fiber and the distributions of the matrix are changed during comeld process, the mechanical properties of comeld composites joints vary from the uncomeld composites. In this paper, the progressive damage method of prediction the strength is developed and programmed by considering the 3-D Tsai-Wu failure criteria and the structural failure criterias based on the 3-D finite element method. And the strength prediction method is applied to predict the strength of comeld joints. Compared with the predicted data and experiments, it is found that the errors between them are very low, which means that the methods developed in this paper are valid.

## S4: Armor Ceramics

### Transparent Materials I

Room: Coquina Salon E

Session Chair: Lisa Franks, US Army TARDEC

**1:20 PM**

**(ICACC-S4-023-2012) Energy effects on the cracking patterns of glass/polymer laminates in ballistic impact (Invited)**

D. Ahearn, J. Ladner, R. Bradt\*, University of Alabama, USA

When cracks develop during the ballistic impact of impact resistant glass/polymer panel laminates, they obtain their energy both from the kinetic energy of the projectile and also from the stored elastic strain energy in the residual stress state of tempered glass. This paper first addresses the role of the kinetic energy for several glass/polymer laminate designs. It then considers the added role of the elastic strain in the target glass panels. In both situations the radial cracks increase linearly with the available energy for crack development.

**1:50 PM**

**(ICACC-S4-024-2012) Edge-on Impact Investigations of Stress and Damage Propagation in Sapphire Single Crystal Plates**

E. Strassburger, Fraunhofer-Institut für Kurzzeitdynamik, Germany; P. Patel, J. McCauley\*, Army Research Laboratory, USA

This paper will review work carried out with a unique, fully instrumented Edge-on Impact (EOI) facility at the Ernst-Mach-Institute (EMI), using a Cranz-Schardin high speed camera, modified for dynamic photoelasticity, to quantify stress wave propagation, damage nucleation and propagation during high velocity impacts. The experimental technique has been used to examine monolithic single crystal sapphire plates (100x100x10 mm) in crystallographically controlled directions impacted at about 400 m/s with both steel solid cylinders and spheres. The plates were impacted as follows: 100X100 large surface r-plane parallel to the a-axis; large surface a-plane parallel and perpendicular to the c-axis; large surface c-plane parallel to a-axis; and impacting perpendicular to r-plane small surface. In certain orientations damage propagation is clearly by macro-cleavage with significant cleavage branching. The velocities of damage and cleavage propagation will be presented.

**2:10 PM**

**(ICACC-S4-025-2012) Radio Frequency Lamination for Curved Windows**

S. M. Allan\*, H. S. Shulman, I. Baranova, M. L. Fall, G. Esquenazi, Ceralink Inc., USA

Radio Frequency (RF) Lamination enables rapid production of laminated glass products including transparent armor. RF lamination eliminates the need for autoclaving by using an RF press with parallel platens to apply uniaxial pressure to a window in addition to RF heating. RF lamination was previously demonstrated on a wide range of flat glass products, however curvature is an important part of many windows used in aerospace and armored vehicles. The development and demonstration of curved glass lamination using RF heating for small automotive windows will be presented. The effects RF parameters of process time, RF power, and pressure on adhesion strength, optical quality and mechanical performance were studied. Temperature labels allowed measurement of the thermoplastic polyurethane interlayer temperature at the various positions around the windows. Energy consumption and process cost comparisons will be made between RF and traditional autoclave lamination.

**2:30 PM**

**(ICACC-S4-026-2012) Effect of Ball Material Properties on Impact Response of SLS Glass at Low Velocities**

A. A. Wereszczak, E. E. Fox, D. J. Vuono, T. G. Morrissey\*, Oak Ridge National Laboratory, USA

In previous quasi-static spherical indentation testing of soda-lime-silicate (SLS) glass, it was conclusively and repeatedly shown that lowering the elastic modulus of the ball material resulted in the causation

of ring crack initiation at lower compressive forces. This was due to differences of elastic property mismatches between indenter ball and target glass and the changes in traction friction caused by those mismatches. Given that, interest existed in the present study to examine if this effect was also operative during the ball impact of SLS glass at low velocities (< 30 m/s or 65 mph). Borosilicate glass, SLS glass, Si<sub>3</sub>N<sub>4</sub>, Al<sub>2</sub>O<sub>3</sub>, and steel balls were used, spanning a range of elastic moduli from 63 to 375 GPa, for the impact testing. It was observed that the onset of impact damage in the SLS tiles was not solely a function of the ball's kinetic energy at this velocity range, and that the effects of elastic modulus mismatch of the ball and SLS glass target could be contributing to the target response too.

### 3:10 PM

#### (ICACC-S4-027-2012) Preparation and Sintering of Al<sub>2</sub>O<sub>3</sub>-Coated Spinel

M. Vu\*, R. Haber, Rutgers University, USA; H. Gocmez, Dumlupinar University, Turkey

Al<sub>2</sub>O<sub>3</sub> was uniformly coated on the surface of magnesium aluminate spinel particles by precipitation and sol-gel techniques followed by heat treatment. The coated powder was then sintered in a SPS furnace at temperatures as low as 1250 - 1350°C. The characterization of the coated powder and sintered pellets was carried out by scanning electron microscopy, X-ray diffraction, hardness testing, and light transmittance techniques. The effect of Al<sub>2</sub>O<sub>3</sub> addition on the hardness and transparency of spinel was investigated. The hardness of spinel was enhanced. The amount of Al<sub>2</sub>O<sub>3</sub> was optimized so as to retain high transparency for spinel samples.

### 3:30 PM

#### (ICACC-S4-028-2012) "Complexion" Based Strategies for Controlling the Microstructure and Properties of Magnesium Aluminate Spinel for Armor Applications

A. Kundu\*, G. J. Ferko, M. P. Harmer, Lehigh University, USA

The research program addresses the challenges of controlling the microstructure and associated properties in magnesium aluminate spinel applying the concept of "grain boundary complexions". Complexion is a new taxonomy for grain boundaries connecting their chemistry, structure and transport properties. Desired transparency in spinel parts is usually achieved with the aid of sintering additives e.g. LiF, often resulting in uncontrollable grain size distributions, higher average grain sizes and abnormally large grains. Two different approaches have been adopted to mitigate this problem. The first involves a fundamental investigation of the formation and stability of various grain boundary phases ("complexions") in spinel with the aid of high resolution electron microscopy as a function of various processing conditions. The grain boundary phases have been induced by controlled doping and preferential segregation of the dopants at the boundaries with proper control of processing conditions. The second approach involves removing intrinsic impurities in commercial spinel powder that affect the grain growth kinetics adversely. A proprietary pretreatment process has been developed for such a purpose. The pretreated powder has been hot-pressed to nearly theoretical transparent parts with average grain size <1 μm without utilizing any sintering additives.

### 3:50 PM

#### (ICACC-S4-029-2012) The Role of Point Defects on the Sintering and Optical Properties of Transparent MgAl<sub>2</sub>O<sub>4</sub> Hot Pressed with LiF

M. Rubat du Merac\*, I. Reimanis, Colorado School of Mines, USA; H. Kleebe, Technical University Darmstadt, Germany; C. Smith, Corning Inc., USA

Magnesium aluminate spinel (MgAl<sub>2</sub>O<sub>4</sub>) has a combination of properties well suited for transparent armor, IR-transparent domes, and possibly UV-transparent windows. However, sintering to the

near-theoretical density required for transparency typically requires use of LiF additive and cold isostatic pressing/sintering or hot-pressing, followed by hot isostatic pressing. LiF reacts with and removes impurities, causes preferential MgO loss, negates dark coloration sometimes observed, and is thought to result in diffusion-enhancing defects. Unfortunately, LiF addition results in grain boundary embrittlement and exaggerated grain growth and remnant LiF results in optical scattering. A better understanding of the function of LiF in the sintering process could lead to better properties and processing methodologies and wider application. An approach based on defect chemistry and characterization using UV-visible photospectroscopy, IR-ellipsometry, Raman spectroscopy, impedance spectroscopy, SEM and TEM is used to understand the role of LiF in defect formation and the effect on densification and optical properties. The relationship between LiF, sintering atmosphere, temperature and pressure profile, defects, and optical properties will be discussed.

### 4:10 PM

#### (ICACC-S4-030-2012) Polished Spinel Directly From the Hot Press

G. Villalobos\*, Naval Research Lab, USA; B. Sadowski, Sotera Defense Solutions, USA; M. Hunt, University Research Foundation, USA; S. Bayya, Naval Research Lab, USA; R. Miklos, Sotera Defense Solutions, USA; W. Kim, Naval Research Lab, USA; I. Aggarwal, Sotera Defense Solutions, USA; J. Sanghera, Naval Research Lab, USA

Polishing is approximately half of the cost of a finished transparent ceramic window. Consequently, we have developed a new process to eliminate post polishing for many applications, thereby reducing the cost of a part. Our use of polished inserts during hot pressing results in a transparent surface on spinel ceramic as it emerges from the hot press die. The inserts eliminate the need to polish the surface after densification and can be used to create both flat and curved surfaces. The polish on the inserts and the insert material itself is very important to the final appearance of the spinel disk. Thermal etching of the inserts can bring to the surface scratches that will be transferred to the finished part. Chemical reaction between the insert and the spinel will also result in an imperfect surface. We have solved these problems and fabricated spinel disks that possess a transmission of 90% of the theoretical value in the visible and infra red wavelength regions after hot pressing with this new process and without any further processing.

### 4:30 PM

#### (ICACC-S4-031-2012) Determining the Strength of Coarse-Grained AlON and Spinel

J. Swab\*, G. Gilde, U.S. Army Research Laboratory, USA; J. Wright, UIC TS, Bowhead Science & Technology, USA; R. Pavlacka, Oak Ridge Institute for Science & Education, USA; S. Kilczweski, Data Matrix Solutions, USA

Transparent aluminum-oxynitride (AlON) and spinel materials are being developed for a variety of applications including transparent armor, electromagnetic windows and as laser hosts. Strength is a common property that is determined for all of these applications. Strength of these materials is typically determined using prismatic beam specimens subjected to four-point flexure as outlined in ASTM C1161 and/or circular disks or square plates in equibiaxial flexure as outlined in ASTM C1499. In both instances the specimens tested are usually only a few millimeters thick and strength-size-scaling is then used to predict the strength of the actual component. However, most of the AlON and spinel materials being developed are comprised of grains hundreds of microns in size. Does the grain size-to-specimen thickness ratio influence the strength measurements? Does strength-size-scaling accurately predict the strength of the larger component? This presentation examines the strength of a coarse-grained AlON and spinel, both with an average grain size in excess of 350 microns, and a sintered spinel with an average grain

size of 1.5  $\mu\text{m}$ . The strength will be determined by applying four-point flexure to specimens of different thicknesses. Equibiaxial flexure strength testing will also be conducted on large plates of each material.

#### 4:50 PM

##### (ICACC-S4-032-2012) A fresh look at why does spinel outperforms sapphire during ballistic tests?

G. Subhash\*, E. J. Haney, University of Florida, USA

Compared to magnesium aluminate spinel, Sapphire has many superior mechanical properties: density 3.97 g/cm<sup>3</sup> vs 3.58 g/cm<sup>3</sup>; Young's modulus 386GPa vs. 277 GPa; Biaxial flexural strength 760 MPa vs. 172 MPa; Vickers hardness 17.4 GPa vs. 14 GPa; and HEL 23GPa vs. 11.3 GPa. However the ballistic performance of sapphire has been reported to be inferior compared to spinel. For comparable aerial density, V50 for spinel has been reported to be almost 300 ft/sec higher than sapphire. To unlock this mystery, we have conducted a range of studies including static indentation, dynamic indentation and ball impact studies and investigated the fundamental mechanisms of fracture development in these two materials. While hardness is an important factor that contributes to superior performance of any armor material, it is not the only factor that determines the performance. A range of mechanisms including decreased tendency for brittle fracture, mixed mode fracture, grain boundary shielding etc., act in favor of spinel whereas interacting cracks and propensity for fracture along preferred crystallographic planes act against sapphire and contribute to lower performance. The details of analysis from various experiments will be presented in detail.

## S7: 6th International Symposium on Nanostructured Materials and Nano-Composites

### Industrial Application of Nanomaterials and One Dimensional Structures

Room: Coquina Salon B

Session Chairs: Ulf Jansson, Uppsala University; Jyh-Ming Ting, National Cheng Kung University

#### 1:30 PM

##### (ICACC-S7-019-2012) Nanostructured Coatings by Cluster Beam Deposition: Method and Applications (Invited)

E. Barborini\*, S. Vinati, R. Carbone, Tethis spa, Italy

One of the key issues to be addressed in order to exploit nanomaterial peculiar properties is the way devices, and surfaces in general, can be functionalized by nanomaterials. To allow the jump beyond lab-scale, deposition techniques are asked to fulfill requirements such as reliability and repeatability, batch deposition, scalability, compatibility with micromachining techniques. Here we show how cluster beam deposition may answer these requests, while offering at the same time a wide library of available nanomaterials, ranging from oxides to noble metals, from carbon to nanocomposites. Cluster beam sources based on electrical discharge and on flame pyrolysis will be described. In both cases, the growth of nanostructured functional film takes place directly onto support surface, once cluster beam reaches it. Cluster soft-assembling generates nanoporosity and, as a consequence, films with large specific surface, which are particularly suited for applications where interaction with solutions or atmosphere has to be favored. Results within chemical sensing field and within biotech field, such as selective capture of peptides and enhanced cell adhesion, as examples of functions that may be added to surfaces or devices by cluster-assembled nanomaterials, will be reported.

#### 2:00 PM

##### (ICACC-S7-020-2012) Copper (II) heteroarylalkenolates: From Molecule to Material

I. Giebelhaus\*, T. Fischer, University of Cologne, Germany; E. Varchkina, M. Rumyantseva, A. Gaskov, Moscow State University, Russian Federation; W. Tyrra, S. Mathur, University of Cologne, Germany

Among the various methods employed to synthesize copper nanostructures, chemical vapor deposition offers a great versatility of controlling the size, morphology and composition of the resulting nanostructures. Given the delicate interplay of precursor chemistry and material properties, reproducible CVD processes demand suitable precursors possessing adequate vapor pressure and stability in the gas phase. In view of the above, the main aims of our work are synthesis, characterization and application of new ligand systems and their copper (II) derivatives which would fulfill all prerequisites of CVD processes. Novel copper (II) heteroarylalkenolates have been successfully used for the deposition of 1-, 2- and 0-D copper nanostructures. Ranging from spherical copper particles over thin films to single copper nanorods the chemical vapor deposition of novel copper (II) compounds offers the possibilities of creating new morphologies and forming novel interesting materials. For example the modification of SnO<sub>2</sub> nanowires with the copper particles and further oxidation of Cu to CuO lead to p-n junction between CuO and SnO<sub>2</sub>. To demonstrate the potential use of CuO decorated SnO<sub>2</sub> nanowires in selective gas detection, we measured the gas sensing properties. This presentation will focus on the synthesis of a new copper (II) precursor family and their application in material synthesis.

#### 2:20 PM

##### (ICACC-S7-021-2012) Use of Copper Nanoparticles to Enhance Thermal Performance of Solar Heat Transfer Fluids

S. Cingarapu\*, E. V. Timofeeva, M. R. Moravek, M. J. Nawrocki, D. Singh, T. Fischer, S. Mathur, Argonne National Laboratory, USA

It is well known that thermal conductivity of base fluids (water, ethylene glycol or their mixtures) can be enhanced by dispersing nanoparticles of various metals and ceramics at various loadings. For concentrating solar power applications, one approach to increase the overall plant efficiency is to improve the thermo-physical properties of the heat transfer fluid. In this regard, we synthesized copper and silica nanoparticles using wet chemistry approaches, and subsequently, dispersed the nanoparticles in a commercial solar heat transfer fluid at various particle loadings. Characterizations such as thermal conductivity, viscosity, and fluid stability were performed. Thermal conductivity enhancements over the base fluids followed the Effective Medium Theory predictions or were higher. Role of surfactant on the stability of the suspensions was investigated. Implications of using the nanoparticle dispersed fluids for the concentrated solar application will be discussed.

#### 2:40 PM

##### (ICACC-S7-022-2012) Development of nanowire based solar cell on multilayer transparent conducting films (Invited)

D. Sahu\*, University of the Witwatersrand, South Africa

Solar cells are attractive candidates for clean and renewable power. Efficient solar-to-electric energy conversion with inexpensive solar cells and materials is one of the most important challenges. New solar cell architectures that can be fabricated using nonconventional nanomaterials can attract extensive attention because of the demand of photovoltaic technologies for large-scale energy production. Novel nanowire-based solar cells are developed on grown superior transparent electrode and active anode materials via structure and surface modification of metal oxide nanowires which gives efficient efficiency. This one dimensional (1D) nanostructures such as nanorods and nanowires are used to improve collection rate of carrier charges

and energy efficiency of solar cells, to demonstrate carrier multiplication and to enable low-temperature processing of photovoltaic devices. The highest efficiency of 5.4% is achieved for the nanowire/nano particle composite solar cell till now. Details of the process and procedure will be discussed during presentation.

### Nanostructured Membranes, Functional Coatings and Nanocomposites

Room: Coquina Salon B

Session Chairs: Emanuele Barborini, Tethis spa; Tim Van Gestel, Forschungszentrum Jülich

**3:20 PM**

#### (ICACC-S7-023-2012) Design of Multifunctional Carbide-based Nanocomposite Coatings (Invited)

U. Jansson\*, Uppsala University, Sweden

Carbide-based coatings with transition metals often form a nanocomposite structure with nanocrystalline carbide grains in an amorphous matrix. Such coatings may exhibit excellent mechanical, tribological and electric properties and have a use in a wide range of applications. Magnetron sputtering offers enormous possibilities to control the properties of these coatings by a careful tuning of the size and distribution of the nanocrystalline grains and the matrix. The present paper will summarize some approaches to design nanostructured carbide coatings in the Ti-Me-C (Me = 3d transition metals) and Me-X-C systems (Me = Ti, Nb, Zr and X = B, Si). In the first case, a metastable solid solution is formed with a weak carbide-forming element such as Al, Ni, or Fe. Theoretical calculations as well as experiments show that it energetically favours to remove carbon from the metastable carbide leading to smaller grains and a more carbon-rich matrix. A potential use of such a concept is self-adaptive coatings which spontaneously form a low-friction graphitic surface in an electric contact. Another approach is to add glass-forming p-elements to a binary metal carbide phase. By a careful tuning of the composition it is possible to form metal glass coatings or coatings with both an amorphous and a nanocrystalline component. Potential applications of these materials will be discussed.

**3:50 PM**

#### (ICACC-S7-024-2012) Synthesis and Electrochemical Performance of SiOC-Carbon Nanotube Composite Nanowire Coatings

R. Bhandavat\*, G. Singh, Kansas State University, USA

Rechargeable battery anodes made from crystalline Si-based nanostructures have been shown to possess high experimental first cycle capacities (~3000 mAh/g), but face challenges in sustaining these capacities beyond initial cycles due to large volume expansion. SiOC is a Si-based polymer derived ceramic, highly stable primarily due to presence of nano-domains that endures adverse chemical and thermal environments. Additionally, a non-covalent functionalization of SiOC with carbon nanotubes could increase the electronic and ionic conductivity of the composite. Here, we demonstrate synthesis of SiOC-CNT composite nanowires as an anode material with enhanced cyclic stability besides high electronic and ionic conductivity. Additionally infrared, X-ray photoelectron spectroscopy and nuclear magnetic resonance spectroscopy results suggest the non-covalent functionalization of CNT with oxygen moieties in SiOC. As a result, sustained battery capacities of ~700mAh/g and first cycle coulombic efficiencies of ~75% were achieved. Future work will involve determination of lithium ion intercalation sites characterized by electron microscopy whereas cyclic voltammetry analysis will access the sequential change in anode chemistry.

**4:10 PM**

#### (ICACC-S7-025-2012) Superhard Nanostructured Coatings Ti-Hf-Si-N, Their Structure and Properties

A. D. Pogrebnjak\*, Sumy State University, Ukraine; A. P. Shpak, Institute for Metal Physics G.V.Kurdyumov NAS of Ukraine, Ukraine; V. M. Beresnev, Kharkov National University, Ukraine; F. F. Komarov, Belarus State University, Belarus; P. Konarski, Tele-Radio Research Institute, Poland; V. V. Uglov, Belarus State University, Belarus; M. V. Kaverin, Sumy State University, Ukraine; D. A. Kolesnikov, Belgorod State University, Russian Federation; N. A. Makhmudov, Samarkand Branch of Tashkent University of Information, Uzbekistan; I. V. Yakyschenko, Sumy State University, Ukraine; V. V. Grudnitskii, Kharkov National University, Ukraine

New Superhard coatings based on Ti-Hf-Si-N featuring high physical and mechanical properties were fabricated. We employed a vacuum-arc source with HF stimulation and a cathode sintered from Ti-Hf-Si. Nitrides were fabricated using atomic nitrogen (N) or a mixture of Ar/N, which were leaked-in a chamber at various pressures and applied to a substrate potentials. RBS, SIMS, GT-MS, SEM with EDXS, XRD, and nanoindentation were employed as analyzing methods of chemical and phase composition of thin films. We also tested tribological and corrosion properties. The resulting coating was a two-phase, nanostructured nc-(Ti, Hf)N and  $\alpha$ -Si<sub>3</sub>N<sub>4</sub>. Sizes of substitution solid solution nanograins changed from 3.8 to 6.5 nm, and an interface thickness surrounding  $\alpha$ -Si<sub>3</sub>N<sub>4</sub> varied from 1.2 to 1.8 nm. Coatings hardness, which was measured by nanoindentation was from 42.7 GPa to 48.6 GPa, and an elastic modulus was E = (450 to 515) GPa. The films stoichiometry was defined for various deposition conditions. It was found that in samples with superhard coatings of 42.7 to 48.6GPa hardness and lower roughness in comparison with other series of samples, friction coefficient was equal to 0.2, and its value did not change over all depth (thickness) of coatings. A film adhesion to a substrate was essentially high and reached 25MPa.

**4:30 PM**

#### (ICACC-S7-058-2012) Nanowire based heterostructures: growth, properties and application to photovoltaics (Invited)

A. Fontcuberta-Morrall\*, Ecole Polytechnique Fédérale de Lausanne, Switzerland

Nanowires are filamentary crystals with a diameter of few to hundreds of nanometers. Thanks to their dimensions they are the perfect playground for fundamental studies and for improving devices such as solar cells. Nanowires are typically obtained by the vapor-liquid-solid method in which gold is used as a catalyst for the gathering of the precursor species and nanowire growth. It has been shown that gold can affect negatively the electronic and optical properties of semiconductors. We fabricate ultra-high purity GaAs nanowires by avoiding the use of gold and by the use of molecular beam epitaxy (MBE). MBE offers also the unique possibility of growing with epitaxial quality on the nanowire facets. Prismatic quantum wells and Stranski-Krastanov quantum dots are obtained with a very high quality, as demonstrated by the optical spectroscopy measurements. Finally, we show how these nanowires are excellent candidates for the fabrication of third generation solar cells.

**5:00 PM**

#### (ICACC-S7-026-2012) P-type conductivity of Mg-doped CuAlO<sub>2</sub> (Invited)

E. Kim\*, M. Kim, M. Oh, S. Kim, Korea Electrotechnology Research Institute, Republic of Korea

There is a considerable technology interest in developing transparent conductive oxide(TCO). Recently p-type TCOs attract attention because of their potential use in transparent optoelectronic devices; such as, light-emitting diodes, laser diodes, solar cells, displays, smart windows, TFTs, and other. CuAlO<sub>2</sub> is a wide band-gap semi-

conductor compound with the delafossite structure, rapidly drawing remarkable attention due to easy formation of its p-type structures. However, few investigations have discussed its defect chemistry in impurity doping for its conductivity modification, especially the effect of ambient atmosphere during doping. In this study,  $\text{CuAlO}_2$  containing Mg impurity substituting for either Cu or Al position has been investigated.  $(\text{Cu}_{1-x}\text{Mg}_x)\text{AlO}_2$  and  $\text{Cu}(\text{Al}_{1-y}\text{Mg}_y)\text{O}_2$  compositions were fabricated by conventional solid reaction method in air atmosphere. As measurements of Hall and Seebeck coefficient, all samples showed p-type property. We suggested the defect chemistry in Mg-doped  $\text{CuAlO}_2$ , from which the carrier concentration was calculated as a function of oxygen partial pressure by considering the formation of native defects. The results of the calculation and measurements showed that Mg ion prefer the Al-site of  $\text{CuAlO}_2$  in air (oxidation) atmosphere, resulting in the acceptor impurity  $\text{Mg}'_{\text{Al}}$ . These may imply, that n- $\text{CuAlO}_2$  can be fabricated by formation of the donor  $\text{Mg}^*_{\text{Al}}$  under controlled oxygen partial pressures.

5:20 PM

**(ICACC-S7-027-2012) Investigation on hybrid composite membrane consisting ammonium phosphate and their characterization**

U. Thanganathan\*, F. Yin, Okayama University, Japan

Fuel cells, in general, are attractive because they provide an innovative alternative to current power sources with higher efficiencies, renewable fuels, and a lower environmental cost. A hybrid material appears to be very attractive material as hybrid matrix for preparing proton exchange membrane (PEM). This work reports the preparation of hybrid composite membranes, with Triammonium phosphate immobilized in the organic/inorganic matrix. The objective of this work is to investigate the influence of dispersed Triammonium phosphate on different membrane properties such as swelling, proton conductivity, and their behavior as electrolyte in PEM fuel cells. The hybrid composite membrane consisting of inorganic/organic hybrids synthesized through sol-gel process was found to offer the proton conductivities of 10–2 S  $\text{cm}^{-1}$  at 100 °C and at relative humidity. These properties make them very suitable candidates for proton exchange membrane fuel cell application. Keywords: Hybrid materials, Proton conductivity, Fuel cells

5:40 PM

**(ICACC-S7-028-2012) Synthesis of Nanostructured Oxidizers for Controlling the Explosive Reactivity of Nanoenergetic Materials**

S. Kim, J. Ahn\*, Y. Kim, Pusan National University, Republic of Korea

In this study, we demonstrate a simple and viable method for controlling the energy release rate and pressurization rate of nanoenergetic materials by controlling the nanostructures and relative elemental compositions of oxidizers.  $\text{CuO-Fe}_2\text{O}_3$  nanoparticles (NPs) and nanowires (NWs) were generated by conventional spray pyrolysis and electrospinning methods. Next, the Al NPs employed as a fuel were mixed with  $\text{CuO}$  NPs or NWs by an ultrasonication process in ethanol solution. Finally, after the removal of ethanol by a drying process, the NPs were converted into nanoenergetic materials (nEMs). The effects of the mass fraction of  $\text{CuO}$  in the  $\text{CuO-Fe}_2\text{O}_3$  bimetallic oxide NPs and NWs on the explosive reactivity of the resulting nEMs were examined by using a differential scanning calorimeter and pressure cell tester (PCT) systems. The results clearly indicate that the energy release rate and pressurization rate of nEMs increased linearly as the mass fraction of  $\text{CuO}$  in the  $\text{CuO-Fe}_2\text{O}_3$  bimetallic oxide NPs increased. This suggests that the precise control of the stoichiometric proportions of the strong oxidizer ( $\text{CuO}$ ) and mild oxidizer ( $\text{Fe}_2\text{O}_3$ ) components in the bimetallic oxide NPs is a key factor in tuning the explosive reactivity of EMs.

**S8: 6th International Symposium on Advanced Processing and Manufacturing Technologies for Structural and Multifunctional Materials and Systems (APMT) in honor of Professor R. Judd Diefendorf**

**Advanced Composite Manufacturing**

Room: Coquina Salon A

Session Chair: Erica Corral, University of Arizona; Shawn Allen, Ceralink

1:30 PM

**(ICACC-S8-019-2012) Processing of Advanced Ceramic Matrix Composites (CMCs) Based on Multifunctional Enhancement Mechanism (Invited)**

S. Dong\*, B. Wu, J. Hu, X. Zhang, Y. Ding, P. He, L. Gao, Z. Wang, H. Zhou, Shanghai Institute of Ceramics, Chinese Academy of Sciences, China

The properties of ceramic matrix composite are highly dependent on the fiber reinforcements, ceramic matrix and the interface/interphase between fiber and matrix. By introduction of multi-walled carbon nanotubes (MWCNTs), reactive nitride particles and ultrahigh temperature ceramic (UHTC) phase, thermal and mechanical properties can be improved through a multifunctional enhancement mechanism. CNTs grown in the fiber preforms act as a second reinforcement. However, CNTs need to be well protected during processing so that it can co-reinforce the CMCs together with the fiber reinforcement. Reactive nitride particles such as silicon nitride ( $\text{Si}_3\text{N}_4$ ) either can be regarded as particle reinforcement to enhance the ceramic matrix, or it can react with free carbon in the matrix to form a strong silicon carbide (SiC) matrix. The reaction between  $\text{Si}_3\text{N}_4$  and free carbon was controlled by the thermodynamic process depending on the decomposition of  $\text{Si}_3\text{N}_4$  to Si and the reaction between Si and C. Since this process is controlled in a very small region, the ceramic matrix will be strengthened without damage of fiber reinforcement. The inclusion of UHTCs phase can potentially improve the properties at very high temperature. However, UHTCs has higher thermal expansion coefficient. Through the formation of multi-layered (SiC/UHTCs)<sub>n</sub> matrix, a strengthened composite will be obtained.

2:00 PM

**(ICACC-S8-020-2012) Graphene Ceramic Composites (Invited)**

L. Walker, V. Marotto, M. Valdez, University of Arizona, USA; M. A. Rafiee, N. Koratkar, Rensselaer Polytechnic Institute, USA; E. L. Corral\*, University of Arizona, USA

Graphene is a promising reinforcement material for use in composite systems due its two exceptional properties and two-dimensional structure. Conventional ceramic matrix composites use one-dimensional reinforcements in order to enhance toughness. However, we find that using graphene to enhance the toughness of bulk silicon nitride ceramics we are able to enhance significantly enhance toughness of our ceramics. Our approach uses graphene platelets (GPL) that are homogeneously dispersed with silicon nitride particles and densified using spark plasma sintering at a densification temperature that enables the GPL to survive the harsh processing environment, as confirmed by Raman spectroscopy. We find that the 100 % alpha-silicon nitride fracture toughness increases by up to ~235% (from ~2.8 to ~6.6  $\text{MPa}\cdot\text{m}^{1/2}$ ) at ~1.5% GPL volume fraction. Most interestingly novel toughening mechanisms were observed that show GPL wrapping and anchoring themselves around individual ceramic grains to resist sheet-pullout. The resulting cage-like graphene structures that encapsulate the individual grains were observed to deflect propagating cracks in not just two- but three-dimensions.

2:20 PM

**(ICACC-S8-021-2012) Contribution to the understanding of the microstructure of first generation Si-C-O fibers**

F. Teyssandier\*, G. Puyoo, S. Mazerat, G. Chollon, R. Paillet, J. Leyssale, Collège de France, France, Collège de France, France University of Bordeaux I, France; F. Babonneau, Collège de France, France

As compared to the most recent SiC-based ceramic fibers, first generation fibers include a significant amount of oxygen and free carbon. Though a large number of papers have been devoted to understanding the microstructure of these fibers, their composition and microstructure are still controversial. This communication is intended to propose a microstructure description of these fibers according to their composition in the Si-C-O isothermal section of the phase diagram. The proposed microstructure is deduced from a large set of characterizations including XRD, Raman, RMN, Auger, XPS, elemental analysis, HRTEM and molecular dynamics simulation. Three NICALON and four TYRANNO fibers are thus characterized. Their oxidation behavior is also presented and discussed.

2:40 PM

**(ICACC-S8-022-2012) Direct 3D printing of composite microstructures**

N. R. Philips\*, B. G. Compton, N. Reilly-Shapiro, M. R. Begley, UCSB, USA

3D inkjet printing allows direct mesostructural control at the micron length scale. Mechanical properties can be tuned for specific applications. The technique is applicable to the wide range of materials enabled by colloidal processing and is directly extendable to large scale fabrication. A current target is the brick and mortar synthetic composites (similar to nacre). With proper tailoring of brick sizes and mortar properties, synthetics can be made to outperform lightweight metals such as aluminum and magnesium. This poster will address existing deposition capabilities and challenges as they relate to microstructure and mechanical properties of an aluminum oxide model system.

**SPS and Micro-Wave Assisted Technology**

Room: Coquina Salon A

Session Chairs: Erica Corral, University of Arizona; Jow-Lay Huang, National Cheng-Kung University

3:20 PM

**(ICACC-S8-023-2012) Study on spark-plasma-sintered beta-Si<sub>3</sub>N<sub>4</sub> based nanocomposites (Invited)**

J. Huang\*, C. Lee, National Cheng-Kung University, Taiwan; H. Lu, 2 Department of Mechanical Engineering, National Chin-Yi University of Technology, Taiping, Taichung 411, Taiwan, Republic of China, Taiwan; P. Nayak, National Cheng-Kung University, Taiwan

A series of  $\beta$ -Si<sub>3</sub>N<sub>4</sub> based nanocomposites were sintered by spark plasma sintering (SPS), and their microstructures were controlled based on the characteristics of rapid heating rate and pulse current in SPS. First, the effect of heating rate on microstructural evolution of monolithic  $\beta$ -Si<sub>3</sub>N<sub>4</sub> is estimated. At a slower heating rate ( $\leq 100$  degree C/min), the nanosized grains are maintained; while anisotropic grain growth is accelerated by applying a rapid heating cycle (200 degree C/min). In addition, the presence of Morie fringes and dislocations have further confirmed that the grain coalescence is one of the possible mechanisms of grain coarsening. After that, the conductive nano-TiC and TiN were incorporated into  $\beta$ -Si<sub>3</sub>N<sub>4</sub>-based nanoceramic. It is found that the  $\beta$ -Si<sub>3</sub>N<sub>4</sub>-based composite containing 5 wt% nano-TiC shows a larger average grain size and aspect ratio compared to monolithic  $\beta$ -Si<sub>3</sub>N<sub>4</sub>-based ceramic. This is possibly because of a leakage current hop across the conductive TiC based grains and causes Joule heating during sintering. This is contrary to the conventional sintering behavior of Si<sub>3</sub>N<sub>4</sub>. By incorporating nanosized TiC and TiN, the pinning effect of the titanium-based phase significantly suppresses the grain growth of  $\beta$ -Si<sub>3</sub>N<sub>4</sub> matrix grains, and a

series of  $\beta$ -Si<sub>3</sub>N<sub>4</sub>-based nanocomposites are thus fabricated successfully in the present study.

3:40 PM

**(ICACC-S8-024-2012) Critical Analysis of Spark Plasma Sintering Scale-up Processing and Production of Complex Shape Parts Assisted by Spark Plasma Joining**

W. Pinc\*, L. S. Walker, University of Arizona, USA; D. Fredrick, Thermal Technologies, USA; E. Corral, University of Arizona, USA

Spark plasma sintering (SPS) uses direct current to rapidly consolidate a wide range of ceramic and metal powders using high temperatures, fast heating rates and high pressure. Despite these advantages of SPS over conventional densification methods, it is not widely used in industrial processes due to concerns about the ability of SPS to produce large, complex shape parts. In study we investigate two specific concerns with SPS scale-up processing of simple geometry parts which are: 1) power requirements for systematically increasing part diameter at elevated temperature and 2) retention of homogenous properties across the diameter of large scale parts. In addition, we investigate methods to enable complex near-net-shape part production with a combination of SPS and spark plasma joining. In order to study scale-up processing and near-net shape complex part production we chose to investigate using ZrB<sub>2</sub>-SiC composite materials due to their high temperature densification (> 1800°C) requirements and their potential use in application as thermal protection system materials. The results of this study will show how to process of larger, complex shaped parts with SPS while maintaining uniform material properties.

4:00 PM

**(ICACC-S8-025-2012) Optical Transparent Nano-structured and Nano-composite Ceramics Prepared by Spark Plasma Sintering**

J. Liu\*, University of California, USA; W. Yao, A. K. Mukherjee, OSRAM SYLVANIA INC., USA

The development of optical transparent nano-structured and nano-composite ceramics has attracted lots of attention due to their excellent optical, mechanical, and functional properties. The applications based on the optical transparent ceramics have been widely spread out quickly. Few new sintering techniques have been recently developed to efficiently prepare the transparent nano-ceramics, such as: spark plasma sintering (SPS) and hot isostatic press. A series of nano-structured and nano-composite transparent ceramics were successfully obtained by SPS, such as: Al<sub>2</sub>O<sub>3</sub>, MgAl<sub>2</sub>O<sub>4</sub>, MgO-Y<sub>2</sub>O<sub>3</sub>, BaTiO<sub>3</sub> and SrTiO<sub>3</sub>. The obtained optical transparent ceramics exhibit both of excellent optical and functional properties. An example is the transparent BaTiO<sub>3</sub> and SrTiO<sub>3</sub> ceramics showed excellent optical properties in both visible and infrared wavelength ranges, and relatively low, and almost temperature independent, permittivity and dielectric loss. This success highlights the potential industry applications of SPS on preparing of optical transparent ceramics.

4:20 PM

**(ICACC-S8-026-2012) In situ carbon nanotube reinforced ceramics via Microwave Assist Technology sintering**

S. M. Allan\*, F. J. Cabe, Ceralink Inc., USA; A. Datye, Florida International University, USA; M. L. Fall, Ceralink Inc., USA; A. Zaretski, K. H. Wu, Florida International University, USA; H. S. Shulman, Ceralink Inc., USA

Microwave Assist Technology (MAT) sintering was used to process alumina and zirconia ceramics with carbon nanotube reinforcement. In-situ carbon nanotube reinforcement was previously demonstrated to yield significant improvements in thermal conductivity and mechanical properties for alumina and zirconia sintered by spark plasma sintering. Carbon nanotubes were grown directly on the ceramic powder surfaces using a vapor deposition process, prior to formation of green body ceramics. The MAT sintering used a combination of electric radiant heat with 2.45 GHz microwaves to provide fast, uni-



form heating of the nanotube reinforced ceramics. Analysis of sintering included density analysis using Archimedes, hardness, thermal conductivity, and microstructure. Microwave sintering will be compared to spark plasma sintering and pressureless sintering performed in previous studies of the zirconia-CNT and alumina-CNT ceramic systems.

**4:40 PM**

**(ICACC-S8-028-2012) FAST Processing of SiC Monolithics and Fiber Reinforced SiC Composites**

S. Gephart\*, J. Singh, A. Kulkarni, Penn State University, USA; R. Shinavski, Hyper-Therm High-Temperature Composites, Inc, USA; A. Calomino, D. Brewer, NASA - Langley Research Center, USA

Field Assisted Sintering Technology (FAST), also known in literature as Spark Plasma Sintering (SPS), is a relatively new technique ideal for sintering high temperature ceramics due to high heating/cooling rates and short processing cycles. SiC is a logical candidate for many applications due to its unique material properties, especially its high hardness and heat resistance at high temperatures. However, it has been well established in literature that sintering of silicon carbide (SiC) to near theoretical density is difficult using conventional methods and require prolonged exposure to high temperatures resulting in large grain growth which lower its performance. This study is focused on sintering of SiC by FAST. In addition, FAST has open an opportunity in fabricating fiber reinforced SiC composites to desired density by controlling various process parameters including temperature, pressure, heating rate and sintering time. Selective results will be shared including hardness, grain-size, flexural strength, and microstructures of SiC and fiber reinforced SiC-composite.

## S9: Porous Ceramics: Novel Developments and Applications

### Structure and Properties of Porous Ceramics II

Room: Coquina Salon C

Session Chair: Thomas Watkins, ORNL

**1:30 PM**

**(ICACC-S9-023-2012) Photoactivities of Porous PEO Coatings on Titanium Plates and Wire Meshes**

L. K. Mirelman\*, B. Clyne, C. Dunleavy, J. Curran, University of Cambridge, United Kingdom

Plasma Electrolytic Oxidation (PEO) offers promise for the production of TiO<sub>2</sub> photoactive surfaces, with the versatility of the production process giving scope for tailoring of microstructural features such as pore size and density, phase constitution, impurity content etc. High purity titanium substrates have been used in the form of plate and wire-based mesh. The PEO coatings were found to predominantly comprise anatase crystal structure, which is known to be beneficial in terms of the efficiency of functioning as a photocatalyst under ultraviolet light. Microstructures and compositions were investigated using a variety of techniques including Scanning Electron Microscopy (SEM) with Energy Dispersive Spectroscopy (EDS), X-ray diffraction with Rietveld analysis and Raman spectroscopy. These studies confirmed that the crystallinity was typically above 90%, while porosity, mainly in the form of fine inter-connected networks of pores, were of the order of 15-20%. These features are expected to be beneficial in terms of photocatalytic efficiency. Work has been carried out on degradation rates of a commercial dye under UV illumination, using the coatings as catalysts, and a study made of the effects of PEO processing conditions, and of the effect of using a mesh, rather than a solid plate, as the substrate. Correlations have been established between these differences and microstructural features.

**1:50 PM**

**(ICACC-S9-024-2012) The Effect of the Water-Silica Interface on Enhanced Proton Transport**

G. K. Lockwood\*, S. H. Garofalini, Rutgers, the State University of New Jersey, USA

Electrochemical studies have shown enhanced proton transport in mesoporous silica containing water, but modeling the kinetic processes underpinning this phenomenon requires molecular simulations that capture both the structural complexity of mesoporous silica and the dissociative properties of water at interfaces. To this end, we have employed a dissociative water potential that matches many properties of bulk and nanoconfined water as well as the chemisorptive behavior of water at the silica surface, and we have simulated the enhanced formation of hydronium ions at these surfaces and shown behavior consistent with ab initio molecular dynamics simulations. In addition to showing the formation of surface silanol (SiOH) sites where protons are strongly bound, our simulations have revealed additional weakly binding proton adsorption sites on the silica surface. These sites contribute to enhanced proton transport beyond that observed in the nanoconfined water phase alone. Thus, this enhanced proton conduction in hydrated mesoporous silica is affected by surface chemistry and topology, and the details of our findings will be discussed.

**2:10 PM**

**(ICACC-S9-025-2012) Intentionally Porous Alumina and Aluminates**

M. Vadala\*, D. C. Lupascu, University of Duisburg Essen, Germany

BaAl<sub>2</sub>O<sub>4</sub> and SrAl<sub>2</sub>O<sub>4</sub> are compounds for the preparation of long lasting phosphor materials with good luminescence properties, such as high initial luminescence intensity, long lasting performance, suitable emitting colour and chemical stability. Recently, barium and strontium aluminates and their related hydrates have also been used as binders for ceramics and refractories. Rare earth doped aluminates serve as an important class of phosphors for phosphorescence lamps and similar applications. It is possible to synthesize these compounds via the conventional solid-state reaction process, using oxides as starting materials. A solid-state reaction process leads to aluminates powders, which are then mixed and sintered to ensure phase formation. In this study we report about BaAl<sub>2</sub>O<sub>4</sub> and SrAl<sub>2</sub>O<sub>4</sub> aluminates and porous light-weight alumina mixtures Al<sub>2</sub>O<sub>3</sub> (95%) + SrCO<sub>3</sub> (5%) and Al<sub>2</sub>O<sub>3</sub> (95%) + BaCO<sub>3</sub> (5%) for use in long lasting glow materials. The compounds were synthesized via solid state reaction, followed by a milling process and then doped. Scanning electron microscopy, porosity and luminescence measurements were carried out. Different values of the surface area and the porosity were generated for the alumina and the aluminates.

**2:30 PM**

**(ICACC-S9-026-2012) Characterizing the Reduction of Ni<sub>x</sub>Mg<sub>1-x</sub>Al<sub>2</sub>O<sub>4</sub>**

B. E. Hill\*, M. E. Miller, K. C. Glass, S. T. Mixture, Alfred University, USA

Treatment of Ni<sub>x</sub>Mg<sub>1-x</sub>Al<sub>2</sub>O<sub>4</sub> with H<sub>2</sub> results in the progressive reduction of Ni with increasing temperature. The resulting cermet is of interest for gas separation and catalytic applications. For compositions  $x < 0.5$ , it has been shown that the vacancy rich spinel structure remains stable with all Ni<sup>2+</sup> removed, up to at least 1000 °C. For compositions  $x = 0.75$  and  $x = 1$ , the spinel phase becomes unstable when approaching full reduction, and forms a transition alumina phase. The addition of a small amount of ZrO<sub>2</sub> (2.5 weight %) has been found to suppress this phase transition and maintain the spinel structure. The formation of a charge compensating oxygen vacancy accompanies the transition of Ni<sup>2+</sup> to Ni<sup>0</sup>. This will be demonstrated through the use of helium pycnometry and in-situ thermogravimetric analysis under flowing hydrogen. Rietveld refinement of room temperature and in-situ high temperature X-ray diffraction data will provide structural and phase fraction information. In-situ TGA gives confirmation of

the refined Ni metal phase fraction by monitoring a mass change due to oxygen evolution. A detailed picture of structural changes, vacancy formation and phase development as a function of composition and reduction temperature will be demonstrated by Rietveld refinement of X-ray diffraction data, He pycnometry, TGA, and in-situ high temperature X-ray diffraction under flowing hydrogen.

### **Mechanical Properties of Porous Ceramics**

Room: Coquina Salon C

Session Chair: Monika Backhaus-Ricoult, Corning Incorporated

#### **3:10 PM**

##### **(ICACC-S9-027-2012) Fracture Toughness of Porous SiC at Elevated Temperature (Invited)**

T. R. Watkins\*, K. J. Wright, A. Shyam, ORNL, USA; R. J. Stafford, Cummins Inc, USA

As diesel particulate filters operate over a range of temperatures, mechanical properties for these porous materials need to be measured to design against failure at elevated temperature. Fracture toughness measurements of porous silicon carbide were performed at temperatures up to 900°C in laboratory air using the double torsion testing methodology. The double torsion tests were performed on rectangular plate specimens fabricated from walls of honeycomb aftertreatment devices. The fracture toughness values were found to be  $0.42 \pm 0.05$ ,  $0.55 \pm 0.03$ ,  $0.90 \pm 0.18$  and  $0.72 \pm 0.20$  MPa $\sqrt{m}$  at 20, 500, 800 and 900°C, respectively. Potential mechanisms for the increase in toughness at elevated temperature will be discussed based on fracture surface observations.

#### **3:40 PM**

##### **(ICACC-S9-028-2012) Failure Stress and Apparent Elastic Modulus of Diesel Particulate Filter Ceramics**

A. A. Wereszczak, E. E. Fox\*, M. J. Lance, Oak Ridge National Lab, USA

Three established mechanical test specimen geometries and methods used to evaluate properties of brittle materials were adapted to the diesel particulate filter (DPF) to evaluate failure initiation stress and apparent elastic modulus of the DPF's ceramics. Testing of the DPF biaxial flexure disk produces a radial tensile stress and crack plane parallel with the DPF's longitudinal axis. Testing of the DPF o-ring specimen produces hoop tension at the DPF's outer diameter (OD) and inner diameter of the test coupon, and crack plane parallel to the DPF's longitudinal axis. Testing of the DPF sectored flexural specimen produces axial tension at the DPF's OD and crack plane perpendicular to the DPF's longitudinal axis. Testing also enables the determination of apparent elastic modulus of the DPF ceramic material. Results show that the apparent elastic modulus of the DPF ceramics is less (e.g. up to an order of magnitude less) than that estimated using sonic- or resonance-based methods. These geometries, stress states, and modes of crack initiation are discussed in context to the DPF's symmetry along with each specimen's ease of fabrication, testing, failure stress determination, viability, and prospects for test standardization. Last, an explanation is offered for why the elastic modulus is relatively low and why their low values are more accurate for predicting thermomechanical stresses in DPFs.

#### **4:00 PM**

##### **(ICACC-S9-029-2012) Strengthening technique of porous alumina using a TEOS solution treatment**

S. Hashimoto\*, R. Hanai, Y. Ito, S. Honda, Y. Iwamoto, Nagoya Institute of Technology, Japan

Porous alumina ceramics have been proposed for high temperature insulators such as porous clinkers in iron and steel-making refractories. Novel refractories with porous clinkers are able to easily maintain a high temperature inside the furnace, which leads to lowered energy cost in the case of steel-making. In order to fabricate porous alumina with excellent properties, anisotropic alumina particles, namely platelets are desirable. Starting powder mixture consisting of

platelets, sintering additive of fine alumina and pore former of corn starch (85 : 10 : 5 in mass ratio) was prepared. The uniaxial pressure in fabricating the green compact body by powder mixture had an influence on the porosity of the alumina body after heating. When green compacts, which had been uniaxially pressed at 1 and 3 MPa, were heated at 1400 C for 1 h, the average porosity and the average compressive strength of the resulting alumina bodies were 66.0 and 63.0%, and 4.6 and 6.3 MPa, respectively. In an attempt to increase the mechanical property of these porous alumina bodies, TEOS (tetraethyl orthosilicate) solution treatment was performed, followed by reheating to 1400 C for 1 h. When a 1.0 mol/l solution was used, the compressive strength of the porous alumina body uniaxially pressed at 1 MPa increased from 4.6 MPa (without solution treatment) to 10.2 MPa, remaining the porosity 65%.

#### **4:20 PM**

##### **(ICACC-S9-030-2012) Elastic Modulus of Porous Cordierite by Flexure Test Method Compared to Sonic/Resonance Test Methods**

R. Stafford\*, K. Golovin, Cummins, Inc, USA; A. Dickinson, Cummins, Inc., USA; T. Watkins, A. Shyam, Oak Ridge National Laboratory, USA

Previous work showed differences in apparent elastic modulus between mechanical flexure testing and sonic/resonance methods. Flexure tests have been conducted using non-contact optical systems to directly measure deflection for calculation of elastic modulus. Sonic and resonance test methods for elastic modulus measurement were conducted on the same material for comparison. The results show significant difference in the apparent elastic modulus for mechanical versus sonic/resonance methods. The significance of the difference in apparent elastic modulus on thermal stress and the hypotheses for these differences will be discussed. Acknowledgement: Research at Oak Ridge National Laboratory was sponsored by the U.S. Department of Energy, Assistant Secretary for Energy Efficiency and Renewable Energy, Office of Vehicle Technologies, as part of the Propulsion Materials Program. Some of the equipment and instrumentation utilized during this investigation was acquired and maintained by the Oak Ridge National Laboratory's High Temperature Materials Laboratory User Program, which is sponsored by the U. S. Department of Energy, Office of Energy Efficiency and Renewable Energy, Vehicle Technologies Program.

#### **4:40 PM**

##### **(ICACC-S9-031-2012) Crack growth during double torsion fracture toughness testing of machined honeycomb ceramics**

J. Zimmermann\*, K. Hoff, J. Westbrook, G. Morgan, T. Meyer, Corning, USA

Crack displacement was captured using high speed videography during a double torsion fracture toughness test in an experimental porous aluminum titanate based ceramic. Double torsion fracture toughness tests have recently been used to evaluate porous ceramics, specifically within the diesel particulate filter industry. Crack velocities and crack paths were evaluated. Specimens were produced from a 300 cells per square inch with wall thicknesses of 330 micrometers (300/13) honeycomb geometry.

#### **5:00 PM**

##### **(ICACC-S9-032-2012) Converting macro to micro-stress and strain in porous and in microcracked ceramics**

G. Bruno\*, Corning Inc., USA; A. N. Levandovskiy, A. M. Efremov, Corning OOO, Russian Federation

We propose an analytical model, capable of distinguishing the contribution of porosity, pore morphology, solid domain stiffness, and microcracking to the macroscopic elastic response of porous ceramics. This model can be used for the evaluation of the dense material properties, making use of microscopic information, such as in-situ neutron diffraction experiments, which reveal the average values of both Young's (E) modulus and Poisson ratio ( $\nu$ ) for the dense domain, and of the pore morphology factor. Extended to microcracked ceramics,

the method can predict the evolution of E with applied load, using the integrity factor. The approach is validated on porous SiC and sintered alumina, and microcracked cordierite. Finite Element Modeling allows calculating the 3D strain and stress under applied uniaxial stress. Stress-strain curves of porous and thermally microcracked materials are generated. FEM can then be used for quantitative prediction of the materials strength and material effective properties variation with the development of thermal microcracks. FEM predictions coincide well with analytical calculations, thus corroborating the validity of the model.

## S14: Advanced Materials and Technologies for Rechargeable Batteries

### Ceramics for Electric Energy Generation, Storage, and Distribution

Room: Coquina Salon H

Session Chairs: Michael Lanagan, Penn State University; Gunnar Westin, Uppsala University

1:30 PM

#### (ICACC-S14-018-2012) High Energy Glass Composites for Pulse Power and Power Electronic Applications (Invited)

M. Lanagan\*, Penn State University, USA

Pulsed power and power electronic systems for energy storage and distribution will require capacitors with higher voltage while maintaining high capacitance. The research challenge can be distilled into a single figure-of-merit, energy density, which captures the materials properties of relative dielectric permittivity and dielectric breakdown strength. Thin glass layers have recently demonstrated very high energy densities ( $> 20$  J/cc) and high temperature stability ( $> 200^\circ\text{C}$ ). This presentation will address the intrinsic and extrinsic contributions to dielectric breakdown strength in glass. In addition, polymer coatings on the glass have been shown to promote self-healing and extend capacitor life after a catastrophic breakdown event. Ceramic materials and composites will be compared in terms of their theoretical energy densities as well as methods to increase high temperature reliability. Large-scale fabrication and characterization glass capacitors will also be presented.

2:00 PM

#### (ICACC-S14-019-2012) Thermoelectric Properties of Selected Phases in the System $\text{Zn}_x\text{In}_y\text{O}_x+1.5y$

M. Amani\*, I. M. Tougas, O. J. Gregory, Department of Chemical Engineering, USA

Combinatorial chemistry techniques were used to rapidly screen materials in the system  $\text{Zn}_x\text{In}_y\text{O}_x+1.5y$  to identify phases and compositions with optimal thermoelectric properties. Zinc rich homologous phases in this system  $(\text{In}_2\text{O}_3)(\text{ZnO})_k$ , ( $k = 3, 4, 5, 7, 9, 11, \text{ and } 15$ ) have been extensively studied for this purpose; however, relatively little experimental work has been performed on phases based in the indium rich end of the system. Furthermore, recent simulations on the  $k = 1$  and 2 phases, which have proven difficult to synthesize, suggest that they have promising thermoelectric properties. Therefore, co-sputtering techniques were employed to form gradients of indium and zinc oxides with smoothly varying compositions. Thermoelectric libraries were fabricated on alumina substrates by patterning them to form hundreds of micro-thermocouples which could be rapidly screened at room temperature for electrical resistivity, Seebeck coefficient, and thermoelectric power factor. These libraries were fully characterized in terms of both composition and heat treatment in nitrogen and air. Bulk ceramics were synthesized from the down-selected materials and their thermoelectric figure of merit was determined as a function of temperature up to  $1050^\circ\text{C}$ .

2:20 PM

#### (ICACC-S14-020-2012) Flexible $\text{Zn}_2\text{SnO}_4/\text{MnO}_2$ Core/shell Nanocable - Carbon Microfiber Hybrid Composites for High Performance Supercapacitor Electrodes

L. Bao, J. Zang, X. Li\*, University of South Carolina, USA

We demonstrate the design and fabrication of a novel flexible nanoarchitecture by facile coating ultra-thin (several nanometers thick) films of  $\text{MnO}_2$  to highly electrical conductive  $\text{Zn}_2\text{SnO}_4$  (ZTO) nanowires grown radially on carbon microfiber (CMFs) to achieve high specific capacitance, high energy density, high power density, and long-term life for supercapacitor electrode applications. The crystalline ZTO nanowires grown on CMFs were uniquely served as highly conductive cores to support a highly electrolytic accessible surface area of redox active  $\text{MnO}_2$  shells and also provide reliable electrical connections to the  $\text{MnO}_2$  shells. The maximum specific capacitances of  $621.6$  F/g (based on pristine  $\text{MnO}_2$ ) by cyclic voltammetry (CV) at a scan rate of  $2$  mV/s and  $642.4$  F/g by chronopotentiometry at a current density of  $1$  A/g were achieved in  $1$  M  $\text{Na}_2\text{SO}_4$  aqueous solution. The hybrid  $\text{MnO}_2/\text{ZTO}/\text{CMF}$  hybrid composite also exhibited excellent rate capability with specific energy of  $36.8$  Wh/kg and specific power of  $32$  kW/kg at current density of  $40$  A/g, respectively, and good long-term cycling stability (only  $1.2\%$  loss of its initial specific capacitance after  $1000$  cycles). These results suggest that such  $\text{MnO}_2/\text{ZTO}/\text{CF}$  hybrid composite architecture is very promising for next generation high performance supercapacitors.

2:40 PM

#### (ICACC-S14-021-2012) Highly efficient spectrally selective solar thermal absorbers by solution processing

G. Westin\*, Uppsala University, Sweden; K. Jansson, Stockholm University, Sweden

Composites consisting of nano-sized metal inclusions in ceramic matrixes are of great interest for many technological applications, such as catalysts, magnetic response materials, transformers, memories, light-weight structural ceramics, durable coatings and spectrally selective solar heat absorbers. Many of these applications require efficient processing lines able to produce nano-materials of complex compositions with optimized micro-structures. Solution based processes provide versatile and efficient routes to complex nano-materials in all shapes such as nano-powders, sponges and thin films. The often direct and simple processing allows for technological exploitation of the processes without the use of complex and size and shape limiting equipment. Here a low cost solution based routes to homo- and heterometallic metallic nano-inclusion materials will be described. Composites with metal particle sizes down to  $2\text{-}5$  nm and metal particle loadings up to  $95\%$  in the ceramic matrix as thin films or highly porous powders will be described for different elemental combinations of matrix and metal inclusions. The  $\text{Ni-Al}_2\text{O}_3$  composite films were optimized as spectrally selective solar heat absorbers with better absorption properties than reported in the literature, as far as we can find, ( $A=97\%$  and  $E=5\%$  at  $100^\circ\text{C}$ ). The process has been scaled up to produce  $50$  bands in a roll-to-roll process.

3:20 PM

#### (ICACC-S14-022-2012) Mesoporous Pseudocapacitive Electrode Materials

B. Saruhan-Brings\*, S. Özkan, Y. Gönüllü, German Aerospace Center, Germany

Electric batteries take long time to re-charge but store greater charges, while capacitors can be charged very rapidly, but suffer from lower energy densities. With new electrodes which introduce pseudo-capacitance and higher surface area, super-capacitors charge rapidly, supply longer energy and have higher energy densities. These features are desirable for a range of applications, in electric vehicles and storage for renewable energy supplies such as wind power which can come in short bursts. Other applications of

super-capacitors and more specifically pseudo-capacitors that combine features of both rechargeable battery and standard capacitor are in mobile digital technologies and flash photography. This work demonstrates the fabrication of mesoporous films by anodisation of metallic plates to yield nano-structuring and/or by anodic deposition, resulting in impressive charge storage behaviour relying on combination of atomic- and nano-scale structures in films. The redox pseudo-capacitance of films is analysed by means of cyclic voltammeter measurements. Capacitive charge-storage properties of mesoporous films made of complex metal-oxides in core + shell architecture are superior to those of non-porous crystalline metal-oxides. Combination of aligned nano-structures (titania) with nano-crystalline redox capable oxides (such as Mn, Co, Ni, Li etc.) may yield intercalating lattice formation to introduce enhanced capacitance.

3:40 PM

### (ICACC-S14-023-2012) Thermal conductivity reduction and thermoelectric performance of ZnO by Multinary Doping

M. Ohtaki\*, Y. Iwano, Kyushu University, Japan

Multinary doping of ZnO with Al and another elements is investigated in order to reduce  $k$ , the phonon part of  $k$ . We have already reported that binary doping of ZnO with Al and Ga significantly reduces  $k$  maintaining fairly high  $S$  values with a metallic temperature dependence, leading to a maximum ZT value of 0.65 at 1247 K. Here we report that binary doping of Al and Cu results in further intense and anomalous reduction of  $k$ , from 40 W/m K for Zn<sub>0.98</sub>Al<sub>0.02</sub>O down to 9 W/m K for Zn<sub>0.96</sub>Al<sub>0.02</sub>Cu<sub>0.02</sub>O at room temperature. Whereas the Al+Cu binary doping strongly deteriorates the electrical conductivity, an additional doping with Ga is found to be successful to recover the  $S$  values. Consequently, the trinary doped sample of Zn<sub>0.96</sub>Al<sub>0.02</sub>Cu<sub>0.01</sub>Ga<sub>0.01</sub>O shows a ZT value of 0.59 at 1237 K. Interestingly, the reduction in  $k$  is twice or more larger by the Cu co-doping than by the Ga co-doping. Investigation of the reduction mechanism of  $k$  is currently underway as well as that to pursue concurrent achievement of high  $S$  and low  $k$ .

4:00 PM

### (ICACC-S14-024-2012) Nanoscale Defect Engineering for High Critical Currents in Epitaxial High Temperature Superconducting (HTS) Tapes

V. Selvamanickam\*, University of Houston, USA; Y. Chen, SuperPower, USA; G. Majkic, S. Tuo, Y. Yao, Y. Bi, X. Tao, N. Khatri, E. Galtsyan, University of Houston, USA; S. Sambandam, SuperPower, USA

HTS thin films grown epitaxially on biaxially-textured templates on flexible metal substrates have been successfully demonstrated as a viable approach to fabricate high performance superconducting tapes for energy applications. We are using a Metal Organic Chemical Vapor Deposition to deposit RE-Ba-Cu-O thin films (RE = rare earth) on a stack of oxide films on a flexible Hastelloy substrate. Since most applications that employ HTS involve high magnetic fields, it is essential that high critical currents are achieved in HTS films in such fields. We have successfully used a self-assembly process to create nanocolumnar defects in RE-Ba-Cu-O films to improve flux pinning in high magnetic fields. Such nanocolumnar defect structures have resulted in more than a two-fold improvement in in-field performance over a range of magnetic fields, temperatures, and field orientations. This improvement in in-field performance was successfully transferred to long-length manufacturing. Additionally, by modification of rare-earth type (RE = Y, Gd, Sm) and content, nanoscale defects have been created along the length of the tape resulting in improved in-field performance in this field orientation. In this presentation, we will discuss engineering of nanoscale defects within epitaxial superconducting films and its impact on critical currents in high magnetic fields.

4:20 PM

### (ICACC-S14-025-2012) Fabrication of 2D/3D Nanostructures using Polymer/Inorganic Nanospheres for Energy Conversion Applications (Invited)

K. Fung\*, C. Ni, National Cheng Kung University, Taiwan

Nanospheres of different materials may be used as a template or a mask to produce nanostructures with unique properties. In this study, PMMA nanospheres were used as the template to fabricate the macroporous Ni/YSZ cermet to be used as the anode of the solid oxide fuel cell. PMMA nanospheres were first impregnated with precursors followed by heating at 1000°C. After removal of PMMA nanospheres, macroporous Ni/YSZ formed with specific surface area as high as 21.64m<sup>2</sup>/g after reduction in H<sub>2</sub>. The methane conversion of Ni/YSZ anode derived from PMMA nanospheres achieved 79% at 900°C. Furthermore, silica nanospheres were used as the mask to fabricate the nanopattern on a glass substrate. First, the monodispersed silica (SiO<sub>2</sub>) nanospheres were uniformly coated on a glass substrate and followed by reactive ion etching (RIE). After RIE etching, the lateral dimensions of pattern varied from 490nm to 620nm depending upon the size of nanospheres. The behavior of light transmitting through this glass substrate was significantly affected by the surface structure of the glass. A TCO thin film was further sputter-coated on the patterned glass substrates using nanosphere lithography method. The results showed that the Haze value of this conducting glass was enhanced to about 10%~15% that is required for thin film solar cell applications in visible wavelength range.

4:40 PM

### (ICACC-S14-026-2012) Improvement of Calcium Cobaltate Thermoelectric Performance by Silver Doping

J. Selig, S. Lin\*, Lamar University, USA; H. Lin, H. Wang, Oak Ridge National Laboratory, USA

Silver doped calcium cobaltate powders (Ca<sub>1-2x</sub>Ag<sub>x</sub>Co<sub>1.62</sub>O<sub>3.86</sub>, x = 0.00 - 0.12) were prepared by Self-propagating High-temperature Synthesis (SHS). SHS process uses a highly exothermic reaction to produce a solid product. Reactant powders are consolidated to a pellet and ignited by an external heat source. After the ignition, the heat released from the reaction is sufficient to sustain the movement of the reaction front until the reactant is completely converted into the product. To study the reaction mechanism, TG-DSC analysis was performed on the reaction mixture to establish the reaction mechanism. Standard SHS variables were investigated, including pellet diameter, density, and oxygen flow rate. K type thermocouples and a short wavelength IR camera were used to measure the temperature history at the pellet centerline and surface temperature during the combustion to determine the velocity of combustion front movement. Products were characterized by XRD for phase purity and SEM for particle size. A planetary mill was used to reduce particle size and increase the specific surface area of produced powders. Our results show that SHS can economically produce thermoelectric oxides with high ZT values and the thermal conductivity of calcium cobaltate decreases when silver is doped to replace calcium.

## FS2: Computational Design, Modeling, and Simulation of Ceramics and Composites

### Novel Simulation Method and Virtual Material Design

Room: Ponce de Leon

Session Chairs: Jian Luo, Clemson Univ; John Lawson, NASA Ames Research Center

1:30 PM

### (ICACC-FS2-020-2012) Kinetic Monte Carlo Simulation of Oxygen Diffusion in Doped Zirconia-Based Materials (Invited)

B. S. Good\*, NASA Glenn Research Center, USA

The thermal stability and low thermal conductivity of yttria-stabilized zirconia (YSZ) is of interest for a variety of technological applications, notably thermal barrier coatings and fuel cell solid state electrolytes. In both applications, oxygen diffusion is of concern. We have

performed kinetic Monte Carlo (kMC) computer simulations of oxygen diffusion in YSZ and similar zirconia-based compounds doped with aliovalent cations. Diffusion barriers consist of pairs of nearest-neighbor cations, and we compute barrier energies using density functional theory. It is usual in such kMC simulations to distribute dopant cations randomly within the computational cell. However, for atoms in any particular species pair it may be energetically favorable for the atoms to either occupy nearest-neighbor positions, or alternatively, to remain isolated. We compute the pairing energetics, and use the results in an additional pre-kMC Metropolis Monte Carlo stage in which the dopants are distributed via species pair exchange. The probabilities of various barrier pair species combinations are obtained from these simulations and used in traditional kMC simulations, from which we obtain results on the dependence of oxygen diffusivity on dopant concentration and temperature.

### 2:00 PM

#### (ICACC-FS2-021-2012) Materials Thermodynamics and Phase Modeling in the Li-Mn-O System (Invited)

H. J. Seifert\*, D. M. Cupid, Karlsruhe Institute of Technology, Germany

The development of advanced lithium ion batteries requires an integrated understanding of the materials thermodynamics and their relationships to electrochemical, thermal and safety cell performances. The system Li-Mn-O encompasses a series of battery active materials which were investigated and thermodynamically modeled in regard to application relevant properties. Additionally the heterogeneous phase equilibria and reactions were investigated and calculated. The results are presented by using different types of phase diagrams, e.g. isothermal sections and potential phase diagrams, respectively. Intensive and extensive thermodynamic properties can be used as diagram axes depending on the particular case of interest. The calculated and experimental data are highly relevant for knowledge-based synthesis and preparation of battery active materials and for electrochemical cell operation. The results with regard to thermodynamic system modeling in the Calphad approach will be shown. In this regard, the crystal chemistry of battery active phases are presented and the influence of nanosize particles on the phase diagram topology will be discussed. The presentation will cover recent results from experimental investigations, theoretical approaches and simulations (ab initio, calphad).

### 2:30 PM

#### (ICACC-FS2-022-2012) Electronic Structure, Bonding, and Optical Properties of Mo Based Alloys in the Mo-Si-B Phase Diagram (Invited)

P. Rulis\*, W. Ching, University of Missouri - Kansas City, USA

Recent progress in the study of the fundamental properties of Molybdenum based alloys from the Mo-Si-B phase diagram will be presented. The ongoing search for materials that can improve the durability and performance of fossil fuel energy conversion systems has strict requirements for materials properties. These alloys are promising candidates for use in coal based power plants operating at elevated temperatures and in corrosive environments. The materials that are focused on in this presentation are MoSi<sub>2</sub>, Mo<sub>3</sub>Si, Mo<sub>5</sub>Si<sub>3</sub>, Mo<sub>5</sub>SiB<sub>2</sub> and Mo<sub>2</sub>B. Mo<sub>3</sub>Si and MoSi<sub>2</sub> are shown to be very stable while Mo<sub>2</sub>B is much less so on the basis of bond order (population overlap) data analysis, electronic structure properties, and charge transfer characteristics. Through such methods, it is expected that the properties and performance attributes of these and other potential materials systems can be judged as a guide to materials processors.

### 3:20 PM

#### (ICACC-FS2-023-2012) Micromechanical Finite Element Simulations and Determination of Effective Properties in Silicon Nitride (Invited)

T. Böhlke\*, J. Wippler, Karlsruhe Institute of Technology, Germany

Silicon nitride is one of the best choices, if a stiff, hard and especially tough material is required for demanding industrial applications. The

aim of our work is to contribute to a better understanding of the reinforcement mechanisms for the fracture behavior of silicon nitride. The intergranular and transgranular crack propagation is, therefore, examined by micromechanical finite element simulations on geometries meant to represent the complex microstructure of silicon nitride. Experimental observations on grain growth and pinning are incorporated into the microstructure generator. The meshes are constructed periodically and used together with a new form of approximate periodic displacement boundary conditions. The constitutive assumptions for the different phases are incorporating thermoelasticity and fracture under maximum principle stresses, whereas the beta-Si<sub>3</sub>N<sub>4</sub> grains are modeled in a transverse-isotropic way. The debonding and post-failure behavior of the grain boundaries is captured by a thermodynamical consistent interface model.

### 3:50 PM

#### (ICACC-FS2-024-2012) A new anisotropic constitutive model for ceramic materials failure

S. Falco\*, C. Dancer, R. Todd, N. Petrinic, University of Oxford, United Kingdom

The lack of understanding of true deformation and failure mechanisms in ceramic materials for armour applications hinders the development of novel materials and the corresponding potential for improved armour solutions. Numerical modelling plays a key role in gaining the required understanding at all relevant length scales. While micro-scale modelling provides new insights into the role of various material characteristics, at the macro-scale such information enables more accurate simulation of the ballistic material behaviour when designing components and structures. Nevertheless, most of the existing macroscopic material models for the numerical simulation of ceramic armour are still based on continuum approaches assuming isotropic material response to impact loading. The constitutive model presented in this work allows for non-isotropic behaviour proposing the tensor damage variable evolution linked directly to the physical properties of crack evolution at lower length scales thus taking into account the discontinuous nature of the material. In the proposed approach, the physical features of cracks and their growth at the grain size level are substituted by explicit simulations, within a multi-scale modelling framework, where macroscopic properties are obtained by numerical homogenization. The constitutive model is compared both against numerical simulations using existing material models and experiments.

### 4:10 PM

#### (ICACC-FS2-025-2012) Inelastic Microstructure Modeling and Design of MMCs with Lamellar Microstructure

R. Piat\*, Y. Sinchuk, Karlsruhe Inst of Technology, Germany

The purposes of this paper are the optimal design and modeling of inelastic behavior of MMCs with lamellar microstructure. The material under consideration consists of the two phases: ceramics (Al<sub>2</sub>O<sub>3</sub>) and aluminum alloy (Al<sub>12</sub>Si) phases. For modeling of the elasto-plastic behavior of the metal the J<sub>2</sub> flow theory was used. The brittle damage model was used for modeling of the failure of the ceramics. Single domain of this material with preferred orientation of lamella was modeled using FE-model and homogenization procedure. Results of the modeling were verified by comparing with experimental data and good corresponding between obtained results was observed. The optimization problem for determination of the sample microstructure with minimal compliance was formulated. The design variables of the posed problem are local orientation of the lamellar domains and the volume fraction of the ceramics in the domain. Solution of the optimization problem is carried out for prescribed volume of the ceramics in the whole specimen. Resulting optimal microstructure were obtained for different geometries of the specimen and for different loading cases. 1. T. Ziegler, A. Neubrand, S. Roy, A. Wanner, R. Piat, Composite Sci. and Tech. 69(5), 620-626 (2009). 2.

J.C. Simo, T.J.R. Hughes, Computational inelasticity (Springer, New York, 2000), p. 392.

**4:30 PM**

**(ICACC-FS2-026-2012) An integrated virtual material approach for ceramic matrix composites**

G. Couegnat\*, W. Ros, T. Haurat, C. Germain, E. Martin, G. L. Vignoles, University of Bordeaux, France

We propose an integrated modeling software suite aiming at a numerical multi-scale simulation of ceramic matrix composites (CMC). This software suite features simulation capabilities for (i) reinforcement weaving design, (ii) matrix infiltration and (iii) mechanical and thermal behavior featuring damage. Numerical methods have been developed either on unstructured meshes or in voxel grid meshes (i.e. plain 3D images), or both. All simulations except matrix deposition by chemical vapour infiltration (CVI) have been developed in Finite Elements formulations; CVI simulation has been coded in random walk algorithms. All simulations are developed in strong relationship with the material microstructure in order to provide a sound basis for experimental validation with respect to actual material samples.

**4:50 PM**

**(ICACC-FS2-027-2012) Microstructure-sensitive extreme value damage response in fully dense ceramic matrix composites with unidirectional plies**

M. Braginsky\*, UES, Inc., USA; C. P. Przybyla, Air Force Research Laboratory, USA

Physically based structure property relations that describe the load induced damage for ceramic matrix composites (CMCs) require an understanding of how the distributed microstructure attributes (e.g., fibers, fiber coatings, defects) influence the damage response. Generally, in materials of engineering significance, the life limiting damage is a function of the extreme value response of the material on the scale of the dominate microstructure attributes. In this work, multiple statistically representative volume elements (SVEs) are instantiated and simulated to sample the microstructure-sensitive extreme value response of fully dense CMCs with unidirectional plies. The load induced damage under various loading conditions is calculated via the XFEM. The distributed microstructure at the locations of the extreme value damage response is described. Correlation functions are applied to quantify the influence of correlated microstructure attributes on the extreme value response.

## FS3: Next Generation Technologies for Innovative Surface Coatings

### Longer Life Solution, Technological Problems and Solutions, and Mass Production

Room: Coquina Salon G

Session Chairs: Jinsam Choi, Gyeongsang National University; Jun Akedo, AIST

**1:30 PM**

**(ICACC-FS3-022-2012) Corrosion protection of non-ferrous metals by SiOxCy(-H) film deposited by atmospheric pressure dielectric barrier discharge (Invited)**

G. Kim, D. Shin, Y. Kim\*, Hanbat National University, Republic of Korea

Aluminum and magnesium alloys can be widely used in automobile, aerospace, and mobile electronics components because of its high strength/weight ratio. However, the non-ferrous alloys have poor corrosion resistance and wear resistance, which restrict its application. The protective organic coating is one of the most convenient methods to greatly improve the corrosion resistance of steels. In this study, we try to deposit SiOxCy(-H) films on the aluminum and magnesium using atmospheric pressure dielectric barrier discharge (DBD) generated by 30 kHz AC to improve their corrosion resistance. The

SiOxCy(-H) films were deposited from a mixture of hexamethylcyclotrisiloxane (HMCTSO), oxygen, and helium. We also used HMDSO as a source of silicon. We investigated the SiOxCy(-H) film properties by Fourier transform infrared spectroscopy (FT-IR), scanning electron microscopy (SEM), atomic force microscopy (AFM), and X-ray photoelectron spectroscopy (XPS). The anti-corrosion behaviors of the coated aluminum and magnesium are evaluated by electrochemical polarization curves. The compositions of SiOxCy(-H) films were controlled from SiOC to SiO<sub>2</sub> by changing flow rates of HMCTSO or HMDSO and oxygen. We will discuss the influences of elemental composition and chemical structure of SiOxCy(-H) films on corrosion behavior of the non-ferrous metals.

**2:00 PM**

**(ICACC-FS3-023-2012) Fabrication of the anisotropic structured BN/Polymer composites with Nanoimprint and Electric Field Process**

T. Nakayama\*, T. Fujihara, H. Cho, S. Endo, H. Kim, Nagaoka University of Technology, Japan; K. Tada, Toyama National College of Technology, Japan; W. Jiang, H. Suematsu, K. Niihara, Nagaoka University of Technology, Japan

The orientation of hexagonal boron nitride (BN) nanosheets was controlled in polymer-based nanocomposite film using microscopic molds while applying a DC electric field. The hexagonal BN nanosheets were dispersed by sonication in a prepolymer mixture of polysiloxane followed by a high speed mixing. The homogeneous suspension was cast on a microscopic mold with different patterns, which is attached to positive electrode during application of electric field before it became cross-linked. Analysis revealed that filament-like linear assemblies of BN nanosheets (LABNs) were fabricated in polysiloxane/BN nanosheet composite films, and BN nanosheets composing LABNs were aligned perpendicular to the film plane with high anisotropy. The anisotropy of BN nanosheets and dimensions of LABNs showed direct relation with thermal property of the composite, and could be changed depending on the type of used microscopic molds. The LABN formation and heat conduction mechanisms induced by the type of microscopic molds and intensity of applied electric fields are discussed.

**2:20 PM**

**(ICACC-FS3-024-2012) Fabrication of De-NOx SCR catalyst over graphene supported vanadium oxides**

H. Kim\*, M. Bae, E. Kim, M. Lee, Korea Institute of Industrial Technology, Republic of Korea

The outstanding properties of graphene make it attractive for applications in various fields. The purpose of this study is to investigate not only the synthesis of a novel graphene supported vanadium oxides as selective catalytic reduction (SCR) catalyst but also the confirmation of the fact of remove effect of De-NOx. The results indicated that vanadium particles were highly dispersed on surface of graphene and made a crystal defect with characters of De-NOx. The structures of the V<sub>2</sub>O<sub>5</sub>/graphene catalysts were characterized by TEM, XRD and the physical-chemical characteristics about measurement of specific area were examined by BET. And then De-NOx evaluation was observed by Micro-Reactor (MR).

**2:40 PM**

**(ICACC-FS3-025-2012) Production of hollow silica nanoparticles as a base material for the functional surface coatings**

T. Hwang, G. Kim\*, Korea Institute of Industrial Technology, Republic of Korea

The structural modification of nanoparticles is becoming more important, since it is believed to give a chance of new functionality otherwise impossible. Among the modifications, the hollow sphere has been a very interesting topic especially in the field of slow-release application. In this work, we successfully prepared hollow spherical nanoparticles of silica with a size ~100 nm from an inverse microemulsion, and we also demonstrated putting smaller silica

nanoparticles of 10 nm in the space. This was done by simply dispersing the nanoparticles in the aqueous phase of microemulsion. By changing the tetraethoxysilane-to-water ration, we could also change the shell thickness of the hollow spheres. The experimental results indicated that the formation of silica shell had started from the border of micelles, and the hollow spheres necessarily trapped the dispersed nanoparticles in the aqueous micelles. We believe this had opened up a possibility of application of the processing technique to the slow-release capsule production.

### 3:20 PM

#### (ICACC-FS3-026-2012) Plasma resistant properties of sol-gel Y<sub>2</sub>O<sub>3</sub> coating on quartz glass windows for semiconductor fabrication equipments

D. Riu\*, Seoul National University of Science and Technology, Republic of Korea; B. Kim, Korea Institute of Industrial Technology, Republic of Korea; C. Oh, KumKang Quartz Co., Republic of Korea

Current semiconductor fabrication processes require extremely low level of particle contaminations from the process chambers for their increased reliability and productivities. As for the high density plasma etching chamber, the windows materials, quartz glasses are used as windows for the chambers. However, during the process, the activated plasma often attacks the window surfaces and easily lose their transparency due to the plasma corrosion related damages. To improve the plasma resistance of the windows, we have applied Y<sub>2</sub>O<sub>3</sub> sol-gel coatings and have evaluated the plasma resistant properties using CF<sub>4</sub>+Ar plasma. Mechanical properties of the Y<sub>2</sub>O<sub>3</sub> coating was also analyzed with nano-indentation and nano-tribometer. We have found that the Y<sub>2</sub>O<sub>3</sub> coating have a superior plasma resistant characteristics and have very good compatibility of the semiconductor process due to its good mechano-tribo-properties.

### 3:40 PM

#### (ICACC-FS3-027-2012) Low-temperature curable TiO<sub>2</sub> paste for the flexible dye-sensitized solar cells

H. Kim\*, J. Park, T. Hwang, Korea Institute of Industrial Technology, Republic of Korea

Dye-sensitized solar cells (DSSC) are attracting more attentions as a next-generation energy harvesting device from research fields and industries as well. The demands are on especially the low-temperature curable TiO<sub>2</sub> for the flexible DSSCs with plastic substrates. Hence, the main purpose of our work is to provide a production method for the paste. We employed the sol-gel chemical method. The production method included synthesis of TiO<sub>2</sub> nanoparticles, formulation of inorganic binder, and stabilization. Importantly, the paste contained no other components than TiO<sub>2</sub>, which is an essential part, since it could avoid the properties' deterioration by the organic binders or stabilizers as in other pastes. Using the paste, we tested the active electrode for a DSSC with a low-temperature curing at < 100 °C. The prepared TiO<sub>2</sub> films were transparent with little haze. The adhesion to an ITO-coated PET was strong enough to build the devices. The XRD analysis revealed the deposited films were mainly in anatase phase. An addition of a small amount of metal nano dots into the paste noticeably enhanced the conversion efficiency, while producing no minus effect on the properties. The experimental results showed that a low-temperature curable TiO<sub>2</sub> paste was successfully synthesized without any organic binders. With the help of metal nano dots' catalytic effect, the conversion efficiency increased even more.

### 4:00 PM

#### (ICACC-FS3-028-2012) Grain orientation control of bismuth layer-structured ferroelectric thick films prepared by aerosol deposition method

M. Suzuki\*, J. Akedo, AIST, Japan

Bismuth layer-structured ferroelectrics (BLSFs) has been regarded as a promising material for applications involving ferroelectric

memories and piezoelectric devices operating at high temperatures due to its large spontaneous polarization (P<sub>s</sub>) and high Curie temperature (T<sub>C</sub>). Since the layered structure leads to a strong anisotropy of the functional properties, it is of great interest to control crystallographic orientation of grains in the form of polycrystalline ceramics and films for achieving superior properties. An aerosol deposition (AD) method, which is based on room temperature impact consolidation (RTIC) phenomena, is attracting attention because it can form thick ceramic layers of simple or complex compositions at a room temperature. In this study, ceramic films of SrBi<sub>2</sub>Ta<sub>2</sub>O<sub>9</sub> (SBTa), Bi<sub>4</sub>Ti<sub>3</sub>O<sub>12</sub> (BiT), SrBi<sub>4</sub>Ti<sub>4</sub>O<sub>15</sub> (SBTi) which are BLSFs family were deposited on glass and Pt/Ti/YSZ substrates by AD method, and their microstructure and polarization properties were investigated. Scanning electron microscopy (SEM) observation revealed that BiT starting raw powder fabricated by a fused salt synthesis had plate-like shaped particles with the size of approximately 1 μm.

### 4:20 PM

#### (ICACC-FS3-029-2012) An Approach to Sinter Yttria Monolith of a Full Density by Using Surface and Interfacial Engineering

J. Choi\*, Gyeongsang National University, Republic of Korea; T. Nakayama, H. Suematsu, Nagaoka University of Technology, Japan; E. Kang, Gyeongsang National University, Republic of Korea

Yttria has widely been used as an additive to enhance the liquid phase sintering of AlN, SiC and SiAlON as well as a stabilizer for zirconia. In recent years, yttria has been attracting huge attention in various semiconductor manufacturing industries because it possesses exceptionally high plasma resistance compared with quartz, alumina and zirconia. For that purpose, large-sized yttria monolithic bodies with a high density are essential, and thus achieving such yttria bodies has been an increasing area of research. In this work, a novel approach to sinter yttria monolith to obtain a full density by using surface and interfacial engineering is presented. The approach includes four steps: coprecipitation with salt bridge from yttria to Y(OH)<sub>3</sub>, modification in surface area by applying nano shape of particles, hot isotatic pressing, and interfacial engineering at grain boundaries by adding dopants such as Gd, Sr, Eu, La, B, Th and P, etc. Interrelationship between surface, interface, grain growth, and defects is discussed in light of achievement of high density yttria bodies.

### 4:40 PM

#### (ICACC-FS3-001-2012) Atomic Layer Deposition of Ru-based Ternary Thin Films for Seedless Copper Electroplating Applications (Invited)

S. Kim\*, Yeungnam University, Republic of Korea

As semiconductor devices are scaled down for better performance and more functionality, Cu-based interconnects suffer from an unwanted increase in the resistivity of the Cu wires due to the size effect on the resistivity of the metal film. One of the solutions to address it is to increase the volume of electroplated-Cu filled into the trench. One can increase the volume of EP-Cu filled into the trench using a thinner but conformal diffusion barrier and seed layer. The portion of Cu in the interconnects structure can be increased further using a direct plating because the electroplating of Cu can be achieved on a diffusion barrier without a seed layer. Ru has been suggested as a diffusion barrier that is compatible with the direct plating of Cu. However, previous studies showed that Ru itself is not a suitable diffusion barrier for Cu metallization due mainly to its poor microstructure with polycrystalline columnar grains. This study developed Ru-based multi-component nanocrystalline thin films with non-columnar grain structure, RuSiN and RuAlO, which are compatible with the direct plating of Cu, using atomic layer deposition (ALD) process. SiN<sub>x</sub> or AlO<sub>x</sub> was incorporated into the Ru by combining the Ru and SiN<sub>x</sub> or AlO<sub>x</sub> ALD cycles, and a ternary thin films, RuSiN and RuAlO, were fabricated and evaluated as diffusion barriers for seedless Cu interconnects.

### FS4: Advanced (Ceramic) Materials and Processing for Photonics and Energy

#### Advanced Materials for Environmental Applications I

Room: Oceanview

Session Chair: J. Morante, IREC and University of Barcelona

**1:30 PM**

#### (ICACC-FS4-009-2012) Hydrolytic Colloidal Routes to Metal Oxide Nanocrystals. Synthetic Principles, Gas-Sensing Devices and Synthesis-Property Relationship (Invited)

M. Epifani\*, CNR-IMM, Italy

A metal oxide sol can be prepared very simply by usual precipitation-precipitation procedures. Is it possible to process the oxide species contained in the sol in order to obtain nanocrystalline species? A positive answer will be given to this question, by using the same chemical agent to promote the nanocrystal formation and at the same time the related growth hindering. The process development will be reviewed, until the most recent version, consisting in a simplified two step hydrolytic-solvolytic processing. The corresponding formation mechanism has been determined as a spatially confined, self-arrested sol-to-gel transition, where the metal oxide nanocrystals are formed during the first few minutes after the injection step. The process is extremely general, providing a broad variety of colloidal oxide nanocrystals ( $\text{SnO}_2$ ,  $\text{ZnO}$ ,  $\text{CeO}_2$ ,  $\text{TiO}_2$ ,  $\text{Fe}_3\text{O}_4$  etc). As an example of application, the remarkable gas-sensing properties of  $\text{SnO}_2$  and  $\text{In}_2\text{O}_3$  nanocrystals will be reviewed. It will be shown that the sensing performance is dominated by the presence of oxygen vacancies in the nanocrystals. In turn, the oxygen vacancies are generated by the synthesis procedure, involving sol-gel colloidal processing in coordinating environment, followed by heat-treatment. This finding finally matched the synthesis of the sensing material with the device performance.

**2:00 PM**

#### (ICACC-FS4-010-2012) Synchrotron based spectroscopic studies of functional materials and systems (Invited)

O. Karis\*, Uppsala University, Sweden

Synchrotron-based spectroscopic investigations of materials, using primarily soft x-rays, has emerged as very sensitive tools for characterization of electronic properties. X-rays allows for elemental and chemical specificity in the measurements, something normally inaccessible with e.g. methods using visible light. Many interesting aspects of the electronic structure in a material concern modifications in the outer valence region. A complication when studying thin films is that also the substrate has valence states overlapping with the states of interest. Using resonant x-ray techniques like x-ray absorption spectroscopy (XAS), resonant inelastic x-ray scattering (RIXS) and resonant photoelectron spectroscopy (RPES) allows this issue to be overcome or at least greatly reduced. We also show examples from our recent activity on characterizing properties in multilayer systems, composites and complex oxides using high kinetic energy photoemission. In particular, the much increased mean free path at higher kinetic energies in combination with the elemental selectivity of the core level spectroscopies in general has led to a regained interest in the use of photoelectron spectroscopy in many areas, as it makes it possible to investigate the electronic structure of materials with a substantially reduced surface sensitivity.

**2:30 PM**

#### (ICACC-FS4-011-2012) Fast Processing of Advanced Ceramics for Sensor and Thermoelectric Applications: The Role of Powder Morphology During Spark Plasma Sintering of Nanopowders (Invited)

O. A. Graeve\*, J. P. Kelly, B. M. Clark, M. A. Alberga, Alfred University, USA

When sintering powders into dense nanograined specimens, the sintering behavior is directly connected to the inherent sinterability of the material and the morphological characteristics of the powders. One could argue that the synthesis process for obtaining powders is the most important decision one is to make in order to obtain fully

dense nanograined specimens effectively, since the characteristics of the powders are related to how the powders are prepared. This talk will present an overview of the state-of-the-art in powder synthesis and spark plasma sintering of powders to obtain nanograined dense compacts. Arguments will be presented connecting morphological characteristics of the powders to the grain size of consolidated specimens by spark plasma sintering. Special emphasis will be placed on the effect of particle size, as determined from dynamic light scattering, on the grain size of sintered compacts. Specific materials to be covered include luthetium oxyorthosilicate (LSO) for gamma-ray detector applications, as well as titania and zinc oxide for thermoelectric applications. For the case of LSO, a thorough analysis of phase development during synthesis and sintering will be presented.

#### Solid State Ionics

Room: Oceanview

Session Chair: Giorgio Sberveglieri, University of Brescia

**3:20 PM**

#### (ICACC-FS4-012-2012) Perovskite thin films and nano-phase powders by alkoxide based synthesis

G. Westin\*, K. Lashgari, A. Pohl, Uppsala University, Sweden; K. Jansson, Stockholm University, Sweden

Thin film perovskite cobaltates, ferrates and manganates are of high importance for many important technological applications including; catalysis, oxygen permeation membranes, high temperature electrode materials, conducting substrates oxide films and IR sensing. Lately a great interest has been paid to multi-ferroics with the focus on single phase of composites containing perovskites. The dominating deposition techniques for such materials are CVD and PVD techniques, but solution based processes may offer more cost efficient alternatives and can be used to coat very large and complex shape substrates. There is however often expressed concern over the quality of solution derived films. Here we describe all-alkoxide based routes to various phase pure polycrystalline and epitaxial perovskites films and nano-phase powders. The highly reactive alkoxides used allow for complete removal of all organics by hydrolysis in air, before heat-treatment, which leads to increased control of the oxide formation by heating. The conversion of gel to perovskite has been studied in detail with a combination of TGA, DSC, TEM-EDS, SEM, XRD and IR spectroscopy for all systems. The importance of the heat-treatment parameters will be discussed and compared within the systems and other chemical deposition routes.

**3:40 PM**

#### (ICACC-FS4-013-2012) Going nano: the impact of boundary effects on the electrical properties of ionically and mixed conducting oxides (Invited)

G. Gregori\*, J. Maier, Max Planck Institute for Solid State Research, Germany

The defect chemistry of nanocrystalline oxides has gained much attention in the last years since, at the nanoscale, their electrical conduction properties drastically change as the boundaries properties become predominant over the bulk. This effect reveals a number of exciting size-induced phenomena and discloses new opportunities to adjust the conduction properties of such materials. In the present contribution, the effect of reducing the grain size on the electrical conductivity of ionic and mixed conductors is discussed. A number of significant examples are presented, which emphasize the huge impact of boundary effects on the transport properties of materials such as  $\text{SrTiO}_3$  and gadolinium-doped  $\text{CeO}_2$ .

**4:10 PM**

#### (ICACC-FS4-014-2012) Synthesis and Characterization of highly textured $\text{BaTiO}_3$ thin film

Z. Zhou\*, University of Florida, USA; Y. Lin, The University of Texas at El Paso, USA; H. A. Sodano, University of Florida, USA

Recently, texture piezoelectric materials have gained much researchers' attention due to the increase in the dielectric and electro-



mechanical properties of materials. In order to produce lower cost and lead free texture piezoelectric materials, this paper introduces a novel method of fabrication textured barium titanate(BaTiO<sub>3</sub>) film on a conductive substrate by transferring oriented rutile TiO<sub>2</sub> nanowires to BaTiO<sub>3</sub> thin film. This fabrication method is based on a two-step hydrothermal process: vertically aligned arrays of TiO<sub>2</sub> nanowire were first grown on Ti substrate then transferred to textured BaTiO<sub>3</sub> film using Ba ions. Thickness of TiO<sub>2</sub> nanowire arrays can be controlled by the concentration of Ti ions, reaction time and temperature. The degree of orientation of BaTiO<sub>3</sub> thin film can be obtained by optimizing the concentration of Ba ions, reaction temperature and time. Scanning Electron Microscopy (SEM) was used to determine the microstructure and film thickness of BaTiO<sub>3</sub> thin film, and X-Ray Diffraction (XRD) was utilized to evaluate the crystal structure and degree of orientation. It was shown that the textured BaTiO<sub>3</sub> thin film has a degree of orientation higher than 73% along [110] axis and a thickness ranging from 3 to 5 $\mu$ m. The enhanced dielectric constant and piezoelectric coupling of the textured BaTiO<sub>3</sub> thin film were also characterized to investigate its potential for sensing and energy harvesting.

4:30 PM

**(ICACC-FS4-015-2012) Upconversion Luminescent Er Doped SrTiO<sub>3</sub>: Site-selected Substitution and Visible-light-driven Photocatalytic H<sub>2</sub> or O<sub>2</sub> Evolution**

J. Shi\*, Xi'an Jiaotong University (XJTU), China; J. Ye, National Institute for Materials Science (NIMS), Japan; L. Ma, Xi'an Jiaotong University (XJTU), China; S. Ouyang, National Institute for Materials Science (NIMS), Japan; D. Jing, L. Guo, Xi'an Jiaotong University (XJTU), China

Photocatalytic water splitting has been acknowledged as a promising way to realize the ideal conversion of solar energy to hydrogen. Oxide semiconducting materials showed an unparalleled stability during photocatalytic reaction. Nevertheless, the ability to utilize visible light was often intrinsically restrained by the wide bandgaps. Accordingly, the electronic band structures of oxide semiconducting photocatalysts were usually tuned by incorporating metal cations to construct new energy bands or localized impurity levels between the bandgaps. However, the redox ability of photogenerated carriers to extract H<sub>2</sub> or O<sub>2</sub> from H<sub>2</sub>O was inevitably reduced. Herein, a series of upconversion luminescent Er doped SrTiO<sub>3</sub> were obtained by a polymerized complex method. Er doped SrTiO<sub>3</sub> with B-site substitution was proved to be a novel, stable, and efficient photocatalyst for visible-light-driven ( $\lambda > 420$  nm) H<sub>2</sub> or O<sub>2</sub> evolution. It was generally suggested that introduction of upconversion luminescent reagents into appropriate host materials was a promising approach to harnessing the low-energy photons for photocatalytic H<sub>2</sub> or O<sub>2</sub> evolution, and that the substitutional sites of doped elements in ABO<sub>3</sub>-type perovskite oxides played a pivotal role in determining the photocatalytic activity.

## S1: Mechanical Behavior and Performance of Ceramics & Composites

### Symposium 1: Poster Session

Room: Exhibit Hall

**(ICACC-S1-P001-2012) Evaluation of ceramic materials and joints using UT and X-Ray**

Y. Nishimura\*, T. Suzuki, N. Kondou, H. Kita, K. Hirao, National Institute of Advanced Industrial Science and Technology, Japan

The possibility of inspecting defects in ceramic materials using UT and X-Ray was studied to investigate the reliability of ceramics materials. Ceramic materials are thought to be unreliable for making large structural components because they are likely to include fatal defects inside and their fractural response are much faster and more drastic than those of metal materials. "Stereo Fabric" is an idea that proposes a method in which a large ceramic product can be assembled of many small blocks. Joints are known to be more likely to fracture than

other parts of ceramic products. In this study, ceramic blocks jointed with silicon sheet, glass or quick-drying adhesives were examined by UT and X-Ray. Joints of silicon sheet or glass could not be distinguished from other parts of component easily by UT or X-Ray. It means mechanically strong joints except that more and larger defects were detected than developers of ceramic products expect. To develop ceramic stereo fabric products, a complete survey or something close to it is required. X-Ray methods and UT methods have to be considered for this. This work was supported by the New Energy and Industrial Technology Development Organization (NEDO) and Ministry of Economy, Trade and Industry as part of the project for the Innovative Development of Ceramics Production Technology for Energy Saving

**(ICACC-S1-P002-2012) Rapid fabrication of a C/SiC Composite with SiC-Powder Slurry Infiltration Method**

T. Hara\*, Tokyo University of Science, Japan; T. Aoki, T. Ogasawara, Japan Aerospace Exploration Agency (JAXA), Japan; Y. Kogo, Tokyo University of Science, Japan

One of the most conventional processing routes of Carbon-fiber-reinforced SiC matrix (C/SiC) composites is the polymer impregnation and pyrolysis (PIP) method. However, due to the low volume yield of pre-ceramic polymers after pyrolysis, repeated PIP is required to obtain high-density C/SiC composites, yielding high processing cost. For the purpose of reducing the processing cost, the space between fibers in a 2D carbon fiber preform was impregnated with SiC powder slurries by a vacuum/pressure assisted infiltration. The experimental results showed that filling fiber preforms with SiC powder slurries in advance can reduce the number of the PIP cycles. In this study, the powder filled preform was further densified by the PIP method and/or the melt infiltration (MI) one to get C/SiC composites. Through these experiments, SiC powder infiltration behavior during a vacuum/pressure assisted slurry infiltration process was discussed, and basic mechanical properties of C/SiC composites fabricated by this process were evaluated.

**(ICACC-S1-P003-2012) Mechanical Behavior of Reaction Bonded Silicon Carbide Exposed to Petroleum and Naptha**

R. P. Silva\*, C. A. Costa, Universidade Federal do Rio de Janeiro - UFRJ, Brazil

The RBSiC is a ceramic material widely used in mechanical seals due to its high hardness, high thermal conductivity, and low coefficient of friction. About its corrosion resistance, the API Standard 682 recommends its use for services where the pH is between 4 and 11. Nevertheless, the present authors did not find any published data about the mechanical behavior of RBSiC after the exposure to oil or oil products. This study evaluates the degradation resistance of RBSiC when immersed in petroleum and naphtha. The studied material had a 2.81 g/cm<sup>3</sup> density, an average four-point bending strength of 193 MPa and modulus elasticity of 270 GPa. The degradation was conducted in petroleum at room temperature and 60 C, and also in naphtha at room temperature. To make the media more severe, all specimens were immersed with 50 MPa applied stress (via 3 point bend) and CO<sub>2</sub> was purged for 30 minutes every week. The immersion periods were 15, 90 and 180 days, in each media. The MOR after immersion in the media showed the material to be insensitive to the tests condition herein reported, namely, no degradation was observed.

**(ICACC-S1-P004-2012) Mechanical characterization of a transparent spinel ceramic**

O. A. Tokariev\*, J. Malzbender, R. W. Steinbrech, Forschungszentrum Jülich GmbH, Germany; L. Schnetter, CeramTec-ETEC GmbH, Germany

Based on macroscopic mechanical tests of transparent MgAl<sub>2</sub>O<sub>4</sub> limits set by the materials properties in testing and reliability are discussed. In particular the elastic modulus and the fracture strength of the brittle material are considered as important properties for the analysis and modeling of stress states and failure. The

experimental limits of standard elastic modulus determination using ring-on-ring testing are highlighted and an approach is outlined to correct the measured apparent values by an analytical relationship. Experimental strength data as a function of stress rate are used to assess the potential effect of slow crack growth yielding the failure time under static loading via a strength – probability – time plot. Furthermore the local strength has been measured using Brinell indentation. Insight on fracture and delamination has been obtained by in-situ observation of the damage process from hardness impressions and scratch testing. The involved local residual stresses could be visualized in the transparent material between crossed polarizers. However, of equal importance for material development and improvement to the statistical data is the knowledge of failure causing defects and the fracture mechanisms. In this respect local mechanical tests and fractography provide valuable information. Light, confocal and scanning electron microscopy supported the defect characterization.

### (ICACC-S1-P005-2012) Synthesis of SiC from Silica-Coated Carbon and Oxidized Silicon Powders

Y. Hwang\*, D. Riu, H. Kang, Seoul National University of Science & Technology, Republic of Korea; D. Chun, Y. Kim, Inocera Inc., Republic of Korea

Among the various SiC synthesis methods, direct reaction of Si and C has its advantage of low synthesis temperature. However it is difficult to control the reaction that rapidly progress, and subsequently coarse powders are obtained. To evade the above difficulty we tried to insert SiO<sub>2</sub> layers between carbon and silicon powders. Two methods have been tried: one is silica coating on the carbon black powder, and the other is oxidization of silicon powders. The mixture of silica-coated carbon and/or oxidized silicon powders were directly synthesized to produce SiC powders. As typical silica coating procedure on carbon black, 3-aminopropyltriethoxysilane (APTES) and tetraethoxysilane (TEOS) solution was dropped into carbon-dispersed ethanol slurry. After 12 hours of reaction, bare or oxidized silicon powders were added under mechanical stirring. The dried mixtures of Si and C were carbonized at 1500 °C for 2 hours in N<sub>2</sub> atmosphere. The shape, size and composition of silica-coated C were observed by transmission electron microscopy. The phase of synthesized SiC was examined by x-ray diffractometer. The morphology and size were examined by scanning electron microscopy and particle size analyzer, respectfully. We sintered SiC into pellet, and its density was measured. The overall characteristics of synthesized SiC powders, the reaction mechanism, and sintering properties are discussed.

### (ICACC-S1-P006-2012) Reaction bonded Si/SiB<sub>6</sub>: effect of carbon additions on composition and properties

S. Salamone\*, M. Aghajanian, O. Spriggs, M Cubed Technologies Inc., USA; S. E. Horner, PM Soldier Protection and Individual Equipment, USA

Silicon Hexaboride (SiB<sub>6</sub>) is an interesting ceramic compound because of its high hardness and low density. With a density of 2.43 g/cc (lower than B<sub>4</sub>C) and a hardness equivalent to SiC, composites made from this material should exhibit enhanced properties. Several Si/SiB<sub>6</sub> composites were fabricated using a reaction bonding technique. This is a flexible, low temperature (as compared to sintering) process that is well suited for making composites with varying amounts of secondary phases, via in-situ formation. X-ray diffraction has revealed the formation of B<sub>4</sub>C and SiC phases in composites of reaction bonded SiB<sub>6</sub>. The ratio of SiB<sub>6</sub> to B<sub>4</sub>C and SiC can be changed with the addition of small quantities of carbon. The compositional changes also affect the physical properties such as density and Young's modulus and the mechanical properties such as hardness and strength. These physical properties are directly related to the final composition (e.g. remaining SiB<sub>6</sub>, B<sub>4</sub>C, SiC and silicon content) of the composite. The following study will correlate the composition and microstructure (including fracture surface analysis) with the mechanical properties.

### (ICACC-S1-P007-2012) Sintering behavior of SiC fiber derived from polycarbosilane

J. Hong\*, Y. Cho, M. Kang, H. Lim, H. Kang, Seoul National University of Science and Technology, Republic of Korea; K. Cho, Korea Institute of Ceramic Engineering and Technology, Republic of Korea; D. Riu, Seoul National University of Science and Technology, Republic of Korea

Stoichiometric silicon carbide fibers have been used for a reinforcement for high temperature SiC/SiC composites. However, the currently commercialized SiC fibers have still some problem in that their microstructures are prone to change during the high temperature composite making process. So, there are several researches to improve the microstructure of the stoichiometric fibers by using high temperature sintering. We have been investigating the pyrolysis and sintering process of polycarbosilane derived SiC fibers. Especially, the oxygen content and the presence of the sintering aid are main concern on the pyrolysis and sintering of pcs fibers. In this study, we present results obtained when we have changed the sintering atmosphere, heating rate and also will discuss the effect of two-step sintering on the microstructure and mechanical properties of the fibers.

### (ICACC-S1-P008-2012) Silicon carbide particle growth during carbothermal reduction of SiO<sub>2</sub> and C mixture

H. Kang\*, J. Cho, D. Riu, Seoul National University of Science and Technology, Republic of Korea; D. Shin, LG Innotek, Republic of Korea

Recently, the need for single crystal SiC wafer are increasing from the power semiconductor and LED industry. High purity silicon carbide powder is an essential source for SiC single crystal growth using PVT process. Normally, high purity silicon carbide particles have been fabricated by carbothermal reduction of SiO<sub>2</sub> and Carbon. However, it is difficult to control the size and the size distribution of the particle during the carbothermal reduction process. In order to control the size of silicon carbide powder, we have examined the effect of seed particles on the size distribution of the resulting products. When 5 % of beta-SiC powder was present in the powder bed, the particle size of the silicon carbide particle sized was increased upto 15 micrometer after 1800°C 3 hours carbothermal reductions. However, when the starting powder was changed slightly from batch to batch, the particle size distribution was significantly affected by the starting powders. Especially, the source of the SiO<sub>2</sub> affected very much on the size distribution of the resulting SiC particles. In this study, we will discuss the effect of seeding particle and starting powder on the silicon carbide particle growth in detail.

### (ICACC-S1-P009-2012) Effect of Ta-doping on Electrical and Dielectric properties of Bi<sub>0.5</sub>(Na<sub>0.5</sub>K<sub>0.5</sub>)<sub>0.5</sub>TiO<sub>3</sub> ceramics

K. Kumar\*, Crystal Lab, India; B. Kumar, University of Delhi, India

Bi<sub>0.5</sub>(Na<sub>0.5</sub>K<sub>0.5</sub>)<sub>0.5</sub>TiO<sub>3</sub> + x wt.% Ta, (x= 0.2, 0.4, 0.6, 0.8 & 1.0 ) piezoelectric ceramics were synthesized by solid state reaction. The dielectric and ferroelectric properties were investigated in detail. A single perovskite phase and formation of composite structure was confirmed using X-ray diffraction (XRD) technique. Pure and Ta-doped BNKT ceramics were analyzed for diffused phase transition behaviour. The temperature dependence of dielectric constant in the temperature range 20-500 °C has revealed two phase transitions from ferroelectric to anti-ferroelectric (T<sub>d</sub>) and antiferroelectric to paraelectric (T<sub>c</sub>) phases. Addition of Ta was found to increase the value of both T<sub>d</sub> and T<sub>c</sub>, thus increasing the usable temperature range of these ferroelectrics. Impedance measurements were made on the prepared sample over a wide range of temperatures (230–400 °C) and frequencies (20 Hz–2 MHz), which show the presence of both bulk and grain boundary effects in the material. The dc and ac conductivities were determined from Nyquist (Cole–Cole) plot. The activation energies for dc and ac conduction were calculated and found to increase with Ta-doping concentration. The activation energy for relaxation was found to increase with Ta concentration till 0.4%, but with further addition of Ta, its value decreases. The electrical properties were analyzed by impedance modulus spectroscopy.

**(ICACC-S1-P010-2012) The study of the variation of mechanical properties with ratio of  $\alpha/\beta$  SiC powders**

H. Shin\*, Y. Kim, D. Chun, Inocera inc., Republic of Korea

This experiment is designed to study effect of ratio of  $\alpha/\beta$  on mechanical properties of SiC. The various mixture of  $\alpha/\beta$  SiC powder was prepared to make liquid-phase sintered SiC with additives of Al<sub>2</sub>O<sub>3</sub> and Y<sub>2</sub>O<sub>3</sub>. Making granules, they are pressed uniaxially with a pressure of 100MPa. Then, the formed body was sintered at 1,960°C for 1hr. in Ar purging atmosphere. Phase analysis, density, strength and hardness were measured and the microstructures of sintered specimen were investigated using SEM. Abnormal grain-growth was observed to have a lower density in case of using 100%  $\beta$  as starting material. XRD analysis showed that all powder of  $\beta$  phase were transformed to a phase. As the content of  $\alpha$  phase increased, there was a tendency that the physical properties increased. It would be compared to the sintered specimen with SiC powder made from direct carbonization method. It will be added that the most moderate method for sintering SiC from DC preparation having a superior properties

**(ICACC-S1-P011-2012) Slurries with organic and inorganic components**

M. Vadala\*, D. C. Lupascu, University of Duisburg Essen, Germany

Slip casting is one of the most widely used preparation methods in ceramics industry, because it allows preparation of compacts with large sizes and complex shapes. A ceramic slurry consists of one or multiple dispersed solid phases in a solvent. In order to produce high dense green bodies by slip casting, incorporating hydrophobic organic components and classically hydrophilic oxides, appropriate solvents and stabilizers have to be chosen. An organic solvent-based slurry is more volatile, and green tapes are achieved easier. An aqueous slurry produces crack-free, uniform green tapes only when all variables are controlled extremely well. In this paper we present different routes to fabricate alumina-based compounds with organic fillers aiming at a process route to generate multi-phase compounds potentially useable in their compacted green state or in some intermediate degree of sintering densification.

**(ICACC-S1-P012-2012) Fracture Behavior and Toughness of Short Carbon Fiber Dispersed SiC Matrix Composites**

R. Inoue\*, Y. Kagawa, H. Kakisawa, The University of Tokyo, Japan

Carbon fiber-dispersed SiC matrix (CF/SiC) composites have been expected for wear component applications. Therefore, understanding of fracture behavior and fracture resistance under various stress concentration sources, such as short- and long- cracks, is important for safety applications. In the present study, effect of the stress concentration on fracture behavior of CF/SiC composite fabricated by melting infiltration process is investigated using disk compression test of notched specimen. Fracture resistance under mode I and mode I+II mixed mode conditions is obtained from the tests. During the test, observation of local damage behavior near a notch tip is carried out. The measured fracture resistances are discussed with the local micro-damage evolution process. Effects of local stress field and associated micro-damage evolution on fracture resistance are also discussed based on the set of experimental evidences.

**(ICACC-S1-P013-2012) Toughening in Graphene Ceramic Nanocomposites**

V. R. Marotto\*, M. A. Valdez, L. S. Walker, E. L. Corral, University of Arizona, USA

Ceramics are ideal materials for high-temperature applications due to their high melting temperature and retention of properties at elevated temperature. However, they have limited toughness for widespread application as a structural material. Therefore, we investigate using two-dimensional graphene platelets (GPL) as novel reinforcements over conventional one-dimensional fiber reinforcements in order to enhance toughness of ceramics. We show that homoge-

neously dispersed GPLs with silicon nitride particles densified, at ~1650°C, using park plasma sintering (SPS) increases fracture toughness of the bulk ceramic by ~235% (from ~2.8 to ~6.6 MPa·m<sup>1/2</sup>) using only 1.5 vol% GPLs. Raman spectroscopy verifies the survivability of the GPLs in the ceramic and at low concentrations (~0.1 vol% GPL) we observe conversion from GPL to nanodiamond. Novel toughening mechanisms show GPL anchoring themselves around ceramic grains to resist sheet pullout. This anchoring mechanism deflects cracks in not just two, but in three dimensions. Analysis of GPL toughness mechanisms and GPL conversion to nanodiamond will be presented.

**(ICACC-S1-P014-2012) Wear Behavior of Ceramic/Metal Composites**

M. Aghajanian\*, B. Givens, M. Watkins, A. McCormick, M. Waggoner, M Cubed Technologies, Inc., USA

Ceramic particle reinforced aluminum metal matrix composites (MMCs) have been well studied due to their utility in various structural and thermal applications. In addition, MMCs have value in various wear applications due to the presence of the hard ceramic phase within the ductile metallic matrix. Potential uses include slurry and dry erosion components in the mining, coal power and paper processing industries where ceramic wear components are not viable due to low fracture toughness (e.g., potential breakage if component is struck with large piece of debris such as a rock). The present work aims to quantify the wear properties of ceramic particle reinforced aluminum as a function of ceramic content and type. Results will be compared to those for traditional unreinforced ferrous and aluminum-based metals. Also, correlation of results with microstructure and properties of the composites will be made. Finally, the wear scars will be examined by SEM to assess failure mode.

**(ICACC-S1-P015-2012) Weave and fiber volume effects in a PIP CMC material system**

G. Ojard\*, E. Prevost, Pratt &amp; Whitney, USA; U. Santhosh, Structural Analytics, Inc.Center, USA; R. Naik, Pratt &amp; Whitney, USA; D. Jarmon, United Technologies Research Center, USA

With the increasing interest in ceramic matrix composites for a wide range of applications, fundamental research is needed in the area of multiple weaves and fiber volume. Understanding of how the material performs with differing weaves and fiber volume will affect the end insertion application. With this in mind, a series of three panels were fabricated via a polymer infiltration process: 8 HS balanced symmetric layup, 8 HS bias weave and angle interlock. From these panels, a series of characterization efforts were undertaken with the sample oriented in both the warp and fill direction: with differing fiber volumes. These tests consisted of tensile, interlaminar shear, interlaminar tensile, in-plane thermal expansion and through thickness thermal conductivity. In addition, micro-structural characterization was done. The results from this testing will be presented, trends reviewed and analysis done.

**(ICACC-S1-P016-2012) Mechanical properties of nacre after cyclic loading**

K. Uno\*, H. Kakisawa, Y. Kagawa, The University of Tokyo, Japan

Nacre, the mother of pearl, has high fracture resistance as a result of its "brick and mortar" structure composed of inorganic (aragonite) plates and organic phase between the plates. The mechanical response of nacre is affected by the interface organic phase, of which mechanical characteristics are attributed to protein modular structures which can be changed through deformation. The objective of this study is focused on the effect of the organic phase structure on mechanical properties of nacre. Cyclic loading is applied to nacre in order to slide the plate interface repeatedly and change the organic structure. Tensile and bending test were done after the cyclic loading. The mechanical response of the nacre depends on the cyclic loading as well as the water content, suggesting that the viscoelastic property

of the organic phase plays an important role in controlling the interface sliding behavior.

### **(ICACC-S1-P017-2012) In-situ Boron Nitride Nanotubes on Ceramic powders by Chemical Vapor deposition**

A. Kumar\*, Florida International University, USA; A. Datye, University of Tennessee, USA; K. Wu, Florida International University, USA; H. Lin, Oak Ridge National Laboratory, USA; J. Hurst, NASA, USA

With the theoretical predication of Boron Nitride Nanotubes (BNNTs) in 1994, there has been an increasing research interest to synthesize BNNTs by various growth techniques. These nanotubes have the similar structure as Carbon Nanotubes (CNTs) with substitution of B and N atoms alternative in graphitic carbon sheet with almost no change in atomic spacing. However the synthesis of BNNTs without impurities and catalysts has a challenging task for future research. Incorporation of the BNNTs in composites has therefore been limited to only ex-situ mixing techniques. Chemical Vapor Deposition (CVD) is a simple and low temperature technique to produce the BNNTs. In the present study, we synthesize the BNNTs on different ceramics powders ( $Al_2O_3$ ,  $Si_3N_4$  and  $SiC$ ) by chemical vapor deposition in  $N_2/NH_3$  atmosphere at low temperature with B-N-O based precursor and therefore, this method leads to synthesis the novel BNNTs-ceramic nano-composite. The morphology of BNNTs has been characterized with SEM, HRTEM and Raman spectroscopy. The phase has been identified with XRD. This success of this method can be an important step forward in producing homogeneous in-situ ceramic – BNNT composites.

### **(ICACC-S1-P018-2012) Study of visualizing of internal defects in ceramic products using UT probe array**

Y. Nishimura, T. Suzuki, National Institute of Advanced Industrial Science and Technology, Japan; K. Fukuda, N. Saito\*, Tokyo National College of Technology, Japan

The possibility of inspecting defects in ceramic materials using UT probe array was studied to investigate the reliability of ceramic products. In making large structural components of many small blocks, such components are likely to include fatal defects inside, particularly in joints, and their fractural response are much faster and more drastic than those of metal materials. Therefore, non-destructive Testing is necessary to detect internal defects. UT probe array can scan the inside of sample and reconstruct the image of internal defects. However, it doesn't takes short to do them. D. Braconnier and S. Hirose proposed methods to reconstruct a image of internal defects in a short time for each. In this study, samples with artificial defects were prepared to simulate defects in ceramics and measured to acquire the data required to reconstruct images. To consider qualities of visualizing by UT array probe, some configurations of the delay time, noise reduction and image reconstruction methods were tried. In the result, the influence of them on visualizing were examined to construct NDT system for inspecting a large ceramic product. This work was supported by the New Energy and Industrial Technology Development Organization (NEDO) and Ministry of Economy, Trade and Industry as part of the project for the Innovative Development of Ceramics Production Technology for Energy Saving.

### **(ICACC-S1-P019-2012) Advanced Ceramics Property Measurements**

J. Salem, NASA GRC, USA; J. D. Helfinstine\*, Corning Inc Retiree, USA; G. Quinn, NIST, USA; S. Gonczyk, Gateway Materials Technology, Inc, USA

Measuring the properties of advanced ceramics is relatively easy – if the proper techniques are known. To help users and producers find established techniques to measure a particular property of a ceramic monolith, composite, or coating, the Advanced Ceramics Committee of ASTM, C-28, has developed dozens of consensus test standards and practices, that give the “what, how and how not, and why” for mechanical, physical, thermal, and performance properties. Using these standards will provide accurate, reliable, and complete data for rigorous comparisons with other test results in your test lab or some-

where else. The C-28 Committee has involved academics, and producers and users of ceramics to write and continually update more than 45 standards since the committee's inception in 1986. Included in this poster will be a pictogram of the C-28 standards and how to obtain individual copies with full details or the complete collection of all of them in one volume. A listing of other committees that might be of interest will be included.

### **(ICACC-S1-P020-2012) Corrosion of titanium carbonitride cermets with a nickel aluminide binder**

M. B. Holmes\*, Z. N. Farhat, G. J. Kipouros, K. P. Plucknett, Dalhousie University, Canada

This study will focus on assessment of the corrosion behaviour of titanium carbonitride ( $Ti(C,N)$ ) and titanium carbide ( $TiC$ ) ceramic-metal composites (or cermets). Despite possessing high strength and resistance to wear, little is known about the corrosion resistance of these materials.  $Ti(C,N)$  and  $TiC$  samples have been prepared through a combination of dry-pressing and melt infiltration, with nickel aluminide ( $Ni_3Al$ ) employed as a metallic binder phase. The effects of the C:N ratio in the  $Ti(C,N)$  starting material, as well as  $Ni_3Al$  volume fraction, were assessed in terms of the cermet resistance to corrosion in a 3.5% NaCl aqueous environment. The samples prepared include:  $TiC_{0.3}N_{0.7}$ ,  $TiC_{0.5}N_{0.5}$  and  $TiC_{0.7}N_{0.3}$ , all with 40 vol.%  $Ni_3Al$ , as well as  $TiC$  with 20-30 vol.%  $Ni_3Al$ . Following the identification of the open circuit potential, Tafel, linear polarization as well as cyclic polarization analyses were performed. This research aims to identify the leading mechanisms driving corrosion of these new  $Ti(C,N)$  based cermets, with the intention of limiting the resulting degradation and prolonging the material's ability to perform in environments wherein corrosion may be a prominent concern.

### **(ICACC-S1-P021-2012) Tensile Behavior and Health Monitoring of SiC/SiC Single Tow Minicomposites**

S. Ramasamy\*, G. Morscher, The University of Akron, USA

SiC/SiC single tow minicomposites processed through chemical vapor infiltration (CVI) of SiC matrix on SiC fibers are the elemental skeletal structure of woven SiC/SiC macro-composites. They provide a simple, versatile, and cost-effective approach to study constituent/property relationships for ceramic matrix composites (CMCs). In this work, single tow minicomposites with constant CVI SiC matrix and variations in other constituents such as fiber types and contents (Hi-Nicalon and Sylramic; 500 or 800 fibers per tow) and interfaces (boron nitride and carbon) between matrix and fibers were studied. Room temperature monotonic tension tests were performed and the influence of matrix and/or fiber cracking on applied load was studied by modal acoustic emission and four-point electrical resistance methods. The results showed that the above-said health monitoring techniques had direct relation to the extent of damages formed during tensile tests. Microscopy of polished sections and fracture surfaces of the failed specimens was performed to understand the extent of damage and failure mechanisms.

### **(ICACC-S1-P022-2012) Low CTE & High Stiffness Diamond reinforced SiC based Composites with Machineable Surfaces for Mirrors & Structures**

M. A. Akbas\*, D. Mastrobattisto, B. Vance, P. Chhillar, P. Jurgaitis, M Cubed Technologies Inc., USA

Reaction bonded SiC composite materials are widely used in precision optic industry thanks to their unique properties such as very high specific stiffness, low thermal expansion coefficient, and high thermal conductivity. Mechanical and thermal stability of reaction bonded SiC composites can be further improved by particulate diamond reinforcement. However, presence of diamond particles in microstructure reduces machinability of the final composite. This problem is resolved by creating hybrid structures which consists of a diamond reinforced core providing thermally and mechanically stable structure and diamond free surfaces machineable to high tolerances. Properties of these structures will be discussed as a function of

diamond reinforcement content and finally microstructure will characterized by SEM to assess interface between SiC/diamond composite core and diamond free surfaces.

**(ICACC-S1-P023-2012) Study of Al<sub>2</sub>O<sub>3</sub> ceramic coating deposited onto carbon fiber reinforced polymer substrate**

G. Sun\*, X. He, J. Jiang, Y. Sun, Center for Composite Materials and Structures, Harbin Institute of Technology, China

To improve the wear resistance of the carbon fiber reinforced polymer composite, alumina ceramic coatings were deposited. Aluminum and ceramic (Al<sub>2</sub>O<sub>3</sub>) coatings were deposited onto the polymer substrate by air plasma spray (APS), microarc oxidation was used to fabricate alumina on the as-sprayed aluminum coating by different deposition voltage. The mechanical properties of the two kinds of alumina coatings made by different methods were examined. The effect of spray parameters (current and spray distance in this paper) on the phase composition, microstructure and mechanical properties was investigated. Shear adhesion strength between the coatings and the substrates were also examined. The results indicate that the deposition parameters have a significant effect on the phase composition, microstructure and mechanical properties of as-sprayed coatings. The maximum shear adhesion strength of the bond coats was 5.21MPa with the current of 180A and 190 mm spray distance. The highest shear adhesion strength of the alumina coating produced by plasma spray technology was 1.13MPa sprayed by the current of 270A and 170 mm spray distance. The hardness of the surface is much improved by the coatings of alumina fabricated by these two kinds of method, which is 13.308 GPa on average.

**(ICACC-S1-P024-2012) Novel Oxide Ceramic Multilayer Structures for High Temperature Applications**

I. Goetschel\*, A. Roosen, University of Erlangen-Nuremberg, Germany

The ceramic multilayer technology which is based on tape cast green sheets has the potential to generate advanced layered composite materials. In this study, high purity oxides of Al<sub>2</sub>O<sub>3</sub>, MgO and MgAl<sub>2</sub>O<sub>4</sub> were used for tape casting and multilayer processing. Tapes of higher thickness up to 8 mm and different microstructures were obtained using grain sizes in the range of 1 μm to 1 mm. Processing of tape casting slurries containing coarse fillers leads to porous microstructures after sintering. By adjusting the multimodal powder mixtures the microstructure of the tapes and their correlated mechanical behavior can be tailored. To improve the thermal shock and corrosion behavior of the carbon-free composites specific multilayer designs had been realized and characterized. The mechanical and thermo-mechanical properties of the sintered tapes and composites will be evaluated and discussed.

**(ICACC-S1-P025-2012) Functionalization and Uniform Dispersion of MWCNTs into PDMS**

S. Sagar\*, N. Iqbal, A. Maqsood, M. Mujahid, M. Shahid, National University of Sciences & Technology (NUST), Pakistan

Carbon nanotubes (CNTs) exhibit excellent mechanical, electrical, magnetic and thermal properties due to their nanometer scale diameter and high aspect ratio. One of the major difficulties encountered during processing of carbon nanotube – reinforced polydimethyl siloxane (PDMS) composite is inability to achieve a uniform dispersion of the nanotubes in liquid PDMS. Multiwall carbon nanotubes were functionalized via HNO<sub>3</sub>– vapours to attain the maximum recovery of FCNTs and uniformly disperse them into polymer matrix via mechanical stirring at 15000 rpm in blending mixture. FTIR and SEM coupled with EDS were confirmed the proper functionalization and uniform dispersion into PDMS respectively.

**(ICACC-S1-P026-2012) Enhancement in Thermal and Mechanical Properties of PDMS via FMWCNTs**

N. Iqbal\*, S. Sagar, M. Khan, M. Mujahid, National University of Sciences & Technology (NUST), Pakistan

Carbon nanotubes have long been recognized as the stiffest and strongest man made materials know to date. The inclusion of car-

bon nanotubes (CNTs) into polymers is anticipated to improve their multifunctional properties. The effect of functionalization on the properties of polydimethyl siloxane (PDMS) and multi wall carbon nanotubes (MWCNTs) nanocomposite is investigated in this work. To make efficient the MWCNTs reinforcement into the polymer matrix, proper dispersion and apposite interfacial adhesion between the FMWCNTs and polymer matrix, MWCNTs have to be functionalized. The properties of nanocomposites were characterized comprehensively using scanning electron microscope (SEM), thermogravimetric analysis (TGA) and mechanical testing. Uniform and proper dispersion of FMWCNTs into PDMS and enhancement in mechanical/thermal properties of nanocomposite prove the efficacy of MWCNTs.

## S4: Armor Ceramics

### Symposium 4: Poster Session

Room: Exhibit Hall

**(ICACC-S4-P048-2012) The Effect of Alumina Microstructure on Acoustic Loss Mechanisms**

S. Bottiglieri\*, Rutgers University, USA

The use of acoustic spectroscopy to accurately obtain valid information relating to material microstructures has been limited to particle sizing in colloidal suspensions. The basis of using ultrasonic testing to obtain feature size information relies upon an understanding of acoustic scattering and absorption loss mechanisms. Studies have been performed which attempt to correlate scattering and absorption in polycrystalline metallic materials with varying results. The goal of the work presented in this paper is to extend the concept of acoustic spectroscopy to build an understanding of how scattering and absorption relates to the microstructure of dense, polycrystalline, aluminum oxide. The effects of acoustic scattering and absorption were studied separately through the use of alumina-based sample sets containing custom engineered microstructures. The microstructure of each sample set was designed to exploit the behaviors of either scattering or absorption. Results show strong correlations between ultrasonic loss mechanisms and different alumina-based microstructures such that quantification relating to average alumina grain size and secondary phase grain size distributions could be obtained.

**(ICACC-S4-P049-2012) Role of Pressure and Strain Rate on Structural Amorphization in Boron Carbide**

G. Subhash\*, D. Ghosh, University of Florida, USA

The reduced performance of B<sub>4</sub>C armor plate for impact against tungsten carbide penetrators beyond a critical velocity has been attributed in the literature to localized amorphization. However, it is unclear if this reduction in strength is a consequence of high pressure or high velocity. Despite numerous fundamental studies under indentation and impact experiments on B<sub>4</sub>C, the roles of strain rate and pressure have not been fully established. Towards this end, rate dependent uniaxial compressive strength and rate dependent indentation hardness, along with Raman spectroscopy, have been employed to show that high strain rate deformation alone (without concurrent high pressure) cannot trigger localized amorphization in B<sub>4</sub>C. In addition, we show that rate dependent indentation hardness can be used to reveal if a given B<sub>4</sub>C ceramic can undergo structural transformation under high pressure and high strain rate loading. It is also argued that when phase transformation does occur in B<sub>4</sub>C, its dynamic properties degrade more severely compared to the static properties. Finally, it is suggested that dynamic hardness, in conjunction with static hardness, can be used as a measurable mechanical property to reveal the incidence of phase transformation in B<sub>4</sub>C without the need for any postmortem TEM or Raman spectroscopy analyses.

### (ICACC-S4-P050-2012) Damage mechanisms and the indentation size effect

L. J. Vandepierre\*, E. Feilden-Irving, R. Birch, N. Ur-Rehman, Imperial College London, United Kingdom; P. Brown, Defence Science and Technology Laboratory, United Kingdom

It is well established that for many ceramics, decreasing the load applied during Vickers hardness testing leads to an increase in the measured hardness. A wide range of theoretical explanations for this indentation size effect have been proposed, and a common feature of these theories is that they predict that the hardness should continue to increase as the load is decreased further. Most of the early observations of this effect were made with micro- and macro- Vickers indenters with load capabilities from ~300 N down to ~0.5 N, but with nano-indenters now capable of accessing lower loads (0.5N – 0.001 N), the experimental results do not conform to the theoretical predictions. Indeed, in many cases the hardness is more or less constant in the entire nano-indentation load range. A key difference between indents made with small and large loads is the accompanying damage due to cracking and the latter clearly increases with load. Therefore a careful study of the correlation of measured hardness, crack length evolution, and cracking patterns was made for a range of aluminium oxides and silicon carbides. Based on these observations it is proposed that the indentation size effect arises as a result of a change in the constraint on indenter penetration due to cracking.

### (ICACC-S4-P051-2012) Improved Modeling and Simulation of the Ballistic Impact of Tungsten-Based Penetrators on Confined Hot-Pressed Boron Carbide Targets

J. C. Lasalvia, C. G. Fountzoulas\*, U.S.Army Research Laboratory, USA

LaSalvia et al studied experimentally the interaction of confined hot-pressed boron carbide (B4C) targets impacted by laboratory-scale tungsten-based long-rod penetrators. To better understand the physics involved, Fountzoulas et al studied by modeling and simulation the ballistic behavior of the above targets. To satisfactorily replicate the experimental damage of the targets during impact, the strength and failure models, the fractured strength constant and fractured strength exponent of  $\sigma_f$ , and the hydro tensile limit were iteratively modified. The fracture of B4C was able to be replicated to some extent but without being able to stop its penetration by the projectile, a disagreement with the experimental observations. Moreover, the simulations resulted in extensive deformation of the Ti6Al4V sleeve, also not observed experimentally. However, the ability of a numerical model to realistically predict the response of ceramic armor to ballistic impact depends mainly on the selection of appropriate material models and availability of appropriate data. The objective of this effort will be to improve the simulating capability of the existing strength and failure material models of the ANSYS/AUTODYN library to be able to accurately model tensile failure in order to accurately simulate the ballistic response of ceramics.

### (ICACC-S4-P052-2012) Microstructure and Mechanical Properties of SiC-TiB<sub>2</sub> Composites

D. King\*, W. G. Fahrenholtz, G. Hilmas, Missouri University of Science and Technology, USA

Mechanical properties of hot pressed silicon carbide – titanium diboride (SiC-TiB<sub>2</sub>) composites were tested at room temperature. SiC-TiB<sub>2</sub> composites containing 10 to 20 vol% TiB<sub>2</sub> as a dispersed phase were fabricated using both spray drying and ball milling techniques to blend the SiC and TiB<sub>2</sub> particles, along with various sintering aids. Billets of SiC-TiB<sub>2</sub> were then hot pressed in the range of 1980 to 2150°C and machined into bars for flexural strength, elastic modulus, and hardness measurements. Flexure testing was performed in four-point bending to determine MOR, Young's modulus and Weibull modulus on bars with two finishes, 600 grit from surface grinding and a 0.25µm diamond slurry polish. Hardness and direct crack growth measurements on polished surfaces were used to determine fracture toughness of both composites. Chevron-notched bars were

also tested in four-point bending to compare fracture toughness results between the two testing methods. The influence of the two processing techniques and the final microstructures on the mechanical properties will be discussed.

### (ICACC-S4-P053-2012) ZnS bulk ceramics fabricated by spark plasma sintering

Y. Wu\*, Alfred University, USA

ZnS is an infrared transparent material with wide applications for IR windows, domes, far-infrared ray cameras, and mid-IR laser materials doped with transition metals, etc. Currently, ZnS bulk materials are fabricated by using chemical vapor deposition method, which is a relative slow and costly process for making large bulk ceramics. Therefore, cost-effective methods for developing transparent ZnS bulk optical ceramics are desirable. In this work, spark plasma sintering has been used to develop ZnS bulk ceramics.

### (ICACC-S4-P054-2012) TEM Phase Study of Silicon Carbide with Coprecipitated Alumina and Yttria as Sintering Aids

S. L. Miller\*, Rutgers University, USA; S. Mercurio, American Standard, USA; J. Michael, Sandia National Laboratory, USA; F. Cosandey, R. Haber, Rutgers University, USA

Coprecipitation of sintering aids into silicon carbide (SiC) is a promising alternative to traditional mixing methods because it provides improved mixing, decreased defect levels and greater control over the structure and properties of the grain boundary phase. SiC with coprecipitated Al<sub>2</sub>O<sub>3</sub> and Y<sub>2</sub>O<sub>3</sub> was liquid phase sintered using spark plasma sintering and compared to the same material prepared through traditional routes. High resolution transmission electron microscopy (HR-TEM) and energy dispersive spectroscopy (EDS) have been used to show the improved dispersion of the sintering aids within the SiC matrix and the presence of a yttrium and aluminum glassy phase within the grain boundaries. Additionally, nanoprobe electron diffraction was used to examine the triple point phases. The fundamental mechanical properties of both coprecipitated and ball milled samples were determined.

### (ICACC-S4-P055-2012) Development of lightweight reaction bonded materials for armor

P. Karandikar\*, S. Wong, M. Aghajanian, M Cubed Technologies, Inc., USA

Reaction bonded SiC (RBSC) and reaction bonded B4C (RBBC) materials have been used successfully for armor applications over the last decade. SiC is inert and does not react with molten silicon during the reaction bonding process. B4C however, can react with molten silicon during the reaction bonding process. These reactions can be used to tailor the microstructure and properties of resultant composite. Addition of alloying elements and reinforcing phase allows further manipulation of the microstructure. For example, diamond is an extremely effective reinforcement due to its very high elastic modulus (1050 GPa), and hardness (12,000 kg/mm<sup>2</sup>). Also, similar to B4C, diamond can react with molten Si forming SiC. This study focuses on processing RBBC with various reactants and reinforcements. The process parameters, particle sizes, reinforcement content, and reinforcement type are systematically varied. The composites produced are subjected to microstructural (optical, SEM, EDAX, and X-ray diffraction), physical, and elastic properties characterization. The resultant process-microstructure-property relationships will be presented in this paper.

### (ICACC-S4-P056-2012) Characterisation of Damage Mechanisms in Commercial Oxide Ceramics Indented Over a Range of Strain Rates

C. J. Dancer\*, J. F. Spawton, S. Falco, N. Petrinic, R. I. Todd, University of Oxford, United Kingdom

Ceramic materials are known to display strain-rate dependent behaviour under impact. We have designed tests to establish the variations in damage mechanisms in three commercial oxide materials (alumina, alumina-zirconia composite and tetragonal zirconia polycrystal). Materials were indented dynamically and quasi-statically using

identical sharp hardened steel projectiles while recording the load profile. Characteristics of both sharp and blunt indentations were observed using scanning electron microscopy and piezospectroscopic mapping. At dynamic strain rates both the depth of the indentation and the residual stress in the material were found to be lower than for quasi-static tests. This was attributed to temperature-induced softening of the projectile. In addition, the residual stress field at the centre of the indentations in zirconia-containing ceramics was tensile, while that for the alumina samples was compressive. This is thought to be due to the transformation of tetragonal zirconia to its monoclinic form during indentation.

**(ICACC-S4-P057-2012) Alumina-Steel Trilayer and Bilayer Penetration: Simulation and the Role of Microcracked Material**

E. A. Gamble\*, B. G. Compton, F. W. Zok, University of California, Santa Barbara, USA

The predictive capability of a mechanism-based constitutive law for ceramic deformation was probed by comparison of finite element (FE) simulations with multilayer penetration experiments. Alumina-steel bilayers and trilayers were impacted with steel spheres over a range of velocities spanning the ballistic limit of the systems. The experimental backface deflection and ballistic limit were used to assess FE results. Reasonable agreement was observed between experiments and FE results. Furthermore, the simulations illuminated the sensitive dependence of armor performance on the post-comminution flow behavior of the ceramic. This flow behavior governs the interaction of the ceramic (and the impactor) with the metal back plate and strongly influences back plate deformation and failure. The implications of this dependence and potential methods for determining the properties of the fragmented material are also discussed.

**(ICACC-S4-P058-2012) Quantifying Ceramic Microstructure Homogeneity through Information Entropy**

A. Portune\*, ARL - ORAU, USA; T. L. Jessen, ARL, USA

Microstructural homogeneity is crucial in determining the performance and mechanical behavior of ceramic materials. Nondestructive characterization techniques have traditionally been employed to ascertain microstructural uniformity by looking for variations in material properties. Methods developed to ascertain homogeneity from characterization results have often been qualitative or subjective in nature. Information entropy offers a distinct solution as an objective representation of the quantity and distribution of data depicting unique microstructural states present in the material. In this study, a methodology for determining information entropy from characterization results was developed and applied to a set of silicon carbide tiles manufactured under different conditions. Entropy values for each measured property were used to assess the homogeneity of a variety of microstructural features, including inclusion concentration and size distribution, grain size distribution, and grain boundary uniformity. Use of information entropy enabled an objective comparison of samples with fundamentally different microstructures and allowed for quantitative ranking based on microstructural homogeneity throughout the sample volume.

**(ICACC-S4-P059-2012) ALON® Transparent Armor**

L. M. Goldman\*, S. Balasubramanian, N. Nag, U. Kashalikar, R. A. Foti, S. Sastri, Surmet Corp., USA

Aluminum Oxynitride spinel (ALON® Optical Ceramic) combines broadband transparency with excellent mechanical properties. ALON's cubic structure means that it is transparent in its polycrystalline form, allowing it to be manufactured by conventional powder processing techniques. Surmet controls every aspect of the manufacturing process, beginning with synthesis of ALON® powder, continuing through forming/heat treatment of blanks, ending with optical fabrication of ALON® armor windows. Surmet has made significant progress in production capability in recent years. Additional expansion of Surmet's manufacturing capability, for larger sizes and higher quantities, is currently underway. ALON® transparent armor repre-

sents the state of the art in protection against armor piercing threats, offering a factor of two in weight and thickness savings over conventional glass laminates. Tiled and monolithic windows have been successfully produced and tested against a range of threats. While the acquisition costs for ALON® armor are considerably higher than those of conventional glass laminates, ALON offers considerable lifecycle cost advantages. The 2x weight savings translates into dramatic savings in fuel costs over the life of an armored vehicle. Furthermore, ALON's extreme durability means fewer field replacements.

**(ICACC-S4-P060-2012) Hardness and Plasticity of Single Crystal SiC**

J. Swab\*, J. McCauley, G. Gazonas, B. Butler, D. Snoha, U.S. Army Research Laboratory, USA

Single crystals of 4H and 6H SiC, in disk form, were fabricated by Fairfield Crystal Technology using a physical vapor transport growth method. X-ray diffraction techniques were used to determine the crystal structure and orientation of both materials. Both disks had the c-axis perpendicular to the flat surfaces of the disk. The Knoop hardness was determined at 15 degree increments around the c-axis using indentation loads of 800 and 2000g (7.85 and 20N). A power law curve-fit was applied to the hardness data to estimate the plasticity as a function of the orientation. This presentation discusses the differences in hardness and plasticity as a function of crystallographic orientation.

**(ICACC-S4-P061-2012) In Depth Study of Cone Cracks in Multi-Layered Transparent Panel Structures by X-ray Computed Tomography**

W. H. Green\*, R. E. Brennan, C. G. Fountzoulas, U.S. Army Research Laboratory, USA

Transparent and opaque materials are used by the Army in protective systems for enhancing survivability of ground vehicles, air vehicles, and personnel. Transparent materials are utilized for face shields, riot gear, and vehicle windows, in addition to other applications for sensor protection, including radomes and electromagnetic (EM) windows. Fracture from low velocity impacts limits visibility and impairs continued vehicle operations. Transparent protective systems typically consist of glass, polymeric and ceramic materials. Impact damage in different multi-layered transparent panel structure types was investigated using a number of nondestructive evaluation (NDE) methods, including phased array ultrasonic testing and x-ray computed tomography (XCT). Some of the damaged specimens exhibited multiple cone cracks in the second glass layer in front of the backing plate. The spatial characteristics of cone cracks were analyzed using geometric data from the XCT scans (images). Quantitative calculations on the extent of the cone spans were performed. Physical cone attributes (e.g., cone angle) were compared to crack damage geometries generated by theoretical simulations of impact damage.

**(ICACC-S4-P062-2012) Effect of Binder Content on the Performance of WC Penetrators**

J. C. Wright\*, UIC TS, Bowhead Science and Technology, LLC, USA; J. J. Swab, L. S. Magness, US Army Research Lab, USA

Tungsten Carbide (WC) has been used as a penetrator in small arms systems largely due to its high strength, hardness, and density. However, the high brittleness of these WC materials leads to fragmentation of the round upon impact at angles other than zero obliquity. The present study investigates the effect of increasing Co binder content on the bending strength, fracture toughness, and penetration performance of WC-Co alloys in the form of cylindrical rods. Fracture toughness of both beam and cylindrical specimens is characterized using the Surface Crack in Flexure (SCF) method presented in ASTM 1421. A method of adapting the SCF method to cylindrical specimens is also investigated.

**(ICACC-S4-P063-2012) Modeling Ceramic Edge on Impact Experiments**

B. Leavy\*, Army Research Lab, USA; E. Strassburger, Ernst Mach Institute, Germany

In the quest to understand the damage and failure of ceramics in ballistic events, a variety of simplified experiments have been developed

to benchmark the behavior. One such experiment is known as the edge on impact (EOI) experiment. In these experiments, an impactor strikes the edge of a thin square plate, and the damage and cracking that occurs on the side free surface is captured in time with the help of high speed photography. If the material of interest is transparent, additional information within the sample can be discerned. Polarizers can be used to determine the stress wave propagation, and photography of internal damage of the sample can be recorded. All this information serves as an excellent benchmark for ceramic and glass models and codes. Simulations of EOI experiments will be shown with the Kayenta material model, highlighting current capabilities and future needs.

### **(ICACC-S4-P064-2012) Nanostructured and large grain spinel: comparison of depth of penetration (DOP) test rubble**

V. T. Viggato, M. J. Magner, L. P. Franks\*, D. N. Hansen, US Army TARDEC, USA

A limited number of Depth of Penetration (DOP) tests were conducted to compare the ballistic performance of nanostructured and large grain spinel manufactured in three-inch diameter by 3/8 thick disks. All disks were optically transparent in the visible spectrum. Rubble was collected from three nanostructured and two large grain ballistic tests and compared using optical and scanning electron microscopes.

### **(ICACC-S4-P065-2012) Strength Testing of Glass Coated Magnesium-Aluminate Spinel**

S. Kilczewski\*, Data Matrix Solutions, USA; R. Pavlacka, Oak Ridge Institute for Science and Education, USA; J. C. Wright, UIC TS Bowhead Science and Technology, LLC, USA; J. J. Swab, US Army Research Laboratory, USA

Coarse-grained Magnesium-Aluminate Spinel has been under investigation for use in numerous applications, including transparent armor windows. While an increase in the strength of currently produced spinel is desired, previous work on the flexure strength of spinel shows little difference between ground or polished specimens. Since polishing does not greatly increase the strength, other mechanisms for the strengthening of spinel are being investigated. One proposed method is the addition of a thin (~200 micron) index matched glass coating. Results from this method will be discussed.

### **(ICACC-S4-P066-2012) Low Temperature Densification and Mechanical Properties of Ultra-hard Boron Suboxide Ceramics**

R. Pavlacka\*, G. Gilde, U.S. Army Research Laboratory, USA

Boron suboxide (B<sub>6</sub>O) is a candidate material for cutting and abrasion applications as well as other applications that benefit from low theoretical density (2.58 g/cc) and very high hardness (Hv100 = 45 GPa). It is difficult to process to full density due, in part, to limitations in previous powder synthesis techniques. As a result sintering has traditionally required various combinations of high temperature, high pressure, specially designed dies, and/or large amounts of sintering aid. A novel boron suboxide powder synthesis procedure has recently been developed that enables the production of fine sinterable powders that require no subsequent milling. Using spark plasma sintering (or field assisted sintering technology) (SPS/FAST), we demonstrate the densification of boron suboxide compacts at lower temperatures and pressures than previously reported. The effect of various sintering aids on densification behavior, indentation hardness, and fracture toughness will be discussed.

### **(ICACC-S4-P067-2012) Acoustic and Mechanical Response of Microstructural Variation in Silicon Carbide Ceramic Materials**

D. Slusark\*, R. Haber, Rutgers University, USA

Silicon carbide (SiC) has many attributes that make it a suitable material for armor applications. Among these are a low relative density when compared with traditional steel armors along with a high elastic modulus, compressive strength, and hardness. The highly covalent bonding in SiC which leads to these beneficial properties makes it a difficult material to produce consistently. The densification of SiC requires the use of high temperatures in conjunction with sintering

aids, which leads to inherent variability within these materials. A study was conducted to determine the effect of microstructural variability on the acoustic and mechanical properties of silicon carbide. A comparison was made between commercially available SiC, as well as samples that had been developed to emphasize specific aspects of the microstructure. These include exaggerated grain growth, increased residual porosity, and enhanced sintering aid content. A combination of ultrasound evaluation, mechanical testing, and microstructural assessment provided the means for comparison.

### **(ICACC-S4-P068-2012) Stress Wave Management in Obliquely Laminated Composite Systems**

C. J. Espinoza Santos\*, The University of Illinois at Urbana Champaign, USA; W. Kriven, The University of Illinois at Urbana Champaign, USA; D. A. Tortorelli, The University of Illinois at Urbana Champaign, USA; M. Silva, The University of Illinois at Urbana Champaign, USA

The purpose of this investigation was to understand the stress wave propagation in multilayer ceramic composite that were designed using gradient-based-topology optimization technique. The laminates were constructed with varying strong and weak layers and were gradually changed their material angle directions every 15 degrees from 0-180 degrees. For this experiment organic alumina tapes were produced as the strong layer. Colloidally-stabilized foam, starch tape, geopolymer and epoxy resin were used as the weak layers and they had respectively millimeter, micrometer and nanometer pore sizes. The flexural strength in the samples was measured as a function of the amount of wt% of alumina loading and number of strong/weak layers. It was found that alumina tapes mixed with weak layers provided crack deflection mechanisms. The multilayer ceramic composites will be tested and are expected to demonstrate stress wave management in a desired trajectory.

## **S9: Porous Ceramics: Novel Developments and Applications**

### **Symposium 9: Poster Session**

Room: Exhibit Hall

### **(ICACC-S9-P109-2012) Local structural characterizations of transition metal cation-doped amorphous silica-based membranes for high-temperature gas separation**

A. Mori\*, K. Higashiguchi, K. Hataya, S. Honda, Y. Iwamoto, Nagoya Institute of Technology, Japan

Microporous amorphous silica-based membranes are well known for their high-temperature hydrogen permselectivity. The selectivity has been explained by the molecular sieve-like property of the amorphous silica having micropores with approximately 0.3 nm in size. In our recent research, metal-organic precursor-derived transition metal cation-doped amorphous silica-based membranes have exhibited a unique high hydrogen permeance at 773 K. However the dominant mechanism for the high permeance has not been clarified yet. In this study, precursor-derived membrane materials were synthesized by the sol-gel method using tetraethoxysilane (TEOS) and an appropriate transition metal nitrate precursor. The synthesized samples were characterized by X-ray diffraction (XRD), temperature programmed reduction (TPR), temperature programmed desorption (TPD) and various spectroscopic analyses such as X-ray photo-emission spectroscopy (XPS), and diffuse reflectance fourier transform infrared spectroscopy (DRIFTS). The study of the oxidation state of the doped metal cation in the amorphous silica, the degree of hydrogen bond formations between the doped metal cation and the Si-OH groups, and the reactivity toward hydrogen at high-temperature are in progress, and results will be summarized and discussed from a view point to develop novel hydrogen-permeative ceramic-based membranes.



**(ICACC-S9-P110-2012) Fabrication of porous zirconia with high volume fraction of closed pores formed by impurities**

T. Umeda, S. Hashimoto\*, Nagoya Institute of Technology, Japan; K. Hirao, N. Kondo, H. Hyuga, Y. Zhou, National Institute of Advanced Industrial Science and Technology (AIST), Japan; S. Honda, Y. Iwamoto, Nagoya Institute of Technology, Japan

A novel technique to make a porous ZrO<sub>2</sub> with high volume fraction of closed pores was studied. It was found that ZrO<sub>2</sub> sintered bodies containing small amount of impurities exhibited larger volume expansion related to the formation of closed pore as heated at high temperatures. These closed pores are considered to be formed due to vaporization of impurities. Particularly, Si, Ti, P and Ca are the possible impurities to form the pores during heating, because the elements were mainly detected by Glow Discharge (GD) mass analysis in the ZrO<sub>2</sub> body having such unusual characteristics. Therefore, in this study, several impurities such as SiO<sub>2</sub>, TiO<sub>2</sub> and/or CaHPO<sub>4</sub> were added to 3 mol% Y<sub>2</sub>O<sub>3</sub> partially stabilized ZrO<sub>2</sub> and formation of closed pores was investigated. A porous ZrO<sub>2</sub> with ~ 30% closed pores was successfully fabricated by adding a few % of impurities and by two step heating technique. Closed pore size and morphology of the porous ZrO<sub>2</sub> bodies were investigated and formation mechanism of the closed pores was discussed in chemical thermodynamics.

**(ICACC-S9-P111-2012) Processing of functional thin films for gas separation membranes and solid oxide fuel cells with sol-gel ink-jet printing**

J. Hoffmann, T. Van Gestel\*, G. Hu, N. Menzler, M. Bram, H. Buchkremer, Forschungszentrum Jülich, Germany

This paper reports novel applications of sol-gel processing, in which ink-jet printing of sols is used to synthesize microporous gas separation membranes and several components of a solid oxide fuel cell (SOFC). In our research, we discovered that ink-jet printing can be applied to coat microporous layers, starting from a conventional alcohol-based nanoparticle sol. Within the framework of different membrane projects, we are currently developing membranes for H<sub>2</sub>/CO<sub>2</sub> separation. Typically, a selectivity > 30 is achieved for amorphous SiO<sub>2</sub> membranes, made by a dip-coating process. To date, we achieved H<sub>2</sub>/CO<sub>2</sub> and H<sub>2</sub>/N<sub>2</sub> selectivities > 50, by optimizing all conditions in the manufacturing procedure (support, sol preparation, mesoporous intermediate layers, ink jet process). These layers have the same thickness of ~100 nm as comparable layers made with dip-coating. In addition, for rapid production, the printing process is combined with a rapid thermal process (RTP), which gives an overall processing time of a few minutes for the membrane. Currently, we are also considering the sol-gel printing process as an alternative for dip- and spin-coating for a wider range of applications. This article shows a few examples of ink-jet printing of SOFC layers, including protective layers for the interconnector, CGO barrier layers and thin film 8YSZ electrolyte layers.

**(ICACC-S9-P112-2012) Fibrous Alumina Scaffolds for Bone Tissue Engineering Applications**

S. Mohanty, S. Dhara\*, IIT Kharagpur, India; A. Rameshbabu, VIT University, India

This study proposes fabrication of green ceramic fibers by wet spinning through ionotropic gelation. The slurry compositions for fiber formation consists 4 wt% chitosan in 2% acetic acid medium with 1:3 weight ratio of aluminum hydroxide in chitosan solution was spun into fiber by wet spinning in sodium tripolyphosphate (STTP) bath through ionotropic gelaion of cationic chitosan. The slurry was optimized by rheological study and the gel formation with STTP was analyzed by the gelation kinetics study. The average diameter of the produced green fiber was ~ 100 μm prior to sintering and was flexible under wet condition. Alpha alumina fibers were obtained when the fibers were calcined at 950 °C for two hours. The fibers had platelet morphology with grain size ~ 4.5 μm when calcined at 1350 °C and transformed into hexagonal platelet morphology when calcined at

1550 °C. Crystallite size of alpha alumina varied between 46 nm to 65 nm. The fibers were shaped into cylindrical scaffolds and sintered scaffolds with density 0.9 g/cc have crushing strength of 0.9 MPa. The sintered fibrous alumina scaffolds were found to have interconnected open porous structure with a compressive strength similar to cancellous bone and may be favourable for tissue in growth while implanted in vivo. This fibrous scaffold may be promising for bone tissue engineering due to their high durability, biocompatibility, and texture properties.

**(ICACC-S9-P113-2012) Obtaining of porous corundum ceramics by utilization of waste rice husk. Investigation of composition, structure and thermal degradation of rice husk**

I. G. Markovska\*, Assen Zlatarov University, Bulgaria

The aim of the present study is to develop a series of porous ceramic materials providing possibilities to control of their porous structure. Two types of industrial waste were used as initial materials - aluminium oxide from oil refining industry and waste rice husk. The methods of differential thermal analysis, scanning electronic microscopy and infrared spectroscopy were used mainly. The rice husk are a potential source of silica containing compounds. The white rice husk ash containing more than 90 mass.% SiO<sub>2</sub> and activated rice husk carbon were obtained thermally in this study. The thermal degradation and the structure of rice husk were investigated. The carbonization of rice husk was carried out in nitrogen medium at temperature of 1000 C and 60 min isothermal heating. The waste γ - Al<sub>2</sub>O<sub>3</sub> is industrial waste from oil industry. It was used as adsorbent or carrier catalyst in several production lines of the petrochemical plant, so it was contaminated with different by type and amount impurities. The contents of impurities decreased after thermal treatment at 1000 C followed by chemical treatment of the product with HCl. Using the recycled alumina and rice husk a series of porous corundum materials were synthesized.

**S14: Advanced Materials and Technologies for Rechargeable Batteries****Symposium 14: Poster Session**

Room: Exhibit Hall

**(ICACC-S14-P133-2012) Si nanowires fabricated by noble metal catalytic etching for Li-ion anodes**

J. Kim\*, S. Baek, J. Park, B. Noh, Daegu Gyeongbuk Insitute of Science & Technology, Republic of Korea

One major problem for practical application of silicon material as anode material in Li-ion batteries is the large volume changes by up to 400 % upon insertion and extraction of lithium. Silicon nanowires have the ability to accommodate large strains without pulverization. We fabricated the silicon nanowires by noble metal catalytic etching method. The HF and AgNO<sub>3</sub> solutions which enable the simultaneous precipitation of Ag particles and etching of silicon are used. The concentration of HF and AgNO<sub>3</sub> was varied. As the concentration of AgNO<sub>3</sub> is increased, the density of silicon nanowires is increased. Beyond 0.05 M of AgNO<sub>3</sub>, the density of silicon nanowires is reduced due to agglomeration of precipitated Ag particles. With the increase of HF concentration, the aspect ratio of silicon nonowires is increased. Si nanowire array films were used as working electrode, and Si substrate was used as current collector. Coin cells were assembled in a glovebox filled with argon atmosphere. The electrochemical properties of each prepared samples with various concentration of HF and AgNO<sub>3</sub> were characterized.

**(ICACC-S14-P134-2012) Effects of Al<sub>2</sub>O<sub>3</sub> Addition on Phase Transition and Ionic Conductivity of The NASICON-type Li<sub>1+x</sub>Al<sub>x</sub>Ti<sub>2-x</sub>(PO<sub>4</sub>)<sub>3</sub> Solid Electrolyte**

K. Fung\*, C. Ni, National Cheng Kung University, Taiwan

LiM<sub>2</sub>(PO<sub>4</sub>)<sub>3</sub> (M=Zr, Ti, Hf) is known to be one of the potential lithium ion conductors. This Nasicon-type network structure has

good chemical stability in the air. However, the pure  $\text{LiM}_2(\text{PO}_4)_3$  still has an ionic conductivity as low as  $10^{-6}$  S/cm. Such a low conductivity may be enhanced by partially substituted  $\text{Ti}^{4+}$  with doping ions. In this study, the NASICON-structured  $\text{LiTi}_2(\text{PO}_4)_3$  was obtained by solid state reaction, and their characteristics were investigated by analyses including X-ray diffraction (XRD), AC impedance measurement, scanning electron microscopy (SEM). After structural analysis of samples with compositions based on the formula of  $\text{Li}_{1+x}\text{Al}_x\text{Ti}_{2-x}(\text{PO}_4)_3$ ,  $x = 0.1 \sim 1.0$ , a single phase was obtained at  $x=0.1 \sim 0.4$ . The samples based on the formula where  $x=0.5 \sim 0.9$ , showed a coexisted phases of rhombohedral and orthorhombic phase ( $\text{Li}_2\text{AlTi}(\text{PO}_4)_3$ , which is isostructural with  $\text{Li}_2\text{FeTi}(\text{PO}_4)_3$ . The lattice parameter reduced due to the substitution of  $\text{Al}^{3+}$  for  $\text{Ti}^{4+}$ . From the SEM micrographs, open porosity and relative density, it showed that the Al addition improved the sintering behavior. The ionic conductivity was affected strongly with the presence of second phase in samples with higher Al content. In this study, the highest conductivity was  $8.16 \times 10^{-4}$  S/cm was obtained with the composition of  $\text{Li}_{1.3}\text{Al}_0.3\text{Ti}_{1.7}(\text{PO}_4)_3$  at room temperature.

### (ICACC-S14-P135-2012) 3D Characterization of Li-ion Batteries and other Porous Composites with Lab and Synchrotron X-ray Microscopes

P. R. Shearing, Imperial College London, United Kingdom; R. Bradley, University of Manchester, United Kingdom; S. H. Lau\*, J. Gelb, Xradia, Inc., USA; N. P. Brandon, Imperial College London, United Kingdom; P. J. Withers, University of Manchester, United Kingdom

Li-ion batteries commonly consist of two porous electrodes divided by a porous separation layer. As is typical of functional materials, there is a direct link between the microstructure of these electrodes and the performance of the cell, but the widely varying length scales make characterization a challenging task. Microstructure is known to affect a broad range of physical phenomena and is intimately linked with capacity, conductivity, charge transfer, and failure. These phenomena in Li-ion batteries occur over a range of length scales, from the formation of SEI layers occurring at the nanometer length scale to the catastrophic failure of battery architectures visible by the naked eye. We describe a non destructive technique using x-ray microscopy (XRM) techniques from both synchrotron and laboratory sources, to study Li-ion battery electrodes from individual electrode particles to full commercial batteries in 3D at multiple length scales (from mm to 50 nm resolution). Examples of the microstructural evolution processes associated with cell performance, degradation and failure mechanisms will be discussed. The use of lab based XRM to characterize other porous composites in 3D at multiscale resolution can also be applied to other materials from ceramics, geomaterials to biomaterials.

## FS2: Computational Design, Modeling, and Simulation of Ceramics and Composites

### Focused Session 2: Poster Session

Room: Exhibit Hall

### (ICACC-FS2-P140-2012) Numerical Simulation of Temperature and Stress Field Evolution Applied to Spark Plasma Sintering

J. Allen\*, C. Welch, J. Peters, US Army Corps of Engineers, Engineer Research & Development Center, USA

Spark plasma sintering (SPS) is a high-amperage, low voltage, powder consolidation technique that employs pulsed direct current (DC) and uniaxial pressure. Over the past several years, SPS has been successfully used to produce a variety of different materials including metals, composites, and ceramics. In this work we present a transient finite element model of aluminum oxide sintering that incorporates a coupled electrical, thermal, mechanical analysis that closely resembles the actual SPS experimental conditions. Within this context, we outline the governing equations that pertain to a balanced energy equation

and include the effects of thermal and electrical contact forces, radiation, and Joule heating. We couple this with the relevant equations pertaining to mechanical displacements and prescribe the necessary initial and boundary conditions for a complete solution. As part of our transient analysis, we also present our implementation of a Proportional Integral Derivative (PID) controller, which (similar to actual experimental conditions) affords the use of a predetermined heating rate conditioned upon a variable voltage. Finally, we discuss implications relating to the temperature and stress fields and suggest possible avenues for improvement.

### (ICACC-FS2-P141-2012) Electronic Structure and Interband Optical Properties of 20 MAX Phase Compounds

Y. Mo, P. Rulis, W. Ching\*, University of Missouri-Kansas City, USA

The electronic structure and interband optical conductivities of 20 MAX phase compounds:  $\text{Ti}_3\text{AC}_2$  (A=Al, Si, Ge),  $\text{Ti}_2\text{AC}$  (A=Al, Ga, In; Si, Ge, Sn; P, As; S),  $\text{Ti}_2\text{AlN}$ ,  $\text{M}_2\text{AlC}$  (M=V, Nb, Cr) and  $\text{Ta}_n\text{AlC}_n$  ( $n=1 \sim 4$ ) are calculated using the first-principles orthogonalized linear combination of atomic orbitals (OLCAO) method. The total density of states (TDOS)  $N(E_f)$  at the Fermi level  $E_f$ , increases with the number of valence electrons. The normalized  $N(E_f)$  correlates well with measured electrical conductivity values. The local configuration of TDOS near the  $E_f$  is used to predict structural stability.  $\text{Ti}_2\text{InC}$ ,  $\text{Ti}_2\text{SC}$  and  $\text{Cr}_2\text{AlC}$  have their  $N(E_f)$  at a local minimum, indicating their intrinsic stability; while  $\text{Ti}_2\text{PC}$ ,  $\text{Ti}_2\text{AsC}$  and  $\text{Ta}_5\text{AlC}_4$  have peaks in TDOS peaks at  $E_f$  suggesting them to be less stable. The interband optical conductivities and their components in the axial and in-plane directions are also calculated and analyzed. Low anisotropy was found for most of these phases except in  $\text{Nb}_2\text{AlC}$  and  $\text{Ta-Al-C}$  series.

### (ICACC-FS2-P142-2012) Crystalline Approximants of SiCO: Implications on Structure and Thermochemistry of Ternary Silicon Oxycarbide

P. Kroll\*, N. Bodiford, UT Arlington, USA

While no ternary crystalline SiCO phase has been observed experimentally so far, recent calorimetric studies have indicated negative enthalpy of formation for some polymer-derived amorphous SiCO compounds. To investigate the energetics in the ternary Si-C-O system, we generated more than 10,000 crystalline SiCO structures over a wide range of possible compositions using the Ab-Initio Random Structure Search (AIRSS) algorithm. DFT calculations are performed within the GGA using the VASP-code. Lowest energy structures of crystalline SiCO for any composition show consistent trends in structural features, which relate closely to those present in the binary constituents: four-fold coordinated Si, four-fold coordinated C, and two-fold coordinated O. Additional "free" carbon increases the likelihood of three-fold coordinated C. Overall, all ternary structures we modeled exhibit positive enthalpy of formation with respect to the crystalline phases of quartz,  $\beta$ -SiC, and graphite. The excess energy  $\Delta E$  turns out to be greater than 0.1 eV per atom for stoichiometric compositions and larger still for structures comprising "free" carbon, providing strong evidence that all ternary SiCO structures are indeed thermodynamically unstable. A comparison to amorphous SiCO yields that at low SiC content the incorporation of SiC in a disordered network is favored over crystalline models.

### (ICACC-FS2-P143-2012) Oxidation mechanism for SiCO: theoretical study on diffusion and reaction of oxygen

P. Kroll\*, B. Xu, B. Kouchmeshky, UT Arlington, USA

Dry oxidation experiments for SiCO show that temperature, carbon content, and thickness of an existing silica layer affect the morphology of the developing  $\text{SiO}_2/\text{SiCO}$  interface. In our computational study we present a rational to interpret the experimental results and to derive a modified Deal-Grove model, which describes oxidation of SiCO. Using density functional calculations, we compute activation energies for various diffusion processes of  $\text{O}_2$  in SiCO. In addition, we

access activation barriers for the reaction of oxygen with the matrix, converting the SiCO into an SiO<sub>2</sub> and releasing CO. Our results indicate that in SiCO glass a reaction of O<sub>2</sub> with sp<sup>3</sup> C of the glass is favored over diffusion of O<sub>2</sub>. Thus, a SiCO glass will exhibit a sharp oxidation from  $\dot{m} = \dot{m}_0$  under these conditions. The reverse process, reduction of CO to either carbidic or graphitic carbon is very unlikely. Overall, our work provides insight into the oxidation resistance of SiCO.

**(ICACC-FS2-P144-2012) Design of ZrO<sub>2</sub>/SiC Composite Materials with very low-thermal conductivity**

B. Kouchmeshky, P. Kroll\*, UT Arlington, USA

We study properties of ZrO<sub>2</sub>/SiC composite materials for engineering applications in which the control of thermal transport is important. Knowledge of the individual contributions of phonons on thermal transport provides us necessary information to focus on most important phonon frequencies. In our study, we select a series of candidate model geometries – different assembly of ZrO<sub>2</sub>/SiC superlattices – and use a virtual testing method to support the design process. The foundation for our concept is the scattering of phonons at interfaces, which may yield destructive interference and low conductivity. Integrating atomistic non-equilibrium molecular dynamics simulations to determine thermal conductivity we provide a proof-of-concept study and deliver best design scenarios of ZrO<sub>2</sub>/SiC composite materials with very low-thermal conductivity.

**(ICACC-FS2-P145-2012) Molecular dynamics simulations of hypersonic velocity impact protection properties of CNT/a-SiC composites**

A. Goodarzi\*, Amirkabir University of Tech., Islamic Republic of Iran; H. Taylor, Imperial College London, United Kingdom

The hypersonic velocity impact protection properties of carbon-nanotube-reinforced amorphous silicon carbide composites are investigated using molecular dynamics simulation. The projectile-impact induced damage to target materials is analyzed for composite targets having perpendicular and parallel alignments of carbon nanotubes with respect to impact direction, and compared to that of pristine amorphous silicon carbide target. It was found that, in the considered range of impact velocities, the penetration depth is approximately the same for both CNT-reinforced composites and pristine a-SiC target. At short time-scales, damage to a target is defined by penetration depth of projectile and density rearrangements taking place in the target material. In the composite with carbon nanotubes aligned parallel to the impact direction, a channeling of damage to deeper regions of the target occurs. In the case of perpendicular alignment, the damage is confined to a narrow region underneath the penetrating projectile. For both considered composite samples, we found that a significant damping of the amplitudes of compressive shock-waves takes place, thus reducing the special extent of damage in composites as compared to that in the pristine a-SiC target.

**(ICACC-FS2-P146-2012) Studies of gas-phase reactivity during chemical vapor deposition of boron carbide**

G. Reinisch, University Bordeaux 1, France; J. Leyssale, CNRS, France; S. Patel, University Bordeaux 1, France; G. Chollon, CNRS, France; G. L. Vignoles\*, University Bordeaux 1, France

Boron carbide is a key constituent of self-healing ceramic-matrix composites, due to its ability to fill matrix cracks by a liquid oxide phase upon oxidation. Its production as protective layers in a multilayered matrix can be performed by Chemical Vapor Infiltration. Since this process is difficult to manage in terms of deposit thickness and quality as a function of processing parameters, a modeling study has been. It features several steps: (i) ab-initio quantum chemical computations using the G3B3 method, (ii) derivation of thermochemical and kinetic data for the main species and reactions involved

in the gas-phase mechanism, (iii) insertion of the obtained mechanism in a 0D thermochemical equilibrium solver and in a 1D chemical kinetic solver. Several specific tools have been developed and applied for a correct treatment of step (ii). An extension of the hindered rotor models with variable kinetic function has been design for a correct computation of partition functions associated to internal rotations in molecules or transition states. The B/3Cl/3H subsystem has received special attention because of transition states without local energy maxima, internal rotations, and reaction product valley bifurcations. Results are compared to experimental data and allow an identification of key species and main reaction pathways during deposition.

**(ICACC-FS2-P147-2012) Image-based 2D Numerical Modeling of Oxide Formation in Self-Healing CMCs**

V. Dréan, INRIA, France; G. Perrot, University Bordeaux 1, France; G. Couegnat, CNRS, France; M. Ricchiuto, INRIA, France; G. L. Vignoles\*, University Bordeaux 1, France

Self-healing Ceramic-Matrix Composites (CMCs) are promising candidates for jet engine hot parts, because of their excellent lifetimes. They are constituted of a 3D arrangement of SiC fiber tows, infiltrated by a multilayer matrix. A pyrocarbon interphase acts as a crack deviator, SiC matrix layers bring stiffness, and boron-containing phases are able to produce above 450°C a liquid oxide which prevents further oxidation by a diffusion barrier effect. This paper introduces an image-based numerical simulation of self-healing under oxidative gases. Existing 0D or 1D models give the time evolution of the oxygen concentration in the weakest fiber of the composite; they deduce from it a global lifetime through an oxygen-controlled slow crack growth rate law. We propose now an approach in which the resolution domain is a 2D FE mesh directly obtained from transverse images of a tow containing the crack. Oxygen diffusion, carbon consumption around the fibers and conversion of boron carbide into boron oxide are simulated. The model solves mass balances for oxygen (gaseous or dissolved), liquid phase height, and consumed heights of pyrocarbon and boron-containing phase. All the heights are considered perpendicular to the image plane (thin layer approximation). Preliminary results of computations performed in images containing several tens of fibers, plus a multilayer matrix, will be displayed and discussed.

**(ICACC-FS2-P148-2012) First Principles Calculations of Boron Carbide**

J. S. Dunn\*, J. C. LaSalvia, U.S. Army Research Laboratory, USA

Boron carbide is the third hardest naturally occurring material after diamond and boron nitride, and has been widely used in armor, abrasives, and nuclear applications. The Army (R. McCuis-ton, 2007) initiated a program to improve its fracture toughness by creating a doped Y-Al-B-Si glassy intergranular film (IGF) at the grain boundary interface. The resulting hot-pressed boron carbide/glass bodies had densities near 90% of the theoretical density. Imperfect glass wetting, high glass viscosity, high glass vapor pressure, and strong boron carbide/glass adhesion prevented complete densification from being achieved. Unfortunately, the compositional design space for doped-glass systems is very large. A method is needed to identify promising regions within this design space to reduce the number of processing experiments. The Density Functional Theory (DFT) approach offers a promising way to explore the wettability, thermodynamic stability, and adhesion strength of doped glassy IGFs within boron carbide. In this study, we develop a bulk model for several different boron carbide compositions and analyze the differences in the electronic structure as a function of composition. We also performed calculations to determine the optimal surface termination for a (0001)-oriented boron carbide slab and study simple adsorption phenomena on its surface.

### FS3: Next Generation Technologies for Innovative Surface Coatings

#### Focused Session 3: Poster Session

Room: Exhibit Hall

#### (ICACC-FS3-P149-2012) Growth behaviors of iron nitride in a low pressure gas nitriding reactor

Y. Kim\*, Hanbat National University, Republic of Korea; K. Moon, Korea Institute of Industrial Technology, Republic of Korea

Nitriding is well known surface treatment process of steels in order to improve the wear resistance, the fatigue endurance and the corrosion resistance. A compound layer that is formed on the surface of the steel in the limited thickness consists mainly of  $\epsilon$ -Fe<sub>2</sub>-3N and/or  $\gamma'$ -Fe<sub>4</sub>N depending on nitriding conditions including gas composition and temperature. The  $\epsilon$ -nitride is better wear and corrosion resistance than  $\gamma'$ -nitride. However,  $\epsilon$ -nitride reduces the fatigue endurance significantly because cracks are easily initiated at the brittle  $\epsilon$ -nitride. In this work, growth behaviors of iron-nitride on carbon steel and alloy steel at low pressure gas nitriding were examined. Surfaces of the steels covered with fine and porous oxide during the pre-oxidation using N<sub>2</sub>O gas. Well faceted particles connected with them were observed after 1 min nitriding. They grew steadily and filled inter-pores during additional nitriding process. From the x-ray diffraction analysis,  $\gamma'$ -iron nitride was dominantly formed at the initial stage but the amount of  $\epsilon$ -iron nitride was rapidly increased as nitriding treatment time. The porous layer was formed on the particles and thickened up to half of nitride layer after 60 min nitriding. The observed growth behaviors were discussed in internal stress related with volume expansion involved in transforming from iron to iron-nitrides.

#### (ICACC-FS3-P150-2012) Fabrication, characterization and mechanical properties of the Y-Ti-O ceramics

S. Amarume\*, Nagaoka university of technology, Japan; H. Lingfeng, University of Wisconsin-madison, USA; N. Tadachika, Nagaoka university of technology, Japan; R. Ramaseshan, Homi Bhabha National Institute, India; Y. Sato, Nagaoka university of technology, Japan; H. Asami, Tomakomai national College of Technology, Japan; T. Suzuki, H. Suematsu, K. Niihara, Nagaoka university of technology, Japan

Oxide Dispersion Strengthened (ODS) steel is high tensile, creep resistance, fatigue strength, it has a value of resistance to radiation damage, which is expected to be applied to next generation fusion reactor. ODS steel is dispersed the Y-Ti-O nanoparticles and its affects to the mechanical properties. However, to evaluate the mechanical properties of nano-particle itself is difficult. Therefore, this study will fabricate a variety of Y-Ti-O oxides can be formed in the steel, its mechanical properties were evaluated. In this experiment, and Y-Ti-O ceramics of various compositions prepared using the hot press method. The mechanical properties, thermal properties were evaluated. The fine structures of the oxides were measured by XRD, SEM and TEM. The mechanical properties of the several kinds of composition of Ti-Y-O ceramics were measured and it was strongly affected by the fine structure of the secondary phase.

#### (ICACC-FS3-P151-2012) Fabrication of the rubber and ceramics electrets with nano second pulsed discharge

M. Mitsuhashi\*, T. Nakayama, S. Endo, M. Terauchi, W. Jiang, T. Suzuki, H. Kim, H. Suematsu, K. Niihara, Nagaoka University of technology, Japan

Electret is a permanently charged dielectric. Therefore, it is expected to be applied to such generators, and electrostatic air purifier. To create an effective electret is a dielectric having a need to create a large charge. Method gives a charge, usually is used to polarize the sample by high-voltage direct current. Here, using the pulse discharge, as well as electronic, are expected to be effectively charged ions to ionize molecules also occur in the air. In this study, by using a semiconductor switching device to create a nano-second pulse power, by which the rubber, polymer, gave a charge to ceramics and composites of

these. It was possible to control the charge as an electret type and power depending on the type of material.

#### (ICACC-FS3-P152-2012) Plasma-Enhanced CVD of Metal Oxide Nanostructures: Growth and Device Applications

A. Mettenboerger\*, A. P. Singh, P. Golus, N. Tosun, S. Mathur, University of Cologne, Germany

Application of tailor-made molecular precursors in plasma-enhanced chemical vapor deposition (PE-CVD) techniques offers a viable solution for overcoming thermodynamic impediments involved in thin film growth. The use of cold plasmas enables the realization of various functional coatings whose application spectrum spans from transparent conductive coatings, scratch-proof films, photoactive to anti-bacterial materials. Over the past decade, we have developed several new precursor systems in order to demonstrate the competitive edge of molecule-based plasma coatings. Our work on a large number of metal oxide systems and their characterization towards microstructure, compositional and functional properties supports the advantages of chemical design in simplifying deposition processes and optimizing functional behaviour. This presentation will focused on how the PE-CVD processed nanostructured films of different metal oxides open up new vistas of material properties, which can be transformed into advanced material technologies. The examples will include application of thin glassy films as barrier and corrosion-resistant coatings, metal oxide nanowires and heterostructures for photoelectrochemical applications.

#### (ICACC-FS3-P153-2012) Non-vacuum type Atomic Layer Deposition of TiO<sub>2</sub> Thin films

W. Kwack\*, S. Kwon, S. Jeong, Y. Jeong, Pusan National University, Republic of Korea

Atomic layer deposition (ALD) has evaluated as an important thin film deposition technique for a variety of applications owing to its inherent abilities such as a digital controllability of sub-atomic level thickness, large area capability, excellent conformality, good reproducibility, simplification of the use of solid precursors, a wide range of film materials, high density, and low impurity level. In spite of its outstanding benefits, however, the major drawbacks of ALD technique are slow growth rate, high cost vacuum process, and the waste of precursors in ALD processes, which make it hard to be adopted in most industries. Hence, a novel method that can solve these drawbacks of conventional ALD process while keeping the inherent advantages of conventional ALD needs to be developed for being widely utilized in various industries. In this study, we proposed a novel non-vacuum type ALD process to solve the drawbacks of conventional vacuum type ALD. Our proposed process had the advantages of wet-process such as low production cost and high deposition rate as well as the advantages of conventional vacuum based ALD such as excellent controllability of thickness, and good step coverage. In addition, we compared the growth characteristics and film properties of TiO<sub>2</sub> thin films prepared by non-vacuum type ALD process with TiO<sub>2</sub> thin films prepared by using conventional ALD.

#### (ICACC-FS3-P154-2012) Flexible piezoelectric thin film by hydrothermal process

S. Lee, Inha University, Republic of Korea; W. Lee, H. Song, C. Kang, Korea Institute of Science and Technology, Republic of Korea; D. Jeong\*, Inha University, Republic of Korea

Flexible piezoelectric films are required for energy harvester or sensors especially for the low mechanical impedance condition. For the film to be flexible, substrates should be also flexible and polymer or thin metal films are suitable for this purpose. However, as the piezoelectric materials were usually heat-treated for the crystallization at the high temperature, polymer materials or thin metal substrates could not be utilized for conventional process. To use the polymer or thin metal substrates, noble process with low processing temperature should be introduced. It is known that hydrothermal process can produce the high crystalline materials below 200 °C. In this research, we

will fabricate the piezoelectric film on flexible substrate and characterize the electrical properties. This flexible piezoelectric film will be promising for high performance energy harvesting and sensors.

**(ICACC-FS3-P155-2012) Synthesis of Dense Nanocrystalline YSZ Coating by Room Temperature Vacuum Cold Spraying**

C. Park\*, K. Baik, Chungnam National University, Republic of Korea

Room temperature vacuum cold spraying (RT-VCS), commonly referred to as aerosol deposition, is a novel technique to form a thick ceramic films with high density and nanocrystalline structure at room temperature. Submicron ceramic particles are accelerated by gas flow in the nozzle up to velocity of several hundred m/s. During interaction with substrate, these particles formed thick, dense, uniform and hard ceramics layers. In this study, a thin 8mol.% YSZ film of ~20nm was produced by vacuum cold spraying and evaluated in terms of microstructural features, gas tightness and ionic conductivity for SOFC application. The sprayed YSZ film comprised nanocrystalline grains of 10-20nm, and was dense enough to satisfy the requirement of gas tightness for SOFC electrolyte. The measured ionic conductivity of sprayed YSZ film at 600-900°C in air was much higher than that of sintered YSZ. The improvement of ionic conductivity was attributed to the formation of nanocrystalline grains.

**(ICACC-FS3-P156-2012) Microstructure Evolution and Electrical Properties of Plasma Sprayed Ba-Ti-O Coating**

K. Baik, D. Lee\*, Chungnam National University, Republic of Korea

In this study, atmospheric plasma spraying has been employed to produce a thick BaTiO<sub>3</sub> coating, and microstructural features and dielectric properties of BaTiO<sub>3</sub> coatings have been investigated. As-sprayed Ba-Ti-O coating was mainly composed of amorphous phase from splat quenching of fully molten droplets. Small amounts of crystalline phase also remained due to incorporation of partially-molten droplets. The as-sprayed amorphous coating was crystallized to BaTiO<sub>3</sub> at low temperatures and a mixture of BaTiO<sub>3</sub> and BaTi<sub>2</sub>O<sub>5</sub> at high temperatures. At 1200°C, the coating was formed an equiaxed grain structure due to sintering effects. Dielectric constant of Ba-Ti-O coatings was rapidly increased from 85 for as-sprayed to 270 for heat-treated at 1200°C. The plasma-sprayed BaTiO<sub>3</sub> coatings were discussed for the application of electrostatic chuck.

**(ICACC-FS3-P157-2012) A study on the ternary elements (X= Cr, Zr, Mo, Cu, Si, B) addition on the Ti-Al-N coating deposited by magnetron sputtering process with single alloying targets**

K. Moon\*, D. Jung, C. Byun, S. Shin, KITECH, Republic of Korea

To improve the properties of TiAlN coating, third elements addition such as Si, B, Cr has been popularly tried. The addition of Si to AlTiN and structurally well manipulation led to the formation of nano-composite coating of TiAlN and Si<sub>3</sub>N<sub>4</sub> phases. This resulted in the super-hardness over 40 GPa and the increase of the oxidation temperature over 1000 °C. However, it is not easy to add Si to the AlTiN by a proper PVD system. In this study, Al-Ti based single alloying targets were prepared by powder metallurgy of mechanical alloying and spark plasma sintering. Also, Si, Cu, Cr, B, Zr, Mo added targets were prepared to improve wear, thermal and oxidation properties. The investigation on the alloying targets showed that their microstructure was nano-sized about 20-30 nm and all the elements were homogeneously distributed. Ternary Ti-Al-based coatings were deposited by unbalanced magnetron sputtering method with various alloying targets. The composition of the coating was almost same with that of the target. Their microstructures and mechanical properties were investigated by XRD, SEM, TEM, nano-indenter, tribometer, etc. The easiness of the nanocomposite structure was reviewed with alloying properties between alloying elements added in the coating.

**(ICACC-FS3-P158-2012) A study on the improvement of the service life of shaft-bushing tribosystems by plasma sulfur nitriding process**

H. Kim\*, K. Kim, J. Kim, Daekeum Geowell, Republic of Korea; K. Moon, C. Byun, KITECH, Republic of Korea

Sliding bearing in a low speed and high load condition is one of the most important parts in the front hinge parts of excavators. The slid-

ing contact between a shaft and a bushing is known to have a microscopic irregularity. Thus the damage of the shaft and the bush are formed irregularly. Especially, the localized plastic deformation of the bush results in a severe damages. In many cases, the damage is accelerated by the presence of dust or sand between the bush and the shaft. The accumulation of microscopic damage in the parts leads to severe wear, sliding noise and final macro-fracture. Thus, the shaft and the bushing need to have the properties of high strength, high wear resistance and good lubrication. Generally, they are surface treated such as nitriding and PTFE coating or nitriding and MoS<sub>2</sub> coating. But such processes are two steps process, that is, they are treated to be nitride in one chamber and then subsequent coated in another chamber. So, if the required properties could be gained by one step process, the production cost would be cut off. In this study, the surface of bushing has been treated by plasma sulfur nitriding process. To estimate the durability of the plasma sulfur nitriding bushing, endurance tests performed and the results will be reported in this present.

**(ICACC-FS3-P159-2012) Development of a dry and wet process for the applications in boundary lubrication area**

K. Moon\*, T. Hwang, KITECH, Republic of Korea

The machinery parts used in boundary conditions should have the properties of high hardness with enough depth from the surface, high wear resistance and good lubrication on the surface. For the enough hardness depth, they are generally treated by nitriding process. For a low friction and a high hardness at the surface, they could be treated by some proper coating process. But in such case, the most important property for the endurance of the duplex coating is adhesion force. So it is very important to manipulate the phase and surface morphology before the coating process. In this study, SiO<sub>2</sub> coating and PTFE coating are tried to be coated on the nitrided steel surface. The polymeric SiO<sub>2</sub> coating and PTFE based coatings are made by Sol-Gel process. The effects of the nitriding phase and surface treatment before coating were examined by scratch tester and indentation tester. Also their wear properties were measured by plate-plate sliding wear measurement method with or without oil addition.

**(ICACC-FS3-P160-2012) A study on the lubrication properties of Diamond Like Carbon coating for industrial applications**

K. Moon\*, J. Kim, KITECH, Republic of Korea; J. Park, Hanyang University, Republic of Korea

DLC films have been applied to diverse industrial fields because of good tribological properties like high hardness, low friction coefficient and chemical stability etc. They have found applications in tribology, mechanics, electronics, biomedicine and even the arts. However DLC has the weakness of high temperature instability and could have bad friction coefficient in moisture, some oil, and even react with solder materials. So in this study, DLC film was post-treated with CF<sub>4</sub> gas to increase the hydrophobic property and the lubrication ability. In this study, DLC films were deposited by PECVD process with C<sub>2</sub>H<sub>2</sub> and Ar gases after the deposition of Si interlayer. And then, to improve super-hydrophobic properties of DLC films, they were treated by CF<sub>4</sub> + Ar gases. The structure of DLC films was confirmed by Raman and the hydrogen contents in the DLC films were measured by RBS and ERD analysis. In additions, the mechanical properties of DLC films were analyzed by scratch tester for adhesion, nano-indenter for hardness and Tribo-meter for wear properties including friction coefficient. Also, it will be reported on the industrial application of the diamond like carbon coating with the improved lubrication property

**(ICACC-FS3-P161-2012) Metal Nitride Coatings for Wear Resistant Aluminum Extrusion Mold**

S. Lee, S. Kim\*, Korea University Of Technology and Education, Republic of Korea

Hard ceramic coatings have increased the life of metal tools, molds and mechanical parts. For example, Ti, Cr and Al based nitrides or carbides thin hard coatings have widely been used for tools because

the coatings also have excellent wear and corrosion resistance. But the application on the aluminum extrusion mold is in the beginning stage, and the wear data did not file up sufficiently. The purpose of this study is to show the friction and wear behaviors of CrN, TiN, CrAlN and TiAlN coated on SKD61 which is applied to Al BM76 extrusion mold. On the wear test, the experimental parameters are the load and counter material's temperature. As results, the friction coefficient increased with load increasing but decreased with counter material's temperature increasing, and those of CrAlN and CrN were lower than those of TiAlN and TiN especially at higher temperature. Wear track with different coatings identified different wear behaviors, that with CrAlN and CrN is abrasive, but that with TiAlN and TiN is adhesive. Therefore, the CrAlN and CrN showed less coating wear rate and counter material's adhesion than the TiAlN, and TiN. Especially, CrAlN showed the lowest wear loss with lower friction coefficient and less adhesion of counter materials at the wide range of wear load and temperature.

### (ICACC-FS3-P162-2012) Temperature Dependent Thermoelectric Properties of Bismuth Antimony Telluride Prepared by Spark Plasma Sintering

K. Lee\*, Y. Jeong, Pusan National University, Republic of Korea

Bismuth antimony telluride (BiSbTe) thermoelectric materials were successfully prepared by spark plasma sintering (SPS). The crystalline BiSbTe ingots were broken into small pieces and then attrition milled into fine powders of about 800 nm under argon gas. Spark plasma sintering was applied on the BiSbTe powders at 240, 320, and 380 °C under a uniaxial pressure of 40 MPa. At all sintering temperature ranges, high density of bulk BiSbTe was successfully obtained. The thermoelectric properties of BiSbTe was evaluated by the dimensionless thermoelectric figure of merits (ZT) defined as  $ZT = \alpha^2 \sigma T / \kappa$ , where  $\alpha$  is the Seebeck coefficient,  $\sigma$  is the electrical conductivity,  $\kappa$  is the thermal conductivity and T is the absolute temperature, respectively. With increasing the sintering temperature, the grain size of BiSbTe was increased and the electrical conductivity ( $\sigma$ ) of BiSbTe was also improved by an increased hall concentration. With increasing the sintering temperature, however, the thermal conductivity ( $\kappa$ ) of BiSbTe was increased due to the decreased phonon scattering caused by the grain growth. Due to the competition of these two contrary effects, the maximum ZT value of 1.14 was achieved at 100 °C for the samples sintered at 380 °C.

## FS4: Advanced (Ceramic) Materials and Processing for Photonics and Energy

### Focused Session 4: Poster Session

Room: Exhibit Hall

### (ICACC-FS4-P163-2012) The Production of Photoactive Coatings by Plasma Electrolytic Oxidation

L. K. Mirelman\*, B. Clyne, C. Dunleavy, J. Curran, University of Cambridge, United Kingdom

Titanium dioxide, particularly in the anatase form, has proven to be a highly efficient photocatalyst under ultraviolet light. A promising approach to producing highly efficient TiO<sub>2</sub> photoactive surfaces is to use the Plasma Electrolytic Oxidation (PEO) process on high purity titanium substrates. The process has been used to create TiO<sub>2</sub> surfaces under a variety of conditions and measurement of phase constitutions as well as surface microstructures has been undertaken. Sodium phosphate-based electrolytes were used and both treatment time and electrolyte concentration were varied whilst current densities were held constant at approximately 20A/dm<sup>2</sup>. X-ray diffraction with initial Rietveld analysis revealed crystallinities above 90 %, predominantly made up of anatase. Scanning Electron Microscopy (SEM) with Energy Dispersive Spectroscopy (EDS) revealed high porosity microstructures typical of those found in PEO microstructures. The degradation of methylene blue under UV illumination,

using the coatings as catalysts, was also investigated and the effects of different electrolytes compared.

### (ICACC-FS4-P164-2012) Crystallization, binding energy and chemical states in ion-implanted TiO<sub>2</sub> nanotubes and nanofibres

I. J. Low\*, Curtin University, Australia; F. W. Yam, Universiti Sains Malaysia, Malaysia; V. De La Prida, University of Oviedo, Spain; M. Ionescu, Australian Nuclear Science & Technology Organisation, Australia

Production of limitless hydrogen fuel by splitting of water using the photo-electrochemical technology is cost-effective and sustainable. To make this an attractive viable technology will require a new materials design concept for TiO<sub>2</sub> photocatalysts. Due to its wide band gap energy, TiO<sub>2</sub> is active only under near-ultraviolet irradiation. However, modified TiO<sub>2</sub> with narrower band gap can be developed so that they are active under visible light irradiation. In this endeavour, ion-implantation has now emerged as an alternative but effective method to improve the separation of the photo-generated electron-hole pairs or to extend the wavelength range of the TiO<sub>2</sub> photo-responses into the visible region. In this paper, we describe the use of synchrotron radiation to investigate (a) the effect of ion-implantation (Cr & Bi) on the crystallization and phase stability at elevated temperature in as-anodized TiO<sub>2</sub> nanotubes and nanofibres, and (b) the binding energy and chemical states in ion-implanted TiO<sub>2</sub>. Depth-profiling of phase composition at the near surface ion-implanted TiO<sub>2</sub> will be evaluated using time-of-flight Secondary Ion Mass Spectrometry (SIMS) and Rutherford Back-Scattering (RBS). The effect of ion-implantation on the electronic state or binding energy of elements at the near surface will be measured using synchrotron x-ray photoelectron spectroscopy.

Wednesday, January 25, 2012

## S1: Mechanical Behavior and Performance of Ceramics & Composites

### In-Situ Evaluations Using X-rays/Neutrons and NDE

Room: Coquina Salon D

Session Chairs: Goffredo de Portu, ISTEC-CNR; Jiengang Sun, Argonne National Lab

8:00 AM

### (ICACC-S1-033-2012) In situ Synchrotron Studies of the Tetragonal to Monoclinic Phase Transformation in Hafnia and Zirconia

R. P. Haggerty, P. Sarin, Z. D. Apostolov, W. M. Kriven\*, University of Illinois at Urbana-Champaign, USA

Using a quadrupole lamp furnace and a novel curved image plate detector the structure of HfO<sub>2</sub> and ZrO<sub>2</sub> have been characterized by high temperature x-ray diffraction. The structural information provided by these experiments allows the properties of the transformation to be further investigated. Using phenomenological theory of martensite crystallography, the strain associated with the transformation from the tetragonal to the monoclinic phase has been described and provides insight into the lack of transformation toughening found in HfO<sub>2</sub>. Further characterization includes determination of the transformation temperature in air, the change in volume associated with the transformation and the temperature hysteresis of the transformation. In addition to transformation properties, the thermal expansion of HfO<sub>2</sub> and ZrO<sub>2</sub> has been thoroughly described as a function of temperature and crystallographic direction. The monoclinic phases of ZrO<sub>2</sub> and HfO<sub>2</sub> have largely anisotropic thermal expansion, which can only be fully described in tensor form, due to the low symmetry of the crystal. A systematic procedure for analyzing the thermal expansion of such low symmetry materials has been developed. Full characterization of the thermal expansion of the crystals has provided insight into the relationship of the bonds in the structure to the expansion on heating.

**8:20 AM****(ICACC-S1-034-2012) Ferroelastic Phase Transformations in Rare-Earth Niobates**

P. Sarin\*, D. R. Lowry, J. Angelkort, Z. D. Apostolov, R. P. Haggerty, W. M. Kriven, University of Illinois at Urbana-Champaign, USA

The rare-earth niobates are known to undergo a reversible, ferroelastic phase transformation from a high temperature, paraelastic, scheelite-type (tetragonal, I41/a) to a ferroelastic, fergusonite-type (monoclinic, I2/a) structure upon cooling. In such transformations only the unit cell shape changes with no apparent change in volume, accompanied with domain rearrangements resulting in ferroelasticity. Such phenomena could lead to shape memory behavior or "smart" ceramic systems with potential for application as large force actuators having spontaneous strains of 6-7 %. The mechanism driving the ferroelastic phase transformation in this class of compounds is not entirely understood. In this study phase transformations in  $\text{YNbO}_4$  and  $\text{LnNbO}_4$  (where Ln = La and Dy), were studied in-situ, at high temperatures using synchrotron X-ray diffraction. The ferroelastic phase transformation in the studied materials was found to be second-order in nature, with highest transformation temperatures observed in the case of  $\text{YNbO}_4$  ( $\sim 861 \pm 2^\circ\text{C}$ ). Changes in lattice parameters, and the spontaneous strain in the ferroelastic phase as functions of temperature will be presented. Atomic rearrangements associated with the transformation of the ferroelastic phases, will be interpreted to elucidate the role of the rare-earth cation in controlling the transformation temperatures.

**8:40 AM****(ICACC-S1-035-2012) In-situ synchrotron x-ray diffraction and thermal analysis study of the cubic to rhombohedral phase transformation in  $\text{Y}_6\text{WO}_{12}$  and its thermal expansion behavior up to  $1500^\circ\text{C}$** 

Z. Apostolov\*, P. Sarin, R. P. Haggerty, W. M. Kriven, UIUC, USA

Rare earth (RE) tungstates exist as several stable compositions, some of which have been studied for their luminescence properties, negative thermal expansion behavior, as potential laser host materials and cation conductors. Most research has been focused on the  $\text{WO}_3$ -rich end of the phase diagram, however, the  $\text{RE}_2\text{O}_3$ -rich half offers some very refractory  $\text{WO}_3$ -compounds for use in high-temperature applications. The objective of this study is to identify any observable trend in the high-temperature properties and elucidate the phase transformation behavior, across its RE members. This presentation will focus on the fcc-to-rhombohedral transformation in the  $\text{Y}_6\text{WO}_{12}$  system, as well as on comparing its thermal expansion properties with the Er and Yb analogues. The phase transformation in  $\text{Y}_6\text{WO}_{12}$  was found to be a thermally activated, heating rate-dependent, interface-controlled continuous ordering process, which occurred over a temperature range. No abrupt change in enthalpy was detected, but a volume change of  $-1.75\%$  on heating was observed with both diffraction and dilatometry. Three dimensional representation of the thermal expansion properties, determined from high temperature XRD data, will also be discussed, in order to understand the role of the RE cation in structural modifications with temperature.

**9:00 AM****(ICACC-S1-036-2012) Investigation of thermal properties of  $\text{ZrP}_2\text{O}_7$  and  $\text{Zr}_2\text{P}_2\text{O}_9$** 

J. Angelkort\*, P. Sarin, Z. D. Apostolov, P. F. Keane, W. M. Kriven, University of Illinois, USA

Zirconium phosphates show only small thermal expansion coefficients and undergo phase transitions induced by changes of temperature. Upon cooling,  $\text{ZrP}_2\text{O}_7$  transforms at  $T_c=290^\circ\text{C}$  into a  $3 \times 3 \times 3$  superstructure of the high-temperature structure involving changes of the molecular conformations of the  $\text{P}_2\text{O}_5$  groups. The monoclinic low-temperature modification ( $\alpha$ -phase) of  $\text{Zr}_2\text{P}_2\text{O}_9$ ,

transforms at  $T_c=1150^\circ\text{C}$  irreversibly into an orthorhombic high-temperature phase ( $\beta$ -phase). A powder sample containing both  $\text{ZrP}_2\text{O}_7$  and  $\text{Zr}_2\text{P}_2\text{O}_9$  phases was used for simultaneous, temperature-dependent x-ray diffraction experiments. This presentation will include thermal expansion behavior of  $\text{ZrP}_2\text{O}_7$  and  $\text{Zr}_2\text{P}_2\text{O}_9$  phases, as determined from the changes in the lattice parameters as functions of temperature. The underlying mechanisms of the phase transitions of the two compounds, based on the analysis of the high- and the low-temperature crystal structures, will also be discussed.

**9:20 AM****(ICACC-S1-037-2012) Microstructures of La-doped Low Thermal Expansion Cordierite Ceramics**

H. Unno\*, KROSAKI HARIMA CORPORATION, Japan; S. Toh, Kyushu University, Japan; J. Sugawara, K. Hattori, KROSAKI HARIMA CORPORATION, Japan; S. Uehara, S. Matsumura, Kyushu University, Japan

La-doped commercial-grade cordierite ceramics have a low thermal expansion coefficient of  $< 0.03$  ppm/K at  $23^\circ\text{C}$  and high dimensional stability with the passage of time. Microstructures of La-doped cordierite ceramics were investigated by transmission electron microscopy (TEM) and X-ray diffraction (XRD) analyses in connection with their thermal expansion properties. Scanning TEM-EDS and electron diffraction analyses revealed that micrometer-sized cordierite grains surrounded by a curved or faceted boundary have several types of inclusions, and La-enriched glassy phases are formed around the grain boundaries. The volume variation behavior of the specimen at temperatures ranging from  $50$  to  $1200^\circ\text{C}$  is almost the same as that of cordierite unit cell characterized by the orthorhombic low-temperature phase (space group Cccm). Therefore, the difference of thermal expansion properties between cordierite grains and glassy phases is thought to be quite small, which is responsible for the high dimensional stability. The specimen once shrinks with increase of the temperature to  $23^\circ\text{C}$ , but it expands further rise in the temperature, drawing a minimum of thermal expansion coefficient. In this conference, the mechanism of low thermal expansion will be discussed in terms of the volume variation behavior of the specimen and the unit cell at around room temperature, the latter is measured by Rietveld analysis of XRD data.

**10:00 AM****(ICACC-S1-038-2012) CTEAS - A GUI based program to calculate coefficients of thermal expansion of crystalline materials from high temperature powder X-ray diffraction**

Z. A. Jones\*, P. Sarin, R. P. Haggerty, W. M. Kriven, University of Illinois at Urbana-Champaign, USA

Thermal expansion of crystalline materials is commonly determined from the change in lattice parameters with temperature. For many low symmetry systems, such as those exhibiting monoclinic or triclinic symmetries, this method is inadequate to describe the anisotropies in crystallographic expansion. CTEAS is a graphical user interface (GUI) based program which enables a user to visualize and understand thermal expansion in both low and high symmetry crystal structures. It converts information on variation in d-spacings of a material with temperature, which is accessible from multiple reflections acquired in a routine high temperature powder X-ray diffraction experiment, into a comprehensive description of thermal expansion properties of the material. Besides generating figures and movies to describe thermal expansion in 3-dimensions, both qualitatively and quantitatively, the thermal expansion of any crystallographic plane or direction can also be calculated. This information can be related to the crystal structure and helps in understanding phase transformation processes, if any, as well as in- and out-of-plane thermal expansion properties of thin films. In summary, CTEAS makes thermal expansion of the most complex crystals easy

to study and understand, rendering it an excellent tool for research and teaching.

**10:20 AM**

**(ICACC-S1-039-2012) On the response of  $Ti_2SC$  &  $Ti_3SiC_2$  to stress studied by in-situ neutron diffraction, nanoindentation and the elasto-plastic self-consistent approach**

M. M. Shamma\*, V. Presser, Drexel University, USA; B. Clausen, D. Brown, Los Alamos National Laboratory, USA; M. Barsoum, Drexel University, USA

In this paper the results of in situ neutron diffraction results on polycrystalline  $Ti_2SC$  and  $Ti_3SiC_2$  samples are presented and modeled via the elasto-plastic self-consistent approach (EPSC). Because  $Ti_2SC$  is the only MAX phase known to date whose response is fully linear elastic below 1 GPa it was chosen to test validity of the EPSC model, as well as, the elastic constants derived from ab initio calculations. Both were found to be valid.  $Ti_3SiC_2$  exhibits kinking nonlinear elastic (KNE) behavior. In this work, using the EPSC model, we show that this behavior cannot be explained by either the activation of 11-21 twins – that are special cases of incipient kink bands or IKBs- nor dislocation pileups on the basal planes since in both cases a permanent plastic stain is predicted. On the other hand, the results are in agreement with the formation of IKBs, the micromechanism proposed to explain KNE behavior.

**10:40 AM**

**(ICACC-S1-040-2012) Depth-resolved strains within thermal barrier coatings from in situ thermo-mechanical characterization using high-energy x-rays**

R. Diaz, M. Jansz, M. Mossaddad, S. Raghavan\*, University of Central Florida, USA; J. Almer, J. Okasinski, Argonne National Laboratory, USA; H. Palaez-Perez, P. Imbrie, Purdue University, USA

The thermo-mechanical effects on the strain evolution within an EB-PVD thermal barrier coating (TBC) is presented in this work using in-situ characterization. Synchrotron x-ray diffraction measurements provided both qualitative and quantitative in-situ data on the strain evolution under a thermal cycle with mechanical loading. The results show that at a critical combination of temperature and load, the stress in the thermally grown oxide (TGO) layer in the TBC reaches a tensile region. These significant findings enhance existing literature showing purely compressive strains within the TGO where mechanical loads have been neglected. The results have important implications on the effects on the overall life of the coating. Quantitative results obtained through peak fitting of the TGO data, show the evolution of strain in-situ over a thermal cycle. Depth resolved quantitative strain is presented as contour plots over a thermal cycle highlighting the complementary strains in the adjacent layers including the bond coat and the TBC with time and temperature. Systematic identification of the appropriate peaks within the multi-layer TBC system provides guidelines for future strain studies using high energy x-rays.

**11:00 AM**

**(ICACC-S1-041-2012) Nondestructive Evaluation of Thermal Barrier Coatings by Optical and Thermal Imaging Methods**

J. Sun\*, Argonne National Lab, USA

Thermal barrier coatings (TBCs) are widely used to improve the performance and extend the life of combustor and gas turbine components. As TBCs become prime reliant, it becomes important to determine their conditions nondestructively to assure the reliability of the components. Nondestructive evaluation (NDE) methods may be used to assess TBC condition for quality control as well as to monitor TBC degradation during service. Several NDE methods were devel-

oped for these applications, including laser backscatter, mid-IR reflectance (MIRR), and thermal imaging based on a multilayer analysis method. Both laser backscatter and MIRR are optical imaging methods and are evaluated under this study for TBC degradation monitoring. For thermal imaging, calibration tests have shown that the multilayer-analysis method developed at Argonne National Laboratory can determine TBC's thermal properties with accuracies comparable to other standard test methods. Because TBC properties change with life that can be measured by thermal imaging, a model for TBC health monitoring based on the property change is proposed. This paper presents these NDE methods and experimental results related to TBC health monitoring.

**11:20 AM**

**(ICACC-S1-042-2012) Investigation of Non-Destructive Evaluation Methods Applied to an Oxide/Oxide Fibre Reinforced Ceramic Matrix Composite**

R. E. Johnston\*, M. R. Bache, Swansea University, United Kingdom; D. Liaptsis, TWI Wales, United Kingdom; I. M. Edmonds, Rolls-Royce plc, United Kingdom

Ceramic matrix composites can contain numerous internal features that can potentially affect their mechanical performance in service applications. Non-destructive investigation techniques for defect evaluation in alumina oxide/alumina oxide ceramic matrix composites (CMC) are presented. Several different non-destructive evaluation (NDE) methods were assessed for their capability to identify the internal structure on varying scale lengths. Internal features included artefacts from the manufacturing process such as porosity, delamination, and microcracking. Artificial defects of varying size were also deliberately introduced within the CMC during the manufacturing phase, to establish a threshold of the resolution for each technique. The NDE methods investigated included X-ray computed tomography, 2-D radiography, flash thermography, and ultrasonics. This then permitted the ranking of each NDE method and set recommendations for their future cost effective employment.

**11:40 AM**

**(ICACC-S1-043-2012) 3D Fracture Behavior Monitoring of a Novel Alumina-Based Refractory and other Composites**

S. H. Lau\*, Xradia, Inc., USA; E. Skierab, J. Malzbender, Forschungszentrum Jülich GmbH, Germany; C. G. Aneziris, TU Bergakademie Freiberg, Germany; R. Steinbrech, Forschungszentrum Jülich GmbH, Germany

Understanding brittle fracture behavior relies to a large extent on detailed information regarding the crack propagation mechanisms in a given microstructure. Experimental results are typically obtained from in-situ crack path observations at the specimen surface and/or from post-mortem analyses of the fracture surfaces. The current work introduces an important complementary approach for non-destructive measurement of the 3D crack path in the interior of the specimen using high resolution x-ray microtomography. Fracture experiments with crack growth observation were carried out as part of the DFG (German Research Association) funded project "Fire", with novel, innovative, carbon-reduced and carbon-free refractory (AZT: 95%  $Al_2O_3$ , 2.5%  $TiO_2$ , 2.5%  $ZrO_2$ ). Microstructural crack path observations were carried out during and after controlled wedge splitting tests with pre-notched specimens of cubic shape (20mm edge length). The crack growth was monitored in-situ on polished surfaces of the specimens by optical (LM) and electron microscopy (SEM). 3D visualization of the crack path in the interior of the specimens was scanned non destructively @ 4.6 micron voxel using a novel lab based X-ray microscope. Extension of 3D characterization of crack evolution under load with temperature, aging and controlled environment for a variety of other composite materials for 4-D imaging will also be discussed.



## S2: Advanced Ceramic Coatings for Structural, Environmental, and Functional Applications

### Thermal Barrier Coatings I

Room: Ponce de Leon

Session Chairs: Uwe Schulz, German Aerospace Center; Eric Jordan, University of Connecticut

8:00 AM

#### (ICACC-S2-001-2012) CMAS degradation of EB-PVD thermal barrier coatings: from solubility of ceramic oxides in CMAS to the development of CMAS-resistant ceramic compositions (Invited)

M. Vidal-Setif\*, N. Chellah, C. Rio, D. Boivin, O. Lavigne, ONERA, France; M. Vilasi, Faculté des Sciences et Techniques, France

The use of TBC on components located in the hot sections of gas-turbine engines has allowed a higher engine operating temperature leading to temperature about 1200°C on the surface of the superalloy coating. At such temperatures, TBC are susceptible to corrosion by molten calcium-magnesium-alumino-silicates (CMAS) resulting from the ingestion of siliceous mineral debris (dust, sand, ash) contained in the hot gases arriving in the turbine. This paper first presents a characterization of the CMAS degradation of an EB-PVD thermal barrier observed on a high pressure turbine blade removed from service. In a second part, we compare these results with those obtained in laboratory scale, using a model CMAS composition. As CMAS corrosion is based on the TBC dissolution and re-precipitation mechanism, the third part of this paper deals with the study of the solubility of ceramic oxides from (ZrO<sub>2</sub>-Y<sub>2</sub>O<sub>3</sub>) and (ZrO<sub>2</sub>-Nd<sub>2</sub>O<sub>3</sub>) systems in molten CMAS. In a last part, various CMAS resistant layers are tested, using dense materials or EB-PVD or PECVD coatings. All are rare-earth zirconates or rare-earth doped zirconium - based oxides. Prevention of CMAS infiltration is obtained through the formation of a dense reaction layer under the main reaction zone between CMAS and doped zirconia.

8:40 AM

#### (ICACC-S2-002-2012) Thermochemical Interaction of EB-PVD Gd<sub>2</sub>Zr<sub>2</sub>O<sub>7</sub> Thermal Barrier Coatings with Artificial Volcanic Ash

P. Mechnich\*, W. Braue, U. Schulz, German Aerospace Center (DLR), Germany

The thermochemical interaction of Gd<sub>2</sub>Zr<sub>2</sub>O<sub>7</sub> EB-PVD coatings with sol-gel derived, artificial volcanic ash (AVA) is investigated in the light of possible impacts of ingested volcanic ashes on turbine engine airfoils with Gd<sub>2</sub>Zr<sub>2</sub>O<sub>7</sub> thermal barrier coatings. The laboratory scale approach was performed by isothermal annealing of EB-PVD Gd<sub>2</sub>Zr<sub>2</sub>O<sub>7</sub> coated coupons with AVA powder deposits and Gd<sub>2</sub>Zr<sub>2</sub>O<sub>7</sub>/AVA powder mixtures. XRD and microstructural analyses reveal a characteristic reaction sequence in the 1000 to 1200°C range, leading to a surface recession of the EB-PVD Gd<sub>2</sub>Zr<sub>2</sub>O<sub>7</sub> coating. Reactions include the decomposition of Gd<sub>2</sub>Zr<sub>2</sub>O<sub>7</sub>, subsequent formation of the apatite-type phase Ca<sub>2</sub>Gd<sub>8</sub>(SiO<sub>4</sub>)<sub>6</sub>O<sub>2</sub> and, depending on the annealing temperature, formation of a tetragonal or cubic polymorph of Gd<sub>2</sub>O<sub>3</sub>-stabilized ZrO<sub>2</sub>. Open coating porosity is partially filled by reaction products and further AVA infiltration is mitigated. The mitigation is closely related to the stability of Ca<sub>2</sub>Gd<sub>8</sub>(SiO<sub>4</sub>)<sub>6</sub>O<sub>2</sub> co-existing with AVA.

9:00 AM

#### (ICACC-S2-003-2012) Recession of EB-PVD YSZ Thermal Barrier Coatings: Interplay of Fe,Ti-rich CMAS-type Deposits and Anhydrite-type CaSO<sub>4</sub>

P. Mechnich\*, W. Braue, German Aerospace Center (DLR), Germany

The CMAS-type recession of yttria-stabilized ZrO<sub>2</sub> (YSZ) thermal barrier coatings (TBC) fabricated by electron-beam physical vapor

deposition (EB-PVD) was examined on ex-service high-pressure turbine blades and in laboratory studies, respectively. CMAS particle deposits observed on turbine blades were found to be Fe,Ti-rich and exhibit a high CaO to SiO<sub>2</sub> ratio. Substantial amounts of anhydrite-type CaSO<sub>4</sub> co-exist. Characteristic YSZ recession scenarios are observed at the TBC/particle deposit interface. CaZrO<sub>3</sub> and the garnet-type phase Ca<sub>3</sub>(Zr,Mg,Ti)<sub>2</sub>(Fe,Al,Si)<sub>3</sub>O<sub>12</sub>, also known as the mineral kimzeyite, are newly formed phases at the YSZ column tips. The formation of CaZrO<sub>3</sub> is explained by a Ca-rich but essentially SiO<sub>2</sub>-free stage, most likely provided by infiltrated CaSO<sub>4</sub>. A CMAS-type deposit providing high concentrations of Fe<sub>2</sub>O<sub>3</sub>, TiO<sub>2</sub>, and SiO<sub>2</sub> favors the formation of kimzeyite. Reaction sequences and microstructural evolution were confirmed in laboratory using EB-PVD YSZ-coated coupons with synthetic powder deposits. Owing to its broad solid solubility range, kimzeyite can level the chemical gradient at the deposit/coating interface; therefore long-term stability of the system is anticipated. On the other hand, the melting temperature of kimzeyite of approximately 1290°C presumably marks an operation limit for YSZ-based TBCs.

9:20 AM

#### (ICACC-S2-004-2012) The Effect of CMAS and Sintering on the Thermomechanical Stability of Plasma-Sprayed TBCs

M. Shinozaki\*, T. W. Clyne, University of Cambridge, United Kingdom

Sintering-driven changes in the microstructure of TBCs, due to prolonged exposure to high temperatures, can impair their thermomechanical stability. In particular, sintering can cause substantial increases in stiffness. These changes can be accelerated by the presence of impurities that segregate to the grain boundaries. In this study, vermiculite (VM) powder was selected as having a composition representative of volcanic ash. Its glass transition was observed to be ~1100°C and its melting temperature is ~1390°C. Selected loadings of VM were introduced onto the surface of free-standing plasma-sprayed yttria stabilized zirconia (YSZ) coatings. The mass of these additions was in the range 0.1 - 5.5 wt.%. After a short initial heat treatment, samples were exposed for periods at elevated temperature, up to 1500°C. The penetration of VM species was monitored by EDX mapping. In order to monitor the thermochemical reaction between VM and YSZ, XRD and Raman spectra was measured as a function of depth into the coating. Changes in the in-plane Young's modulus was also monitored. Finally, the effect of VM-assisted sintering on the spallation resistance of TBCs was investigated using specimen sprayed onto dense alumina and YSZ substrates. These measurements show that CMAS deposits potentially have a severe effect on TBC lifetime.

10:00 AM

#### (ICACC-S2-005-2012) Cyclic life of EB-PVD thermal barrier coatings having novel compositions

U. Schulz\*, German Aerospace Center, Germany

Advanced aero engines focuses on reduced specific fuel consumption and increased thrust-to-weight ratio which calls for increased temperatures. Thermal barrier coatings (TBCs) are applied to increase lifetime and efficiency of highly loaded turbine blades and vanes. New top coat chemistries have been developed that offer low thermal conductivity, improved sinter resistance and phase stability, and for some compositions improved resistance against CMAS attack. The current research deals with the investigation of the cyclic life of two new TBCs deposited on top of NiCoCrAlY coated superalloy bars. Two different top coats were investigated, namely Gadolinium Zirconate and Dysprosia-stabilized Zirconia. All top coatings had been deposited by Electron-beam physical vapor deposition. The cyclic life was investigated at 1100°C in a conventional furnace cycle test. Cyclic life was compared between single layers, double layers that consisted of a 7 YSZ base layer underneath the new top coats, and conventional 7 YSZ TBCs. Surprisingly, the new TBC single layers showed a longer

life than the double layer coatings. The microstructure after depositions and after TBC failure was analyzed by SEM with special emphasis on TGO formation. The failure pattern varied among the different top coats in terms of spalled area and type of spallation.

**10:20 AM**

**(ICACC-S2-006-2012) Multilayered Thermal Barrier Coating Architectures for High Temperature Applications**

D. E. Wolfe, M. P. Schmitt, Penn State University Applied Research Lab, USA; D. Zhu, NASA Glenn Research Center, USA; A. K. Rai\*, R. Bhattacharya, UES, Inc., USA

Pyrochlore oxides of the rare earth zirconates are excellent candidates for use as thermal barrier coating (TBC) materials in highly efficient turbine engine operation at elevated temperatures ( $>1300^{\circ}\text{C}$ ). Pyrochlore oxides have most of the relevant attributes for use at elevated temperatures such as phase stability, low sintering kinetics and low thermal conductivity. One of the issues with the pyrochlore oxides is their lower toughness compared to the currently used TBC material viz. yttria (6 - 8 wt. %) stabilized zirconia (YSZ). In this work, arguments are advanced in favor of a multilayered coating approach to enhance erosion performance by improving toughness and lowering thermal conductivity of the TBCs. Unique multilayered coating design architectures were fabricated with alternating layers of pyrochlore oxide viz  $\text{Gd}_2\text{Zr}_2\text{O}_7$  and low  $k$  TBC ( $t'$  and cubic phase rare earth oxide doped YSZ) utilizing electron beam physical vapor deposition (EB-PVD) technique to reduce overall rare earth oxide content. Microstructure, phase, erosion resistance and thermal conductivity of the as-fabricated multilayered coatings were evaluated and compared with that of the single layered coatings.

**10:40 AM**

**(ICACC-S2-007-2012) Defect-dependent thermal conductivity of tetragonal yttria-stabilized zirconia**

A. M. Limarga\*, D. R. Clarke, Harvard University, USA

The low intrinsic thermal conductivity, combined with the porosity incorporated in the coating, has made tetragonal prime yttria-stabilized zirconia ( $t'$ -YSZ) the material of choice for thermal barrier coatings to protect the metallic components in turbine hot sections. The densification and evolution of coating microstructure have been considered to be the primary cause for the increase of coating conductivity during high-temperature service. In this work, we evaluate the evolution of thermal conductivity of fully dense nanocrystalline tetragonal zirconia with high temperature aging. It is found that the thermal conductivity is dependent on the grain size and the phase composition in YSZ as the metastable tetragonal undergoes phase separation to yttria-lean tetragonal and yttria-rich cubic phases at high temperature. These results provide an insight on how the thermal protection efficiency of the coatings evolves during service and how to design a new generation TBC with superior performance and high-temperature stability.

**11:00 AM**

**(ICACC-S2-008-2012) Implications of the  $c/t'$  Transformation on Characterization Efforts of Thermally Aged TBCs**

J. A. Krogstad\*, M. Lepple, UCSB, USA; Y. Gao, D. M. Lipkin, GE Global Research, USA; C. G. Levi, UCSB, USA

Accurate characterization of the phase evolution in traditional yttria-stabilized zirconia thermal barrier coatings (TBCs) becomes more critical as the maximum use temperature of these TBCs is ultimately limited by the rate of destabilization. X-ray diffraction has been traditionally used to track the decomposition of the metastable  $t'$ -phase into its equilibrium components, a yttria-rich cubic phase and a yttria-lean tetragonal phase, the later of which is transformable to the monoclinic phase upon cooling leading to a deleterious volume expansion and potential microcracking. The transformability of a product phase can be estimated from the nominally linear relationship be-

tween  $\text{YO}_{1.5}$  content and unit cell parameters. However, the accuracy of this relationship is compromised as the tetragonality of the unit cell approaches unity, due in part to the ambiguous nature of the  $c/t'$  transformation. Careful examination of the transition region between tetragonal and cubic symmetry has revealed that several factors may influence the unit cell parameters as determined by x-ray diffraction. If these factors are not properly considered, the relationship between unit cell parameters and dopant concentration may be significantly skewed in the yttria-lean range, resulting in mischaracterization of transformability.

**11:20 AM**

**(ICACC-S2-009-2012) Development of pyrochlore materials for thermal barrier coatings deposited by suspension plasma spraying**

A. Joulia\*, Centre Européen de la Céramique, France; S. Rossignol, Centre Européen de la Céramique, France, Centre Européen de la Céramique, France; M. Vardelle, M. Huger, S. Foucaud, Centre Européen de la Céramique, France; E. Renard, CNES, France; D. Tchou-Kien, Centre Européen de la Céramique, France, Centre Européen de la Céramique, France; CNES, France

Nowadays, thermal barrier coatings (TBCs) are widely used in gas turbine engines for aircraft propulsion. They provide a thermal insulation and protect hot-section metallic components from combustion environments at elevated temperatures. The most used ceramic topcoat is yttria stabilized zirconia in industrial TBC system, which is able to operate at temperatures below  $1200^{\circ}\text{C}$ . Thus, the development of new advanced ceramic materials and new coating architectures is essential to increase engine operating temperature ( $T > 1200^{\circ}\text{C}$ ) in order to enhance their efficiency and their performance. Among the potential candidates for TBCs, the rare earth ceramic materials are promising due to their low thermal conductivity and their high melting point. Most of TBCs are deposited by conventional EB-PVD and Plasma Spray processes. A new processing method consists in injecting suspensions of sub-micrometer particles into the plasma torch. The aim of this work is to develop new microstructures for TBCs applications by suspension plasma spraying. The process advantages are to decrease thermal conductivity and enhanced strain tolerance so the coating life time compared to APS TBCs. Another study is also focused on the synthesis of pyrochlore materials by sol-gel method as well as their phase transformation under reducing and oxidizing atmospheres at  $1400^{\circ}\text{C}$ .

**11:40 AM**

**(ICACC-S2-010-2012) Structures of  $(\text{La}_x\text{Gd}_{1-x})_2\text{Zr}_2\text{O}_7$  Oxide Systems for Thermal Barrier Coatings (TBCs)**

S. Kim\*, K. Kwak, S. Lee, Y. Oh, Korea Institute of Ceramics Engineering and Technology, Republic of Korea; B. Jang, National Institute of Materials Science, Japan; H. Kim, Korea Institute of Ceramics Engineering and Technology, Republic of Korea

Among candidates for future TBCs investigated recently, fluorite and pyrochlore oxides are two prevailing materials. While the cubic fluorite phase of rare-earth oxide has the space group of  $\text{Fm}\bar{3}(-)m$ , the cubic pyrochlore phase corresponds to the space group  $\text{Fd}\bar{3}(-)m$ . Furthermore, the pyrochlore structure is characterized by the cation occupancy of the special crystallographic sites and the oxygen vacancy at the 8a site. This ordering of cations in the pyrochlore structure results in more superlattice peaks in XRD compared with the fluorite structure. In this study, phase structures of  $(\text{La}_x\text{Gd}_{1-x})_2\text{Zr}_2\text{O}_7$  oxide systems are investigated.  $(\text{La}_x\text{Gd}_{1-x})_2\text{Zr}_2\text{O}_7$  systems are comprised by selecting  $\text{La}^{3+}/\text{Gd}^{3+}$  as A-site ions and  $\text{Zr}^{4+}$  as B-site ions in  $\text{A}_2\text{B}_2\text{O}_7$  pyrochlore structures. Either fluorite or pyrochlore or mixture of both appears with contents of A-site cation after heat treatment. For the developed phases among  $(\text{La}_x\text{Gd}_{1-x})_2\text{Zr}_2\text{O}_7$  compositions, crystallographic structures and microstructures are characterized by using X-ray diffraction, Raman spectroscopy, or transmission electron microscopy.

## S4: Armor Ceramics

### Transparent Materials II

Room: Coquina Salon E

Session Chair: James McCauley, Army Research Laboratory

8:00 AM

#### (ICACC-S4-033-2012) Nondestructive Characterization of Low Velocity Impact Damage in Transparent Laminate Systems

R. E. Brennan\*, W. H. Green, C. G. Fountzoulas, U.S. Army Research Laboratory, USA

Multi-layer, multi-material transparent laminate systems are used to enhance protection efficiency for ground vehicle windshield and window applications while ensuring sufficient visibility for the operator. Impact damage caused by low velocity strikes may result in crack formation in the transparent materials or delaminations between layers, which can impair visibility and adversely affect performance. In this effort, several different series of conventional and novel transparent laminate systems have been nondestructively evaluated in a pre-impact, baseline state using visual, cross-polarization, x-ray, and ultrasound characterization. After subjecting the laminate systems to a series of low velocity impact tests, the same nondestructive methods were used for characterization of the post-impact state. By combining nondestructive and destructive testing, damage mechanisms were identified at critical velocity and energy conditions to help establish damage tolerance levels for transparent protective systems. In addition to experimental testing, 2D and 3D modeling studies were concurrently performed for initial development of a transparent laminate system failure model. The combination of experimental and modeling results will be utilized for comparison of transparent laminate systems to achieve improved visibility and protection capabilities.

8:20 AM

#### (ICACC-S4-034-2012) XCT Diagnostics of Ballistic Impact Damage in Transparent Armor Targets

J. Wells\*, Office of Naval Research Global, United Kingdom

This paper introduces results of the non-invasive XCT damage diagnostics for transparent armor targets made available via the DARPA Topological Light Weight Armor Program, TCLA-Phase II. The study was conducted by the author as Principal Investigator while at The Johns Hopkins University before assuming his current position with ONR Global. TA target samples were originally 14in x 14 in. x 2 in. thick and consisted of several layers of transparent materials. One such target was examined using a 9 MeV x-ray facility, and the remaining 3 targets were reduced in size to a 12 in. diameter x 2 in. thick geometry and were scanned with a 450 kv meso-scale XCT facility. Finally, a 4 in. x 8 in. x 2 in. reduced size sample was water jet cut from one 12 in. diameter target sample to be capable of being scanned by the Zeiss 225 kV microfocus tomography facility. Diagnostic results at various resolution levels will be shown and discussed. This effort was directed at establishing an initial baseline for the state-of-the-art, SOA, of non-invasive XCT impact damage diagnostics modality for the characterization and development of improved glass/ceramic/polymer layered transparent armor architectures.

### Opaque Materials I

Room: Coquina Salon E

Session Chair: James McCauley, Army Research Laboratory

8:40 AM

#### (ICACC-S4-035-2012) Opportunities in Protection Materials Science and Technology for Army Applications (Invited)

E. L. Thomas\*, Rice University, USA

A year long National Academy study of light weight materials for protection of military personnel and light vehicles was completed in July, 2011. Ceramics play an important role in body armor and in vehicle armor including transparent armor. Protection materials by design in

order to enhance the performance of the material and material systems and to more rapidly develop armors is a critical need. The use of advanced computational and experimental methods to understand the mechanisms of deformation and failure due to ballistic and blast threats is key to success in this endeavor. Recommendations of the report will be presented and discussed. The report is available for free pdf download at [http://www.nap.edu/catalog.php?record\\_id=13157](http://www.nap.edu/catalog.php?record_id=13157)

9:10 AM

#### (ICACC-S4-036-2012) The Outlook for Ceramic in Future Vehicle Armor Solutions

M. Price\*, Vector Strategy, USA

This study describes the qualitative and quantitative outlook, trends, and demand for ceramic in future vehicle armor solutions. Secondary and primary research is completed to determine the future demand for ceramic in vehicle armor solutions. Interviews with suppliers, vehicle OEMs, armor manufacturers, and government/military personnel yield an assessment of the future for vehicle armor ceramics. An extensive model of material usage based on anticipated vehicle procurement programs, protection levels, vehicle surface area coverage, and armor material technologies yields a quantitative forecast of ceramic in vehicle armor applications. Technology advancements, escalating threats, and cost/weight tradeoffs are considered. The study concludes that although ceramic will be incorporated more frequently in vehicle armor solutions due to escalating threats, weight considerations, improved manufacturing processes, novel designs, and new material technologies; the declining procurement rates of armored vehicles and armor kits will constrain growth in armor ceramics for the next 5 to 10 years. This conclusion is valid unless the US becomes involved in a contingency operation beyond the scope of those it is currently involved in. Although ceramic armor technology will continue to improve and evolve, the market and demand for ceramic armor will be constrained due to lower vehicle and armor procurement by the US government.

9:50 AM

#### (ICACC-S4-037-2012) Discrimination of Basic Influences on the Ballistic Strength of Opaque and Transparent Ceramics

A. Krell\*, E. Strassburger, Fraunhofer EMI, Germany

The study addresses (1) the impact of (i) ceramic microstructure and (ii) mechanical (stiffness, strength) data of the ceramic/backing composite on ceramic fragmentation (size, shape) and projectile erosion, and (2) indirect influences of the microstructure via mechanical properties (Young's modulus  $E$ , hardness, HEL, bending/compressive strength,  $KIc$ ) which may govern the abrasive destruction of the penetrator. Regarding the highly dynamic interaction, the study had to find out if all mechanical parameters must be dynamically recorded for understanding the ballistic performance. Different ceramics in front of different backings (steel, aluminum, glass) exhibited a 3-fold hierarchy of influences: 1. Top priority is the mode of ceramic fragmentation governed by ceramic micro-structure and dynamic stiffness (i.e. not by Young's modulus  $E$ ) of the ceramic/backing composite. These influences also affect the relative importance of dwell and penetration phases. 2. On a middle rank,  $E$  and the dynamic stiffness of the ceramic are responsible for the projectile deformation during dwell. 3. On penetration, a high abrasive effect caused by a high ceramic hardness depends on the size of the ceramic debris. Compared with these influences, all strength data were weakly correlated with the ballistic figure. This hierarchy explains frequent apparently contradictory experimental results of the past.

10:20 AM

#### (ICACC-S4-038-2012) Using Hardness Tests to Determine Plasticity & Predict Impact Performance of Ceramics

C. Hilton\*, Oak Ridge Institute for Science & Education, USA; J. McCauley, J. Swab, US Army Research Lab, USA; E. Shanholtz, Oak Ridge Institute for Science & Education, USA

The importance of hardness to the gross impact performance of ceramic materials has been well documented. Although many studies

have shown that harder ceramics generally perform better in armor applications, the relationship between hardness and impact performance is not currently understood well enough to be useful for materials development. Additionally, some research has suggested that a ceramic material's ability to deform in an inelastic manner, or its "bulk plasticity", may also play an important role in its potential to resist penetration. Methods of quantifying the bulk plasticity of ceramic materials are, however, extremely limited. In a recent study, McCauley and Wilantewicz (M&W) proposed a novel technique in which Knoop Hardness measurements were used to 1) quantify the bulk plasticity in SiC materials and 2) predict the transition velocities of these ceramics. This study further investigates the method of M&W by extending the technique to additional ceramic materials. Additionally, the robustness of the method is examined through the use of multiple operators and multiple hardness testing units.

**10:40 AM**

**(ICACC-S4-039-2012) An Evaluation of the Relationship between Indentation Size Effect and Ballistic Performance in a Range of Ceramic Materials**

D. Hallam\*, A. Miller, M. Robinson, University of Surrey, United Kingdom; P. Brown, A. Heaton, B. James, Dstl, United Kingdom; P. Smith, J. Yeomans, University of Surrey, United Kingdom

Whilst it is not possible to specify the most advantageous microstructural arrangement and associated values of materials parameters of a ceramic material intended for use in protection from a ballistic event, it has been hypothesised that exhibiting some amount of plastic deformation prior to catastrophic failure is desirable. In essence, if the ceramic can be prevented from fracturing, or more likely, if there is a time delay between impact and fracture (dwell) then the material is a more effective armour material. A recent study has used Knoop hardness indentation size effect (ISE) curves to provide a semi-quantitative measure of plasticity. This was then shown to correlate with transition velocities, indicative of dwell, for a number of ceramic materials. The current study extends that work by presenting the Knoop hardness ISE curves from a range of oxide and non-oxide ceramic materials and examining the relationships between the derived plasticity values and microstructural parameters, quasi-static and ballistic fracture modes and the ranking of the materials in ballistic tests.

**11:00 AM**

**(ICACC-S4-040-2012) Colloidal Processing Method and Mechanical Properties Analysis of Silicon Carbide Ceramics sintered by SPS**

R. Bianchini, S. Miller, R. Haber\*, Rutgers University, USA

A chemical precipitation processing technique is used to introduce sintering aids into silicon carbide powders. Maintaining the SiC suspension at 9.5 pH allows for the yttrium oxide and aluminum nitride to homogeneously coat SiC particles by electrostatic attraction. These systems are densified via spark plasma sintering at various temperatures to investigate the properties and effectiveness of the colloidal processing. The improved mixing reduces defects and modifies silicon carbide microstructures as compared to conventionally prepared systems. Mechanical and microstructural properties of compositional variations in sintering aids are evaluated and measured to ball milling. Differences in grain boundary phases have been observed through X-ray diffraction and shown to affect cracking behavior.

**11:20 AM**

**(ICACC-S4-041-2012) Effect of Boron Carbide Additive Size and Morphology on Spark Plasma Sintered Silicon Carbide**

V. DeLucca\*, R. A. Haber, Rutgers Univ, USA

Silicon carbide is a versatile material used in many demanding applications for its high hardness, high strength, and good thermal properties. While the effects of boron carbide on the sintering behavior of silicon carbide have been studied extensively, the role of boron car-

bide additive size and morphology has not. In this study the effect of boron carbide additive particle size and morphology on the microstructure and ultrasound response of spark plasma sintered (SPS) silicon carbide ceramics is examined. Several silicon carbide samples were made using carbon and boron carbide as sintering aids, maintaining constant additive concentration while varying the boron carbide additive source. Ultrasonic nondestructive characterization techniques and field emission scanning electron microscopy (FESEM) were used to characterize the sintered bodies.

**11:40 AM**

**(ICACC-S4-042-2012) Multi-depth imaging in complex ceramics with a microwave interference scanning system**

K. Schmidt\*, J. Little, Evisive, inc., USA; W. Ellingson, ERC Company, USA; L. P. Franks, W. Green, US Army, USA; G. Jefferson, US Air Force, USA

A microwave interferometry nondestructive evaluation (NDE) system has been improved to permit simultaneous capture of the responses from multiple frequencies, producing layered volumetric images of complex ceramic structures. This has the effect of moving the interference phase angle through the depth of the inspected part. The technique has been used to image composite ceramic armor and ceramic matrix composite components, as well as other complex dielectric materials. The system utilizes Evisive-Scan microwave interference scanning technique. Validation tests include artificial and in-service damage of ceramic armor surrogates and ceramic matrix composite samples. Validation techniques include micro-focus x-ray and computed tomography imaging. The microwave interference scanning technique has demonstrated, using various ceramic materials, detection of cracks, interior laminar features and variations in material properties such as density. The multi-layer image from phase angle manipulation yields depth information, and extent of feature depth information, which was not previously achievable in a single scan. It requires access to only one surface, and no coupling medium. Data are not affected by separation of layers of dielectric material, such as outer over-wrap. The paper will present application examples.

## **S7: 6th International Symposium on Nanostructured Materials and Nano-Composites**

### **Nanotubes, Nanowires and Other One-dimensional Structures**

Room: Coquina Salon B

Session Chairs: Aleksander Gurlo, Technische Universitaet Darmstadt; Jason Graetz, Brookhaven Natl Lab

**8:00 AM**

**(ICACC-S7-029-2012) Exploring organic-inorganic interfaces in silica-based nanomaterials by a combined spectroscopic and modelling approach (Invited)**

F. Babonneau\*, N. Folliet, T. Azaïs, C. Gervais, LCMCP / UPMC-Paris6 & CNRS, France; E. Tielens, Université Pierre et Marie Curie and CNRS, France; C. Bonhomme, LCMCP / UPMC-Paris6 & CNRS, France

A large number of applications of silica are related to their surface properties and more specifically to the interactions between the surface sites and organic or even biological entities. Moreover these interactions can be tuned by a proper functionalization of the surface. The organic/silica interfaces in various systems, have been investigated using a combined spectroscopic and modelling approach. Multinuclear solid-state NMR techniques have been used to probe proximities between the silica surface sites and the various organic functions that may interact. In parallel, a representative model for the hydroxylated surface of amorphous silica characterized by means of periodic DFT calculations was used to model these interactions. This allowed calculating the NMR parameters, to compare them to the experimental data and to validate the proposed structural model for the

organic-silica interfaces. Two main systems that can be used for drug delivery applications will be discussed: ordered mesoporous silica, and silica coated liposomes.

**8:30 AM**

**(ICACC-S7-030-2012) Use of Nanotubular Electrodes in Electrochemical Applications (Invited)**

B. Saruhan\*, Y. Gönüllü, S. Özkan, German Aerospace Center, Germany

$\text{NO}_x$  is a common air pollutant that is associated even at the ppb level, with poor air quality and breathing difficulties and greenhouse effects.  $\text{NO}_x$  is produced during combustion processes independent of the fuel quality. Sensing of  $\text{NO}_2$  at high and low temperatures is essential for human health and protection of nature. The super-capacitors charge more rapidly than batteries, supply longer energy and have higher power densities. These features are desirable for a range of applications such as electric vehicles and storage for renewable energy supplies such as wind power. This presentation reports the use of doped/undoped nano-tubular  $\text{TiO}_2$ -layers as  $\text{NO}_2$ , CO and  $\text{H}_2$  sensors at temperatures up to  $500^\circ\text{C}$  for concentrations varying from 10 to 50 ppm and from 25 to 75 ppm and 100-500 ppm, respectively. Doping  $\text{TiO}_2$  with Al and Cr yields favourable properties regarding sensors selectivity and sensitivity. Moreover, the studies carried out in our group shows that aligned or interlocking nano-structured and nano-crystalline redox capable oxides introduce enhanced capacitance and higher energy densities, extending the operation limits of the super-capacitors.

**9:00 AM**

**(ICACC-S7-031-2012) Investigation of Optical and Electronic Properties of Mn Doped ZnO Nanowires and Devices**

R. Prabhakar\*, N. Mathews, G. Kr, S. Pramana, J. Kochupurackal, NTU, Singapore; B. Varghese, C. Sow, NUS, Singapore; S. Mhaisalkar, NTU, Singapore

Mn doped ZnO nanowires were prepared by carbo-thermal reduction method. ZnO powder was mixed with  $\text{MnCl}_2$  salt at an appropriate atomic ratio to achieve doping of ZnO nanowires. Silicon substrates were coated with a layer of Au of 2 nm thickness and this layer acted as the catalyst for nanowire growth. Structural morphology of the nanowires was studied using Scanning electron microscope (SEM) and Transmission electron microscope (TEM). Crystal structure and chemical composition of nanowires were studied by Raman spectroscopy and XRD. Photo-luminescence spectroscopy and absorption studies, were performed on the Mn doped ZnO nanowires. Single Nanowire devices were fabricated by Focused Electron Beam (FEB) and its charge transport properties were studied in dark and under laser light illumination.

**9:20 AM**

**(ICACC-S7-032-2012) Recent advances in membrane development for  $\text{CO}_2$  free fossil power plants**

T. Van Gestel\*, Forschungszentrum Jülich, Germany, Forschungszentrum Jülich, Germany; Forschungszentrum Jülich, Germany; S. Baumann, M. Ivanova, W. Meulenber, H. Buchkremer, Forschungszentrum Jülich, Germany

This overview paper focuses on the actual developments in ceramic gas separation membranes in our institute, in particular membranes with a selective transport for  $\text{H}_2/\text{CO}_2$  and  $\text{O}_2/\text{N}_2$  gas mixtures. We consider the development of such membranes for application in future pre-combustion and oxyfuel-combustion coal and gas power plants. For  $\text{H}_2/\text{CO}_2$  separation,  $\text{SiO}_2$  based membranes are considered, due to their promising combined values of selectivity and flux. A sol-gel dip-coating method is used to prepare the membranes, which results in the deposition of thin microporous layers (thickness ~100 nm) with an average selectivity > 30 and the required  $\text{H}_2$  flux. As an alternative, dense  $\text{H}_2$  transport membranes are also investigated. These membranes are made of crystalline  $\text{Ln}(\text{WO})_{12}$  proton-

conducting materials and exhibit an infinite separation factor, but a comparably low  $\text{H}_2$  flux, requiring the development of thin film layers. For processes with oxyfuel combustion,  $\text{O}_2$  transport membranes are investigated. Our current membranes are made of a mixed electron and ion conducting perovskite material (LSCF, BSCF) by a graded tape-casting process. These membranes have also an infinite separation factor and by lowering the thickness to ~10  $\mu\text{m}$ , a flux > 10  $\text{ml}/\text{min}\cdot\text{cm}^2$  has been achieved. Research is currently directed towards the development of thinner membranes with a thickness of ~1  $\mu\text{m}$  using a nano-particle deposition process.

**Nanostructured Materials and their Application**

Room: Coquina Salon B

Session Chairs: Florence Babonneau, LCMCP / UPMC-Paris6 & CNRS; Bilge Saruhan-Brings, German Aerospace Center

**10:00 AM**

**(ICACC-S7-033-2012) Preparation of n- and p-type metal oxide nanowires and nanostructures for chemical sensing (Invited)**

E. Comini\*, G. Faglia, M. Ferroni, A. Ponzoni, D. Zappa, G. Sberveglieri, Brescia University CNR-IDASC, Italy

Metal oxide chemical sensors are investigated from more than five decades, thanks to their ability to change electrical properties with the surrounding gas atmosphere. Yamazoe showed in 1991 that reduction of crystallite size went along with a significant increase in gas sensing performances. Therefore the challenge became the fabrication of materials with small crystallite size which keep their stability over long-term operation at high temperature. Single crystalline nanowires are very stable and when the lateral dimensions are sufficiently small they are good candidates for chemical sensing. In 2002, the field of metal oxide nanowires underwent a significant expansion and became one of the most active research areas within the nanoscience community. Nowadays it is almost a decade from the first presentation of metal oxide nanowires as chemical sensors. Significant advances have been made both in terms of preparation procedures and their integration into functional sensing devices, while progress in fundamental understanding of their functional properties is slow-moving. In fact, the full integration still remains a challenge that has been wisely approached in different ways. In this presentation we will review the most recent developments in bottom up and top down approaches for chemical sensors application.

**10:30 AM**

**(ICACC-S7-034-2012) Selective Chemical Vapor Deposition for Enhanced Gas Sensing Applications**

T. Fischer\*, I. Giebelhaus, S. Mathur, University of Cologne, Germany

Metal oxide semiconductors are versatile materials for gas sensor applications due to their reversible change in electrical properties upon adsorption of different gaseous analytes. Major drawbacks for a widespread application still remain, as high operating temperatures and therefore a low power efficiency hinder an autonomous operation of these devices. Especially safety and security applications demand nowadays more efficient sensors which combine enhanced selectivity, sensitivity and long term stability with low power consumption. Metal oxide nanowires are a promising class of materials as they provide a large surface area (large surface to volume ratio) for more sensitive gas sensors, but still offer only poor stability when used as single wires. We describe a novel method of a site selective chemical vapor deposition (CVD) technique, which enables the growth of metal oxide nanowires directly on multifunctional substrates. Unlike classical fabrication techniques no additional bonding of the active material is necessary. More stable devices can be produced, as no single nanowires, but bundles of nanowires are grown directly on the contacting electrodes. Moreover direct analytical tools, like in situ mass spectrometry and NMR spectroscopy provide a detailed insight into the ongoing decomposition reactions during the CVD process.

10:50 AM

**(ICACC-S7-035-2012) Catalysts, Membranes and Sensors for the Hydrogen Economy: Design, Synthesis and Characterization (Invited)**

A. Gurlo\*, M. Bazarjani, R. Riedel, Technische Universitaet Darmstadt, Germany

Tunable synthesis of nanocomposites possessing desired functionalities has received considerable attention in the last decades. In the field of the hydrogen economy such materials are applied as catalysts for hydrogen production, hydrogen storage materials, hydrogen separation membranes, and hydrogen sensors. In the present work we report a precursor-based approach towards composite materials composed of polymeric matrix with incorporated nanoscaled metallic, oxide and nitride particles. After thermal treatment under desired conditions (temperature, ambient gas) such polymeric nanocomposites transform into ceramic nanocomposites. Their porosity is tuned by an appropriate choice of thermolysis and annealing conditions. Case studies include the synthesis and characterization of (i) superparamagnetic and catalytically active nanocomposites of polysilazane in-situ modified with nickel nanoparticles, (ii) nanoporous silicon oxycarbonitride ceramics in-situ modified with nickel nanoparticles, (iii) photocatalytically active composites of siloxane-based polymers modified with tungstite nanoparticles, and (iv) metal nitride-silicon oxycarbonitride ceramic composites.

11:20 AM

**(ICACC-S7-036-2012) Nano-scale lithium batteries for in operando electron microscopy studies (Invited)**

J. Graetz\*, F. Wang, D. Zeng, Brookhaven Natl Lab, USA; T. McGilvray, University of California San Diego, USA; N. Dudney, Oak Ridge National Laboratory, USA; Y. S. Meng, University of California San Diego, USA; Y. Zhu, Brookhaven Natl Lab, USA

Transmission electron microscopy (TEM) studies of lithium battery materials have revealed valuable information on nano-scale changes in the chemistry, structure and morphology of electrodes and interfaces occurring during (de)lithiation. Nonetheless, observation of these phenomena in operando remains challenging. In this work, two methods are being pursued to prepare nano-scale batteries, with a target thickness  $\leq 100$  nm that can function in the TEM environment. In the first method, nanowires or thin films are deposited directly onto a TEM grid while a counter electrode of Li metal is deposited onto a biasing tip along with a solid electrolyte. In a second method the nano-batteries are fabricated from larger solid-state thin film micro-batteries using a focused ion beam. In this case, the nano-batteries are prepared by first cutting out a section of the battery, lifting out the lamella, mounting it to a specially designed TEM grid and finally, thinning down a "window" to  $\sim 100$  nm. The fabrication procedure, along with the advantages and disadvantages of the different cell designs and chemistries will be discussed. Preliminary microstructural analysis on each layer and the interface of the solid-state thin-film batteries will also be presented.

11:40 AM

**(ICACC-S7-037-2012) A Simple Greener Route to Metal Chalcogenide Nanoparticles (Invited)**

N. Revaprasadu\*, M. N. Mntungwa, P. V. S. R. Rajasekhar, O. A. Nejo, A. A. Nejo, University of Zululand, South Africa

There have been many reported synthetic routes to metal chalcogenide nanoparticles. The so called 'hot injection' precursor route is a common route to the controlled synthesis of these materials. The route involves the use of a chalcogenide source and a metal salt injected into a coordinating solvent typically an alkylamine. The pioneering work made use of metal alkyls as the metal source. Subsequently the use of 'greener' substitutes such metal oxides became more popular. In this paper we describe the results obtained by using a novel facile solution based/thermolysis route. This method involves the reaction by the addition of an aqueous suspension or solution of a metal salt (chloride, acetate, nitrate or carbonate) to a freshly pre-

pared NaHE (where E = S, Se or Te) solution. The isolated bulk material was then dispersed in tri-octylphosphine (TOP) and injected into pre-heated hexadecylamine (HDA) at temperatures of 190, 230 and 270 °C for 2 h. Examples of the following semiconductor materials will be discussed in detail: CdSe, PbS, PbTe and CdTe. The reaction conditions were varied to achieve morphological control of the particles. The growth mechanism of the materials was influenced by parameters such as metal salt and reaction temperature. The absence of any volatile, toxic or pyrophoric precursors makes the route simple, environmentally benign with potential for scale up.

**S8: 6th International Symposium on Advanced Processing and Manufacturing Technologies for Structural and Multifunctional Materials and Systems (APMT) in honor of Professor R. Judd Diefendorf**

**Green Manufacturing**

Room: Coquina Salon A

Session Chairs: Richard Sisson, Worcester Polytechnic Institute; Hiroshi Tsuda, Osaka Prefecture University

8:00 AM

**(ICACC-S8-029-2012) Incorporating Global Issues, Green Manufacturing and Innovation into Materials Processing Education**

R. D. Sisson\*, Worcester Polytechnic Institute, USA

In today's global, environmentally conscious, innovation economy materials engineers need education and experience in these important new topics. At WPI we have developed an integrated systems engineering approach to imbue these topics into existing courses and projects. In this paper the integration effects at all academic levels (first year -senior year - graduate courses and projects) will be presented and discussed. The importance of student team projects and knowledgeable mentoring will be emphasized.

8:20 AM

**(ICACC-S8-030-2012) Raw Material Scarcity and its Impact on the US Advanced Ceramic Technology**

M. D. Hill\*, Trans-Tech Inc., USA

Raw material considerations play a considerable role in the engineering activities of many US corporations manufacturing ceramic products. Historical data will be presented exploring the causes of scarcity and various measures taken by governments, universities and industrial groups will be evaluated. Such considerations play a central role in the technology development roadmaps and how they are implemented. The impact of current raw materials scarcity such as that of the rare earth elements are central considerations for a number of advanced technology applications. Data will be presented which can serve as a predictive model for the supply and demand for various raw materials in the near term and long term timeframe. Finally, pro-active strategies will be discussed on handling scarcity issues with an emphasis on aligning research and development activities to address current and potential future issues involving the supply of critical raw materials.

8:40 AM

**(ICACC-S8-031-2012) Lithium ion battery recycling**

Y. Wang\*, D. Apelian, Worcester Polytechnic Institute, USA

Lithium ion (Li ion) batteries are extensively used because of their high energy density, good cycle life, high capacity, etc. The rechargeable Li ion battery market was  $\sim$  \$4.6 billion in 2006 and is expected to grow to more than \$6.3 billion by 2012. Also lithium ion batteries are gradually being used for large applications, such as hybrid or electrical vehicles and grid systems. At present, Li ion batteries such as the ones used in cell phones and laptops are not widely recycled. We be-

lieve that such an open loop industrial cycle is not sustainable; it is our strong conviction that we must develop and establish viable Li ion battery recycling methodologies. We recycle Li ion batteries through low temperature chemical methods and active materials can be synthesized during recycling process; this will reduce energy usage, environmental damage, lead to economically viable processes, and strengthen our national security position.

**9:00 AM**

**(ICACC-S8-032-2012) Green-Conscious Ceramic Injection Moulding**

O. Weber\*, T. Hanemann, Karlsruhe Institute of Technology, Germany

Injection moulding provides an opportunity to produce complexly shaped micro components. The advantage of this technique is most of all the possibility to manufacture in high numbers of pieces with near-net-shape geometries without any post-processing steps. The present work focuses on the development of an alternative binder system for the application in micro ceramic injection moulding consisting of environmentally friendly polyethylene glycol (PEG) and polyvinyl butyral (PVB). In comparison to conventional binders based on wax this new combination has an important profit that the liquid pre-debiding step takes place in water and not in a toxic organic solvent such as hexane. In addition, these compounds allow further process simplifications by its economic and timesaving benefits. The results presented here cover all process steps from feedstock preparation to sintering of final micro parts. In comparison to literature significantly higher filler loadings with zirconia powder (TZ-3YS-E) of 55 vol% were achieved and reproducibly injection mouldable. The solvent debinding experiments showed that the best dimensional stability was found at room temperature where about 94% of the PEG-content was extracted after only 2 hours. Furthermore, removal of polymers can be performed just thermally without any deformation. A concluding sintering at 1450°C led to final defect-free products with a high density close to 100%.

**9:20 AM**

**(ICACC-S8-033-2012) High Volume Production for High Performance Ceramics**

W. J. Walker\*, Federal-Mogul Corporation, USA

Ceramic insulators for spark plugs are produced at a rate of more than 4 million parts per day worldwide. With advances in engine technology, these insulators must withstand increasingly harsh service environments and must deliver reliable performance over constantly increasing service lifetimes. Critical properties include dielectric breakdown strength and mechanical strength. One of the keys to achieving these performance goals is the processing methods. Because of the high production volumes and low cost requirements, powder compaction remains the preferred method for manufacturing spark plug insulators, but advances in all aspects of the processing ensure that performance improvements can be achieved.

**Joining and Integration**

Room: Coquina Salon A

Session Chairs: Richard Sisson, Worcester Polytechnic Institute; Hiroshi Tsuda, Osaka Prefecture University

**10:00 AM**

**(ICACC-S8-034-2012) TEM observation of the Ti interlayer between SiC substrates during diffusion bonding (Invited)**

H. Tsuda\*, S. Mori, Osaka Prefecture University, Japan; M. C. Halbig, M. Singh, NASA Glenn Research Center, USA

Silicon carbide (SiC) is an enabling material for a wide variety of high-temperature and extreme environment applications because of its high temperature thermomechanical properties, and thermal stability. However, limitations in the geometries that can be produced in current processing methods hinder the wider utilization of silicon carbide-based materials. To overcome these problems, one cost-effective solution for fabricating large, complex-shaped components is

through the joining of simpler shaped ceramics. In this study, titanium (Ti) was selected as an interlayer between silicon carbide substrates during diffusion bonding. Interlayers consisted of 10 and 20 micron thick Ti foils and physical vapor deposited (PVD) Ti coatings. Diffusion bonding was performed at 1200°C or 1250°C for 2 h. From the polished cross-sections of the joined samples, transmission electron microscope (TEM) specimens were prepared by focused ion beam (FIB). In all specimens, 3C-SiC was observed. Also, twin spots and the streaks perpendicular to the [111] direction of SiC in SAD pattern were observed. Based on the analyses of SAD patterns,  $Ti_3SiC_2$  was found in all specimens. It is known that there existed not only  $Ti_3SiC_2$  but also other phases, such as  $Ti_5Si_3C_x$  in the reacted interlayer between SiC substrates at high temperature. Detailed analysis of the formed phases in the bonded region will be presented.

**10:20 AM**

**(ICACC-S8-035-2012) Hybrid ceramic-metal tubes for steam pipes**

C. Spatz\*, Fraunhofer-Center Lightweight design for high temperature environments, Germany; N. Langhof, W. Krenkel, University of Bayreuth, Germany

In order to meet the energy demand in the future, steam power plants with steam temperatures up to 700 °C are planned, enabling net efficiencies over 50 %. Current austenitic steel tubes are limited in their life time due to tertiary creep. In order to use these steel tubes for an extended period of time, this paper describes technology approaches to reinforce these metallic tubes with outer ceramic fiber reinforcements. CMCs as well as matrix-free fiber reinforcements have been investigated as so-called compound tubes. In addition finite element modeling is used to calculate the tensile stresses in the outer reinforcement which occur due to the higher coefficient of thermal expansion of the steel tube. The FE model utilizes temperature dependent material properties of the ceramic-metal hybrid tube, and examines the influence of geometry factor on the studied material concept. Material systems as well as the results of FE modeling are discussed with respect to the process temperature and other specifications.

**10:40 AM**

**(ICACC-S8-036-2012) Joining of Alumina by Alumina-Zirconia Interlayer under low pressure and high temperature**

N. Kondo\*, M. Hotta, H. Hyuga, K. Hirao, H. Kita, National Institute of Advanced Industrial Science and Technology (AIST), Japan

Joining of alumina by alumina-zirconia interlayer was reported in the 1980's ~ 90's. Alumina-zirconia composite is a well-known superplastic material. Superplastic behavior of the interlayer was used for joining, therefore, joining was carried out at elevated temperatures of 1400 ~ 1600C and under mechanical pressure of a few ~ 10 MPa. Recently, large alumina components are needed for industrial use. One possible technique to make large components is joining. Thus, the authors refocus the joining technique by using superplastic alumina-zirconia interlayer. To actualize superplastic behavior of the interlayer, high mechanical pressure or high temperature is required. In this work, joining under low mechanical pressure and high temperature was tried. Joining of alumina under 0.2MPa and 1700C was successfully done. No residual pores exist at the joined interface. Bend specimens cut from the joined body exhibited strength of 310MPa. (Research supported by METI, Japan, as part of the Project "Innovative Development of Ceramics Production Technology for Energy Saving")

**11:00 AM**

**(ICACC-S8-037-2012) Low temperature joining of boron carbide ceramics**

K. Sekine\*, Stereo Fabric Research Association, Japan; T. Kumazawa, Mino Ceramic Co., Ltd., Japan; W. Tian, Stereo Fabric Research Association, Japan; H. Hyuga, H. Kita, National Institute of Advanced Industrial Science and Technology (AIST), Japan

Boron carbide (B4C) ceramics have the properties of light weight, high elastic modulus and high hardness. For these advantages, they

are expected to be used as components for semiconductor. The semiconductor apparatus size is increasing for throughput enhancement nowadays. Therefore it is necessary to produce large size ceramic components. Low temperature joining process is the key technology for producing large size ceramic components. In this study, therefore, joining of B4C ceramics using Al was investigated. Briefly, B4C ceramic plates with dimensions of 20mm×20mm×4mm were prepared as base materials. Al sheet was set on the 20mm×4mm face and was sandwiched between two B4C ceramic plates. Joining was conducted by heating the specimen to a temperature range of 700°C to 1100°C in vacuum. The average four-point bending strength of B4C joint was close to that of the B4C base material. Based on the microstructural observations, we found that Al and B4C were bonded directly and Al infiltrated into B4C microcracks easily. The fracture origins were generally within the base materials instead of the joint locations. This work was supported by New Energy and Industrial Technology Development Organization (NEDO) and Ministry of Economy, Trade and Industry (METI), as part of the Innovative Development of Ceramics Production Technology for Energy Saving project.

**11:20 AM**

### **(ICACC-S8-038-2012) Joining of alumina by using polymer blend**

K. Kita\*, N. Kondo, National Institute of Advanced Industrial Science and Technology (AIST), Japan; Y. Izutsu, Stereo Fabric Research Association, Japan; H. Kita, National Institute of Advanced Industrial Science and Technology (AIST), Japan

Polymer blends containing polycarbosilane (PCS) and polymethylsilsesquioxane (PMSQ) were prepared and joining of alumina by using the polymer blends and aluminum foil had been investigated for the purpose of development of ceramic joining method with energy reduction during joining and metal reduction in joined ceramics. Aluminum and silica (SiO<sub>2</sub>) layer directly reacts by heating and can be made into silicon-alumina oxide such as mullite and it was considered that this react would be helpful to the purpose. The former investigation that joining of alumina by using PCS and aluminum foil shows an inert atmosphere and 1073K pyrolysis enable alumina with SiO<sub>2</sub> layer to join each other. However, silicon carbide (SiC) layer derived from PCS on alumina can be made by 1073K heating and cannot get exfoliation, making of SiO<sub>2</sub> layer on alumina derived from the SiC layer needs 1673K heating. In the case of PMSQ, it consists of the amount of Si-O groups and gets hard by heating at less than 473K, however, the layer of PMSQ on alumina cause exfoliation easily. We paid attention to polymer blend method in order to make good use of these advantages of these polymers because there are some reports of the validity of the method, and we shed light on the effect of the polymer blend and the joining method.

**11:40 AM**

### **(ICACC-S8-039-2012) Diffusion Bonding of Rigid Alumina Pieces Using Porous Alumina Interlayers**

H. Miyazaki\*, M. Hotta, H. Kita, National Institute of Advanced Industrial Science and Technology, Japan; Y. Izutsu, Stereo Fabric Research Association, Japan

Huge alumina components with a size of more than 2 m are now required in chemical plants and semiconductor industries to improve productivity. For such a demand, joining ceramics parts with a height of 1 m to form such huge assemblies is necessary since both machining and sintering of giant green bodies are usually difficult. However, conventional joining technique using glass as an interlayer can not be used since high purity of the joint is required to prevent product contamination for these applications. In order to fabricate an alumina joint with pure alumina interlayer, a pure alumina slurry with dispersant was sandwiched by an alumina plate couple in this study. The slurry was dried in the gap of faying surfaces and sintered at 1650 °C without substantial external pressure. Macro defects, which limit the strength, such as large cavities and lateral interfacial cracks were not observed in the porous joints when the concentration of slurry was

optimized. An average of flexural strength of more than 280 MPa was attained at room temperature for the joint prepared from a slurry with solid content of 42.2 vol%, although the porosity of the interlayer was ~20%. By controlling the interlayer microstructure, high quality diffusion bonds of alumina could be made without either joining pressure or perfectly flat surfaces.

## **S9: Porous Ceramics: Novel Developments and Applications**

### **Applications of Porous Ceramics**

Room: Coquina Salon C

Session Chair: James Zimmermann, Corning

**8:00 AM**

### **(ICACC-S9-033-2012) The State of the Diesel Particulate Filter (DPF) (Invited)**

M. Murtagh\*, Corning Incorporated, USA

Prevailing global environmental concerns over mobile and stationary diesel emissions prompted strict legislation incrementally implemented over the first decade of the 21st century. The standards established by the new emissions legislation posed a significant materials science and engineering challenge. New requirements demanded greater efficiency from existing emissions after-treatment (catalyst support systems, i.e. catalytic converters), as well as engine modifications. The challenge of acquiring means to meet the stricter standards generated the emergence of some innovative approaches. As a result, heavy and light duty diesel engine manufacturers (in North America, Europe and Japan) were faced with the challenge of implementing rapidly developing technologies to meet the environmental legislation for particulate matter (PM) and oxides of nitrogen (NO<sub>x</sub>) emissions. This presentation will review the state of the diesel particulate filter (DPF) past, present and future, covering wall flow filter material choices, i.e. cordierite, silicon carbide, and aluminum titanate, and the wall flow DPF design considerations, such as component filtration (efficiency & pressure drop), thermomechanical, and thermochemical properties derived from the fixed integration of both the macro and microstructural attributes.

**8:30 AM**

### **(ICACC-S9-034-2012) Ultra High Porosity Acicular Mullite Ceramic Designed for Filtration of Diesel Particles and Reduction of NO<sub>x</sub> (Invited)**

A. J. Pyzik\*, B. Newman, R. Ziebarth, M. Malanga, Dow Chemical Company, USA

Broad implementation of diesel engines requires significant reduction of NO<sub>x</sub> and particulate matter (PM) from the engine exhaust. Today's trend to combine these functions into one substrate has potential for reducing system size and overall cost. However, the large amount of catalyst needed for NO<sub>x</sub> control (Lean NO<sub>x</sub> Trap or Urea SCR) reduces porosity and increases back pressure, thus increasing fuel consumption. This paper describes development of an experimental ultra-high porosity acicular mullite ceramic to be used for combined NO<sub>x</sub> reduction and filtration of soot in diesel engines. Acicular mullite honeycombs having porosities between 75 and 85% showed high strength, excellent NO<sub>x</sub> reduction and pressure drop that is comparable to state of the art commercial filters without any catalyst coating. The effect of increased porosity on mechanical properties, especially on flexural strength, are investigated and discussed in comparison to other high porosity ceramics. The ability of high porosity acicular mullite to combine several functions into one substrate provides the promise of lower cost for the entire emission treatment system without compromising performance.



9:00 AM

**(ICACC-S9-035-2012) Solid foam monoliths as supports for zeolite catalysts**

W. Schwieger\*, A. Inayat, S. Lopez, Friedrich-Alexander-Universität Erlangen Nürnberg, Germany; H. Freund, Max-Planck-Institut, Germany; A. Schwab, T. Zeiser, Friedrich-Alexander-Universität Erlangen Nürnberg, Germany

The development and application of structured reactors have been triggered by the requirements of low pressure-drop and high surface area for reactions with very low residence times and high space velocities. Structured monolithic reactors can be considered as a very open macro porous system in which the surfaces can be utilized as the carrier for active components useful as a catalyst in a desired reaction. Such a surface modification of the monolith surface with an additional porous material results in a hierarchically organized system. In this regard the use of appropriate materials like microporous zeolites permits the development of a hierarchical organization of the porosity on two (micro-/macro) or three different (micro-/meso-/macro) levels. Thus, hierarchically organized structured zeolitic composites can benefit from both, the zeolitic function (e.g. separation, activity) and the function of the support (e.g. mechanical stability, pressure drop reduction, mass transport). This contribution will review of recent trends and advances in the field of hierarchical zeolitic composites with a special emphasis on the characteristics of open-cellular ceramic foams used as (non-reactive as well as reactive) supports. It will be shown that it is very important to identify the role played by the methods and/or supports with respect to the characteristics of the final hierarchical structures.

9:20 AM

**(ICACC-S9-036-2012) Immobilization of Silver-Modified Nitrogen-Doped Anatase TiO<sub>2</sub> Nanoparticles on Porous Rutile TiO<sub>2</sub> Ceramic Foam and its Photocatalytic Disinfection on *E. coli* bacteria under Visible Light Illumination**

C. Sun, Q. Li\*, L. Cao, S. Gao, Institute of Metal Research, Chinese Academy of Sciences, China; J. K. Shang, University of Illinois at Urbana-Champaign, USA

The immobilization of silver-modified nitrogen doped anatase TiO<sub>2</sub> (TiO<sub>2</sub>/Ag<sub>2</sub>O) on porous rutile TiO<sub>2</sub> ceramic foam was conducted via a two-step process. Monolith rutile TiO<sub>2</sub> ceramic foam with open macropores was prepared by the dispersion of TiO<sub>2</sub> nanoparticles into a polymer foam template followed with a high temperature sintering process. Silver-modified nitrogen-doped TiO<sub>2</sub> nanoparticles were then immobilized onto the porous rutile TiO<sub>2</sub> ceramic foam through a sol-gel process. This photocatalytic ceramic foam possesses an excellent photocatalytic microorganism disinfection effect as demonstrated by its disinfection of *E. coli* under visible light illumination. The immobilization of photo-activated TiO<sub>2</sub>/Ag<sub>2</sub>O could avoid the possible dispersion of nanoparticles into the environment, while the porous rutile TiO<sub>2</sub> ceramic foam has a relatively high compressive strength of 0.11 Mpa to endure the pressure of water in flow-through water treatment devices and its 3D interconnected pores facilitate the passage of water and the efficient contact of microorganisms in water with photo-activated TiO<sub>2</sub>/Ag<sub>2</sub>O nanoparticles. Its unique properties are beneficial for its potential applications in the water treatment for the microorganism disinfection.

**S5: Next Generation Bioceramics****Porous Bioceramics - Joint Session with Symposium 9 on Porous Ceramics**

Room: Coquina Salon C

Session Chairs: Eldon Case, Michigan State University; Aldo Boccaccini, University of Erlangen-Nuremberg

10:00 AM

**(ICACC-S5-001-2012) Requirements for Bioactive Bone Implants from a Medical Device Company's Perspective (Invited)**

J. Rouleau\*, M. Reiterer, Medtronic, USA

The transition from restorative to regenerative therapies is perhaps the biggest trend in the medical device industry for 21 century. In the

past, medical devices mostly relied on mechanical and electrical engineering to improve patient health, and less on fundamentally curing diseases. The high cost of repeated medical procedures, increasing life expectancy, and lofty patient expectations call for regenerative therapies. One long standing area of research interest is bone replacements since non-bioactive solid materials may lead to complications such as limited bone attachment, periprosthetic bone remodeling, or revision surgeries due to patient growth. This talk will review fundamentals of in vivo ossification and clinical requirements for bioactive bone replacements. Finally, the presentation will discuss clinical requirements that are used to derive a set of desired design guidelines. These guidelines include biochemical and mechanical properties that are considered to be important for robust product performance.

10:30 AM

**(ICACC-S5-002-2012) Fabrication of Carbonate Apatite – PLGA Hybrid Foam Bone Substitute**

G. M. Munar\*, M. L. Munar, K. Tsuru, Kyushu University, Japan; S. Matsuya, Fukuoka Dental College, Japan; K. Ishikawa, Kyushu University, Japan

Porous carbonate apatite foam is a potential bone substitute material since it approximates the morphology and mineral phase of bone. One drawback however, is the poor mechanical properties for sufficient handling. A useful method to improve the mechanical property is by reinforcing it with organic material such as biodegradable polymer. This study reports the preparation of carbonate apatite – PLGA hybrid foam for improved mechanical strength and osteoconductivity. Carbonate apatite foam was prepared by hydrothermal treatment of alpha-tricalcium phosphate foam in carbonate solution at 150°C for 24 hours. Carbonate apatite powder was synthesized from vaterite and disodium hydrogen phosphate aqueous solution at 37°C. The carbonate powder was mixed with 10wt% PLGA solution then coated on carbonate apatite foam using freeze-vacuum technique. The obtained carbonate apatite – PLGA hybrid foam showed interconnecting porous structure with average porosity of 85%. Compressive strength was as high as 0.35 MPa from 0.04 MPa. X-ray diffraction and FT-IR showed carbonate apatite as the primary mineral phase. In conclusion, carbonate apatite – PLGA hybrid foam with improved mechanical properties and approximates the mineral composition and morphology of the cancellous bone, was prepared based on dissolution – precipitation reaction and can be a potential bone substitute of scaffold for tissue engineering.

10:50 AM

**(ICACC-S5-003-2012) Sustained Release of a Monoclonal Antibody from Porous Silica**

J. S. Andrew\*, University of Florida, USA

Localized and controlled delivery of drugs is of current interest for the treatment of age related macular degeneration (ARMD). Systemic administrations of drugs for ocular diseases require large and potentially toxic doses to deliver only a small fraction of drug at the target. In light of this, intravitreal injection has become the standard method for administering drugs to the eye. However, the short half-life of drugs in the vitreous requires frequent injections. Each injection introduces risk of infection or hemorrhage, which can lead to permanent vision loss. To overcome these limitations, biocompatible and biodegradable nanoporous silica (SiO<sub>2</sub>) microparticles were used to load and release the monoclonal antibody bevacizumab via electrostatic adsorption. This electrostatic adsorption allows bevacizumab to be concentrated by ~120x (300 mg bevacizumab per gram of porous SiO<sub>2</sub>). These particles allow for high drug loading, controlled release, as well as a simple optical method for monitoring release in a clinical setting. In vitro drug release profiles were characterized by an enzyme linked immunosorbent assay (ELISA). The nanostructured delivery system described here provides the first example of sustained release of a bio-functional monoclonal antibody from a porous ceramic, where approximately 90% of drug is released over a period of one month.

11:10 AM

**(ICACC-S5-004-2012) Porosity-property relationships for bioceramics – is the volume fraction porosity an adequate descriptor in some cases? (Invited)**

E. D. Case\*, Michigan State University, USA

The function of porous hydroxyapatite, other bioceramics and for brittle materials in general may often depend on the details of the distribution of pore shape, size and location with a given specimen. However, when the physical properties of those porous materials are characterized, which properties are sensitive to the microstructural details of porosity and which can be simply described as functions of the total volume fraction porosity,  $P$ ? For example, the evidence is overwhelming for links between the microstructural details and the fracture strength of a given specimen, but what about properties such as Young's modulus, shear modulus, Poisson's ratio, thermal conductivity and electrical conductivity? Are there conditions under which the porosity-dependence of these properties can be adequately described using only by the volume fraction porosity? The questions posed above will be discussed and related to processing.

11:30 AM

**(ICACC-S5-005-2012) Novel Cu-doped bioactive glass (45S5) derived scaffolds for bone tissue engineering**

A. Hoppe, D. Hiller, S. Narayan Rath, U. Knesser, A. R. Boccaccini\*, University of Erlangen-Nuremberg, Germany

Bioactive glasses and glass derived 3D glass ceramic scaffolds are being developed for bone tissue engineering applications due to their high bioactivity and stimulating effects on bone cells. Copper ions have been shown to have beneficial effects on human osteoblast cells and to stimulate vascularization. The goal of this study was to incorporate Cu ions into the bioactive glass network and to use their therapeutic effects when Cu is released upon dissolution of the scaffold. Cu-doped 45S5 bioactive glass was used for fabrication of 3D porous scaffold via the foam replica method. Acellular in vitro studies revealed a very high bioactivity of the Cu-doped scaffolds indicated through fast formation of carbonated hydroxyapatite layer (CHA) after 3 days of immersion in simulated body fluid (SBF). The kinetics of the glass-ceramic scaffold transition to calcium phosphate was confirmed through XRD, FT-IR and SEM analysis. Cell tests with rat-derived mesenchymal stem cells (rMSCs) were performed showing good biocompatibility of Cu-doped samples, whereby RNA / RT-PCR analysis as well as ALP staining were performed. Further, the specific effect of Cu-ions on the activity of the HNE marker (end product of lipid peroxidation) was investigated using human osteosarcoma cells (HOS) in a MTT assay indicating accumulation of HNE on the scaffolds.

11:50 AM

**(ICACC-S5-006-2012) Microstructures and physical properties of biomorphic SiSiC ceramics manufactured via LSI-technique**

S. Weber\*, R. Jemmali, D. Koch, H. Voggenreiter, German Aerospace Center, Institute of Structures and Design, Germany

Biomorphic SiSiC ceramic composites were produced by liquid silicon infiltration (LSI) process. These materials are based on activated coal (ACBC) and wood fibers (MDF). Microstructural characteristics in green-, carbon- and SiSiC-body modification were investigated by analyzing curved structures (type charcoal) and planar structures (type MDF). Therefore polished and unpolished specimens have been examined with scanning electron microscopy (SEM), microfocus X-ray computed tomography (CT) and respective evaluation software. Focused on the objective of near net shape reproducibility for the ceramic composites, different shrinkage and silicon uptake behavior were identified. Furthermore, significant capillarities, densities and porosities could be determined and valued regarding the objective and highest possible SiC content. The appearing different SiSiC microstructures influence the physical properties of SiSiC ceramics

such as flexural strength, Young's modulus and hardness, which were detected with standardized testing methods.

**S12: Materials for Extreme Environments: Ultrahigh Temperature Ceramics (UHTCs) and Nanolaminated Ternary Carbides and Nitrides (MAX Phases)**

**Structural Stability under Extreme Environments I**

Room: Coquina Salon F

Session Chair: Luc Vandeperre, Imperial College London

8:00 AM

**(ICACC-S12-001-2012) Oxidation Mechanisms in UHT and MAX Phase Ceramics (Invited)**

W. E. Lee\*, B. Cui, E. Eakins, D. D. Jayaseelan, Imperial College, United Kingdom; P. Brown, DSTL, United Kingdom

To understand oxidation in UHTCs & MAX phases we have investigated microstructural evolution of oxide scales formed over a range of temperatures. Ti<sub>2</sub>AlC and Ti<sub>2</sub>AlN, have been examined. In Ti<sub>2</sub>AlC from 1100-1300C an outer rutile layer & a thicker protective Al<sub>2</sub>O<sub>3</sub> layer grow whose densification appears to be aided by the presence of CO. >1400C Al<sub>2</sub>TiO<sub>5</sub> forms on reaction between TiO<sub>2</sub> and Al<sub>2</sub>O<sub>3</sub> leading to cracking & loss of oxidation protection. In Ti<sub>2</sub>AlN oxidation is more complex involving formation of mixed rutile, anatase and Al<sub>2</sub>O<sub>3</sub> layers which become dense from 900-1100C and under which a void layer forms possibly via a Kirkendall effect and NO<sub>x</sub> gas. With increasing temperature Al<sub>2</sub>TiO<sub>5</sub> and a series of void layers additionally form and the gaseous NO<sub>x</sub> generated has no beneficial effect on densification. Attempts have been made to control oxidation in UHTCs such as ZrB<sub>2</sub>, ZrB<sub>2</sub>-SiC, HfB<sub>2</sub> and HfB<sub>2</sub>-SiC using additive phases, eg, to increase the viscosity of any liquid phase formed or provide protective refractory phases at high temperatures. SiC additions are effective in forming protective silica but only in static environments and to ~1600C. For higher temperature applications, RE<sub>2</sub>O<sub>3</sub> additions lead to formation of a dense HfO<sub>2</sub> or ZrO<sub>2</sub> scale also containing RE zirconates and hafnates. Such ceramic systems, producing self-generating refractory oxidation barriers or dense scales, show promise in providing oxidation resistance.

8:20 AM

**(ICACC-S12-002-2012) Testing SiC fiber-reinforced ZrB<sub>2</sub> sharp component in supersonic regime**

L. Silvestroni\*, F. Monteverde, CNR-ISTEC, Italy; R. Savino, DIAS – University of Naples, Italy; D. Sciti, CNR-ISTEC, Italy

Ultra-high-temperature ceramics are currently the most promising materials for thermal protection structures, like wing leading edges in next generation space vehicles flying at hypersonic speed or/and re-entering the earth's atmosphere, which are characterized by sharp profiles to increase performances and maneuverability. In this contribution, the aero-dynamic behaviour of a very sharp ZrB<sub>2</sub>-SiC fiber composite is tested in a plasma wind tunnel in supersonic regime. A wedge with curvature radius of 0.1 mm was exposed to four runs in a temperature range 1400-1680°C for a total time of about 17 minutes. The wedge survived the test with minimal dimension change. The microstructural modifications induced by the hot stream were used as input values for computational fluid dynamics which furnished as output the temperature gradient along the wedge profile. Microstructural changes induced by oxidation are compared to those of a ZrB<sub>2</sub>-SiC particles ceramic machined in the same shape and exposed to similar aero-dynamic conditions. On the oxidised surface of the fiber-reinforced composite large deposits of carbon were observed due to active oxidation of SiC, which was hardly detected on ZrB<sub>2</sub>-SiC particles composites. The different way SiC fibers and particles oxidise could significantly affect the thermal conductivity and consequently the overall aero-thermal response of the composites.

8:40 AM

**(ICACC-S12-003-2012) High-Temperature Oxidation Testing of UHTC Composites**

A. Paul\*, S. Venugopal, J. Binner, B. Vaidyanathan, Loughborough University, United Kingdom; P. Brown, A. Heaton, Dstl, United Kingdom

Carbon preform-UHTC powder composites aimed for hypersonic applications have been prepared by a slurry impregnation route. Five different UHTC compositions have been selected for impregnation, viz. ZrB<sub>2</sub>, ZrB<sub>2</sub>-20 vol%SiC, ZrB<sub>2</sub>-20 vol%SiC-10 vol%LaB<sub>6</sub>, HfB<sub>2</sub> and HfC. The impregnated preforms were further densified with pyrolytic carbon using chemical vapour deposition. The samples have been analysed for depth of impregnation and UHTC powder distribution using X-ray micro-CT, FEGSEM and EDAX; the depth of impregnation was found to be more than 3 mm for all the samples produced. Oxidation and high temperature resistance were studied using a purpose-built oxyacetylene torch test facility at temperatures above 2500°C for 30 s and 1 min. Very recently, some tests have also been performed for >2 mins. The mass loss and depth of erosion were determined and the samples were analysed using the same characterisation techniques outlined above. The results will be presented and discussed. Early experiments to improve the oxidation resistance by fibre coating have been carried out and will also be presented. The conclusions are that hafnium-based UHTC impregnated samples appear to offer the greatest resistance to ultra high temperature oxidation; as yet, it is unknown whether this is due to the chemistry of the Hf-based systems or UHTC particle size since these powders were also the coarsest. Further work is continuing to investigate this.

9:00 AM

**(ICACC-S12-004-2012) Protection against oxidation, by CVD or SPS coatings of Hafnium Carbide and Silicon Carbide, on Carbon/Carbon composites**

A. Allemand\*, CEA, France; Y. Le Petitcorps, O. Szwedek, Universite de BORDEAUX, France; N. Teneze, P. David, CEA, France

The hafnium carbide compound is an ultra high refractory ceramic; as a result it could be of interest for the protection of carbon/carbon composites against oxidation at high temperatures. However HfC and most of these metallic carbides present a non stoichiometric composition with carbon vacancies. As a consequence, the oxidation resistance is poor at low temperatures (500-1000°C). In order to overcome this main drawback the HfC can be associated with a carbide (SiC) presenting a better oxidation resistance at lower temperatures. Two coating routes have been studied; the first one is the Chemical Vapour Deposition which enables to obtain very thin coatings and the second one is the Spark Plasma Sintering technique which permits to get new microstructures of coatings. This study describes the CVD conditions for the deposition of HfC from the metallic hafnium pellets to get hafnium chlorides followed by the reduction of the chlorides by H<sub>2</sub> and the deposition of HfC with the methane as carbon precursor. In an other hand, SPS has permitted to sinter, on Carbon substrate, ultra high refractory ceramic powders with a significant amount of SiC. The sintering conditions to obtain an uncracked coating will be presented as well as microstructures and oxidation tests.

9:20 AM

**(ICACC-S12-005-2012) Experimental methods for reliable oxidation measurements of ultra-high temperature ceramics up to 1600°C**

M. Miller-Oana\*, L. S. Walker, W. R. Pinc, E. L. Corral, University of Arizona, USA

During hypersonic flight, vehicles need materials such as ultra-high temperature ceramics (UHTCs) for thermal protection systems (TPS) in order to withstand temperatures greater than 2000°C, extreme heat fluxes, all in the presence of varying gas mixtures. Therefore, understanding the effect of test environment on the oxidation behavior of these materials that is relevant to the application environ-

ment is important. We examine the oxidation behavior of ZrB<sub>2</sub>-SiC composites by investigating the ratio of total specimen edge length to total specimen surface area, developing reliable oxidation testing methods, and studying the effect of testing environment with various gas flow rates by comparing oxidation measurements in the box, tube, and TGA furnaces. In situ mass gains during ZrB<sub>2</sub>-SiC oxidation are measured with thermogravimetric analysis (TGA) at 1400, 1500, 1600°C from 15 to 60 minutes. Reproducible oxidation rates are not obtained due to varying edge length and surface area of ZrB<sub>2</sub>-SiC composites. Using identical test conditions, mass gains during heating range from 0.93% to 0.14% for total specimen edge length to surface area ratios of 1.28 and 0.33, respectively. For reliable and reproducible data, sample parts with a ratio less than 0.5 should be used for oxidation testing due to the reduced effect of edge and corner oxidation compared to bulk (planar) oxidation.

**Structural Stability under Extreme Environments II and Novel Processing Methods I**

Room: Coquina Salon F

Session Chairs: Martin Magnuson, IFM; William Lee, Imperial College

10:00 AM

**(ICACC-S12-006-2012) Charged particle irradiation of (Ti,Zr)<sub>3</sub>(Si,Al)C<sub>2</sub>: structural disorder and thermal diffusivity**

M. Le Flem\*, X. Liu, S. Doriot, T. Cozzika, CEA Saclay, France; D. Rochais, CEA Le Ripault, France; I. Monnet, CIMAP, France

MAX phases and especially Ti<sub>3</sub>SiC<sub>2</sub> based compounds have been recently considered as potential candidates for core components in some future nuclear reactors. Despite tolerance to damage and good thermal conductivity, the impact of radiation on microstructure and properties is a very recent worry. Irradiation with charged particles has already highlighted the resistance to amorphisation of Ti<sub>3</sub>SiC<sub>2</sub>, but the progressive increase in structural disorder with dose needs to be specified, especially in terms of possible occurrence of saturation and impact on properties. In this work, (Ti,Zr)<sub>3</sub>(Si,Al)C<sub>2</sub> compounds fabricated by IMR, Shenyang (China) were irradiated with 95 MeV Xe ions up to 4.5×10<sup>15</sup> cm<sup>-2</sup>. The effect of dose and temperature on microstructure and hardness was investigated through XRD analyses, TEM examinations and nanoindentation measurements. Photoreflectance was used to estimate the change in thermal diffusivity. Both Ti<sub>3</sub>(Si,Al)C<sub>2</sub> and (Ti,Zr)<sub>3</sub>(Si,Al)C<sub>2</sub> exhibited no significant evolution up to 10<sup>13</sup> cm<sup>-2</sup>. Higher doses induced change in surface topology and occurrence of atomic disorder highlighted by High Resolution TEM and XRD analyses. An increase in hardness was highlighted and the thermal diffusivity was obviously strongly affected by irradiation, especially in the area of implanted ions. Above 1×10<sup>15</sup> cm<sup>-2</sup>, a plateau in hardness suggested a saturation in irradiation damage.

10:20 AM

**(ICACC-S12-007-2012) Behaviour under ion-irradiation of Cr<sub>2</sub>GeC and Cr<sub>2</sub>AlC**

M. Bugnet, T. Cabioch\*, V. Mauchamp, M. Jaouen, University of Poitiers, France

Recently, MAX Phases have attracted much attention in the irradiation community since they are considered as new materials which could be incorporated in core components of future gas cooled fast nuclear reactors. Promising results were obtained on Ti<sub>3</sub>SiC<sub>2</sub> and Ti<sub>3</sub>AlC<sub>2</sub> since no amorphization was obtained even after very large fluences ion-irradiations. In the present study, the behaviour under ion irradiation of epitaxial Cr<sub>2</sub>AlC, Cr<sub>2</sub>GeC thin films deposited onto sapphire substrates by high temperature magnetron sputtering were studied in situ in a TEM and ex situ by XRD. Cross-sections of these films were irradiated at room temperature with 340 keV Xe<sup>2+</sup> ions (nuclear energy loss) and 6 MeV Au<sup>3+</sup> ions (electronic energy loss). In both cases, amorphization of the chromium based MAX phases were

obtained, on the contrary of titanium based MAX Phases. This amorphization takes place for lower fluences with  $\text{Xe}^{2+}$  ions than  $\text{Au}^{3+}$  ions and only nuclear losses have to be considered to explain our observations. Furthermore, whereas the amorphization of  $\text{Cr}_2\text{AlC}$  seems to originate in a defects accumulation process, evidences of direct impact damages are obtained for  $\text{Cr}_2\text{GeC}$ . The presented results clearly indicate that the behaviour under irradiation of MAX phases strongly varies with the chemistry of these compounds.

**10:40 AM**

### (ICACC-S12-008-2012) High Strain Rate Deformation Behavior of Nanolaminated Titanium Aluminum Carbide

S. Abotula, University of Rhode Island, USA; S. Basu, M. Radovic\*, Texas A&M University, USA; A. Shukla, University of Rhode Island, USA

A unique combination of ceramic and metallic properties of  $\text{Ti}_2\text{AlC}$  makes it a suitable candidate for applications in extreme conditions involving high strain rate deformation. The quasi-static deformation behavior of  $\text{Ti}_2\text{AlC}$  exhibits fully reversible hysteretic behavior independent of strain rates. This rather uncommon behavior in fully-dense ceramics has been attributed to formation of dislocation based incipient kink bands, a precursor to irreversible kink bands (KB). To understand the dynamic deformation behavior of the  $\text{Ti}_2\text{AlC}$ , Split Hopkinson Pressure Bar (SHPB) compression experiments have been performed in 1500-5000/s strain rate range and 27 -1150 oC temperatures range. At room temperature, the failure stress and strain show little dependence on strain rate, whereas the failure stress drops considerably at temperatures above 900 oC. Unlike other structural ceramic materials,  $\text{Ti}_2\text{AlC}$  does not exhibit brittle failure but rather a softening after failure initiation and a more graceful failure. SEM of the fracture surfaces reveals the laminated nature of  $\text{Ti}_2\text{AlC}$  and significant amount of KB formation. As discussed herein, the formation of KBs is argued to be the primary reason behind energy dissipation and crack bridging in  $\text{Ti}_2\text{AlC}$ , resulting in the softening and graceful failure observed during the SHPB experiments.

**11:00 AM**

### (ICACC-S12-009-2012) Growth of $\text{Ti}_3\text{SiC}_2$ single crystals (Invited)

D. Chaussende\*, T. Ouisse, CNRS - Grenoble INP, France

Even if the growth of bulk  $\text{Ti}_3\text{SiC}_2$  single crystals is not driven by any identified application, its study has a twofold objective. First, the availability of such crystals could allow an accurate measurement of the basic physical properties of such materials. For instance, the  $\text{Ti}_3\text{SiC}_2$  outstanding anisotropy, closely related to its layered crystalline structure, has only been partially described. Second, it should provide some basic physico-chemical data necessary for a perfect monitoring of  $\text{Ti}_3\text{SiC}_2$  synthesis. The present paper will give an overview of the previously reported growth methods, with a special emphasis put on what can be learnt from them. It will then be shown how liquid phase growth of  $\text{Ti}_3\text{SiC}_2$  at high temperature (1700°C) has permitted to tackle some fundamental aspects of crystal growth which were previously restricted to very simple chemical systems, such as pure metals deposited with atomic scale control.

**11:20 AM**

### (ICACC-S12-010-2012) Growth and electrical transport properties of $\text{Cr}_2\text{GeC}$ thin films

P. Eklund\*, Linköping University, Sweden; M. Bugnet, V. Mauchamp, S. Dubois, C. Tromas, Université de Poitiers, France; J. Jensen, Linköping University, Sweden; L. Piraux, L. Gence, Université catholique de Louvain, Belgium; M. Jaouen, T. Cabioch, Université de Poitiers, France

Although a relatively little researched member of the MAX-phase family,  $\text{Cr}_2\text{GeC}$  exhibits a number of traits that render it interesting from a fundamental-research point of view, such as its very high reported thermal expansion coefficient and its anomalously high density of states at the Fermi level. Therefore, we are interested in  $\text{Cr}_2\text{GeC}$ . For synthesis of this phase, thin-film growth is a potentially

important approach because of the relative ease with which numerous MAX phases can be epitaxially grown. Here, we report growth of phase-pure  $\text{Cr}_2\text{GeC}$  directly onto  $\text{Al}_2\text{O}_3(0001)$  at temperatures above 700 – 800 °C. These films have an epitaxial component and a large secondary grain population with (10-13) orientation. Deposition onto  $\text{Al}_2\text{O}_3(0001)$  with a  $\text{TiN}(111)$  seed layer and onto  $\text{MgO}(111)$  yielded globally epitaxial  $\text{Cr}_2\text{GeC}(0001)$  with a virtually negligible (10-13) contribution. In contrast, films grown at 500 – 600 °C are polycrystalline  $\text{Cr}_2\text{GeC}$  with (10-10)-orientation and exhibit surface segregations of Ge because of the fast Ge-diffusion rates along the basal planes. The room-temperature resistivity of our samples is 53 – 66  $\mu\Omega\text{cm}$ . Temperature-dependent resistivity measurements from 15 to 295 K show that electron-phonon coupling is important and anisotropic, which emphasizes that the electrical transport properties cannot be understood in terms of ground state electronic structure calculations only.

**11:40 AM**

### (ICACC-S12-011-2012) MAX phase formation by intercalation upon annealing of $\text{TiC}_x/\text{Al}$ ( $0.4 \leq x \leq 1$ ) bilayer thin films

J. Schneider\*, A. Abdulkadhim, D. Music, T. Takahashi, F. Munnik, RWTH Aachen University, Germany

$\text{TiC}_x/\text{Al}$  bilayer thin films were synthesized using combinatorial magnetron sputtering to study the influence of C content on the reaction products at different annealing temperatures. Based on energy dispersive X-ray analysis calibrated by elastic recoil detection analysis data, x in  $\text{TiC}_x$  was varied from 0.4 to 1.0. Film constitution was studied by X-ray diffraction before and after annealing at temperatures from 500 to 1000°C. The formation of  $\text{TiC}_x$  and Al in the as-deposited samples over the whole C/Ti range was identified. Upon annealing  $\text{TiC}_x$  reacts with Al to form the Ti-Al based intermetallics. Already at 700°C, the formation of MAX phases (space group  $P63/mmc$ ) is observed at  $x \leq 0.7$ . Based on the comparison between the C content induced changes in the lattice spacing of  $\text{TiC}_x$  and  $\text{Ti}_2\text{AlC}$  as well as  $\text{Ti}_3\text{AlC}_2$ , we infer the direct formation of MAX phases by Al intercalation into  $\text{TiC}_x$  for  $x \leq 0.7$ .

## S14: Advanced Materials and Technologies for Rechargeable Batteries

### Lithium Metal Air Batteries and Beyond Lithium Batteries

Room: Coquina Salon H

Session Chair: Reza Shahbazian Yassar, Michigan Technological University; Gabriel Veith, ORNL

**8:00 AM**

### (ICACC-S14-027-2012) Exploring the active electrochemistry in lithium-oxygen batteries using gas-phase mass spectrometry (Invited)

B. D. McCloskey\*, IBM, USA

As a result of their high theoretical specific energy, Li-air batteries have attracted considerable attention as possible energy storage devices for electric vehicles and other high energy applications. However, numerous scientific challenges remain unsolved in the pursuit of attaining a high capacity, coulombically efficient Li-air battery. This presentation will highlight IBM's current efforts to understand the nature of Li-O<sub>2</sub> electrochemistry, with the main goal of improving Li-air battery cyclability and capacity. A particular emphasis will be given to studies which employed Differential Electrochemical Mass Spectrometry (DEMS) to analyze stability of aprotic electrolytes and the effect of various electrocatalysts in Li-O<sub>2</sub> cells. Other topics will include the use of an internal redox probe to correlate capacity limitations with cell cathode electrical passivation, and in-situ and ex-situ analysis of electrodeposits formed on the cathode during discharge.

8:30 AM

**(ICACC-S14-028-2012) Understanding Reactions in Lithium-Air Batteries (Invited)**

G. M. Veith\*, N. J. Dudney, J. Nanda, J. Howe, Oak Ridge National Laboratory, USA

One major obstacle for the design of a practical Li-air battery is the non-rechargeability of prototype Li-air cells, likely because the discharge products have poor solubility in most electrolytes and form a solid phase on carbon cathodes [Ogasawara 2006]. In order to design catalysts to promote the decomposition of discharge products we have to determine the final products. This presentation will describe the results of characterization studies performed to determine the discharge products formed during cycling and how these discharge products change as a function of catalyst, electrolyte composition, and oxygen pressure. Specific emphasis will be placed on Raman, Fourier Transform Infrared, and X-ray photoelectron spectroscopies. In addition, scanning Auger spectroscopy will be used to demonstrate changes in discharge product composition as a function of time from Li-air cells using aprotic solvents, such as ethylene carbonate/dimethyl carbonate with Li salts such as LiPF<sub>6</sub>. Finally these results will be summarized to predict reaction mechanisms with specific catalyst structures. Acknowledgements: Research sponsored by the Laboratory Directed Research and Development Program of Oak Ridge National Laboratory, managed by UT-Battelle, LLC, for the U. S. Department of Energy. References: Ogasawara, T., Debart, A., Holzapfel, M., Novak, P., Bruce, P.G., Journal of the American Chemical Society, 128, 1390 (2006).

9:00 AM

**(ICACC-S14-029-2012) Effect of Al on the phase stability and conductivity of Li<sub>7</sub>La<sub>3</sub>Zr<sub>2</sub>O<sub>12</sub>**

J. Wolfenstine\*, J. Allen, Army Research Laboratory, USA; J. Sakamoto, E. Rangasamy, R. Malony, Michigan State University, USA

There is an interest in the garnet Li<sub>7</sub>La<sub>3</sub>Zr<sub>2</sub>O<sub>12</sub> (LLZO) as a possible Li-ion conducting solid electrolyte for use in Li/Li-ion solid-state, Li-air and Li-sulfur batteries because, of its stability with Li and high lattice conductivity (5 x 10<sup>-4</sup> S/cm) at room temperature for the cubic structure. LLZO can also exist with a tetragonal structure. The conductivity of the tetragonal phase at room temperature is approximately 2 orders of magnitude lower than that for the cubic structure. Thus, it is important to understand how to prepare the cubic phase. It has been suggested that the presence of an impurity such as Al is required to stabilize the cubic structure at room temperature. However, there has been no detailed study to determine how the phase stability of LLZO is influenced by the Al concentration. Consequently, a systematic study involving the deliberate and precise addition of Al to LLZO was undertaken and the results evaluated using x-ray diffraction (XRD), inductively coupled plasma (ICP) analysis and nuclear magnetic resonance (NMR). Furthermore, once the critical amount of Al was determined it was decided to use this information to prepare powders of cubic LLZO and consolidate them using uniaxial hot-pressing to determine the ionic and electronic properties of a dense pellet and compare to values determined using conventional sintering.

9:20 AM

**(ICACC-S14-030-2012) Li<sub>4</sub>SiO<sub>4</sub>-Li<sub>3</sub>PO<sub>4</sub> solid solution ion conducting layers for lithium batteries**

L. Cheng\*, L. Zhang, J. Cabana, G. Chen, M. Doeff, T. Richardson, Lawrence Berkeley National Laboratory, USA

The possibility of using materials in the Li<sub>4</sub>SiO<sub>4</sub>-Li<sub>3</sub>PO<sub>4</sub> system as protective layers on the Li electrode to prevent dendrites has been investigated. Li<sub>4</sub>SiO<sub>4</sub>-Li<sub>3</sub>PO<sub>4</sub> solid solutions were prepared by solid state reactions. X-ray diffraction (XRD) was used to characterize the phases. Pellets made from the material with a composition of 60% Li<sub>3</sub>PO<sub>4</sub> (60LP) and sintered at 900°C showed the highest conductivity

with 4.5x10<sup>-6</sup> Ω<sup>-1</sup>cm<sup>-1</sup>. The addition of 0.5 wt% lithium borate (LB) into 60LP aids sintering without sacrificing ionic conductivity. Spraying and radio frequency sputtering were used to deposit thin films onto anodized aluminum oxide (AAO) substrates. The films have been characterized by XRD and scanning electronic microscope (SEM)/energy dispersive X-ray Spectroscopy (EDS). The amorphous and crystalline thin films were compared in terms of morphology and conductivity. Detailed elemental analyses were done by using Rutherford Backscattering Spectrometry (RBS)/Nuclear Reaction Analysis (NRA). The electrochemical stability of the prepared phases against lithium was studied in Li-Li symmetric cells. Both Li-Si-P-O and Li-Si-P-B-O solid electrolytes were found to have stable voltage profiles during cycling with no deleterious reactions. Additional confirmative insight on the electrochemical stability of the phases was obtained from Li/liquid electrolyte/60LP cells.

10:00 AM

**(ICACC-S14-031-2012) Analytical tools for advanced Li-S batteries (Invited)**

R. Dominko\*, M. Patel, National Institute of Chemistry, Slovenia; R. Demir-Cakan, ALISTORE-ERI, France; M. Gaberscek, National Institute of Chemistry, Slovenia; M. Morcrette, J. Tarascon, ALISTORE-ERI, France

The rechargeable Li-S batteries are considered as a promising technology due to their high energy density and being cost effective. Their practical use is faced with two major problems: (i) a low intrinsic conductivity and (ii) loss of active material. Latter is reflected with a capacity loss during cycling and low efficiency. Generally, low intrinsic conductivity can be overcome by maintaining the active material in an intimate contact with an electron conductive matrix. With an aim to find a suitable electrochemical environment and to avoid the loss of active material (polysulphide shuttle-lock) we need to understand the mechanism of Li-S battery and influence of each component on cycling stability and efficiency. Within this we are developing several different in-situ electrochemical and spectroscopic techniques which can detect the formation of soluble and non-soluble intermediate products. In this presentation we report on the applicability of a modified multi electrode Swagelok cell which enables in-situ detection of soluble polysulphides in the electrolyte during Li-S battery operation and we show the design and results obtained using in-situ cell for UV-Vis and Raman spectroscopies. For instance, in the normalized conditions (amount of electrolyte, geometry, electrochemical conditions, ...), quantitative and qualitative differences in terms of polysulfides between different solvents, composites, salts can be observed.

10:30 AM

**(ICACC-S14-032-2012) Non-Aqueous Single-Metal Redox Flow Batteries (Invited)**

C. W. Monroe\*, A. A. Shinkle, A. Sleightholme, L. T. Thompson, University of Michigan, USA

Redox flow battery (RFB) systems store energy in liquid electrolytes, rather than solid electrodes. Their charge capacity can be changed independently of the reactor size by increasing the liquid volumes, making them promising for grid-scale use. A main goal of RFB development is to raise the energy density above 30 Wh/L. The energy density of an RFB electrolyte scales with the concentration of the redox-active species and the equilibrium voltage. Existing RFBs, such as the aqueous all-vanadium or Zn-Br hybrid, use aqueous electrolytes. The ease of water electrolysis limits aqueous RFBs to voltages below 1.4 V. We have identified several single-metal RFB chemistries that function in non-aqueous solvents. These novel non-aqueous RFBs are based on electrochemical disproportionation of transition-metal coordination complexes. Complexes of V, Cr, and Mn with the acetylacetonate ligand have been tested and show that cell voltages of up to 3.5 V can be achieved in acetonitrile solutions. Minimal literature exists regarding the non-aqueous electrochemistry of these complexes. Studies of reaction kinetics and degradation mechanisms will be reported in detail, along with a survey of diagnostic techniques, using the non-aqueous vanadium RFB as an example. We will discuss how changing

ligand structure affects energy density and cell potentials of vanadium RFB electrolytes. Other challenges, including separator selection, will be addressed.

**11:00 AM**

**(ICACC-S14-033-2012) In-situ Fabrication of Porous Carbon Supported  $\alpha$ -MnO<sub>2</sub> Nanoparticles at Room Temperature: Application for Rechargeable Li-air Battery (Invited)**

J. Lu\*, Y. Qin, Z. Chen, Y. Ren, K. Amine, Argonne National Laboratory, USA

Lithium-air cells can be considered the 'holy grail' of lithium battery because they offer a significantly superior theoretical energy density to conventional lithium-ion system. In this study, porous carbon supported MnO<sub>2</sub> nanoparticles synthesized at room temperature have been explored as an electrocatalyst for rechargeable Li-air cells. Both high-energy XRD and XAFS analyses showed that the prepared MnO<sub>2</sub> exhibited tetragonal crystal structure ( $\alpha$ -MnO<sub>2</sub>), which has been proved as one of the most efficient catalysts to facilitate the reaction on charge in the Li-air cell. Under the current synthetic approach,  $\alpha$ -MnO<sub>2</sub> was uniformly distributed onto the surface of carbon support, while the porous structure and surface area of carbon are still well persevered. As a result, the as-prepared catalysts demonstrated a superior electrochemical behavior, which can deliver 1000 mAh/g of capacity (carbon + electrocatalyst) using the current density of 0.05 mA/cm<sup>2</sup> during the initial discharge. The charge potential has been significantly lowered to 3.7 V compared to most of the reported data, which are above 4.0 V. The reaction is reasonably reversible during the early cycles. The mechanism of the capacity fade has also been investigated by analyzing the cathode electrode at different stages using X-ray photoelectron spectroscopy (XPS) technique.

**11:20 AM**

**(ICACC-S14-034-2012) The Spinel Block Integrity in the  $\beta''$ -Alumina Structure**

D. P. Birnie\*, Rutgers University, USA

The  $\beta''$ -alumina structure is examined in detail and an analysis is presented of the three dimensional integrity of the lattice. The layer structure that is responsible for the very high sodium conduction rate is the specific focus. Layers that are derived from the cubic spinel structure are interleaved by more open honeycomb pathways where rapid ion diffusion takes place. The three dimensional rigidity of the spinel-block in this structure makes it possible to accurately quantify the conduction layer thickness based only on the hexagonal unit cell dimensions, as suggested originally by Harbach in 1983. His assumption was that the spinel-block behaves as a 3D isotropic medium (as it would in the parent cubic spinel structure), expanding or contracting in all directions equally as changes are made in the composition. The resulting simple equation he derived is tested rigorously against the many published single crystal and powder full structure determinations that have been made on the  $\beta''$ -alumina-family compounds. Excellent correlation is found substantiating that the spinel block remains isotropic in its physical shape as various solid solution adjustments are made. This paves the way for simpler diffraction analysis of the structure than has previously been done. (Work conducted while on sabbatical at GE Research Labs in Bangalore, India, academic year 2010/11.)

**11:40 AM**

**(ICACC-S14-035-2012) Exploration of Enhanced Beta Alumina Sintering using Microwave Assist Technology**

M. Fall\*, S. Allan, H. Shulman, F. Cabe, Ceralink Inc, USA

Beta (double prime) alumina is an ion conducting ceramic, making it an important solid electrolyte material for both tubular and planar sodium batteries. The performance of this ceramic membrane is critical to the overall efficiency of batteries and therefore improvements are of great interest. Ceralink has been exploring the use of Microwave Assist Technology (MAT), a combined radiant heat and microwave

method to reduce firing time and temperature for densification, which can improve sodium retention. Higher sodium levels increases the ionic conductivity performance of the ceramic. The MAT manufacturing method also has significant energy savings implications. This presentation will show the initial results for sintering and analysis of both prototype tubular and planar beta alumina electrolytes.

## **FS3: Next Generation Technologies for Innovative Surface Coatings**

### **Low Friction Coating**

Room: Coquina Salon G

Session Chairs: Oyelayo Ajayi, Argonne National Laboratory; Tim Hosenfeldt, Schaeffler Technologies GmbH & Co. KG

**8:20 AM**

**(ICACC-FS3-030-2012) Advances in Multi-functional Nanocomposite Coatings for Demanding Automotive Applications (Invited)**

A. Erdemir\*, O. L. Eryilmaz, Argonne National Laboratory, USA

Multi-functional nanocomposite coatings of the hard nitride, carbide, and boride types hold great promise in further enhancing performance, efficiency, and durability of many moving mechanical assemblies in advanced automotive systems. In particular, composite coatings with super-hardness, toughness and low-friction can markedly improve durability and efficiency of these systems. Most of the multi-functional coatings owe their attractive properties to the very unique chemical and structural architectures that they possess. The latest coatings are based on nano-scale multilayers and/or composite architectures providing superlow friction and extreme resistance to wear and scuffing. In this presentation, the design principles for a new class of nanocomposite coatings providing super low-friction and wear will be introduced. For the structural and chemical design of such coatings, we use an innovative approach which is based on the principles of a crystal-chemical model. This model is proven to be very useful in the selection of specific coating ingredients which appear to be very critical for the superior mechanical and tribological properties of resultant coatings under severe sliding conditions. Recent laboratory and engine test results demonstrated much superior performance and durability for components that were protected by these designer coatings.

**8:50 AM**

**(ICACC-FS3-031-2012) Interactions Between Amorphous Carbon Coatings and Engine Oil Additives: Prediction of the Friction Behavior Using Optimized Artificial Neural Networks (Invited)**

E. Schulz\*, T. Beitsprecher, Friedrich-Alexander-University Erlangen-Nuremberg, Germany; Y. Musayev, T. Hosenfeldt, Schaeffler Technologies GmbH&Co. KG, Germany; S. Tremmel, S. Wartzack, H. Meerkamm, Friedrich-Alexander-University Erlangen-Nuremberg, Germany

Amorphous carbon coatings are more and more used in combustion engines. In the valve train these coatings are applied in order to fulfill legislative guidelines concerning energy efficiency and CO<sub>2</sub> emissions. Up to now the effect of interactions between additives and such coatings on the friction is not sufficiently understood. Especially the high complexity of valve train systems and large experimental effort needed for a coating development show the need for a specific prediction of the friction behavior. Since an analytical prediction in such complex systems is not possible, always empirical studies are needed to determine the tribological behavior. This article presents the development and optimization of different multilayer artificial neural networks (ANNs) to predict the friction behavior on basis of tribological test data. For this a multitude of experiments were carried out by using various tribological test equipments whereby input parameters like type of coating, base oil, additives, temperature, pressure, etc. were varied systematically. The predictive capabilities of the ANN models were validated with experimental results. With a systematic

variation of the learning rate and structure of the ANNs, a correlation coefficient from 0.69 up to 0.85 and relative absolute error of about 13% to 21% could be achieved.

#### 9:20 AM

##### (ICACC-FS3-032-2012) The effect of Cu content on the microstructure and wear properties of MoN- Cu Nanocomposite coatings deposited by reactive magnetron sputtering with single alloying target

K. Moon\*, H. Lee, D. Jung, S. Shin, KITECH, Republic of Korea

To reduce energy consumption and wear problems of engine parts, it has been tried to deposit the MoN-Cu thin coatings showing high hardness and low friction. This kind of nano-composite coating is generally made by PVD process using double targets of Mo and Cu. However, during the deposition with two targets, it is not easy to control the exact composition and to deposit homogeneous coating of large scale specimens. In this study, it has been tried to make the single Mo-Cu alloying targets with the various Cu contents among 5-50 at.% in which it has been tried to find out the composition showing the best friction coefficient and surface hardness. The nanocomposite coatings with various Cu contents were prepared by reactive magnetron sputtering process with the single alloying targets in Ar+N<sub>2</sub> atmosphere. The microstructure changes of the coatings were investigated by using XRD, SEM and EDS and TEM. The mechanical properties of MoN-Cu coatings were evaluated by using nanoindenter, wear testers such as ball on disc method and plate on plate method. It is shown in this study that the optimum Cu content for the better low friction properties will be decided between 5-50 at.% Cu.

#### 10:00 AM

##### (ICACC-FS3-033-2012) Performance Evaluation of Hard Ceramic Coatings for Tribological Applications (Invited)

O. Ajayi\*, C. Lorenzo-Martin, D. Singh, N. Demas, G. Fenske, Argonne National Laboratory, USA

Tribological components involve solids in contact and relative motion during operation. This is accompanied by friction, surface damage and wear, ultimately loss of functionality. Under sliding, rolling or sliding/rolling contact there are three predominant failure modes, namely scuffing, contact fatigue, and general wear. To mitigate these failures and ensure reliability and durability of tribological component surfaces, lubrication (solid and fluid) is employed. Hard thin-film ceramic coatings are increasingly being used to enhance the reliability and durability of tribological interfaces. Since there are varieties of thin film hard coatings, appropriate performance evaluation is needed to determine the appropriateness of different coatings for different applications. This presentation discusses performance evaluation of thin-film hard coatings for tribological applications using the systematic tribology approach. In the approach, the basic tribological failure mechanisms are first determined, and then test protocols are developed to reproduce the failure mechanisms. Appropriate test protocols can then be used evaluate thin film coatings for specific applications. Of course, there are tribology specific quality control tests required for thin film coatings. Some of these will be discussed as well.

#### 10:30 AM

##### (ICACC-FS3-034-2012) Nanocrystalline Diamond Coatings on WC-Co with W or Ti Interlayer (Invited)

B. Na, I. Kim, J. Myung, C. Kang\*, Korea Polytechnic University, Republic of Korea

We have used W or Ti as an interlayer material between WC-Co and diamond coatings in order to suppress the detrimental effect of Co. The metal interlayer was deposited at 70°C on the surface polished WC-Co substrate under Ar in an RF magnetron sputtering system. After scratching the metal deposited specimens in an ultrasonic bath containing nanometer diamond powders, the nanocrystalline dia-

mond films were deposited at 600°C on the metal layers in a 2.45 GHz microwave plasma CVD system. Parameters of deposition were microwave power of 1.2kW, the chamber pressure of 110Torr, and the Ar/CH<sub>4</sub> ratio of 100/1sccm. The resulting films were comprised of 0.3~0.5 μm thick interlayer and 1.5~5.0 μm thick diamond coatings. The W interlayer exhibited better results than the Ti interlayer in terms of the growth rate and surface roughness of diamond films. As measured by scratch tester, the adhesion of the coated films to the substrate was more than 30 N regardless of the interlayer. The coefficient of friction on the diamond films with W or Ti interlayer was measured as 0.12 whereas that on the bare WC-Co was 0.40. The excellent adhesion of nanostructured diamond on WC-Co substrate was believed to lead to reliable wear behavior. In summary, both W and Ti interlayers can enhance diamond nucleation and adhesion on WC-Co substrate and thus facilitating the formation of adherent diamond coatings on WC-Co tools.

#### 10:50 AM

##### (ICACC-FS3-035-2012) Electronic and Grain Boundary Structure Control for Hardening in Chromium Oxynitride Based Thin Films

H. Suematsu\*, T. Suzuki, Nagaoka University of Technology, Japan; J. Shirahata, UNION TOOL CO., Japan; K. Suzuki, T. Nakayama, K. Niihara, Nagaoka University of Technology, Japan

Various nitrides have been developed for hard coatings on cutting tools. By demands for higher machining speed and less lubricant consumption, the hardness of the coatings must be increased. Recently, we revealed that oxygen partial substitution in CrN could be possible by pulsed laser ablation and induced hardening. Furthermore, newly synthesized (Cr,Mg)(N,O) thin films showed HV= 4200 which exceeded the hardness of CrN. From the X-ray absorption spectroscopy and electron energy loss spectroscopy (EELS), the Cr-K and L absorption edge was shifted to low energy, which was thought to be caused by the increase in ionicity of Cr. Using this Cr(N,O) based compounds, industrial applications took place. Thin films of (Cr,Si)(N,O) deposited by a magnetron sputtering showed a peak in hardness. From precise field emission transmission electron microscopy and EELS observations, until the formation of soft grain boundary layers of Cr-Si-O, hardness was increased monotonically with the increase in Si content. From the above results, it was found out that electronic and grain boundary structure control can improve the hardness of Cr(N,O) based thin films.

#### 11:10 AM

##### (ICACC-FS3-036-2012) Low friction coatings for automotive and industry application in high volume production (Invited)

T. Hosenfeldt\*, Schaeffler Technologies GmbH & Co. KG, Germany

Modern components and systems for automotive and industrial applications have to meet various requirements in multiple technical fields. Apart from properties that affect the part itself – like geometry, stiffness, weight or rigidity – the surface properties must be adjusted to the growing environmental requirements. This includes measures for corrosion and wear protection, for optimum electrical or thermal conductivity and for optical purposes. Beyond those, coatings are increasingly used to reduce the friction losses of car components, improve fuel efficiency and reduce CO<sub>2</sub>-emissions. This article describes how to use surface technology as a modern design element for components and systems to enable the increasing requirements on market leading automotive and industrial products. Therefore, Schaeffler has developed and established a coating tool box for customized surfaces to apply the right solutions for all that needs and requests with the corresponding coating system made by PVD-/ PACVD-, spraying or electrochemical technology. For innovative products it is extremely important that coatings are considered as design elements and integrated in the product development process at a very early stage. In this article tribological coatings are viewed within a holistic and design-oriented context.

**11:40 AM**

**(ICACC-FS3-037-2012) Industrial large scale production of PVD/PECVD coatings for automotive components (Invited)**

R. Tietema\*, R. Jacobs, D. Doerwald, T. Krug, Hauzer Techno Coating BV, Netherlands

PVD coatings have been introduced in the automotive industry in the beginning of the 1990's. The production of large scale of coatings on automotive components, started with carbon based coatings on components for high pressure diesel injection. These coatings had to provide wear protection in that period and were inevitable for the function of the new technology. The increased engine power as a consequence of the introduction of the HP injection gave an avalanche effect leading within a few years to the replacement of engine parts in both the valve train and power train by engine parts, designed with coatings for wear resistance. These coatings were mainly carbon based, but also non-carbon based coatings have found their way to automotive parts. Today most commonly coatings used are CrN and DLC coatings. In the beginning of this century, new regulations were introduced for the reduction of CO<sub>2</sub> emission. This gave again a boost to the market of DLC coatings for their low friction properties. Here started the introduction on valve train components. Other CO<sub>2</sub> emission reduction measures in automotive industry that have been introduced more recently to improve engine efficiency include weight reduction, engine down sizing, start stop engines, hybrid engines and partial cylinder shut off.

## FS4: Advanced (Ceramic) Materials and Processing for Photonics and Energy

### Photoelectrochemical Systems

Room: Oceanview

Session Chair: Eric Diau, National Chiao Tung University

**8:00 AM**

**(ICACC-FS4-016-2012) Nanostructured hybrid materials for energy applications (Invited)**

D. Ma\*, G. Chen, D. Wang, INRS, Uni. Quebec, Canada; J. Baral, University of Quebec at Montreal, Canada; H. Zhao, B. Gonfa, S. Desinan, R. Nechache, INRS, Uni. Quebec, Canada; N. Wu, West Virginia University, USA; V. Truong, Concordia University, Canada; M. El Khakani, INRS, Uni. Quebec, Canada; R. Izquierdo, University of Quebec at Montreal, Canada; F. Rosei, INRS, Uni. Quebec, Canada; R. Rosei, Trieste University, Italy

I will present two types of nanostructured hybrid materials, designed for photovoltaic (PV) and catalysis applications, respectively. The first type is based on the attachment of quantum dots (QDs) onto one-dimensional nanostructures and the second type is known as core@shell structures. Harvesting near infrared (NIR) photons represents an attractive approach to improve the energy conversion efficiency of organic PVs. We have realized controlled hybridization of NIR PbS QDs with carbon nanotubes (CNTs) and further integrated them into poly(3-hexylthiophene). The nanohybrid cell show considerably enhanced power conversion efficiency, which is attributed to the significantly extended absorption in NIR by PbS QDs and the effectively enhanced charge transportation due to CNTs. We have also realized controlled hybridization of PbS QDs with TiO<sub>2</sub> nanobelts, which show markedly extended "effective" sensitization up to 1400 nm. As for catalysis, using noble metals as shell materials in a core-shell nanoparticle (NP) configuration is a promising strategy with significant economic advantages because it maximizes the precious element's surface to volume ratio. We have synthesized a novel Ni-core@Ru-shell NPs via developing a new organometallic approach and such formed core-shell structures show remarkable performance in the hydrolysis of ammonia borane, in addition to superparamagnetic properties.

**8:30 AM**

**(ICACC-FS4-017-2012) Creating polymer nanostructure for organic photovoltaic devices (Invited)**

C. Luscombe\*, N. Doubina, S. Boyd, M. Yuan, University of Washington, USA

Semiconducting polymers are actively under development for use in light-weight, flexible, disposable organic light-emitting diodes, and thin-film transistors. A key application which is currently attracting a lot of interest for semiconducting polymers is their use in organic photovoltaic devices (OPVs). The main drive for developing OPVs is the lower cost associated with their manufacturing, because of the fact that organic semiconducting polymers can be solution processed. Poly(3-hexylthiophene) (P3HT) remains one of the most commonly used polymers in organic photovoltaics due to its desirable electronic properties. Both the Yokozawa and the McCullough groups developed methods for the synthesis of highly regioregular P3HT with controlled molecular weights and narrow molecular weight distributions using the 1,3-bis(diphenylphosphino)propane nickel(II) chloride (NiCl<sub>2</sub>(dppp)) catalyzed polymerization of Grignard-type monomers. The drawback of this synthetic methodology is that it is not possible to initiate the polymerization from an external moiety. This is necessary for the synthesis of more complex polymer architectures such as brushes, star and block copolymers. Our work towards obtaining these complex architectures will be presented.

**9:00 AM**

**(ICACC-FS4-018-2012) Two photon polymerization of inorganic-organic hybrid materials (Invited)**

P. R. Miller, UNC/NCSU Joint Department of Biomedical Engineering, USA; A. Ovsianikov, A. Koroleva, Laser Zentrum Hannover e. V., Germany; S. D. Gittard, B. N. Chichkov, R. Narayan\*, UNC/NCSU Joint Department of Biomedical Engineering, USA

Due to their unusual properties, including chemical inertness, high hardness, and optical transparency, inorganic-organic hybrid materials have been utilized in a variety of technological applications, including medical device applications. We will describe the use of two photon polymerization for creating structures with microscale and/or nanoscale features out of inorganic-organic hybrid materials. In two photon polymerization, nearly simultaneous absorption of two photons from an ultrafast laser (e.g., titanium:sapphire femtosecond laser) is used for selective polymerization of a photosensitive resin. A variety of structures, including scaffolds for tissue engineering, have been created out of inorganic-organic hybrid materials using two photon polymerization. In addition, translation of this approach for large-scale processing will be considered.

**9:20 AM**

**(ICACC-FS4-019-2012) Plasma-Enhanced CVD of Hematite: Photoelectrochemical Water Splitting for Hydrogen Production**

A. P. Singh\*, A. Mettenboerger, P. Golus, N. Tosun, S. Mathur, University of Cologne, Germany

The use of metal oxide semiconductor as a solar energy harvesting element in photoelectrochemical cell for water splitting is a topic of growing interest for solar energy conversion to chemical fuel. Metal oxide thin films can be deposited by a variety of methods available. However, plasma-enhanced chemical vapor deposition (PE-CVD) technique offer a viable solution for the deposition of various type of metal oxide thin films with tunable structural, optical, electrical and morphological properties. This talk will present how properties of hematite thin film can be changed by PE-CVD technique by changing the process parameter. In this work, thin films of hematite were prepared at different RF-power using iron pentacarbonyl as a precursor with oxygen as reactive gas. The resulting thin films were used as a photoelectrode in photoelectrochemical cell to study the solar water oxidation under illumination in 1M NaOH electrolytes. The  $\alpha$ -Fe<sub>2</sub>O<sub>3</sub> photoanodes deposited at high RF-power, an enhancement in the photocurrent density was observed. These results demonstrate



that the controlled growth of hematite film with tunable morphology provides an efficient photoanode for photoelectrochemical water splitting application which is obtained by the proper choosen of process parameters. Results will be presented during the talk.

### Photovoltaics

Room: Oceanview

Session Chair: Andreas Ruediger, INRS-EMT

#### 10:00 AM

##### (ICACC-FS4-020-2012) Fabrication and Characterization of Sulfur-doped Titania Nanotube Arrays for Highly Efficient Dye-Sensitized Solar Cells (Invited)

E. W. Diau\*, L. Li, National Chiao Tung University, Taiwan

In this lecture, I will present our recent results for highly efficient DSSC based on a series of one-dimensional (1D) TiO<sub>2</sub> nanostructures through modifications of structural morphologies and compositions in order to improve the charge-collection efficiency of the device. One example is given below. The original TiO<sub>2</sub> nanotube (TNT) arrays of ~25 micrometers in length were produced by a typical anodization method, and a hydrothermal post-treatment was employed to effectively dope the sulfur element into the TNT substrate. The XRD results indicate that the anatase phase of TNT can be produced at a low-temperature condition after the hydrothermal process. The XPS results further confirm that the sulfur cations were firmly intercalated into the surface of TNT with the amounts of the S-dopants increasing as the concentrations of the precursor increase. The photovoltaic performances of the S-doped devices exhibit a systematic trend with the best performance occurring on the device with a middle doping amount. The IMPS/IMVS measurements were carried out to understand the electron-transport and charge-collection properties of the S-doped devices. A charge-unbalance model was proposed to reasonably explain the enhanced photocurrents and the trend of device performance for those S-doped TNT devices under investigation.

#### 10:30 AM

##### (ICACC-FS4-021-2012) Carbon-based transparent conductors for solar applications: from Carbon Nanotubes to Graphene (Invited)

G. Fanchini\*, University of Western Ontario, Canada

Large-area graphene thin films and low-density networks of carbon nanotubes are of interest for a number of applications, such as flexible field-effect transistors on plastics and transparent electrodes for solar cells. The interest in these novel transparent and conducting thin films stems from their ease of preparation at room temperature, for instance by vacuum filtration of suspensions of graphene oxide, graphene flakes and single-wall carbon nanotubes (SWNTs). Our results suggest that this method can be generalized to prepare thin films and devices on virtually any type of substrate. We will show how optical and in-situ Raman spectroscopy, along with electrical characterization, can be used to understand the optical and electronic properties of thin films from SWNTs and graphene. We will point out the necessity to consider intrinsic birefringence in modeling the optoelectronic properties of our films and optimising their use in optoelectronic devices. Finally, we will present our current work involving the application of graphene and SWNT thin films in next-generation organic solar cells from polyaromatic molecular crystals. Specifically, we will demonstrate how graphene thin films and carbon nanotubes networks can be used to prepare "smart" solar cells with tunable open circuit voltage.

#### 11:00 AM

##### (ICACC-FS4-022-2012) Optimizing Nanomorphology in Bulk Heterojunction Organic Photovoltaics (Invited)

Y. Lam\*, Nanyang Technological University, Singapore, Singapore; Y. Lam, RWTH Aachen University, Germany; T. Salim, Nanyang Technological University, Singapore, Singapore; B. Bräuer, Stanford University, USA; S. Sun, A. Grimsdale, Nanyang Technological University, Singapore, Singapore

Currently, the best conversion efficiencies OPV adopts the concept of bulk heterojunction (BHJ), in which p-type donor material is

blended with n-type fullerene acceptor to form the photoactive layer sandwiched between electrodes with different work functions. Power conversion efficiencies (PCE) of BHJ-based OPV devices in excess of 5% has been demonstrated for the binary blends of fullerene derivatives with thiophene based polymers. High PCEs can only be obtained when both donor and acceptor form optimal morphology with interpenetrating nanoscale network favorable for both exciton dissociation and charge transport. Thermal/solvent annealing, solvent additive and use of preformed polymer nanostructures have been applied to BHJ to induce a more thermodynamically stable and optimally phase-separated blend morphology. Some of these approaches to obtain optimal nanostructures will be discussed. To boost the performance of OPV BHJ devices, a simple yet effective method to improve device performance is to generate ternary blends through incorporation of dopant materials with superior optical and electrical properties into the original mixture. Here in the second part of the talk, I will also present some work relating of such systems. I will also talk about the criteria for such systems to work.

#### 11:30 AM

##### (ICACC-FS4-023-2012) Post Porosity Plasma Protection A new platform to integrate $k < 2.4$ porous ultra low-k materials (Invited)

G. Dubois\*, T. J. Frot, W. Volksen, T. Magbitang, D. Miller, IBM Almaden Research Center, USA; R. L. Bruce, M. Lofaro, S. Purushothaman, IBM T. J. Watson Research Center, USA

Integration of porous low dielectric constant materials constitutes a major roadblock in the reliable manufacturing of back end of the line (BEOL) wiring for the advanced technology nodes [1]. The two main issues for Ultra low-k (ULK) materials are their low mechanical properties and high sensitivity to plasma induced damage (PID). We have developed a new class of bridged oxycarbosilane (OCS) type materials with unique stiffness [2,3], and a novel process to enable their integration [4]. The Post Porosity Plasma Protection (P4) consists of refilling the pores of the fully cured porous ULK with an organic material prior to patterning, integrating the protected ULK and thermally removing the filler at the end of the process. We demonstrate the enormous potential of our integrated solution (materials at  $k < 2.4$  and P4 process) on blanket films and its compatibility with integration of single damascene structures at relaxed ground rules. [1] W. Volksen et al., Chem. Rev., 110, pp.56-110, 2010 [2] G. Dubois et al., Adv. Mater., 19, pp.3989-3994, 2007 [3] M.S. Oliver et al., Adv. Funct. Mater., 20, pp. 2884-2892, 2010 [4] T. Frot et al., Adv. Mater., 23, pp. 2828-2832, 2011

#### 12:00 PM

##### (ICACC-FS4-024-2012) Hydrothermal synthesis of epitaxial BiFeO<sub>3</sub> for bulk photovoltaics

I. Velasco Davalos\*, R. Nechache, A. Ruediger, INRS-EMT, Canada

Bismuth ferrite (BFO) has a remarkably large piezoelectric coefficient; it has a polar and a magnetic order parameter at the same time. The interesting photovoltaic properties have reiterated a strong interest in the bulk photovoltaic effect, also known as the photogalvanic effect in early literature. Epitaxial BFO films were successfully produced on STO (100) via hydrothermal synthesis which is an excellent alternative route due to its low cost mass production. Bi<sub>2</sub>O<sub>3</sub> and FeO(OH) were used as precursors with NH<sub>4</sub>OH as mineralizer. The crystallization and film growth were carried out in a batch reactor under autogeneous pressure that corresponds to vapor pressure of water at different conditions e.g. temperature and reaction times. The obtained films were characterized by X-ray diffraction (XRD), atomic force microscopy (AFM), scanning electron microscopy (SEM), X-ray photoelectron spectroscopy (XPS) and photovoltaic response (PV) with help of a solar simulator. We confirm the significant photovoltaic effect reported in literature and provide first data on the anisotropy of the bulk photovoltaic tensor.

### S1: Mechanical Behavior and Performance of Ceramics & Composites

#### Environmental Effects of Ceramics and Composites

Room: Coquina Salon D

Session Chair: Jacques Lamon, CNRS

##### 1:30 PM

#### (ICACC-S1-044-2012) Evaluation of impact damage resistance of SiC/SiC composites in tension and in static fatigue at high temperatures

J. L. Lamon\*, M. Picard, E. Maillet, P. Reynaud, N. Godin, M. R'Mili, G. Fantozzi, CNRS, France

Resistance to foreign object damage (FOD) is a key issue to ensure structural reliability in service for ceramic matrix composites. This paper investigates the resistance to foreign object damage of a 3D SiC/Si-B-C composite (Snecma Propulsion Solide -Bordeaux, France). Prior to mechanical loading or to static fatigue at high temperatures (450°C and 650°C) impact damage was generated by quasi-static indentation using a spherical steel punch of 9 mm diameter. Stress induced damage during the tensile and the fatigue tests was evaluated using unloading-loading cycles and acoustic emission monitoring. At room temperature, intense acoustic emission was detected at impact notch tips at the beginning of tensile loading, but the tensile behavior was unchanged when comparing to the reference one measured on the as-fabricated specimens. Impact damage insensitivity was assessed using plots of composite failure stress vs damage characteristics. Whatever the temperature, the impacted specimens survived as long as the as-fabricated specimens, more than 1000 hours under 80 MPa. Damage at 650°C seemed to be less significant, probably due to the matrix self-healing phenomenon. Comparison of residual strengths confirmed impact damage insensitivity of tensile and fatigue behavior at temperatures < 650°C.

##### 1:50 PM

#### (ICACC-S1-045-2012) Tension-compression fatigue of a Hi-NiCALON/SiC ceramic matrix composite at 1200°C in air and in steam

M. Ruggles-Wrenn\*, T. Jones, Air Force Institute of Technology, USA

Tension-compression fatigue behavior of a non-oxide ceramic composite with a multilayered matrix was investigated at 1200°C in laboratory air and in steam environment. The composite was produced via chemical vapor infiltration (CVI). The composite had an oxidation inhibited matrix, which consisted of alternating layers of silicon carbide and boron carbide and was reinforced with laminated Hi-Nicalon™ fibers woven in an eight-harness-satin weave (8HSW). Fiber preforms had pyrolytic carbon fiber coating with boron carbon overlay applied. Tension-compression fatigue behavior was studied for fatigue stresses ranging from 80 to 300 MPa at a frequency of 1.0 Hz. The R ratio (minimum stress to maximum stress) was -1.0. Fatigue run-out was defined as  $2 \times 10^5$  cycles. Fatigue limit was 80 MPa in air and in steam. The presence of steam decreased the fatigue life of specimens tested above the fatigue limit. Specimens that achieved fatigue run-out were subjected to tensile tests to failure to characterize the retained tensile properties. The material retained 100% of its tensile strength. Reduction in tensile modulus was limited to 68.4% while the change in compressive modulus was negligible. Composite microstructure, as well as damage and failure mechanisms were investigated.

##### 2:10 PM

#### (ICACC-S1-046-2012) Notch Sensitivity of Fatigue Behavior of a Hi-NiCALON/SiC Ceramic Composite at 1200°C in Air and in Steam

M. Ruggles-Wrenn\*, G. Kurtz, Air Force Institute of Technology, USA

Effects of holes on the fatigue behavior of a non-oxide ceramic composite with a multilayered matrix was investigated at 1200°C in laboratory air and in steam environment. The composite was produced via chemical vapor infiltration. The composite had an oxidation inhibited

matrix, which consisted of alternating layers of silicon carbide and boron carbide and was reinforced with laminated woven Hi-Nicalon fibers. Fiber preforms had pyrolytic carbon fiber coating with boron carbon overlay applied. The effect of holes on fatigue performance was studied in tension-tension fatigue tests performed at frequencies of 0.1, 1.0, and 10 Hz with fatigue stresses ranging from 80 to 140 MPa in air and from 100 to 140 MPa in steam. The R ratio (minimum stress to maximum stress) was 0.05. Fatigue run-out was defined as  $10^5$  cycles at 0.1 Hz and as  $2 \times 10^5$  cycles at 1.0 and 10 Hz. Presence of steam had little influence on fatigue performance at 1.0 Hz, but noticeably degraded the fatigue lifetimes at 0.1 Hz. The fatigue life was notch insensitive in air and in steam. Specimens that achieved run-out were tested in tension to failure to characterize the retained tensile properties. Prior fatigue in air and in steam caused significant reduction in tensile strength and modulus. Composite microstructure, as well as damage and failure mechanisms were investigated.

##### 2:30 PM

#### (ICACC-S1-047-2012) High Temperature Strength and Corrosion Resistance of Silicon Carbide to Silicon Carbide Joints Used in Heat Exchangers and Other Joining Arrays

H. Anderson\*, J. R. Fellows, C. A. Lewinsohn, M. A. Wilson, Ceramatec, Inc., USA

Ceramic heat exchange systems and other ceramic arrays depend on the ability to join various ceramic components into reliable high strength systems. Ceramic heat exchangers are increasingly important for use as high temperature recuperators or chemical synthesis modules where efficient heat transfer is required. Applications may include gas turbines, Solid Oxide Fuel Cells or synthesis gas generators. Other joined arrays may also include satellite dishes, armor systems, or microchip packaging. Each of these applications has thermal gradients that create differential stresses in joints where materials and thermal conditions can be discontinuous. In most cases, the joint material is characterized for strength at room temperature, yielding comparable data; however, as these joints are used at high temperatures, other factors influence the strength of the joint. Room temperature strength data may therefore be incomplete for use in ceramic heat exchanger design. This research discusses the room temperature and high temperature strength of various joining materials, including a newly developed joining material that meets the strength of monolithic silicon carbide, and also the effects upon the strength after joint exposure to various corrosive environments.

#### Reliability

Room: Coquina Salon D

Session Chair: Dietmar Koch, Institute of Structures and Design

##### 3:20 PM

#### (ICACC-S1-048-2012) Prediction of mechanical behavior of continuous fiber reinforced ceramics (Invited)

D. Koch\*, S. Hofmann, K. Tushkev, Institute of Structures and Design, German Aerospace Center, Germany

Today, broad application of CMC is limited due to the lack of accurate prediction methods of mechanical behavior. Main reason is that simple approaches like rule of mixture are not sufficient to describe precisely the properties which strongly depend on the manufacturing process, fiber lay-up and orientation. Finite element based (FE) analysis is a promising way to calculate and design structural components. With only few experimental tests under tensile, shear and interlaminar loading sufficient input data are generated for FE analysis. The properties are evaluated and recalculated using inverse laminate theory to describe the virtual transverse isotropic behavior of unidirectional reinforced plies. The resulting FE model homogenizes the properties of fiber, matrix, and interphase and allows the calculation of any reinforcement angles of CMC specimens if there are no voids. For design of components, however, additionally the effect of defects should be considered. With help of computer tomography (CT) a de-

tailed image of CMC components can be achieved and converted to FE mesh with the above mentioned properties. Then, crack propagation in the real CMC structure can be simulated and critical crack shapes and sizes can be identified. The proposed combination of inverse laminate theory and CT analysis represents an important step towards enhanced prediction of properties of CMC components.

**3:40 PM**

**(ICACC-S1-049-2012) Prediction of lifetime in fatigue using equivalent energy of acoustic emission sources in ceramic matrix composites**

E. Maillet\*, N. Godin, M. R'Mili, P. Reynaud, J. Lamon, G. Fantozzi, INSA-Lyon MATEIS, France

Ceramic Matrix Composites (CMCs) are anticipated for use in aeronautical engines. Expected lifetimes in service conditions that are of thousands of hours are unattainable during laboratory tests. The objective of this paper is to propose an Acoustic Emission (AE) based approach to lifetime prediction for CMCs. The energy of AE events is used as a measure of stress induced damage during static fatigue at high temperature on woven SiCf/[Si-B-C] composites. An equivalent energy of AE sources is calculated for each AE event from the signal energy received at two sensors in order to eliminate effects of attenuation due to propagation distance. The effects of attenuation due to damage are also corrected using calibration tests. Thus the equivalent energy is shown to provide a satisfactory estimate of damage. A method of real-time analysis of associated energy release has been developed. It allows the identification of a characteristic time that was found to represent 55% of the measured rupture time. This critical time reflects a critical local energy release assessed by the applicability of the Benioff law.

**4:00 PM**

**(ICACC-S1-050-2012) Lessons Learned from Failure Analyses of Electronic Components**

R. Tandon\*, Sandia National Lab, USA

For high-consequence applications of commercial passive electronic components, accelerated aging and over-tests are employed; when failures occur, analysis of their origins/modes provide insights into improving materials, processes or designs. We describe the methods employed, lessons learned and corrective actions from five such failures. Optical and SEM fractography, strength testing, and fracture mechanics principles were employed to understand the causes. The first two examples are fracture of a single crystal quartz-beam timing resonator in mechanical shock, and of polycrystalline alumina in a thick-film resistor during vibration loading. The third is a "glue-spalling" fracture of a thick film resistor during thermal cycling. The fourth study is that of a Kovar-glass seal interface delamination, due to mishandling, that compromised the hermeticity of a transistor. The final study describes the failure of a glass-body diode which is attributed partly to strain imposed during thermal cycling by the protective polymer coating. Sandia is a multi-program laboratory operated by Sandia Corporation, a Lockheed Martin Company, for the United States Department of Energy's National Nuclear Security Administration under Contract-DE-AC04-94AL85000.

**4:20 PM**

**(ICACC-S1-051-2012) Alumina-Silicon Carbide Laminated Composites with Tailored Strength**

F. De Genua\*, V. M. Sglavo, University of Trento - Italy, Italy

Three laminated structures made of stacking of alumina composite layers with up to 30 vol% of SiC particles were designed to induce tailored residual stress and fabricated by tape casting and lamination followed by Spark Plasma Sintering (SPS) at 1700°C under a pressure of 30 MPa. As-produced or pre-indented monoliths and multilayered materials were mechanically characterized by four point bending tests to evaluate the influence of residual stresses on the fracture

strength and reliability. The engineered laminates showed an average strength equal to 550 MPa, 559 MPa and 605 MPa, sensibly larger than the resistance of pure alumina (417 MPa). The strength variability is also sensibly suppressed being always lower than 10%. The multilayers strength values remained invariant also on samples damaged with Vickers indentation at loads as high as 100 N. Fractographic analysis allowed to associate such mechanical performances to a peculiar crack propagation, consisting of stable growth of surface defects up to the most compressed layer and crack arrest before the final catastrophic failure.

**4:40 PM**

**(ICACC-S1-052-2012) Experimental and numerical study on application of a CMC nozzle for high temperature gas turbine**

K. Nita\*, Y. Okita, C. Nakamata, IHI Corporation, Japan

Ceramic Matrix Composites (CMC) is promising material for advanced gas turbine engines because its allowable temperature is approximately by 200degC higher than those of conventional Ni-base super alloys. In this study, a thermal shock test using a nozzle cascade rig and numerical thermal stress analyses have been conducted in order to confirm healthiness of a CMC nozzle under an engine emergency shut down (thermal shock) condition, which is the most severe of any gas turbine engine operations. In the thermal shock test, gas temperature dropped immediately from 1100 to 150degC within a few second by fuel cut-off and the temperature fields of the CMC nozzle surface were measured by using infrared (IR) cameras. Important dimensionless numbers, such as Reynolds number[4x10<sup>5</sup>], are approximately equivalent to those of typical gas turbine engines. After the test, the CMC nozzle was examined by X-ray CT scanner and no crack was found. The numerical thermal stress analyses using the temperature field obtained in the thermal shock test were conducted to confirm the locations where high thermal stress was generated. In conclusion, by these studies it is confirmed that the CMC nozzle has sufficient durability from a practical viewpoint and the mechanism of the thermal stress generation in the CMC nozzle.

## **S2: Advanced Ceramic Coatings for Structural, Environmental, and Functional Applications**

### **Thermal Barrier Coatings II**

Room: Ponce de Leon

Session Chairs: Yutaka Kagawa, The University of Tokyo; Douglas Wolfe, Penn State University Applied Research Lab

**1:30 PM**

**(ICACC-S2-011-2012) Foreign Object Damage Behavior of Thermal Barrier Coatings in Airfoil Components (Invited)**

D. Faucett, M. Ayre, J. Wright, S. Choi\*, Naval Air Systems Command, USA

Thermal barrier coatings (TBCs), due to their brittle nature, are highly susceptible to damage by impacting particles when the impacting kinetic energy exceeds certain limits. The damage, termed foreign object damage (FOD), results in various issues/problems to coatings as well as to substrates from delamination to cracking to catastrophic failure depending on the severity of impact. Extensive FOD testing has been conducted using a ballistic impact gun for actual airfoil components coated with YSZ TBCs (APS or EB-PVD). A range of impact velocities from 50 to 340 m/s was applied in conjunction with three different projectile materials of hardened steel, silicon nitride, and borosilicate ball projectiles. The damage was characterized with respect to variables such as impact velocity, projectile material, and coating material. A resultant phenomenological model will be also presented to describe the impact and delamination behavior of the coatings.

2:00 PM

### (ICACC-S2-012-2012) Solid Particle erosion of thermal spray and physical vapour deposition thermal barrier coatings

F. Cernuschi\*, C. Guardamagna, L. Lorenzoni, Ricerca per il Sistema Energetico, Italy; R. Vassen, Forschung Zentrum Jülich, Germany; K. von Niessen, Sulzer Metco AG, Switzerland; C. Giolli, Turbocoating SpA, Italy; S. Capelli, Ricerca per il Sistema Energetico, Italy; F. Bossi, Politecnico di Milano, Italy

Thermal barrier coatings (TBC) are used to protect hot path components of gas turbines from hot combustion gases. Electron beam physical vapour deposition (EB-PVD) coatings have a columnar microstructure that guarantees high strain compliance and better solid particle erosion than PS TBCs. The main drawback of EB-PVD coating is the deposition cost that is higher than that of air plasma sprayed (APS) TBC. Nowadays segmented APS coatings and PS - PVD have been developed to improve solid particle erosion of plasma sprayed TBCs. In this perspective standard porous APS, segmented APS, EB-PVD and PS - PVD were tested at 700°C in a solid particle erosion jet tester, with EB-PVD and standard porous APS being the two reference systems. Tests were performed at impingement angles of 30° and 90°, representative for particle impingement on trailing and leading edges of gas turbine blades and vanes, respectively. Microquartz and alumina were chosen as the erodents. After the end of the tests, the TBC microstructure was investigated using electron microscopy to characterise the failure mechanisms taking place in the TBC.

2:20 PM

### (ICACC-S2-013-2012) Structure Evolutions and Thermal Conductivities of Yttria-Lanthanum Zirconate Solid Solutions

Y. Wang\*, F. Yang, P. Xiao, University of Manchester, United Kingdom

Structure evolutions and thermal conductivities of yttria-lanthanum zirconate (Y<sub>2</sub>O<sub>3</sub>-La<sub>2</sub>Zr<sub>2</sub>O<sub>7</sub>) solid solutions, covering the full composition range from La<sub>2</sub>Zr<sub>2</sub>O<sub>7</sub> to Y<sub>2</sub>Zr<sub>2</sub>O<sub>7</sub>, have been studied in this paper. It has been found that the crystal structure of the solid solutions changes gradually from pyrochlore to defect fluorite with an increase in the yttria content. Below a critical yttria content, Y<sub>3+</sub> mainly substitutes La<sub>3+</sub>, whereas above the critical value it substitutes both La<sub>3+</sub> and Zr<sub>4+</sub>. The Y<sub>2</sub>O<sub>3</sub>-La<sub>2</sub>Zr<sub>2</sub>O<sub>7</sub> solid solutions show lower thermal conductivities than their end members La<sub>2</sub>Zr<sub>2</sub>O<sub>7</sub> and Y<sub>2</sub>Zr<sub>2</sub>O<sub>7</sub>. Glasslike thermal conductivities which nearly approach the amorphous limit have been observed within a certain yttria content range. The results are discussed from both the classic phonon-defect scattering theory and the possible "rattling" effect. The low and temperature-independent thermal conductivities make the Y<sub>2</sub>O<sub>3</sub>-La<sub>2</sub>Zr<sub>2</sub>O<sub>7</sub> solid solutions promising candidates for high temperature thermal barrier coatings (TBCs) materials.

2:40 PM

### (ICACC-S2-014-2012) Gd<sub>2</sub>Zr<sub>2</sub>O<sub>7</sub>-YSZ composite for high temperature corrosion resistant thermal barrier coatings

M. Jarligo\*, D. E. Mack, R. Vaßen, IEK-1, Forschungszentrum Jülich GmbH, Germany

Integrated Gasification Combined Cycle (IGCC) is currently one of the most attractive technologies for the high-efficiency use of coal. However, the insulative thermal barrier coating (TBC) applied on turbine blades of an IGCC engine is greatly affected by the operating environments under high thermo-mechanical stresses and corrosion attack. Improved materials systems able to protect engine components against aggressive temperatures and compositions of exhaust gases are therefore in demand. Gadolinium zirconate from the pyrochlore system with high thermal stability has recently been found to resist high temperature corrosion attack in aero-engines. In addition, yttria stabilized zirconia (YSZ) ceramic TBC has outstanding mechanical properties. Since Gd<sub>2</sub>Zr<sub>2</sub>O<sub>7</sub> is very costly, a composite with YSZ can have additional benefits of durability and affordability. Various compositions of Gd<sub>2</sub>Zr<sub>2</sub>O<sub>7</sub>-YSZ feedstock were therefore pre-

pared and deposited into coatings by atmospheric plasma spraying. Spray parameters were optimized to achieve the desired microstructure. Corrosion resistance test was conducted isothermally in an oven at 1250°C using a corrosion agent with composition obtained from collected deposits on IGCC gas turbine blades. The reaction products and microstructure were evaluated using X-ray diffraction (XRD) and scanning electron microscope (SEM).

3:20 PM

### (ICACC-S2-015-2012) Challenges and Solutions to TGO Stress Measurement in Engine Run Gas Turbine Components (Invited)

E. Jordan\*, M. Majewski, C. Kelley, J. Lake, M. Renfro, University of Connecticut, USA; W. Hassan, W. Brindley, Rolls Royce, USA

Photoluminescent piezospectroscopy is capable of measuring the stress in thermally grown alpha alumina oxides (TGOs) that form on the bond coat (BC) below the thermal barrier coating (TBC). The stress values show a consistent trend with respect to remaining life fraction for some BC-TBC combinations and present an opportunity for retirement for cause for some types of TBCs. Unfortunately, real engine parts are exposed to environmental contamination, including for example calcium, aluminum, magnesium and silica (CMAS). We have begun to measure stresses on engine run turbine components and discovered that environmental contaminants containing alumina generate photoluminescent signals that obscure the TGO signal. In this presentation, we will describe a pulsed laser method of cleaning TBC surfaces where the laser ablation is controlled using laser induced breakdown spectroscopy, which allows the ablation to be stopped as soon as significant TBC materials begin to be removed. The cleaned surface allows measurements of TGO stress to be made but some false signals remain which must be censored from the collected data. A data censoring method will also be described.

4:00 PM

### (ICACC-S2-016-2012) Interfacial Delamination of Modeled APS-TBCs under Shear Loading: Effect of Difference in Chemical Composition of Bond Coat

M. Hasegawa\*, S. Yamaoka, Yokohama National University, Japan

Mechanical properties are examined on modeled APS-TBCs in order to understand the effect of the difference in chemical composition and microstructure of bond coat (BC) on interfacial mechanical property between thermally grown oxide (TGO) and BC. The chemical composition of NiAl alloys was Ni-26Al, Ni-40Al and Ni-40Al-10Pt (mol%), respectively. NiAl alloys selected as BC alloys were heat treated in a vacuum at 1413 K for 1 to 10 hours. After heat treatment, modeled TBCs were formed by air plasma spraying of YSZ to NiAl alloys. The formed modeled TBCs were heat exposed at 1323 K for 10 to 200 hours. Yield stress  $\sigma_y$  of the NiAl alloys decreases and decohesion strain energy release rate  $\Gamma$  increases with the increase in heat treatment time. The increase in  $\Gamma$  might be attributed to the increase of the process zone size ahead the decohesion front due to the decrease of  $\sigma_y$ . The TGO thickness increases with the increase in heat exposure time independently of the chemical composition of BC NiAl alloy.  $\Gamma$  decreases monotonically with the increase in heat exposure time.

4:20 PM

### (ICACC-S2-017-2012) Methods for Measurement and Analysis of Stress Components in Anisotropic TGO Growth Layer formed after Thermo-mechanical Fatigue Tests of EB-PVD Y<sub>2</sub>O<sub>3</sub>-ZrO<sub>2</sub> TBCs

R. Kitazawa\*, H. Kakisawa, Y. Kagawa, The University of Tokyo, Japan

A method for measurement of stress components in thermally grown oxide layer with anisotropic undulation behavior has been developed. EB-PVD Y<sub>2</sub>O<sub>3</sub>-ZrO<sub>2</sub> TBC system is subjected to in-phase (IP) and out-of-phase (OP) thermo-mechanical fatigue tests. Stress components in formed TGO layer have been measured using polarized piezo-spectroscopy. Experimental procedures for obtaining stress

components from the measured piezo-spectroscopy results are discussed. Origin of the measured stress components is discussed. The stress components depend on both anisotropic undulation morphology and growth conditions, respectively. That is, the average stress and stress components depend on history of the applied thermal and mechanical loadings.

**4:40 PM**

**(ICACC-S2-018-2012) Degradation of EB-PVD TBCs and (Ni,Pt)Al Coatings by Mixture of Sodium and Potassium Sulfate at 950°C**

L. Zhou\*, S. Mukherjee, Y. Sohn, University of Central Florida, USA

Environmental stability of thermal barrier and (Ni,Pt)Al coatings due to combustion by-product of fuel impurities has been examined owing to recent interests in bio-derived (e.g., algae-derived) fuels. Pure sodium sulfates (Na<sub>2</sub>SO<sub>4</sub>), potassium sulfates (K<sub>2</sub>SO<sub>4</sub>) and three of their mixtures with different weight ratio were prepared by mechanically grinding and their high temperature interactions were investigated in a laboratory furnace at 950°C with electron beam physical vapor deposited (EB-PVD) 8 wt.% Y<sub>2</sub>O<sub>3</sub> stabilized ZrO<sub>2</sub> (YSZ) thermal barrier and Pt-modified β-NiAl bond coatings. The corroded samples were characterized by X-ray diffraction and scanning electron microscopy equipped with energy dispersive spectroscopy. The results showed severe damages occurred in the bond coat while no chemical reactions or phase transformations occurred in the YSZ. For the (Ni,Pt)Al bond coat, mixed salts caused the most damage with sulfide formation dispersed throughout.

**5:00 PM**

**(ICACC-S2-019-2012) Monitoring TBC Delamination Propagation during Cyclic Tests for Building of Lifting Models**

G. Witz\*, M. Esquerre, H. Bossmann, Alstom (Switzerland) Ltd, Switzerland

Thermal barrier coatings lifetime prediction and understanding if their failure mechanism is a key requirement for enabling using the full potential benefit of the coating in terms of reduction of cooling requirements. Usually, lifetime prediction is based on furnace cyclic tests of coated samples together with visual inspection. This methodology does not allow monitoring accurately the coating delamination process and leads to highly scattered data. In this work, the use of pulse thermography for monitoring coating delamination is presented. This leads to the opportunity to better characterise the delamination kinetic and evaluate quantitatively some parameters describing this mechanism. Various parameters describing the delamination kinetic will be discussed and experimental data will be presented showing how they can be used for developing of lifting models.

### **S3: 9th International Symposium on Solid Oxide Fuel Cells (SOFC): Materials, Science and Technology**

#### **SOFC Applications and Technology Overview**

Room: Coquina Salon H

Session Chairs: Narottam Bansal, NASA Glenn Research; Prabhakar Singh, Connecticut Global Fuel Center

**1:30 PM**

**(ICACC-S3-001-2012) Recent Developments in the SECA Program (Invited)**

B. White\*, Dept. of Energy, USA

The development of an electric power generation technology that efficiently and economically utilizes coal while meeting current and projected environmental and water conservation requirements is of crucial importance to the United States. With that objective, the U.S. Department of Energy (DOE) Office of Fossil Energy (FE), through the National Energy Technology Laboratory (NETL), is leading the research and development of advanced solid oxide fuel cells (SOFC) as a key enabling technology. The FE Fuel Cell Program is embodied

in the Solid State Energy Conversion Alliance (SECA). Alliance participants include industrial teams, national labs, small businesses, and academia. Progress and recent developments in the SECA program will be presented.

**2:00 PM**

**(ICACC-S3-002-2012) Long-term evaluation of Ce-modified (Mn,Co) spinel coating for SOFC application in a 3-cell short stack geometry (Invited)**

Y. Chou\*, E. C. Thomsen, J. Choi, J. W. Stevenson, G. G. Xia, J. F. Bonnett, W. E. Voldrich, Pacific Northwest National Lab, USA

Ce-modified (Mn,Co) spinel coating is currently studied as a candidate coating for metallic interconnect for planar solid oxide fuel cells (SOFCs). The coating was applied via an ultrasonic sprayer onto ferritic stainless steel AISI441, followed by two steps heat treatment in different atmospheres. In order to mimic the actual SOFC conditions, the coated AISI441 interconnect plates were assembled in a 3-cell short stack using a commercial cell (Ni/YSZ supported YSZ electrolyte with LSM cathode) of 2"x2". The short stack was tested at 800°C for long-term (6000h) at a constant current mode with mixed fuel of H<sub>2</sub>:N<sub>2</sub>=1:1 versus air. Periodic impedance and I-V sweeps were conducted at every 500h. Over the long-term testing periods, two of the three cells showed poor stability while one was rather stable with minimum degradation. Upon completion the stack was disassembled for post mortem analysis. The coated interconnect plates were sectioned for detailed microstructure and interfacial characterization. The stability of Ce-modified (Mn,Co) spinel coating will be discussed.

**2:30 PM**

**(ICACC-S3-003-2012) Performance of electrolyte supported cells based on thin electrolyte (Invited)**

M. Kusnezoff\*, N. Trofimenko, Fraunhofer IKTS, Germany; J. Olenick, K. Olenick, ENRG, USA

3YSZ electrolytes with thickness of 90-150 μm are well known as robust and inexpensive substrates for ESC manufacturing. The main disadvantage of 3YSZ is a relatively low ionic conductivity compared to 8YSZ or scandia doped zirconia. If the thickness of electrolyte can be reduced down to 45-21 μm the electrolyte impact on the cell ASR decreases up to 0,15-0,07 Ωcm<sup>2</sup> respectively. It can be shown that for electrolytes with thickness of 45 μm the electrodes on basis of uLSM/10ScSZ and NiO/8YSZ or Ni/CGO could be optimized to provide low bending during manufacturing and good performance (ASR of 0,3 Ωcm<sup>2</sup>@850°C). The operation of manufactured cells in fuel cell and electrolysis mode has been tested and the degradation phenomena analysed.

#### **SOFC Applications and IC Development**

Room: Coquina Salon H

Session Chairs: Jeffry Stevenson, PNNL; Mihails Kusnezoff, Fraunhofer IKTS

**3:20 PM**

**(ICACC-S3-004-2012) Highlighting DOE EERE Efforts for the Development of SOFC Systems for APU and Stationary Applications (Invited)**

D. Peterson\*, D. Papageorgopoulos, Department of Energy, Office of Energy Efficiency and Renewable Energy, USA

The Fuel Cell Technologies (FCT) Program, within the US Department of Energy's (DOE) Office of Energy Efficiency and Renewable Energy (EERE), represents a comprehensive portfolio of activities that address the full range of technological and non-technological barriers facing the development and deployment of fuel cell and hydrogen technologies. The Program conducts focused efforts to enable widespread commercialization of fuel cell and hydrogen technologies in diverse sectors of the economy. In particular, the Program

pursues a technology neutral approach and maintains a diverse portfolio of activities aimed at reducing cost and improving both durability and performance of fuel cell systems for a range of applications. This presentation will emphasize the Program's efforts in developing fuel cell systems for truck auxiliary power units (APU), as well as for stationary applications, including combined heat and power, remote power, and energy storage (reversible fuel cells). While the Program supports a portfolio of fuel cell technologies for these applications, this presentation will focus on SOFC system development, highlighting challenges, strategy, and progress toward meeting DOE market-driven technical and cost targets. Recent research, development, and demonstration achievements for SOFC activities ranging from materials R&D to field demonstrations also will be provided.

### 3:50 PM

#### (ICACC-S3-005-2012) La(1-y)Ca<sub>y</sub>Ti(1-x)Mn<sub>x</sub>O<sub>3</sub> as an interconnect material for solid oxide fuel cells

N. Raeis Hosseini\*, H. Yoon, N. Sammes, J. Chung, Pohang University of Science and Technology (POSTECH), Republic of Korea

Despite the fact that LaCaCrO<sub>3</sub> perovskite oxide satisfies all the crucial requirements for use as an interconnect material in SOFCs, it still faces some sintering problems because of chromium vaporization at elevated temperature. To overcome this problem, alternative interconnect materials involving La doped SrTiO<sub>3</sub> have been recently suggested. In this work we investigate the influence of Mn doping on the sintering behavior, electrical conductivity, thermal expansion and microstructure of La<sub>1-y</sub>Ca<sub>y</sub>Ti(1-x)Mn<sub>x</sub>O<sub>3</sub> (LCTM) ( $y=0.5, 0 \leq x \leq 1$ ) as an interconnect material. Thus a series of ceramic compounds of LCTM were prepared via a modified Pechini method. XRD patterns of the calcined powders and sintered bars confirmed the single phase formation of the orthorhombic perovskite. Thermogravimetric analysis revealed weight loss for LCTM powder as a function of Mn doping. Microstructural characteristics of the fracture surface accompanied with a 99% theoretical density verified dense and compact grains. The electrical conductivity, in both oxygen and Ar/5% H<sub>2</sub> (as oxidizing and reducing environments respectively) was measured on sintered bars of LCTM and it was found that the electrical activation energy for conduction increased as a function of Mn content. In addition, manganese doping elevated the thermal expansion coefficient (TEC) of LCTM to be equal to that of 8 mol% YSZ electrolyte.

### 4:10 PM

#### (ICACC-S3-006-2012) Coating Optimization of Commercialized MnCoO-CeO spinel and the Effect of Thickness on Electrical Conductivity

J. Choi\*, J. W. Stevenson, S. Ryan, M. Chou, Pacific Northwest National Lab, USA

Ferritic stainless steel interconnects are generally used in planar type SOFC stacks, due to their low-cost, chromia scale-forming behavior, and good thermal expansion match to other stack components. However, volatile Cr-containing species, which originate from the oxide scale, can poison the cathode material in the cells and subsequently cause power deterioration in the device. A conductive MnCo spinel coating has been developed for preventing cathode poisoning and to provide low electrical resistance in SOFC stacks. It is essential that the spinel coating be sufficiently dense to block the Cr-containing species volatilization, this paper will summarize development of an ultrasonic spray coating method and optimization of the commercialized spinel material using design of experiment methodology with Taguchi and ANOVA analysis. Then, observed the thickness effect on electrical conductivity with long-term test. The results of this work demonstrate the possibility of automated mass production of dense conductive spinel-coated interconnect materials.

### 4:30 PM

#### (ICACC-S3-007-2012) A High H<sub>2</sub>S Tolerant Ni-GDC Anode with a GDC Barrier Layer

C. Xu\*, P. Gansor, J. W. Zondlo, K. Sabolsky, E. M. Sabolsky, West Virginia University, USA

The solid oxide fuel cell (SOFC) can use a variety of hydrocarbon fuels, such as coal-syngas or natural gas. The Ni-based cermet is a cost-effective SOFC anode material for these hydrocarbon fuels. However, trace impurities, such as H<sub>2</sub>S, in the fuel can cause degradation of cell performance by poisoning the Ni-based anode. In this research, Ni/gadolinium doped ceria (Ni-GDC) hybrid anodes with different architectures and Gd doping levels were exposed to synthesized syngas and H<sub>2</sub> with various concentrations of H<sub>2</sub>S at 800°C under constant current density. The tests showed that the cells with a GDC barrier layer were resistant to H<sub>2</sub>S up to 1000 ppm in wet H<sub>2</sub> and 100 ppm in syngas during long-term tests. On the other hand, cells without the barrier layer had a significantly lower tolerance for the H<sub>2</sub>S impurity. All tests were evaluated periodically using electrochemical methods. A reference electrode was placed on one cell to monitor changes in the anode and cathode polarization resistances. Post-mortem analysis of the SOFC anode was performed using SEM/EDS and XPS. The mechanisms of H<sub>2</sub>S poisoning and tolerance of the Ni-GDC anode with/without the GDC barrier layer are analyzed and discussed.

### 4:50 PM

#### (ICACC-S3-008-2012) Composite Interconnector for SOFC

S. Somov\*, Solid Cell Inc., USA; O. Graeve, Alfred University, USA; S. Ghosh, RocCera LLC, USA; H. Nabielek, Solid Cell Inc., USA

The interconnect is a key SOFC component. Metallic alloys and conductive ceramic oxides are traditional interconnect materials, but have shortcomings. Solid Cell has developed a composite SOFC interconnect that enables matching the CTE to specific SOFC designs. It is based on nickel and titanium oxides doped by niobium oxide, with copper oxide as a sintering agent. Its general equation is  $(1-z)[xNi+(1-x-y)TiO_2+yNb_2O_5]+zCuO$ ; x, y & z are corresponding parties of weight. Investigation included varying the composition, particle size, fabrication method and sintering procedure. Electrical conductivity, mechanical properties and chemical stability in oxidizing and reducing atmospheres at high temperature were evaluated. The CTE was matched to YSZ. Tests demonstrated good mechanical stability at high temperature, corrosion resistance and high electrical conductivity. The material was chemically stable in oxidizing and reducing atmospheres at high temperature. The material has several advantages compared to lanthanum chromates and Crofer 22APU. It does not contain chromium that is poisonous to cathodes. It has an adjustable CTE, dependent on the ratio of its metallic and oxide phases. It has high electrical conductivity ~103 Ohm-cm<sup>-1</sup> and it's made from inexpensive materials. Its mechanical properties are similar to metals, because nickel constitutes the largest part of the composite – mechanical stability > 900°C, yet flexible to resist cracking.

### 5:10 PM

#### (ICACC-S3-009-2012) Stability against chromium poisoning in ferritic cathodes

A. Arregui\*, L. Rodriguez, University of Trento, Italy; S. Modena, M. Bertoldi, Sofcpower S.p.A., Spain; V. Sglavo, University of Trento, Italy

The stability of a new promising barrier against chromium poisoning in SOFC cathodes was successfully studied in 500 h durability tests with two different cathode compositions. (La<sub>0.6</sub>Sr<sub>0.4</sub>)<sub>0.95</sub>FeO<sub>3-δ</sub>/Sm<sub>0.2</sub>Ce<sub>0.8</sub>O<sub>2</sub> (70:30 w/w) and (La<sub>0.6</sub>Sr<sub>0.4</sub>)<sub>0.995</sub>Co<sub>0.2</sub>Fe<sub>0.8</sub>O<sub>3-δ</sub>/Gd<sub>0.1</sub>Ce<sub>0.9</sub>O<sub>2</sub> (50:50 w/w) cathodes screen printed on commercially available anode-supported planar half-cells containing a La<sub>0.5</sub>Sr<sub>0.5</sub>CoO<sub>3</sub> layer to facilitate current collection were put in contact with a Crofer22 APU mesh current collector coated with the novel material. The cathode was 30 μm thick after sintering at

1050°C. The experiments were carried out at 700°C with 75 ml/cm<sup>2</sup> of dry air; such conditions have been previously shown to be the most stable processing/operation conditions of the ferritic cathodes. Moreover, since air humidification was found to be the second degradation source after chromium poisoning for cells of the actual characteristics, the influence of air humidification in the chromium evaporation and barrier effectiveness was also evaluated.

**5:30 PM**

**(ICACC-S3-010-2012) Component interactions after long-term operation of an SOFC stack with LSM cathode**

J. Malzbender\*, P. Batfalsky, R. Vassen, V. Shemet, F. Tietz, Forschungszentrum Jülich, Germany

The reliable long-term operation of stacks with low degradation rate is a prerequisite for the commercialization of solid oxide fuel cell (SOFC) technology. In order to understand degradation mechanisms a detailed post-test analysis of operated stacks is of main importance. This work reports the results of a post-test analysis of a SOFC stack with lanthanum strontium manganite (LSM) cathode operated under steady-state conditions for 19000 h. In particular the microstructural and chemical analysis of the relevant metallic and ceramic components are reported. The interconnects were coated with a (Mn,Co,Fe)<sub>3</sub>O<sub>4</sub> spinel by atmospheric plasma spraying which hindered the Cr evaporation into the cathode compartment. The diffusion of Mn from the (La,Sr)MnO<sub>3</sub> cathode into the 8YSZ electrolyte led to local enrichment at grain boundaries which might have been responsible for the degradation via electronic pathways leading to a partial short-circuiting across the electrolyte. However, the ultimate failure of the stack was a result of a weakening and fracture of the 8YSZ electrolyte grain boundaries by the local Mn enrichment.

## S4: Armor Ceramics

### Opaque Materials II

Room: Coquina Salon E

Session Chair: Matthew Bratcher, U.S. Army Research Laboratory

**1:20 PM**

**(ICACC-S4-043-2012) Submicron Theoretically Dense Boron Carbide via Pressureless Sintering**

C. S. Wiley, R. Speyer\*, Verco Materials, LLC, USA

Boron carbide powder compacts were pressureless sintered and post-HIPed to theoretical density with uniform and sub-micrometer grains, yielding a 7% increase in Vickers hardness than our previous best. The high-purity powders used were of substantially lower cost than in our previous developments. Ti- and C-bearing additives were used in a form which facilitated intimate mixing with the powder. The powder had a narrow particle size distribution, which inhibited the driving force for grain growth in the latter stages of sintering. Carbon was used in its traditional role of reacting away boron oxide coatings on B<sub>4</sub>C particles. This carbon; however, was largely extracted from the final sintered and HIPed microstructure through reactions which formed carbon monoxide gas and hard, finely dispersed TiB<sub>2</sub> phases isolated at triple points.

**1:40 PM**

**(ICACC-S4-044-2012) Submicron Boron Carbide Synthesis Through Rapid Carbothermal Reduction**

S. L. Miller\*, F. Toksoy, W. Rafaniello, R. Haber, Rutgers University, USA

Highly pure submicron boron carbide powder has been synthesized by rapid carbothermal reduction. A specially designed furnace maintains the temperature of a boron oxide containing precursor below its melting temperature until just prior to entering the furnace hot zone at 1600-2000°C. The rapid heating of the precursor results in increased nucleation and the subsequent formation of small crystallites. The resulting powder morphology consists of very fine, highly pure,

equiaxed crystallites with a narrow size distribution. The average size, distribution, and morphology is affected by the carbon source and reactor temperature. Further, these powders are shown to have a boron to carbon molar ratio of 4:1 for true stoichiometric B<sub>4</sub>C. As the mechanical properties of boron carbide have been shown to depend heavily on stoichiometry, the properties of dense bodies produced from these powders should compare favorably to other boron carbide ceramics. The use of spark plasma sintering (SPS) and relatively low sintering temperatures to densify these powders enabled fine grained microstructures to be produced.

**2:00 PM**

**(ICACC-S4-045-2012) Pressure Induced Amorphization as a Function of Comminution in Boron Carbide**

D. Maiorano\*, R. Haber, V. Domnich, Rutgers University, USA

Boron carbide has been of interest in high strength structural ceramic applications for many years, yet has been of limited usability because of anomalous fracture at very large stresses due to pressure induced amorphization. Recent studies have focused upon determining when this pressure induced amorphization occurs, and whether it may occur during typical powder processing. This work has shown clearly that pressure induced amorphization regularly occurs during jet milling, a common industrial comminution technique during the production of boron carbide. Spectra from Raman microspectroscopy and Fourier Transform InfraRed Spectroscopy have both displayed amorphization as a result of comminution.

**2:20 PM**

**(ICACC-S4-046-2012) Understanding the high-pressure phase transitions in Silicon-doped Boron Carbide**

V. Bhakhri\*, Imperial College London, United Kingdom; J. Proctor, T. Scheler, University of Edinburgh, United Kingdom; S. G. Macleod, Imperial College London, United Kingdom; E. Gregoryanz, University of Edinburgh, United Kingdom; F. Giuliani, Imperial College London, United Kingdom

Boron Carbide is an extremely hard ceramic material with potential as a light weight ceramic armor. However, under shock-loading conditions or non-hydrostatic unloading, amorphization occurs at pressures, as low as 25 GPa. Boron Carbide's strength against impact and therefore its applications as a superhard material are limited by this pressure-induced amorphization. It has recently been proposed theoretically that, of the various polytypes that make up Boron Carbide, it is the collapse of the B<sub>12</sub>(CCC) polytype that causes the experimentally observed pressure-induced amorphization. Furthermore, it has been proposed that if Boron Carbide is Silicon-doped, the B<sub>12</sub>(CCC) polytype leading to the premature failure in Boron Carbide can be practically completely eliminated leading to the development of a material with a Hugoniot Elastic Limit exceeding 40 GPa. In this work we have fabricated Silicon doped Boron Carbide nanowires and have then tested them in diamond anvil cells up to 60 GPa while monitoring their crystal structure by hard synchrotron X-ray diffraction (I15, Diamond light source, UK). These results are consistent with a suppression of the amorphization due to the incorporation of Silicon. Furthermore, high resolution transmission electron microscopy of the material before and after loading in the diamond anvil cells will also be presented.

**2:40 PM**

**(ICACC-S4-047-2012) Investigation of ISE in a Commercial SiAlON**

E. R. Shanholtz\*, J. C. LaSalvia, Army Research Lab, USA

Knoop indentation was conducted at various loads (1 – 200N) to examine the mechanical behavior of a commercially-available gas-pressure sintered Silicon Aluminum Oxynitride (SiAlON). The hardness was found to decrease with an increase in load; a phenomenon known as the Indentation Size Effect (ISE). The ISE was analyzed in accordance with Meyer's Law, Proportional Specimen Resistance (PSR) model, and a Multi-Fractal Scaling (MFS) model. The MFS model yielded three loading regimes in which the indentation behavior distinctly different. Scanning Electron Microscopy (SEM) was

used to examine the characterize features within the indents in each of these loading regimes in an effort to identify mechanistic differences. Crack lengths as a function of load were also measured. Experimental procedures and results are presented and discussed.

### 3:20 PM

#### (ICACC-S4-048-2012) Further Results on Nanocrystallization Features in Ballistically-Impacted Boron Carbide

J. C. LaSalvia\*, E. R. Shanholtz, U.S. Army Research Laboratory, USA

Observations of nanocrystallization features in a hot-pressed boron carbide impacted at high-velocities with cemented carbide spheres were previously reported. These features were observed immediately beneath the impact site (compression) and in association with cone cracks. The localized nature of these features reflects the importance of shear stress and resulting deformation on their formation. Nanocrystallization suggests solid-state amorphization and possibly melting. These features were subjected to scanning electron microscopy, energy-dispersive spectroscopy, micro-X-ray diffraction, micro-Raman spectroscopy, and nanoindentation in an effort to better understand them. Thermodynamic-based considerations and atomistic modeling findings are presented in an attempt to explain the origin of these features.

### 3:40 PM

#### (ICACC-S4-049-2012) Raman Spectroscopic Analysis of Nano Zirconia Toughened Alumina for Ceramic Armour Applications

S. Huang\*, J. Binner, B. Vaidhyanathan, Loughborough University, United Kingdom; P. Brown, Defence Science and Technology Laboratory (DSTL), United Kingdom; C. Hampson, Morgan Advanced Ceramics Limited, United Kingdom; C. Spacie, Morganite Electrical Carbon Ltd, United Kingdom

The brittleness of ceramic armour can limit their ability to resist multiple ballistic impacts. Toughened ceramics, such as zirconia toughened alumina (ZTA), have been considered as a potential armour material. In the present work, fully dense ZTA with varied zirconia content (10-20 wt%) and yttria additions (1.5 and 3 mol%) were prepared using single and two-stage sintering to achieve a range of alumina (0.5-1.5  $\mu\text{m}$ ) and zirconia (100-350 nm) grain sizes. Raman spectroscopy was used in particular to investigate the effect of the zirconia grain size on the zirconia transformability after Vickers indentation. The result indicated that, as expected, with a larger grain size, a higher transformability was observed. In addition, the dislocation density and residual stress in the alumina phase was studied using Cr<sup>3+</sup> fluorescence spectroscopy and it was found that, with the increasing transformability, the dislocation density was reduced and the residual stress transferred from compressive to tensile. After split Hopkinson pressure bar testing, the phase transformation and residual stress of the samples were also analysed using Raman spectroscopy. The toughening effect induced by zirconia phase transformation upon impact was confirmed. It is hoped that by January 2012 results will have been obtained for actual ballistic testing of the ZTA samples and, if so, they will also be presented.

### 4:00 PM

#### (ICACC-S4-050-2012) Metal-complexionized alumina ceramics

A. Lawrence\*, Lehigh University, USA

The purpose of this study is to explore the potential and conditions for forming atomic-scale thermodynamically stable interface-stabilized metallic phases (so-called complexions) at the grain boundaries in alumina. The material of choice is alumina doped with copper and/or titanium in the range of a few hundred ppm. In previous studies this system has shown indirect evidence of a nanoscale metallic copper phase. The material was sintered using spark plasma sintering, and then annealed for various times and temperatures under different partial pressures including those obtained by using an N<sub>2</sub>-5%H<sub>2</sub> and an O<sub>2</sub> atmosphere. Grain growth kinetics were studied using SEM and grain boundary structure and composition were investigated using high resolution transmission electron microscopy. The results are compared to those found in initial studies done at Lehigh.

### 4:20 PM

#### (ICACC-S4-051-2012) Processing, Sintering and Dynamic Mechanical Behavior of 8Y-TZP Doped Carbide Based Cermets

A. Ozer, Gebze Institute of Technology, Turkey; X. Nie, Purdue University, USA; Y. K. Tur, Gebze Institute of Technology, Turkey; W. M. Kriven\*, University of Illinois at Urbana-Champaign, USA; W. Chen, Purdue University, USA

Beyond the cutting tool applications, carbide cermets have gained interest for their outstanding fracture toughness among advanced ceramics. Their relatively high hardness, strength, toughness and even high temperature oxidation resistance made them a promising candidate for both high speed cutting tool and high temperature-impact resistant applications. In this study, Cr<sub>3</sub>C<sub>2</sub>-NiCr cermets were fabricated and were doped with 4wt% 8Y-TZP to investigate the sintering properties and mechanical properties as well as dynamic mechanical behavior with Split Hopkinson Pressure Bar Tests. All cermets were produced at 1350°C. Hardness was measured by Vickers(HV10), strength and fracture toughness (SENB) were evaluated by 3 point bending tests and dynamic mechanical behavior was characterized by SHPBs. While non-doped cermets having a hardness of 10GPa, a strength of 800MPa and a fracture toughness of 10 MPa $\sqrt{\text{m}}$ ; the doped cermets showed a hardness of 9GPa, a strength of 700MPa and a fracture toughness of 12 MPa $\sqrt{\text{m}}$ . Their fracture toughness values increase by 20%, by sacrificing some hardness.

### 4:40 PM

#### (ICACC-S4-052-2012) Surface preparation of alumina for improved adhesive bond strength in armour

A. Harris\*, University of Surrey, United Kingdom; S. Burnage, G. Miles, B. Vaughan, Lockheed Martin UK - Amptill, United Kingdom; J. Yeomans, P. Smith, University of Surrey, United Kingdom

Surface treatments of alumina have been investigated to determine if a range of preparations can increase the bond strength when using a toughened epoxy adhesive. Three surface conditions have been assessed: as-fired; grit blasted; and krypton fluoride excimer laser treated. A range of techniques have been used to characterise the surfaces: scanning electron microscopy, energy dispersive x-ray spectroscopy, x-ray photoelectron spectroscopy, profilometry and sessile drop. Compared with the as-fired surface, the grit blasted surface was rougher with poorer wettability, possibly due to surface contamination. It was found that the laser melted and vaporised the alumina, slightly increasing the surface roughness. The laser treatment led to an increased surface energy, which has been tentatively linked to observed chemical changes in the surface composition. The adhesive bond strength was assessed by testing joints in tension and shear. It was found that the laser treated surface demonstrated the greatest improvement in bond strength, with a cohesive failure of the adhesive in tension. A failure at the interface occurred in shear for all samples and in tension for the as-fired and grit blasted samples. Thus, it has been demonstrated that modifications to the surface of alumina can be used to alter the bond strength and the locus of failure.

## S5: Next Generation Bioceramics

### Advanced Processing of Bioceramics I

Room: Coquina Salon C

Session Chairs: Min Wang, The University of Hong Kong; Jerome Chevalier, INSA-LYON

### 1:30 PM

#### (ICACC-S5-007-2012) Interfaces in Biocomposites (Invited)

C. Bonhomme\*, UPMC, France

The role of interfaces in biosolids and biomaterials is of paramount importance. The physical and biochemical properties of such materials depend fundamentally on the hybrid connections between organic and inorganic components. The questions related to the detailed characterization and understanding of the interfaces remain fully



open. In this presentation, full combination of spectroscopy and ab initio calculations will be presented.

**1:50 PM**

**(ICACC-S5-008-2012) Electrospinning and Electrospun Fibrous Structures for Medical Applications (Invited)**

M. Wang\*, The University of Hong Kong, Hong Kong

Formhals' patent in 1934 gave birth to what is nowadays called "electrospinning". But the technique was little used until the 1990s when it was shown that electrospun micro- and nanofibers could have applications in diverse fields including filtration, sensors, cosmetics, etc. In the biomedical field, electrospun fibrous structures are studied as tissue engineering scaffolds and drug/biomolecule delivery vehicles. Ultrafine fibers can be electrospun from many biopolymers and their composites, offering distinctive advantages as nanofibrous tissue engineering scaffolds. For the potential use as delivery vehicles, the loading and release behaviour of incorporated drugs/biomolecules may be modulated for emulsion electrospun or co-axial electrospun fibers. In recent years, advances in electrospinning have overcome some technological problems, resulting in fibrous structures of distinctive features that are helpful for body tissue regeneration and for controlled drug/biomolecule delivery. This paper gives an overview of our research in using different electrospinning techniques to form various fibers and fibrous structures. Critical factors in conventional electrospinning, negative-voltage electrospinning, emulsion electrospinning, co-axial electrospinning and dual-source dual-power electrospinning are discussed. The biological performance of some fibrous scaffolds is also presented.

**2:10 PM**

**(ICACC-S5-009-2012) Organic-Inorganic Scaffolds for Bone Substitute Applications (Invited)**

J. Chevalier\*, P. Marianna, N. Ginsac, L. Gremillard, S. Meille, J. Chenal, L. Chazeau, C. Gauthier, INSA-LYON, France

Two alternative strategies are presented to develop organic inorganic composites for bone substitute applications and bone repair. On one side, we show the effect of polymer impregnation on mechanical properties of bioceramic scaffolds. Biphasic calcium phosphate (BCP: 70% hydroxyapatite, 30%  $\beta$ -tricalcium phosphate) scaffolds characterized by a bimodal pore size distribution (i.e. containing both micro- and macro- pores) and a global porosity of 70% are chosen as starting materials. Scaffolds are then impregnated by polycaprolactone. We show that during bending tests, polymer phase formed fibrils while the crack propagates, just as collagen fibrils bridge microcracks in real bone. This leads to a very important increase in energy to failure. On the other side, we present how polymer-Bioglass® composites can be simply processed to complex shapes like screws or fusion cages by injection molding. The content of Bioglass® in the composite and the parameters of injection play a critical role on bioactivity, mechanical properties and resorption rate in vitro. Composites with 30 wt.% of Bioglass® particles show a good balance between bioactivity and degradation rate. In vivo studies confirm the interest of such composites for clinical applications.

**2:30 PM**

**(ICACC-S5-010-2012) Direct foaming of a sponge-like bioactive glass/gelatin composite scaffold for bone tissue engineering**

D. Nadeem\*, University of Bristol, United Kingdom; X. Yang, University of Leeds, United Kingdom; B. Su, University of Bristol, United Kingdom

A composite of sol-gel derived bioactive glass powder (70S30C, Med-Cell) and porcine gelatin (Type-A, Sigma Aldrich) was used to fabricate, through direct foaming, a sponge-like bioresorbable scaffold for bone tissue engineering. The composite was developed to provide a viable alternative to synthetic-polymer based scaffolds, allowing directed regeneration of tissue through an openly porous architecture. The fabricated scaffold was characterised through x-ray microtomog-

raphy and light microscopy whilst its acellular and cellular bioactivity were assessed through apatite formation in simulated body fluid and through dental pulp stem cell cultures, respectively. Characterisation showed a 3-dimensionally porous and interconnected structure, with an average pore size suitable for cellular infiltration and tissue growth. Apatite deposition on the surface of the composite was found to be comparable to that of pure bioactive glass, a highly bioactive (Class A) material and successful cell cultures on samples of the composite scaffold establish its biocompatibility. With respect to degradation, modification of dehydrothermal treatment parameters was shown to induce varying degrees of crosslinking whilst the use of genipin, to supplement the dehydrothermal treatments, provides a means of further modifying the rate of degradation to suit longer term applications.

**Advanced Processing of Bioceramics II**

Room: Coquina Salon C

Session Chairs: Masahiro Yoshimura, National Cheng Kung University; Leif Hermansson, Doxa AB

**3:10 PM**

**(ICACC-S5-011-2012) Possible Degradation-Tolerable Zirconia Ceramics for Biomedical Applications (Invited)**

M. Yoshimura\*, C. Hwang, National Cheng Kung University, Taiwan

In the application of Zirconia, particularly Y-TZP, in biomedical areas, Low-Temperature Degradation (LTD) caused by the phase transformation from Tetragonal (T) to Monoclinic (M) is believed to be the most serious problem. From T to M transformation is accelerated in wet environments and high temperatures, thus autoclave treatments of Zirconia specimens for their sanitization might cause their fatal breakdowns. Recent our study, however, has suggested a strategy to avoid such failures. That is, in micro- and nano-structure controlled samples, the bending strength (4 point test) has not decreased or rather increased with the increase of M contents in the surface. That was 540 MPa for autoclaved at RT-60 C, changed to 580 MPa after 134 C, then reached to 650 MPa after 200 C treatments. The surface of the last sample has been transformed into 100% M, but it has not cracked at all. Those results could be explained by a simple Griffith criteria. This study is clearly suggesting that some Zirconia Ceramics may be useful in some Biomedical areas if we admit them having relatively low strength, say 650 MPa or so. They can be called as Degradation-Tolerable Zirconia Ceramics

**3:40 PM**

**(ICACC-S5-012-2012) ZBLAN glass ceramics for X-ray Imaging (Invited)**

J. Johnson\*, University of Tennessee Space Institute, USA; C. Passlick, Martin-Luther-University of Halle-Wittenberg, Germany; S. Schweizer, Fraunhofer Center for Silicon Photovoltaics, Germany

ZBLAN (Zirconium, Barium, Lanthanum, Aluminum, and Sodium Fluorides) glass-ceramic materials are being developed as scintillators and storage phosphors mainly for applications in medicine. Substitution of barium fluoride for barium chloride allows the precipitation of barium chloride nanoparticles with a fluoride glass matrix, which can either store electron-hole pairs or lead to scintillation upon x-ray excitation when doped with a suitable optical activator, such as europium. X-ray diffraction (XRD) has shown a particular phase of the barium chloride nanoparticles to be allied with either storage or scintillation. The hexagonal phase is synonymous with scintillation and the orthorhombic phase is synonymous with the storage mechanism. Extensive characterization of the materials for x-ray imaging applications has taken place to determine the exact composition and structure/property relationships. In situ transmission electron microscopy is ongoing to explore the interface kinetics between the nanoparticles and glass matrix. These results will be presented.

4:00 PM

**(ICACC-S5-013-2012) Laser deposition of bioactive glasses on titanium alloys (Invited)**

S. R. Paital, Y. Xiang, J. Du, N. Dahotre\*, University of North Texas, USA

Bioactive coatings on metal implants can help the integration of the implants to the host tissue thus extending the life time of load bearing prosthetics. Bioactive coatings such as hydroxyapatite have been applied to metal implants using conventional techniques such as but not limited to PECVD, thermal spray, PVD methods. These coatings however suffer stability issues due to weak bonding to the alloys substrates. In this paper, high energy laser based technique was employed to deposit bioactive glass coatings on the Ti-6Al-4V alloys. Bioactive glasses were synthesized using the melt and quench process. The water quenched glasses were ball milled to obtain fine glass powders which were used as coating precursor during laser deposition. The phase composition and surface morphology of the deposited coatings are systematically studied using XRD and SEM respectively. The surface elemental compositions of the coatings were studied using XPS and the coating/substrate interfacial structures were examined using high resolution TEM. It is found that Ca-P based bioactive phases in association with sound metallurgical bonding could be achieved with the laser deposition technique. In addition, molecular dynamics simulations were performed to study the atomic structure of bioactive glasses and their interfaces with metal substrates to understand the surface and interfacial features of these coatings.

4:20 PM

**(ICACC-S5-014-2012) Aspects of Antibacterial Nanostructurally Integrating Ca-aluminate Based Biomaterials (Invited)**

L. Hermansson\*, Doxa AB, Sweden

This presentation will give an overview of Ca-aluminate based materials and the use within the nanostructural biomaterials field. The presentation describes typical features of the Ca-aluminate material with regard to chemistry and microstructure developed as well as application possibilities within odontology, orthopedics and drug delivery. Special focus will be on the microstructure developed which is in the nanosize range. The nanostructure including pores size below 5nm in these structures opens up for some specific applications related to dental applications where antibacterial and bacteriostatic aspects are of importance, and as thin coating on implants within dental and orthopaedic applications. Another field where nanosize porosity is essential is within drug delivery systems for controlled release of medicaments.

4:40 PM

**(ICACC-S5-015-2012) Hydroxyapatite, TCP and Bioglass Coatings for Biomedical Applications made by High Velocity Suspension Flame Spraying (HVSFS)**

R. Gadow\*, A. Killinger, N. Stiegler, University of Stuttgart, Germany

Osteoconductive and bioresorbable ceramic coatings on prosthetic devices improve or enhance the in-growth behavior and/or long term mechanical stability of the implant under various load conditions. Cell growth and osteocyte proliferation are improved on plasma and HVSFS sprayed calcium phosphate and bioglass coatings. TCP as a bioresorbable coating can be used on bioresorbable substrates as PDLLA-implants. Thermal spraying of suspensions containing particles of submicron or nano size offers new possibilities in coating development and gives access to new application fields. Spraying suspensions by means of HVSFS, results in coatings with a refined microstructure and a layer thickness, ranging from 20 - 50  $\mu\text{m}$ . HVSFS is a novel thermal spray process developed at IFKB, for direct processing of submicron and nanosized particles. Thermally sprayed HAP coatings have been tested for various biomedical applications due to the fact that HAP is a material capable of forming a direct and firm biological fixation with surrounding bone. The deposited coatings were mechanically characterized and phase content of the coat-

ings was evaluated using XRD. The bond strength of the composites were analyzed by the pull-off method and compared for different spraying conditions. The applied coatings were further characterized by in-vitro tests with SBF and MG63 cell lines.

## S7: 6th International Symposium on Nanostructured Materials and Nano-Composites

### Bio-active Nanomaterials and Nanostructured Materials for Bio-medical Applications

Room: Coquina Salon B

Session Chairs: Sonia Estrade, Universitat de Barcelona; Cheng Sun, Nanyang Technological University ERI@N

1:30 PM

**(ICACC-S7-038-2012) Optimizing Iron Oxide Nanoparticles as Diagnostic Tracers for Magnetic Particle Imaging (Invited)**

D. Burdinski\*, Cologne University of Applied Sciences, Germany; C. Bohlander, N. Haex, H. Grull, Philips Research, Netherlands

Purpose: Magnetic particle imaging (MPI) is a novel diagnostic imaging modality that holds the promise for quantitative and particularly fast tomographic imaging. MPI signal generation relies on the use of magnetic nanoparticles (MNPs) as tracer material, because it directly probes their magnetic moment. The magnetic properties of MNPs used today in prototype MPI scanners have not been optimized for maximum signal intensity. The particle magnetic properties strongly depend on composition, shape, and size and can therefore be optimized by varying these parameters in a systematic synthetic approach. Methods: Monodisperse MNPs of varying size, shape, and composition were synthesized following various synthetic procedures. Suitable MNPs were encapsulated in liposomal carriers to generate supramolecular tracers. The MPI response of the nanoparticles was evaluated using magnetic particle spectroscopy. Results: The experimental results indicate a variation in the MPI signal intensity as a function of MNP size and shape, which greatly depended on the chosen synthetic procedure. The tracer-based signal intensity was improved by encapsulating suitable MNPs in liposomal carriers. Conclusions: MNPs with a greatly improved MPI-response were obtained in a synthetic approach yielding spherical magnetite particles with a diameter of about 15 nm.

2:00 PM

**(ICACC-S7-039-2012) Water-soluble and Biocompatible Superparamagnetic Magnetite Nanoparticles for Enhanced Magnetic Resonance Imaging (MRI)**

L. Xiao\*, University of Cologne, Germany; D. F. Brougham, E. K. Fox, Dublin City University, Ireland; F. Kiessling, University Hospital Aachen-RWTH, Germany; N. Feliu, B. Fadeel, Karolinska Institutet, Sweden; S. Mathur, University of Cologne, Germany

Ultrasmall superparamagnetic iron oxide nanoparticles (USPIONs) coated with oxidized vitamin C (OVC) were synthesized by a simple hydrothermal method. The as-prepared OVC-USPIONs have an average core size of 5.1 nm and exhibit good crystallinity and high magnetization saturation value (47 emu.g<sup>-1</sup>). The strong capping effects of the OVC on the surface of the particles impart to the USPIONs an excellent solubility and stability in water, PBS buffer and cell cultures. Detailed NMR analysis of the suspensions provides insight into the magnetic order within the colloid and demonstrates the suitability of this highly biocompatible material as negative contrast agents for MRI. Phantom experiments on the contrast agent (clinical 3 T MRI scanner) reveal an enhanced r2/r1 ratio of 36.4 (r1= 5 s-1mM<sup>-1</sup> and r2= 182 s-1mM<sup>-1</sup>) by comparing with the clinically approved SPIOs and USPIOs. The biocompatibility of the OVC-USPIONs was confirmed by the primary human monocyte-derived macrophages (HMDM) via LDH assay, as primary cell cultures are a better reflec-

tion of the in vivo situation than transformed cancer cell lines. To further assess the effects of OVC-USPIONS on HMDM, the secretion of tumor necrosis factor (TNF)- $\alpha$  (a pro-inflammatory cytokine) was determined, and no cytokine secretion was seen upon incubation with OVC-USPIONS.

**2:20 PM**

**(ICACC-S7-040-2012) Application of Nanomaterials in Drug Targeting (Invited)**

N. Nagib Afifi\*, German University in Cairo, Egypt

Drug targeting using nanomaterials as drug carriers is gaining advantage over other carriers such as liposomes and erythrocytes for being more stable, more reproducible and accordingly more practically applicable. In fact, drug targeting is transferred from a sophisticated research domain to important marketed or possibly marketed pharmaceutical formulations due to the application of nanomaterials. Nanomaterials used as drug carriers can be particles of different natural, semi-synthetic or synthetic substances or vesicles such as niosomes and related structures. The latter have the advantage of flexible application for targeting both lipophilic drugs carried in the lipophilic layer and hydrophilic drugs carried in the hydrophilic core. Such vesicles are also more suitable for the targeted transfer of biomaterials such as DNA for gene therapy as well as enzymes, hormones or metabolites for treating diseases due to deficiency of such biomaterials. Nanomaterials can be used for passive drug targeting depending on their physical properties e.g. size and surface charge as well as their chemical nature. Nanomaterials are also used for active targeting by attaching antigen-specific antibodies or receptor-specific ligands. Physical targeting of drugs is also applied using PH sensitive or thermosensitive nanomaterials as well as substances of magnetic activity such as magnetite.

**2:40 PM**

**(ICACC-S7-041-2012) Biological application of nanomaterials: Benefits versus risk**

O. Heikal\*, German University in Cairo, Egypt

Nanomaterial safety is becoming an increasingly debatable issue that has intensified over the past years. The small size and particular shape, large surface area and surface activity, which make nanomaterial attractive in many medical, environmental and energy applications, may contribute to their toxicological profile. Regarding their safety assessment, nanomaterial cannot be treated in the same manner as chemical compound. Therefore, the establishment of principles and test procedures to ensure safe use of nanomaterial in the marketplace is urgently required.

**Synthesis and Characterization Techniques for Nanostructures**

Room: Coquina Salon B

Session Chairs: Eun Dong Kim, Korea Electrotechnology Research Institute; Dirk Burdinski, Cologne University of Applied Sciences

**3:20 PM**

**(ICACC-S7-042-2012) Advanced Transmission Electron Microscopy Solutions for Nanoscience Problems**

S. Estrade\*, J. M. Rebled, L. Yedra, A. Eljarrat, L. López Conesa, F. Peiró, Universitat de Barcelona, Spain

In Nanoscience and Nanotechnology it is well known that the quality and nature of interfaces, the possible presence of crystalline defects, the shape and morphology of a nanoobject, as well its chemical composition and local electronic state determine the physical and chemical behavior of this nanoobject, and, thus, its suitability for an application in fields such as biomedicine, energy storage, electronics or spintronics. In the present work we will consider the advanced TEM characterization of several nanosystems: We will present a detailed characterization of CFO nanocolumns embedded in a highly distorted tetragonal BFO matrix grown on a LAO substrate, with special

focus on the interface formed by the two CFO and BFO film phases and between them and the substrate; we will also present the TEM-EELS characterization of core-shell  $\text{SnO}_2/\text{FeO}_x$  1D nanostructures, where EELS allowed to determine the nature of the iron oxide and to assess the wrapping of the  $\text{SnO}_2$  shell around the  $\text{FeO}_x$  core; we will give the quantitative EELS characterization and tomographic reconstruction of  $\text{MnOx}/\text{MnOy}$  bi-magnetic core-shell nanoparticles, where EELS allowed telling the core from the shell; and, finally, we will present the tomographic reconstruction of complex oxide mesoporous structures.

**3:50 PM**

**(ICACC-S7-043-2012) Electrical characterization of individual metal-oxide nanowires using AC impedance spectroscopy**

G. Karra Raveendran\*, J. Kochupurackal, H. Yizhong, S. G. Mhaisalkar, Nanyang Technological University, Singapore

Fundamental electrical characterization of individual nanowires is a critical step in understanding the nanowire based device behaviour. With growing applications of metal-oxide nanowires, newer techniques need to be explored to elucidate their device dependent properties. Impedance spectroscopy is performed on individual nanowire devices of  $\text{Fe}_2\text{O}_3$ ,  $\text{ZnFe}_2\text{O}_4$  fabricated using electron beam induced deposition (EBID) in a focused ion beam system (FIB). Due to high sensitivity of the measurement, EBID was chosen for fabrication and measurements were performed in a probe station under vacuum environment, minimizing every possibility of stray capacitance from contacts. The mobility of the majority charge carriers in the nanowire was extracted using modified space charge limited current (SCLC) analysis for the nanowire geometry. The trapping kinetics of the charge carriers were analyzed by measuring the impedance of the nanowires as a response to the perturbation of the applied AC modulation. The analysis of the capacitance and phase information obtained from presents us with the distribution of traps and other morphological imperfections like grain boundaries in the nanowire. The interpretation of the impedance and capacitance spectra provides us with key material parameters and serves as direct measurements for trap kinetics.

**4:10 PM**

**(ICACC-S7-044-2012) Mobility Edge in High-Performance Transistors Based on Aligned Tin Oxide Nanonets (Invited)**

C. Sun\*, Nanyang Technological University, Singapore; N. Mathews, Nanyang Technological University, Singapore; L. H. Wong, Nanyang Technological University, Singapore; S. G. Mhaisalkar, Nanyang Technological University, Singapore

There has been a growing interest in semiconducting nanostructures such as nanowire networks due to their potential applications on large-area, low-cost and flexible substrates. We have shown that highly oriented tin oxide ( $\text{SnO}_2$ ) nanowire network based devices could be fabricated through contact printing which showed excellent device characteristics. We have proposed that the degradation of the nanonet FET performance with the increasing channel length is due to the nanowire junctions which will form an energy barrier during the electron transfer. Recently, we characterized the  $\text{SnO}_2$  nanonet FET under controlled environment with the temperature firstly lower down to 77K. In order to eliminate the other factors rather than nanowire-nanowire junction effect, devices with three different channel lengths (45, 100 and 200 $\mu\text{m}$ ) were tested and compared. It has been revealed that for the device with smaller channel length, a clear mobility edge was observed in accordance with the predication of Mott's model. At low carrier concentrations, the mobility increases with the increasing temperature while beyond a threshold carrier density, the mobility decreases. Through calculations and predictions, it showed that this threshold carrier density tends to have a right shift with the increase of channel lengths which indicates the large energy barrier for electron carriers existing at the nanojunction sites.

4:30 PM

**(ICACC-S7-045-2012) Low temperature (< 150 deg C) synthesis of TiO<sub>2</sub> photoanodes for use in plastic substrate flexible dye-sensitized solar cells (Invited)**

J. Ting\*, C. Hsu, National Cheng Kung University, Taiwan

The electrodes in typical DSCs are supported on indium-tin-oxide (ITO) coated glass substrate, making the cells rigid. However, considering the weight reduction and flexibility, substrates such as ITO-coated poly (ethylene terephthalate) and ITO-coated poly (ethylene naphthalate) are receiving increasing interests. One of the challenges faced by FDSCs is to have well-connected TiO<sub>2</sub> nanoparticles in the photoanode after low-temperature synthesis. In the case of plastic flexible substrate FDSCs, the necking is impossible to occur and organic additive remains at the low synthesis temperatures, typically < 150 deg C. This paper reports our recent research results on plastic substrate flexible FDSCs. Several issues, including a new approach for the synthesis of the so-called TiO<sub>2</sub> beads, two modified techniques for the fabrication of TiO<sub>2</sub> photoanodes, the use of a novel gel-electrolyte, have been addressed. The resulting photoanodes and high efficiency cells were subjected to analyses using X-ray diffraction, Raman spectroscopy, high-resolution transmission electron microscopy, scanning electron microscope, the Brunauer-Emmett-Teller method, UV-visible spectroscopy, solar simulator, incident photon-to-electron conversion efficiency measurement, electrochemical impedance spectroscopy, and intensity-modulated photocurrent/photovoltage spectroscopy.

5:00 PM

**(ICACC-S7-046-2012) Electrospinning of Nanocomposite Scaffolds for Bone Tissue Engineering: Emitting Electrode Polarity and Charge Retention**

H. Tong, M. Wang\*, The University of Hong Kong, Hong Kong

It is well known that the polarity and density of electrical charges on a biomaterials surface affect the behaviour of cells seeded on the biomaterial. In conventional electrospinning to produce fibrous tissue engineering scaffolds, high positive voltages are normally used. In the current study, negative voltage electrospinning (NVES) of nanocomposite scaffolds and charge retention were investigated. For comparisons, positive voltage electrospinning (PVES) of scaffolds was also conducted. Carbonated hydroxyapatite (CHA) nanoparticles were firstly synthesized. Using NVES or PVES, CHA/PHBV nanocomposite scaffolds with CHA content up to 15wt% were made. Fibers and scaffolds were analyzed using various techniques (SEM, TEM, EDX, TGA, FTIR, etc.). The diameter of PHBV and CHA/PHBV fibers were 3 to 6 microns. The average diameter generally increased with increasing polymer solution concentration but decreased with increasing working distance. Increasing applied voltage rendered larger fiber diameters for PVES but smaller fiber diameters for NVES. PVES and NVES rendered fibrous scaffolds bearing positive and negative charges, respectively. The retained charge increased with increasing applied voltage, no matter whether PVES or NVES was employed. Both PHBV and CHA/PHBV fibrous scaffolds retained around 30% of the initial charge after 1 week of electrospinning.

5:20 PM

**(ICACC-S7-047-2012) Nanoparticle Toxicity for Mycobacteria in Biofilms and the Planktonic State**

I. Nettlehip\*, C. Larimer, M. Islam, A. Ojha, University of Pittsburgh, USA

It has been recently discovered that waterborne mycobacteria and other human pathogens are relatively concentrated in showerhead biofilms where they can become detached and inhaled as aerosols. While there is a growing literature on the effect of nanoparticles on bacteria such as E. Coli, little is known about their effect on mycobacteria. This study will compare the effect of silver nanoparticles on mycobacteria biofilms and mycobacteria in the planktonic state. The effect of nanoparticles on three different species of planktonic

mycobacteria and one silver resistant mutant were evaluated. The strikingly different toxicity for silver nanoparticles observed for the different species will be discussed in terms of the environment in which these bacteria are commonly found. Additionally, the effect of nanoparticles on the growth of mycobacteria biofilms on ceramic surfaces was studied. The differences in nanoparticle toxicity for planktonic bacteria and biofilms will be discussed in terms of the inherent differences between these two stages in the life cycle of bacteria.

5:40 PM

**(ICACC-S7-048-2012) Antimicrobial properties of copper and silver loaded silica nanomaterials**

S. Santra\*, P. ManiPrasad, R. Menezes, University of Central Florida, USA

Antimicrobial properties of copper (Cu) and silver (Ag) ions have been widely studied. Hundreds of nanotech based consumer products are now available in the market which uses antimicrobial Ag nanoparticles. Cu and Cu alloy based touch surfaces are shown to be effective in controlling bacterial infection. In this talk, I will present our research on synthesis and characterization of sol-gel silica nanoparticle/nanogel materials loaded with antimicrobial Cu and Ag. Structure/morphology and antimicrobial properties of the silica nanoparticle/nanogel delivery system with and without containing the active agent (Cu or Ag) will be discussed. We have tested antimicrobial properties of these materials against both gram-negative (E. Coli and Xanthomonas Alfalfae) and gram-positive (B. Subtilis) bacteria. Our results on Cu nanomaterials showed improved antibacterial efficacy of Cu loaded silica nanomaterial over its Cu source while the concentration of metallic Cu remained the same. Several materials characterization techniques (such as HRTEM, XRD and XPS) were used to understand structure-property (anti-bacterial) relationship using Cu loaded silica nanoparticle/nanogel nanomaterial.

## **S8: 6th International Symposium on Advanced Processing and Manufacturing Technologies for Structural and Multifunctional Materials and Systems (APMT) in honor of Professor R. Judd Diefendorf**

### **Novel Processing**

Room: Coquina Salon A

Session Chairs: Ian Nettlehip, University of Pittsburgh; Yi-Bing Cheng, Monash University

1:30 PM

**(ICACC-S8-040-2012) The Processing of Materials Systems for Perfusion Bioreactors used in Regenerative Medicine (Invited)**

I. Nettlehip\*, A. Finoli, E. Schmelzer, J. Gerlach, University of Pittsburgh, USA

Implementation of regenerative medicine therapies will require widespread availability of human stem cell and tissue products. In-vitro expansion and maintenance of stem cells from available stem cell sources will be a key requirement. In this presentation the appropriate bioreactor technologies will be briefly reviewed with emphasis on the more "physiologic" perfusion bioreactors. The basic design requirements for porous ceramics bioreactor core materials will be considered in terms of the necessary levels of structure previously identified for scaffold materials while referring to the characteristic features of the in-vivo stem cell "niche" or microenvironment for both hematopoietic stem cells and hepatic stem cells. The main example will be the processing of multiscale porous calcium phosphate ceramics scaffolds containing hydrogel and hollow fiber membranes. In particular, the ways in which the design is being altered to accommodate the processing of a vascular system in the ceramic core will be discussed. Additionally, a heat treatment process that can be used to produce multiphase calcium phosphate ceramics in highly porous hydroxyapatite will be presented.

2:00 PM

**(ICACC-S8-041-2012) Optimization of the sintering process for multi-layer CGO membranes by in situ techniques**

A. F. Kaiser\*, Risø DTU National Laboratory for Sustainable Energy, Denmark; A. S. Prasad, Banaras Hindu University, India; S. P. Foghmoes, Risø DTU National Laboratory for Sustainable Energy, Denmark, Risø DTU National Laboratory for Sustainable Energy, Denmark; Banaras Hindu University, India; V. Esposito, Risø DTU National Laboratory for Sustainable Energy, Denmark

Thin film gadolinium doped ceria (CGO) membranes on a Ni-YSZ support have shown high oxygen fluxes of  $16 \text{ Nml cm}^{-2} \text{ min}^{-1}$  at  $1173^\circ\text{C}$  for syngas reaction. For other membrane reactor applications, e.g. oxidative coupling of methane, different catalysts are required and the Ni-YSZ support was replaced by a porous CGO support. The preparation of the resulting CGO bi-layers, using 2 mol.-%  $\text{Co}_3\text{O}_4$  as sintering aid, was investigated by in-situ optical dilatometry and Van der Pauw conductivity measurements. Optical dilatometry confirmed that the addition of  $\text{Co}_3\text{O}_4$  allowed a significant reduction of the sintering temperature of the CGO membrane of around  $250^\circ\text{C}$ . The support porosity could be optimized and shape instabilities (warping, delamination) minimized. In-situ Van der Pauw conductivity measurements, used as a complementary tool, showed different phases of CGO layer densification in air. Particularly, the cobalt oxide assisted sintering process of CGO showed a wide range of conduction mechanism. In accordance with dilatometry results, different energies  $E_a$  for the conductivity were related to the densification during heating, isothermal sintering treatment and to cooling after densification. Changes in the electrical properties of the multi-layer system were attributed to the presence of the  $\text{Co}_3\text{O}_4$ , suggesting the arrangement of a percolating cobalt oxide network at the CGO grain boundaries.

2:20 PM

**(ICACC-S8-042-2012) Quantitative validation of a multi-scale model of pyrocarbon chemical vapor infiltration from propane**

G. L. Vignoles\*, W. Ros, University Bordeaux I, France; G. Chollon, F. Langlais, CNRS, France; C. Germain, University Bordeaux, France

The Chemical Vapor Deposition (CVD) or Infiltration (CVI) of pyrocarbons is a key step in the preparation of carbon-fiber reinforced carbon-matrix composites and reinforced carbon foams. Here, a simultaneous control of the deposit homogeneity in the porous medium (i.e. fibrous arrangement, or carbon foam) and of the pyrocarbon nanotexture is highly desirable, since it determines directly the material's thermal and mechanical properties. Pyrocarbon is usually prepared by the thermal cracking of hydrocarbons like propane or methane. The present contribution reports an integrated multi-scale model of pyrocarbon infiltration from pure propane, featuring: (i) a model for gas-phase reactions during the precursor pyrolysis, (ii) an identification of the deposition reactions leading to specific pyrocarbon microstructures, thanks to CFD computations, (iii) numerical tools for multi-scale simulations of CVI and (iv) a finite element solver for reactor scale simulation. The porous medium structures were acquired at various scales by X-ray CT; previous studies on pyrocarbon CVD have allowed the construction of a consistent chemical mechanism featuring gas-phase and deposition reactions. Numerical simulations based on this data were performed and compared favorably to actual CVI experiments. Guidelines for a correct control of deposit homogeneity and microstructure are given.

2:40 PM

**(ICACC-S8-043-2012) Fabrication of Dendritic Electrodes for Solid Oxide Fuel Cells by Using Micro Stereolithography**

N. Komori\*, K. Noritake, Osaka University, Japan; S. Tasaki, S. Kirihara, Osaka University Joining and Welding Research Institute, Japan

Dendritic electrodes composed of yttria stabilized zirconia (YSZ) and nickel oxide (NiO) were fabricated for solid oxide fuel cells. The dendritic structures constructed from micrometer order ceramic rods

with coordination numbers of 4, 6, 8, and 12 were designed in computer graphic application. Range of aspect ratios determined by the rod diameters and lengths were valued from 0.75 to 3.00. Gaseous fluid properties and stress distributions in the dendritic electrodes were simulated and visualized by using finite volume methods. The dendritic lattice with 12 coordination number was verified to exhibit the largest surface area and smooth fluid transparent characteristics. By using micro stereolithography, the optimized dendritic structure of 100-500  $\mu\text{m}$  in lattice constants was successfully fabricated. Slurry paste of photo sensitive acrylic resin with nanometer sized YSZ and Ni particles were applied on a substrate homogeneously at 5  $\mu\text{m}$  in layer thickness. Cross sectional images were exposed on the slurry surface at 2  $\mu\text{m}$  in part accuracy. Through these stacking processes, lattice structures were formed. These composite precursors were dewaxed at  $600^\circ\text{C}$  for 2 hs and sintered at  $1400\text{-}1500^\circ\text{C}$  for 2 hs. Microstructures and composite distributions were observed by using a scanning electron microscope and a energy dispersive X-ray spectroscopy.

3:20 PM

**(ICACC-S8-044-2012) Sol-gel processing of TiC Composites (Invited)**

Y. Cheng\*, J. Zhing, Monash University, Australia; S. Liang, Central South University, China; K. Wang, H. Wang, T. Williams, Monash University, Australia; H. Huang, The University of Queensland, Australia

A templated sol-gel process has been developed to produce nano structured titanium carbide materials, in which a titanium alkoxide was used as a source of the oxide, furfuryl alcohol as a carbon source and P123 (EO20PO70EO20) as a surfactant. The co-templated sol-gel process produced a homogeneous gel which became an amorphous mesoporous Ti-O-C composite after heating to  $550^\circ\text{C}$  under nitrogen, where the P123 phase was removed and polyfurfuryl alcohol decomposed into carbon. Mesoporous carbon-bonded titanium-carbide ceramics with a high specific surface area, ultra fine grains (10-50 nm) and high crystallinity were synthesized from direct carbothermal reduction ( $1100\text{-}1450^\circ\text{C}$ ) of the monolithic Ti-O-C precursor. The nano sized carbide grains are bonded into bulk materials by ploy(furfuryl alcohol) (PFA) derived nanocrystalline carbon framework because of its "bridge", "entanglement" and "adhesive" effects. The epitaxially grown graphenes are found to bond on the (111) plane of TiC grains. The bonding of graphitic carbon layers on carbide grains support the nanostructure and also result in the desired combination of functional and mechanical properties.

3:40 PM

**(ICACC-S8-045-2012) Preparation of highly crystalline nano zeolites by bead milling and post-milling recrystallization method**

T. Wakihara\*, J. Tatami, K. Komeya, T. Meguro, Yokohama National University, Japan

Organic template-free synthesis of nano zeolite has been an important subject of both scientific and industrial applications. Most research has focused on the fabrication of nano zeolite by a bottom up approach, that is, control of zeolite nucleation and crystal growth during the hydrothermal synthesis. Here we show a new method for the production of nano zeolite powder by a top-down approach. In this study the zeolite was first milled to produce a nano powder. This technique can cause destruction of the outer portion of the zeolite framework and hence cause pore blocking, which deactivates various properties of the zeolite. To remedy this, the damaged part was recrystallized using a dilute aluminosilicate solution after bead milling. As a result of the combination of bead milling and post-milling recrystallization, nano zeolite A (LTA type zeolite) about 50 nm in size with high crystallinity was successfully obtained.

4:00 PM

**(ICACC-S8-046-2012) Phase Pure SiAlON Ceramics from Pre-ceramic Polymers Filled with Nano-particles**

E. Bernardo\*, G. Parciannello, S. Pilati, P. Colombo, University of Padova, Italy

$\alpha$ -SiAlON and  $\beta$ '-SiAlON ceramics have been successfully prepared by the heat treatment in nitrogen, at relatively low temperatures (not

exceeding 1550°C), of commercial polysiloxanes and polysilazanes, respectively, filled with Al<sub>2</sub>O<sub>3</sub> and Si<sub>3</sub>N<sub>4</sub> nano-particles. O<sup>-</sup>-SiAlON ceramics exploit the phase separation of the SiOC ceramic residue, typically provided by polysiloxanes, into silica, SiC and free carbon. The free carbon is intended to promote reduction and nitridation reactions, whereas SiC is left as secondary phase, in the form of nanocrystals. Improvements in phase purity (i.e. development of only one SiAlON phase in addition to SiC), structural integrity and density are achievable by the modulation of the C content, e.g. by adding carbon black or phenolic resin, and by the insertion of SiC micro-particles as passive fillers, thus obtaining SiC-SiAlON composites. Pure low z-value β<sup>-</sup>-SiAlON (Si<sub>5.6</sub>Al<sub>10.4</sub>O<sub>0.4</sub>N<sub>7.6</sub>) exploit the high yield of Si and N of perhydropolysilazane, mixed with a conventional polysilazane, combined with a low Al<sub>2</sub>O<sub>3</sub> addition; the developed formulation is promising for the production of phosphor materials, due to the observed luminescence of samples doped with Eu<sub>2</sub>O<sub>3</sub> (1 wt%).

**4:20 PM**

### (ICACC-S8-047-2012) Novel Cladding Technologies of Thermal Nanoparticle Spraying and Patterning

S. Kirihara\*, Y. Itakura, Y. Uehara, S. Tasaki, Osaka University, Japan

Thermal nanoparticle spraying and patterning had newly developed as novel cladding technologies to create fine ceramic layers and geometrical intermetallic patterns. As raw materials of the coating process, nanometer sized alumina or zirconia particles of 100 - 200 nm in average diameter were dispersed into liquid resins at 50 - 70 % in volume fraction. The obtained thixotropic slurries were sputtered by using compressed air jet of 3 - 5 atm in gas pressure, and the slurries mist were blew into the arc plasma with an argon gas spray of 50 slpm in flow rate. On steels substrates, the ceramic layers of 10 - 50 μm in thickness were formed at 300 gpm in supply rate. Subsequently, thermal nanoparticles patterning for intermetallics drawing had been developed successfully. Pure copper or aluminium particles were dispersed into the photo solidified liquid resins at 50 - 60 % in volume fraction. The slurry were spread on the stainless steel substrates with 50 μm in layer thickness, and micro patterns were drawn and fixed by using an ultra violet laser scanning of 100 μm in spot size. The patterned pure metal particles were heated by the argon arc plasma spraying, and the intermetallic or alloy phases with high hardness were created through reaction diffusions. These geometric patterns can control the stress distributions on the material surfaces and improve the mechanical behaviors effectively.

**4:40 PM**

### (ICACC-S8-048-2012) Fabrication and Characterization of Zeolite-geopolymer Hybride Materials

S. Hashimoto\*, H. Takeda, T. Iwata, S. Honda, Y. Iwamoto, Nagoya Institute of Technology, Japan

Fly ash discharged from coal-fired power plant is mainly consisting of an amorphous aluminosilicate phase, quartz and mullite. So far, as an attractive reuse method of the fly ash, zeolite conversion technique has been developed. On the other hand, geopolymer bulk bodies have been also fabricated from fly ash using an alkali solution treatment. However, formation condition between zeolite and geopolymer was quite different in concentration of alkali solution. Nevertheless, the authors were able to develop the novel zeolite-geopolymer composite bulk materials from fly ash using a stepwise treatment of alkali solution. After packing the compact of coal fly ash mixed with 3.5 mol/L of sodium hydroxide solution inside a cylindrical plastic mold at 80 C and 50 % in relative humidity, the plastic mold was released and then the compact was immersed into 3.5 mol/L of sodium hydroxide solution at 80 C for 48 h. When the resultant compact was further cured at 80 C and 50 % in relative humidity for 7 days, zeolite-geopolymer composite bulk materials could be formed finally. The specific surface area and compressive strength of the bulk body sample was 21.4 m<sup>2</sup>/g and 29.0 MPa, respectively. According to quantitative analysis by means of XRD technique, the contents of the formed Na-P type zeo-

lite and geopolymer were estimated to be approximately 28.2 % and 20 % in mass ratio, respectively.

**5:00 PM**

### (ICACC-S8-049-2012) Influence of Nd<sub>2</sub>O<sub>3</sub> on Willemite Crystalline Glazes

N. Sharma\*, L. K. Sharma, H. Kaur, N.A.S. (P.G.) College, India

Crystalline glazes contain large numbers of macroscopic two-dimensional spherulites, each of 5 μm (micron) or less in width. The crystals start growing as microscopic spots in the glaze, called seeds. For the formation of these seeds, the glaze is first fired to peak temperature to thoroughly melt all of its ingredients and then cooled to the crystal-growing temperature, where the crystals start growing on the seeds and appear as the macroscopic structures. The longer the glaze is held at that temperature (soaking time), the larger the crystals grow. These wonderful shapes of distinctly different colour from their background are the result of manipulating the glaze formula and the cooling rate of the kiln. The whole of this shape is coloured by the penetration of a colouring oxide into the crystal and is clearly seen against the background. Here, in this paper we have added three different percentages (1.0, 3.0, and 5.0 wt%) of neodymium oxide (Nd<sub>2</sub>O<sub>3</sub>) as the colourant to see the effect on basic willemite crystals. The macroscopic and microscopic changes in the crystals were compared with the crystal sample containing willemite glaze without any colourant through XRD (X-Ray Diffraction) and SEM (Scanning Electron Microscopy). The effect of change in soaking time at peak temperature on Nd<sub>2</sub>O<sub>3</sub> added glaze was also examined.

## S12: Materials for Extreme Environments: Ultrahigh Temperature Ceramics (UHTCs) and Nanolaminated Ternary Carbides and Nitrides (MAX Phases)

### New Methods for Joining

Room: Coquina Salon F

Session Chairs: Erica Corral, University of Arizona; Guo-Jun Zhang, Shanghai Institute of Ceramics

**1:30 PM**

### (ICACC-S12-013-2012) Spark Plasma Joining of Ultra-High Temperature Ceramics with Zirconium-Boron Filler Materials

W. Pinc\*, L. S. Walker, University of Arizona, USA; Z. Wing, Advanced Ceramics Manufacturing, USA; E. L. Corral, University of Arizona, USA

Ultra-high temperature ceramics (UHTCs) such as ZrB<sub>2</sub>-SiC are ideal materials for thermal protection systems (TPS) in hypersonic vehicles due to their refractory properties. However, forming TPS relevant shapes from ceramics is difficult, costly, and time consuming. Therefore a novel joining method is required which will preserve both room and high temperature mechanical and oxidation properties of the bulk UHTCs. Our newly developed method of ceramic joining called spark plasma joining is used to rapidly join ZrB<sub>2</sub>-SiC to itself and form a seamless joint microstructure that exhibits identical high temperature mechanical and oxidation properties to the baseline ceramic composite. ZrB<sub>2</sub>-SiC substrates are joined by use of filler materials composed of zirconium and boron powder mixtures and a spark plasma sintering furnace is used to rapidly heat the substrates which allows for joining to be complete in under 30 minutes. This setup produces no joint region, instead the two substrate's microstructures are uninterrupted across the joint. As a result, the room and high temperature flexural strengths of the joined substrates and the oxidation resistance are equal to the baseline ZrB<sub>2</sub>-SiC material.

1:50 PM

**(ICACC-S12-014-2012) Effect of Current Density on the In Situ Temperature Measurement During Rapid Joining of ZrB<sub>2</sub>-SiC Using a Spark Plasma Sintering Furnace**

W. Pinc\*, L. Walker, University of Arizona, USA; Z. Wing, Advanced Ceramics Manufacturing, USA; E. L. Corral, University of Arizona, USA

A spark plasma sintering (SPS) furnace uses pulsed direct current to rapidly heat ceramic powders using high heating rates (600°C/min). We have developed a method of joining ultra-high temperature ceramics using an SPS furnace called, spark plasma joining (SPJ). During this process we believe that the current to play a significant role in SPJ and a we study the effect of current density through the parts in order to understand the role of current during joining. The samples are insulated to various components of the graphite die that holds the samples, forcing current through the samples or through the die. We measure the temperature gradient between the sample and die in each case using direct measurements taken at the specimen within the die. In this study we examine the effect of insulating the sample or die from current flow on the temperature differences between the die wall and ZrB<sub>2</sub>-SiC substrates during SPJ. It is found that altering the current path had significant effects on sample temperature, resulting in large temperature gradients between the die and samples which are characterized up to 1800 °C.

2:10 PM

**(ICACC-S12-015-2012) Effect of Carbon Additions on the Thermal and Electrical Properties of Hot Pressed ZrB<sub>2</sub>**

G. Harrington\*, G. E. Hilmas, W. G. Fahrenholtz, Missouri S&amp;T, USA

Due to its prevalence in the processing of commercial ZrB<sub>2</sub> powders, carbon is a major impurity that affects the densification behavior, and the resulting thermal and electrical properties, of ZrB<sub>2</sub>. As-received commercial ZrB<sub>2</sub> powder with up to 1 wt% carbon additions with an additional 1 wt% ZrH<sub>2</sub> to adjust for stoichiometry were studied. ZrB<sub>2</sub> and ZrH<sub>2</sub> powders, along with phenolic resin as a carbon source, were milled using ZrB<sub>2</sub> ball milling media in order to avoid contamination from typical milling media (i.e., WC or SiC). Pyrolysis of the phenolic resin was completed in the hot press die at 600°C to form amorphous carbon. Hot pressing was performed at 2100°C under a 32MPa pressure until ram travel stopped for 10 minutes to achieve the maximum density for each composition. The effects of carbon content on the density and microstructure were investigated. In addition, thermal diffusivity and heat capacity were measured using the laser flash method and used to calculate thermal conductivity. Electrical resistivity was also evaluated for each material to investigate the electrical and phonic contributions to thermal conductivity.

2:30 PM

**(ICACC-S12-016-2012) Thermal Properties of ZrB<sub>2</sub>-TiB<sub>2</sub> Solid Solutions**

M. Thompson\*, W. G. Fahrenholtz, G. Hilmas, Missouri University of Science and Technology, USA

The elevated temperature thermal diffusivity, heat capacity, and thermal conductivity were characterized for zirconium diboride (ZrB<sub>2</sub>) ceramics with TiB<sub>2</sub> additions. Microstructural information including grain size, the presence or absence of a grain boundary phase, and second phase distributions were characterized. Thermal conductivity was calculated as a function of temperature from measured thermal diffusivity and heat capacity values. Models that combine microstructural information like grain size, amount of an additive, and porosity were used to estimate the impact of solid solution on thermal conductivity. The electron contribution to thermal conductivity was calculated from measured electrical resistivity and used to estimate the phonon contribution to thermal conductivity. Separation of phonon and electron contributions enables the analysis of each component using the brick-layer or Bloch-Grüneisen models to further analyze the effects of grain boundaries or solid solutions on thermal

conductivity. The lack of property data above 1500°C and the need for robust thermal properties for input to thermomechanical simulations were the primary motivations for this study.

2:50 PM

**(ICACC-S12-017-2012) Lattice thermal conductivity of ultra high temperature ceramics (UHTC) ZrB<sub>2</sub> and HfB<sub>2</sub> from atomistic simulations**

J. W. Lawson\*, NASA Ames Research Center, USA; M. S. Daw, Clemson University, USA; C. W. Bauschlicher, NASA Ames Reseach Center, USA

Ultra high temperature ceramics (UHTC) including ZrB<sub>2</sub> and HfB<sub>2</sub> have a number of properties that make them attractive for applications in extreme environments. One such property is their high thermal conductivity. Computational modeling of these materials will facilitate understanding of fundamental mechanisms, elucidate structure-property relationships, and ultimately accelerate the materials design cycle. Progress in computational modeling of UHTCs however has been limited in part due to the absence of suitable interatomic potentials. Recently, we developed Tersoff style parameterizations of such potentials for both ZrB<sub>2</sub> and HfB<sub>2</sub> appropriate for atomistic simulations. As an application, Green-Kubo molecular dynamics simulations were performed to evaluate the lattice thermal conductivity for single crystals of ZrB<sub>2</sub> and HfB<sub>2</sub>. The atomic mass difference in these binary compounds leads to oscillations in the time correlation function of the heat current, in contrast to the more typical monotonic decay seen in monoatomic materials such as Silicon, for example. Results at room temperature and at elevated temperatures will be reported.

**Novel Processing Methods II**

Room: Coquina Salon F

Session Chairs: Marion Le Flem, CEA; Miladin Radovic, Texas A&amp;M University

3:30 PM

**(ICACC-S12-018-2012) Synthesis and crystal growth of MAX-phases from molten metals (Invited)**

H. Hillebrecht\*, D. Kotzot, H. Leuckeroth, M. Kleczek, University of Freiburg, Germany

Most of the investigations on bulk material of MAX-phases were done on sintered polycrystalline samples. This has consequences (Folgen) on the Especially the measurement of anisotropic properties like hardness or conductivity is restricted. Precise site parameters (interatomic distances), occupation factors, formation of solid solutions, superstructures, stacking faults. Disadvantage: information Using molten metals as a flux and/or solvent we were able to grow single crystals of MAX-phases.

3:50 PM

**(ICACC-S12-019-2012) Hysteresis in MAX phases (Invited)**

W. J. Clegg\*, C. Humphrey, University of Cambridge, United Kingdom; F. Giuliani, Imperial College, United Kingdom

MAX phases show very easy slip on the basal plane, and a very pronounced hysteresis on loading and unloading, which has been attributed to the growth and shrinkage of incipient kink bands. An alternative explanation for the hysteresis is that the anisotropy of plastic flow allows some grains to plastically deform, while others remain elastic. In this paper, we explore whether such a mechanism might occur using in-situ diffraction to characterise the evolution of elastic and plastic strains in the grains of a polycrystalline Ti<sub>3</sub>SiC<sub>2</sub> upon cyclic loading to 500 MPa. It is found that such effects are significant and might account for the hysteresis without the need to invoke incipient kink bands, consistent with observations in other systems, including single crystals.

### 4:10 PM

#### (ICACC-S12-020-2012) Processing and Mechanical Properties of Ti<sub>2</sub>AlC Reinforced with Alumina Fibers

K. Jeon, S. Basu, F. Schaff, Texas A&M University, USA; M. W. Barsoum, Drexel University, USA; M. Radovic\*, Texas A&M University, USA

Fully dense Ti<sub>2</sub>AlC composites, reinforced with 5 to 15 vol.% of uniformly dispersed alumina, Al<sub>2</sub>O<sub>3</sub>, fibers (Nextel 720, Nextel 610, and ALBF1), were processed. The Ti<sub>2</sub>AlC powders and Al<sub>2</sub>O<sub>3</sub> fibers were dispersed in water and slip cast to form green bodies. The latter were densified by pressureless sintering or hot isostatic pressing at different temperatures. The fabricated samples were characterized by X-ray diffraction, scanning electron microscopy with energy-dispersive spectroscopy, and porosimetry. Their elastic properties, fracture toughness and hardness values were determined using resonant ultrasound spectroscopy, double torsion and Vickers hardness, respectively. While the elastic moduli and hardness of the Ti<sub>2</sub>AlC composites increased moderately with the addition of 5-15 vol.%, fibers, the fracture toughness values showed significant increase due to crack bridging and fiber pull-outs at the crack tip. The role of the SiO<sub>2</sub> impurity in the different fibers on the fiber-matrix interface strength and toughening is discussed in some detail

### 4:30 PM

#### (ICACC-S12-021-2012) Crystallisation and annealing of Cr<sub>2</sub>AlC: a Raman investigation

V. Vishnyakov\*, P. Dobrosz, J. Colligon, Manchester Metropolitan University, United Kingdom

Cr<sub>2</sub>AlC films up to 2 μm thick have been deposited by ion sputtering from combined elemental targets onto Silicon and Stainless Steel at room and elevated substrate temperatures. Some depositions were conducted with simultaneous 300 eV Ar<sup>+</sup> ion bombardment of the growing film with atom to ion ratio at around 1. The material was annealed by laser or thermally in air and in vacuum at temperatures around 700 C. As-deposited and annealed films have hardness at around 17 GPa. Raman spectra of as-deposited films show characteristic but not well-structured 211 MAX-phase like bands in the region of 100-400 cm<sup>-1</sup>, CrC enhanced by Al bands in the region below 1000 cm<sup>-1</sup> and broad amorphous Carbon D-band. After annealing a Cr<sub>2</sub>AlC nano-phase is well-formed and the MAX-phase region in the Raman spectra becomes well structured. Surprisingly, Carbon also develops a G-band signature, the amplitude of which is proportional to annealing time, and this probably indicates the presence of some carbon nano-clustering in the system. This carbon can be partially responsible for the low initial friction coefficient. Ion assistance during film deposition or annealing in air or by laser significantly suppresses development of Carbon bands. Film crystallisation in air develops shallow surface oxides visible in Raman only as Chromium Oxide. The oxidation only proceeds to depth of approximately 120nm which is less than 7% of total film thickness.

### 4:50 PM

#### (ICACC-S12-022-2012) Effect of lattice anisotropy on plasticity mechanisms in Ti<sub>2</sub>AlN studied by in-situ compression of micro-pillars under synchrotron micro-beam

L. Thilly\*, J. Roa, A. Guittion, P. Villechaise, C. Tromas, A. Joulain, University of Poitiers, France; C. Marichal, S. Van Petegem, H. Van Swygenhoven, Paul Scherrer Institut, Switzerland

Ti<sub>2</sub>AlN is a MAX ternary nitride. Its deformation mode consists of kink and shear bands which are attributed to the very anisotropic nano-layered structure with very high c/a ratio (=4.5) where basal dislocation slip is mostly operative leading to kinking nonlinear elastic (KNE) properties. The micro-mechanism suggested to explain KNE properties is the incipient kink band (IKB). To date, direct evidence for the existence of IKBs, is lacking; the purpose of the present work is therefore to study the elementary deformation mechanisms of MAX phases and more generally the effect of lattice anisotropy:

polycrystalline Ti<sub>2</sub>AlN samples have been characterized by EBSD to obtain full knowledge of the crystalline orientation of the individual grains. Several single crystalline micro-pillars have been fabricated from selected grains by focused ion beam (FIB) milling and in-situ compressed under micro-focused x-ray beam at the MicroXAS beamline of the Swiss Light Source (PSI). The compression of the micro-pillars, associated with in-situ micro-diffraction, shed light on the intrinsic deformation mechanisms: the simultaneous recording of the applied compressive stress-strain curve and of the Laue patterns allows associating the onset of micro- and macro-plasticity and/or non-linear elasticity, with the local lattice characteristics.

### 5:10 PM

#### (ICACC-S12-023-2012) Effects of Porosity and Pore Size on Room Temperature Thermal Conductivity and Mechanical Properties of Porous Ti<sub>2</sub>AlC

L. Hu\*, S. Basu, R. Benitez, I. Karaman, M. Radovic, Texas A&M University, USA

The ternary compound Ti<sub>2</sub>AlC is one of the best studied of machinable ternary carbides from so-called MAX phases family. Although the properties of fully dense Ti<sub>2</sub>AlC have been well characterized, little is known about processing and properties of porous Ti<sub>2</sub>AlC. In this work, we demonstrate a simple and inexpensive way to process porous Ti<sub>2</sub>AlC with controlled porosity and pore-size distribution, using NaCl as the pore former. Porous Ti<sub>2</sub>AlC with porosity ranging from 5 to 75 vol.% and different pore size levels, i.e 45-90 μm, 180-250 μm and 355-500 μm, were successfully pressureless sintered at 1400 °C. The effects of porosity on the room temperature thermal conductivity, elastic moduli and compressive strength of Ti<sub>2</sub>AlC are determined. It follows that porosity becomes a useful microstructural parameter that can be used to tune thermal and mechanical properties of Ti<sub>2</sub>AlC.

### 5:30 PM

#### (ICACC-S12-024-2012) Properties of Hot-Pressed Ti<sub>2</sub>AlC Obtained by SHS Process

L. Chlubny\*, J. Lis, AGH-University of Science and Technology, Poland

Some of ternary materials in the Ti-Al-C system are called MAX-phases and are characterised by heterodesmic layer structure. Their specific structure consisting of covalent and metallic chemical bonds influence their semi-ductile features locating them on the boundary between metals and ceramics. These features may lead to many potential applications, for example as a part of a ceramic armour. Ti<sub>2</sub>AlC is one of this nanolaminate materials. Self-propagating High-temperature Synthesis (SHS) was applied to obtain sinterable powders of Ti<sub>2</sub>AlC. Intermetallic compounds were used as a precursors in the synthesis. For densification of obtained powders hot-pressing technique was used. Phase composition of dense samples was examined by XRD method. Properties such as hardness, bending strength, fracture toughness and elastic properties were determined.

### 5:50 PM

#### (ICACC-S12-025-2012) Deposition of MAX-phases coating by cold spray

S. Rech, A. Trentin, A. Patelli, A. Surpi, S. Vezzù\*, CIVEN, Italy; P. Eklund, J. Frodelius, L. Hultman, Linköping University, Sweden; J. Glor, Sandvik AB, Sweden

Currently, magnetron sputtering is the most used technique to deposit MAX-phase thin films. Yet, magnetron sputtering does have limitations: thickness of few micrometers, difficulty in covering large areas and cost. As an alternative, thermal spray techniques have been studied to deposit thin and thick coatings. However, the high temperatures there involved produce coatings with a significant fraction of oxides. In this context, cold-spray is an attractive technology because of low deposition temperature, high productivity and large-area coverage. Here Ti<sub>2</sub>AlC was deposited onto aluminium and steel by using



an industrial CGT-Kinetic®4000 deposition system. Sandvik's Maxthal®211 was used as feedstock material. Compact coatings with thickness of 60 micrometers were deposited onto steel substrates. XRD showed no difference with respect to original powders, the coating is mainly Ti<sub>2</sub>AlC with a fraction of Ti<sub>3</sub>AlC<sub>2</sub>. A few percent of intermetallics and TiC were also detected. The coating morphology has been also evaluated by LOM and SEM. Some critical aspects such as the need to improve the growth of the coating and the adhesion on hard materials will be discussed. Further investigations on cold spray deposition with blended and surface engineered powders have been carried out in order to obtain thicker coatings.

## Global Young Investigators Forum

### Frontiers in Ceramic Sensors I

Room: Coquina Salon G

Session Chairs: Thomas Fischer, University of Cologne; J. Daniel Prades, Universitat de Barcelona

1:30 PM

#### (ICACC-GYIF-001-2012) A hunt for scientific opportunities: the business of science

E. V. Timofeeva\*, Argonne National Laboratory, USA

Future and prospective scientists are driven by curiosity, a passion for learning, and the excitement of discovery. However, little consideration is usually paid to the reality that science is a business as well. A scientist should be able to identify those career paths which combine passion and research within avenues of societal impact and market realities. It takes a coherent vision, planning, resource management, social networking, and persuasion. In this presentation we will discuss what constitutes scientific opportunities, where to look for them, financing them, and how to address the critics. Some opportunities come around only once in a lifetime, it is better to be prepared for them.

1:50 PM

#### (ICACC-GYIF-002-2012) Influence of the electrodes on a SnO<sub>2</sub> thick film sensor: DRIFTS and sensors study

S. Rank\*, N. Barsan, U. Weimar, University of Tuebingen, Germany

A chemoresistive SnO<sub>2</sub> based gas sensor allows for measuring the resistance of the sensing layer between two electrodes in order to provide information about the chemical composition of the ambient atmosphere. It is well documented that besides making possible the resistance measurement, the noble metal electrodes have an impact on the sensing performance because of various reasons. Some of them are purely electric in nature – the electrode gap determines the number of grain-grain boundaries – but there is also an important chemical influence due to the catalytic processes taking place at the three phase boundary: electrode/metal oxide/ambient atmosphere. In this work we report on operando measurements performed on screen printed thick-film SnO<sub>2</sub> sensors on Al<sub>2</sub>O<sub>3</sub> substrates and on the corresponding model systems for the electrode-metal oxide interface: mixtures between SnO<sub>2</sub> powders and micrometric Au and Pt powders. The measurements were performed in dry and humid air backgrounds in the presence of various CO and H<sub>2</sub> concentrations. The experimental methods are DRIFT and DC electrical measurements. The findings, illustrating the impact of the different nature of the electrodes on the surface species nature and concentration as well as the differences in sensing performance, shed light of the underlying elementary processes.

2:10 PM

#### (ICACC-GYIF-003-2012) Field-effect gas sensor for high water vapor environments

O. Casals Guillen\*, University of Barcelona, Spain; T. Becker, EADS Deutschland GmbH, Germany; P. Godignon, IMB-CNM-CSIC, Spain; A. Romano-Rodriguez, University of Barcelona, Spain

Pt/TaOx/SiO<sub>2</sub>/SiC Metal-Insulator-Semiconductor capacitors are proposed to monitor the presence of fuel remains or byproducts of

the catalytic reaction in the exhaust gases of hydrogen or hydrocarbon-based fuel cells. The devices' response to hydrogen, hydrocarbons and CO has been studied in atmospheres with extremely high concentrations of water vapor (up to 40% by volume ratio of water vapor to nitrogen), in presence of CO<sub>2</sub> and temperatures above 200 C. In absence of other gases, the capacitors are almost insensitive to the presence of water vapor. When hydrogen is introduced in the gas chamber the response of the sensor towards this gas decreases with increasing amount of water vapor in the gas mixture. However, a saturation is seen above 30%, giving rise to a nearly water vapor independent hydrogen sensing behavior. Similar behavior has been observed for the device response to small hydrocarbons such as ethane or ethene. On the contrary, the device response to CO has been found to be independent of the water vapor concentration. Under the harshest measuring conditions, the devices are sensitive to all the gases under study down to 1ppm hydrogen, 2ppm CO, 100ppm of ethane and 25ppm of ethene. In order to propose suitable sensing mechanisms, the device's response to the different gases and mixtures of interest for full cell monitoring will be correlated with the most recent approaches to heterocatalysis on Pt surfaces.

2:30 PM

#### (ICACC-GYIF-004-2012) FSP synthesized In<sub>4</sub>Sn<sub>3</sub>O<sub>12</sub>, a novel gas sensing material

J. Kemmler\*, University of Tübingen, Germany; S. Pokhrel, L. Mädler, University of Bremen, Germany; N. Barsan, U. Weimar, University of Tübingen, Germany

Semiconducting Metal Oxide (SMOX) based gas sensors are widely used in practical applications due to their good sensitivity to various classes of gases, simplicity of use and low cost. There are two main issues that hinder SMOX based devices to even broader applicability, namely their limited sensitivity, when target gases are in the sub-ppm concentration range, and the selectivity. Therefore new materials are researched, to overcome this problem. In the course of our study, we used Flame Spray Pyrolysis (FSP) to directly deposit the sensing layer, in situ, on the sensor substrate. To prove the stability of the material, XRD studies on powders of the sensing material was performed, as well as the evaluation of the baseline resistance and the sensor signal over time. We have been able to demonstrate that a highly doped phase is responsible for selective sensing of formaldehyde. This phase which is In<sub>4</sub>Sn<sub>3</sub>O<sub>12</sub> is metastable and is proven to be stable for more than 3 Months at operation conditions. Accordingly, we think that this research opens a new field of investigation on this specific and on other ternary phases in terms of selectivity and sensing mechanisms. This is especially exciting because of the proven ability of FSP to rapidly fabricate sensors to which we demonstrated that it is possible to add the quenching of metastable phases with possible unknown properties.

### Frontiers in Ceramic Sensors II

Room: Coquina Salon G

Session Chairs: Sven Rank, University of Tuebingen; Elena Timofeeva, Argonne National Laboratory

3:10 PM

#### (ICACC-GYIF-005-2012) Synthesis and Application of Doped TiO<sub>2</sub> based nano structures

Y. Goenuellue\*, B. Saruhan Brings, German Aerospace Center, Germany

For decades, TiO<sub>2</sub> is one of the most important transition metal oxides with its excellent chemical stability, semi-conductive properties, non-toxicity and low cost. In recent years, TiO<sub>2</sub> nano tubes have received considerable attention because of their large surface area and strong adsorption capabilities. A great deal of research work has been done on various synthesis techniques and applications of TiO<sub>2</sub> nano tube arrays such as anodization of titanium and its alloy, hydro-thermal synthesis or anodic aluminium oxide template method. In this work, nano tubular TiO<sub>2</sub> structures were synthesized with several

methods such as template free method or direct anodization from titanium or its alloys. As prepared nano-tubular TiO<sub>2</sub> structures were modified with different kind of elements such as Cr, Ni, Ba, Al or etc. In conclusion, nano structured and modified TiO<sub>2</sub> layers showed better results than bulk TiO<sub>2</sub> layers in different application. The nano-structured TiO<sub>2</sub>-gas sensor has faster and more stable response toward CO and NO<sub>2</sub> than the reference TiO<sub>2</sub> sensor. In addition, Cr doping in to nano tubular TiO<sub>2</sub> layers response makes the sensor layer more sensitive and selective towards NO<sub>2</sub>. In summary, different kind of TiO<sub>2</sub> layers and M<sup>+</sup> doped TiO<sub>2</sub> were synthesized with different methods and characterized their properties in each application area.

**3:30 PM**

**(ICACC-GYIF-006-2012) Chemical sensors based on individual metal oxide nanowires: breakthroughs accomplished and pending challenges**

J. Prades\*, Universitat de Barcelona, Spain; F. Hernandez-Ramirez, Institut de Recerca en Energia de Catalunya (IREC), Spain; R. Jimenez-Diaz, A. Romano-Rodríguez, Universitat de Barcelona, Spain; J. Morante, Institut de Recerca en Energia de Catalunya (IREC), Spain

Single-crystalline semiconductor metal oxidenanowires exhibit novel structural and electrical properties attributed to their reduced dimensions, well-defined geometry and the negligible presence of grain boundaries and dislocations in their inside. This facilitates direct chemical sensing mechanisms at their surfaces upon exposure to gas molecules, making them promising active device elements for a new generation of chemical sensors. Furthermore, metal oxide nanowires can be heated up to the optimal operating temperature for gas sensing applications with extremely low power consumption due to their small mass, giving rise to devices more efficient than their nanoparticle-based counterparts. Here, the current status of development of sensors based on individual metal oxidenanowires is surveyed, and the main technological challenges which act as bottleneck to their potential use in real applications are presented.

**3:50 PM**

**(ICACC-GYIF-007-2012) Thermal and chemical stability of metal oxide nanowire based gas sensors**

A. Ponzoni\*, CNR-IDASC SENSOR Lab and University of Brescia, Italy; C. Baratto, CNR-IDASC SENSOR Lab and University of Brescia, Italy; E. Comini, CNR-IDASC SENSOR Lab and University of Brescia, Italy; G. Faglia, CNR-IDASC SENSOR Lab and University of Brescia, Italy; G. Sberveglieri, CNR-IDASC SENSOR Lab and University of Brescia, Italy

In this work we analyze the stability of gas sensors based on metal oxide nanostructures. We analyze both thermal and chemical (arising from exposure to aggressive gases) stability. The former arise from the high working temperature (usually 200 – 500 °C depending on the target gas) of metal oxide gas sensors, which induce the coarsening of crystallites within the sensitive layer. Thermal stability is checked over a period of six months, using carbon monoxide as probe molecule due to its non-poisoning interaction. Poisoning effects are studied with respect to DMMP, a simulant of Sarin nerve agent, which is well known to leave phosphorous compounds over the oxide surface, inhibiting with time the layer reactivity to gases. Two different nanostructures have been used in this work: metal oxide nanowire bundles (NW), prepared by evaporation-condensation method, and on nanoparticle layers (NP), prepared through thin film technology. Results indicate that both NWs and NPs exhibit an asymptotic drift in their conductance  $G$  during thermal-stability test. The same drift is observed with both  $G_{\text{air}}$  and  $G_{\text{gas}}$ , so that the response, calculated as  $G_{\text{gas}}/G_{\text{air}}$  results nearly stable within the six-month period. Differently, poisoning effects induced by DMMP exposure revealed quite critical already during the first exposures. For example, the response to ethanol decreased appreciably after each exposure to DMMP.

**4:10 PM**

**(ICACC-GYIF-009-2012) Click chemistry based magnetic nanoparticles for targeted drug delivery on breast carcinoma**

B. Kumar\*, N. Puvvada, S. Rajput, G. Dey, A. Pathak, M. Mandal, Indian Institute of Technology, India

Breast cancer is most prevailing cause of cancer deaths around world-wide. Despite of numerous efforts across globe for its treatment still it remains a great challenge by conventional chemotherapy. Nanoparticle mediated drug delivery were been implemented to solve several limitations of conventional chemotherapy as nonspecific biodistribution and targeting, lack of water solubility, cytotoxicity of drugs and low therapeutic indices at target tumor site. In current study, we employed tamoxifen drug (FDA approved in 1990) for targeted delivery against breast cancer to reduce its side effects. In present study we prepared MnFe<sub>2</sub>O<sub>4</sub> by chemical precipitation method and resultant samples were characterized using FTIR spectroscopy and X-ray diffraction. Further, tamoxifen loaded chitosan coated MnFe<sub>2</sub>O<sub>4</sub> was prepared. The drug entrapment efficiency was found around 57%. The morphology of prepared samples was analyzed by TEM and particle size distribution was determined. In addition, magnetic measurements of resultant samples were analyzed by SQUID.

## **FS4: Advanced (Ceramic) Materials and Processing for Photonics and Energy**

### **Multiferroics for Photovoltaics**

Room: Oceanview

Session Chair: Christine Luscombe, University of Washington

**1:30 PM**

**(ICACC-FS4-025-2012) Multiferroics for photovoltaics (Invited)**

R. Nechache\*, INRS & NAST, Canada

Driven by a rapid depletion of fossil fuel resources and a rise of environmental concerns, scientists have start to investigate candidate materials for thin films photovoltaic (PV) cells as a critical step for alternative and sustainable energy production. The availability of lower band gap magnetic-ferroelectric oxides (i.e. multiferroic) Bi<sub>2</sub>FeCrO<sub>6</sub> (BFCO) present an alternative pathway for highly efficient separation of photoexcited carriers. As ferroelectric, multiferroic (MFs) material, which exhibit strong bulk photovoltaic effect, have advantages compared with traditional semiconductor-based solar energy conversion materials: no need to any p/n junction and no limitation of the photo-voltage. Furthermore, the electron-electron interaction governing the magnetic ordering in MFs, leads to smaller gaps resulting in an improvement of the photocurrent generation process. MFs offer a fundamentally different route to enhance the solar energy conversion efficiency and show potential for visible-light photovoltaic devices. Here we review recent progress of our group in the exploration of novel oxide materials – both thin film and nanostructures – in pursuit of two major research thrusts: MF and solar energy conversion. We will present, the controlled growth and characterization of MF BFCO thin films and nanostructures via pulsed laser deposition. The investigation of the optical and PV properties of this material will be discussed in details.

**2:00 PM**

**(ICACC-FS4-026-2012) Ferroelectric thick and thin films with large piezoelectric and electrocaloric effect (Invited)**

M. Kosec\*, Jožef Stefan Institute, Slovenia, Jožef Stefan Institute, Slovenia, Jožef Stefan Institute, Slovenia, Jožef Stefan Institute, Slovenia, Jožef Stefan Institute, Slovenia, CO NAMASTE, Slovenia

Processing strategies for highly efficient ferroelectric thick and thin films are discussed. Examples include synthesis of PMN-PT relaxor-ferroelectric thick films, lead free KNN based ferroelectric thick films with high piezoelectric response and PLZT thin films with giant EC effect. Mechanochemical activation was intro-

duce in synthesis of ceramic powder followed by sintering in protective atmosphere. This enables to get dense thick films with homogeneous microstructure that reflect in high piezoelectric properties of PMN-PT and KNN thick films respectively. The piezoelectric properties of KNN are further increased by crystallographic texturing. PLZT thin films with giant EC effect are made by chemical solution deposition on platinised Silicon. Special attention was given to get chemically homogeneous films with columnar structure.

**2:30 PM**

**(ICACC-FS4-027-2012) On the relevance of interfaces in bulk photovoltaics (Invited)**

A. Ruediger\*, INRS-EMT, Canada

The bulk photovoltaic effect, formerly known as the photogalvanic effect, creates a substantial separation of photoexcited carriers in the volume of polar media i.e. pyro-, and ferroelectrics. Its technological relevance has so far been negligible due to the large band gap of ferroelectrics and the corresponding high internal resistance, incompatible with the requirements of a power source. Recent progress on those multiferroic materials with a ferroelectric and a magnetic order parameter have reiterated interest in this field as the magnetic ordering reduces the band gap into and below the visible range for some materials. Even though these devices would operate without need for a pn-junction, the charge transport to and from the electrodes will be as crucial as in conventional photovoltaics. But the most critical point is the high anisotropy of the third rank bulk photovoltaic tensor which requires a favourable orientation of the thin film structure with respect to the electrodes. It is this tensor that determines the direction of the photocurrent which immediately limits the use of unpoled, polycrystalline samples. The presentation will elaborate on criteria for appropriate materials, interfaces and discuss some recent results on the understanding of the microscopic origins of charge separation and conduction.

**Advanced Materials for Environmental Applications II**

Room: Oceanview

Session Chair: Mauro Epifani, CNR-IMM

**3:20 PM**

**(ICACC-FS4-028-2012) Organic electrochemical transistors in sensing and bioelectronics (Invited)**

F. Cicoira\*, Polytechnique Montréal, Canada

The vision of organic electronics, which uses as semiconductors carbon-based molecules, is to enable technologies that will revolutionize the way we generate, manipulate and display information. Organic electronics experienced tremendous development since the 1990s, when organic light emitting diodes OLEDs, organic thin-film transistors (OTFTs), and organic photovoltaics (OPVs) became the subjects of intense research and development. As a result of these efforts, organic electronic devices are becoming ubiquitous in our society. My research deals with the application of organic electronics to the interface with biology, termed organic bioelectronics. Organic electronic materials have emerged as ideal candidates for bioelectronics because of their ease of processing, softness and synthetic tunability of electronic properties. My research focused on organic electrochemical transistors (OECTs), a class of devices particularly attractive for applications in sensing and bioelectronics. OECTs can be operated in aqueous electrolytes as ion-to-electron converters, thus providing an interface between the worlds of biology and electronics. I will talk about the working mechanism of sensors based on OECTs and I will show how unconventional lithographic patterning can guide the design of novel device architectures.

**3:50 PM**

**(ICACC-FS4-029-2012) Hydrogen and CO<sub>2</sub> reduction as sun light fuel precursors using metal oxide nanostructures (Invited)**

T. Andreu, C. Fabrega, A. Parra, M. Manzanara, C. Reza, IREC, Catalonia Institute for Energy Research, Spain; J. Arbiol, ICREA Institució Catalana de Recerca i Estudis Avançats and Institut de Ciència de Materials de Barcelona, ICMAB-CSIC, Spain; J. R. Morante\*, IREC, Catalonia Institute for Energy Research, Spain

Metal oxide nanowires/nanotubes offer significant properties for high efficient sunlight absorption and large active areas for effective chemical surface reaction promoting hydrogen generation or CO<sub>2</sub> reduction. The surface of these nanostructured metal oxides can be decorated with high density of quantum dots or multi metallic clusters to enhance the absorption of the solar spectrum or to increase the catalytic reaction ratio. Interfaces between the decorated quantum dots and the supporting nanostructure was studied with detail to model the influence of these interface characteristics in the formed heterostructure and simulate the charge transfers mechanisms. Influence of the technology route will be checked. Likewise the quantum dot surface stabilities were also detailed. Charge generation and separation mechanisms will be discussed and correlated with efficiencies and estimated limits. Bimetallic nanoparticles were in parallel analyzed as promoters of the CO<sub>2</sub> chemical reduction. In both cases the capability for extending the photoelectrochemical activity towards the visible range will be discussed. The potential to built photoreactor and developing its engineering will also be explored and their associated efficiency estimated according to the paramount outstanding for the next future in achieving efficient methodologies to give directly sun fuels instead of photovoltaic electricity.

**4:20 PM**

**(ICACC-FS4-030-2012) Functionalized carbon nanotube and graphene devices for nanoscale chemical and biological sensing (Invited)**

K. Balasubramanian, T. Kurkina, R. Sundaram, M. Burghard, K. Kern\*, Max Planck Institute for Solid State Research, Germany

Carbon in both its one-dimensional (carbon nanotubes - CNTs) and two-dimensional (graphene) allotropic forms is emerging to be a major candidate for a number of on-chip device applications. Chemical functionalization routes designed to expand the spectrum of realizable applications bring in specialized properties that are unattainable in these systems in their pristine form. Our focus is on the use of electrochemistry both as a preparative and as an analytical tool for the design and operation of sensing devices based on single-wall CNTs (SWCNTs) and graphene. The use of nanostructures for analytical purposes brings in key advantages such as higher sensitivity and shorter response times. The first part will focus on the use of electrochemistry as a preparative tool, to functionalize the surface of contacted SWCNTs and graphene flakes. We have designed a generic route to attach a wide spectrum of receptors on to the surface of carbon nanostructures either in a covalent or non-covalent manner. The receptors range from simple organic moieties through nanoparticles to biomolecules. The second part will deal with the use of functionalized carbon nanostructure devices as highly sensitive analytical tools for the detection of gaseous, chemical and biological species.

**4:50 PM**

**(ICACC-FS4-031-2012) Advanced nanocomposite materials for functional magnetic refrigeration (Invited)**

H. Srikanth\*, M. Phan, University of South Florida, USA

Magnetic refrigeration, based on magnetocaloric effect (MCE) has several advantages over conventional gas compression techniques, such as higher energy efficiency, compactness and environmental safety. We discuss some of the key aspects of nanocomposites such as refrigerant capacity for energy-efficient magnetic refrigeration. Two case studies are presented -our recent discoveries of enhanced MCE

and RC in mixed phase manganites and clathrate based composites. In the first case, enhanced MCE is demonstrated in nanocrystalline  $\text{La}_{0.35}\text{Pr}_{0.275}\text{Ca}_{0.375}\text{MnO}_3$  is discussed. While the conventional trend is reduction of magnetization and MCE with nanostructuring, we show that the opposite is true in this class of manganites with competing magnetic phases. In the second case, we highlight our findings on clathrate composites. While  $\text{Eu}_8\text{Ga}_{16}\text{Ge}_{30}$  clathrates are widely known for their excellent thermoelectric properties, our recent discoveries of large MCE and RC in the clathrates and their composites make them unique for dual functional thermoelectric and thermomagnetic cooling applications. We have achieved a very large RC of 794 J/kg at 5T over a 70K in the  $\text{Eu}_8\text{Ga}_{16}\text{Ge}_{30}$  - EuO composites, which is the largest value ever achieved among the existing materials for magnetic refrigeration around 77K. Optimum cooling in this range is critical for enhancing the quantum efficiency in IR detectors.

## S2: Advanced Ceramic Coatings for Structural, Environmental, and Functional Applications

### Symposium 2: Poster Session

Room: Exhibit Hall

#### (ICACC-S2-P027-2012) Original in-situ method to quantify the SiC active oxidation rate in Ar/H<sub>2</sub>O gas mixtures at very high temperatures

M. Q. Brisebourg\*, F. Rebillat, F. Teyssandier, LCTS, France

Oxidation behavior of silicon carbide under Ar/H<sub>2</sub>O gas mixtures is investigated at very high temperatures (>1700°C) in order to further understand both the active and passive oxidation kinetics as well as transition between these two oxidation regimes. Experiments are conducted by Joule heating TEXTRON SCS-6 fiber samples inside an air-tight vessel under different Ar/H<sub>2</sub>O mixtures at atmospheric pressure. Temperature is regulated by means of a computer-assisted control loop consisting of a two-color pyrometer and a power supply delivering electrical current to the sample. The variation of the electrical current is used to monitor the oxidation rate. Active oxidation rate is found to increase linearly with PH<sub>2</sub>O, and to be almost independent of temperature up to 2100°C. Above 2100°C, a significant increase of the oxidation rate is observed. Thermal decomposition of SiC is found to be responsible for the increase of the oxidation rates above 2100°C. All experimental results are compared to simulation results obtained from a 3D finite volume approach of transport phenomena inside the vessel. For the active regime, they are in good agreement with simulation results. This feature suggests that oxidation kinetic is in our vessel mainly limited by species transport through a natural convection boundary layer.

#### (ICACC-S2-P028-2012) Silicon Carbide Nanotube Oxidation at High Temperatures

N. Ahlborg\*, The Ohio State University, USA; D. Zhu, NASA Glenn Research Center, USA

Silicon Carbide Nanotubes (SiCNTs) have high mechanical strength and also many potential functional applications. In this study, SiCNTs were investigated for use in strengthening high temperature silicate and oxide materials for high performance ceramic nanocomposites and environmental barrier coating bond coats. The high temperature oxidation behavior of the nanotubes was of particular interest. The SiCNTs were synthesized by a direct reactive conversion process of multiwall carbon nanotubes and silicon at high temperature. Thermogravimetric analysis (TGA) was used to study the oxidation kinetics of SiCNTs at temperatures ranging from 800°C to 1300°C. The oxidation mechanisms were also studied.

#### (ICACC-S2-P029-2012) Actual Toughness of Environmental Barrier Oxide Coatings on SiC/SiC Substrate

T. Matsumoto\*, H. Kakisawa, Y. Kagawa, The University of Tokyo, Japan

Fracture toughness of ceramic coating layer depends on laminate structure and substrate composites; usually largely different from that

without substrate composites. In the present study, the effects of thermal stress/strain and elastic constraint on fracture toughness of environmental coating layer are studied using well-identified model coating systems. Oxide multilayer coatings, which consist of alumina and mullite etc., are done on a surface of SiC/SiC or SiC and fracture toughness of the layer is measured by indentation method and bending test. The effect of residual stress is evaluated using different combination of multilayer and substrate thickness. Through the set of experimental results, discussions are focused on the change of toughness due to intrinsic factors of the entire coating system.

#### (ICACC-S2-P030-2012) Thermal Conductivity and Microstructure of Y<sub>2</sub>O<sub>3</sub>-ZrO<sub>2</sub> Coatings Fabricated by EB-PVD

B. Jang\*, H. Murakami, National Institute for Materials Science, Japan; J. Sun, Argonne National Laboratory, USA; S. Kim, Y. Oh, H. Kim, Korea Institute of Ceramic Engineering and Technology, Republic of Korea

Thermal barrier coatings (TBCs) manufactured by electron beam-physical vapor deposition (EB-PVD) have been favored because their unique microstructure offers the advantage of superior tolerance to mechanical strain and thermal shock at the high temperatures which gas turbines are operated. This work describes the properties of thermal conductivity and microstructure of EB-PVD coatings. 2~8mol%Y<sub>2</sub>O<sub>3</sub> doped ZrO<sub>2</sub> coatings were deposited by EB-PVD using a 45 kW electron gun. The coated samples were prepared with coating thicknesses in the range of 200~500µm. The laser flash method and thermal imaging measurement were used to measure the thermal conductivity of coated samples. The Y<sub>2</sub>O<sub>3</sub> doped ZrO<sub>2</sub> coatings consist of porous-columnar grains containing nano pores. Nano sized pores could be observed around feather-like grains as well as inside of columnar grains. The thermal conductivity of the coatings decreases with increasing porosity. This result was attributed to the decrease of mean free path due to the enhancement of phonon scattering at pores. The influence of Y<sub>2</sub>O<sub>3</sub> addition and microstructure on the thermal conductivity of Y<sub>2</sub>O<sub>3</sub> doped ZrO<sub>2</sub> coatings will also be discussed.

#### (ICACC-S2-P031-2012) Mesoporous Ti-Si-O-C composite thin film obtained by metalorganic chemical vapor deposition

S. M. El-sheikh\*, O. A. Fouad, Y. Y. Ahmed, Central Metallurgical Research and Development Institute, Egypt

New quaternary Ti-Si-O-C mesoporous thin film obtained by metalorganic chemical vapor deposition (MOCVD) with the using of titanium iso-propoxide (TIP) and Tetraethylorthosilicate (TEOS) as procurers have been investigated. The influences of several parameters such as substrate temperature, deposition time and carrier gas on deposition of mesoporous Ti-Si-O-C thin films were also studied. XRD data at low angle indicated that the produced film in a mesoporous structure. On the other hand, the results indicated that the deposition time and substrate temperatures play a very important role especially on the morphology and composition of the final deposited film. While, the carrier gas has limited effect not only on the composition of the final film produced but also on the morphology of the produced film. The composition of the film formed at 700°C in presence of hydrogen gas was mainly Ti, Si, O and C with a nano-spherical core shell shape as SEM and EDX were obtained. These nano-spherical particles core shell were growth to long nano-rods by increasing the substrate temperature and the deposition time as SEM and EDX were obtained. KeyWords: mesoporous Ti-Si-O-C, thin film, MOCVD

#### (ICACC-S2-P032-2012) Nanostructured Coating Process by Inductively Coupled Plasma Assisted Magnetron Sputtering

S. Chun\*, D. Seo, D. Yoon, Mokpo National University, Republic of Korea

The generation of high density plasma is important for plasma assisted deposition, because high density plasma can be used as an activation source for lowering the substrate temperature and enhancing the film quality. A higher plasma density will result in a higher degree of ionization of the metal atoms in the gaseous phase, which enables

maximum control over deposited films. Inductively coupled plasma (ICP) with an ion density of up to  $10^{12}/\text{cm}^3$  can be produced simply by attaching an RF coil to an existing facility. In this presentation some examples of applying ICP to the deposition of hard and wear resistant coatings will be shown. Acknowledgment Following are results of a study on the "Human Resource Development Center for Economic Region Leading Industry" Project, supported by the Ministry of Education, Science & Technology (MEST) and the National Research Foundation of Korea (NRF).

**(ICACC-S1-P033-2012) The Effect of Erbium and Ytterbium Oxide on the Creep Properties of 10 % SiC containing SiAlON Ceramics**

D. Turan\*, A. Uludag, Y. Deniz, S. Kayhan, Anadolu University, Turkey

SiAlON ceramics are important materials for high temperature applications and their use at high temperatures depends on their behavior under creep conditions. Creep properties of silicone nitride materials are largely controlled by the amount and type of sintering additives and the amount and type of crystallinity after sintering. In this work, we investigate the effect of Yb and Er doping on the crystallinity of SiAlON samples after sintering and heat treatment by using x-ray diffraction analysis and their effect on the creep behavior of these materials. The creep tests were carried out at  $1350^\circ\text{C}$  under 100 MPa load. It is found that after sintering and heat treatment different crystalline phases were formed for Yb and Er doping. The type of crystalline phase also found to affect the creep performance of SiC containing SiAlON materials. In this presentation, atomic scale observations and the relationship between the atomic scale microstructure and mechanical and luminescence properties will be demonstrated.

**(ICACC-S1-P034-2012) The Effect of Ytterbium and Cerium Oxide Double Doping on Atomic Scale Microstructure and Properties of SiAlON Ceramics**

S. Turan\*, H. Yurdakul, Anadolu University, Turkey; J. C. Idrobo, Oak Ridge National Laboratory, USA; S. J. Pennycook, Vanderbilt University, USA; E. Okunishi, JEOL Ltd., Japan

SiAlON ceramics are used in different applications such as cutting tools and luminescent materials due to their better mechanical and optical properties. These properties are largely controlled and can be tailored with the amount and type of sintering additives. In this work, we investigate the effect of Yb and Ce double doping on the atomic level microstructure of SiAlON samples by using high resolution Z-contrast scanning transmission electron microscopy as well as conventional scanning and transmission electron microscopes. The mechanical properties of fully densified samples were characterized by hardness and toughness measurements. In addition, the performance of the samples under real cutting conditions were determined and compared with commercial products. Luminescence properties were also measured. In this presentation, atomic scale observations and the relationship between the atomic scale microstructure and mechanical and luminescence properties will be demonstrated.

### S3: 9th International Symposium on Solid Oxide Fuel Cells (SOFC): Materials, Science and Technology

**Symposium 3: Poster Session**

Room: Exhibit Hall

**(ICACC-S3-P035-2012) CdMnS Thin Film Synthesis using CBD: Application in Photoelectrochemical Cell**

J. S. Dargad\*, N. S. Korde, Dayanand Science College, Latur, MS, India, India

A dilute magnetic semiconductor (DMS, CdMnS) thin film based photoelectrochemical cell is fabricated and studied. CDMnS DMS thin films are synthesized on both glass and stainless steel substrates using a chemical bath deposition process. The preparative parameters (such as growth temperature, time, reaction pH, pre-

cursor concentrations, etc) were optimized to yield characteristically oriented films. The layer thickness was found to be decreased with an increase in Mn concentration. The composition of the as-grown samples was determined by an EDS technique. The electrochemical cells were then formed out of these series of films as the active photoelectrodes, an electrolyte and a counter electrode. The cells were then characterized through their dark and photosensing properties. The other cell parameters were determined from these studies and the cell performance has been evaluated with a special reference to Mn concentration in CdS. A significant enhancement in performance has been observed for a cell with electrode composition of  $x = 0.01$ .

**(ICACC-S3-P036-2012) Investigation of novel solid oxide fuel cell cathodes based on impregnation of  $\text{SrTi}_x\text{Fe}_{1-x}\text{O}_{3-\delta}$  into ceria-based backbones**

M. Brinch-Larsen\*, M. Sogaard, J. Hjelm, H. L. Frandsen, Risø DTU, Denmark

SOFC cathodes were prepared by impregnation of  $\text{SrTi}_x\text{Fe}_{1-x}\text{O}_{3-\delta}$  (STFx) into a porous backbone of  $\text{Ce}_{0.9}\text{Gd}_{0.1}\text{O}_{1.95}$  (CGO). STFx was chosen as literature indicates very high oxygen surface exchange rate, high ionic conductivity and electrochemical stability as a thin film electrode. Symmetric cells were prepared by screen printing and sintering porous CGO backbones onto both sides of a CGO electrolyte tape. The porous backbones were subsequently infiltrated with STFx,  $x = 0; 0.1; 0.2; 0.3; 0.4$  and  $0.5$ . The electrochemical performance was measured using impedance spectroscopy, where the performance has been monitored as a function of the maximum temperature ( $T_{max}$ ) the electrodes have been subjected to. The results were tried correlated with scanning electron microscopy and high-temperature x-ray diffraction. The catalysts with  $x = 0$  and  $x = 0.1$  performed the best with polarization resistances of  $4 \Omega\text{cm}^2$  and  $3.8 \Omega\text{cm}^2$ , respectively, during testing in an air atmosphere at  $600^\circ\text{C}$ . In addition it was found that the best performance was obtained for  $T_{max} = 600\text{-}700^\circ\text{C}$ . The relatively low performance is attributed to a rather low electronic conductivity of STFx, limiting the electrode performance. Continued work includes impregnation in an optimized backbone structure with higher electronic conductivity and rationalization of the results using micro structural modeling.

**(ICACC-S3-P037-2012) Interface and grain boundary effects on the electrical conductivity of epitaxial and nanocrystalline ceria thin films**

G. Gregori\*, M. C. Göbel, Max Planck Institute for Solid State Research, Germany; X. Guo, Shanghai Institute of Ceramics, Chinese Academy of Sciences, China; J. Maier, Max Planck Institute for Solid State Research, Germany

In the present study, 10 mol% Gd-doped as well as undoped ceria films, grown with pulsed laser deposition on different substrates and at different deposition temperatures, were investigated with the purpose of further understanding the role of interface as well as grain boundary effects on the electrical conductivity. For some samples, both conductivity and activation energy vary as a function of film thickness suggesting the presence of interface effects between film and substrate. Interestingly, the interface contribution can be clearly detected in the case of polycrystalline films grown on  $\text{SiO}_2$ , whereas only minor interface effects can be detected for the epitaxial films grown on  $\text{Al}_2\text{O}_3$ . As expected, the conduction properties of the nanocrystalline films are dominated by grain boundary effects which also influence the interface conductivity contribution. Particularly intriguing is the case of the nanocrystalline, 10 mol% Gd-doped films with extremely small grain size (10 nm), which exhibit unusual properties such as a partially electronic conductivity under oxidizing conditions and low temperatures. The results are discussed in the framework of the general space charge model.

### (ICACC-S3-P038-2012) Development of GDC-(LiNa)CO<sub>3</sub> Nano-Composite Electrolytes for Low Temperature Solid Oxide Fuel Cells

R. Chockalingam\*, A. K. Ganguli, S. Basu, Indian Institute of Technology, India

Nano composite electrolytes made of gadolinium doped ceria and a bi-phase mixture of lithium carbonate and sodium carbonate salts are investigated with respect to their crystal structure, morphology and electrical conductivity. The addition of mixed salts reduced the sintering temperature of Gadolinium doped ceria by forming a eutectic melt at 497°C and improved the ionic conductivity especially at low temperature. The results derived show formation of a single fluorite phase which appears to be stable up to 800°C. Electrochemical impedance spectroscopy (EIS) measurements were performed to estimate the total ionic conductivity of gadolinium doped ceria with varying amounts of lithium-sodium carbonate and the results show that the ionic conductivity increased up to 25 wt% carbonate and thereafter decreased. The typical nature of the impedance spectra of the composite shows the possibility of coexistence of multi ionic transport or existence of space charge effect at the interface of Gd-CeO<sub>2</sub>/(LiNa)CO<sub>3</sub> phase. The composite containing 25 wt% carbonate shows conductivity ranging from 0.1751-0.239 S cm<sup>-1</sup> within the temperature range of 400-600°C. Single cells fabricated with NiO-GDC-25 wt% (LiNa)CO<sub>3</sub> as anode||GDC-(LiNa)CO<sub>3</sub> electrolyte||Li<sub>2</sub>O-NiO-25 wt% (LiNa)CO<sub>3</sub> cathode, tested at 500°C using hydrogen as fuel and air as oxidant delivers a maximum power density of 500mW/cm<sup>2</sup>.

### (ICACC-S3-P039-2012) Sintering and thermo-mechanical behavior investigation of strontium and cobalt doped LaCrO<sub>3</sub> ceramic interconnect

C. R. Sousa\*, W. Acchar, L. Silva, UFRN, Brazil; S. Castanho, IPEN, Brazil

The unit cells of the solid oxide fuel cell (SOFC) are separated by means of interconnects, which serve as electrical contact between the cells. Lanthanum Chromite (LaCrO<sub>3</sub>) has been the most common material used as interconnect in SOFC due to its physical and mechanical properties. This work investigates the sintering behavior and the thermo-mechanical behavior of the strontium and cobalt doped LaCrO<sub>3</sub> ceramic interconnect. The material was sintered at 1600 °C during 4 hours and characterized by X-ray diffraction, flexural strength at room temperature, hardness test and scanning electron microscopy (SEM). The material shows flexural strength values of 52 MPa and hardness of 5,982 GPa. The microstructure analyses show an intergranular and intragranular fracture mode.

### (ICACC-S3-P040-2012) Fabrication of Dual Layer Ceramic Interconnect on a NiO-YSZ Anode Support for Flat Tubular Solid Oxide Fuel Cells

M. Yoon\*, H. Hwang, Inha University, Republic of Korea; R. Song, Korea Institute of Energy Research, Republic of Korea

Interconnect materials of solid oxide fuel cells (SOFCs) can be roughly classified into metals and ceramics. In case of metals, Fe-Cr based alloys are mainly used, which have a high electronic conductivity, ease of fabrication and low cost. However they have poor oxidation resistance. Insulating oxide scale is formed under the oxidizing atmosphere. In case of ceramics, Sr or Ca doped LaCrO<sub>3</sub> based materials have been extensively studied. Although they have a high electrical conductivity and phase stability, Sr doped LaCrO<sub>3</sub> suffers from poor sinterability. On the other hand, Ca doped LaCrO<sub>3</sub> has a Ca migration problem at the NiO-YSZ anode interface. In addition, Fe-Cr based alloys or LaCrO<sub>3</sub> based interconnects can lead to volatile Cr (VI) species such as CrO<sub>3</sub> and CrO<sub>2</sub>(OH)<sub>2</sub> at high temperatures, which diffuse to the cathode and degrade SOFC performance. In this study, Y doped SrTiO<sub>3</sub> was synthesized by solid state reaction and evaluated as ceramic interconnect for SOFCs. An Y doped SrTiO<sub>3</sub> coating layer was fabricated on a NiO-YSZ anode support by screen printing and co-firing process. Sr doped LaMnO<sub>3</sub> was also coated on the Y doped SrTiO<sub>3</sub> layer to improve the performance under the oxidizing atmosphere. The area specific resist-

ance of the dual layer ceramic interconnect was measured both in air and hydrogen atmospheres. The gas tightness was confirmed by Ar leakage test.

### (ICACC-S3-P041-2012) Methane Oxidation behavior of Perovskite Type Catalysts for Solid Oxide Fuel Cells

J. Yoon\*, INHA university, Republic of Korea; B. Choi, M. Ji, Korea Institute of Ceramic Engineering and Technology, Republic of Korea; H. Hwang, INHA university, Republic of Korea

Recently, there is growing interest in developing oxide anode materials for direct hydrocarbon solid oxide fuel cell. In addition to high electronic and ionic conductivities, the catalytic activity is very important requirement for SOFC anode materials if the hydrocarbons are used as a fuel. It is well known that the perovskite-type oxide materials show excellent catalytic activity for hydrocarbon oxidation reaction. In general, there are two types of oxidation reactions such as complete and partial oxidation for hydrocarbons, and these are classified by the operation temperatures and CH<sub>4</sub>/O<sub>2</sub> ratio. But, the mechanism and active site of oxidation reaction for hydrocarbon have not been understood clearly. In this study, a perovskite-type (R<sub>x</sub>Sr<sub>1-x</sub>)(MyTi<sub>1-y</sub>)O<sub>3-δ</sub> (R=Y or La, M=Fe, Ni or Mn) catalysts were synthesized using Pechini method. And their catalytic activity for methane oxidation was investigated using fixed-bed gas reactor and gas chromatography

### (ICACC-S3-P043-2012) Characterization of scandium doped lanthanum strontium ferrite as cathodes for solid oxide fuel cells

J. Park\*, J. Zou, H. Yoon, J. Chung, POSTECH, Republic of Korea

Scandium oxide has been used as a doping element to improve the cathode performance of various perovskite based systems. LSFSc having various zinc contents (La<sub>0.6</sub>Sr<sub>0.4</sub>Fe<sub>1.0-x</sub>Sc<sub>x</sub>O<sub>3-δ</sub>, x = 0, 0.05, 0.1, 0.2) were prepared by the EDTA-citrate method. The prepared LSFSc powders, having well-indexed peaks, were investigated via measurement of their electrical conductivity, polarization resistance, microstructure, reaction order and electrochemical properties. When scandium was substituted for 5mol% of iron on the B-site, it showed the best performance towards cathode ORR due to the increase in oxygen vacancy concentration. Further, when incorporated with 50wt% of YSZ particles, its Rp values decreased by 70% while the MPD increased by 40%. It can be concluded that the minor doping of elements having constant oxidation state, such as Sc<sup>3+</sup>, produce positive effects on the electrochemical properties of SOFC cathodes.

### (ICACC-S3-P044-2012) Preparation and evaluation of Ca<sub>3-x</sub>BixCo<sub>4</sub>O<sub>9+δ</sub> (0 < x ≤ 0.5) as novel cathodes for intermediate temperature-solid oxide fuel cells

J. Zou\*, J. Park, H. Yoon, T. Kim, J. Chung, Pohang University of Science and Technology, Republic of Korea

The misfit compounds Ca<sub>3-x</sub>BixCo<sub>4</sub>O<sub>9+δ</sub> (x = 0.1~0.5) are synthesized via conventional solid state reaction and evaluated as cathode materials for intermediate temperature solid oxide fuel cells (IT-SOFCs). The structures of powders are investigated by x-ray diffraction, scanning emission microscopy, thermogravimetry analysis and oxygen temperature-programmed desorption. The monoclinic Ca<sub>3-x</sub>BixCo<sub>4</sub>O<sub>9+δ</sub> powders exhibit good thermal stability and chemical compatibility with Ce<sub>0.8</sub>Sm<sub>0.2</sub>O<sub>2-γ</sub> electrolyte. The Ca<sub>2.9</sub>Bi<sub>0.1</sub>Co<sub>4</sub>O<sub>9+δ</sub> shows the higher catalytic activity and electrical conductivity with the maximal conductivity of 655.9 S cm<sup>-1</sup>. Among the investigated compositions, Ca<sub>2.9</sub>Bi<sub>0.1</sub>Co<sub>4</sub>O<sub>9+δ</sub> shows the best cathodic performance. The maximum power densities of the NiO/Ce<sub>0.8</sub>Sm<sub>0.2</sub>O<sub>2-γ</sub> anode-supported single cells fabricated with the Ce<sub>0.8</sub>Sm<sub>0.2</sub>O<sub>2-γ</sub> electrolyte layer and Ca<sub>2.9</sub>Bi<sub>0.1</sub>Co<sub>4</sub>O<sub>9+δ</sub> cathode reach 332, 245 and 144 mW cm<sup>-2</sup> at 700 °C, 650 °C and 600 °C respectively, which is attributed to its best catalytic activity and lowest total polarization resistance values. All the preliminary results indicate that Ca<sub>2.9</sub>Bi<sub>0.1</sub>Co<sub>4</sub>O<sub>9+δ</sub> is a promising candidate as an IT-SOFC cathode material.

**(ICACC-S3-P045-2012) n-Dodecane reforming over Ni-YSZ cermet catalysts with K<sub>2</sub>Ti<sub>2</sub>O<sub>5</sub>**

T. Kim\*, H. Kim, J. Chung, POSTECH, Republic of Korea

n-dodecane reforming has a serious coke formation problem which results in failure of the reformer, in contrast to reforming of light hydrocarbons. Ni-YSZ cermet is commonly used as an anode material for solid oxide fuel cells (SOFC) because it has excellent electrochemical performance. It can be used as an n-dodecane reforming catalyst because Ni has a catalytic activity for hydrocarbon fuels. However, it has a serious coke formation problem, and hence K<sub>2</sub>Ti<sub>2</sub>O<sub>5</sub> was added as a soot oxidation catalyst. A Ni-YSZ cermet catalyst with K<sub>2</sub>Ti<sub>2</sub>O<sub>5</sub> additives was studied under two types of n-dodecane reforming (Steam, Autothermal reforming) with various GHSV conditions. The appearance of deactivation of the Ni-YSZ catalyst was quite different. Ni-YSZ cermet was synthesized by mixing NiO and YSZ by ball milling for three days. It was then sintered for 5 hours at 1000°C, and reduced at 800°C under H<sub>2</sub> for 3 hours. K<sub>2</sub>Ti<sub>2</sub>O<sub>5</sub> was prepared using the solid state method. These powders were physically mixed in an agate mortar using absolute ethanol. The catalyst powders were characterized by XRD and SEM. The catalyst performance for n-dodecane reforming was tested at 800°C. The reformate gas was analyzed using a gas chromatograph equipped with a TCD and FID. After the reaction had finished, the amount of coke in the catalysts was measured using an SEM image and TPO. The relation between the amount of coke and the GHSV was also investigated.

**(ICACC-S3-P046-2012) Deposition of Mn<sub>1.5</sub>Co<sub>1.5</sub>O<sub>4</sub> thin films by thermal co-evaporation on Crofer 22APU interconnects for chromium poisoning SOFC electrolyte protection purpose**

M. Bindi\*, D. Beretta, Edison.S.p.A., Italy; F. Smeacetto, L. Ajitdos, Polytechnic of Turin, Italy

We report on the in-situ growth and characterisation of thin MnCo<sub>2</sub>O<sub>4</sub>:Mn<sub>2</sub>CoO<sub>4</sub>=1:1 (Mn<sub>1.5</sub>Co<sub>1.5</sub>O<sub>4</sub>) solid solution films deposited on Crofer 22APU alloy by reactive thermal co-evaporation for its possible application as protective coating material in solid oxide fuel cells (SOFC). The correct phase was synthesised by a two step-process and the structure of the resulting thin films were characterized by means of X-ray theta-2theta Bragg-Brentano diffractometry and by Field Emission Scanning Electron Microscopy. Furthermore electric analysis were carried out in air in order to measure the conductivity properties of the produced samples, from room temperature up to 800°C. Work is actually focused to the 10 x 10 cm<sup>2</sup> sized interconnects coating for following SOFC stacks assembly.

**(ICACC-S3-P047-2012) A Comparative assessment of Chromium Evaporation from Bulk and Surface Aluminized Iron and Nickel Base Alloys**

L. Ge\*, P. Singh, University of Connecticut, USA

Chromium evaporation from bulk and aluminized iron and nickel base alloys has been measured in flowing humidified air environment (3-12% H<sub>2</sub>O) and 800-950°C temperature range utilizing a transpiration technique. Surface morphology of oxidized samples has been examined for scale morphology and chemistry using XRD, FESEM, FIB, TEM and EDS. A comparative assessment of Cr evaporation from bulk and aluminized alloys will be presented, along with the nature and performance of the coating. Role of scale morphology and initial stages of oxidation on scale evaporation will be discussed. Localized breakdown of scale and loss of protection will be presented and discussed.

**(ICACC-S3-P170-2012) Structure, morphology and transport properties of rapidly quenched YSZ**

M. Dragan\*, A. Verma, University of Connecticut, USA; P. Strutt, NanoCell Systems Inc., USA; R. Maric, University of Connecticut, USA

Metastable nanostructured 8-YSZ powders were synthesized using a pyrolytic melting or vaporization of an aerosol-solution precursor in a DC-arc plasma, followed by rapid quenching which produced ho-

mogeneous nanoceramic materials. The surface chemistry and structure of rapidly quenched YSZ influenced the oxygen ion transport. The conductivity of YSZ was found to be strongly dependent on both crystallinity and phase transformation. The evolution of the crystalline structure and phase evolution has been explored and related with the transport properties of the material system. Impedance spectroscopy was utilized to distinguish between the bulk intrinsic and grain boundary conductivity at different testing conditions. In this work the structure, morphology, and transport properties of rapidly quenched YSZ will be discussed. Preliminary findings will be presented and the physical and electrical properties of rapidly quenched nano-size YSZ powder will be compared with bulk samples.

## S5: Next Generation Bioceramics

### Symposium 5: Poster Session

Room: Exhibit Hall

**(ICACC-S5-P069-2012) In Vitro Evaluation of Silicate and Borate Bioactive Glass Scaffolds Prepared by Robocasting of Organic-Based Suspensions**

A. M. Deliormanli\*, M. N. Rahaman, Missouri University of Science and Technology, USA

Porous three-dimensional scaffolds of silicate (13-93) and borate (13-93B3) bioactive glass were prepared by robocasting and evaluated in vitro for potential application in bone repair. Organic-based suspensions were developed to limit degradation of the bioactive glass particles, and deposited layer-by-layer to form constructs with a grid-like microstructure. After binder burnout, the constructs were sintered for 1 hour at 700°C (13-93 glass) or 570 °C (13-93B3 glass) to produce scaffolds (porosity ≈ 50%) consisting of dense bioactive glass struts (300 μm in diameter) and interconnected pores of width 400 μm. The mechanical response in compression and the conversion of the scaffolds to hydroxyapatite (HA) were studied as a function of immersion time in a simulated body fluid (SBF). As fabricated, the 13-93 and 13-93B3 scaffolds had compressive strengths far higher than the values for human trabecular bone. When immersed in the SBF, the borate 13-93B3 scaffolds showed a far faster conversion rate to HA hydroxyapatite than the silicate 13-93 glass, but also a sharper decrease in strength. Based on their high compressive strength and bioactivity, the scaffolds fabricated in this work by robocasting could have potential application in bone repair and regeneration.

**(ICACC-S5-P070-2012) Evaluation of Borate Bioactive Glass Scaffolds with Different Pore Sizes in a Rat Subcutaneous Implantation Model**

A. M. Deliormanli\*, M. N. Rahaman, Missouri University of Science and Technology, USA

Borate bioactive glass has been shown to convert faster and more completely to hydroxyapatite and to enhance new bone formation in vivo when compared to silicate bioactive glass (such as 45S5 and 13-93 bioactive glass). In this work, the effect of the borate glass microstructure on its ability to support tissue ingrowth was evaluated in vivo in a rat subcutaneous implantation model. Bioactive borate glass scaffolds, designated 13-93B3 (composition: 5.5 Na<sub>2</sub>O, 11.1 K<sub>2</sub>O, 4.6 MgO, 18.5 CaO, 3.7 P<sub>2</sub>O<sub>5</sub>, 56.6 B<sub>2</sub>O<sub>3</sub>; wt%), with a grid-like microstructure (porosity ≈ 50%) and pore widths of 300, 600, and 900 μm were prepared by a robocasting technique. The scaffolds were implanted subcutaneously for 4 weeks in Sprague Dawley rats. Silicate 13-93 glass scaffolds with the same microstructure were used as the control. Histology and scanning electron microscopy were used to evaluate conversion of the bioactive glass implants to hydroxyapatite, as well as tissue ingrowth and blood vessel formation in the implants. The effects of the scaffold microstructure on tissue infiltration, blood vessel formation, and mineralization are presented and discussed.

### (ICACC-S5-P071-2012) The effect of silicocarnotite on the behavior of rat bone marrow stromal cells

C. Ning\*, W. Duan, Shanghai Institute of Ceramics, Chinese Academy of Sciences, China

In the present study, the effects of a new bioceramic, silicon containing calcium phosphate ceramic (silicocarnotite,  $\text{Ca}_5(\text{PO}_4)_2\text{SiO}_4$ , CPS), on the proliferation and osteoblastic differentiation of rat bone marrow stromal cells (rat BMSC) have been investigated in comparison with the classical bioceramic hydroxyapatite (HA). The silicocarnotite showed the similar cell attachment behavior with HA. However, rat BMSCs proliferated more significantly on CPS disk than on HA disk. Moreover, The analysis of osteoblast-related genes, including Runx-2, osteopontin (OPN) and bone sialoprotein (BSP), indicated that CPS ceramics enhanced the expression of osteoblast-related genes. It also implied that silicon may enhance cell differentiation in a certain concentrations.

## S7: 6th International Symposium on Nanostructured Materials and Nano-Composites

### Symposium 7: Poster Session

Room: Exhibit Hall

### (ICACC-S7-P072-2012) Evolution of structure, microstructure and hyperfine properties of nanocrystalline FeAl powders

Z. Hamlati\*, University of Blida, Algeria; A. Guittoum, Nuclear Research Center of Algiers, Algeria; S. Bergheul, University of Blida, Algeria; M. Azzaz, U.S.T.H.B, Algeria

Iron–aluminum alloy of Fe–28% Al composition was prepared by mechanical alloying (MA) of the elemental powders. The phase transformations and structural changes occurring in the studied material during mechanical alloying were investigated by X-ray diffraction (XRD), scanning electron microscopy (SEM), Mössbauer spectroscopy and magnetic measurement. The final product of the MA process was the nanocrystalline Fe(Al) solid solution with a mean crystallite size of 10 nm. The complete formation of bcc-FeAl solid solution is observed after 4 h of milling. The Mössbauer spectra show different behaviors with the increase of milling time. Indeed, after 4 h, the Mössbauer spectrum shows the presence of a singlet and sextet. After 8 h of milling, the paramagnetic phase disappears leading to the appearance of a sextet, with a mean hyperfine field,  $H_{\text{hf}}$ , equal to 24.18 T which is characteristic of  $\text{DO}_3'$  structure. For the higher milling time i.e. 24 h, the Mössbauer spectrum was analyzed with two components. The first one with equal to 29.9 T is still indicative of ordered  $\text{DO}_3$ , however, the second with a value of 10.25 T is characteristic of the fine domain B2 ordered structure.

### (ICACC-S7-P073-2012) Low Temperature Solution based Synthesis of ZnO and Ag admixed ZnO Nanoparticles (NPs) their Structural and Optical Characterization

J. Singh\*, P. Kumar, R. S. Tiwari, O. N. Srivastava, B H U, India

Looking at its huge range of applications of ZnO nanostructured can be considered as a technological material. Simple and green production techniques for ZnO and other nanostructured material can enhance the detection of their unusual properties. In this context water-based wet chemical synthesis technique for ZnO and Ag admixed ZnO nanocrystals are explored in this work. High productive yield of the ZnO and Ag admixed ZnO nanocrystals with different Ag contents is successfully synthesized through a simple wet chemical method at the low temperatures in the absence of surfactants. The as synthesized products were characterized by X-ray diffraction (XRD), transmission electron microscopy (TEM), Fourier transform IR (FTIR), UV-Vis spectroscopy, and photoluminescence spectroscopy. The size of the nanoparticles was found to increase with the increasing Ag content. Large blue-shifts relative to the bulk exciton absorption of ZnO were observed in the absorption and PL spectra of the

pure ZnO and Ag admix ZnO. The emission intensity of PL spectra of Ag admixed ZnO sample has been found to decrease considerably with respect to that of pure ZnO sample. NaOH plays multiple roles in the formation of pure ZnO NPs and Ag admix ZnO NPs.

### (ICACC-S7-P074-2012) Physical-Chemical, Mechanical, Thermal, and Radiation Resistance of Hard and Super-Hard Nano-Structured Coatings

A. D. Pogrebnyak\*, Sumy Institute for Surface Modification, Ukraine; M. Tashmetov, Institute of Nuclear Physics, NAS of Uzbekistan, Uzbekistan; M. Il'yashenko, Sumy State University, Ukraine; N. Makhmudov, Samarkand Branch of Tashkent State University of Information, Uzbekistan; V. Beresnev, Kharkov National University, Ukraine; A. Shpylenko, Sumy State University, Ukraine; I. Kulik, M. Kaverin, Sumy Institute for Surface Modification, Ukraine; V. Baidak, A. Dem'yanenko, Sumy State University, Ukraine

The report deals with investigation results on structure and properties of hard Zr-Si-N, Zr-Ti-N, and super-hard Zr-Ti-Si-N coatings of 1.8 to 3.2  $\mu\text{m}$  thickness. Coated samples were  $\gamma$ -irradiated during several months in a reactor and cobalt gun. Hardness of Zr-Si-N coatings was 28 to 32 GPa, that of Zr-Ti-N reached 35  $\pm$  2.6 GPa, and hardness of Zr-Ti-Si-N was 40 to 48 GPa. Thermal annealing of coated samples to 550°C increased their hardness to 53 GPa, and subsequent  $\gamma$ -quantum-irradiation under 108 to 109 Grey essentially decreased their hardness. Nano-grain sizes increased as a result of annealing and subsequent  $\gamma$ -quantum-irradiation. Inter-layers of amorphous phase ( $\alpha$ - $\text{Si}_3\text{N}_4$ ) surrounding nano-grains (Zr, N)-nc, ... (Zr, Ti)N-nc increased by several per cent, which seemed to be related to enhanced processes of relaxation-accelerated diffusion.  $\gamma$ -quantum-irradiation of samples with super-hard coatings till high-temperature annealing resulted in a shift of hardness maximum to 150°C (as a result of subsequent annealing in vacuum) closer to the beginning of temperature interval.

### (ICACC-S7-P075-2012) Real-Time Oxidation Kinetics of Dielectric-Embedded Ag Nanoparticles: Revealing Physicochemical Properties via In Situ Optical Microspectroscopy

K. McAlpine\*, J. A. Jimenez, M. Sendova, New College of Florida, USA

This study was designed to find the barrier for the oxidation of Ag NPs embedded in an aluminum oxide matrix deposited on quartz undergoing heat treatment. *In situ* optical microspectroscopy was used to obtain absorption spectra, whose respective peaks decayed exponentially with an increase in temperature. Analyzing through first-order kinetics yielded an activation energy of 33  $\text{kJ mol}^{-1}$  as determined from an Arrhenius plot.

### (ICACC-S7-P076-2012) Insitu Synthesis of Multi-Walled Carbon Nanotubes/ Al<sub>2</sub>O<sub>3</sub> Nanocomposite With Non-metallic ZrO<sub>2</sub> Catalyst by Chemical Vapor Deposition

A. Kumar\*, J. Karpf, D. Amit, K. Wu, Florida International University, USA

Since the discovery of CNTs by Iijima, significant progress has been made towards many applications of CNTs, especially in the area of composite materials. Our group has studied various MWNT/ceramics nanocomposites for armor and biomedical applications. In the present study, we have synthesized the MWNTs/ $\text{Al}_2\text{O}_3$  nanocomposites with zirconia nanoparticles as nonmetallic catalyst for in-situ direct growth of CNTs using the thermal CVD process, to avoid the problem associated with the metallic catalysts, which generally react with the matrix materials in the composite. This nonmetallic catalyst is expected to improve the properties of the nanocomposite materials as compared with those fabricated using metallic catalysts. In this study we have succeeded in precipitating  $\text{ZrO}_2$  nanoparticles by wet chemistry on the  $\text{Al}_2\text{O}_3$  powders and studied the effect of the weight percentage of  $\text{ZrO}_2$ , the sintering temperature, and growth time on the properties of the spark-plasma sintered MWNT/ $\text{ZrO}_2$ / $\text{Al}_2\text{O}_3$  composites. The morphology of MWNTs has been characterized with SEM and Raman spectroscopy, and the percentage of CNTs has been characterized with TGA.



**(ICACC-S7-P077-2012) Synthesis and Characterization of Boron/Nitrogen Incorporated Diamond-Like-Carbon Thin Films**

L. Zhang\*, Q. Yang, Y. Li, Y. Tang, C. Zhang, L. Yang, University of Saskatchewan, Canada

Boron (B) and/or nitrogen (N) incorporated diamond-like-carbon (DLC) composite thin films have been synthesized from a simultaneous ion beam deposition of DLC films and ion beam sputtering of boron carbide (B<sub>4</sub>C) and boron nitride (BN) targets, respectively. Raman Spectroscopy, Scanning/Transmission Electron Microscopy, Atomic Force Microscopy, X-ray Photoelectron Spectroscopy and synchrotron-based Near Edge X-ray Absorption Fine Structure were applied to investigate the film microstructure, morphology, electronic structure and bonding state. Nanoscratch tests were conducted using a nanoanalyzer to measure the mechanical properties of the synthesized films including both hardness and elastic modulus, as well as to evaluate the adhesion property. The electronic structure, bonding state and mechanical properties of the B/N incorporated DLC films were compared with those of unincorporated DLC film, and the relationships between the processing conditions, structure and properties were addressed.

**(ICACC-S7-P078-2012) Photocatalytic degradation of waste liquid from biomass gasification in supercritical water with simultaneous hydrogen production**

W. Tang\*, D. Jing, S. Guo, J. Yin, L. Guo, State Key Laboratory of Multiphase Flow in Power Engineering, China

Photocatalytic water splitting by solar light and biomass gasification in supercritical water both are considered as the most promising routes for renewable hydrogen production. The waste liquid from biomass gasification in supercritical water contains various kinds of organic compounds. To couple these two systems together, we tried photocatalytic degradation of waste liquid from biomass gasification in supercritical water. Here organic compounds in the waste liquid were supposed to act as the sacrificial agents in the photocatalytic system. In the present work, we compared hydrogen production performances by the anaerobic photocatalytic reforming of waste liquid from biomass gasification in supercritical water among various kinds of photocatalysts such as oxide semiconductors like Na<sub>2</sub>Ti<sub>2</sub>O<sub>4</sub>(OH)<sub>2</sub> nanotubes, NaTaO<sub>3</sub>, sulfide semiconductors like ZnIn<sub>2</sub>S<sub>4</sub>. These photocatalysts have been characterized by XRD, TEM, BET and XRF et al. Here, we use waste liquid from glucose cellulose and glycerol gasification in supercritical water respectively. Various reaction parameters were investigated, such as different gasification temperature and the pH value of the waste liquid. It was demonstrated that gasification in supercritical water and photocatalytic water splitting can be coupled together.

**(ICACC-S7-P079-2012) Graphitic Carbon Nitride Doped with Silicon for Improved Visible-light-Driven Photocatalysis**

P. Wu\*, J. Shi, L. Guo, Xi'an Jiaotong University, China

In this work, a series of Si-doped graphitic carbon nitride (g-C<sub>3</sub>N<sub>4</sub>) were conveniently synthesized through polymerization of melamine and Si source. Some basic physical and chemical properties of these metal-free semiconductors were characterized by X-ray diffraction (XRD), Fourier transform infrared spectrometer (FTIR) spectra, scanning electron microscope (SEM), UV-visible diffuse reflectance spectra (UV-Vis) and Brunauer-Emmett-Teller (BET) surface area measurement. The XRD patterns of all the prepared materials were dominated by the characteristic (002) peak at 27.48 of a graphitic, layered structure with an interlayer distance of d=0.33 nm, indicating that the introduction of Si did not destroy the graphitic structure. The photocatalytic H<sub>2</sub> productions from an aqueous solution containing sacrificial reagent triethanolamine under visible-light irradiation over the series of Si-doped C<sub>3</sub>N<sub>4</sub> were also evaluated. As the initial mole ratio of Si to C increased from 0 to 0.5, the photocatalytic activity was improved about 1.5 times. The mechanism of the better photocatalytic activity based on Si doping was revealed.

**(ICACC-S7-P080-2012) Remarkable enhancement of photocatalytic hydrogen evolution over Cd<sub>0.5</sub>Zn<sub>0.5</sub>S by bismuth-doping**

S. Peng, R. An, Y. Li\*, Nanchang University, China; G. Lu, S. Li, Lanzhou Institute of Chemical Physics, Chinese Academy of Science, Lanzhou, China

Bi<sup>3+</sup> doped Cd<sub>0.5</sub>Zn<sub>0.5</sub>S photocatalysts were prepared by a simple hydrothermal method, and characterized by X-ray diffraction (XRD), scanning electron microscopy (SEM), transmission electron microscopy (TEM), X-ray photoelectron spectroscopy (XPS), energy dispersive X-ray spectroscopy (EDX), BET and UV-Vis absorption spectroscopy techniques. When Bi<sup>3+</sup> doping content is lower, the doping ions lie at the surface lattice sites, whereas when the doping content is higher, the ions also enter the bulk lattice sites. Their photoactivities were evaluated by hydrogen evolution from aqueous solution containing Na<sub>2</sub>S and Na<sub>2</sub>SO<sub>3</sub> as a hole scavenger under visible light ( $\lambda \geq 420$  nm) irradiation. Bi<sup>3+</sup> doping enhances markedly photocatalytic activity. When Bi<sup>3+</sup> doping content is 0.10 mole %, the photocatalyst exhibits the highest activity, and the average apparent quantum yield amounts to 9.71% during 30 h irradiation. The possible mechanism was discussed.

**(ICACC-S7-P081-2012) Fabrication of CdS-ZnO core/shell Nanofibers by Electrospinning and Their Photocatalytic Activity**

W. Yan\*, G. Yang, Xi'an Jiaotong University, China

Core/shell 1D materials have been extensively pursued in recent years and a variety of methods have been demonstrated to generate core/shell nanostructures from many kinds of materials, such as self-assembly, CVD, pyrolysis, plasma sputtering decoration, electrospinning and template synthesis etc. Electrospinning has been proved to be a versatile and effective method for the manufacturing of micro-scale to nano-scale fibers continuously, thus it attracts much attention as a new promising route to obtain materials featuring core-shell structure. In this article, CdS/ZnO core-shell nanofibers were prepared successfully by typical single-nozzle electrospinning, with subsequent simple thermal decomposition. The SEM and TEM results indicated that core-shell fibers with a diameter of 200-350 nm and shell thickness of 50 nm was obtained when PVP/zinc acetate/cadmium acetate/Thiocarbamide composite nanofibers was calcinated at 480 °C for 4h. The EDS analysis results showed that the core fiber is CdS and the shell layer is ZnO. Hydrogen evolution measurements from photocatalytic water splitting using the ZnO/CdS core/shell nanofibers as photocatalysts were carried out. The ZnO/CdS core/shell nanofibers exhibit a much higher ability for H<sub>2</sub> evolution than that of the sole CdS or ZnO. The highest H<sub>2</sub> evolution rate was up to 600  $\mu$ mol h<sup>-1</sup>g<sup>-1</sup> under light irradiation at wavelength of 420nm.

**(ICACC-S7-P082-2012) Structural, Optical and Photoelectrochemical Characterization of Hydrogen Plasma Treated TiO<sub>2</sub> Thin Films**

A. Mettenboerger\*, A. P. Singh, P. Golus, N. Tosun, S. Mathur, University of Cologne, Germany

TiO<sub>2</sub> thin films which are of particular interest as photovoltaic materials have limitations due to its high band gap energy. In this study, we report a novel method for the fast fabrication of visible and IR light absorbing black TiO<sub>2</sub> thin films by plasma enhanced chemical vapor deposition (PE-CVD) technique. This method is based on the *in situ* synthesis of both the titanium dioxide matrix and its hydrogenation. The novelty of this method is the deposition and hydrogenation of metal oxide films in a single reactor at various temperatures which allows the formation of homogeneous films with relatively low surface roughness. This variability is very important because it allows the optical properties of TiO<sub>2</sub> films to be tuned over a visible and IR range. XRD analysis exhibits the formation of pure anatase phase of TiO<sub>2</sub> after the hydrogenation. The UV-Visible-IR spectrum exhibits that the absorption edge of the hydrogenated TiO<sub>2</sub> films shifted towards the visible and IR region. Photoelectrochemical characterization carried out under 1 Sun illumination in 1M NaOH electrolyte exhibits the much higher photocurrent density as compared to conventional TiO<sub>2</sub> films.

### (ICACC-S7-P083-2012) One-dimensional heterostructures based on $\text{SnO}_2/\text{Nb}_2\text{O}_5$ and $\text{SnO}_2/\text{Fe}_2\text{O}_3$ core-shell architectures and functional applications

R. Fiz\*, T. Fischer, M. Hoffmann, A. P. Singh, S. Mathur, University of Cologne, Germany

Quasi-one-dimensional (1D) metal oxide nanostructures are considered ideal building blocks for nanodevice fabrication. Heterostructures represent the innovating step in the development of novel device nanostructures. Due to the new characteristics of the heterojunctions it is possible to design materials with unique properties and functionalities showing great advantages compared to their single component counterparts. In this work the controlled fabrication of  $\text{SnO}_2/\text{Nb}_2\text{O}_5$  and  $\text{SnO}_2/\text{Fe}_2\text{O}_3$  core-shell heterostructures by metal-organic chemical vapor deposition is presented. The influence of morphology and crystal structure on the material properties was studied by means of SEM/EDX, HR-TEM and XRD. Analysis of the electrical conductance shows proper band-gap alignment between shell-core materials and high conductivity through the  $\text{SnO}_2$  core. Finally, the integration of these heterostructures in different applications such as gas sensors and photoelectrochemical water splitting has been investigated.

### (ICACC-S7-P084-2012) Fabrication and Characterization of a Novel Nanostructured Solar Diode Sensor

A. Gad\*, M. Hoffmann, H. Shen, S. Mathur, University of Cologne, Germany

Gas sensors have various applications in safety and security application as well as air quality monitoring. The major disadvantage of the well established metal oxide gas sensors, is the high operation temperature of these devices, which demands a reliable power supply and limits its operating time. For recording a resistance change in the active material proportional of the target gas concentration, operation temperatures of 300-500 °C are necessary to ensure stable working conditions. Developments in reducing the power consumption of these systems have already reached a limit by employing micro-machined substrates and pulsed operation modes. Recent developments focus on autonomous, self-powered devices, which combine sensing and power generation units. The described solar diode sensor is based on a solar cell consisting of a n-type metal oxide and p-type silicon. A targeted activation of the p-n-junction with CdS, CdSe, CdTe, PbS or CuO forms a room temperature gas sensor, which changes its open-circuit voltage depending on the concentration of the absorbed target gas molecules under solar light irradiation. A first prototype of this novel gas sensing mechanism is presented including full structural, mechanical and operational investigations.

### (ICACC-S7-P085-2012) Novel Precursor Libraries for Gas Phase Synthesis of Functional Metal Oxide Coatings and Nanostructures

L. Brueckmann\*, C. Hegemann, J. Schlaefer, I. Giebelhaus, G. Fornalczyk, L. Appel, W. Tyrna, S. Stucky, S. Mathur, University of Cologne, Germany

Recent advances in material science also depend on the availability of suitable precursors for material synthesis. Different synthetic routes, like gas phase and liquid phase synthesis, demand different chemical and physical properties of the applied precursors, to achieve the desired purity, phases or morphologies of the final material. Up to date only a few precursors are commercially available and especially the application of various materials in gas phase deposition is still hindered due to a lack of suitable starting materials. We would like to introduce a new versatile precursor library for gas phase and liquid phase synthesis of metal oxides which is based on a metal derivatives of  $\beta$ -heteroaryl-alkenolates. These air-stable, non-toxic, volatile compounds yield pure metal or metal oxide coatings in chemical vapor deposition processes and are available through well established chemical synthesis in a multi-gram scale. Next to monometallic compounds also multi-metallic precursors are available, which opens the way to complex materials obtained from a single source. The synthesis of the compounds as well as their molecular structure, verified via X-Ray diffraction and NMR-spectroscopy, will be described. More-

over their volatility, decomposition pathways and the resulting metallic and ceramic products are studied in depth.

### (ICACC-S7-P086-2012) Metal Oxide Nanoparticles for Biomedical Applications

L. Wortmann\*, L. Xiao, O. Arslan, S. Mathur, University of Cologne, Germany

In recent years metal oxide nanoparticles have emerged as versatile tools for drug delivery and imaging techniques in biomedical applications. While superparamagnetic iron oxide magnetite nanoparticles serve as excellent biocompatible contrast agents in magnetic resonance imaging systems, silica nanoparticles or nanospheres are used as vehicles for targeted drug delivery. For a wide spread application a reliable and scalable synthetic approach is needed which involves biocompatible and non-toxic reagents in order to minimize the probability of contamination. This contribution will demonstrate new synthetic approaches of nanoparticle and core shell nanostructures, combined with cell culture studies for assessing the biocompatibility of various metal oxide nanoparticles produced via different synthetic approaches. The effect of different functionalizations of the nanoparticles' surface on the metabolism of these nanostructures and the release of embedded molecules is also studied.

### (ICACC-S7-P088-2012) Structural and Optical Studies of ZnO & Mg doped ZnO Nanowires

J. Singh\*, R. S. Tiwari, O. N. Srivastava, B H U, India

ZnO represents a material where the properties (e.g. band gap, exciton binding energy, optical and electrical properties) are strongly sensitive to its structure, including the morphology, aspect ratio, size, orientation and density of the crystal. Herein, undoped and Mg doped zinc oxide ( $\text{Mg}_x\text{Zn}_{1-x}\text{O}$ ,  $x=0, 5, 10$  and  $20$  at. %) nanowires were successfully synthesized by two step process. Initially, ZnO nanowires were grown by thermal evaporation of Zn powder under oxygen atmosphere and then Mg powder were doped with the as grown ZnO nanowires by solid state reaction route at low temperature  $\sim 500$  °C. Energy dispersive x-ray spectroscopy (EDAX), transmission electron microscopy (TEM), X-ray diffraction (XRD) and UV-Visible absorption spectra analysis revealed that the Mg doping on ZnO nanowires induces lattice strain in ZnO which furthermore increases the band gap of  $\text{Mg}_x\text{Zn}_{1-x}\text{O}$ . XRD patterns reveals that pure and Mg doped ZnO nanowires are crystalline with wurtzite structure. Rietveld analysis of XRD data also confirms the wurtzite structure and a continuous compaction of the lattice (in particular, the c-axis parameter) as x increases. Strong UV emission and weak visible emission of Mg doped ZnO nanowires were investigated by photoluminescence (PL) spectra. A possible mechanism of Mg doping on ZnO has been discussed in detail through PL spectra.

### (ICACC-S7-P089-2012) Strengthening Effect of Kaolinite on Porous Kaolinite-Silica Nanocomposites

K. Lu\*, W. Li, J. Walz, Virginia Tech, USA

Kaolinite is found to be effective in modifying the microstructure of freeze-cast kaolinite-silica nanocomposites and modifying the sintering behavior of the silica nanoparticles. In this work, the reinforcing effects of kaolinite on porous kaolinite-silica composites are investigated. It has been found that the strength of the fabricated porous composites depends simultaneously on kaolinite concentration and sintering temperature. Experiments show that the maximum strengths of the different temperature sintered composites occur at different kaolinite loadings. This unique strengthening effect is attributed to both kaolinite particle geometry and new phase formation. This improvement of the flexural strength is achieved without significantly sacrificing the porosity. The strength and porosity with different solids loading at the maximum strength compositions are also studied.

### (ICACC-S7-P090-2012) Preparation of novel SiC nanostructures by arc plasma heat treatment method

B. B. Nayak, B. K. Mishra\*, IMMT, India

Nanostructures of silicon carbide like nanorods, nanotubes, nanowires provide potential scope for applications in field emission

devices, quantum devices, sensors and ultra high strength composites. While SiC nanorods are now used in R&D for developing cold cathode field emission display (FED) such as television, flexible thin film computer screen, atomic force microscope (AFM) tip, SiC nanowires (NWs) and nanocables (NCs) have drawn attention for possible application as catalyst supports, reinforcement materials in nanocomposites and components for nanoelectromechanical systems. SiC is one such few compound which does not melt but undergoes dissociation above 22000C in a non-oxidizing atmosphere. The dissociation completes at around 28250C. By taking advantage of the non-melting and dissociative property of the carbide, effort has been made to prepare various nanostructures, including rods, tubes, ropes, wires, etc. by adopting a selective removal of Si (in vapour form) at high temperature followed by recombination reaction with the dissociated carbon left out in solid matrix. An arc plasma reactor was employed to produce temperature of the order of 30000C for causing dissociation of SiC. Ar plasma generated in the arc was ingeniously used so as not to strike the SiC powder directly. Heating of the powder was done indirectly in the arc reactor by cathode heating technique.

#### (ICACC-S7-P091-2012) Nanostructured Zr-doped Hematite Thin Films for Photoelectrochemical Water Splitting

P. Kumar\*, P. Sharma, R. Shrivastav, S. Dass, V. R. Satsangi, Dayalbagh Educational Institute, India

Photoelectrochemical (PEC) water splitting using solar energy represents a holygrail in energy science due to clean and renewable hydrogen production. This paper, thus, reports an investigation on the influence of method of preparation and Zr doping on photoelectrochemical performance of nanostructured hematite thin films. Two simple and economical methods-electrodeposition and spray pyrolysis were used for preparation of nanostructured hematite thin films on fluorine-doped tin oxide (FTO) substrate. Photoelectrochemical results were analyzed with the help of XRD, SEM, XPS, Raman and UV-Vis absorption spectroscopy. Raman spectra indicated partial transformation of hematite to  $Fe_3O_4$  (magnetite) phase of iron oxide after doping of Zr. Hematite thin films were used as photoelectrode in PEC cell and current-voltage characteristics were recorded under visible light illumination. Electrodeposited samples exhibited much better photoresponse as compared to spray pyrolytically deposited samples. 2 at% Zr doped electrodeposited iron oxide sample exhibited best photocurrent density  $\sim 3.0$  mA/cm<sup>2</sup> and solar to hydrogen conversion efficiency  $\sim 1.84$  % at 0.7V/SCE. Maximum values of donor density and flatband potential for this sample, as obtained from Mott-Schottky characterization, also supported the best performance of 2 at% Zr doped electrodeposited iron oxide sample.

#### (ICACC-S7-P092-2012) Enhanced Photoelectrochemical Response of Doped BaTiO<sub>3</sub> for Solar Hydrogen Generation: Experiments and First-Principles Analysis

S. Dass, S. Upadhyay\*, J. Shrivastava, A. Solanki, S. Choudhary, N. Singh, V. Sharma, P. Kumar, Deemed University, India; V. R. Satsangi, Dayalbagh Educational Institute, Deemed University, India; R. Shrivastav, Deemed University, India; U. V. Waghmare, Jawaharlal Nehru Centre for Advanced Scientific Research, India

Hydrogen is a recyclable and clean fuel, as it generates water after its use in combustion, and the water can be split to generate hydrogen back. The latter is a crucial step and can be facilitated through use of a photocatalyst in splitting of water into hydrogen gas by accessing solar energy, another important source of energy for the planet. The present work aims to investigate the effect of Fe and Ru doping on BaTiO<sub>3</sub> for its possible application in photoelectrochemical splitting of water using both first-principle based DFT calculations and experiments. BaTiO<sub>3</sub> with 0.5 – 4.0 at.% Fe & Ru doping is synthesized via polymeric precursor route and characterized with X-Ray Diffractometer (XRD), Scanning Electron Microscopy (SEM), High Resolution Transmission Electron Microscopy (HR-TEM), UV-Vis Spectroscopy, Mossbauer Spectroscopy. The origin of the observed activity in the visible range is traced through calculated electronic structure to

the electronic states associated with Fe at energies within the band-gap. A reasonable agreement between the changes in measured spectra and those in calculated electronic structure augurs well for a judicious use of first-principles calculations in screening of dopants in design of doped oxide materials with enhanced photoelectrochemical activity, such as that of Fe-doped BaTiO<sub>3</sub> demonstrated here.

#### (ICACC-S7-P093-2012) Solubility of NiO in Pechini-derived ZrO<sub>2</sub> Examined with SQUID Magnetometry

J. T. White, I. E. Reimanis, Colorado School of Mines, USA; J. R. O'Brien, Quantum Design, Incorporated, USA; A. Morrissey\*, Colorado School of Mines, USA

ZrO<sub>2</sub> ceramics containing NiO are crucial in energy conversion applications, such as solid oxide fuel cell anodes, and also in structural components such as plasma-sprayed thermal barrier coatings for jet engine turbine blades. However, the effect of NiO on phase stability and microstructure of ZrO<sub>2</sub> is not well-understood. The present study examines the solubility of NiO in ZrO<sub>2</sub> by x-ray diffraction, TEM, and SQUID magnetometry. Lattice parameter measurements from a similar, established oxide system, NiO-10YSZ, were first used to show that SQUID magnetometry can effectively measure solubility. ZrO<sub>2</sub> specimens with 0, 0.5, 1, 2, 3 and 5 percent by mol NiO were prepared via the Pechini method. The specimens were calcined in air at 500, 600, and 1000°C. The paramagnetic response of the specimens measured with SQUID magnetometry revealed that up to 5 percent by mol NiO is soluble in ZrO<sub>2</sub> for specimens calcined at 500 and 600°C. The relatively large solubility compared with NiO-10Y SZ occurs due to the very fine grain size (5 - 10 nm). The fine grain size is also responsible for stabilizing the tetragonal phase of ZrO<sub>2</sub>. At the 1000°C calcination temperature, the ZrO<sub>2</sub> is entirely monoclinic, exhibits larger grains (> 45 nm), and only dissolves about 0.5 percent by mol or less NiO. The correlations between grain size, ZrO<sub>2</sub> polytype, and NiO addition are discussed.

#### (ICACC-S7-P094-2012) Optimisation of Spray Freeze Dried Nanozirconia Granules

Y. Zhang\*, J. Binner, C. Rielly, B. Vaidhyanathan, Loughborough University, United Kingdom

Granulation of nanostructured 3 mol% yttria stabilised zirconia (3YSZ) has been investigated via spray freeze drying to achieve flowable and crushable granules to be used for subsequent die pressing. The precursor nanosuspension with a primary particle size of  $\sim 16$  nm has been concentrated to 55 wt% (16.8 vol%) solid contents via a patented technique, followed by spraying into liquid nitrogen via a twin-fluid atomiser at a controlled spray flow rate. Spherical granules with good flowability have been achieved via a subsequent freeze drying process at -62oC, 50 mtorr conditions for 48 hours, whilst up to 56% green density has been obtained after die pressing a specific size fraction of the granules, viz. 125 to 250  $\mu$ m, at a conventional pressing pressure of 200 MPa. A density of 99.5% of theoretical after sintering has been achieved using both conventional radiation two step sintering and microwave hybrid sintering. Controlling the size fractions of the spray freeze dried granules has also been investigated to improve the production efficiency. Granules retaining good crushability for die pressing are in the size range 125 to 250  $\mu$ m, which have been achieved with yields of  $\sim 50$ % by weight via atomisation, whilst only  $\sim 30$  wt% granules in this size range were produced in previous research at Loughborough University using an ultrasonic spray process.

#### (ICACC-S7-P095-2012) Chemical Vapor Deposition Growth of Carbon Nanotubes on Carbon Fiber

W. McKinley\*, K. Wu, Florida International University, USA; A. Datye, University of Tennessee, USA; M. Gomes, J. Karpf, A. Zaretski, Florida International University, USA

A method to grow Carbon Nanotubes (CNT) on Carbon Fibers (CF) by chemical vapor deposition (CVD) is studied with various catalysts and CF surface conditions. CF is a low density, high strength material which has many applications in composites. CNT's have shown

excellent mechanical and thermal properties. The two main barriers to utilizing the properties of such a composite have been uniform distribution of the CNT's within the matrix and interfacial bonding of the CNT's to the substrate. Uniform distribution has been achieved by stirred CVD growth of CNT's directly on the CF. It is proposed that a high interfacial strength can be realized by the Carbon to Carbon bond. The synthesis parameters are studied in relation to the interaction of the catalyst with the various CF surface modifications. The distribution of CNT's are examined using SEM and the characteristics are investigated using TEM and Raman. The surface conditions under study are with sizing intact, with sizing removed via chemical process and pyrolyzed sizing. Cobalt catalyst concentrations from 0.1 %wt to 5 %wt are examined for each surface condition. The results show optimal growth on the pyrolyzed sizing CF surface with a catalyst content of 0.6 %wt.

### (ICACC-S7-P096-2012) Titania Suspension for Fabrication of Micron Feature Arrays via Template-assisted Approach

K. Lu\*, Y. Liang, Virginia Tech, USA

In this study, TiO<sub>2</sub> nanoparticle suspension is guided by polymeric templates during shaping to fabricate novel micron feature arrays. TiO<sub>2</sub> nanoparticle suspensions are made using polyethylene glycol (PEG) as the dispersant under ball milling. Polydimethylsiloxane (PDMS) molds are used to regulate and confine nanoparticles into pre-determined pattern arrays. The effects of PEG with different molecular weights are investigated, and the surface wettability between the molds and the TiO<sub>2</sub> nanoparticle suspensions has been studied. The results show that PEG 400 has the best dispersibility and the suspension has better wetting on Au coated PDMS surfaces, which decrease the adherence of TiO<sub>2</sub> nanoparticle features to the PDMS mold. Micron feature arrays (ranging from 1 μm to 2 μm) are obtained. The fundamental understanding of the process is discussed.

### (ICACC-S7-P097-2012) Enhanced Properties of Multiferroic Nanocomposite Materials

J. Starr, J. S. Andrew\*, University of Florida, USA

Multiferroic materials exhibit both ferromagnetic and ferroelectric properties, which tend to be mutually exclusive in single-phase materials. Therefore, composite materials are the obvious approach to developing a material with both a high electric permittivity and high magnetic permeability. In composite systems the magnetoelectric effect arises from the mechanical coupling between magnetostrictive and piezoelectric phases. Magnetoelectric coupling in composite systems is an interfacial phenomenon. To enhance this coupling, the interfacial area between the two phases should be maximized. This can be accomplished using nanoparticles, which have a large surface area-to-volume ratio. Ceramic multilayer multiferroic materials are plagued with porosity and cracking at the interfaces between the two phases, resulting in reduced performance. To avoid the limitations of these ceramic composites nanostructured ferroelectric polymer-magnetic nanoparticle (PVDF-Ni<sub>0.5</sub>Zn<sub>0.5</sub>Fe<sub>2</sub>O<sub>4</sub>) and BaTiO<sub>3</sub>-CoFe<sub>2</sub>O<sub>4</sub> composites with enhanced properties have been prepared via electrospinning. The effects of the electrospinning processing conditions on resultant material properties including the fiber morphology, crystallinity and the crystalline structure of the nanocomposites were investigated. SQUID magnetometer and dielectric measurements were also performed to determine the materials' magnetic and dielectric properties.

### (ICACC-S7-P098-2012) Laser-Induced Enhanced Plasmonic Response in Ag Nanocomposite Glasses Monitored in Real Time via In Situ Optical Microspectroscopy

J. A. Jimenez\*, University of North Florida, USA; M. Sendova, New College of Florida, USA

Ag nanoparticle (NP) doped glasses displaying dissimilar surface plasmon resonance (SPR) spectral features were prepared by melting and heat treatment (HT) processes, and subsequently irradiated with a ns Nd:YAG laser operating at 532 nm (fluence of 150 mJ/cm<sup>2</sup>).

Laser treatment was observed to produce a plasmon absorption vanishing effect, pronounced for the more red-shifted SPR peaks. The resulting non-plasmonic photo-fragments are most likely neutral Ag clusters and/or atoms, as suggested by photoluminescence spectroscopy measurements. Additional structural elucidation by Raman spectroscopy shows no significant modification of glass structure induced by the laser. In situ monitoring of the plasmonic evolution during HT of a sample showing complete SPR vanishing after irradiation revealed an enhanced temperature- and time-dependent optical response. Transmission electron microscopy shows that the resulting NPs are clustered, and have a small size and narrow distribution. Strong electrodynamic interactions between closely spaced NPs seem to be the cause for the peculiar SPR development.

## S8: 6th International Symposium on Advanced Processing and Manufacturing Technologies for Structural and Multifunctional Materials and Systems (APMT) in honor of Professor R. Judd Diefendorf

### Symposium 8: Poster Session

Room: Exhibit Hall

### (ICACC-S8-P099-2012) Research in Recycling Technology of Fiber Reinforced Polymers by Superheated Steam: Effect of Surface Treatment on Recycled Glass Fiber

J. Shi\*, Interdisciplinary Graduate School of Science and Technology of Shinshu University, Japan; R. Kobayashi, J. Katou, L. Bao, Faculty of Textile Science and Technology, Shinshu University, Japan

In order to achieve the good adhesion between unsaturated polyester resin and recycled glass fibers on which there were some char impurities, a surface treatment should be carried out to remove them. Soaked recycled glass fibers in two different solution- acetone and haita (a kind of kitchen lotion) for 4 to 24 hours. Then surface cleaning was performed. Recycled glass fibers were washed in acetone and haita for 1 hour respectively by ultrasonic cleaning machines. After surface cleaning, the recycled glass fibers were remanufactured to glass fiber reinforced polymers (GFRP). Bending test was carried out to evaluate the effects of detergent and soaking time. Samples of washed, recycled and virgin fibers were analyzed by using scanning electron microscopy to determine visual signs of residual char impurities. SEM pictures showed char impurities would decrease after surface cleaning by ultrasonic cleaning machines. Although haita can make work life more environmental friendly, SEM micrographs indicated that there were less residual char impurities on glass fiber which cleaned by acetone. Results of bending test showed that bending strength of remanufactured GFRP can be preserved about 90% of that of virgin GFRP. The recycled glass fibers were able to be used as a feed-stock for remanufactured GFRP with high Mechanical properties.

### (ICACC-S8-P100-2012) Microstructure and Dielectric Properties of MnCO<sub>3</sub> and Nb<sub>2</sub>O<sub>5</sub> Doped BaTiO<sub>3</sub>-ceramics

V. Mitic\*, V. Paunovic, J. Purenovic, J. Nedin, Faculty of Electronic Engineering, Serbia; M. Miljkovic, Laboratory for Electron Microscopy, Serbia

The goal of the present investigation was to study the influence of MnCO<sub>3</sub> and Nb<sub>2</sub>O<sub>5</sub> on BaTiO<sub>3</sub>-ceramics microstructure properties. Samples were prepared from Murata BaTiO<sub>3</sub>, MnCO<sub>3</sub> and Nb<sub>2</sub>O<sub>5</sub> powders and sintered up to 1350°C. Microstructure properties of BaTiO<sub>3</sub>-ceramics doped from 0.5 to 1.5 wt % of MnCO<sub>3</sub> and Nb<sub>2</sub>O<sub>5</sub> have been studied using scanning electronic microscopy method. The purpose of this paper was to determinate the correlation between technological parameters and microstructural characteristics of BaTiO<sub>3</sub>-ceramics with MnCO<sub>3</sub> and Nb<sub>2</sub>O<sub>5</sub>, as well as to determine the influence of additives on the microstructure of BaTiO<sub>3</sub>-ceramics

materials. Obtained results provided determination of the influence of  $\text{MnCO}_3$  and  $\text{Nb}_2\text{O}_5$  on structure as well as on final electrical and ferroelectric properties of  $\text{BaTiO}_3$ -ceramics. The model of impedances, between clusters of ceramics grains, especially with fractal pyramids by Sierpinski, has been presented and calculations of microcapacitance generated in grains contacts of doped  $\text{BaTiO}_3$  have been performed.

**(ICACC-S8-P101-2012) Additives for the Preparation of Al- $\text{Al}_2\text{O}_3$ -Precursor Powders**

N. Holstein\*, T. Schloridt, University of Applied Science Koblenz, Germany; R. Janssen, Hamburg University of Technology, Germany; J. Kriegesmann, University of Applied Science Koblenz, Germany

The concept of Reaction-Bonded-Aluminum-Oxide (RBAO) processing provides the basis for technologies of several advanced ceramic composites. Therefore the preparation of a fine grained, homogeneously precursor is a fundamental requirement for the corresponding ceramics exhibiting dense and uniform microstructures and hence good mechanical properties. RBAO precursor powders were prepared using 45 vol.-% aluminum and 55 vol.-% alumina powders, respectively. The relating powder-mixtures were wet-ground in an attrition mill using non-aqueous milling liquids. Owing to this intensive grinding process, the resulting metal ceramic powder mixtures are extremely reactive. The consequence is formation of oxide and hydroxide during and after the milling process because of the hygroscopic and pyrophoric properties of fine-grained metal powders. Organic additives like stearic acid and citric acid can passivate the surface of the metal powder particles, which inhibits the formation of hydroxides. Their effectiveness is characterized by thermogravimetric analysis and resistance to hydrolysis. The resulting higher aluminum proportion after grinding promotes the reaction bonding process. Furthermore the use of additives enables the manufacturer to adjust the surfaces of the metallic powder particles so that they act either in a hydrophobic or in a hydrophilic manner. This is important for the subsequent shape-forming process.

**(ICACC-S8-P102-2012) Laser machining of melt infiltrated ceramic matrix composite**

G. Ojard\*, Pratt & Whitney, USA; D. Jarmon, United Technologies Research Center, USA; D. Brewer, NASA - Langley Research Center, USA

As interest grows in considering the use of ceramic matrix composites for critical components, the response of the ceramic matrix composites to differing machining and the resulting machined surface condition needs to be understood. To this end, this work presents the characterization of a Melt Infiltrated  $\text{SiC}/\text{SiC}$  machined by different methods. While a range of machining approaches were considered, only diamond grinding and laser machining were performed on a series of tensile coupons. The tensile coupons were exposed to a steam environment while under stress. The samples were then tested for residual tensile capability. The data clearly differentiated the laser machining as having the better capability for the samples tested. These results along with micro-structural characterization will be presented.

**(ICACC-S8-P103-2012) De- $\text{NO}_x$  Evaluation of SCR Catalyst Fabricated Using Aluminum Dross**

M. Bea\*, H. Kim, K. Kim, M. Lee, Korea Institute of Industrial Technology, Republic of Korea

Aluminum dross waste is an unavoidable by-product of the aluminum production process. It forms at the surface of the molten metal as the latter reacts with the furnace atmosphere. Furthermore, it has not been sufficiently recycled yet. The purpose of this study is to investigate the De- $\text{NO}_x$  evaluation of  $\text{V}_2\text{O}_5$ - $\text{WO}_3$ - $\text{TiO}_2$ - $\text{Al}_2\text{O}_3$  Selective Catalyst Reduction (SCR) prepared using recycled Al-dross. Al dross was used as precursors  $\text{Al}_2\text{O}_3$  As to experimental procedures, Al dross was classified according to its size. The Al dross smaller than 300 $\mu\text{m}$  was leached with sodium hydroxide solution to extract the remaining aluminum from the dross into the solution, and then alu-

minum hydroxide precipitate was recovered from the leached liquor. The recycled Al dross was made into SCR catalyst by mixing with  $\text{WO}_3$ ,  $\text{V}_2\text{O}_5$  and  $\text{TiO}_2$ . The  $\text{NO}_x$  removal activity and sulfur tolerance of SCR catalyst with respect to the contents of  $\text{Al}_2\text{O}_3$  were observed by MR(Micro-Reactor). SCR using aluminum dross are comparable with that of the commercial products.

**(ICACC-S8-P104-2012) Effect of Debinding and Sintering Condition on Thermal Conductivity of Pressureless Sintered AlN Ceramics**

S. Lee\*, Mokpo National University, Republic of Korea; S. Na, S. Kim, S. Go, YJC CO., LTD., Republic of Korea

Aluminum nitride (AlN) has excellent properties such as high thermal conductivity and electrical resistivity, whereas it has some disadvantage such as low sinterability. In this study, the effect of debinding condition, yttria additive content and sintering time on thermal conductivity of AlN was examined. Spray dried AlN powders containing 1~3 wt% yttria additive and PVB binder were heated at 600 °C in air or nitrogen atmosphere for debinding and then pressureless sintered at 1900 °C in nitrogen atmosphere for 2~5 h. All AlN specimens showed higher thermal conductivity as the additive content and time increase. The thermal conductivity of AlN specimens was promoted by the addition of yttria because of the yttria addition could reduce the oxygen contents in AlN lattice. Also, thermal conductivity was improved by the increase of sintering time because of the uniform distribution and the elimination of secondary phases from the grain boundary due to the evaporation. In the case of the debinding effect, the AlN specimen treated in nitrogen atmosphere showed higher thermal conductivity and darker grey color. The measured thermal conductivity of AlN specimen added 3 wt% yttria and sintered at 1900 °C for 5 h after debinding in nitrogen atmosphere was 180~200 W/mK.

**(ICACC-S8-P105-2012) Thermal and Dielectric Properties of Metal Substrate Coated for Ceramic-Based Insulating Thin Film**

S. Honda\*, Y. Takeuchi, Nagoya Institute of Technology, Japan; N. Komada, Meijyo University, Japan; H. Usami, Meijyo University, Japan; Y. Iwamoto, Nagoya Institute of Technology, Japan

Ceramic-based composite thin film was fabricated on an aluminum substrate for adding the insulative ability. After the surface of aluminum substrate was modified by ceramic particles, amorphous silica thin film layer could be successfully coated using spin coating by in-situ formation below 423 K through ammonia-catalyzed oxidation of perhydropolysilazane (PHPS). The FT-IR and SEM analysis were clarified that thin amorphous silica layer with a thickness of approximately 1 micron was successfully fabricated on an aluminum substrate. Relationships between the ratio of the ceramic particles/silica of the composite film, thickness, and thermal diffusivity, dielectric breakdown properties were evaluated. Amorphous silica-based composite thin film could be synthesized on an aluminum substrate at room temperature by surface modification treatment followed by PHPS coating and subsequent oxidation. The surface modification treatment was found to be effective for minimizing the decrease in the thermal conductivity and increasing in the electrical resistance of the aluminum substrate by the surface composite thin layer formation.

**(ICACC-S8-P106-2012) Structural and optical properties of  $\text{Zn}_{1-x}\text{Mg}_x\text{O}$  blue phosphors synthesized by chemical solution method**

Y. Inata\*, Nagoya Institute of Technology, Japan; K. Inoue, Mie Prefecture Industrial Research Institute, Japan; S. Honda, S. Hashimoto, Y. Iwamoto, Nagoya Institute of Technology, Japan

Hexagonal  $\text{Zn}_{1-x}\text{Mg}_x\text{O}$  exhibits high luminescent efficiency under the low-voltage cathodoluminescence conditions, and thus can be expected to use as a novel blue phosphor for Vacuum Fluorescent Display (VFDs). However, the maximum Mg content in  $\text{ZnO}$  is 2 mol% by the conventional solid state reaction method, and the emission is green-like blue. Chemical solution method is an attractive synthesis method to realize the Mg-heavy doping to  $\text{ZnO}$  because the chemical

composition of the materials can be strictly regulated by using metal-organic monomer precursors such as metal alkoxides. In this study, Mg-heavy doped hexagonal Zn<sub>1-x</sub>Mg<sub>x</sub>O solid solutions were successfully synthesized by the chemical solution method. The formations of the solid solutions were identified by assigning their crystal structures together with the evaluations of their lattice constants using XRD analyses. The optical properties of the solid solutions were analyzed by PL measurement and investigated the emission blue shift by the Mg-heavy doping. In addition to their investigations, Hexagonal Zn<sub>1-x</sub>Mg<sub>x</sub>O thin films were fabricated by the chemical solution method. Their structural and optical properties will be also reported at the conference.

**(ICACC-S8-P107-2012) Mechanochemical Synthesis of ReB<sub>2</sub> Powder**  
N. Orlovskaya, Z. Xie\*, M. Klimov, H. Heinrich, D. Restrepo, R. Blair, C. Suryanarayana, University of Central Florida, USA

ReB<sub>2</sub> was recently reported to exhibit high hardness and low compressibility, which both are strong functions of its stoichiometry, namely Re to B ratio. Most of the techniques used for ReB<sub>2</sub> synthesis reported 1:2.5 Re to B ratio because of the loss of the B during high temperature synthesis. However, as a result of B excess, the amorphous boron, located along the grain boundaries of polycrystalline ReB<sub>2</sub>, would degrade the ReB<sub>2</sub> properties. Therefore, techniques which could allow synthesizing the stoichiometric ReB<sub>2</sub> preferably at room temperature are in high demand. Here we report synthesis of ReB<sub>2</sub> powders using mechanochemical route by milling elemental crystalline Re and amorphous B powders in the SPEX 8000 high energy ball mill for 80 hours. The formation of boron and perhenic acids are also reported after mechanochemically synthesized ReB<sub>2</sub> powder was exposed to the moist air environment for a twelve month period of time.

**(ICACC-S8-P108-2012) Flash sintering mechanisms in fully dense yttria-stabilized zirconia**  
J. Downs\*, University of Trento, Italy; R. Raj, University of Colorado, USA; V. M. Sglavo, University of Trento, Italy

The flash sintering phenomena has recently been well documented but the underlying mechanisms are still under investigation. In this work, DC I-V characterization of samples of fully dense 8YSZ was done. Fully dense samples show similar flash regime behaviors that have been seen in green bodies while eliminating the associated dimension changes. Characterization was done using four point measurements at various isotherms from 500-900C in static air. Conductivity measurements were made from low voltage to the onset of flash sintering behavior with respect to grain size and voltage ramping rate. Initial studies showed that there is no retention or change of sample conductivity after a sample has reached the flash regime. This would also suggest that there is little grain growth in the presence of the electric field despite the high temperatures reached while the samples are being internally heated. Results also often show the initiation of a secondary conduction mechanism or a region of stability where there is a non-continuous change in resistance. Then the sample transitions into a non-linear zone characterized with the runaway current and passage into the flash sintering regime. The passage through these transitions is suspected to be the point where flash sintering is initiated as a result of additional carriers.

## S10: Thermal Management Materials and Technologies

### Symposium 10: Poster Session

Room: Exhibit Hall

**(ICACC-S10-P114-2012) Examination of the Interconnectivity of SiC in a Si:SiC Composite System and the Effects on Thermal Properties**

A. Marshall\*, M Cubed Technologies, Inc., USA

Composites of silicon carbide particles (SiCp) and silicon (Si) are fabricated by the reactive infiltration of molten Si into preforms of

said particles and carbon. Depending upon the application, these materials can be used in many situations due to their favorable properties including high hardness, low thermal expansion, high thermal conductivity and high stiffness. Through heat treatment methods, necking of the SiCp is promoted in the pre-infiltration state which will allow further tailoring of material properties. This study examines the effects of firing temperature and firing time on Young's modulus, thermal expansion, thermal conductivity, and the interconnectivity of the SiCp. Interconnectivity will be examined through optical microscopy methods, SEM analysis, and mechanical means.

**(ICACC-S10-P115-2012) Extremely high thermal properties of Boron Nitride-epoxy composite with high orientation**

K. Miyata\*, T. Yamagata, Denki Kagaku Kogyo Kabushiki Kaisha, Japan; T. Adschiri, Tohoku University, Japan

Electronic packaging materials are used in a wide range of devices. The heat transfer in electronic packaging materials is becoming important issue, as the demands in denser and faster circuits intensify year by year. Thus, composite materials of high thermal conductivity filler and matrix resin attract keen attentions in this field, and many R&Ds have been reported recently. In this paper, we demonstrate that extremely high thermal conductivity with maintaining high dielectric strength could be obtained for the boron nitride-epoxy matrix composite materials by the high orientation of fillers. We made the composite using flake-like boron nitride crystals with anisotropic thermal conductivity, and epoxy resin. In this study, we established an advanced share-applying technology, which can increase the filling ratio of the fillers and at the same time orient the fillers (either vertically or horizontally) in epoxy matrix. The thermal conductivity of this composite corresponded well with estimation. Then, the result of this study shows excellent properties, which match with the requirement of the devices: Thermal conductivity of 36.2 W/mK, dielectric strength of 25kV/mm, and the coefficient of thermal expansion of 1.8ppm at 80vol% of boron nitride, which are obviously better properties than alumina (Al<sub>2</sub>O<sub>3</sub>) ceramic materials.

## S11: Nanomaterials for Sensing Applications: From Fundamentals to Device Integration

### Symposium 11: Poster Session

Room: Exhibit Hall

**(ICACC-S11-P116-2012) Theoretical Modeling of NH<sub>3</sub> Adsorption on SnO<sub>2</sub>**

F. Shao\*, Institut de Recerca en Energia de Catalunya (IREC), Spain; N. López, Institut Català d'Investigació Química (ICIQ), Spain; F. H. Ramírez, Institut de Recerca en Energia de Catalunya (IREC), Spain; J. D. Prades, Universitat de Barcelona, Spain; J. R. Morante, Institut de Recerca en Energia de Catalunya (IREC), Spain

In order to unveil the detailed sensing mechanism of NH<sub>3</sub> in the mostly find metal oxide material SnO<sub>2</sub>, we applied ab-initio density function theory simulation to analyze the reactivity of NH<sub>3</sub> molecules onto the (110) rutile surface of SnO<sub>2</sub>. In this work, the generalized gradient approximation (GGA) and the revised Perdew-Burke-Ernzerhof (rPBE) exchange correlation functional were used. The adsorption energies of NH<sub>3</sub> molecule on different surface sites were calculated and the optimized adsorption configurations were determined. In addition, nudged elastic band (NEB) method was applied in order to find the transition states and activation energy barriers of the postulated reaction routines involving surface bridging O. This information will help us to predict the kinetics of metal oxide sensors and evaluate their experimental behavior. The theoretical results will be compared to experimental measurements obtained with gas sensors made up of individual SnO<sub>2</sub> nanowires (Fig.2). Finally, a critical analysis of the performance of SnO<sub>2</sub> nanowires as ammonia sensors on the basis of both the theoretical and experimental approach will be presented.

**(ICACC-S11-P117-2012) Nanowire based gas sensors in wireless and power-autonomous detector systems**

J. Llosa, Universitat de Barcelona, Spain; M. Martínez de Marigorta, J. Bécarea, WorldSensing, S.L.N.E., Spain; O. Monereo, J. Prades\*, Universitat de Barcelona, Spain; F. Hernandez-Ramirez, Institut de Recerca en Energia de Catalunya (IREC), Spain; I. Vilajosana, WorldSensing, S.L.N.E., Spain; S. Mathur, Universität zu Köln, Germany; A. Cirera, Universitat de Barcelona, Spain

For years the need of heating the sensing materials has kept the power needed to operate conductometric gas sensors, such as the ones based on metal oxides, above the mW range. Today, the self-heating effect in nanowires allows us to reduce such value to a few  $\mu\text{W}$ . This minute power requirements makes possible considering, for the first time, energy harvesting techniques as a suitable power sources for such applications. After the first proof-of-concept devices, we present now the fully functional prototypes that integrate individual nanowires, wireless communications and energy harvesting and accumulation systems that features fully autonomous operation. The control and communication functionalities are based on the Atmel ZigBit module. All these components rendered power consumption values lower than 30 $\mu\text{W}$  using duty cycling techniques. The power processing subsystem relays on a Si-based photovoltaic panel that stores its energy in a rechargeable battery using a supercapacitor to improve the battery life and the number of charging cycles. The system displays an autonomous response to gases such as CO, NO<sub>2</sub>, NH<sub>3</sub>, temperature and humidity that can be recorded remotely with the help of a small embedded computer or a common PC. Stress test showed that the system can keep operating in real Sun illumination conditions continuously without component failure or power drain.

**(ICACC-S11-P118-2012) Insight into ethanol sensing mechanism and its relation with humidity using individual SnO<sub>2</sub> nanowires**

J. Prades, Universitat de Barcelona, Spain; F. Hernandez-Ramirez, J. Morante\*, Institut de Recerca en Energia de Catalunya (IREC), Spain

Time resolved spectroscopy using individual nanowires was applied to study the sensing mechanisms based on the chemical interaction of ethanol molecules with the SnO<sub>2</sub> surface and the potential influence of different active sites present or generated at the surface of the metal oxides. Due to the limitation of the thermal inertia response of the system, study has been performed at temperature below 215degC. In this range, there is a predominance of the absorbed molecular oxygen instead that mono atomic oxygen. Under these conditions, the response against different ethanol conditions and humidity's ranging from dry ambient to 100% of humidity at room temperature has been studied with details from the sensor response amplitudes and response time constant. At these conditions, the results confirm that ethanol molecule is decomposed giving rise to a water molecule. Likewise, it is found that is this one the responsible of the electrical signal obtained from the conductometric measurement. Data have been probed with those obtained from simple humidity effect. It corroborates the sensing mechanism associated to the ethanol detection, its simulation and , at the same time, it shows the powerful of the used experimental techniques for studying and characterizing sensing materials in order to collect data for ab initio simulation as well as for adequate sensing material selection.

**(ICACC-S11-P119-2012) Metal oxide mesoporous structures for resistive CO<sub>2</sub> gas sensors**

T. Andreu, M. Manzanares, J. Morante\*, Catalonia Institute for Energy Research (IREC), Spain; J. Morante, University of Barcelona, Spain

Metal oxide mesoporous structures decorated with catalyst additives are proposed as sensing materials for CO<sub>2</sub>. High conductometric sensor responses to CO<sub>2</sub> are presented with  $R_{\text{gas}}/R_0 > 20$  at 1000 ppm and sensitivity, slope of  $\log R_{\text{gas}}/R_0$  versus  $\log [\text{CO}_2]$ , approximately of 1. Usually, the potential CO<sub>2</sub> detection using conductometric based gas sensors is still hidden for effects such as gas diffusion, layer porosity, gas exhausting phenomenon or not optimized nanomaterial for transduction processes. The proposed sensing materials are based

on CaO functionalized In<sub>2</sub>O<sub>3</sub> mesoporous structures that present very small size nanocrystals, about 10nm, to enhance the effects of the CO<sub>2</sub> chemical to electrical transduction on the resistance variation. Moreover, these mesoporous materials have a high level of porosity, porous diameter about 12 nm, to facilitate the gas diffusion through the sensing material. These characteristics have been complemented by selecting the thickness of the sensing layer between the compromise for reducing the baseline resistance, as the reduced size and the catalyst introduction increase highly this resistance, and for avoiding gas consumption and, hence, CO<sub>2</sub> exhauster zones through the layer. In such frame, In<sub>2</sub>O<sub>3</sub> has been identified better reception material than other usual metal oxides and alkaline earth as reliable additives enhancing the detection of CO<sub>2</sub> molecules.

**S12: Materials for Extreme Environments: Ultrahigh Temperature Ceramics (UHTCs) and Nanolaminated Ternary Carbides and Nitrides (MAX Phases)****Symposium 12: Poster Session**

Room: Exhibit Hall

**(ICACC-S12-P120-2012) Thermal expansion and structural parameters of Cr<sub>2</sub>(Al<sub>x</sub>Ge<sub>1-x</sub>)C studied by X-ray diffraction**

T. Cabioch\*, University of Poitiers, France; P. Eklund, Linköping University, Sweden

MAX phases form isostructural solid solutions both on M-, A-, and X-sites. This allows studies of the correlation of structure and chemistry with physical properties and offers the possibility for property tuning. In this study, porous samples containing mainly the Cr<sub>2</sub>Al<sub>x</sub>Ge<sub>1-x</sub>C MAX phase were obtained by pressureless sintering (4h at 1400°C, Ar flow) of Cr, Al, Ge and graphite powders. The evolution of the structure (lattice parameters, coordinate  $z_{\text{Cr}}$ , ...) as a function of the aluminum content x was studied at room temperature by Rietveld refinement of XRD patterns. A linear evolution of the lattice parameters as well as that of  $z_{\text{Cr}}$  is obtained. XRD patterns obtained from room temperature up to 800°C allow to deduce the thermal expansion  $\alpha_a$  and  $\alpha_c$  of the lattice parameters, a and c respectively. Whereas  $\alpha_a > \alpha_c$  for Cr<sub>2</sub>AlC ( $\alpha_a = 16.3 \times 10^{-6} \text{ K}^{-1}$ ;  $\alpha_c = 13.2 \times 10^{-6} \text{ K}^{-1}$ ), it is the inverse for Cr<sub>2</sub>GeC ( $\alpha_a = 14.6 \times 10^{-6} \text{ K}^{-1}$ ;  $\alpha_c = 18.6 \times 10^{-6} \text{ K}^{-1}$ ). These measurements confirmed that these two studied compounds behave the largest values of thermal expansion of the MAX phases known up to now. Furthermore, an almost linear evolution of the  $\alpha_a$  and  $\alpha_c$  thermal expansion coefficient is obtained when x is varied, an isotropic behavior ( $\alpha_a = \alpha_c$ ) being even obtained for x=0.5. This study clearly confirms the possibility of tuning some of the MAX phase properties by synthesizing solid solutions.

**(ICACC-S12-P121-2012) Ultrarefractory carbides for applications in Concentrating Solar Power systems**

D. Sciti\*, L. Silvestroni, ISTECC-CNR, Italy; J. Sans, L. Charpentier, M. Balat-Pichelin, L. Mercatelli, CNRS, France; E. Sani, CNR, Italy

Solar thermal technology is a safe and cost-effective energy supply. The maximum operating temperatures of a solar power plant are usually less than 900 K because of the rapid degradation of its components. However, the efficiency of solar thermal power plants increases rapidly with increasing working temperatures, so that the problem has to be solved by improving the high temperature stability, especially of the receiver. This work is devoted to the characterization of pure and doped ZrC and TaC, in terms of room and high temperature thermo-mechanical and optical properties, in view of their possible application as solar absorbers. High-temperature emissivity of UHTC carbides is compared to that of Silicon Carbide, as the latter is conventionally used in volumetric solar absorbers. The measurements show a lower emissivity of Zirconium Carbides and Tantalum Carbides with respect to SiC at all the investigated temperatures, from 1100 to 1400 K. This demonstrate that UHTC carbides have favorable

emissivity properties, arising in a good thermal energy storage capability with minimal radiative losses. In addition, high temperature oxidation of a ZrC composite in a solar facility is conducted in the temperature range 1800-2400 K in air, in order to partially reproduce the operating conditions of a high-temperature solar receiver.

### (ICACC-S12-P122-2012) Effect of Oxy-acetylene Torch Test Flame Conditions on the Ablation Resistance of Ultra-High Temperature Ceramic Composites at Elevated Temperatures

M. A. Valdez\*, W. R. Pinc, L. S. Walker, E. L. Corral, University of Arizona, USA

The extreme aero-thermal environments that hypersonic vehicles undergo require materials for thermal protection systems (TPS) that exhibit a strong degree of high temperature mechanical and oxidation resistant properties, such as ZrB<sub>2</sub>-SiC. However, in order to evaluate the suitability of a material for TPS application, oxidation testing facilities that simulate the extreme environment of hypersonic flight must be used. An oxy-acetylene torch can simulate the high heat fluxes and temperatures that TPS materials undergo during flight. The oxy-acetylene torch flame, however, is not clean and contains many species not normally found in the hypersonic flight environment. Therefore in order to understand how the flame chemistry affects oxidation, we measured ablation rates of ZrB<sub>2</sub>-SiC (25 vol %) using a stoichiometric flame as well an oxygen-rich flame at 1500 and 1700°C. Scanning electron microscopy (SEM) is used to analyze the ablated surfaces as well as the cross-sections of the samples. The results of this test will allow us to determine the optimal oxy-acetylene torch conditions for future oxidation tests of high temperature materials.

### (ICACC-S12-P123-2012) Mechanical Properties & Residual Thermal Stresses of Spark Plasma Sintered ZrB<sub>2</sub>-SiC Composites

R. Stadelmann\*, N. Orlovskaya, University of Central Florida, USA; V. Sglavo, University of Trento, Italy

Ultra High Temperature Ceramic (UHTC) ZrB<sub>2</sub>-10, 20, 30wt%SiC composites are of high interest for hypersonic air-breathing vehicles. In this work ZrB<sub>2</sub>-10, 20, 30wt%SiC UHTC composites were produced by Spark Plasma Sintering (SPS) technique. After sintering, almost dense ceramics with ~ 5-8% porosity were produced. Their mechanical properties, such as Young's modulus, 4-point bending strength, and SEVNB fracture toughness were measured. In addition, the attempt was made to determine the thermal residual stresses in SiC phase of two phase composites by using micro-Raman spectroscopy. The results show that these materials are a possible candidate for hypersonic air-breathing vehicles with its high Young's modulus, ability to withstand high temperatures, and a relatively low density.

### (ICACC-S12-P124-2012) Oxidation-resistant ZrB<sub>2</sub>-SiC composites

A. Goodarzi\*, Amirkabir University of Tech., Islamic Republic of Iran; H. Taylor, Imperial College London, United Kingdom

Oxidation resistance tests were carried out on hot-pressed ZrB<sub>2</sub>-20 vol%SiC using an oxyacetylene torch. The temperature of the oxidized specimens exceeded 2200 C. The mass and linear oxidation rates of the ZrB<sub>2</sub>-20 vol%SiC composites for 10 min were -0.23 mg/s and 0.66 lm/s, respectively. The surface layer appeared dense and adherent with the exception of a few burst bubbles and craterlets. No macro-cracks or spallation were detected after oxidation, suggesting that these composites possess a super oxidation resistance. The microstructure of the surface and cross-section of the oxidized specimens were studied by scanning electron microscopy along with energy dispersive spectrometry and X-ray diffraction. The oxidation mechanism was also discussed. The formation of high pressure gaseous phases (i.e., B<sub>2</sub>O<sub>3</sub> and SiO) led to the generation of a significant amount of pores. SiC was no longer responsible for the improvement in oxidation resistance of the composites in the present case. ZrO<sub>2</sub> recrystallized into a dense coherent subscale, which protected the underlying ceramic from catastrophic oxidation.

### (ICACC-S12-P125-2012) Tensile Creep of Coarse-Grained Ti<sub>2</sub>AlC in the 900-1150 °C Temperature Range

D. J. Tallman\*, M. Abdelmalak, M. Barsoum, Drexel University, USA

The tensile creep of coarse-grained, CG, Ti<sub>2</sub>AlC samples, in the 1000-1150 degreesC temperature, T, and 5 MPa to 70 MPa stress, sigma, ranges, respectively, was studied. The creep behavior is characterized by three regimes: an initial, a secondary where the creep rate is at a minimum, (epsilon)over dot(min), and a tertiary regime. In the secondary regime (epsilon)over dot(min) is given by: (epsilon)over dot(min)(s)^(-1) = epsilon(0)exp(10.5+/- .5)(sigma/sigma(0))(2.46+/-0.4) exp(-222 +/- 34 kJ/mol/RT) where sigma(0) = 1 MPa and epsilon(0) = 1 s^(-1). The times to failure are given by: t(f) (s) = exp(-2.46 +/- 0.6)(epsilon)over dot(min)^(-1). Not surprisingly, the results presented herein confirm that, as in the case of Ti<sub>3</sub>SiC<sub>2</sub>: dislocation creep is the dominant mechanism. At about 220 KJ/mol, the creep activation energy was roughly half its value for Ti<sub>3</sub>SiC<sub>2</sub>. However, at 2.5±0.5, the stress exponents were comparable.

### (ICACC-S12-P126-2012) Study of NiTi-MAX Phase Composites Prepared via Spark Plasma Sintering

A. Kothalkar\*, L. Hu, S. Basu, F. Schaff, I. Karaman, M. Radovic, Texas A&M University, USA

Shape memory alloy (SMA) – MAX phase composites were fabricated by spark plasma sintering (SPS) of equiatomic NiTi and Ti<sub>3</sub>SiC<sub>2</sub> or Ti<sub>2</sub>AlC powders at temperatures in the range of 960-1000°C under 100 MPa uniaxial load. The microstructure and phase composition along the interfaces of these two-phase composites were studied using Scanning Electron Microscopy (SEM) and Energy-Dispersive Spectroscopy (EDS). The phase evolution near the interfaces in SPSed composites depends significantly on sintering temperature, because of the formation of Ni-Ti liquid phase at temperatures higher than 980°C. The martensitic phase transformation in the NiTi – MAX phase composites was confirmed by Differential Scanning Calorimetry (DSC). Thermo-mechanical properties of the composites are discussed in detail, along with practical implications of the results on inducing compressive stresses in ceramic MAX phases through phase transformations in SMA.

### (ICACC-S12-P127-2012) Interfacial Study between Ti<sub>3</sub>SiC<sub>2</sub> and NiTi Shape Memory Alloy via Diffusion Bonding

A. Kothalkar\*, S. Basu, P. Mahaffey, M. Radovic, I. Karaman, Texas A&M University, USA

Herein we report the study of Ti<sub>3</sub>SiC<sub>2</sub> and NiTi diffusion bonded joints in the range of 800 to 1200°C. The microstructure of the interfacial layer, formed at different temperatures and after different bonding times, has been characterized using scanning electron microscopy and microprobe elemental analysis to determine its phase composition and mechanism of diffusion bonding. At 1200°C, the bonding mechanism observed is liquid phase whereas solid state diffusion bonding was observed at lower temperatures. The interfacial layers form by diffusion of Si from Ti<sub>3</sub>SiC<sub>2</sub> into the interface and its subsequent reaction with NiTi to form Ni-Ti-Si ternary phases. Elastic modulus and hardness of different phases present in the interfacial layer are determined using nanoindentation. Vickers hardness data shows considerably higher hardness at the interface layer compared to both Ti<sub>3</sub>SiC<sub>2</sub> and NiTi. High fracture toughness of the interfacial bonding phases is confirmed by the absence of any significant cracking near the indents.

### (ICACC-S12-P128-2012) Thermal atomic displacements in select MAX phases through first-principles phonon calculations

N. Lane\*, Drexel University, USA; A. Togo, Kyoto University, Japan; L. Chaput, Université de Nancy, France; G. Hug, ONERA-CNRS, France; M. Barsoum, Drexel University, USA

MAX phases are known to possess an unusual combination of properties, including high thermal and electrical conductivity, relatively low Vickers hardness, exceptional damage tolerance and thermal



shock resistance, thermal stability, high stiffness, and excellent damping capabilities. All these properties are heavily dependent on the phonon spectrum. The atomic motion behavior at elevated temperatures is especially important in considering their high-temperature damping as well as their thermal and electrical conductivities. Experimental and theoretical studies of  $\text{Ti}_3\text{SiC}_2$  and  $\text{Ti}_3\text{GeC}_2$  have suggested that certain MAX phases exhibit correlated atomic motion, which may be due to the strongly localized low frequency modes where the atoms move to avoid collision. In this study, we model the temperature dependence of atomic displacements based on the phonon spectrum determined by first principles calculations based on density functional theory. We will present results on the time- and space-averaged thermal displacements, as well as the interatomic distance between atom pairs averaged over time, all determined from the phonon density of states. The effects of the chemical bonding, stoichiometry, and mass of the constituent atoms will be discussed and compared with experimental results from high-temperature neutron diffraction.

**(ICACC-S12-P129-2012) Microstructural characterization and compression properties of  $\text{TiC}_{0.61}/\text{Cu}(\text{Al})$  composites synthesized from Cu and  $\text{Ti}_3\text{AlC}_2$  powders**

Z. Huang, School of Mechanical and Electronic Control Engineering, China; V. Gauthier-Brunet, J. Bonneville, Institut PPRIME, France; H. Zhai, School of Mechanical and Electronic Control Engineering, China; A. Joulain, S. Dubois\*, Institut PPRIME, France

A new sub-micro-layered  $\text{TiC}_{0.61}/\text{Cu}(\text{Al})$  composite has been prepared by hot-pressing a mixture of 50 vol.%  $\text{Ti}_3\text{AlC}_2$  and 50 vol.% Cu powders at 1150 C and 30 MPa. Compression properties of the composites were tested. It is demonstrated that the composite has an unusual microstructure made up of sub-micro-sheet layered of  $\text{TiC}_{0.61}$  and Cu(Al) alloy within one  $\text{Ti}_3\text{AlC}_2$  particle; both the width of the  $\text{TiC}_{0.61}$  and Cu(Al) layers are  $\sim 150$  nm.  $\text{Ti}_3\text{AlC}_2$  is decomposed into  $\text{TiC}_{0.61}$  phase whereas Al atoms provided by  $\text{Ti}_3\text{AlC}_2$  are dissolved and diffuse into the liquid Cu at high temperature. Compression tests were performed at constant strain rate in the temperature range 20–800 C. Due to the strong interface bonding between  $\text{TiC}_{0.61}$  and Cu(Al) phase, composites exhibit high  $\sigma_{0.2\%}$  and ultimate compressive strength.  $\sigma_{0.2\%}$  is 786 MPa and 660 MPa, and the ultimate compressive strength is 1,13 GPa and 1 GPa at 20 and 200 C, respectively. Plastic deformation takes place in the Cu(Al) matrix. Activation volumes were measured by the stress relaxation technique at different temperatures. At 200 C, the effective activation volume,  $V_{\text{eff}}$ , is as low as 25  $b^3$  and weakly strain dependent, indicating that a single mechanism controls plastic flow in both the micro and macro plastic stages. Wavy slip lines are observed suggesting that cross-slip may be the dominant deformation mechanism.

**(ICACC-S12-P130-2012) Structure and properties of oxide coatings on Al-Cu and Al-Mg alloys**

A. D. Pogrebnjak\*, Sumy State University, Ukraine; M. K. Kylyshkanov, Serikbayev East Kazakhstan state technical University, Kazakhstan; Y. N. Tyurin, The E.O.Paton Electric Welding Institute, Ukraine; A. S. Kaverina, I. V. Yakushchenko, Sumy State University, Ukraine

The new research on the protective oxide coatings based on  $\text{Al}_2\text{O}_3$  (Si, Mn) in aluminum alloys by electrolytic plasma oxidation were provided. The analysis is performed using scanning electron microscopy, SEM with EDS (energy dispersive microanalysis), X-ray diffraction (XRD), Rutherford backscattering of ions (RBS)  $4\text{He}^+$  and protons nanoindenter and tests of the wear, friction and acoustic emission. The results showed that coatings are formed with good quality, high hardness and wear resistance, and with low thermal conductivity. It was found that, along with  $\text{Al}_2\text{O}_3$ , there are also present in the coating such elements Si, Mn, C and Ca. The stoichiometry of the coating is determined. The density and hardness of the coating on the substrate Al-Cu is close to the values of  $\alpha\text{-Al}_2\text{O}_3$  phase, and of the coating deposited on the substrate Al-Mg, - 1.5 times less.

## S13: Advanced Ceramics and Composites for Nuclear Applications

### Symposium 13: Poster Session

Room: Exhibit Hall

**(ICACC-S13-P131-2012) Processing of ultrafine Silicon Carbide Powder by Silicon–Carbon and Silica–Carbon Reactions**

S. Sagar\*, R. Srinivasan, S. Ashok Kumar, Bhabha Atomic Research Centre, India

Silicon Carbide (SiC) ceramics find application as structural components in high temperature reactor and fusion reactor research facilities in the form of both monoliths and coating on metallic surfaces. Processing of these components require sinter-active powders. Hence synthesis of silicon carbide powders by silicon – carbon and colloidal silica – charcoal reactions was studied. Phase pure powder formation occur in the temperature range of 1425 to 15750C as shown by TG-DTA and XRD studies. The powders formed were highly agglomerated ( $D_{50} \sim 10\mu$ ) with faceted dense particles and porous agglomerates of finer particles in case of the former and later reactions respectively. A pH of  $\sim 9$  and slurry solid loading of 30 volume percent were found to be optimum for dispersion (z.p.  $\sim -30\text{mV}$  and Newtonian flow) conditions for effective wet grinding. Powders with a  $D_{50}$  of  $\sim 1\mu\text{m}$  with all particles  $< 10\mu\text{m}$  were formed by wet grinding by planetary milling. The powders thus obtained could be hot pressed to  $>85\%$ T.D. and coated to form adherent film by slurry based dip coating.

**(ICACC-S13-P132-2012) Characterization of Electrodeposited FCCI barrier by ionic liquid for SFR**

S. Jee\*, S. Lee, Y. Yoon, Yonsei Univ, Republic of Korea

The great attention has been shown to the unique properties of a metal fuel, such as high thermal conductivity, high proliferation resistance, ease of fabrication, and a good compatibility for the sodium in Sodium-cooled Fast Reactor (SFR) for burning the long-lived fission products. However, It has several problems to use the U-Pu-Zr metal fuel directly since a fuel-clad chemical reaction (FCCI) caused by the eutectic reaction between actinide elements (U, Pu) and a cladding material based on stainless steel at above 650 degree C. It is necessary that the novel research for the interaction barrier to prevent the FCCI between the cladding and the metal fuel with high strength and adhesion without the cladding wastage. To maximize the performance of a diffusion barrier, the Zr thin film was deposited by electrodeposition using Zirconium chloride and ionic liquid ( $\text{ZrCl}_4 / 1\text{-ethyl-3-methylimidazolium chloride}$ ). The Zr thin film was analyzed for crystalline structure, atomic composition, and interaction barrier effect. This result suggested that Zr thin film, even with the thickness below  $\mu\text{m}$  level, has very high possibility as an effective barrier against FCCI.

## Global Young Investigators Forum

### GYIF Poster Session

Room: Exhibit Hall

**(ICACC-GYIF-P166-2012) Nanocrystalline ferrites  $\text{Ni}_x\text{Zn}_{(1-x)}\text{Fe}_2\text{O}_4$ : acid sites on the surface and sensor properties**

A. Kazin\*, M. Rumyantseva, Moscow State University, Russian Federation; V. Prusakov, I. Suzdalev, Y. Maximov, V. Imshennik, S. Novochikhin, Semenov Institute of Chemical Physics, Russian Federation; A. Gaskov, Moscow State University, Russian Federation

Ferrites are commonly used in electromagnetic devices. Currently, they are used to apply in gas sensors (resistive type) as a material of a sensitive layer. This trend is developing promisingly, because of the opportunities in modifying the properties of ferrites (band structure and nature of active sites on the surface) by changing the cation composition. The main aim in this research was to investigate the relationships between sensory properties and measured characteristics. Series of compounds with the general formula  $\text{Ni}_x\text{Zn}_{(1-x)}\text{Fe}_2\text{O}_4$  was synthesized by pyrosol using the appropriate metal nitrates, sensor

activity has been studied with reducing gases NH<sub>3</sub> (6–50 ppm) and ethanol vapor (15 – 100 ppm). It was established that the changes in the composition affect the number and strength of acid sites. Increasing the proportion of zinc in the ferrite leads to an increase in the number of strong acid sites on the surface. With the increase in the proportion of nickel an increase in number of weak and medium acid sites is observed. In conclusion, it was established that the decrease in the proportion of strong surface acid sites leads to an increase in sensor activity in the detection of ammonia. For ethanol an inverse relationship occurs.

### **(ICACC-GYIF-P167-2012) Influence of ZnO(Ga) defect structure on sensor properties to ammonia**

N. Vorobyeva\*, M. Rumyantseva, A. Gaskov, E. Konstantinova, D. Grishina, Moscow State University, Russian Federation

Materials based on porous ZnO are widely investigated since they are promising for utilizing as gas sensors. The aim of this work was to study the unusual nanocrystalline ZnO(Ga) sensor properties to ammonia, namely the inversion of sensor signals to NH<sub>3</sub> in the middle temperature region (523–573 K). The sensor responses at 373–723 K were assessed from in situ DC conductance measurements on thick films. Electron paramagnetic resonance (EPR) spectra were recorded before and after NH<sub>3</sub> treatment of ZnO(Ga) powders at different temperatures. In as-prepared sample two types of paramagnetic centers were observed: single ionized oxygen vacancies and radicals O<sub>2</sub><sup>-</sup>. Annealing in NH<sub>3</sub> at 373 K for 1 h resulted in an increase of oxygen vacancies concentration. The signal from oxygen radicals was still observed. However NH<sub>3</sub> treatment at 573 K led to a 2.4-fold decrease of oxygen vacancies concentration and appearance of a new signal attributed to N<sub>2</sub><sup>-</sup> radicals instead of O<sub>2</sub><sup>-</sup> radicals. The formation of N<sub>2</sub><sup>-</sup> radicals could indirectly indicate on nitrogen incorporation into the lattice of ZnO(Ga), which is known to be an acceptor dopant. To conclude, a comparative EPR study and DC conductance measurements allow to attribute the inversion of NH<sub>3</sub> sensor signals to changes in the donor and acceptor defect concentration in the surface layer of ZnO(Ga).

### **(ICACC-GYIF-P168-2012) Oxygen isotope exchange study on SiO<sub>2</sub>-supported mixed 3d-metal oxides with spinel structure**

D. Frollov\*, Y. Kotovshikov, I. Morozov, A. Boltalin, A. Fedorova, Moscow State University, Russian Federation; E. Sadovskaya, Boreskov Institute of Catalysis, Russian Federation; V. Ivanov, Kurnakov Institute of General and Inorganic Chemistry, Russian Federation

3d-Metal oxides with spinel structure are well-known catalysts for hydrocarbons and CO oxidation. To estimate their potential catalytic activity temperature-programmed oxygen isotopic exchange (TPIE) can be used. Some oxides with spinel structure (Co<sub>3</sub>O<sub>4</sub>, CuMn<sub>2</sub>O<sub>4</sub>, Cu<sub>0.6</sub>Co<sub>1.2</sub>Mn<sub>1.2</sub>O<sub>4</sub>) supported on high surface area SiO<sub>2</sub> were prepared and studied by TPIE in 570–1070 K temperature range. All supported samples showed the ability to exchange up to 100% of oxygen both in spinel and SiO<sub>2</sub> phases, while pure silica sample does not catalyze oxygen exchange up to 1173 K. It can be assumed that the increased mobility of the oxygen support connected with realization mechanism of oxygen exchange, similar to a well-known spillover mechanism. It was shown that supported Cu<sub>0.6</sub>Co<sub>1.2</sub>Mn<sub>1.2</sub>O<sub>4</sub> oxide have the greatest activity as compared with unsupported one as well as supported Co<sub>3</sub>O<sub>4</sub> and CuMn<sub>2</sub>O<sub>4</sub> in terms of heteroexchange rates, calculated on 1 g of spinel phase. The optimal content of active phase was found to be 10 wt %. To conclude, the depositing of spinel on SiO<sub>2</sub> surface led to the effect of synergism in activation of the SiO<sub>2</sub> and spinel in oxygen isotope exchange reaction.

### **(ICACC-GYIF-P169-2012) Photoconductivity of nanocrystalline SnO<sub>2</sub> sensitized with colloidal CdSe quantum dots**

A. Babynina\*, R. Vasiliev, O. Maslova, M. Rumyantseva, A. Gaskov, Moscow State University, Russian Federation

Photoconductivity of composite thick films based on the nanocrystalline SnO<sub>2</sub> matrix sensitized with colloidal CdSe quantum dots was

investigated. Transient and steady-state dependences of photoconductivity were studied. The sensitized SnO<sub>2</sub> samples showed considerable photoconductivity up to 300 times with 5 mW/cm<sup>2</sup> illumination at the wavelength of excitonic transition of QDs. Photoconductivity time and intensity dependences show power-law behavior together with slow response and relaxation with characteristic times about hours related to disordered SnO<sub>2</sub> nature. The samples showed high photoresponse stability for periodic illumination switching over 10000 cycles. Photoresponse of samples depends dramatically on the annealing temperature of SnO<sub>2</sub> films: the largest photoconductivity together with shortest relaxation time was observed for the SnO<sub>2</sub> sample annealed at 700 C compared to low annealing temperature that attributed to structural defect concentration.

## **FS1: Geopolymers, Inorganic Polymers, Hybrid Organic-Inorganic Polymer Materials**

### **Focused Session 1: Poster Session**

Room: Exhibit Hall

### **(ICACC-FS1-P136-2012) Influence of activating solution's composition on products stability and thermomechanical properties of volcanic ash-based geopolymers**

P. N. Lemounga, U. F. Chinje Melo, University of Yaoundé, Cameroon; M. Delplancke, Université Libre de Bruxelles, Belgium; H. Rahier\*, Vrije Universiteit Brussel, Belgium

Geopolymers have emerged in recent years as a possible alternative in supplying building materials with limited environmental impact compared to OPC. These materials can be synthesized with a wide range of natural occurring aluminosilicate materials, including volcanic ashes readily accessible in several countries with past or present volcanism. Here we present the influence of the activating solution's composition on products stability and (thermo)mechanical properties of geopolymers made from a Cameroonian volcanic ash. NaOH, KOH solutions and silicate solutions with low modulus were tested. The reactivity of the systems is studied with DSC. A NaOH solution seems to be the fastest activator, but still the reaction is very slow at room temperature. Typically the samples are cured at 90°C for at least 2 days, but the mechanical strength increases substantially up to 7days at 90°C. The influence of particle size on the reactivity is looked at. For practical reasons the volcanic ash is ground and sieved to a grain size below 400µm, but the largest particles only act as a reactive filler. The smaller particles dissolve in the activating solution as can be seen by SEM. The results obtained suggest the possible use of the synthesized materials for building applications and low temperature refractories up to about 700–800°C.

### **(ICACC-FS1-P137-2012) Thermal Resistance Properties of Geopolymers Containing Ground Granulated Blast Furnace Slag**

J. Eichler\*, T. Metroke, Universal Technology Corporation, USA; M. Henley, Air Force Research Laboratory, USA

Ground granulated blast furnace slag (GGBFS) was added to geopolymers prepared from mixtures of fly ash (FA) and granulated blast furnace (GBFS). Due to its reduced particle size, the GGBFS readily releases Ca<sup>2+</sup> ions under alkaline activation conditions used during geopolymer synthesis, the incorporation of which may aid in strength development and decrease set time. Thermal resistance properties (residual compressive strength, cracking tendency, dimensional stability, etc.) were determined as a function of temperature ranging from ambient to 1000 °C. In general, the additive was found to shorten the setting time at ambient temperature of the geopolymer paste, as determined using Vicat needle analysis in accordance with ASTM C191. Additionally, when incorporated in concentrations less than 10%, the GGBFS additive did not degrade the thermal resistance properties of the FA-based geopolymer. The results of this study indicate that both ambient set time and thermal resistance of the geopolymer materials may be tailored by varying the amount of GGBFS added during synthesis.

**(ICACC-FS1-P138-2012) Properties of low calcium fly ash based geopolymer pastes**

Y. Choi\*, J. Kim, G. Moon, Y. Cho, B. Lee, S. Jung, Korea Comformity Institute, Republic of Korea

Use of fly ash based geopolymers in concrete manufacturing has environmental benefit as its production requires less energy. The alkali activation of fly ash is a chemical process differing from hydration of Portland cement. In this process, fly ash mixed with alkaline solutions (NaOH, KOH, Na<sub>2</sub>CO<sub>3</sub> and waterglass solutions) and subjected to mild temperature curing (40~100°C). The experimental program of this paper was to study effect of heating curing conditions, particle size distribution of fly ash, Na<sub>2</sub>O(alkali) content, SiO<sub>2</sub>/Na<sub>2</sub>O mol ratio on the performance of fly ash based geopolymer paste specimens. Geopolymer pasts manufactured with four blaine fineness of fly ash, alkali content (4% ~8%) and SiO<sub>2</sub>/Na<sub>2</sub>O mol (0.6~1.4). These specimens were subjected to various temperature exposure (40~90°C) and duration (6~48hour), its performance was evaluated on the basis of strength. In addition, mineralogical analysis and microstructure of fly ash based geopolymer were studied by X-ray Diffraction (XRD), scanning electron microscopy (SEM), Fourier-transform infrared (FTIR) spectroscopy and mercury intrusion porosimetry (MIP). Also, the leaching test of fly ash mixed with various concentration of sodium hydroxide solution was performed for different time intervals and leachates were analyzed in terms of silica and alumina contents.

**(ICACC-FS1-P139-2012) Effect of elevated temperature exposure on the performance of fly ash based geopolymer**

Y. Choi\*, J. Kim, B. Lee, S. Jung, Korea Comformity Institute, Republic of Korea

Geopolymers are an alternative to Portland cement that can be used to produce concrete without the considerable carbon dioxide emissions. Among the aluminosilicate materials, metakaolin and fly ash are the most favorable raw materials for geopolymer production. However the limited availability and high cost are the problems for metakaolin based geopolymer, therefore most of the recent research on geopolymer utilizes fly ash as the binder. The experimental investigation of this paper was to study effect of Na<sub>2</sub>O(alkali) content, SiO<sub>2</sub>/Na<sub>2</sub>O mol ratio and elevated temperature exposure on the performance of fly ash based geopolymer paste specimens. Geopolymer pasts manufactured with varying alkali content (4% ~8% of fly ash weight) and SiO<sub>2</sub>/Na<sub>2</sub>O mol (0.6~1.4) were subjected to elevated temperature up to 900oC and its performance was evaluated on the basis of weight loss, strength loss after temperature exposure. In addition, mineralogical changes due to elevated temperature exposure were studied by XRD. Investigation of microstructure as well as microprobe analysis was performed using scanning electron microscopy (SEM), Fourier-transform infrared (FTIR) spectroscopy and mercury intrusion porosimetry (MIP).

**Thursday, January 26, 2012**

**S1: Mechanical Behavior and Performance of Ceramics & Composites****Processing-Microstructures-Properties Correlations I**

Room: Coquina Salon D

Session Chairs: Yanchun Zhou, Aerospace Research Institute of Materials & Processing Technology; Dechang Jia, Harbin Institute of Technology

**8:00 AM**

**(ICACC-S1-053-2012) Microstructure and Mechanical Property Characterization of Si<sub>0.5</sub>C<sub>1.5</sub>N<sub>0.8</sub>Al<sub>0.3</sub> Ceramics Produced by Mechanical Alloying and Subsequent Hot-pressing (Invited)**

D. Jia\*, D. Ye, Z. Yang, Z. Sun, Y. Zhou, Harbin Institute of Technology, China

Amorphous Si<sub>0.5</sub>C<sub>1.5</sub>N<sub>0.8</sub>Al<sub>0.3</sub> powders have been prepared by mechanical alloying (MA) technique using c-Si, h-BN, graphite and

Al as starting materials. The investigated results showed that MA Si<sub>0.5</sub>C<sub>1.5</sub>N<sub>0.8</sub>Al<sub>0.3</sub> powders were completely amorphous. Solid-state nuclear magnetic resonance spectra have improved Si and C atoms are intimately mixed at atomic levels and aluminum is present as mixed state of AlN<sub>4</sub>, AlN<sub>5</sub>/AlO<sub>4</sub> and AlN<sub>6</sub>. X-ray photoelectron spectroscopy results indicated that chemical bonds between Si, B, C, N and Al elements could be formed for the MA powders. Si<sub>0.5</sub>C<sub>1.5</sub>N<sub>0.8</sub>Al<sub>0.3</sub> powders were consolidated by hot pressing at 1800°C under a pressure of 30 MPa in Ar and N<sub>2</sub>, respectively. The sintering atmosphere had a great influence on the microstructures and mechanical properties of the ceramics. For the ceramics sintered in argon, flexural strength, fracture toughness, elastic modulus and Vickers' hardness were 421.9MPa, 3.40MPa·m<sup>1/2</sup>, 174.1GPa, and 12.74GPa, respectively. For the ceramics sintered in nitrogen, the mechanical properties increased, except for the Vickers' hardness, and the values of the above properties were 526.8 MPa, 5.25 MPa·m<sup>1/2</sup>, 222.1 GPa, and 11.63 GPa, respectively.

**8:30 AM**

**(ICACC-S1-054-2012) Microstructure Evolution from Mechanically Alloyed Amorphous SiBCN Powder to Hot Pressed Nanocrystalline Ceramic**

P. Zhang\*, D. Jia, Z. Yang, X. Duan, Y. Zhou, Harbin Institution of Technology, China

Organic Polymer derived SiBCN ceramics are well known for their nice oxidation resistance, thermal and mechanical stability at high temperature. However, the polymer pyrolysis technology uses expensive chemical reagents, and will probably bring pores or cracks in product. In this work, mechanical alloying and hot pressing were utilized to fabricate amorphous SiBCN powder and nanocrystalline ceramic. A mixture of silicon, boron nitride and graphite was high-energy ball milled to synthesize SiBCN powder, which was then sintered at 1500oC-1900oC and 80MPa pressure in nitrogen atmosphere. It is shown that the milled SiBCN powder has fairly well amorphous structure, as detected by XRD and TEM. Sintered at 1500oC, nanocrystallines with size of 3nm-5nm are embedded in amorphous matrix. With temperature increasing, the content of crystallized SiC gets more, and their diameters also become larger and larger. However, BNC is still amorphous, which seems not to be dependent on temperature. While the sintering temperature is 1900oC, SiC crystalline has a statistical size of 96nm, which is encompassed and separated by amorphous BNC. The crystallization process and the final nanocrystalline structure are similar to that of polymer derived SiBCN ceramics. Hence, mechanical alloying is believed to be potential in developing new amorphous or nanocrystalline materials.

**8:50 AM**

**(ICACC-S1-055-2012) Effect of AlN content on the microstructure and mechanical properties of BN-based composites**

Z. Tian, D. Jia\*, Z. Yang, X. Duan, Y. Zhou, Harbin Institute of Technology, China

In this study, AlN was introduced into hot pressed BN-SiO<sub>2</sub>-AlN composites as reinforcement. The effect of AlN content on the microstructure and mechanical properties was systematically investigated. XRD (X-ray diffraction) results indicated that a new phase of Si<sub>3</sub>AlON<sub>7</sub> appeared when AlN was added. Amorphous silica can be observed when AlN content was lower than 5 vol%. While AlN content was higher than 10 vol%, amorphous silica disappeared. At the same time, the relative amount of Si<sub>3</sub>AlON<sub>7</sub> increased with raised AlN. Mechanical properties results indicated that the bending strength and fracture toughness of BN-SiO<sub>2</sub>-AlN ceramics was improved with added AlN. As the AlN content increased, the bending strength and fracture toughness of BN-SiO<sub>2</sub>-AlN ceramics firstly increased and then decreased, the elastic modulus slightly increased. The composite with 5vol.% AlN exhibited the highest bending strength (247.0 MPa) and fracture toughness (4.02 MPam<sup>1/2</sup>), which was 57.5% and 40.6% higher than that of BN-SiO<sub>2</sub>(30vol.%) ceramics, while the elastic modulus was 10.2% higher than the latter.

9:10 AM

### (ICACC-S1-056-2012) Utilizing Pressure-Induced Transformations for Toughening of Ceramics

S. Ramalingam\*, I. E. Reimanis, C. E. Packard, Colorado School of Mines, USA

A novel mechanism for transformation toughening of ceramic composites using pressure-induced transformations is proposed.  $\beta$ -eucryptite ( $\text{LiAlSiO}_4$ ) transforms to  $\epsilon$ -eucryptite at about 0.8 GPa hydrostatic pressure. The transformation is characterized with nanoindentation on single- and poly-crystals, and in-situ diamond anvil cell-Raman spectroscopy. A micromechanical model that captures toughening from the dilatation during transformation and anti-toughening from tensile thermal residual stresses in the matrix predicts a net increase in toughness for zirconia/ $\beta$ -eucryptite composites compared with zirconia. To validate these results, composites of zirconia with eucryptite of various particle sizes and volume fractions are made by hot pressing. This research identifies the key parameters required for achieving transformation toughening using pressure-induced phase transformations.

9:40 AM

### (ICACC-S1-057-2012) Microstructural Variations in Bulk Monoclinic $\text{Y}_2\text{O}_3$ Transformed under High Pressure

S. Deutsch\*, J. F. Al-Sharab, B. H. Kear, S. D. Tse, Rutgers University, USA

A high pressure/high temperature (HPHT) apparatus has been developed to effect a cubic to monoclinic transition in bulk polycrystalline  $\text{Y}_2\text{O}_3$ , for the first time. Previously, diamond anvil cells were used to achieve the high processing pressures necessary for this transformation, and then only in powder. Adjusting the HPHT processing pressure from 3-8 GPa at 1000°C has resulted in a number of striking microstructural changes, with final grain sizes ranging from tens of nanometers to hundreds of microns. With increasing processing pressures, the grain size nucleation rate increases and growth rate decreases. The phase transformation can be reversed via subsequent HPHT processing. Partial conversion has been shown to be possible, resulting in a cubic-monoclinic  $\text{Y}_2\text{O}_3$  self-nanocomposite. Complete conversion from cubic to monoclinic and back to the cubic phase has also resulted in net grain size refinement, from 1.5  $\mu\text{m}$  starting material to 40 nm. Work is underway to determine if other lanthanide sesquioxide materials, such as  $\text{Er}_2\text{O}_3$  and  $\text{Yb}_2\text{O}_3$ , can be reversibly transformed in a similar manner. This work reports on the structural changes of  $\text{Y}_2\text{O}_3$  under high pressure/high temperature processing as the cubic to monoclinic transformation is observed for the first time in a bulk material.

10:00 AM

### (ICACC-S1-058-2012) Mechanical Properties of Zirconia Toughened Alumina with 10-24 vol-% 1Y-TZP Reinforcement

F. Sommer\*, R. Landfried, F. Kern, R. Gadow, University of Stuttgart, Germany

Structural ceramics as ZTA require high bending strength, fracture toughness and wear resistance. In order to achieve optimum mechanical properties processing and compositional parameters have to be adjusted. ZTA ceramics with an yttria content of 1 mol-% and zirconia contents ranging from 10-24 vol-% were hot pressed at 1475°C and 50 MPa axial pressure. The stabilization of the reinforcement phase in ZTA with yttrium oxide was performed by coating of monoclinic zirconia nanopowders via the nitrate route and subsequent blending with sub-micron size alumina. Three different dwell times of 1-3 h were applied to test the sensitivity of the coated powder to heat treatment conditions. Mechanical and microstructural properties were investigated. Highest bending strength and fracture toughness were determined for the 1 mol% Y 17 vol-% ZTA sample. Stabilizer contents have to be carefully adjusted to the zirconia contents to obtain best mechanical properties. Variation in dwell within the limits chosen has only a minor influence. Results overmatch previous studies of ZTA ceramics with higher yttria contents of 1,5 - 2 mol-%

and identical zirconia contents of 10-24 vol-%. Thus significant influencing factors for an optimized composition of ZTA ceramics, such as vol-% of TZP phase in combination with stabilizer content could be successfully identified for best mechanical properties.

10:20 AM

### (ICACC-S1-059-2012) Tailoring microstructures in mullite for toughness enhancement

D. Glymond\*, Imperial College London, United Kingdom; M. Vick, M. Pan, Naval Research Laboratory, USA; F. Giuliani, L. Vandeperre, Imperial College London, United Kingdom

Mullite is considered a promising candidate for future structural applications such as ceramic recuperators in turbo propelled engines, due to highly favourable properties at elevated temperatures. In order for it to be viable for structural applications its relatively weak fracture toughness needs to be improved. A reliable way of improving fracture toughness in a range of materials has been to tailor the microstructure to contain elongated grains capable of bridging cracks. In this paper, the tailoring of mullite microstructures using a range of processing methods will be reported: reactive sintering of mixtures of alumina and silica, sol-gel synthesis of mullite and the use of sol-gel derived additives for commercial mullite powders. The differences in morphologies produced as well as the influence on indentation fracture toughness will be described.

10:40 AM

### (ICACC-S1-060-2012) Microstructural, Thermal, Electrical and Mechanical Characterisation of Silica Matrix Composites reinforced with Carbon Nanotubes

T. Subhani\*, Imperial College London, United Kingdom; M. Mackovic, E. Spieker, A. R. Boccaccini, University of Erlangen-Nuremberg, Germany; M. S. Shaffer, W. E. Lee, Imperial College London, United Kingdom

MWCNTs were incorporated in a dense  $\text{SiO}_2$  matrix to explore their effect as nano-reinforcement. Colloidal processing by heterocoagulation of  $\text{SiO}_2$  nanoparticles on acid-treated MWCNTs produced composite powders with homogeneous dispersion of nanotubes, which were consolidated by cold isostatic pressing and pressureless sintering. MWCNT- $\text{SiO}_2$  composites with nanotubes up to 10wt% (13.3vol%) had high densities (>96% relative density), which were characterised by mechanical, thermal, electrical and microscopical examination. XRD showed an amorphous glass matrix with low degree of crystallisation (<3%). SEM and TEM revealed well dispersed nanotubes without any indication of large nanotube agglomerates. Selected area electron diffraction (SAED) analysis revealed the presence of cristobalite only in the  $\text{SiO}_2$  matrix but not at MWCNT/ $\text{SiO}_2$  interfaces. A sharp increase in the electrical conductivity was observed in composites corresponding to eight orders of magnitude. Thermal conductivity improved linearly with an increase in nanotube loadings and similar trend of linear improvement was observed in the mechanical properties when composites were tested for hardness, elastic modulus and indentation fracture toughness. The effect of the diameter and aspect ratio of nanotubes on the mechanical and functional properties of the composites were also investigated.

11:00 AM

### (ICACC-S1-061-2012) Influence of Carbon Doping on the Mechanical Properties of Alumina

N. A. Yahya\*, R. I. Todd, University of Oxford, United Kingdom

Previous studies have shown that the addition of silicon carbide (SiC) nanoparticles to alumina changes the fracture mode from intergranular to transgranular and in doing so improves the wear resistance. The reason for this is not clear but the grain boundary chemistry may be involved. SiC usually contains free carbon and therefore the aim of current study was to investigate the influence of small amounts of carbon doping on the fracture mode and wear properties of alumina. The microstructure and properties of alumina doped with 0, 0.012, 0.036 and 0.050 wt% carbon were studied. Alumina showed mainly

intergranular fracture. Its wear resistance and the percentage of surface grains pulled out were dependent on grain size. The addition of carbon in alumina changed the fracture mode to mainly transgranular. The wear resistance improved significantly and was insensitive to grain size. The percentage of surface grains pulled out was lower compared to pure alumina and was also independent of grain size. The strengths of pure and doped alumina were compared and will also be presented.

11:20 AM

**(ICACC-S1-062-2012) Relationship between the number density of coarser defects and strength and their fluctuations in dry-pressed ceramics**

S. Tanaka\*, S. Goi, R. Furushima, K. Uematsu, Nagaoka University of Technology, Japan

The objective of this study is to examine between coarser defects and mechanical property such as strength and their fluctuations by simulation based on characteristics of coarser defects analysis and experiments. The number densities of coarser defects were assumed to be given by the power function,  $f=Ac^{-n}$ . The number density of coarser defects increased with increasing parameter A, and the distribution of are narrowed with increasing n. The strengths distributions were simulated by the assumed power functions of coarse defects. The average strength was related to a function of A and n. The Weibull modulus was related to a function of n. In experimental, coarser defects in engineering ceramics were characterized by the optical microscopy with thinned ceramics. There were many coarse defects originated from the interstices of granules in the die-pressed compact. The number distribution of coarser defects could be approximated by the power function as assumed above. The simulation of strength and its distribution agreed very well with the measured strength.

11:40 AM

**(ICACC-S1-063-2012) The Preparation and microstructure of ZrC based ceramics**

R. Zhidan\*, L. Yufu, Southeast University, China

ZrC based ceramics were prepared by reactive melt infiltration. The various mass ratios of original materials (C,ZrC and resin powders) and the pressure were optimized to obtain a porous carbon/carbon (C/C) skeleton. The zirconium melt was then infiltrated into the porous C/C at temperatures higher than the melting point of zirconium to obtain ZrC based composites. The microstructural features of the composite were revealed by optical microscopy (OM), X-ray diffraction (XRD) and scanning electron microscopy (SEM). It was found that the composite matrix is composed of continuous ZrC, island-like ZrC particle, residual carbon and little impurities. Finally, the hardness and toughness of the composites were also studied.

## S2: Advanced Ceramic Coatings for Structural, Environmental, and Functional Applications

### Environmental Barrier Coatings and Protective Coating-Component Systems for Extreme Environments

Room: Ponce de Leon

Session Chairs: Peter Mechnich, German Aerospace Center (DLR); Sung Choi, Naval Air Systems Command

8:00 AM

**(ICACC-S2-020-2012) Hot gas corrosion and EBC development of non-oxide ceramic materials (Invited)**

H. Klemm\*, A. Bales, K. Schoenfeld, A. Michaelis, Fraunhofer IKTS, Germany

Caused by the steady increasing energy price and the stronger requirements in environmental protection the main focus of future

generations of gas turbines will be emphasized on an increased efficiency with a simultaneous reduction of the emissions. These goals can be obtained only by higher hot gas temperatures. Ceramic materials offer high potential for application in gas turbines. Significant progress has been achieved in the development of high-temperature stable ceramic materials; however, commercial applications in the hot gas path of gas turbines were rather limited. Caused by the high water vapor pressure in combination with high temperatures and gas velocities, corrosion processes at the surface of the materials were observed resulting in significant material loss. Hence, environmental barrier coatings (EBC) have been presented to be the solution to protect the ceramic materials. Systematic studies on the hot gas corrosion of non-oxide ceramics (monolithic and CMC) have been performed with and without EBC. Oxidation processes were found to be an important factor for the hot gas stability of the CMC materials. Based on a detailed understanding of both oxidation and corrosion processes at elevated temperatures general concepts for the development of environmental barrier coatings for non-oxide ceramic materials will be provided.

8:40 AM

**(ICACC-S2-021-2012) The effect of oxidation resistant fillers on bond-coats for EBC on silicon-based ceramics**

C. Lewinsohn\*, H. Anderson, J. Johnston, Ceramtec, Inc., USA; R. Bhatt, D. Zhu, NASA Glenn Research Center, USA

Multilayer, environmental barrier coating (EBC) systems, based on polymer-derived bond coat layers, have been shown to improve the hydrothermal corrosion resistance of silicon nitride and silicon carbide-based materials. Use of silicon-based ceramics could dramatically improve efficiency in combustion systems by allowing increased operating temperatures and could reduce harmful emissions. Environmental barrier coatings, however, are required to enable silicon-based ceramics to have usable lifetimes in propulsion and energy conversion systems. This work will investigate the effect of additions of oxidation resistant filler materials to polymer-derived bond coats for EBCs. The results of approaches to accommodate differences in coefficient of thermal expansion and densification behavior during coating processing will be described. In the current work, additional data will be provided showing that the bond coat system can be adapted to monolithic and composite silicon carbide. Initial results on the high-temperature durability of these coatings will be presented.

9:00 AM

**(ICACC-S2-022-2012) Thermal Stability and Expansion Properties of Rare Earth Monosilicates**

P. Sarin\*, D. R. Lowry, Z. D. Apostolov, J. Angelkort, Z. A. Jones, W. M. Kriven, University of Illinois at Urbana-Champaign, USA

Rare earth monosilicates are promising materials for environmental barrier coatings (EBCs) for Si-based composites. They have a low coefficient of thermal expansion (CTE), good phase stability, chemical compatibility with the underlying mullite or mullite+BSAS ( $(1-x)\text{BaO}-x\text{SrO}-\text{Al}_2\text{O}_3-2\text{SiO}_2$ ,  $0 \leq x \leq 1$ ) coat, and are significantly less volatile than BSAS in water vapor. Understanding the thermal stability and expansion properties of these materials is essential to develop coherent and oxidation resistant EBCs. In this study, powder samples of  $\text{Y}_2\text{SiO}_5$  and  $\text{Ln}_2\text{SiO}_5$  (where Ln = Gd, Dy, Er or Yb) were synthesized by the organic steric-entrapment method. All the compositions exhibited a monoclinic low temperature phase which transformed to a monoclinic high temperature phase, irreversibly. High temperature powder XRD studies were conducted using synchrotron radiation to elucidate the crystallographic changes, resulting in volume changes, accompanying the transformation. This presentation will provide an atomistic look into the phase transformation mechanisms, and explain the anisotropies of the thermal expansion properties of the  $\text{Y}_2\text{SiO}_5$  and  $\text{Ln}_2\text{SiO}_5$  phases. Direction dependence of CTEs in each material system will be explained crystallographically, and the role of the

rare-earth cation type in defining the observed behavior will also be discussed.

**9:20 AM**

**(ICACC-S2-023-2012) Thermal Expansion and Phase Transitions of Rare Earth Disilicates**

T. Key\*, E. E. Boakye, UES / AFRL, USA; K. F. Presley, R. S. Hay, AFRL, USA

Rare earth disilicates are of interest as environmental thermal barrier coatings for SiC based composites. The thermal expansion and phase stability of  $\text{Re}_2\text{Si}_2\text{O}_7$  (Re=Y, Ho, Er) in the  $\alpha$ ,  $\beta$  and  $\gamma$  phases was examined by XRD at temperatures between 20 °C and 1200 °C. Lattice parameters and phase fractions were determined from Rietveld refinement of powder diffraction data. The total thermal expansion coefficient tensors for single crystals were calculated from the lattice parameter data as a function of temperature and compared to TMA performed on bulk samples. The triclinic  $\alpha$  phase was approximately twice as expansive as the monoclinic  $\beta$  and  $\gamma$  phases were, and it partially transformed into the beta phase at 1200 °C.

**10:00 AM**

**(ICACC-S2-024-2012) Develop Eu<sup>3+</sup> doped YPO<sub>4</sub> Environmental Barrier Coating for Self-health-monitoring (Invited)**

Y. Wang\*, W. Liu, L. Cheng, Northwestern Polytechnical University, China

Luminescence of europium doped yttrium phosphate (YPO<sub>4</sub>:Eu) environmental barrier coatings (EBCs) has been developed as a means of self-monitoring. The corrosion behavior of YPO<sub>4</sub>:Eu in water-vapor and molten salt is investigated as well as the effect of these corrosion environments on the intensity of luminescence. By comparison of these results, the relationship between the extent of corrosion of YPO<sub>4</sub> and the change in luminescence intensity ratio is determined. Preliminary data suggest that the YPO<sub>4</sub>:Eu can monitor the microstructural damages including structural perturbations, phase changes and chemical reactions. The results also indicate that the intensity ratio from luminescence spectra can be used as nondestructive evaluation (NDE) technology for EBCs.

**10:30 AM**

**(ICACC-S2-025-2012) Testing of Candidate Rigid Heatshield Materials at LHMEI for the Entry, Descent, and Landing Technology Development Project**

S. Sepka\*, ERC/NASA-Ames, USA; R. Beck, S. White, NASA Ames Research Center, USA

To further the technologies required to land heavy (~40 metric ton) masses on Mars, material testing was done at the Wright-Patterson Air Force Base Laser Hardened Materials Laboratory (LHMEI) Two laser exposures were applied. The first, which was given to all test models, was at 450 W/cm<sup>2</sup> for 60 seconds to simulate an aerocapture maneuver. The second exposure was at 115 W/cm<sup>2</sup> for 100 seconds to simulate a planetary entry. The second exposure was given to only one model of each tested material. The results described herein were part of a material screening program of vendor-supplied, proposed heat shield materials. This work was part of NASA's Entry Descent and Landing (EDL), Technology Development Project (TDP), Thermal Protection Systems (TPS) element, rigid materials development task. The goal of this task was to develop low density, rigid material systems with an appreciable weight savings over PICA while improving its material response performance. In addition, new technologies, such as having PICA-like materials in honeycomb to avoid a gapped tile system or having materials with variable density through-the-thickness were studied. For these tests, seven different materials were tested: PICA (representing the baseline configuration), 3DQP, BPAFG, CC/CALCARB, LM-MonA, P28/P15, and PIRAS-22. Results from the testing are summarized herein.

**11:00 AM**

**(ICACC-S2-026-2012) A SiC/SiC-MoSi<sub>2</sub>-ZrB<sub>2</sub> double-layer oxidation resistant coating for carbon/carbon composites**

H. Li\*, X. Yao, Y. Zhang, X. Shi, Northwestern Polytechnical University, China

A SiC/SiC-MoSi<sub>2</sub>-ZrB<sub>2</sub> double-layer oxidation protective coating for carbon/carbon (C/C) composites was prepared by two-step pack cementation. The microstructures of the as-prepared multilayer coating were characterized by XRD and SEM analyses. The oxidation resistance and the effects of high temperature oxidation resistance and thermal shock on the mechanical properties of the coated C/C composites were investigated. The results show that the coating characterized by excellent oxidation resistance could effectively protect C/C composites from oxidation for 500 h with only 0.5% weight loss at 1773 K. The flexural strength of C/C composites after preparing the coating decreased and the fracture behavior changed from the pseudo-plastic fracture to brittle mode. After oxidation at 1773 K for 30 h or thermal shock between 1773 K and room temperature for 20 cycles, the flexural strength of the coated specimens decreased accordingly, and the plastic increased.

**11:20 AM**

**(ICACC-S2-027-2012) Novel PDC based composite coating to protect mild steel in very harsh environments**

G. Motz\*, M. Guenther, U. Glatzel, A. Schuetz, University of Bayreuth, Germany; K. Wang, R. K. Bordia, University of Washington, USA

To improve the energy efficiency of e.g. waste incineration plants an increase of the firing temperature up to 700 °C is one of the most important demands. The higher working temperature in combination with the aggressive combustion gases and the abrasive ash particles require a very stable environmental barrier coating to protect the steel components of the heat exchanger. For this application a double layer polysilazane-based environmental barrier coating system for steel consisting of a perhydropolysilazane bond coat and a polysilazane-based glass/ceramic composite top coat has been developed. After application of the layers by simple dip- or spray coating processes and subsequent drying a thermal treatment in air at 700 °C leads to uniform, dense and crack-free composite coatings with a remarkable thickness up to 100 µm and an excellent adhesion to the mild steel substrate. Microstructural analysis by SEM and XRD demonstrates the homogeneous dispersion of the hard ceramic ZrO<sub>2</sub> filler particles within the amorphous PDC matrix, whereas the glass filler seals the coating system. Cyclic oxidation tests up to 700 °C and corrosion tests in representative salt melts proved the effectivity of the coating system to protect mild steel in harsh environments.

**11:40 AM**

**(ICACC-S2-028-2012) In-situ observation of the active/passive transition of SiC oxidation under Ar/O<sub>2</sub> gas mixtures at very high temperatures**

M. Q. Brisebourg\*, F. Rebillat, F. Teyssandier, LCTS, France

Oxidation behavior of silicon carbide under Ar/O<sub>2</sub> gas mixtures is investigated at very high temperatures (>1700°C) in order to further understand both the active and passive oxidation kinetics as well as transition between these two oxidation regimes. Experiments are conducted by Joule heating TEXTRON SCS-6 fiber samples inside an airtight vessel under different Ar/O<sub>2</sub> mixtures at atmospheric pressure. Temperature is regulated by means of a computer-assisted control loop consisting of a two-color pyrometer and a power supply delivering electrical current to the sample. The variation of the electrical current is used to monitor the oxidation rate. Active oxidation rate is found to increase linearly with PO<sub>2</sub>, and to be independent of gas flow rate and of temperature up to 2100°C. Passive oxidation kinetics at 1700°C follows parabolic variation and is independent of PO<sub>2</sub>. All experimental results are compared to simulation results obtained from a 3D finite volume approach of transport phenomena inside the vessel. For the active regime, experimen-

tal and simulated results are in good agreement. This suggests that oxidation kinetics is mainly limited by species transport through a natural convection boundary layer.

### S3: 9th International Symposium on Solid Oxide Fuel Cells (SOFC): Materials, Science and Technology

#### Electrode Materials and Microstructural Engineering I

Room: Coquina Salon H

Session Chairs: Briggs White, Dept. of Energy; S. Elangovan, Ceramtec, Inc.

#### 8:00 AM

##### (ICACC-S3-011-2012) Improved Anodic Performance of $\text{Ce}(\text{Mn,Fe})\text{O}_2\text{-La}(\text{Sr})\text{Fe}(\text{Mn,Co})\text{O}_3$ Composite Oxide For Direct Hydrocarbon Type SOFCs (Invited)

T. Ishihara\*, T. Shin, Y. Ju, Kyushu University, Japan

One of the great advantages of SOFCs is the direct usage of hydrocarbon for fuel, however, because of carbon formation, direct use of hydrocarbon for fuel is highly difficult. In our previous study, we found that  $\text{Ce}(\text{Mn,Fe})\text{O}_2\text{-La}(\text{Sr})\text{Mn}(\text{Fe})\text{O}_3$  oxide composite shows high anodic activity to  $\text{C}_3\text{H}_8$  and  $\text{C}_4\text{H}_{10}$ . In this study, effects of small amount of additives to  $\text{La}(\text{Sr})\text{Fe}(\text{Mn})\text{O}_3$  was studied for further improvement of power density. Among the examined dopant, doping small amount of Co and Pd to  $\text{La}(\text{Sr})\text{Fe}(\text{Mn, M})\text{O}_3$  is highly effective for increasing the power density of the cell. The maximum power density of the cell was achieved a value of  $0.6\text{W}/\text{cm}^2$  at 1073 K, which is almost double to the cell with using non doped  $\text{La}(\text{Sr})\text{Mn}(\text{Fe})\text{O}_3$ . The electrical conductivity of the doped  $\text{La}(\text{Sr})\text{Mn}(\text{Fe})\text{O}_3$  was also studied and the total conductivity in hydrogen atmosphere increases by doping Co or Pd. Therefore, improved power density could be explained by the improved conductivity in fuel atmosphere. Another advantage of oxide anode is tolerance against reoxidation. In this study, influence of re-oxidation treatment of anode on the power density is also studied. The power density negligibly decreased by exposure to air at 1073 K for several times, and so high stability against reoxidation is clearly demonstrated.

#### 8:30 AM

##### (ICACC-S3-012-2012) Silver Based Composite Cathodes for High Performance SOFCs

A. Sarikaya\*, V. Petrovsky, F. Dogan, Missouri University of Science and Technology, USA

Performance and stability of cathode materials play a critical role in the development and future applications of the solid oxide fuel cells (SOFCs). Ag based electrodes are among the most vulnerable components of the SOFCs due to their operation in oxidizing atmospheres at high temperatures near the melting temperature of pure Ag. Ag based LSM (lanthanum-strontium manganite) composite electrodes performed without degradation of the electrical properties and any significant changes of the porous microstructure for >2000h at 800°C in air. Relying upon the results obtained, LSCF (lanthanum-strontium-cobalt ferrite) and LSF (lanthanum-strontium ferrite) as well as LSM composites of Ag were manufactured by polymeric precursor infiltration technique in order to investigate various Ag composites for SOFC cathode applications. LSF and LSCF have higher ionic conductivity than LSM and often used as single component cathodes. Ag-LSF and Ag-LSCF composite cathodes have potential to show higher stability with lower cathode overpotentials and work as combined cathode-current collector layer. Recent results on the relationship between the composition, microstructural development and electrochemical properties of the composite cathodes will be discussed.

#### 8:50 AM

##### (ICACC-S3-013-2012) Production and Characterization of Micro-Tubular Solid Oxide Fuel Cells

M. Casarin\*, R. De la Torre Garcia, V. M. Sglavo, University of Trento, Italy

In order to broaden the tubular SOFCs use in transportation and portable applications it is mandatory reducing the operating temperature and cell dimensions. In particular, when the diameter of cells is decreased, characteristics such as volumetric power density and thermo-cycling ability are increased. However, as the cell diameter is scaled down the current collection becomes a fundamental issue due to the ohmic losses caused by long current paths. Several approaches have been proposed to reduce such ohmic losses, one of the most effective ways are developing more efficient current collection architectures. In the present study, anode supported micro-tubular SOFCs with a compliant current collector were produced. This innovative current-collection configuration allows a homogeneous current collector distribution along the cell length by inserting a spiral nickel wire within the anode with two terminals available for the electrical connections. Characteristics such as different cell length/diameter and anode with graded porosity were considered during processing in order to improve the cell performance. The cell with diameter of ~1.2 mm and active area of ~0.75 cm<sup>2</sup> consists of NiO/YSZ for anode, YSZ for electrolyte, and a bi-structured cathode layer based YSZ/LSM and pure LSM sequentially deposited by dip coating.

#### 9:10 AM

##### (ICACC-S3-014-2012) In-situ XRD of Operating LSCF Cathode Suggests Gradual Compositional Change

J. S. Hardy\*, J. W. Templeton, D. J. Edwards, Z. Lu, J. W. Stevenson, Pacific Northwest National Laboratory, USA

A research capability recently developed at Pacific Northwest National Laboratory makes it possible to simultaneously perform electrochemical testing of an anode-supported solid oxide fuel cell (SOFC) while collecting x-ray diffraction (XRD) data from its cathode. During over 60 hours of cell operation, XRD of the cell's LSCF-6428 cathode found that the diffraction peaks arising from the LSCF gradually shifted to lower angles, indicating lattice expansion. Rietveld refinement determined that the cubic lattice parameter for LSCF was increasing at an average rate of 0.00004 Å per hour. Correlation of this rate to published reports of the effects of compositional changes on the crystal lattice of LSCF indicate that the loss of up to 0.0007 of either Sr or Co per hour from the chemical formula for LSCF-6428 could account for such an expansion. A comparison of SEM-EDS elemental maps of the tested cell to a duplicate cell that was not tested also indicate increased Sr and Co diffusion out of the cathode during cell operation.

#### 9:30 AM

##### (ICACC-S3-015-2012) Performance and Accelerated Degradation of Infiltrated Cathode Systems for Solid Oxide Fuel Cells (Invited)

A. Call\*, M. Shah, S. A. Barnett, Northwestern University, USA

Solid Oxide Fuel Cell (SOFC) cathodes consisting of ionic conducting scaffolds infiltrated with mixed ionic and electronic conducting (MIEC) nanoparticles have exhibited some of the smallest reported polarization resistances. However, few studies investigate the long term degradation of these high performance cells. Symmetric cell cathodes were prepared via wet infiltration of  $\text{La}_{0.6}\text{Sr}_{0.4}\text{Co}_{0.2}\text{Fe}_{0.8}\text{O}_3$  (LSCF) or  $\text{Sr}_{0.5}\text{Sm}_{0.5}\text{CoO}_3$  (SSC) nanoparticles into porous  $\text{Ce}_{0.9}\text{Gd}_{0.1}\text{O}_{1.95}$  (GDC) scaffolds. Electrochemical impedance spectroscopy (EIS) measurements were completed at 600°C in air to simulate intermediate operating temperature and conditions. Initial polarization resistances ( $R_p$ ) as low as 0.23  $\Omega\text{cm}^2$  and 0.11  $\Omega\text{cm}^2$  were obtained for the LSCF-GDC and SSC-GDC systems, respectively. The cells were then subjected to accelerated degradation by aging at temperatures between 650°C and 850°C. Scanning Electron Microscopy (SEM) was performed on

samples at different aging times to determine the size evolution of the MIEC nanoparticles within the GDC scaffold. Along with intrinsic materials properties of the starting materials, this information was used in a composite cathode model to make predictions on  $R_p$  and long term degradation. Results correlating changes in  $R_p$  to microstructural changes observed during life tests will be presented.

### Electrode Materials and Microstructural Engineering II

Room: Coquina Salon H

Session Chairs: Briggs White, Dept. of Energy; S. Elangovan, Ceramtec, Inc.

#### 10:00 AM

##### (ICACC-S3-016-2012) Investigation of Microstructural Effect of Ni-Yttria Stabilized Zirconia for SOFC Anode (Invited)

T. Suzuki\*, K. Hamamoto, B. Liang, T. Yamaguchi, H. Sumi, Y. Fujishiro, National Institute of Advanced Industrial Science and Technology, Japan; B. Ingram, J. Kropf, J. D. Cater, Argonne National Laboratory, USA

Microstructural effect of solid-oxide fuel cell anode on the fuel cell performance has been investigated using XAFS analysis. The microstructure of the anode consisting of conventional Ni-yttria stabilized zirconia (YSZ) has been controlled by the co-sintering temperature with the electrolyte. Impedance analysis has clearly shown that the overpotentials for the gas transport and the electrochemical reactions improve for the anode prepared at lower co-sintering temperatures. XAFS Observation has shown the oxidation status of Ni in the anode sensitively, which may indicate the reaction sites for oxide ions and the fuel.

#### 10:30 AM

##### (ICACC-S3-017-2012) Manganese induced Structural Modifications in Yttria Stabilized Zirconia (YSZ)

M. K. Mahapatra\*, N. Li, W. Ahmad, M. Aindow, P. Singh, University of Connecticut, USA

Role of manganese oxide on the structural modifications in 8 mol% yttrium stabilized zirconia (YSZ) has been investigated. YSZ pellets (>95% density) were embedded in manganese dioxide powder and sintered at 1000-1400°C for 2-10 hrs. in air. Changes in the crystal structure, manganese diffusion profile and interface morphology were studied using a variety of analytical techniques. It is found that cubic YSZ transforms into tetragonal structure and the surface morphology changes from planar to undulated/wavy structure. The mechanisms of the structural and morphological changes of the YSZ are discussed along with its implication on the electrode/electrolyte interfacial stability of solid oxide fuel cell.

#### 10:50 AM

##### (ICACC-S3-018-2012) Interactions of Electrolyte-(La<sub>0.8</sub>Sr<sub>0.2</sub>)xMnO<sub>3</sub> Air Electrode-Interconnect Tri-layers for Solid Oxide Fuel Cells (Invited)

K. Lu\*, T. Jin, Virginia Tech, USA

In solid oxide fuel cell operation, electrical current plays an important role for the air electrode interaction with electrolyte and interconnect and long-term cell performance. In this study, (La<sub>0.8</sub>Sr<sub>0.2</sub>)xMnO<sub>3</sub> (LSM) air electrodes with different stoichiometry ( $x = 0.95, 1, \text{ and } 1.05$ ) are fabricated on the surface of yttria stabilized zirconia (YSZ) and put in contact with AISI 441 stainless steel interconnect. The simulated half cells are thermally treated at 800°C for 500 h under a 200 mA/cm<sup>2</sup> current density. YSZ/LSM interfacial interaction and the reaction of volatile chromium species on the LSM surface are characterized. Different LSM stoichiometry leads to different interfacial reactions and Cr deposition amounts. Mn is a critical species for the Cr deposition under polarization. Excessive Mn in LSM lessens the formation of La-containing phase at the YSZ/LSM interface and accelerates Cr deposi-

tion. Deficient Mn in LSM leads to extensive interfacial reaction with YSZ, forming more La-containing phase and inhibiting Cr deposition.

#### 11:10 AM

##### (ICACC-S3-019-2012) Investigation of cobalt-free perovskite Ba<sub>0.95</sub>La<sub>0.05</sub>FeO<sub>3-δ</sub> as a cathode for proton-conducting solid oxide fuel cells

L. Yan, X. Xue\*, University of South Carolina, USA

Cobalt-free perovskite Ba<sub>0.95</sub>La<sub>0.05</sub>FeO<sub>3-δ</sub> (BLF) was synthesized. The conductivity of BLF was measured with a DC four-point technique. The thermal expansion coefficient of the BLF was measured using a dilatometer. The BaZr<sub>0.1</sub>Ce<sub>0.7</sub>Y<sub>0.2</sub>O<sub>3-δ</sub> (BZCY7) electrolyte based proton conducting solid oxide fuel cells (SOFCs) were fabricated. A composite cathode with BLF+BZCY7 was used to mitigate the thermal expansion mismatch with the BZCY7 electrolyte. The polarization processes of the button cell NiO-BZCY7/BZCY7/BZCY7-BLF were characterized using the complicated electrochemical impedance spectroscopy technique. The open circuit voltage of 0.982V, 1.004V, and 1.027V was obtained at 700oC, 650oC, and 600oC respectively while the peak power density of 325mWcm<sup>-2</sup>, 240 mWcm<sup>-2</sup>, and 152 mWcm<sup>-2</sup>, was achieved accordingly.

#### 11:30 AM

##### (ICACC-S3-020-2012) Freeze-Tape Casting for the Design of Anode and Cathode Materials in [1#11#]Solid Oxide Fuel Cells (SOFCs)

J. Bunch\*, Y. Chen, University of South Carolina, USA; M. May, Citadel, USA; F. Chen, University of South Carolina, USA

Solid oxide fuel cells (SOFCs) have tremendous commercial potential due to their high efficiency, high energy density, and flexible fuel capability, operating on both hydrogen and hydrocarbon-based fuels. The material and fabrication challenges of SOFCs are highly research and well documented. The design for this type of fuel cell is critical if this technology will become widely used and accepted. The method proposed is a novel technique known as freeze-tape casting. This method is used to prepare the anode by tailoring to desired porosity. By using these method to optimize this technology this will provide advances within fuel cell research so that one day a viable sustainable energy source will be available.

#### 11:50 AM

##### (ICACC-S3-021-2012) Liquid Tin Anode Direct JP-8 Fuel Stack Performance and System Development

M. Koslowske\*, J. Brodie, C. MacKean, J. Bentley, T. Tao, CellTech Power, LLC, USA

CellTech Power's direct fuel Liquid Tin Anode-Solid Oxide Fuel Cell (LTA-SOFC) has demonstrated operation on un-reformed or un-processed carbonaceous fuels. Cell development has improved performance on direct JP-8 and direct solid fuel (coal and biomass) over the last several years. For complex liquid fuels such as JP-8, the LTA-SOFC has shown high performance 170 mW/cm<sup>2</sup> and high efficiencies >30%. The material system has demonstrated fast thermal cycling (>100), and performance longevity (> 1000 hrs H<sub>2</sub>) with 1.2% degradation. Current efforts are focused on manufacturing and testing of sub-stack panels, testing stacks and developing a prototype direct JP-8 system. In this presentation, the performance of JP-8 long term (>1000 hrs) testing with the LTA-SOFC single cell will be shown. Also, cell improvements will be summarized resulting in an optimized cell design. Stack development and performance on JP-8 will be reviewed. Finally, a direct JP-8 standalone system prototype based on the LTA-SOFC will be introduced and performance results will be presented.



## S5: Next Generation Bioceramics

### Bioinspired, Biomimetic, and Biologically-derived Ceramics I

Room: Coquina Salon C

Session Chairs: Xiaodong Li, University of South Carolina; A. Cuneet Tas, University of Oklahoma, College of Dentistry

8:00 AM

#### (ICACC-S5-016-2012) Granules of brushite and octacalcium phosphate from marble (Invited)

A. Tas\*, University of Oklahoma, USA

Brushite (DCPD, dicalcium phosphate dihydrate,  $\text{CaHPO}_4 \cdot 2\text{H}_2\text{O}$ ) and octacalcium phosphate (OCP,  $\text{Ca}_8(\text{HPO}_4)_2(\text{PO}_4)_4 \cdot 5\text{H}_2\text{O}$ ) granules with millimeter sizes were prepared by using marble (calcium carbonate) granules as the starting material. The method of this study simply comprised of soaking the marble granules in aqueous solutions containing phosphate and/or calcium ions at temperatures between 20 and 37 C. This process did not cause any size change between the initial marble and final brushite or octacalcium phosphate granules. Such DCPD and OCP granules could be useful in maxillofacial, dental and orthopedic void/bone defect filling and grafting applications. Samples were characterized by X-ray diffraction, inductively-coupled plasma atomic emission spectroscopy, and scanning electron microscopy.

8:20 AM

#### (ICACC-S5-019-2012) Bio-inspired synthesis of bone-like matrix

Y. Wang\*, N. Nassif, T. Azaïs, G. Laurent, M. Giraud-Guille, F. Babonneau, Laboratory of la chimie de la matiere condensee de Paris, France

Bone is a complex composite material composed of an organic matrix (mainly collagen) with inorganic nanocrystals (apatite) that strengthen it. The biological apatites are non-stoichiometric carbonate-containing plate-shaped nanocrystals. A better characterization of molecular interactions between these components is fundamental to improve understanding of bone formation. In the present work, specific experimental conditions based on a diffusion method have been developed to induce precipitation of biological-like apatite in solution as well as within a collagen matrix. In this tissue-like collagen apatite matrix, size and distribution of apatite crystals are recreated as in bone. We have investigated the structure of those nanocrystals and compared them with biological apatite. Characterization by X-ray powder diffraction shows that the collagen matrix influences the crystallite size of apatite. We then relied on solid-state NMR experiments to probe the local environment of several sites, and thus gain insights into the complex structure of such substituted apatite. Results obtained from  $^{31}\text{P}$  MAS NMR spectra highlight the impact of the dense organic matrix on the environment of the phosphates anions. In parallel, the collagen apatite matrix was used as a simplified model for investigating the molecular interactions between the organic matrix and the mineral phase by NMR.

8:40 AM

#### (ICACC-S5-017-2012) Unveiling the Strengthening and Toughening Mechanisms of Nacre – Lessons from Nature (Invited)

X. Li\*, University of South Carolina, USA

Nacre is a natural nanocomposite with superior mechanical strength and eminent toughness. What is the secret recipe that Mother Nature uses to fabricate nacre? What roles do the nanoscale structures play in the strengthening and toughening of nacre? Can we learn from this to produce nacre-inspired nanocomposites? The recent discovery of nanoparticles in nacre is summarized, and the roles these nanoparticles play in nacre's

strength and toughness are elucidated. It was found that rotation and deformation of aragonite nanoparticles are the two prominent mechanisms contributing to energy dissipation in nacre. The biopolymer spacing between nanoparticles facilitates the particle rotation process. Individual aragonite nanoparticles are deformable. Dislocation formation together with deformation twinning were found to play an important role in the plastic deformation of individual nanoparticles, contributing remarkably to the strength and toughness of nacre upon dynamic loading. This talk also presents future challenges in the study of nacre's nanoscale structure and mechanical properties.

9:00 AM

#### (ICACC-S5-018-2012) Antibiotics-incorporated Apatite and Apatite/Collagen Coatings on NiTi Shape Memory Alloy Formed by Electrochemical Deposition (Invited)

W. Lee, M. Wang\*, The University of Hong Kong, Hong Kong

NiTi shape memory alloys (SMAs) are attractive metallic biomaterials due to their shape memory and superelastic properties. By forming a bioactive coating on NiTi SMAs, namely, an apatite or apatite/collagen coating, the release of cytotoxic Ni ions from NiTi SMAs may be minimized while the bioactivity of implants is provided. Furthermore, antibiotics-incorporated coatings may minimize/prevent implant-associated infections. In the current investigation, antibiotics-loaded apatite or apatite/collagen coatings were formed on a NiTi SMA through electrochemical deposition. Two antibiotics, tobramycin and vancomycin, were used separately for the coatings and the in vitro release of antibiotics was studied. The apatite coating and apatite/collagen composite coating exhibited different drug loading levels and loading efficiency. It was found that the amount of antibiotics incorporated into the coatings and their in vitro release behaviours were controlled by the type of antibiotics, the concentration of an antibiotic in the electrolyte and the speed of coating formation. Tobramycin showed better incorporation than vancomycin, which was due to differences in drug chemical structure and molecule size. In the in vitro release study, antibiotics of a smaller molecule size appeared to be released faster.

9:20 AM

#### (ICACC-S5-020-2012) UV-irradiation modifies chemistry of anatase layer pertinent to in vitro apatite nucleation (Invited)

K. Uetsuki, S. Nakai, Y. Shirosaki, S. Hayakawa, A. Osaka\*, Okayama University, Japan

Implant surface must be so modified sometimes as to form strong bond to host tissues. Chemically pure titanium has been provided with anatase layer that induces spontaneous apatite deposition under physiological conditions, and hence it has bone-bonding ability. The anatase layer derived from chemical oxidation with  $\text{H}_2\text{O}_2$  and subsequent calcination (CHT samples) could be enhanced in such ability by UV irradiation, because it would experience certain chemical modifications: decrease or increase in Ti-O- or Ti-OH and Ti-O(H)-Ti which are considered as active sites for apatite nucleation. When in vitro apatite deposition was examined using Kokubo's simulated body fluid (SBF), UV irradiation in air (UVa) reduced the apatite-forming ability of the anatase layer, but UV irradiation on the samples in water (UVw) enhanced the ability. Those results were correlated to the change in the fraction of Ti-OH and Ti-O(H)-Ti, derived from O 1s X-ray photoelectron spectroscopy. Analysis of the number and size of the semi-spherical particles and their surface-coverage as a function of the soaking period lead to a model: proper assembly of those sites (Ti-OH and Ti-O(H)-Ti) should only give rise to induction of apatite nucleation, analogous to the fact that lattice matching would ease deposition of a crystal with a different structure but with a similar arrangement of particular ions.

### Bioinspired, Biomimetic, and Biologically-derived Ceramics II

Room: Coquina Salon C

Session Chairs: Federico Rosei, INRS; Akiyoshi Osaka, Okayama University

**10:00 AM**

#### (ICACC-S5-021-2012) Nanoscale Properties of Implantable Biomaterials (Invited)

F. Rosei\*, INRS, Canada

Modifying the nanoscale structure of materials allows to tailor and optimize their properties [1]. Our strategy rests on using nanomaterials, specifically creating nanopatterns that act as surface cues [2,3] and affect cell behavior. We developed a chemical treatment of Ti-based materials that produces a unique nanostructured topography [4], showing that chemical oxidation is a general strategy that affects biocompatibility [5]. The treatment generates multifunctional surfaces that selectively promote the growth of certain cells while inhibiting others, without using growth factors. Nanostructured Ti surfaces selectively inhibit fibroblastic cell growth [4] and promote osteogenic cell activity [6-9] *in vitro*. Further enhancement of biocompatibility may be provided by coating with spider silk, whose structural/functional properties are currently being studied [10,11]. [1] F. Rosei, *J Phys Cond Matt* 16, 1373 (2004). [2] F. Cicoira, F. Rosei, *Surf Sci* 600, 1 (2006). [3] F. Variola et al, *Small* 5, 996 (2009). [4] F. Variola et al, *Biomaterials* 29, 1285 (2008). [5] F. Vetrone et al, *Nanolett* 9, 659 (2009). [6] L. Richert et al, *Adv Mater* 20, 1488 (2008). [7] F. Variola et al, *Adv. BioMater.* 11, B227 (2009). [8] F. Variola, A. Nanci, F. Rosei, *Appl. Spect.* 63, 1187 (2009). [9] L. Richert et al, *Surf. Sci.* 604, 1445 (2010). [10] C.P. Brown et al, *Nanoscale* 3, 870 (2011). [11] CP Brown et al, *Nanoscale* in press (2011).

**10:20 AM**

#### (ICACC-S5-022-2012) Bioactive Glass Scaffolds for Bone Tissue Engineering (Invited)

M. N. Rahaman\*, Missouri University of Science and Technology, USA

Despite considerable work over many decades, the repair of segmental bone loss remains a challenging clinical problem. Current treatments such as bone allografts and custom metal augments are expensive and have serious limitations. Bioactive glass is unique in its ability to convert to hydroxyapatite *in vivo*, in addition to its proven osteoconductivity and ability to bond firmly to hard and soft tissues. This paper will provide a review of our recent work to create bioactive glass scaffolds that can be used for the repair of large defects in load-bearing bones, such as segmental defects in the long bones resulting from trauma, war, or disease. Bioactive glass scaffolds with controllable conversion rates to hydroxyapatite, with compressive strengths comparable to those of trabecular and cortical bones, and with the ability to enhance new bone ingrowth and angiogenesis *in vivo* will be described. The creation of optimized bioactive glass scaffolds for the repair of segmental bone loss will be discussed.

**10:40 AM**

#### (ICACC-S5-023-2012) Residual stress and phase transformation in zirconia restoration ceramics (Invited)

M. Allahkarami, J. C. Hanan\*, Oklahoma State University, USA

A ceramic based dental restoration's service life is limited to a few years until catastrophic fatigue cracking. With patient life expectancy continuing to increase, and limits on available bio compatible material options, the need for more engineering approaches to crown design continuous to grow. The next generation of multi layer ceramic restorations can rely on designing the manufacture process and geometries to control residual stresses at the contact surface and internal interfaces. As an example, having compressive residual stress beneath the applied external load, increases damage resistance and prevents crack initiation. Measurement techniques interpreting inter-

nal stress states are lacking. At different locations on a typical zirconia-porcelain crown, residual stress as large as  $\pm 400$  MPa and tetragonal to monoclinic phase transformation were measured using microdiffraction (Bruker D8).

**11:00 AM**

#### (ICACC-S5-032-2012) Structural Investigation of substituted Hydroxyapatites : Strengths of Solid State NMR (Invited)

F. Babonneau\*, T. Azaïs, LCMCP / UPMC-Paris6 & CNRS, France; C. Coelho, IMPC / UPMC-Paris6 & CNRS, France; C. Bonhomme, LCMCP / UPMC-Paris6 & CNRS, France

The richness of the apatite structure is an extraordinary ability to accept substitutions and vacancies. The apatite structure can incorporate a wide variety of ions, of the same or of different charge, which affect both its cationic and anionic sub-lattices. This property is intimately related to its adaptability to the biological functions of different tissues. This presentation will illustrate how multinuclear solid-state NMR methods can be efficiently used to describe the structure of nanosized substituted hydroxyapatites. The particular cases of carbonate and silicate substitution will be discussed.

**11:20 AM**

#### (ICACC-S5-025-2012) Preparation and Characterization of Mg-based Silicate Bioceramics from a Pre-ceramic Polymer Filled with Nano-particles (Invited)

E. Bernardo\*, P. M. Dias, P. Colombo, University of Padova, Italy; L. Treccani, U. Hess, K. Rezwan, University of Bremen, Germany

Forsterite ( $Mg_2SiO_4$ ) ceramics have been successfully prepared by a not previously reported approach, consisting of the heat treatment of silicone resins embedding MgO nano-particles as "active" filler. The combined reactivity of oxide nano-particles and silica derived from the ceramic conversion of the silicone resins allowed high yields of forsterite (F) even at the very low temperature of 900°C. This condition was exploited to minimize the thermal decomposition of commercial hydroxyapatite micro-particles (HAp), inserted as secondary, "passive" filler, thus leading to forsterite-hydroxyapatite composites, with different balance between the phases (from 75 wt.% F-25 wt.% HAp to 25 wt.% F-25 wt.% HAp). A similar approach was employed for the synthesis of Ca-Mg silicates, such as diopside ( $CaMgSi_2O_6$ ) and akermanite ( $Ca_2MgSi_2O_7$ ), obtained by using both MgO and  $CaCO_3$  nano-particles as fillers. Akermanite (Ak), being produced in conditions of superior phase purity than diopside, was taken as a matrix for further ceramic composites, i.e. akermanite-hydroxyapatite composites. Both F-HAp and Ak-HAp composites may be suitable for use in bone tissue engineering application and, by several *in vitro* tests, their biocompatibility and bioactivity is currently investigated.

## S7: 6th International Symposium on Nanostructured Materials and Nano-Composites

### Synthesis, Functionalization, Processing and Self-assembly of Nanoparticles I

Room: Coquina Salon B

Session Chairs: Gunnar Westin, Uppsala University; Kathy Lu, Virginia Tech

**8:00 AM**

#### (ICACC-S7-049-2012) ZnO nanoparticle-based surface templating (Invited)

K. Lu\*, B. Chen, K. Ramsburg, Virginia Tech, USA

In this study, ZnO feature arrays are fabricated by casting a high solid loading ZnO nanoparticle suspension in PDMS molds. The pattern arrays on the PDMS molds are obtained using an imprint lithography

method in combination with patterned silicon cores. ZnO nanoparticle suspension is prepared using 20 nm ZnO nanoparticles at different pH values and in the presence of different dispersants. The effect of the pH value and dispersant on the maximum solids loading is examined. Different surface modifications of the PDMS molds influence the wettability of the ZnO nanoparticle suspension on them. The volume shrinkage during the transformation from ZnO nanoparticle suspensions into ZnO solid features inside the PDMS mold features is explored. The minimum diameter and the maximum aspect ratio of the ZnO features that can be obtained by this templating method are studied.

#### 8:20 AM

##### (ICACC-S7-050-2012) Thin complex oxide, composite and metal coatings through solution processes (Invited)

G. Westin\*, Uppsala University, Sweden; K. Jansson, Stockholm University, Sweden; A. Pohl, Uppsala University, Sweden

The development of many materials related renewable energy, such as solar-cells catalysts, photo-catalysts and batteries require complex nano-structured materials, where different parts are optimized for different functions. Often the materials should consist of a nano-structure with an ultra thin coating of 1-5 nm thickness that e.g. protect against recombination with an electrolyte, inhibit corrosion or particle growth or provide a co-catalyst to a photo-catalyst. As the knowledge in these areas increase rapidly due to the immense experimental and theoretical research made, more and more complex materials are desired where homo and multiphase thin coatings are one of the key components. There is however a need to develop efficient processes to produce such coatings since the technological exploitation for energy applications requires low cost high rate processing. We describe solution based, flexible coatings for formation of thin coatings in the range 1-5 nm containing various oxides, oxide-metal composites and metals. Systems that will be discussed are; transition metal oxides, M-oxide composites with metal particle sizes around 1-2 nm (M=Ni,Co,Pt...), and metal films with a focus on Ni-metal. The processes are based both on alkoxides and organically complexed salts depending on the system in mind. The processes have been applied on oxide systems such as ZnO nano-particles and wires and TiO<sub>2</sub>.

#### 8:50 AM

##### (ICACC-S7-051-2012) Hot wire and spark pyrolysis as simple new routes to silicon nanoparticle synthesis (Invited)

M. R. Scriba\*, CSIR, South Africa; D. T. Britton, M. Harting, University of Cape Town, South Africa

Recently, printed electronics, based on silicon nanoparticle ink, has emerged as a new route to the production of electronic devices on flexible media. For electron transport these nanoparticles must be free of an oxide layer and contain dopants. Silicon nanoparticles produced by plasma pyrolysis, laser ablation or chemical routes often do not meet these requirements. We have investigated hot wire and spark pyrolysis as simple new routes to the production of doped silicon nanoparticles using silane or a mixture of silane and diborane or phosphine as precursor, at a pressure between 40 and 800 mbar. For both processes, all particles produced are monocrystalline. While hot wire pyrolysis always results in multifaceted particles with a mean diameter of 32 nm, spark pyrolysis produces spherical particle with a 40 nm average diameter. A simple method of resistance measurement on compressed powder showed that most silicon powders are electrically active while those that are not have been shown by TEM analysis to contain an oxide layer on their surface. XPS results support these observations and in addition offer proof of successful boron and phosphorus doping of these silicon nanoparticles. The results clearly demonstrate that hot wire and spark pyrolysis offer a new simple route to the production of monocrystalline doped silicon nanoparticles suitable for printed electrical devices.

#### 9:20 AM

##### (ICACC-S7-052-2012) Materials modelling for electrochemical applications (Invited)

T. T. Jaervi\*, L. Mayrhofer, L. Pastewka, M. Moseler, Fraunhofer Institute for Mechanics of Materials IWM, Germany; T. Kaib, S. Kaib-Haddadpour, S. Dehnen, Philipps-University Marburg, Germany; H. F. Andersen, K. Möller, Fraunhofer Institute for Silicate Research (ISC), Germany

Addressing the immense challenges on clean energy storage, imposed by emission-free energy and transport technologies, requires development of both new materials and ways of nanostructuring them for maximum efficiency. Thus materials science is expected to provide solutions for electrochemical systems ranging from batteries and supercapacitors to photochemistry, just to name a few examples. In this talk, we will review our recent work, aiming to address some of the above questions, with emphasis on modelling electrochemical systems on scales from electronic structure to classical atomistic simulations. Addressing the materials question, we will present results on several novel materials, which are promising for energy storage applications. We show how classical mean-field charge-transfer models can be derived from quantum methods via the tight-binding formalism. Models similar to traditional variable-charge models can be obtained and readily incorporated into existing molecular dynamics codes. The effectiveness of the model is demonstrated for metallic carbon nanotubes and graphene, where a Li-C potential can be constructed, capable of describing Li-intercalation into carbonaceous anodes in biased systems, fully incorporating long-range electrostatics.

##### Synthesis, Functionalization, Processing and Self-assembly of Nanoparticles II

Room: Coquina Salon B

Session Chairs: Kathy Lu, Virginia Tech; Ashok Singh, Defence Institute of Advanced Technology

#### 10:00 AM

##### (ICACC-S7-053-2012) Mechanism-Based Design of Precursors for the Deposition of Inorganic Films and Nanoparticles (Invited)

L. McElwee-White\*, D. Wei, T. J. Anderson, University of Florida, USA

A chemistry-based approach to designing precursors for the deposition of inorganic films and nanoparticles requires consideration of the physical properties of the precursor compound and its probable decomposition pathways, both in the gas phase and on the surface during growth. Among the standard techniques for the elucidation of decomposition pathways in organometallic compounds that will be discussed in this context are NMR kinetics, mass spectrometry, DFT calculations, Raman spectroscopy and small molecule structure determination by single crystal X-ray diffractometry. Information on the precursor chemistry found through these means will be correlated to properties of the deposited materials including composition (AES, XRD), growth kinetics (X-SEM) and bonding states (XPS). These issues will be discussed in the context of deposition of tungsten carbonitride thin films on silicon wafers using the tungsten imido complexes  $WCl_4(NR)(CH_3CN)$  [ $R = Ph, ^iPr, allyl$ ] and the tungsten hydrazido complexes  $WCl_4(NNR_2)(CH_3CN)$  [ $R_2 = Me_2, Ph_2, -(CH_2)_5-$ ]. Deposition of gold nanoparticles on nanostructured silver substrates will also be discussed. This work was financially supported by the US National Science Foundation through the NSF-CCI Center for Nanostructured Electronic Materials (grant CHE-1038015 to LMW and WDW) and through grant CHE-0911640 to LMW and TJA.

#### 10:30 AM

##### (ICACC-S7-054-2012) Plasma-enabled, environment-friendly nanomaterials synthesis: from precursor-free silicon nanowires to catalyst-free vertical nanotubes and graphenes (Invited)

K. Ostrikov\*, CSIRO Materials Science and Engineering, Australia

In my presentation, I will discuss several examples of uniquely plasma-enabled nanomaterials for applications in energy conver-

sion and storage, sensing, opto- and nanoelectronics. The first example shows a simple, uniquely plasma-enabled and environment-friendly process to reduce the thickness of vertically standing graphenes to only 4–5 graphene layers and arranging them in dense, ultra-large surface area, ultra-open-edge-length, self-organized and interconnected networks. The approach for the ultimate thickness reduction to 1–2 graphene layers is also discussed. In the second example, a simple, rapid, catalyst-free synthesis of complex patterns of long, vertically aligned multiwalled carbon nanotubes, strictly confined within mechanically-written features on a silicon surface is presented. Our results contribute to enabling direct integration of graphene structures into presently dominant Si-based nanofabrication platform for next-generation nanoelectronic, sensor, biomedical, and optoelectronic components and nanodevices. It will also be discussed how low-temperature plasma-specific effects contribute to the solution of (i) effective control of nucleation and growth; (ii) environmental friendliness; and (iii) energy efficiency critical issues in semiconducting nanowire growth.

**11:00 AM**

**(ICACC-S7-055-2012) CNT based nanocomposite strain sensor for structural health monitoring (Invited)**

A. K. Singh\*, Defence Institute of Advanced Technology, India

Laboratory synthesized CNTs were used to make nanocomposite of different loadings in PMMA polymer. Before use, CNTs were characterized at different stages of purification using TGA, Raman, FTIR, XRD, SEM, and HRTEM. Obtained CNTs were about 10 nm in dia and about 0.5  $\mu\text{m}$  in length and MWNT in nature. The prepared nanocomposites were characterized for their electrical behaviour. The corresponding I-V behaviour indicates that the films have metallic behaviour close to room temperature. The peppered MWNT/PMMA nanocomposite films were used for strain sensor application for structural health monitoring by fixing it onto a Al cantilever beam. The change of resistance of each strain sensor was measured by Data Acquisition System (DT 80 De Logger) with respect to the displacement due to bending of the cantilever beam. Full bridge circuit was used to measure change in resistance to minimize the errors due to temperature variations. Performance of strain sensor was studied under different conditions. The strain sensor results closely matched with standard strain gauge sensor under static as well as dynamic condition. It showed consistent piezoresistive behavior under repetitive straining and unloading, and good resistance stability. The developed CNT nanocomposite strain sensor followed the free vibration pattern similar to pattern of standard reference strain sensor demonstrating good static and dynamic response.

**11:20 AM**

**(ICACC-S7-056-2012) Microwave Assisted Synthesis of Si(B)CN-MWCNT Free-Standing Paper for High Temperature Applications**

R. Bhandavat\*, G. Singh, W. Kuhn, Kansas State University, USA; E. Mansfield, National Institute of Standards and Technology, USA

We demonstrate an environment friendly and time saving method for synthesis of a polymer-derived ceramic (PDC)-MWCNT composite using microwave irradiation at 2.45 GHz. The process takes about 10 minutes for the polymer to ceramic conversion as compared to hours required by conventional methods. The successful conversion of polymer coated carbon nanotubes to ceramic composite is chemically ascertained by FT-infrared, X-ray photoelectron spectroscopy and transmission electron microscopy. The permittivity measurements confirm high microwave nanotube interaction resulting in large heat generation necessary for polymer to ceramic conversion. The free-standing paper was then prepared by vacuum filtration of the composite nanowires, stable in air up to  $\sim 800^\circ\text{C}$ . The paper will find applications in high temperature membranes, thermal sensors and rechargeable battery anode.

**11:40 AM**

**(ICACC-S7-057-2012) Carbon nanotube - Nanocrystalline diamond composite coatings: processing conditions and growth mechanism**

S. Vasudevan\*, J. Rankin, Brown University, USA; B. Walden, Trinity college, USA; B. W. Sheldon, Brown University, USA

Microwave assisted plasma chemical vapor deposition (MPCVD) has been employed to fabricate Carbon nanotube (CNT) – Nano-crystalline Diamond (NCD) composite thin films which are envisaged as excellent wear resistant coatings. The growth conditions used for forming the NCD matrix can etch the CNTs, hence the balance between NCD growth and hydrogen induced carbon loss from the CNTs is critical. The fabrication of such CNT/NCD composite films was investigated over a range of different conditions and the material was characterized with Raman spectroscopy and TEM. Analysis of the growth mechanisms will also be discussed.

## **S8: 6th International Symposium on Advanced Processing and Manufacturing Technologies for Structural and Multifunctional Materials and Systems (APMT) in honor of Professor R. Judd Diefendorf**

**Processing, Structure and Properties**

Room: Coquina Salon A

Session Chairs: Vojislav Mitic, Faculty of Electronic Engineering; Junichi Tatami, Yokohama National University

**8:10 AM**

**(ICACC-S8-050-2012) Texturing Technologies for Group IVB Metal Diboride Ceramics (Invited)**

G. Zhang\*, Shanghai Institute of Ceramics, China

TiB<sub>2</sub>, ZrB<sub>2</sub> and HfB<sub>2</sub> ceramic materials, including the monolithic ceramics and their composites, show a good combination of various properties, such as high strength, high electrical conductivity, good chemical corrosion and oxidation resistance. Especially, diborides based ultra-high temperature ceramics (UHTCs) with chemical and physical stability at high temperatures (e.g., above 2000°C) and in reactive atmospheres (e.g., monatomic oxygen) are key materials for applications in liquid/solid rocket engines and thermal protective systems of hypersonic flight (nose cones and leading edges). In this presentation group IVB metal diborides including TiB<sub>2</sub>, ZrB<sub>2</sub> and HfB<sub>2</sub> were investigated and characterized by texturing the material microstructures. Highly textured ZrB<sub>2</sub>-SiC and HfB<sub>2</sub>-SiC UHTCs with c-axis orientation were prepared via strong magnetic field alignment (SMFA) during slip casting, followed by spark plasma sintering. Results showed that hardness on SS surface (perpendicular to magnetic field) was superior to that on TS surface. Oxidation resistance demonstrates obvious anisotropy. ZrB<sub>2</sub>-MoSi<sub>2</sub> ceramics with in situ formed ZrB<sub>2</sub> platelets have been successfully prepared by reactive hot pressing, and furthermore, textured ZrB<sub>2</sub>-MoSi<sub>2</sub> ceramics were manufactured by hot forging. The microstructure features, formation mechanisms and the relationships with material properties will be discussed.

**8:40 AM**

**(ICACC-S8-051-2012) Contact Surface Influence on Microstructure and Dielectric Properties of Doped BaTiO<sub>3</sub>-ceramics**

V. Mitic\*, V. Paunovic, J. Purenovic, Faculty of Electronic Engineering, Serbia; S. Jankovic, Faculty of Mathematics, Serbia; V. Pavlovic, Faculty of Agriculture, Serbia

The effects of rare-earth ions dopants on modified BaTiO<sub>3</sub>-microstructure have been studied in this investigation. Microstructural and compositional studies were performed by SEM and EDS system.

BaTiO<sub>3</sub>-ceramics doped up to 1.0 wt% of Ho<sub>2</sub>O<sub>3</sub> were prepared by conventional solid state procedure and sintered up to 1380°C for four hours. Dielectric characteristics, as dielectric constant and dielectric loss, have been done in the frequency range from 20Hz to 1MHz. After using fractal method, grains shapes reconstruction and intergranular contacts have been successfully done. The area of grains surface was calculated by using fractal correction which expresses the irregularity of grains surface through fractal dimension. Also, we developed the new contact surfaces probability approach and method. The results indicate that, fractal and statistics methods provide better and more precise describing, predicting and modeling the grain shape and relations between the BaTiO<sub>3</sub>-ceramic structure and dielectrical properties in further circuits' integrations and devices miniaturization.

#### 9:00 AM

##### (ICACC-S8-052-2012) Numerical Analysis of Fracture Behavior in Anisotropic Microstructures

H. Serizawa\*, S. Tomiyama, T. Hajima, H. Murakawa, Osaka University, Japan

As one of the numerical methods for examining microstructural fracture behavior in the virtual polycrystalline model, the finite element method with interface element has been developed, where the isotropic elastic-plastic deformation of grain or the debonding & slipping at grain boundary could be demonstrated. However, the mechanical properties of grain and grain boundary should be anisotropic due to the grain orientation. So, in this research, the effect of these anisotropies on microstructural fracture behavior was studied by assuming the orthotropic property in grain due to grain orientation and by considering the variation of grain boundary strength caused by the misorientation between neighbor grains. Also, the influence of plastic deformation in grain on fracture behavior was examined by employing the theory of crystal plasticity. As the results assuming the grain orientation, it was revealed that the anisotropic property of grain boundary would be a dominant factor of the fracture process and the computed result would have a good agreement with the experiment by selecting the appropriate value of interaction between opening and slipping deformations at grain boundary. Moreover, it was found that the stress concentrations due to both the mismatch between neighbor grains and the slipping at grain boundary could be demonstrated by using the theory of crystal plasticity.

#### 9:20 AM

##### (ICACC-S8-053-2012) Grain boundary structures of silicon nitrides with Lu<sub>2</sub>O<sub>3</sub>-SiO<sub>2</sub> and Lu<sub>2</sub>O<sub>3</sub>-Yb<sub>2</sub>O<sub>3</sub>-SiO<sub>2</sub> additives

K. Fukunaga\*, AIST, Japan; N. Kondo, H. Kita, T. Ohji, National Institute of Advanced Industrial Science and Technology (AIST), Japan; T. Saito, Japan Fine Ceramics Center, Japan; Y. Ikuhara, The University of Tokyo, Japan

Mechanical properties of silicon nitrides are strongly depending on their sintering additives. Lu<sub>2</sub>O<sub>3</sub>-based sintering additives are advantageous to achieve high temperature strength. Some of the authors previously reported that 1) High temperature strength of this system strongly depends on Lu<sub>2</sub>O<sub>3</sub>/SiO<sub>2</sub> ratio. 2) Fracture toughness as well as high temperature strength are improved by adding small amount of Yb<sub>2</sub>O<sub>3</sub>. To understand their mechanical properties in relation to their compositions, atomic scale direct observation of their grain boundaries is strongly needed. Recently high-angle annular dark-field scanning transmission electron microscopy (HAADF-STEM) and annular bright-field scanning transmission electron microscopy (ABF-STEM) have been developed. By using these techniques, location of Si, N, Lu, Yb, etc. can be defined in atomic scale. In this work, grain boundary structures of three silicon nitrides, Si<sub>3</sub>N<sub>4</sub> - 8Lu<sub>2</sub>O<sub>3</sub> - 2SiO<sub>2</sub> (wt.%) (8L), Si<sub>3</sub>N<sub>4</sub> - 9Lu<sub>2</sub>O<sub>3</sub> - 1SiO<sub>2</sub> (9L) and Si<sub>3</sub>N<sub>4</sub> - 7.9Lu<sub>2</sub>O<sub>3</sub> - 0.1Yb<sub>2</sub>O<sub>3</sub> - 2SiO<sub>2</sub> (LY), were examined by HAADF-STEM and ABF-STEM. It was found that atomic location at grain boundaries were different in these three systems. For example, 1) Lu<sub>2</sub>O<sub>3</sub> was detected at grain boundaries in 9L, but was not in 8L. 2)

Yb was detected at grain boundary in LY. Mechanical properties were discussed in relation to the grain boundary structures.

#### 10:00 AM

##### (ICACC-S8-054-2012) Amorphous Silicon nitride - Carbon nanotube composite coatings: the impact of nanotube structure and density on mechanical properties

S. Vasudevan\*, B. W. Sheldon, K. Sena, Brown University, USA

Chemical vapor infiltration was employed to produce composite carbon nanotube (CNT) reinforced coatings with excellent mechanical properties. This approach uses vertically aligned CNT (VACNT) arrays fabricated by chemical vapor deposition (CVD) on a bilayer Fe/Al<sub>2</sub>O<sub>3</sub> catalyst. Controlled variation of the catalyst thickness and/or annealing temperature was used to modify the CNT structure, defect population and CNT density. The composite coatings were fabricated by infiltrating silicon nitride matrix in to these VACNT arrays using low pressure CVD. The carbon structure in the initial arrays and the composites were analyzed with Raman spectroscopy, while the elastic properties and fracture toughness of the composites were investigated with nanoindentation. The present work focuses on understanding how these mechanical properties are affected by two key features: the density of the CNT arrays and the defect structure of the CNTs. These effects were systematically controlled through careful synthesis of the materials.

#### 10:20 AM

##### (ICACC-S8-055-2012) Development of electrical discharge machinable ZTA ceramics with 24 vol.-% of TiC, TiN, TiCN, TiB<sub>2</sub> and WC as electrically conductive phase

R. Landfried\*, F. Kern, R. Gadov, University of Stuttgart, Germany

The Electrical Discharge Machining of electrically conductive ceramics enables an economical production of tools and molds containing cavities with high aspect ratio and sharp inner edges. In order to develop ED machinable high strength and toughness ceramics for high wear applications ZTA ceramics with addition of 17 vol.-% 1.5Y-TZP and 24 vol.-% of TiC, TiN, TiCN, TiB<sub>2</sub> and WC as electrically conductive phases were hot pressed at 60 MPa and temperatures ranging from 1475°C to 1550°C. Mechanical and electrical properties were investigated. The influence of the electrically conductive phase on the surface quality after ED-machining (die sinking and wire-EDM) was analyzed. The mechanical properties and machining quality were found to depend significantly on the type of conductive phases. While WC leads to highest bending strength of 1120 MPa, TiB<sub>2</sub> leads to highest toughness of 7.6 MPa√m and lowest roughness after wire ED machining. ZTA-TiC samples with strength of 1050 MPa and toughness of 6.1 MPa√m show best machinability and surface qualities after die sinking. High end tools and molds of novel conductive ZTA composites can be ED machined at high precision with narrow dimensional tolerances.

#### 10:40 AM

##### (ICACC-S8-056-2012) Electrical conductivity of CNT-dispersed Si<sub>3</sub>N<sub>4</sub> ceramics fabricated by using HfO<sub>2</sub> as a sintering aid

M. Matsuoka\*, S. Yoshio, J. Tatami, T. Wakihara, K. Komeya, T. Meguro, Yokohama National University, Japan

The study to give electrical conductivity by dispersing carbon nanotubes (CNT) into silicon nitride (Si<sub>3</sub>N<sub>4</sub>) ceramics has been carried out in recent years. However, the density of Si<sub>3</sub>N<sub>4</sub> ceramics were degraded and CNTs disappeared after firing at higher temperatures because CNTs prevent Si<sub>3</sub>N<sub>4</sub> from densification and there is a possibility that CNTs react with Si<sub>3</sub>N<sub>4</sub> or SiO<sub>2</sub>. In order to suppress the reaction and the disappearance of CNTs, lower temperature densification is needed. In this study, HfO<sub>2</sub> was added to Si<sub>3</sub>N<sub>4</sub>-Y<sub>2</sub>O<sub>3</sub>-Al<sub>2</sub>O<sub>3</sub>-AlN-TiO<sub>2</sub> system to fabricate CNT-dispersed Si<sub>3</sub>N<sub>4</sub> ceramics at lower temperatures. It was observed that CNTs remained in the sintered body. By using HfO<sub>2</sub> as a sintering aid, we succeeded in fabricating dense CNT-dispersed Si<sub>3</sub>N<sub>4</sub> ceramics from lower temperatures. Samples adding

HfO<sub>2</sub> showed higher electrical conductivity than that of samples without HfO<sub>2</sub>. It has been reported that HfO<sub>2</sub> improved the oxidation resistance of silicon carbide compositionally graded graphite. In our study, HfO<sub>2</sub> suppressed the disappearance of CNT due to the reaction with Si<sub>3</sub>N<sub>4</sub> or SiO<sub>2</sub>. Consequently, it was shown that HfO<sub>2</sub> promoted the densification of Si<sub>3</sub>N<sub>4</sub> and it improved electrical conductivity of CNT-dispersed Si<sub>3</sub>N<sub>4</sub> ceramics.

11:00 AM

### (ICACC-S8-057-2012) Electrically Conductive Si<sub>3</sub>N<sub>4</sub>/TiN Nanocomposites Prepared by Pressureless Sintering of TiN-Coated Si<sub>3</sub>N<sub>4</sub> Powder

K. Krnel\*, Jozef Stefan Institute, Slovenia; A. Maglica, Lek d.d., Slovenia; T. Kosmac, Jozef Stefan Institute, Slovenia

Electrically conductive Si<sub>3</sub>N<sub>4</sub>/TiN nanocomposites have been fabricated by pressureless sintering of TiN-coated Si<sub>3</sub>N<sub>4</sub> powders. The silicon nitride powder was coated with various amounts (10–35 vol. %) of nano-sized TiO<sub>2</sub> particles by an in-situ gel precipitation of titanium hydroxides in Si<sub>3</sub>N<sub>4</sub> aqueous suspension. The TiN nanoparticles on the Si<sub>3</sub>N<sub>4</sub> powder surface were formed by nitridation of TiO<sub>2</sub> in a NH<sub>3</sub> gas flow at 900 deg.C. The TEM analysis indicated that the Si<sub>3</sub>N<sub>4</sub> particles are uniformly coated with TiN nanoparticles exhibiting a narrow size distribution and the average size of 5 nm. In the presence of Y<sub>2</sub>O<sub>3</sub> and Al<sub>2</sub>O<sub>3</sub> sintering additives dense and homogeneous Si<sub>3</sub>N<sub>4</sub>/TiN composites were fabricated and verified for the relative density, flexural strength and electrical resistivity. The values of flexural strength and electrical resistivity of composites decreased with the increase in TiN content. The composite containing 24 vol. % of TiN exhibited flexural strength of 360 MPa and electrical conductivity of 3.6 x 10<sup>3</sup> Ω<sup>-1</sup>m<sup>-1</sup>.

11:20 AM

### (ICACC-S8-058-2012) The influence of SiC coating on the ablation of ZrB<sub>2</sub>-coated Carbon/Carbon composites prepared by low pressure chemical vapor deposition

D. Yao\*, H. Li, Q. Fu, X. Shi, K. Li, X. Yao, Northwestern Polytechnical University, China

To improve the anti-ablation of carbon/carbon (C/C) composites, a new type of ablation protective multilayer coating has been produced by supersonic plasma spray and low pressure chemical vapor deposition. XRD and SEM analysis show, the coating produced by supersonic plasma spray was ZrB<sub>2</sub>, the outer coating protected by low pressure chemical vapor deposition was SiC. Oxycetylene ablative test shows that, the ablative linear/mass rates of ZrB<sub>2</sub> coated C/C are 0.175%/0, 3.762%/0.151%, 9.189%/5.332% at about 2173K for 20s, 40s, 60s, respectively, and the ablative linear/mass rates of SiC-ZrB<sub>2</sub> coated C/C only -0.183%/0.155%, 2.349%/0.177%, 5.626%/3.212% at about 2173K for 20s, 40s, 60s, respectively. The ablation of C/C composites was primarily due to chemical corrosion and mechanical denudation, and oxygen diffusing through the penetrable cracks in the coating.

11:40 AM

### (ICACC-S8-059-2012) Physical and mechanical properties of nano- and microstructure of Al<sub>2</sub>O<sub>3</sub> and Zr<sub>2</sub>O<sub>3</sub> oxide coatings

A. D. Pogrebnyak\*, Sumy State University, Ukraine; V. M. Beresnev, Kharkov National University, Ukraine; A. S. Kaverina, Sumy State University, Ukraine; D. A. Kolesnikov, Belgorod State University, Russian Federation; I. V. Yakuschenko, M. V. Ilyashenko, Sumy State University, Ukraine; N. A. Makhmudov, Samarkand branch of the Tashkent State University of Informatics, Uzbekistan

With the use of AFM, nanohardness and elastic modulus measuring, as well as measurements of the forces of cohesion, the friction coefficient by means of a scratch test, oxide coatings of Al<sub>2</sub>O<sub>3</sub> and Zr<sub>2</sub>O<sub>3</sub>, obtained by magnetron sputtering of Al (Zr) were investigated. The hardness of the coating Al<sub>2</sub>O<sub>3</sub>, nanostructured film deposited on

TiN, increased as compared with the coating deposited on steel. A comparison of the morphology of samples obtained by reactive magnetron sputtering synthesis and a source of RF plasma using oxygen ions was carried out. The mechanical characteristics of hardness, elastic modulus, adhesion strength and friction coefficient of obtained coatings were investigated.

## S11: Nanomaterials for Sensing Applications: From Fundamentals to Device Integration

### Sensing Devices I

Room: Oceanview

Session Chair: Francisco Hernandez-Ramirez, Catalonia Institute for Energy Research

8:00 AM

### (ICACC-S11-001-2012) Integration and testing of quasi-one-dimensional tin oxide nanomaterials in chemical microsensors (Invited)

K. D. Benkstein\*, E. N. Dattoli, C. B. Montgomery, S. Semancik, National Institute of Standards & Technology, USA; S. Donthu, V. Dravid, Northwestern University, USA

Nanomaterials, owing to proposed benefits in sensor performance, are increasingly popular as research topics for next-generation chemical-sensing devices. Challenges still remain for integration, systematic characterization and evaluation of the materials in operational devices. In that context, three configurations of quasi-one-dimensional tin oxide materials on gas-phase chemical microsensors will be discussed: poly-crystalline nanowires and patterned nanolines, and single-crystalline nanowires. Each material was integrated into sensing devices, using varied methods, as aligned arrays of multiple nanomaterials. The poly-crystalline nanowires were aligned across electrodes using di-electrophoretic techniques, the nanolines were patterned on the surface using soft-electron-beam-lithography, and the single-crystalline nanowires were integrated using force-contact transfer. Functionality included in the MEMS device structure is critical for evaluating the materials by enabling sensor modulation for fundamental and application-based evaluation of the nanomaterials. Temperature control plays a primary role in affecting sensor-analyte interactions, and modulated gate voltages are also shown to be useful in elucidating sensing mechanisms and enhancing sensor performance. The presentation will conclude with a comparison of the varied devices with respect to integration and performance.

8:30 AM

### (ICACC-S11-002-2012) Structural and Electrical Characterization of BaTiO<sub>3</sub> Nanorods

K. Zagar\*, Jozef Stefan Institute, Slovenia; F. Hernandez-Ramirez, Catalonia Institute for Energy Research (IREC), Spain; J. Prades, University of Barcelona, Spain; J. Morante, Catalonia Institute for Energy Research (IREC), Spain; A. Recnik, M. Ceh, Jozef Stefan Institute, Slovenia

1-D BaTiO<sub>3</sub> nanorods are a potential candidate for energy-harvester systems and sensors. In order to explore potential applications of BaTiO<sub>3</sub> nanorods, we report on the processing and on their structural and electrical characterization. BaTiO<sub>3</sub> nanorods were synthesized using the electrophoretic deposition of a BaTiO<sub>3</sub> sol into the aluminium oxide template, followed by annealing. Resulting BaTiO<sub>3</sub> nanorods were characterized by electron microscopy techniques. To study electrical properties, BaTiO<sub>3</sub> nanorod devices were fabricated by focused ion beam nanolithography techniques. Obtained BaTiO<sub>3</sub> nanorods had diameters of approximately 250 nm, with an average length of 10–25 μm. The BaTiO<sub>3</sub> nanorods were polycrystalline and composed of well-crystallized and pseudo-cubic BaTiO<sub>3</sub> grains. A hexagonal BaTiO<sub>3</sub> polymorph was also present as a minor phase and its formation was triggered by reduction of Ti<sup>4+</sup> to Ti<sup>3+</sup>. Electrical measurements performed on single BaTiO<sub>3</sub> nanorod showed resistivity values between 10 and 100 ohmcm, which corresponds to typical

values for oxygen-deficient BaTiO<sub>3</sub>. Single BaTiO<sub>3</sub> nanorods were tested as proof-of-concept humidity sensors. The measurements of electrical resistivity of single nanorods in varying humidity environment showed reproducible response, thus demonstrating that BaTiO<sub>3</sub> nanorods can be integrated in more complex circuit architectures with functional capacities of a humidity nano-sensor.

#### 8:50 AM

##### (ICACC-S11-003-2012) NH<sub>3</sub> Sensing with Single SnO<sub>2</sub> Nanowire and the Humidity Influence

F. Shao\*, Catalonia Institute of Energy Research (IREC), Spain; R. J. Diaz, University of Barcelona, Spain; F. H. Ramirez, Catalonia Institute of Energy Research (IREC), Spain; J. D. Prades, University of Barcelona, Spain; S. Mathur, Inorganic Chemistry, Germany; J. R. Morante, Catalonia Institute of Energy Research (IREC), Spain

Abstract Gas sensing properties of SnO<sub>2</sub> nanowires (NW) toward NH<sub>3</sub> in dry and humid environments were studied. NH<sub>3</sub> sensing experiments were performed on individual SnO<sub>2</sub> nanowire based resistive sensors, where SnO<sub>2</sub> nanowires were grown by a CVD method. The transient curves of the nanowires' resistance were carefully mapped to determine their sensitivity and response time. The decreases of resistance in expose to NH<sub>3</sub> indicate the reducing property of NH<sub>3</sub>. These devices showed moderate sensitivity to NH<sub>3</sub> with R<sub>0</sub>/R<sub>gas</sub> value accounted ranges from 1.05 to 1.6 when 500ppb to 200ppm NH<sub>3</sub> were applied. The optimal working temperature was found between 200°C to 250°C depending on the sensors tested. On the contrary, The experimental response was relative slow at the temperatures below 200°C. By mixing the background flow with humidified gas, the influence of H<sub>2</sub>O molecule on the sensors' behavior was explored. Humidity has resulted in a lower sensor response and indicated a competitive adsorption mechanism of H<sub>2</sub>O molecule on SnO<sub>2</sub> surface with NH<sub>3</sub>. In this contribution, the abovementioned analysis will be presented and its application to future sensing prototypes will be discussed.

#### 9:10 AM

##### (ICACC-S11-004-2012) Effects of the UV illumination and temperature on the conductometric detection of CO using SnO<sub>2</sub> nanowires from room temperature

J. Prades, Universitat de Barcelona, Spain; F. Hernandez-Ramirez, J. Morante\*, Institut de Recerca en Energia de Catalunya (IREC), Spain

Solely a few numbers of studies have been reported on the effects of the illumination onto metal oxides when these materials are used as gas sensing materials. However, photons with enough energy, UV range, are able to generate a depopulation of absorber oxygen molecules. It can be considered as equivalent to get a reduced surface with direct access to cationic sites around the Sn ion positions. Usually, thin or thick films suffer from strong absorption of the high energy photons and it is difficult to achieve a homogenous and uniform experimental condition in the whole sensing material. Unlike it, individual nanowire offers ideal conditions to analyze the UV photons effects on the conductometric measurement as gas sensor. In this contribution we report on the CO molecule interaction with SnO<sub>2</sub> surface depending of the reduction degree which becomes depending on the UV flux and the temperature as the oxygen molecule absorption is function of it. The CO molecule is a heteropolar molecule with a lightly basic character that under reduced conditions shows preference for the cationic sites and producing then an increase of the sensing material resistance. On the contrary, when the oxidation degree of the surface increased, CO molecules interact mainly with the absorbed oxygen according to the classically described reaction.

#### 10:00 AM

##### (ICACC-S11-005-2012) Nanowire Chemiresistors: The Devices Where the Joule Heating is Beneficial (Invited)

A. Kolmakov\*, Southern Illinois University at Carbondale, USA

Different from microelectronics components the semiconductor nanowires allows rational use of Joule heating and heat dissipation

balance in the detection scheme. We have tested three different detection principles using self-heating, thermally induced metal-insulator transition and catalytic heat conversion. It was shown that using these principles the realization of the standard redox type sensing can be realized via consuming only tens of microwatts of energy. Under certain conditions, the required energy can be harvested from the environment. The benefits and limitation of these approaches will be discussed.

#### 10:30 AM

##### (ICACC-S11-006-2012) Improved gas selectivity to the humidity using self-heated nanowires in pulsed-operation

J. Prades\*, Universitat de Barcelona, Spain; F. Hernandez-Ramirez, Institut de Recerca en Energia de Catalunya (IREC), Spain; T. Fischer, M. Hoffmann, R. Müller, Universität zu Köln, Germany; N. López, Institut Català d'Investigació Química (ICIQ), Spain; S. Mathur, Universität zu Köln, Germany; J. Morante, Institut de Recerca en Energia de Catalunya (IREC), Spain

One of the main limitations of conductometric gas sensors based on metal oxides is the poor selectivity and important cross sensitivity to common interfering gases such as humidity. Any of the several solutions proposed so far (i.e. (1)selective absorbing filters, (2)catalytic additives (3)sensor arrays and pattern recognition algorithms or (4) working temperature modulation) yield to a partial solution to the problem. It has recently been reported that self-heating effect in individual metal oxide nanowires, can also be used to modulate the sensors' temperature profile at higher pulsing frequencies, making available the direct observation of the kinetics associated with the chemical interactions between the metal oxide and the gases of interest. In this contribution we will demonstrate the feasibility of using this approach in individual SnO<sub>2</sub> nanowires for the quantitative analysis of CO and H<sub>2</sub>O in gas blends. Finally, experimental response and recovery times of individual SnO<sub>2</sub> nanowires toward oxidizing and reducing gases obtained with the here-proposed methodology were related to the reaction barriers predicted by theoretical models and other experimental techniques.

#### 10:50 AM

##### (ICACC-S11-007-2012) Combined Resistive-Surface Ionisation Gas Sensor Response in Individual Nanowires

F. Hernandez-Ramirez, Institut de Recerca en Energia de Catalunya (IREC), Spain; J. Prades\*, Universitat de Barcelona, Spain; A. Hackner, EADS Innovation Works, Germany; T. Fischer, Universität zu Köln, Germany; G. Müller, EADS Innovation Works, Germany; S. Mathur, Universität zu Köln, Germany; J. Morante, Institut de Recerca en Energia de Catalunya (IREC), Spain

One of the main limitations of conductometric gas sensors based on metal oxides is the poor selectivity and important cross sensitivity to common interfering gases such as humidity. In this contribution, gas detection experiments were performed with individual tin dioxide (SnO<sub>2</sub>) nanowires specifically configured to observe surface ion (SI) emission response towards representative analyte species. The high selectivity of these SI sensors emerges from the dissimilar sensing mechanisms of those typical of standard resistive-type sensors (RES). Therefore, by employing this detection principle (SI) together with RES measurements, better selectivity than that observed in standard metal oxide sensors could be demonstrated. Herein, parallel nanowire device (PND) configurations were used. PNDs consist of a pair of nanowires running parallel to each other while being separated by a small air gap of less than 1 micron width. We present an equivalent circuit model of a PND and show how its observable output parameters can be related to the two orthogonal SI and RES responses. Simplicity and specificity of the gas detection as well as low-power consumption make these single nanowire devices promising technological alternatives to overcome the major drawbacks of solid-state sensor technologies, providing extremely useful information.

### **S12: Materials for Extreme Environments: Ultrahigh Temperature Ceramics (UHTCs) and Nanolaminated Ternary Carbides and Nitrides (MAX Phases)**

#### **Processing, Structure and Property Relationships**

Room: Coquina Salon F

Session Chairs: Yutaka Kagawa, The University of Tokyo; James Zimmermann, Corning

**8:00 AM**

#### **(ICACC-S12-026-2012) Mechanical Behavior of ZrB<sub>2</sub>/SiC Particulate Composites Produced with varying SiC Particle Sizes**

J. Watts\*, G. Hilmas, W. G. Fahrenholtz, Missouri University of S & T, USA

The addition of SiC particulate to ZrB<sub>2</sub> increases the strength, fracture toughness, thermal shock resistance, and hardness, among other properties. Previous research has indicated a correlation between the size of the SiC particles within the composite and the flexural strength of that composite. The current study has expanded the range of SiC particle sizes studied and focused on further understanding the correlation between SiC particle size and mechanical properties. Composites were prepared with final maximum SiC particle sizes ranging from 4.4 to 18 μm. Hardness and elastic modulus remained constant for composites containing SiC particles 11.5 μm and smaller while the flexural strength exhibited a  $1/c^{1/2}$  type relationship over the same particle size range. However, strength, hardness, and elastic modulus all exhibited a sudden decrease for composites with maximum SiC particle sizes larger than 11.5 μm. Analysis of the mechanical properties, as well as the microstructure of the composites, indicated that microcracking occurred when the maximum SiC particle size exceeded 11.5 μm.

**8:20 AM**

#### **(ICACC-S12-027-2012) TaB<sub>2</sub>-based ceramics: microstructure, mechanical properties and oxidation resistance**

L. Silvestroni\*, S. Guicciardi, C. Melandri, D. Sciti, CNR-ISTEC, Italy

Among ultra-high temperature ceramics, major attention has been devoted to zirconium and hafnium borides and carbides. Tantalum composites remain a less explored class of ceramics. In this contribution, TaB<sub>2</sub>-based ceramics were hot pressed with addition of 5-10 vol% MoSi<sub>2</sub>. Temperatures in the range of 1680-1780°C led to relative density around 90-95%. The microstructure was studied through X-ray diffraction, scanning and transmission electron microscopy and the results enabled the rebuilding of the densification mechanisms occurring upon sintering. The hardness was about 18 GPa, the fracture toughness 4.6 MPam<sup>1/2</sup> and the room temperature flexural strength was around 630 MPa, but abruptly decreased to 220 MPa at 1200°C. The composite containing 10 vol% of MoSi<sub>2</sub> was tested in a bottom-up furnace in the temperature range 1200-1700°C for 30 minutes. The microstructure appeared covered by a SiO<sub>2</sub> layer, but the bulk remained unaltered up to 1600°C. At 1700°C the specimen vaporized. Nanoindentation was employed on the oxidized cross section to detect eventual mechanical properties modification associated to Chemical/microstructural change. TaB<sub>2</sub> compounds are extremely stable until a threshold temperature, but, once this limit is overcome, very fast decomposition occurs. The absence of a steady intermediate state can result catastrophic if operating temperatures are not well known.

**8:40 AM**

#### **(ICACC-S12-028-2012) Densification Behavior and Mechanical Properties of ZrB<sub>2</sub> Processed Using Spark Plasma Sintering**

D. Pham\*, W. R. Pinc, L. S. Walker, E. L. Corral, University of Arizona, USA

Zirconium diboride (ZrB<sub>2</sub>) is an ultra-high temperature ceramic with a set of properties that make it ideal as a thermal protection system (TPS) material for hypersonic application. However, processing

fully dense ZrB<sub>2</sub> typically requires the use of sintering additives that modifies material properties. This study focuses on processing ZrB<sub>2</sub> without the use of additives by spark plasma sintering (SPS) and compares them to ceramics processed by pressureless sintering (PS) and hot pressing (HP). Ball-milled (BM) and ball-milled heated treated (BMHT) ZrB<sub>2</sub> achieve >99% theoretical densities by SPS at 1850°C with a 35MPa load in 5 minutes. Although heat treatment in a tube furnace slightly reduces the oxygen content of BM powder from 0.91wt% oxygen to 0.63 wt% oxygen, the densification profiles obtained by in situ position measurements of the loading ram shows that BM powder begins the densification process at 1200°C compared to BMHT at 1500°C. Residual oxygen content in the ceramic after sintering is extremely low, being reduced to 0.18 wt% and 0.28wt% for BM and BMHT ceramics. Microstructural analysis by SEM and mechanical properties of fully dense ceramics SPS at 1850°C are performed. SEM micrographs show how the microstructure changes with increasing temperature. Grain sizes are  $3.8 \pm 1.7 \mu\text{m}$  and  $4.2 \pm 1.7 \mu\text{m}$  for BM and BMHT ceramics, respectively.

**9:00 AM**

#### **(ICACC-S12-029-2012) High-temperature bending strength of ZrB<sub>2</sub>-20vol%SiC ceramics (Invited)**

G. Zhang\*, J. Zou, Shanghai Institute of Ceramics, CAS, China; C. Hu, T. Nishimura, Y. Sakka, H. Tanaka, Nano Ceramics Center, NIMS, Japan; J. Vleugels, O. Van der Biest, Katholieke Universiteit Leuven, Belgium

ZrB<sub>2</sub>-SiC particulate composites are regarded as the baseline materials in ultra-high temperature ceramics (UHTCs) family. The densification process, microstructure tailoring, oxidation/ablation resistance, thermo-physical and mechanical properties of ZrB<sub>2</sub>-SiC composites have been well investigated during the last ten years. In this presentation, the high temperature bend strength of ZrB<sub>2</sub>-20vol%SiC ceramics (ZS) and its degradation mechanisms up to 1600°C in high purity argon atmosphere were investigated. The specimens were dense ZS ceramics fabricated by hot pressing using self-synthesized high purity ZrB<sub>2</sub> and commercial SiC powders as raw materials. According to the analysis of the fracture mode, crack origin and internal friction curve of ZS ceramics, its strength degradation above 1000°C is considered to be the results of grain boundary softening, grain sliding together with the formation of cavitations and cracks near the SiC grains on the tensile side of the specimens. The strength retention of ZS at 1600°C was 84% (460±31 MPa), obviously higher than the reported values in literature, mainly benefiting from the high purity powders of ZrB<sub>2</sub>. By the way, the fracture of ZS ceramics below 1000°C was mainly originated from the flaws induced by the machining process.

**9:20 AM**

#### **(ICACC-S12-030-2012) Room Temperature Fatigue of Ultra High Temperature ZrB<sub>2</sub>-SiC Ceramic Composites**

N. Orlovskaya\*, R. Stadelmann, University of Central Florida, USA; T. Graule, J. Kuebler, Swiss Federal Laboratories for Materials Science and Technology, Switzerland; M. Lugov, Institute for Problems of Materials Science, Ukraine; C. Aneziris, M. Neubert, TU Bergakademie Freiberg, Germany

The goal of this study is to characterize time dependent mechanical behavior of ZrB<sub>2</sub>-30 wt% SiC composite under static and cyclic loading at room temperature. The fatigue testing of the hot pressed composites was performed in different environments, such as dry and humid air, as well as water. While slow crack growth experiments under static loads were performed in humid air, the cyclic fatigue tests were performed in dry and humid air, as well as water environment. In static tests, the shielding stress intensity factor decreased both the total effective stress intensity factor at the crack tip and the crack growth rate. In cyclic tests these crack interactions and the shielding stress intensity factor become increasingly reduced with increasing number of cycles due to wear, and crack growth rate



becomes higher. It was observed that the cracks grow faster in cyclic fatigue tests in comparison with static experiments, which can be explained by degradation of bridging interactions between the two crack surfaces and corresponding decrease of a shielding stress intensity factor. It was found that water accelerates crack growth in ZrB<sub>2</sub>-30wt%SiC ceramics and the higher humidity in the environment was used during the mechanical testing, the higher crack growth rate was observed. The effect of humidity on fatigue behavior of ZrB<sub>2</sub>-30wt%SiC composite is similar to such effect for crack growth in glass.

### Novel Characterization Methods

Room: Coquina Salon F

Session Chairs: Jochen Schneider, RWTH Aachen University; Jeremy Watts, Missouri University of S & T

#### 10:00 AM

##### (ICACC-S12-031-2012) Identification of new stable MAX phases with tunable properties (Invited)

J. Rosen\*, The department of Physics, Chemistry and Biology, Linköping University, Sweden

Nanolaminated materials are attractive from the point of view of fundamental science and applications, including for example anisotropic mechanical, electronic and magnetic properties. Focusing on these characteristics, we will here present results showing the potential of known as well as predicted new MAX phases. First-principles calculations have been used to study trends in phase stability for potential magnetic MAX phases. Results will be presented for a range of carbides, where we show example of atomic configurations being used to tune the magnetism between different states. Furthermore, the effect of doping and alloying on the mechanical and electronic properties of Ti<sub>2</sub>AlC will be presented, suggesting a wide range of properties attainable with varying dopant concentration. The above mentioned theoretical predictions have been tested experimentally by thin film deposition through arc as well as sputtering methods. Predicted new MAX phases have successfully been synthesized, and selected properties evaluated, in accordance with observations from theory.

#### 10:20 AM

##### (ICACC-S12-032-2012) Synthesis, microstructural characterization and transport properties of Ti<sub>2</sub>Al[C<sub>x</sub>N(1-x)]<sub>y</sub> MAX phase solid solutions

W. Yu, V. Gauthier-Brunet, T. Cabioch, Institut PPRIME, France; L. Gence, L. Piraux, Université Catholique de Louvain, Belgium; Z. Buck, J. Hettinger, S. Lofland, Rowan University, USA; M. Barsoum, Drexel University, USA; S. Dubois\*, Institut PPRIME, France

Using Ti, TiC, AlN and Al reactant powder mixtures, sub-stoichiometric Ti<sub>2</sub>Al[C<sub>x</sub>N(1-x)]<sub>y</sub> (y<1) MAX phase solid solutions have been successfully synthesized by hot isostatic pressing. Rietveld refinement is used to carefully characterize the structure and the octahedron and trigonal prisms distortion parameters as a function of the C content in Ti<sub>2</sub>Al[C<sub>x</sub>N(1-x)] solid solutions. Four point probe resistivity measurements were performed as a function of temperature on Ti<sub>2</sub>AlN, Ti<sub>2</sub>AlC<sub>0.25</sub>N<sub>0.75</sub>, Ti<sub>2</sub>AlC<sub>0.4</sub>N<sub>0.6</sub>, Ti<sub>2</sub>AlC<sub>0.5</sub>N<sub>0.5</sub>, Ti<sub>2</sub>AlC<sub>0.75</sub>N<sub>0.25</sub> and Ti<sub>2</sub>AlC samples. The ideal resistivity,  $\rho_i(T)$ , obtained from the Matthiessen law only depends on the charge carrier-phonon coupling; i.e. it does not depend on defect and impurity densities. As the ideal resistivity varies linearly with the temperature in the range 100-300 K, one can obtain information on the charge carrier-phonon coupling from the slope of the linear variation. The slopes, in the range 0.1-0.16  $\mu\text{ohm.cm.K}^{-1}$ , provide evidence of a relatively strong charge carrier-phonon coupling in MAX phase materials. It is also demonstrated that charge carrier-phonon scattering is more efficient in solid solutions than in the two end-members. Moreover, the charge carrier-phonon scattering increase in sub-stoichiometric

solid solutions indicates that vacancies are potential scatterers of charge carriers.

#### 10:40 AM

##### (ICACC-S12-033-2012) A first-principles investigation of the phase stability of known and hypothetical MAX phases

M. Dahlqvist\*, B. Alling, J. Rosén, Thin Film Physics Division, Sweden

There are a large number of MAX phases which has been experimentally studied and even more have been considered theoretically. The crucial question for the latter *in silico* hypothetical phases is if they can exist in reality, i.e. be synthesized experimentally. In this work we present our systematic theoretical method to investigate the phase stability of MAX phases with respect to competing crystal phases. As a case study, we use an important subset of the  $M_{n+1}AX_n$  phases:  $M = \text{Sc, Ti, V, Cr, or Mn}$ ,  $A = \text{Al}$ , and  $X = \text{C or N}$ . Through a combination of Density Functional Theory and the simplex linear optimization procedure, including all known and hypothetical competing phases, we identify the set of most competitive phases for the relevant composition for  $n = 1-3$  in each system. Our approach avoids *ad hoc* choices of competing phases, which may lead to incorrect indication of phase stability. Our calculations completely reproduce experimental occurrences of stable MAX phases, and this study can thus be seen as a Benchmark test. Based on here presented results, our method is established as a reliable tool that can be, and has been, used as guidance for further search of potentially existing undiscovered multi-component phases, such as new  $M_{n+1}AX_n$  phases, before time consuming and expensive experimental investigations are attempted.

#### 11:00 AM

##### (ICACC-S12-034-2012) The MAX Phases: The Next Horizons (Invited)

M. Barsoum\*, Drexel University, USA

Today research on the MAX phases is a worldwide endeavor. Currently, most of their properties are fairly well understood and surprises are far and few between. This begs the question: what next? In this talk I outline a number of possible future research directions. Probably the most important is to endow the MAX phases with functionality by engineering a band gap and/or magnetism. Another is to develop metal matrix composites with exceptional properties. A third is to selectively remove the A-group element from the MAX phases to create 2-D solids that we are labeling - in analogy to graphene - MXenes. In this talk I will review our work on Mg-MAX and Al-MAX composites. I will also review our recent work on the exfoliation of MAX phases to create MXenes and their many potential uses.

#### 11:20 AM

##### (ICACC-S12-035-2012) Zero-Recession Lightweight Ablators with UHTC surface layers

T. Aoki\*, M. Mizuno, T. Suzuki, T. Ogasawara, Y. Ishida, K. Fujita, T. Yamada, Japan Aerospace Exploration Agency, Japan

This presentation reports the processing, properties and arc jet testing results of UHTC-infiltrated lightweight ablators developed at Japan Aerospace Exploration Agency (JAXA). These materials are composed of a low-density carbon fiber preform surface-densified with an ultra-high-temperature ceramic (UHTC). The low-density CMCs are further impregnated with a phenolic resin. The surface UHTC layer is formed in order to improve the oxidation and erosion resistances. At present, HfC-SiC, ZrC-SiC and SiC are formed as an anti-recession layer. The densities of UHTC-infiltrated lightweight ablators are ranging from 0.35 to 0.55 g/cm<sup>3</sup>. The thermal and recession behaviors are evaluated by arc jet testing at cold wall heat fluxes from 0.9 to 2.0 MW/m<sup>2</sup> and surface pressures from 1.9 to 4.3 kPa. The test results indicate that surface densification with UHTCs is highly effective for the reduction of surface recession within the examined heating conditions.

11:40 AM

### (ICACC-S12-036-2012) Effect of Transition Metal Additives on the Oxidation Behavior of ZrB<sub>2</sub>

M. Kazemzadeh Dehdashti\*, W. G. Fahrenholtz, G. E. Hilmas, Missouri University of Science and Technology, USA

The effect of transition metal additives on the oxidation behavior of ZrB<sub>2</sub> ceramics was investigated. Weight gain, scale microstructure and scale thickness of hot pressed pure ZrB<sub>2</sub> and ZrB<sub>2</sub> containing 4, 6 or 8 mol% of W or Nb were studied. Specimens were oxidized at temperatures ranging from 700-1600°C in flowing air. The results indicated that the samples containing metal additives had improved oxidation resistance compared to pure ZrB<sub>2</sub>. It was observed that the surfaces of the samples oxidized at 800-1200°C were covered by a liquid/glassy phase. For pure ZrB<sub>2</sub>, the glassy phase evaporated at higher temperatures leaving a porous ZrO<sub>2</sub> scale behind. Oxidation of ZrB<sub>2</sub> containing either Nb or W at 1200-1600°C resulted in the formation of three-layer oxide scales. The oxide layer next to the unoxidized ZrB<sub>2</sub> consisted of zirconia and metal oxide particles. This layer was covered by a boron-zirconia-metal oxide liquid/glass layer. The last layer consisted of zirconia-metal oxide particles precipitated from the liquid phase as a result of evaporation of boron at high temperatures. The higher stability of the glassy phase in these samples was attributed to the increase in solubility of boron in the zirconia-boron-metal oxide liquid phase, resulting in improved oxidation resistance for ZrB<sub>2</sub> samples containing Nb or W.

## S13: Advanced Ceramics and Composites for Nuclear Applications

### Ceramics for Nuclear Reactors and Fuels

Room: Coquina Salon E

Session Chair: Lance Snead, ORNL

8:00 AM

### (ICACC-S13-001-2012) Some Lessons Learned at the Fukushima Accident (Invited)

A. Tokunishi\*, U. Idaho, USA; S. M. McDevitt, Texas A&M, USA

The Fukushima nuclear station with 6 BWRs co-located on the coast of Japan withstood a 9.0 earthquake and a large-scale tsunami on March 11, 2011. All six units were constructed via US-Japan collaboration. In spite of the immediate shut down of all units based on ground acceleration and initial decay heat cooling, loss-of-offsite-power initiated a loss-of-coolant accident; overall a 'beyond design basis accident'. The spent fuel pools in lightly-structured buildings above the reactor also lacked cooling. Several H<sub>2</sub> explosions later and many months since '3/11', Japan now faces a 20-year cleanup effort. Evidence suggests that 3 cores have partially-to-fully melted. The scale of cleanup will be very large. In the years ahead one of the challenges will be characterizing the (UO<sub>2</sub>) fuel, including MOX fuel in Unit 4. The fuel is housed in Zircaloy cladding. Based on the 'burn-up' of the fuel at the time of the accident and the subsequent lack of decay heat cooling, the thermal condition of the fuel, cladding and coolant during the accident progression dictated the eventual state of fuel/cladding materials. Since only an approximate progression sequence will eventually be known, there will be inherent uncertainties in the likely condition of intact and possibly fragmented oxide fuel form. We will provide a quick perspective on the Fukushima accident, technical/non-technical lessons learned and oxide fuel issues.

8:30 AM

### (ICACC-S13-002-2012) Thermo-mechanical aspect of SiC/SiC composite fuel cladding in LWR (Invited)

S. Higuchi\*, Y. Kawaharada, F. Kano, Toshiba Corporation, Japan

Nuclear fuel in Light Water Reactor (LWR) is required to be more safely as well as more efficiently in the future. In this context, the fuel cladding materials other than current zirconium-based alloy are one

of the aims of the fuel studies. Silicon carbide-based ceramic composite (SiC/SiC composite) is discussed as a promising structural material for the purpose. In this paper, application of the SiC/SiC materials to LWR fuel cladding is discussed from the viewpoint of thermo-mechanical behavior in normal operation and transient condition. Bonded fiber silicon carbide composite is used for the estimation of the fuel performance because of its excellent thermal conductivity. The materials properties such as thermal conductivity are modeled into FEMAXI-6 computer code to calculate fuel thermo-mechanical behavior. Behavior in accident condition is also qualitatively noticed.

9:00 AM

### (ICACC-S13-003-2012) Thermochemistry of Fully Ceramic Matrix Coated Particle Fuel

T. M. Besmann\*, Oak Ridge National Laboratory, USA

A recent concept for accident tolerant LWR fuel has been the use of coated particle (TRISO) fuel within an SiC matrix. Some of the historical issues for this fuel may still be of concern such as kernel migration and fission product palladium attack of the SiC particle coating layer. Other issues such as behavior of the matrix SiC under loss of coolant accident conditions will need to be newly explored. This presentation will cover a number of the issues from a thermochemical perspective, including potential means for mitigating negative interactions. This research was sponsored by the U.S. Department of Energy through the Office of Nuclear Energy-Fuel Cycle R&D Program at Oak Ridge National Laboratory.

9:20 AM

### (ICACC-S13-004-2012) Processing of inert SiC matrix with TRISO coated fuel by liquid phase sintering

K. Shimoda\*, T. Hinoki, Kyoto University, Japan; K. A. Terrani, L. L. Snead, Y. Katoh, Oak Ridge National Laboratory, USA

SiC is promising material for nuclear application especially due to its outstanding property of high thermal conductivity and exceptional low-radioactivity. It is proposed to replace the current uranium oxide fuel pellets for light water reactors with the ceramic micro-encapsulated uranium compacted within SiC inert matrix in the DOE's Deep Burn Program. In this study, nanostructured SiC by liquid phase sintering of SiC nanopowder was proposed as an inert SiC matrix for compact-packing of surrogate TRISO fuel particles. Sintering additives like Y<sub>2</sub>O<sub>3</sub> and Al<sub>2</sub>O<sub>3</sub> were used in addition to SiC nanopowder in the amount of 0-10 wt%. Powder mixtures including 40 vol% of fuel particles were hot-pressed at 1800-1900 C under 0-20 MPa. The influences of process parameters (selection of SiC nanopowder, sintering temperature and applied pressure) on porosity and remained sintering additives (amount and distribution) in inert SiC matrix were evaluated, based on the detail microstructural characterization. The second phase formed during hot-pressing was identified by XRD and microstructure was characterized by FE-SEM with EDS and TEM. The samples sintered at 1800 C showed lower relative density and more remained additives between fuel particles and matrix in comparison with those obtained at 1900 C. The more amount of additives improved relative density and mechanical properties even when applied pressure reduced.

10:00 AM

### (ICACC-S13-005-2012) SiC-Coated HTGR Fuel Particle Performance (Invited)

M. J. Kania, -, USA; H. Nabilek\*, K. Verfondern, Forschungszentrum Juelich, Germany

After completing fuel development for AVR and THTR with BISO coated particles, the German program continued toward a new program utilizing TRISO coated particles in spherical fuel elements for advanced HTGR concepts directed to process heat application, direct-cycle electricity production with a gas turbine in the primary circuit, and conventional steam generation. In coated particle develop-

ment, the combination of low-temperature-isotropic (LTI) inner and outer PyC layers surrounding a strong, stable SiC layer greatly improved manufacturing conditions and the subsequent contamination and defective particle fractions in production fuel elements. In addition, this combination provided improved mechanical strength and a higher degree of solid fission product retention, not known previously with HTI-BISO coatings. The improved performance of the HEU (Th,U)O<sub>2</sub> and LEU UO<sub>2</sub> TRISO fuel systems was successfully demonstrated in three primary areas of development: manufacturing, irradiation testing under normal operating conditions, and accident simulation testing. Good irradiation performance for these elements was demonstrated under normal operating conditions to 12 % FIMA and in accident conditions not exceeding 1600°C

**10:30 AM**

**(ICACC-S13-006-2012) Modeling of Microstructural Evolution in Nuclear Fuels during Service (Invited)**

V. Tikare\*, Sandia National Laboratories, USA

Nuclear fuels experience unique microstructural evolution as a result of thermal and irradiation conditions, and fission that they experience during service. These result in a host of unusual processes including the generation, transport and release of fission gases; swelling due to fission product generation; formation of high-burnup rim structures; and component segregation. The ability to simulate these microstructural changes at the meso-scale would enhance the ability to understand, predict and control the engineering performance and service life of many different fuel forms in a variety of reactors. We present a model that combine two traditional microstructural evolution models, phase-field and Potts, to address all the evolution processes listed above. This hybrid Potts-phase field method is an efficient and effective method with many advantages. It can simulate microstructural evolution on a sufficiently large scale to provide engineering properties directly or generate constitutive models to inform continuum engineering scale models. It can couple multiple physical processes such as coarsening, diffusion, nucleation, recrystallization, phase transformations, and others that neither model can simulate alone, but combining them allows the hybrid to address all the processes simultaneously in a coupled simulation.

**11:00 AM**

**(ICACC-S13-007-2012) The Role of Defect Structure on the Sinterability of Non-stoichiometric Oxide Fuel**

J. B. Henderson\*, Netzsch Instruments NA, USA; A. T. Nelson, D. D. Byler, K. J. McClellan, Los Alamos National Laboratory, USA

Even though oxide fuel possesses some non-ideal attributes, it is still used in the vast majority of LWRs. As a result, after 50 years it is still the subject of intense study. A great deal of work has been focused on characterizing key parameters which control sintering and therefore fuel quality and performance. Despite the impressive body of literature on this subject, many unresolved questions remain. Clearly, the defect structure controls diffusion, which in turn controls sintering. The purpose of this work was to gain a better insight into the interrelationship between defects and diffusion and their effect on the sinterability of UO<sub>2+x</sub> and CeO<sub>2-x</sub>, as well as (U,Ln)O<sub>2+x</sub> (where Ln=La,Ce,Pr,Nd,Gd) systems, by using a combination of mass change, evolved gas, specific heat, transition energetics, sintering and XRD data. Focus was placed on quantifying the effect of parameters such as PO<sub>2</sub>( $\Rightarrow$  O/M) and heating rate on the evolution of the defect structure and diffusion mechanisms on the single-component oxides. Further, sintering data on (U,Ln)O<sub>2+x</sub> systems were used to help explain the complex diffusion blocking mechanisms which occur in the above-mentioned mixed oxides. These mechanisms impede sintering and can lead to incomplete densification. The results of this work will be presented and discussed in detail.

**11:20 AM**

**(ICACC-S13-008-2012) Thermal Conductivity of Multiphase Ceramics for Inert Matrix Nuclear Fuel**

D. A. Men\*, M. H. Sullivan, D. R. Mumm, J. P. Angle, M. M. Chan, University of California, Irvine, USA; M. K. Patel, K. E. Sickafus, Los Alamos National Laboratory, USA; M. L. Mecartney, University of California, Irvine, USA

Candidate inert matrix materials should have thermal conductivity significantly higher than UO<sub>2</sub> to avoid central melting, a high melting point, good radiation stability, and good solubility for fission by-products, especially the actinides. The Mecartney group has prepared four-phase ceramics composed of (a) Y<sub>2</sub>O<sub>3</sub> stabilized ZrO<sub>2</sub> (YSZ) and CeO<sub>2</sub> as isostructural low thermal conductivity surrogates for UO<sub>2</sub>, (b) Al<sub>2</sub>O<sub>3</sub> as the heat conducting phase, (c) MgAl<sub>2</sub>O<sub>4</sub> for good amorphization resistance, and (d) LaPO<sub>4</sub> as the radionuclide-bearing phase. After mixing powders by attritor milling, multiphase samples were sintered at temperature from 1400-1600°C for times from 1-4 hours. Phase composition evaluated by XRD and SEM found that certain compositions promoted the formation of magnetoplumbite. The thermal conductivity of the composites is evaluated experimentally using a unique apparatus designed by the Mumm group. The experimental results will be compared to computational results derived in the Mecartney group using the OOF2 software program from NIST. Both computational and experimental results will be compared to values for pure YSZ to determine the enhancement of thermal conductivity. The results of irradiation experiments at LANL with 10 MeV Au<sup>2+</sup> ions with a fluence of 1×10<sup>16</sup> ions/cm<sup>2</sup> at 500°C substrate temperature as evaluated by SEM and TEM will also be reported.

**11:40 AM**

**(ICACC-S13-009-2012) Structure and Property Relationship in Spark Plasma Sintered UO<sub>2</sub> pellets**

G. Subhash\*, E. McKenna, G. LiHao, A. Cartas, J. Tulenko, R. Baney, University of Florida, USA

UO<sub>2</sub> powder has been sintered at a range of temperatures using spark plasma sintering technique. The sintered material density varied between 85-97% theoretical density. Ultrasonic measurements (both shear and longitudinal wave measurements) were conducted on sintered disks to determine their modulus and Poisson's ratio. The evolved microstructure was investigated using SEM and optical microscopy. Hardness measurements were conducted using a Vickers indentation tester. In addition, thermal conductivity measurements were also conducted. These measurements and their relationship to the evolved microstructure as well as a comparison to UO<sub>2</sub> produced by other methods will be discussed in detail during the presentation.

## Global Young Investigators Forum

### Frontiers in Ceramic Hybrid Materials and Composites for Biomedical Applications

Room: Coquina Salon G

Session Chairs: Satoko Tasaki, Osaka University; Eva Hemmer, Tokyo University of Science

**8:00 AM**

**(ICACC-GYIF-010-2012) Fluorescent Carbon Nanowires for Targeted Drug Delivery for Breast Cancer Therapy and Optical Imaging (Invited)**

N. Puvvada\*, B. Kumar, N. Babu, H. Kalita, M. Mandal, A. Pathak, Indian Institute of Technology Kharagpur, India

In the present study, we report for the very first time the use of functionalized fluorescent carbon nanowires as potential nanocarriers of antitumor agents for the treatment of breast cancer. The fluorescent carbon nanowires have been prepared through microwave irradiated heating of chitosan and have been characterized using FTIR spectroscopy and X-ray diffraction. Further, the drug loading has been

carried out through click chemistry approach which was established through NMR studies while the surface charge was ascertained through zeta potential measurements. The drug entrapment in carbon material was determined by HPLC. Hemocompatibility of the carbon nanowires was identified through hemolytic assay. Efficacy of the drug loaded carbon nanocarriers for the treatment of breast cancer was ascertained through cell proliferation assay (MTT), phase contrast & confocal laser fluorescence microscopy studies, and through cell cycle analysis were performed on MCF 7 cells. The present study therefore indicates that functionalized fluorescent carbon nanowires could not only serve as a promising, effective and safe means of administering therapeutic agents for breast cancer therapy but could also be used for monitoring therapeutic responses of anti-tumor agents in a patients through optical imaging.

### 8:20 AM

#### (ICACC-GYIF-011-2012) Design, Fabrication and *In Situ* Surface Modification of the Selectively Doped Advanced ZnO Nanohybrid Materials and their Biological Activities (Invited)

K. Namratha\*, K. Byrappa, S. Rajesh, V. Ravishankar Rai, University of Mysore, India

In recent years, the interest in the biological activities of ZnO nanomaterials and nanohybrid materials is fast growing. The design, fabrication and in situ modification of selectively doped (W, Mo, Pd, Ag in the concentration range 1–3 wt% ) ZnO nanohybrid materials were carried out using novel solution routes such as hydrothermal and solvothermal techniques within the temperature range (150 – 250 °C), with an autogeneous pressure and an experimental duration of 12 to 16 hours. *In situ* surface modification was carried out using gluconic acid, oleic acid, and n-butylamine, etc. The experimental products were freeze-dried and subjected to a systematic characterization using powder XRD, FTIR, UV-VIS, SEM Positron Annihilation, Photoluminescence spectroscopy (PALS), BET surface area, zeta potential measurements, etc. The antifungal activity of the selectively doped ZnO designer nanohybrid materials with different concentrations was evaluated for pathogenic *Candida* spp. by means of the determination of the minimum inhibitory concentration (MIC), minimum fungicidal concentration (MFC), and the time-dependency of yeasts growth inhibition. This biological activity has been investigated systematically with respect to the concentration of surfactant, size of the particles, shape and the type of dopant metal in these ZnO nanohybrid materials.

### 8:40 AM

#### (ICACC-GYIF-012-2012) Covalent Immobilization and Time Dependent Release of Sparfloxacin on SiO<sub>2</sub>@FeOx Nanoparticles

L. Wortmann\*, University of Cologne, Germany; N. El-Gamel, Cairo University, Egypt; K. Arroub, S. Mathur, University of Cologne, Germany

The exceptional properties of iron oxide nanoparticles as superparamagnetism, chemical stability, non-toxicity and biocompatibility have lead to their wide spread of use for biomedical applications. One field of interest is their application as drug delivery systems, whereby the surface modification with biologically relevant functionalities is essential to lower their cytotoxicity and facilitate their targeting functionality. A physiologically conductive silica shell around the iron oxide particles is the tool of preference to simplify the biomolecule attachment. However, the synthesis of nanoparticles with a well defined surface chemistry including its utilization to link and delink a bioactive component by an appropriate chemical trigger as well as synthesizing a uniform silica shell still remains a synthetic challenge. Herein we report the synthesis of SiO<sub>2</sub>@FeOx nanoparticles with a tunable shell thickness which were used as carriers for the covalent immobilization and release of the antimicrobial drug sparfloxacin (SPHX). SPHX loaded particles exhibit time-dependent drug release, with no measurable in vitro cytotoxicity, making the drug@nanoparticle conjugates potentially relevant for nanomedical applications.

### 9:00 AM

#### (ICACC-GYIF-014-2012) Bio-inspired synthesis of bone-like matrix (Invited)

Y. Wang\*, N. Nassif, T. Azaïs, G. Laurent, M. Giraud-Guille, F. Babonneau, University Pierre et Marie Curie (UPMC), France

Bone is a complex composite material composed of an organic matrix (mainly collagen) with inorganic nanocrystals (apatite) that strengthen it. The biological apatites are non-stoichiometric carbonate-containing plate-shaped nanocrystals. A better characterization of molecular interactions between these components is fundamental to improve understanding of bone formation. In the present work, specific experimental conditions based on a diffusion method have been developed to induce precipitation of biological-like apatite in solution as well as within a collagen matrix. In this tissue-like collagen apatite matrix, size and distribution of apatite crystals are recreated as in bone. We have investigated the structure of those nanocrystals and compared them with biological apatite. Characterization by X-ray powder diffraction shows that the collagen matrix influences the crystallite size of apatite. We then relied on solid-state NMR experiments to probe the local environment of several sites, and thus gain insights into the complex structure of such substituted apatite. Results obtained from <sup>31</sup>P MAS NMR spectra highlight the impact of the dense organic matrix on the environment of the phosphates anions. In parallel, the collagen apatite matrix was used as a simplified model for investigating the molecular interactions between the organic matrix and the mineral phase by NMR.

### Frontiers in Ceramic Chemistry and Biomedical

#### Applications

Room: Coquina Salon G

Session Chairs: Laura Wortmann, University of Cologne

### 10:00 AM

#### (ICACC-GYIF-015-2012) Fabrication of Ceramics Implants with Biocompatibility Structures by Using Laser Scanning Stereolithography

S. Tasaki\*, S. Kirihara, Osaka University, Japan

Ceramics implants of dental crown models with thin shell structures and sponge bone models with ordered porous structure were fabricated successfully in micrometer orders by using laser scanning stereolithography and powder sintering processes. Graphic models of the components could be designed sterically considering to biocompatibilities by using graphic applications with supports of computer tomography systems. These data were converted into numerical file sets of cross sectional images through slicing operations. Subsequently, bioceramics powders of alumina, zirconia, hydroxyapatite and calcium phosphate were dispersed into photo sensitive acrylic resins at 45-70 volume %. The obtained slurries were spread on a substrate with 25-50 μm in layer thickness by a mechanical blade. An ultraviolet laser beam of 100 μm in spot size was scanned on the slurry surface to create cross sectional images. Through these automatic micro stacking processes, the dental crown models were fabricated. These composite precursors were dewaxed and sintered in the air atmosphere, and uniformly dense and defect free microstructures could be obtained successfully. The mechanical properties were measured by conventional tensile testing, and fluid transmittances or stress distributions were visualized by finite element simulation methods.

### 10:20 AM

#### (ICACC-GYIF-016-2012) PEG-*b*-PAAc Modified Gd<sub>2</sub>O<sub>3</sub>:Er<sup>3+</sup>, Yb<sup>3+</sup> Nanostructures as Over-1000-nm Near-Infrared Fluorescence Biomarkers

E. Hemmer\*, T. Yamano, H. Takeshita, T. Fujiki, H. Kishimoto, Tokyo University of Science, Japan; R. B. Goldfarb, National Institute of Standards and Technology (NIST), USA; K. Soga, Tokyo University of Science, Japan

Bioimaging is an important tool for the visualization of cellular phenomena and as a diagnostic tool in medicine. Lanthanide containing

compounds are promising candidates to overcome the problems of commonly used organic dyes. In particular, near-infrared (NIR) absorbing and emitting materials are attractive because the use of NIR light reduces phototoxicity and scattering. Er<sup>3+</sup> and Yb<sup>3+</sup> doped inorganic host materials are known for their upconversion and NIR emission under 980-nm excitation. In this study, Er<sup>3+</sup> and Yb<sup>3+</sup> ions were doped into a Gd<sub>2</sub>O<sub>3</sub> nanoparticle or nanorod matrix in order to introduce multifunctionality, namely luminescence and magnetism. For biomedical applications, biocompatibility of the nanomaterials was achieved by surface modification with PEG-*b*-PAAc. Variation of the modification conditions (temperature, stirring time, sonication or stirring) had a strong influence on the physico-chemical properties of the resulting nanostructures. The suitability of the obtained nanostructures for over-1000-nm NIR *in-vivo* fluorescence bioimaging (OTN-NIR-IFBI) was analyzed by *in-vitro* studies, which demonstrated good biocompatibility, as well as by *in-vivo* investigation of their biodistribution in mice organs. Magnetic characterizations show that PEG-*b*-PAAc modified Gd<sub>2</sub>O<sub>3</sub>:Er<sup>3+</sup>,Yb<sup>3+</sup> nanostructures are promising candidates for application as opto-magnetic biomarkers.

**10:40 AM**

**(ICACC-GYIF-017-2012) Immunotoxicity Assessment of Carbon-Based Nanomaterials (Invited)**

F. Torres-Andon\*, Karolinska Institutet, Sweden; L. Xiao, University of Cologne, Germany; H. Salminen-Mankonen, S. Tuomela, University of Turku and Abo Akademi University, Finland; R. Autio, Tampere University of Technology, Finland; R. Lahesmaa, University of Turku and Abo Akademi University, Finland; A. Shvedova, West Virginia University, USA; S. Mathur, University of Cologne, Germany; B. Fadeel, Karolinska Institutet, Sweden

The novel characteristics of engineered nanomaterials that are essential for successful and innovative applications might also lead to negative health effects. Here we performed a comparative study of the interactions of single-walled carbon nanotubes (SWCNT), graphene oxide, and hollow carbon spheres (HCS) with cells of the immune system. Graphene is a two-dimensional (2-D) nanomaterial composed of layers of carbon atoms forming six-membered rings; SWCNT is a 1-D nanomaterial formed by the rolling of graphene sheets into hollow tubes, and HCS are carbon-based nanospheres (3-D). Owing to their novel electrical, optical, mechanical and chemical properties, these carbon-based nanomaterials are currently of great interest for a variety of technological as well as biomedical applications. The materials were first confirmed to be free from endotoxin contamination. We then compared the effect of the carbon-based nanomaterials on cell viability and production of pro- and anti-inflammatory cytokines using primary human monocyte-derived macrophages (HMDM). We also monitored cellular uptake of these materials using transmission electron microscopy. Finally, we performed global gene expression analyses of HMDM exposed to the nanomaterials. The latter results may enable us to define nanomaterial-specific changes in gene expression i.e. 'nanotoxicogenomic' signatures.

**11:00 AM**

**(ICACC-GYIF-018-2012) Novel scaffolds made from metallic ion doped bioactive glasses: fabrication and characterization (Invited)**

A. Hoppe\*, Institute of Biomaterials, Germany; D. Hiller, U. Kneser, University of Erlangen, Germany; A. R. Boccaccini, Institute of Biomaterials, Germany

Bioactive glasses, such as standard 45S5 Bioglass®, have been widely used in the field of bone tissue engineering due to their high bioactivity and stimulating effects on osteogenesis and angiogenesis. The greater understanding of molecular mechanisms and chemical pathways dictating the interaction between materials and cells will allow constructing tissue specific scaffolds with tailored chemistry, surface topography, porosity and ion release kinetics, which will induce the desired biological effect in the physiological environment. Melt-derived Cu-doped 45S5 bioactive glass was used to fabricate 3D porous scaffold via foam replica method. Acel-

lular *in vitro* studies revealed a very high bioactivity of the Cu-doped scaffolds indicated through fast formation of carbonated hydroxyapatite layer (CHA) after 3 d of immersion in simulated body fluid (SBF). Kinetics of this glass-ceramic scaffolds transition to calcium phosphate was confirmed through XRD, FT-IR, and SEM analysis and was monitored with micro ion-beam measurements. Cell tests with human-derived mesenchymal stem cells (hMSCs) were performed showing good biocompatibility of Cu-doped samples. Further RNA / RT-PCR analysis as well as ALP staining will be used to identify specific effects if the copper ions on osteogenic differentiation of hMSCs.

**11:20 AM**

**(ICACC-GYIF-019-2012) Science in between Fun, Funding and Fundamentals (Invited)**

T. Fischer\*, University of Cologne, Germany

Emerging young researchers face the challenge on how to position themselves on the global science market. As science is becoming more and more interdisciplinary and interconnected on an international scale, new possibilities arise for working on more complex projects, but also new skills are essential for long lasting scientific success. This talk wants to point out some aspects on planning a modern science career, which includes unlocking funding possibilities, developing communication skills and creating strong collaboration networks.

**11:40 AM**

**(ICACC-GYIF-020-2012) On the optical measurement of interlaminar stress-strain response of double notched compression specimens from woven Carbon/Carbon composites**

T. Krause\*, University of Bremen, Germany; S. Ladisch, Fraunhofer Institute for Mechanics of Materials, Germany; K. Tushtev, University of Bremen, Germany; R. Schäuble, Fraunhofer Institute for Mechanics of Materials, Germany; G. Grathwohl, University of Bremen, Germany; D. Koch, Institute of Structures and Design, Germany

Ceramic Matrix Composites (CMC) are engineered for quasi-plastic behavior when stressed in the in-plane direction. Out-of-plane (or interlaminar) strength is about one order of magnitude lower than in-plane properties, making interlaminar failure a key issue for CMC failure. They are commonly regarded as purely brittle, assuming a linear stress strain relationship followed by sudden fracture. In this study, the interlaminar shear stress vs. shear strain relation is examined and related to the CMC lay-up. The present work focusses on the recording of double notched compression tests by a two camera system and calculation of resulting deformations by means of gray value correlation. Twill weave Carbon/Carbon composites were tested until interlaminar shear failure occurred. Gray value correlation leads to a deformation pattern of the entire shear specimen. The shear zone is limited to a small area around the middle plane of the specimen, with significantly higher shear along the future crack plane. Influence of the choice of the area of analysis is demonstrated. Deformations are transformed into shear stress – shear strain curves. It is shown that interlaminar shear can be divided into a linear-elastic part and pseudo-plastic part at which the shear plane is degraded stepwise. Relation to fracture pattern is used to support the results.

### S1: Mechanical Behavior and Performance of Ceramics & Composites

#### Processing-Microstructure-Properties Correlations II

Room: Coquina Salon D

Session Chairs: Michael Halbig, NASA Glenn Research Center; Lalit Sharma, Central Glass Research Insititute

1:30 PM

#### (ICACC-S1-064-2012) Investigation of the Mechanical Properties of an Oxide/Oxide Fibre Reinforced Ceramic Matrix Composite

R. E. Johnston\*, M. R. Bache, Swansea University, United Kingdom; D. Thompson, Umeco Composite Structural Materials, United Kingdom; P. J. Withers, S. Van Boxel, Manchester University, United Kingdom; I. M. Edmonds, Rolls-Royce plc, United Kingdom

Alumina based oxide-oxide ceramic matrix composites offer improved resistance to high temperature oxidation compared to systems based on silicon carbide (e.g.  $\text{SiC}_f/\text{Al}_2\text{O}_3$  or  $\text{SiC}_f/\text{SiC}$ ). This will be a critical requirement where applications are envisaged in oxidising environments at temperatures approaching 1200°C. The mechanical behaviour of these oxide-oxide systems, either in response to direct mechanical or indirect thermal loading, requires a thorough understanding prior to considering such CMCs for engineering service. A comprehensive programme of research has assessed the mechanical performance of a novel alumina oxide-alumina oxide CMC at room temperature plus a range of elevated temperatures between 600°C and 1200°C. Mechanical properties including monotonic tension, flexural strength, inter-laminar shear strength, low cycle fatigue and creep have all been evaluated. Throughout the study, detailed non destructive inspections were conducted. Post test fractography then offered a fundamental insight into damage accumulation and failure mechanisms which could be related back to the original condition of supply. Fracture under a wide variety of testing modes was preceded by fibre-matrix de-cohesion across various length scales within the composite, i.e. between plies, fibre bundles and individual fibres.

1:50 PM

#### (ICACC-S1-065-2012) Stochastic models of fragmentation of brittle fibers or matrix in ceramic matrix composites

J. L. Lamon\*, CNRS, France

Modelling of matrix fragmentation during tensile loading, is critical to determination of composite deformation and non-linear stress-strain behaviour, to the development of optimized composites and the design of structural components. The present paper compares the fragmentation strength distributions predicted using various models including: - the well-known Monte Carlo simulation method based on chain-of-segments model and fiber strength distribution. This model has been widely used to simulate fragmentation of fibers in polymer or metal matrix. - Fragment dichotomy model based on failures and flaw strength distributions in successive fragments. This model has been validated in previous papers by comparison to experimental results - and Bayesian chain-of-elements model based on flaw strength distribution in the fiber. This model is proposed in this paper. These models are discussed. They were compared to experimental series of fragmentation stresses obtained during tensile tests on SiC matrix composites reinforced with SiC or C fibers. Matrix failures were detected using either acoustic emission counts or SEM inspection during the tests. The influence of preponderant factors was anticipated.

2:10 PM

#### (ICACC-S1-066-2012) Oxide Fiber Composites with cellular YAG/ZrO<sub>2</sub>-matrices

T. Wamser\*, J. Lehmann, S. Scheler, W. Krenkel, Ceramic Materials Engineering, Germany

In the future oxide fiber composites (OFC) will be used in turbine engines as well as in furnace- and chemical applications increasingly.

This material class has outstanding properties due to its high temperature strength and damage-tolerant fracture behavior even in corrosive oxidizing atmospheres. Furthermore, OFC can be used as a lightweight material because of the low density. In this contribution, a novel freeze casting process for the manufacturing of cellular oxide fiber composite is presented. The method is based on an ultrasonic assisted infiltration of fabrics with aqueous, gelatin-containing slurries which can be laminated subsequently. After a freeze-drying process the laminate can be sintered. The innovative approach is based on the design of the matrix by influencing the growth of ice crystals during the freezing of water with organic additives such as glycerol and gelatin. It is shown that an optimized porosity can reduce shrinkage during sintering and thus the strength and the fracture behavior can be improved significantly. This effect can be explained by an in-situ densification of the matrix by the growth of the ice-crystals. To increase the strength further a vacuum-infiltration of the porous matrix with metal organic precursors is provided. The novel method is demonstrated on the basis of Nextel™610/ YAG-ZrO<sub>2</sub> composites. The bending strength of the novel damage-tolerant cellular OFC is above 250 MPa.

2:30 PM

#### (ICACC-S1-067-2012) Mechanical and microstructural characterization of C/C-SiC manufactured via triaxial and biaxial braided fiber preforms

F. Breede\*, M. Friess, D. Koch, H. Voggenreiter, Institute of Structures and Design, German Aerospace Center (DLR), Germany; V. Frenzel, K. Drechsler, University of Stuttgart, Germany

Carbon-carbon silicon carbide (C/C-SiC) composite plates were manufactured via triaxial and biaxial braided fiber preforms. The liquid silicon infiltration (LSI) method was used to achieve the SiC matrix. In a first processing step intermediate modulus carbon fiber (T800 12k) preforms were manufactured via braiding technique which generates typical fiber orientations. In the next step the fiber preforms were processed to CFRP green bodies by warm pressing (using phenolic resin) as well as by resin transfer molding (RTM, using aromatic resin). The CFRPs have a fiber volume content of about 60 percent.  $\pm 45^\circ$  and  $\pm 75^\circ$  fiber orientation were selected for this study. The main objective of this work was to investigate the mechanical properties under tensile and bending loads at room temperature depending on fiber orientation and processing route. The change in fiber orientation as well as the influence of triaxial fiber preforms in contrast to biaxial fiber preforms will be explained. The use of different CFRP process techniques results in different final matrix structures and therefore in different microstructures of the resulting C/C-SiC composites which will be compared based on CT and SEM analysis.

2:50 PM

#### (ICACC-S1-068-2012) Influence of Fiber Fabric Density and Matrix Fillers as well as Fiber Coating on the Properties of OXIPOL Materials

S. Hoenig\*, E. Klatt, M. Friess, D. Koch, C. Martin, I. Naji, German Aerospace Center, Germany

Higher efficiency of jet engine and environmental friendly use are promised via an increase of the combustion temperature. Oxide ceramic matrix composites (CMC) are reliable candidates for this purpose. Within this scope, the German funded project HiPOC (High Performance Oxide Ceramics) supports the further development of OXIPOL (Oxide CMC based on Polymers) materials at the German Aerospace Center (DLR) in Stuttgart. The OXIPOL materials studied in this work are manufactured via the polymer infiltration and pyrolysis process (PIP) and reinforced with alumina fibers (Nextel 610, 3M). A variation of the fiber fabric density (i.e. filament count) and the fiber volume content is firstly investigated. Moreover, the influence of ceramic fillers on the interlaminar shear strength (ILSS) as well as the influence of different types of fiber coating (fugitive and

lanthanum phosphate coating) on mechanical behavior are discussed. This work showed that OXIPOL materials with lower filament count present a more homogeneous fiber coating in the bundle and a better matrix infiltration, leading to an improvement in mechanical properties.

**3:20 PM**

**(ICACC-S1-069-2012) Innovative clay-cellulosic biosourced composite: formulation and processing**

G. Lecomte-Nana\*, ENSCI - GEMH, France; O. Barré, C. Nony, Société Bibliotek, AVRUL Dpt Incubateur, France; G. Lecomte, ENSCI - GEMH, France

The present research work is in line with sustainable and environment conscious development through the use of natural raw materials for the processing of biosourced products. The main scope is to manufacture a new class of products for future application as protection barriers for delicate objects towards fire and flooding. The main requirements that must be fulfilled for such application are: flame resistance, waterproof, good permeability and adequate flexural strength (> 2 MPa). Kaolinitic-illitic raw clays were selected as starting materials regarding their specific behaviors. Various clay-fiber compositions were prepared and optimized regarding the final required characteristics. Three surfactants were used to improve the rheological behavior of the system. Moreover, a peculiar shaping process was developed in order to obtain satisfying products, consolidated without sintering. The optimized formulation consists of a clay-fiber mixture with a fiber/clay ratio of 0.13. The key characteristics obtained for this product are: M0 class, resistance towards water seeping of 90 min and flexural strength of 7 MPa.

**3:40 PM**

**(ICACC-S1-070-2012) Shape-memory effect in glassy carbon**

Y. Shinoda\*, T. Akatsu, F. Wakai, Tokyo Institute of Technology, Japan

The shape-memory effect is a phenomenon wherein a material that is deformed into a specific shape recovers its original shape on exposure to an external stimulus. Thermally induced shape-memory effects have been reported in a variety of materials, such as metallic alloys, ceramics, hydrogels and polymers. The shape-memory effect in metallic alloys such as Ni-Ti-based alloys is based on a martensitic phase transformation and reversal without diffusion. On the other hand, characteristics such as shape recovery and shape fixity in polymers and hydrogels are a result of the difference in viscoelastic behavior above and below the glass transition temperature. Shape-memory materials have attracted recent attention because of the potential for significant practical applications as well as scientific interest. Glassy carbon is a material composed of only carbon atoms, and its mechanical properties are similar to those of glass or ceramics; they are hard and brittle, and fracture surfaces are glass-like in appearance. Glassy carbon exhibits superviscoelastic behavior at elevated temperatures because of its unique microstructure. Here, we report the shape-memory effect in glassy carbon using its large viscoelastic properties at elevated temperatures. The shape-memory effect in glassy carbon can be practically applied in many situations, such as couplings between graphite parts or as actuators and sensors operating under ultra-high temperature.

**4:00 PM**

**(ICACC-S1-071-2012) Novel Silicon Carbide Composites without Interface Layer**

T. Hinoki\*, K. Shimoda, Y. Park, Kyoto University, Japan

Novel conceptual silicon carbide composites were developed applying porous silicon carbide matrix. The composites consist with just silicon carbide fiber and crystalline porous silicon carbide matrix without fiber/matrix interphase like carbon. The silicon carbide matrix was formed with carbon powder by liquid phase sintering or reaction sintering method. The porous silicon carbide matrix was formed following decarburization process. The composites showed pseud-ductile behavior and complicated fracture behavior due to frictional stress at debonded fiber/matrix interface. Three point flexural

strength was approximately 300 MPa in case of the material with 30 % porosity. Silicon carbide composites require fiber/matrix interface layer like carbon for pseud-ductile fracture behavior. The control of thickness and quality for the interface layer is very difficult, although it is the key to determine mechanical properties of the composites. The novel composites showed pseud-ductile behavior without the interface layer. It is easy to fabricate uniform material and reduce the material cost significantly. The carbon interface layer is the weakest link in some cases in particular for oxygen environment at high temperature. The novel material just consists with silicon carbide and applicable for various severe environment.

**4:20 PM**

**(ICACC-S1-072-2012) Bonding of Silicon Carbide Ceramics to Metals using Particulate Reinforced Ag-Cu-Ti Alloys**

M. C. Halbig\*, NASA Glenn Research Center, USA; B. P. Coddington, University of Wisconsin-Madison, USA; R. Asthana, University of Wisconsin-Stout, USA; M. Singh, Ohio Aerospace Institute, USA

CVD silicon carbide was bonded to itself and to molybdenum and tungsten using two Ag-Cu-Ti braze alloys reinforced with SiC particulates. Powders of the braze alloys, Ticusil (68.8Ag-6.7Cu-4.5Ti, TL: 900°C) and Cusil-ABA (63Ag-35.3Cu-1.75Ti, TL: 815°C) were premixed with 5, 10 and 15 wt% SiC particulates (nominal size: ~20 µm). All joints were processed in vacuum and examined using optical microscopy (OM), scanning electron microscopy (SEM), energy dispersive spectroscopy (EDS), and Knoop microhardness testing. The SiC particles were randomly distributed within the braze matrix and well-bonded to it via reaction with the Ti that segregated at particle/braze interfaces. The SiC particles with Ti-rich interfaces promoted the nucleation of the Cu-rich secondary phase that precipitated on the particle surface. The loss of Ti in the reaction involving SiC particulates did not impair the bonding of the SiC substrate which also showed Ti segregation, reaction layer formation and good bonding. Thus, reinforcing the braze matrix with SiC particulates can provide the dual benefits of metallurgically well-bonded substrates and reinforced joints with enhanced strength. The loss in the braze ductility due to reinforcement and ability to accommodate thermal stresses may be compensated by the decrease in the coefficient of thermal expansion (CTE) of reinforced joints.

**4:40 PM**

**(ICACC-S1-073-2012) Biaxial Flexure tests of Carbon Fiber – SiC Matrix Hybrid Ceramics**

N. Nakagawa\*, Japan Ultra-High Temperature Materials Research Center, Japan; S. Aonuma, Covalent Materials Co., Japan; S. Guo, National Institute for Materials Science, Japan; K. Goto, Japan Aerospace Exploration Agency, Japan; Y. Kagawa, University of Tokyo, Japan

Carbon fiber reinforced SiC matrix composites (C/SiC) have several superior properties, high strength, high thermal shock resistance, tribological properties and low density. Therefore, C/SiC hybrid ceramics are expected for applications in high performance brake system, instead of the existing cast steel and C/C composite. In this study, we had successfully fabricated short carbon fiber reinforced SiC ceramic matrix composites by using Si melting infiltration method. Strength testing of hybrid ceramics materials in biaxial rather than uniaxial flexure offer useful advantages.

**5:00 PM**

**(ICACC-S1-074-2012) Strategies to Optimize the Strength and Toughness of Ceramic Laminates**

R. Bermejo\*, Montanuniversitaet Leoben, Austria; L. Sestakova, O. Sevecek, Materials Center Leoben Forschung GmbH, Austria; Z. Chlup, Academy of Sciences of the Czech Republic, Czech Republic; R. Danzer, Montanuniversitaet Leoben, Austria

Layered ceramics are, compared to conventional monolithic ceramics, a good choice for highly loaded structural applications having improved fracture toughness, strength and mechanical reliability (i.e. flaw tolerant materials). The use of tailored residual

compressive stresses in the layers is a key parameter to adjust these properties. In this work two types of ceramic laminates are analyzed which have external or internal compressive stresses. The most important factors having influence on the strength and toughness of these laminates are discussed. Experimental bending tests are performed to investigate the crack propagation through the layers. A fracture mechanics analysis is employed to estimate the crack growth resistance of the material as a function of the crack length. It is found that the proper selection of a suitable mismatch strain (responsible for the generation of residual stresses), volume ratio of the layer materials and thickness and distribution of individual layers are crucial to achieve a high toughness and/or a high lower limit (threshold) for strength in ceramic laminates. Design guidelines to avoid cracking of layers associated with high residual stresses are also provided. Design criteria to optimize strength and toughness in advanced ceramics to be used in engineering applications are established.

**5:20 PM**

### **(ICACC-S1-075-2012) High Pressure Seawater Impingement Resistance of High Purity Aluminum Oxides**

T. S. Dyer\*, Energy Recovery Inc, USA; R. Quiazon, Energy recovery Inc, USA; M. Rodgers, Rio Tinto Alcan, France

High purity alumina is used to make energy recovery devices for seawater desalination. These devices reduce energy consumption of large SWRO water factories by up to 60%. SWRO applications are unusual for ceramics since they are continuous and combine corrosive and abrasive conditions with prolonged cavitation energy. Selecting a starting material for a product formulation is critical. High purity, raw, specialty alumina ceramic powders have been developed with minimized soda and silica levels. Available products included the now obsolete RAC45B, which has been replaced by P172HPB targeting levels of <0.03% soda and <0.02% silica. Though similar products are available in the market, aluminas made from these raw materials perform differently in seawater impingement. Super ground, >99.5% alumina powders, including Alcan P172HPB, were processed into samples using ERI spray dry, CIP, and sintering processes. These ceramic coupons, along with commercial ceramic coupons, were subjected to a modified ASTM G134 – 95 cavitation test. After testing, surface roughness increased to 100 to 200  $\mu\text{m}$ . Cavitation damage appears to correlate with hardness and Archimedes density. Fired density data also reveals that the Alcan P172HPB densifies equal to or better than the RAC45B it is intended to replace. In general, raw materials with overall lower impurity levels appear to perform better in SWRO conditions.

**5:40 PM**

### **(ICACC-S1-076-2012) Production and study of stability of Ca<sub>2</sub>AlNbO<sub>6</sub> ceramics in crude petroleum for their application in petroleum extraction industry**

Y. P. Yadava\*, M. M. Lima, J. S. Oliveira, R. A. Sanguinetti Ferreira, Universidade Federal de Pernambuco, Brazil

In the present work niobium based complex cubic perovskite oxide Ca<sub>2</sub>AlNbO<sub>6</sub> ceramics were fabricated and studied their stability in crude petroleum environment for the manufacture of inert ceramic embedding for temperature sensors used in petroleum extraction. Ca<sub>2</sub>AlNbO<sub>6</sub> ceramic powder was prepared through thermo-mechanical processing. Structural characteristics of calcined material was investigated by powder X - ray diffraction, which presented a single phase complex cubic perovskite structure with lattice parameter  $a = 7.8826\text{\AA}$ . Compacted Ca<sub>2</sub>AlNbO<sub>6</sub> ceramics were sintered at 1300C during 24 hours in ambient atmosphere. Microstructure of the sintered ceramics was studied by scanning electron microscopy and mechanical behavior was studied by Vicker's micro-hardness testing. Sintered ceramics were submerged in crude petroleum for 45 days. Ceramics were taken out from the petroleum periodically and sub-

jected to structural, microstructural and mechanical characterizations. Results showed that ceramics submerged in crude petroleum did not suffer any change at any stage of submersion.

## **S2: Advanced Ceramic Coatings for Structural, Environmental, and Functional Applications**

### **Coatings to Resist Wear, Erosion and Extreme Environments**

Room: Ponce de Leon

Session Chairs: Oyelayo Ajayi, Argonne National Laboratory; Irene Spitsberg, Kennametal

**1:30 PM**

### **(ICACC-S2-029-2012) Investigation of Coating Failure Behavior under Extremely High Impact and Sliding Load Conditions (Invited)**

J. F. Su, X. Nie\*, H. Hu, University of Windsor, Canada

Hard coatings deposited by PVD/CVD processes are widely used for increasing the lifetime of tools and components. Pin-on-disc tribotests, scratch and impact tests are currently applied to study failure mechanisms of the hard coatings at the laboratory level. However, such tests cannot simulate working conditions of coatings under extremely high loads where impact and sliding motions are also involved, such as in Advanced High Strength Steel (AHSS) stamping applications. In this project, a newly-developed impact-sliding wear tester was used to evaluate the wear resistance and failure behavior of three typical coatings (TiAlN, CrN and TiC) on AISI D2 substrates (hardened or nitrided) under two load combinations (80N/200N and 200N/400N impact/pressing forces). Morphology of the coatings in areas of the impact-sliding wear tracks were observed and analyzed using Scanning Electron Microscopy and energy-dispersive X-ray spectrometry. Selected coating samples were dissected along the impact-sliding wear tracks to investigate the coating failure behavior. Fatigue cracking, chipping and peeling of coatings as well as counterface material transfer were found to be the main failure mechanism. The testing methodology was effective and explicit in evaluation of PVD and CVD coating performance under extremely high impact/sliding load conditions.

**2:00 PM**

### **(ICACC-S2-030-2012) Modeling and Ab-Initio Simulation of Amorphous Coatings (Invited)**

P. Kroll\*, UT Arlington, USA

With increasing computational resources, both in methods and computer power, much progress has been made in advancing our understanding in complex materials systems. Simulations at the atomistic length scale have indicated significant influence of variations in elemental character, distribution of atoms and chemical bonding on basic properties such as adhesion, strength, and thermal properties. In this talk we will present results of our efforts combining modeling with electronic structure calculations. We focus on amorphous ceramic coatings, in particular on silicon based advanced ceramics. Examples include the adhesion and delamination of hard SiCN coatings on steel, oxidation of SiCO, and thermal transport in HfSiCNO.

**2:30 PM**

### **(ICACC-S2-031-2012) Effect of stoichiometry of ceramic interlayers pre-coated on WC-Co on diamond coatings by MPCVD**

Y. Li\*, Y. Tang, L. Zhang, Q. Yang, A. Hirose, University of Saskatchewan, Canada

Direct coating of well adherent diamond films on WC-Co cutting tool inserts is usually restrained by the low diamond nucleation density and weak interfacial bonding. In this work, stoichiometry-grad-



ent carbide/nitride interlayers by ion beam deposition were studied to overcome this drawback. The interlayers and the diamond coating deposited on them using a microwave plasma enhanced chemical vapor deposition method were characterized by Rockwell indentation testing, scratching testing, nanoanalyzer, scanning electron microscopy, X-ray diffraction, X-ray photoelectron spectroscopy and synchrotron based x-ray absorption spectroscopy. The results have demonstrated that the gradient carbide/nitride interlayers with a thickness down to few hundred nanometers can significantly improve the diamond nucleation density and the interfacial adhesion of diamond to WC-Co cutting tools.

### 3:10 PM

#### (ICACC-S2-032-2012) Effect of Hard Coatings on Tribochemical Film Behavior in Lubricated Sliding Contact

M. Lorenzo Martin\*, O. O. Ajayi, S. Torrel, N. Demas, G. Fenske, Argonne National Laboratory, USA

Tribological components such as gears and bearings engaged in sliding or rolling contacts are made of ferrous materials. In order to reduce friction and wear, lubricants are often applied to components. The lubricants are usually formulated with additives such as anti-wear, friction modifier, anti-oxidant, etc. These additives react with the ferrous materials surface to form tribochemical surface films. To date, additives are formulated primarily to react with ferrous surfaces. A variety of hard thin-film coatings are increasingly being used in tribological components. These coatings enhance the friction and wear behavior of the components. There are significant uncertainties on the impacts of thin film coatings on reactions of lubricant additives on coated surfaces in lubricated sliding contact. In this study, we evaluated the friction and wear behavior of several commercially available thin-film ceramic coatings when lubricated with unformulated and fully formulated synthetic lubricants. In tests with unformulated lubricant, friction coefficient behavior is similar as the uncoated steel. While in tests with fully formulated lubricants, a variety of behaviors was observed for different coatings. These behaviors are explained in terms of the differences in tribochemical film formation and properties on the coatings surfaces.

### 3:30 PM

#### (ICACC-S2-033-2012) Evaluations of Multilayer Coatings for Galvanic Corrosion Resistance Applications

C. Qu, Alfred University, USA; R. Kasica, NIST, USA; R. Wei, Southwest Research Institute, USA; E. McCarty, 4. Materials Technologies Consulting, USA; J. Fan, D. Edwards, G. Wynick, X. Wang\*, Alfred University, USA

Magnesium alloy materials are utilized in some vehicles due to their low mass densities. The challenge is to mitigate the galvanic corrosion when a magnesium alloy part is fastened with a carbon steel bolt. Current solutions involve aluminum fasteners, isolators and sleeves. On an aluminum metal surface, natively grown aluminum oxide may exist and its thickness may vary from one spot to the other. The aluminum parts can only partially isolate steel and steel fasteners from magnesium in some random locations. To electrically insulate steel parts away from magnesium (AZ31) parts, three layer coatings are applied on the carbon steel parts. The layer stacking sequence is silicon nitride, aluminum oxide and UV curable aluminum oxide. Based on zero-resistance ammeter measurement and ASTM B 117 salt spray testing, the three layer coating mitigates the galvanic corrosion better than that provided by aluminum. Materials properties, corrosion testing results will be provided, along with the measured mechanical properties.

### 3:50 PM

#### (ICACC-S2-034-2012) Formation of nano dispersed ceramic-metallic composite coatings

R. Saha\*, M. A. Farrokhzad, T. I. Khan, University of Calgary, Canada

The use of electrodeposited composite coatings with a nano dispersed ceramic particles have been widely considered for industrial applications in the recent years due to their enhanced hardness and

wear resistance properties. In this study, nickel coating reinforced with a dispersion of nano sized Al<sub>2</sub>O<sub>3</sub> particles was developed using electrodeposited technique and the coatings were investigated with respect to hardness and wear properties. The effects of post-deposition heat treatment on the morphology of the composite coatings were also studied. The microstructural features of the coatings were characterized by scanning electron microscopy and energy dispersive x-ray spectroscopy. Micro-indentation and wear tests were conducted to evaluate the hardness and wear resistance, respectively, of the deposited layer. The results showed that the hardness and the wear properties of the coatings increased with an increase of ceramic particles in the composite coating. The post-deposition heat treatment softens the coated layer.

### 4:10 PM

#### (ICACC-S2-035-2012) Nanoindentation and tribological properties of magnetron sputtered WC-C coatings

F. Lofaj\*, M. Ferdinandy, P. Hornak, Institute of Materials Research of SAS, Slovakia; G. Cempura, AGH-UST, Poland

Nanoindentation and tribological properties of thin DC and RF magnetron sputtered WC-C coatings were investigated in order to optimize deposition technology from the viewpoint of achieving nanocomposite structure with improved hardness and friction behavior. The coatings were deposited under variable pressure and ion energy conditions and their structure and properties were investigated using scanning and transmission electron microscopy with EDX-ray spectroscopy, atomic force microscopy, Raman spectroscopy, instrumented indentation and ball-on-disc tribological testing at room and elevated temperatures, respectively. Additional grazing incidence X-ray measurement confirmed the presence of WC1-x phase and of large compressive stresses. High resolution TEM visualized 10-30 nm WC nanocrystals. Iterative approach applied to the variations of deposition conditions based on mechanical properties resulted in the increase of indentation hardness up to approximately 35 GPa, which is more than 50% increase compared to commercially available WC-C coatings and the coefficient of friction obtained at room temperature was below 0.2. Rapid increase of COF at elevated temperatures was attributed to local chemical interactions between the coating and steel ball in the oxidizing environment resulting in the formation of unstable transfer film with high COF.

### 4:30 PM

#### (ICACC-S2-036-2012) Enhancing the performance and lifetime of ceramic components in critical applications through the use of carbon based coating technology

C. H. Walker\*, Diamond Hard Surfaces Ltd, United Kingdom

The advantages of using ceramics in mechanical components are well known, however on their own they have limitations in some application areas. This paper will present an overview of carbon coatings as potentially applied to ceramics in high speed rotating applications where marginal lubrication conditions are an issue. We will discuss different classifications of materials, their background, characteristics, advantages and disadvantages, application requirements and some of the work we have done on our materials with customers in the field of mechanical seal faces. The paper will discuss end user requirements and why ceramics alone no longer meet customer needs in many critical applications. We will also discuss future potential developments to further enhance performance.

### 4:50 PM

#### (ICACC-S2-037-2012) Rare earth oxide reinforced Al<sub>2</sub>O<sub>3</sub>-TiO<sub>2</sub> ceramics coating for metal matrix in petroleum industry

Y. P. Yadava\*, S. A. Rêgo, C. E. Mendes, R. A. Sanguinetti Ferreira, Universidade Federal de Pernambuco, Brazil

Recent findings of largest known pre-salt petroleum reservoir on earth in Brazil have generated intense demand for new materials capable of withstanding direct contact with the crude petroleum as it is

a highly corrosive and chemically reactive fluid. Petroleum drilling equipments, storage tanks and transportation systems suffer constant physical stress caused by chemical attack of crude petroleum. Ceramics present high chemical stability and therefore can be used as protective coatings to solve the problem. However, fragile nature of the ceramics needs improvement in their mechanical properties. For this purpose we have produced rare-earth oxide (CeO<sub>2</sub>, La<sub>2</sub>O<sub>3</sub>) reinforced Al<sub>2</sub>O<sub>3</sub>-TiO<sub>2</sub> ceramic composites in proportions of 5-20 wt% TiO<sub>2</sub> with high mechanical strength, through thermo-mechanical processing and sintering techniques. To evaluate the possibility of using these ceramics as protective coatings of metallic matrix of crude petroleum storage and transportation systems, we have studied the physico-chemical and mechanical stability of these materials in crude petroleum originated from petroleum wells of Sergipe region of Brazil. These studies presented satisfactory results for the use of rare earth oxide reinforced Al<sub>2</sub>O<sub>3</sub>-TiO<sub>2</sub> ceramic composites with 15-20 wt% TiO<sub>2</sub> and 2 wt% of rare earth oxides for inert coating of metallic parts for petroleum extraction industry.

**5:10 PM**

**(ICACC-S2-038-2012) A Novel Hybrid Nanomanufacturing Ceramic Coating and Surface Engineering Process: Cubic Boron Nitride Coating, a Case Study**

A. Malshe\*, NanoMech Inc., USA; W. Jiang, University of Arkansas, USA

Additive and subtractive manufacturing processes are in growing demand for high level of functionality for meeting increasing challenges of higher productivity and sustainable manufacturing. Innovations in hybrid manufacturing where multiple processes are combined to provide improved capabilities and allowing new opportunities that have never been possible previously. Authors present a platform of hybrid process combining capability of electric field assisted deposition of nano particles of ceramic integrated with second and even third phases of ceramic materials infiltrated using chemical vapor deposition. This hybrid platform called TuffTek has allowed the realization of world's first cubic boron nitride (cBN) composite coated carbide tools for machining and wear parts applications. This talk discusses materials, process and resulting performance of cBN-TiN and related materials for machining hard materials. Speaker will also disseminate potential opportunities not only in machining but also in electronics, biomedical and other applications.

### **S3: 9th International Symposium on Solid Oxide Fuel Cells (SOFC): Materials, Science and Technology**

#### **Mechanical and Thermal Properties**

Room: Coquina Salon H  
Session Chairs: Toshio Suzuki, National Institute of Advanced Industrial Science and Technology; Yeong-Shyung Chou, Pacific Northwest National Lab

**1:30 PM**

**(ICACC-S3-022-2012) Weibull strength variations between room temperature and high temperature Ni-3YSZ anode supports**

D. J. Curran\*, H. Lund Frandsen, S. Rasmussen, P. Vang Hendriksen, DTU, Denmark

Solid oxide fuel cells are made up of numerous individual ceramic cells with each of these cells being integral to the functioning of the fuel cell. One of the most relevant failure mechanisms of a fuel cell is fracture of the individual cells, with even catastrophic failure of one cell resulting in temporary interruption, reduced efficiency, increased degradation and/or the complete termination of energy production. Although individual cells consist of a number of functioning layers, the bulk of the mechanical strength is determined by the support layer. This research investigates the effect of fuel cell

operating temperatures on the Weibull strength of Ni-3YSZ support layers, tested by the 4-point bend method, using room temperature (RT) measurements as a reference for high temperature (HT) tests. Additionally, the possible effects of cell reduction on the Weibull strength are also investigated. A sample set of 30 is used to give viable statistical results. Volume scaling is used for comparison of the Weibull strengths to results in the literature, which additionally allows the direct comparisons of the 4-point bend test method to previous ring-on-ring tested cells. Preliminary results, between cells tested at RT and HT, indicate that cell operation at elevated temperature reduces the Weibull strength of the cell.

**1:50 PM**

**(ICACC-S3-023-2012) (Sc<sub>2</sub>O<sub>3</sub>)<sub>0.1</sub>(CeO<sub>2</sub>)<sub>0.01</sub>(ZrO<sub>2</sub>)<sub>0.89</sub> / (Y<sub>2</sub>O<sub>3</sub>)<sub>0.08</sub>(ZrO<sub>2</sub>)<sub>0.92</sub> layered electrolytes**

Y. Chen\*, N. Orlovskaya, University of Central Florida, USA; J. Neutzler, J. Sightler, X. Huang, University of South Carolina, USA; T. Graule, J. Kuebler, Empa, Swiss Federal Laboratories for Materials Science and Technology, Switzerland

(Sc<sub>2</sub>O<sub>3</sub>)<sub>0.1</sub>(CeO<sub>2</sub>)<sub>0.01</sub>(ZrO<sub>2</sub>)<sub>0.89</sub> (SCSZ) has superior ionic conductivity in the intermediate temperature range (700~800 °C) for the operation of solid oxide fuel cells (SOFCs), but it does not exhibit good phase stability and reliability in comparison with yttria-stabilized zirconia (YSZ). To improve it, the layered electrolyte structures with YSZ outer layers and SCSZ inner layers were designed and manufactured. One goal to design such layered structures was to protect SCSZ against destabilization during the operation by placing more stable YSZ material on the outer surfaces of the electrolyte. Another goal was to create thermal compressive stresses on the outer surfaces, which would increase the fracture toughness of the layered composite and therefore its mechanical strength. It was calculated that at 800 °C compressive residual stress exists in outer layers and tensile stress appears in inner layers. The stress state can be adjusted by the layers thicknesses ratio. The biaxial flexure strength at RT and 800 °C of electrolytes was tested via a ring on ring method, and the primary analysis showed the enhancement of flexure strength in SCSZ/YSZ electrolytes at 800 °C. The Arrhenius plots show the ionic conductivities approximately follow the predicted value by a simple resistor-in-series model, and the high ionic conductivity in the intermediate temperature range can be maintained in the layered designs.

**2:10 PM**

**(ICACC-S3-024-2012) Thermomechanical Degradation Behavior of SOFC Materials**

H. Lee, E. R. Kupp\*, G. L. Messing, Penn State University, USA

Many energy systems such as SOFCs are processed from, and composed of, layered ceramic components supported on a rigid substrate. These systems are processed at and operate at a range of thermal cycles and transients. The reliability and costs of the energy system depend on the ability to predict what conditions lead to degradation and failure-causing stresses that arise during operation and processing. By measuring the viscoelastic properties (E, η) of the individual components as a function of temperature we can model the stress states in the energy system during processing and operation. With this knowledge we can understand how to adjust materials, processing and operation conditions to avoid failure. We have developed testing techniques, such as cyclic loading dilatometry (CLD) and creep beam bending (CBB), to measure the thermomechanical properties of individual ceramic components as a function of relative density and microstructure (i.e. porosity and grain size) at typical processing and operation temperatures. SOFC cathode materials such as LSCF, LSCF-GDC, LSM, LSM-YSZ, and YSZ were analyzed during this study. Material sintering behaviors (e.g., shrinkage, warpage, densification) and thermomechanical responses (e.g., viscosity, Poisson's ratio) were determined using CLD and CBB on both individual materials and laminar composites prepared by tape casting.

2:30 PM

**(ICACC-S3-025-2012) Characterization of Zirconia by Means of Thermoanalytical Methods: From the Green Body to Dense Bulk Ceramics**

E. Post\*, NETZSCH Geraetebau GmbH, Germany; B. Fidler, NETZSCH Instruments North America, LLC, USA

ZrO<sub>2</sub> is a very important high-temperature oxide ceramics due to its wide application range varying from refractory materials to thermal barrier coatings to fuel cell membranes. Depending on the application, the physical and chemical properties can be determined using different stabilizing oxides, different grain sizes or sintering temperatures. The influences of these modifications can be studied very effectively with thermoanalytical methods which are very powerful tools for the characterization of ceramic raw materials, the production of the ceramic sintering bodies and last but not least, for assessment of the quality of the final product. By means of classical analytical methods such as thermogravimetry (TG), differential scanning calorimetry (DSC) or dilatometry, the sintering behavior and binder burnout can be studied and optimized. The Laser Flash Technique yields the thermal diffusivity values of both the green bodies and of all intermediate phases to the final product. Based on the thermal diffusivity, specific heat (e.g. obtained from DSC measurements) and density (dilatometer results), the thermal conductivity can then be calculated. With the example of ZrO<sub>2</sub> measurement results, the accompanying possibilities of Thermal Analysis based on the green body to the final ceramics are presented in this article.

**SOFC Electrolyte and Seal**

Room: Coquina Salon H

Session Chairs: Tatsumi Ishihara, Kyushu University; Prabhakar Singh, Connecticut Global Fuel Center

3:10 PM

**(ICACC-S3-026-2012) Evaluation of Approaches to Improving Long Term Stability of Solid Oxide Electrolysis Stack (Invited)**

S. Elangovan\*, J. J. Hartvigsen, F. Zhao, D. Larsen, I. Bay, Ceramtec, Inc., USA

The reverse functionality of solid oxide fuel cells (SOFC) operating as solid oxide electrolysis cells (SOEC) is an attractive feature that benefits from recent advances in SOFC technology. While such reversible operation is routinely demonstrated, certain degradation mechanisms are unique to SOEC mode of operation. The major sources of degradation are identified to be: delamination of air electrode, chromium poisoning of air electrode, and metal interconnect corrosion under high steam exposure. The choice of current distribution layer is also critical for high performance and long-term stability. In collaboration with Idaho National Laboratory under the DOE Nuclear Hydrogen Initiative and with support from the Office of Naval Research, systematic evaluation of various materials was undertaken to address the stability issues. Significant reduction in degradation rate has been achieved by the use of new electrode materials set and protective coatings on interconnects. A modified current collection layer was found to provide higher performance. An overview of recent evaluation and operational results will be presented.

3:40 PM

**(ICACC-S3-027-2012) A Techno-Economic Model of Solid Oxide Electrolysis Systems for H<sub>2</sub> or Syngas Production**

J. J. Hartvigsen\*, S. Elangovan, D. Milobar, Ceramtec, Inc., USA

Solid oxide electrolysis cells (SOEC) offer an efficient route for production of hydrogen and syngas from electric power. Employing CO<sub>2</sub> free power sources enables production of hydrogen for industry, transportation fuels and recycling CO<sub>2</sub> into synthetic liquid fuels, without the CO<sub>2</sub> emissions associated with conventional processes. Further, production of high value, storable and transportable fuels from intermittent renewable energy resources provides a more compatible load model than the real-time demand model of the grid, which in turn will enable a much greater reliance on clean but inter-

mittent energy sources. Efficiency, flexibility and environmental advantages are insufficient motivation for adoption of this technology. It must also be economically competitive. The specific energy requirement varies with the cell operating voltage and steam flow rate. A map of performance in operating voltage and steam flow space was developed. The performance map was extended to depict a variety of techno-economic parameters such as cost of electricity, cost of capital and cost of specific capital elements such as the SOES stack within the operating space. These cost elements were combined in an overall cost of hydrogen map, to guide both system design and operating conditions. This was not intended to be a manufacturing cost study and therefore assumed widely accepted SOFC cost target values.

4:00 PM

**(ICACC-S3-028-2012) Improved Air Electrode Materials for Solid Oxide Electrolysis Cells**

M. Keane\*, A. Verma, P. Singh, University of Connecticut, USA

High temperature steam electrolysis using solid oxide electrolysis cells (SOECs) offers high efficiency and potential for cost effective and large scale production of hydrogen. SOECs typically consist of an yttria stabilized zirconia electrolyte, perovskite air electrode, and nickel-zirconia cermet fuel electrode (Air/LSM//YSZ//Ni-ZrO<sub>2</sub>/H<sub>2</sub>-H<sub>2</sub>O) and operate at 850 °C. Degradation at the air electrode - electrolyte interface remains a major contributor to electrical performance degradation. A wide variety of tailored manganite and ferrite perovskite (bulk and composite A and B-site doped) and nickelate air electrodes have been synthesized using a citrate process and tested in symmetric half and full cell configurations. Electrolysis cells were tested at 840 °C for 100 hours under a constant voltage. Phase changes and microstructural evolution at the electrode-electrolyte interfaces have been studied using electron microscopy, energy dispersive x-ray spectroscopy, and x-ray diffraction techniques. Electrode morphology, interfacial reactions, and compound formation will be presented.

4:20 PM

**(ICACC-S3-029-2012) Compliant sealing glass for SOFC applications: electrical stability with YSZ and alumina coating under DC loading (Invited)**

Y. Chou\*, E. C. Thomsen, J. Choi, W. E. Voldrich, J. W. Stevenson, Pacific Northwest National Lab, USA

A commercial silicate based sealing glass (SCN-1) is currently evaluated as a candidate sealing glass for solid oxide fuel applications. The glass contains about 17% alkalis and remains vitreous during heat treatment, unlike the conventional sealing glass which turns into a rigid glass-ceramics after heat treatment. In this presentation we will evaluate the electrical stability in dual environments at various elevated temperatures (700, 750, and 800°C) under DC loading of 0.8V. The SCN-1 glass is used to seal two AISI441 small square coupons with or without alumina and YSZ coating. High temperature apparent electrical resistivity was monitored for 500-1000h. The results of electrical resistivity and the interfacial reaction and microstructure development under DC loading is presented and discussed. Overall the compliant glass showed good electrical stability with apparent resistivity much greater than all SOFC elements, except for the uncoated one at 800°C.

4:50 PM

**(ICACC-S3-030-2012) Viscous Sealants for Intermediate Temperature Solid Oxide Fuel Cells (Invited)**

M. O. Naylor\*, S. Misture, J. Shelby, Kazuo Inamori School of Engineering, Alfred University, USA

Several silicate based glasses were studied for application as viscous sealants for SOFCs. Several gallium and germanium containing compositions retain a large amorphous content after 1400h at 850 °C in air and remain highly amorphous at 650-750 °C. Powdered samples

of the glasses have been heat treated up to 1500h at 750 and 850 °C in air to evaluate crystallization and interactions with 8YSZ and aluminumized stainless steel. Alkali containing galliosilicate glasses are excellent glass-ceramic sealants at 850 °C, while non-alkali compositions are suited for operating temperatures near 750 °C. Viscous flow behavior of powdered samples was studied using hot-stage microscopy. Select sealants exhibit minimal interaction with 8YSZ substrates after 1500h. Less viscous glasses penetrate ~10µm into the 8YSZ grain boundaries, while more viscous compositions tend to crystallize at the interface. Initial test seals between 8YSZ and aluminumized stainless steel survive thermal cycling, suggesting that some glasses are appropriate for the SOFC application.

### 5:10 PM

#### **(ICACC-S3-031-2012) Glass-ceramic sealant in planar SOFC short stack; thermal cycle stability and chemical compatibility with stack components**

F. Smeacetto\*, M. Salvo, P. Leone, M. Santarelli, G. Ortigoza Villalba, Politecnico di Torino, Italy; M. Bindi, Edison Spa, Italy; L. C. Ajitdoss, M. Ferraris, Politecnico di Torino, Italy

The design, operation and electrical behavior of a SOFC short planar stack (based on anode-supported cells) and the performance of the glass ceramic sealant inside the stack are discussed. The time-evolution of the cell voltage was investigated with respect to chromium poisoning issues, in order to study the stability and effectiveness of the glass-ceramic (boron and barium-free silica-based) sealant; the cell open circuit voltage was demonstrated to be fully achieved (at 800°C up to 500 hours) by employing the glass ceramic sealant. The stack performance was also evaluated during thermal cycles from RT to 800°C. In order to stop chromium evaporation from the metallic interconnect a MnCoO<sub>4</sub> protective coating was applied on Crofer22APU by thermal co-evaporation technique. The compatibility between the glass-ceramic sealant and the MnCoO<sub>4</sub> protective coating, as well as their electrical behaviour is also presented and discussed. The Crofer22APU/glass-ceramic sealant/cell was submitted to post-mortem examination after the long-term stack experiment. Cross-sections of joined samples were characterized by SEM and EDS analysis, in order to evaluate thermal cycle stability and chemical compatibility of the glass-ceramic sealant with the stack components.

### 5:30 PM

#### **(ICACC-S3-032-2012) Development of Viscous Sealing Glasses for Solid Oxide Fuel Cells**

C. Kim\*, MO-SCI Corporation, USA; R. K. Brow, Missouri University of Science and Technology, USA

We have formulated and tested several glass compositions that could be used as viscous seals for Solid Oxide Fuel Cells (SOFCs). The glasses possess desirable viscosity characteristics- that is, they have softening points in the temperature range expected for SOFC operations (650-850°C), so cracks that might form in the glass on thermal cycling should reseal upon reheating through a 'viscous healing' mechanism. The new glasses have relatively low liquidus temperatures (< 800°C) and do not exhibit significant crystallization when held at SOFC operational temperatures. Excessive crystallization could change the viscous behavior and may jeopardize the viscous healing characteristics of the seal. In addition, the new glasses wet both aluminumized SS441 and NiO/YSZ substrates, forming hermetic seals. Properties of the glasses and hermetic test results will be discussed.

### 5:50 PM

#### **(ICACC-S3-033-2012) Effect of environmental exposure on the microstructural stability of two alkali barium silicate glasses**

A. Shyam\*, R. Trejo, V. García-Negrón, A. Ladouceur, M. Kirkham, D. McClurg, Z. Ladouceur, E. Lara-Curzio, Oak Ridge National Laboratory, USA

Solid oxide fuel cell (SOFC) glass seals are expected to retain their functional characteristics for at least 40,000 hours under severe oper-

ating conditions. To assess the durability of two alkali barium silicate glasses and their compatibility with SOFC-relevant materials, test specimens consisting of glass beads sintered onto alumina and 8YSZ substrates were exposed to air and a gas mixture of steam+H<sub>2</sub>+N<sub>2</sub> at 800°C for various periods of time. The effect of long-term environmental exposure (~10,000 hours) on the phase and microstructural stability of the glass and its physical, thermal and mechanical properties was investigated and the results will be reported. The evolution of microstructural features such as pores and crystalline phases that have a direct bearing on the sealing properties was documented. Models for the temporal evolution of these features were implemented and will be discussed. This work was sponsored by the US DOE - SECA Core Technology Program at Oak Ridge National Laboratory. Experimental facilities at ORNL's High Temperature Materials Laboratory User Program were used in this investigation, the HTML User Program is funded by the U. S. Department of Energy, Office of Energy Efficiency and Renewable Energy, Vehicle Technologies Program.

## S5: Next Generation Bioceramics

### **Advanced Processing of Bioceramics III**

Room: Coquina Salon C

Session Chair: Aldo Boccaccini, University of Erlangen-Nuremberg

### 1:30 PM

#### **(ICACC-S5-026-2012) Metal Matrix-Bioactive Glass Composite Coatings via Flame Spray (Invited)**

J. A. Nychka, G. M. Nelson\*, Univ of Alberta, Canada; A. G. McDonald, University of Alberta, Canada

A metal matrix-bioactive glass ceramic composite coating was produced via the flame spray deposition technique. The porous coatings, targeted for bone fixation and orthodontic devices, were made from blended powders of titanium alloy (Ti-6Al-4V) and bioactive glass (45S5). Flame spray was used to manufacture different ratios of metal matrix to ceramic powder under different deposition conditions, which resulted in different levels of porosity. Coatings were characterized using cross-sectional metallography and optical microscopy, X-ray diffraction (XRD), scanning electron microscopy (SEM), and Fourier transform infrared spectroscopy (FTIR). Bioactive response was characterized with immersion testing in simulated body fluid (SBF) up to 14 days. Hydroxyapatite (HA) was detected within 7 days immersion in SBF for composite coatings; no HA was observed after 14 days on the pure titanium alloy negative control coating. The presence of HA on the metal matrix-bioactive glass composite coating, and lack thereof on the titanium alloy control, suggests that incorporation of bioactive glass could be used to increase the bioactivity of porous metal-matrix coated implants, and potentially shorten tissue integration times.

### 2:00 PM

#### **(ICACC-S5-027-2012) Composite materials with biomimetic apatite matrix for bone substitution (Invited)**

D. Grossin, F. Brouillet\*, C. Rey, CIRIMAT Carnot institut (Toulouse university), France

The purpose of this study was to elaborate and characterize composite materials for bone substitution with improved mechanical properties. These materials were made of bioceramic matrices reinforced with fibrous polymeric particles. A non conventional technique, spark plasma sintering (SPS), was used to consolidate this new biomaterial at very low temperature(150°C). The composite is constituted of a biomimetic apatite, a highly bioactive mineral, associated with Micro-crystalline Cellulose (MCC) a natural polymer with low chemical reactivity, high compressibility and high thermal resistance. The effect of MCC/apatite ratio (0-20% w/w) was investigated and related to physico-chemical and mechanical properties. Samples obtained by SPS were characterized by various techniques such as FTIR, XRD, SEM. Brazilian test

was used to determine the tensile strength of the material. The similar particle size (100  $\mu\text{m}$ ) of the two compounds favoured a homogeneous mixing which was preserved after consolidation. Indeed the composite appeared as a dense material containing dispersed and oriented aggregates of MCC. The various physico-chemical analyses on the composite material showed a preservation of the interesting characteristics of the biomimetic apatite. An important improvement of the tensile strength of the innovative composite material was obtained with the increase of the polymer weight fraction.

### 2:30 PM

#### (ICACC-S5-028-2012) Fracture Origins in a High Strength Dental Porcelain

G. Quinn\*, American Dental Association foundation, USA; K. Hoffman, American Dental Association foundation, USA; J. Quinn, American Dental Association foundation, USA

Fractographic analysis of dental porcelains is often difficult due to the coarse microstructure and resulting roughness of the fracture surfaces. Previous studies with lab scale test coupons have identified occasional large pores or contact damage sites as fracture origins. Systematic identifications of fracture origins in test specimens are rare. In this study, we found and characterized every fracture origin in twenty-six high-strength Vita Mark II feldspathic porcelain bend bars. The results were correlated to the microstructure which had no less than five crystalline phases. Multiple flaw types were present and a fractographically labeled Weibull plot was prepared. We found: baseline microstructural feature (BMF) flaws, pore-bubbles, inclusions, and two types of grinding flaws. The flaws were correlated with the overall Weibull distribution which had a moderate Weibull modulus of 18.0 (90% confidence interval: 13.1 – 22.2). One unique new flaw type was a subset of spherical pores. Isolated pores in the interior, no matter how large, were harmless and did not cause fracture. In contrast, the ones that touched an exposed outer surface or were near to another pore-bubble were strength limiting flaws. This poses an interesting dilemma for reliability analysis: volume-distributed pore flaws can be strength limiting, but only if they touch a free surface or another pore.

### 2:50 PM

#### (ICACC-S5-029-2012) Cellular response to ionic dissolution products from bioactive glasses and glass-ceramics (Invited)

A. R. Boccaccini\*, A. Hoppe, University of Erlangen-Nuremberg, Germany

Bioactive glasses, e.g. 45S5 Bioglass, have been shown to exhibit stimulating effects on osteogenesis and angiogenesis. The exact mechanism of interaction between the ionic dissolution products of such inorganic materials and human cells are not fully understood, which has led to a large number of studies published in literature during the last decade investigating the effect of dissolution products of silicate bioactive glasses (BGs) and glass-ceramics related to osteogenesis and angiogenesis. More recently several advances made in fabricating silicate scaffolds doped with trace elements (e.g. Sr) and investigations on the effect of these elements on the scaffold biological performance have confirmed the enhancement of bioactivity of materials in the context of tissue engineering including, for instance, Sr-doped BGs showing increased osteoblast activity. The greater understanding of molecular mechanisms and chemical pathways dictating the interaction between materials and cells will allow the design of tissue specific scaffolds with tailored chemistry, surface topography, porosity and ion release kinetics, leading to the desired biological effect and new tissue regeneration. This presentation will give an overview of the biological response to ionic dissolution products released from bioactive glasses and glass-ceramics highlighting the areas requiring for further investigations.

## Advanced Processing of Bioceramics IV

Room: Coquina Salon C

Session Chair: Steven Jung, Mo-Sci Corporation

### 3:30 PM

#### (ICACC-S5-030-2012) Fabrication of custom specific dental crown through green stage machining of ceramics

S. Mohanty, S. Dhara\*, IIT Kharagpur, India

The manufacturing of biomedical implants is always a challenging task owing to their variation in size and shapes for one off custom specified product. Closer fitness of the implants is always the prior requirement to achieve higher success rate in clinics. Artificial denture is one such component where size and shape variation is always evident from one to another even for same patient. With the advent of modern technology, higher consumption of processed food is leading to high occurrence of dental carries and gingivitis, which requires removal/replacement of dentures. For fabrication of dental crown, various materials are like glass, ceramics, porcelain and acrylic polymers/resins are used. Direct molding technique may not work for ceramics/glass based crown due to associated shrinkage during sintering. Direct machining of ceramics in to exact size and shape may be preferred choice using CAD/CAM for custom specified product like dental crown. Machining of sintered ceramics is always challenging due to their high hardness and low fracture toughness. Present study proposes top down green stage machining of ceramics for development of dental crown using model image of 3D laser scanned data for custom specific product. The machined and sintered ceramics are characterized for surface quality, anisotropic shrinkage, mechanical strength and microstructure as well.

### 3:50 PM

#### (ICACC-S5-031-2012) Heterogeneous structure of hydroxyapatite and in vitro degradability (Invited)

S. Hayakawa\*, T. Ohiwa, Y. Shirosaki, A. Osaka, Okayama University, Japan; J. Christian, BAM, Germany

It is well known that hydroxyapatite (HAp) decomposes by heat-treatment, accompanied by forming partially dehydrated oxyhydroxyapatite, or forming tricalcium phosphate ( $\alpha$ -TCP), and then decomposed HAp has a disordered structure. However, it is not clear how the disordered structure of HAp influences biodegradability. In this study, HAp sample was synthesized by various processing method such as solid-state reaction and hydrothermal reaction, and was characterized in terms of their chemical composition, apatite lattice defects and in vitro biodegradability. XRD revealed that the prepared samples composed of single phase HAp. On the other hand, 1D and 2D solid-state NMR analysis showed that the prepared HAp sample consisted of not only crystalline HAp but also disordered phase. The in vitro biodegradability was discussed by using a novel structure model for nano-crystalline HAp, in which the nano-crystals consist of a crystalline HAp core covered with a disordered surface layer (core-shell model) proposed by Jäger et al.

### 4:10 PM

#### (ICACC-S5-024-2012) Carbonate Apatite Formation During The Setting Reaction of Apatite Cement

A. Cahyanto\*, I. Artilia, K. Tsuru, K. Ishikawa, Faculty of Dental Science, Kyushu University, Japan

Mechanism of the replacement of apatite cement (AC) to bone has not fully been understood. Some researchers claimed that AC was replaced to bone, while others said there was no replacement at all. Since AC shows good osteoconductivity, the key may be resorption of AC by osteoclasts. Also, the different observations to the replacement of AC to bone may be caused by the different setting condition up to the clinical cases. One of the factors may be the formation of carbonate apatite ( $\text{CO}_3\text{Ap}$ ) on its surface. We have reported that  $\text{CO}_3\text{Ap}$  was easily replaced to bone. There may be a chance that AC might convert

to CO<sub>3</sub>Ap in the body environment even if AC is free from carbonate. The aim of this study was to investigate whether or not carbonation process occurred in AC. As an AC, equimolar mixture of tetracalcium phosphate and dicalcium phosphate anhydrous was employed. After mixing with water, the paste was allowed to harden in the presence and absence of CO<sub>2</sub> at 37°C and 100% humidity. B-type CO<sub>3</sub>Ap was found when allowed to set under CO<sub>2</sub> atmosphere. The CO<sub>3</sub><sup>2-</sup> content gradually decreased with the depth from the cement surface. We concluded therefore that CO<sub>3</sub>Ap formation in AC may relate to the replacement of AC to bone.

### 4:30 PM

#### (ICACC-S5-033-2012) Potential Toxicity of Bioactive Borate Glasses In-vitro and In-vivo (Invited)

S. Jung\*, Mo-Sci Corporation, USA; R. Brown, Missouri University of Science and Technology, USA; L. Bonewald, University of Missouri - Kansas City, USA; D. Day, Missouri University of Science and Technology, USA

Potential toxicity of a bioactive borate glass was evaluated using in-vivo animal models in soft tissue and bone and in-vitro cell culture using MLOA5 late osteoblast/early osteocytes cells. No toxicity was found between bioactive borate glass and subcutaneous tissue, in the liver, and only normal incidental changes in rat kidney. Bone growth across porous scaffolds composed of randomly oriented borate glass fibers was significantly higher than for a scaffold composed of a borosilicate or a silicate bioactive glass (13-93) fibers after 12 weeks in-vivo,  $p < 0.05$ . In-vitro cell culture on bioactive glasses showed that under static culture conditions, borate glass disks tended to inhibit the growth of MLOA5 cells, but when the disks were pre-reacted (in culture medium or a dilute phosphate solution) the cell proliferation is significantly increased to levels similar to 45S5 bioactive glass. The present work, along with literature data, show that bioactive borate glasses are biocompatible in-vivo and are not toxic to adjacent hard or soft tissues, or internal organs such as the kidney and liver, at the relatively high, estimated concentrations ( $\sim 126\text{mg/kg/day}$ ). Based on the present results and literature data, boron released from the borate glasses was not toxic in a dynamic environment such as the body and should be considered for use in humans and other mammals for soft and hard tissue engineering applications.

### 4:50 PM

#### (ICACC-S5-034-2012) Investigation of the local environment of cations in apatites and bone

D. Laurencin\*, Université Montpellier 2, France; M. E. Smith, University of Warwick, United Kingdom; F. Fayon, UPR3079 CNRS, France; N. de Leeuw, University College London, United Kingdom; C. Gervais, C. Bonhomme, Université Pierre et Marie Curie, France

In order to fully understand the structure and functionalities of bone, it is necessary to analyze the local environment of the cations present in the material, such as calcium, which is the most abundant, and sodium and magnesium, which are trace elements of biological importance. Determining the structural role of these ions is not straightforward, and despite the numerous studies of bone mineral, very few investigations on the local environment of cations have been reported so far. Here, it will be shown how solid state NMR is well adapted to the study of cationic environments in bone: - concerning calcium, results of natural abundance <sup>43</sup>Ca solid state NMR experiments of equine bone and bovine tooth samples will be presented and compared to Ca K-edge X-ray absorption spectroscopy analyses, in order to show how they can inform on the calcium coordination shell. - in the case of sodium, high resolution <sup>23</sup>Na solid state NMR studies will be presented, which bring the first direct evidence that some sodium is located inside the apatite phase in bone. - concerning magnesium, it will be shown that the combination of multinuclear solid state NMR and computational modeling can inform on the location of Mg in the apatite phase. For each cation, we will emphasize how to interpret the NMR data and how to best perform the experiments.

### 5:10 PM

#### (ICACC-S5-035-2012) Preparation of Magnesium-containing TiO<sub>2</sub> Ceramic Layer on Titanium by Hydrothermal Treatment and its in vitro Bioactivity

X. Shi\*, M. Nakagawa, A. Valanezhad, K. Tsuru, K. Ishikawa, Faculty of Dental Science, Kyushu University, Japan

Surface modification on titanium was carried out in order to improve its bioactivity. Pure titanium was hydrothermally treated in 0.1 mol/L MgCl<sub>2</sub> solutions with pH 5.5, 7.5 and 9.5, at 200°C for 24 h. Surface morphology, roughness, wettability and chemical composition were characterized before and after treatment. Simulated body fluid (SBF) was employed to examine apatite forming ability. MC3T3-E1 cells were cultured and initial cell attachment, morphology, and proliferation were evaluated. After hydrothermal treatment, nano-sized precipitations were observed and these surfaces showed superhydrophilicity. Ti-O-Mg bond was formed on titanium surface and high pH benefited the combination of Mg. Apatite spheres were observed on hydrothermally treated samples after immersion in SBF for 2 days. Hydrothermal treatment in MgCl<sub>2</sub> solution improved initial cell attachment, but cell adhesion was reduced on high Mg-containing Ti. Cell spreading was obviously enhanced on Mg-containing samples compared with untreated or those treated in distilled water. Proliferation results showed hydrothermal treatment in MgCl<sub>2</sub> solution accelerated multiplication of cells on titanium surface. The hydrothermal treatment in MgCl<sub>2</sub> solution was expected to be an effective method to fabricate titanium implant with good bioactivity.

## S10: Thermal Management Materials and Technologies

### Characterization of Thermal Management Materials

Room: Coquina Salon B

Session Chair: Andrew Gyekenyesi, OAI/NASA GRC

### 1:30 PM

#### (ICACC-S10-001-2012) Modeling Thermal Mechanical Properties of TPS (Thermal Protection Systems) and Porous Ceramics with a novel 3D X-ray Microscope

S. H. Lau\*, Xradia, Inc., USA; T. H. Squire, J. W. Lawson, Nasa Ames Research Center, USA

Thermal mechanical properties of C fiber based ceramics such as advanced TPS materials can be traced, in part, to the internal microstructure of the material. Finite element analysis (FEA) of these microstructures can lead to better understanding of material performance and help define the most advantageous direction for further material development for improved performance. There are two general approaches to developing FEA models for material microstructures. The first is to construct idealized finite element meshes using regular patterns of grains or fibers based on assumed geometry of the microstructure. We utilize the second approach, which is to use 3D images of the actual microstructure of the PICA (Phenolic impregnated carbon ablator), a state of art, light weight heat shield material developed by NASA, and measured directly and non invasively with a novel lab based x-ray microscope @ tomography resolution of 0.5 micron pixel, enhanced with phase contrast. 3D FEA mesh was superimposed over the tomography images and transient, thermal analyses performed. Analysis of the 3-D model of the TPS material shows how the non-uniform distribution of the carbon fibers affects the conduction of energy through the material. Applications of x-ray microscopy in Ultra High Temp Ceramics; for porosity and in situ characterization will also be discussed.

### 1:50 PM

#### (ICACC-S10-002-2012) Measurement of Thermal Conductivity of Graphitic Foams

K. Alam\*, K. Drummond, Ohio University, USA

Highly conductive graphitic foams are currently being studied for heat sink and thermal storage applications. This paper describes the

experimental research at Ohio University to determine the thermal conductivity of graphitic carbon foam. The standard methods for determination of thermal conductivity generally work well for solid materials, but these methods may produce significant errors with graphitic foams because of convection and interface resistance. Therefore, a method has been developed in which the open celled graphitic foam is infiltrated by a low conductivity polymer. The resulting composite is a dense solid that can be measured accurately by classical methods. It is shown that the presence of the polymer has negligible effect on the thermal conductivity of the graphitic foam; therefore, the bulk conductivity of the foam is well approximated by the conductivity of the infiltrated foam.

### 2:10 PM

#### (ICACC-S10-003-2012) Potential of Black Alumina Coatings: Effect of Thickness on Thermal behaviors

H. Kakisawa\*, M. Yamazoe, Y. Kagawa, The University of Tokyo, Japan

Black polycrystalline alumina has been developed to change thermal properties of white alumina. The black alumina is heated rapidly and is cooled slowly compared with white alumina. The thermal behavior difference is also dependent on thickness. In the present study, temperature-time relations during heating and cooling of the black alumina are measured under quasi-steady state cooling and unsteady state cooling processes. The results confirm that a cooling rate of the black alumina is lower than that of white alumina. The rate also depends on the thickness of the black alumina. Discussions are made to explain the unique thermal behavior of the black alumina from coating application points.

### 2:30 PM

#### (ICACC-S10-004-2012) Thermal Conductivity of Wood-Derived Graphitic Carbon and Carbon/Copper Composites

M. Johnson\*, K. Faber, Northwestern University, USA; H. Wang, Oak Ridge National Lab, USA

The thermal conductivity of porous graphite and graphite/copper composites is of great interest in thermal management applications. Factors such as pore volume, distribution, and composite structure strongly affect thermal properties. Samples for this study are prepared using wood pyrolysis and copper electrodeposition techniques and thermal conductivities are measured via the laser-flash technique. Wood, possessing a naturally optimized, anisotropic honeycomb-like microstructure, offers a unique porous precursor, which may be pyrolyzed to yield a graphitic scaffold with a microstructure replicating that of the original wood. Composite structures are fabricated via electrodeposition, a room temperature method for infiltrating copper into very high aspect ratio porosity without damaging the porous carbon scaffold structure. While methods exist to model properties, such as thermal conductivity, in multi-phase systems, the use of natural materials with naturally varying microstructures increases the complexity of such analysis. Modeling techniques, including finite element methods, are used to evaluate the effects of porosity and pore size distribution on the thermal conductivity of the carbon scaffold and results are compared to experimentally determined values. Composite materials are similarly evaluated based upon copper fraction and connectivity.

### Processing and Integration Strategies for Thermal Management Materials

Room: Coquina Salon B

Session Chair: Andrew Gyekenyesi, OAI/NASA GRC

### 3:10 PM

#### (ICACC-S10-005-2012) Bonding Ceramic Parts for High Temperature Applications using Pre-ceramic Polymer based Adhesives

H. Chen\*, T. A. Parthasarathy, M. K. Cinibulk, M. Chen, AFRL, USA

Pre-ceramic polymer based adhesives were developed for bonding ceramic composite sheets to ceramic foams as part of a hybrid ther-

mal protection system. The adhesives were prepared by dispersing ceramic particles and/or active metal compounds in three types of pre-ceramic polymers. After curing and pyrolysis, the adhesive converts to a solid ceramic bond layer between the composite and the foam. The transition of the adhesives during curing and pyrolysis were characterized using TGA, XRD, and SEM. X-Ray CT was utilized to observe defects within the bond layer and at the interfaces. The bond strength was evaluated using a tensile test method. Surface properties, adhesive formulations, curing and pyrolysis conditions were studied for their effects on the microstructure of the bond layer and bond strength. The objective is to identify an adhesive and a process that will produce a strong bond between ceramic composite and foam for high temperature applications. This work was partially supported through the U.S. Air Force Contract FA8650-10-D-5226.

### 3:30 PM

#### (ICACC-S10-006-2012) Bonding High Conductivity Graphite Foams to Metals for Thermal Management Applications

R. Asthana\*, University of Wisconsin-Stout, USA; M. Singh, C. E. Smith, A. L. Gyekenyesi, Ohio Aerospace Institute, USA

High-conductivity graphite foams (density: 100 to 800 kg.m<sup>-3</sup>) were vacuum brazed to titanium, copper-clad-molybdenum, Inconel-625, and 430 stainless steel using conductive Ag-Cu-Ti and Ag-Cu-Pd braze alloys. The brazed joints were characterized using optical microscopy (OM), scanning electron microscopy (SEM), energy dispersive spectroscopy (EDS), and mechanical testing. Both types of brazes yielded microstructurally sound joints that exhibited braze penetration into the porous foam as well as interface enrichment with Ti (notably in joints made using Ag-Cu-Ti brazes). In the case of Inconel-625 and 430 stainless steel, chromium enrichments at the foam surface were observed. Tension test on the foam/Ti joints made using Ag-Cu-Ti braze alloys revealed that the brazed joints had sufficient strength so that failure always occurred in the foam away from the braze. This behavior was true for both low- and high density foam joints. Steady-state heat conduction calculations of thermal resistance reveal the potential for use of foam/metal joints in light-weight thermal management applications such as avionic heat sinks and heat exchangers.

### 3:50 PM

#### (ICACC-S10-007-2012) Fabrication and thermal properties of diamond-copper composite produced by the pulse plasma sintering technique (PPS)

M. Rosinski\*, L. Ciupinski, A. Michalski, K. J. Kurzydowski, Warsaw University of Technology, Poland

Miniaturization of micro-electronic devices leads to a considerable increase of heat dissipated by electronic circuits. To increase further the packing density of micro-electronic circuits, new materials with better heat conductivity are required. Another requirement is that these materials should have a thermal expansion coefficient comparable with that of the microelectronic substrate material. Among known materials, the best heat conductivity is shown by diamond. In the form of CVD-produced layers, diamond is used for substrates in micro-electronic devices, but in this application it has a drawback in that its thermal expansion coefficient greatly differs from that of semiconductor materials. Materials which are expected to combine a high thermal conductivity with a thermal expansion coefficient close to that of semiconductor materials are Cu/diamond composites. The thermal conductivity and expansion coefficient of these composites can be easily controlled by modifying their composition. However, it is known, that there is a very weak bonding between diamond particles and pure copper matrix in the consolidated composite. Improvements in properties of the composite was achieved by using PPS method and copper with carbide-forming elements to increase the interfacial bonding between Cu matrix and diamond particles.

4:10 PM

### (ICACC-S10-008-2012) Improving the heat transfer efficiency of synthetic oil with silica nanoparticles

E. V. Timofeeva\*, M. R. Moravek, D. Singh, Argonne National Laboratory, USA

The introduction of nano-sized particles to heat transfer fluids (nanofluids) is an emerging thermal management concept with implications in many disciplines including power generation, transportation, microelectronics, chemical engineering, aerospace and manufacturing. In this study we assess the possible benefits of adding silicon dioxide nanoparticles and surfactant to an aromatic high temperature heat transfer fluid. The heat transfer properties of synthetic oil (Therminol 66) used for high temperature applications (150°C to 400°C) are shown to improve by introducing 15 nm silicon dioxide nanoparticles. Stable suspensions of inorganic nanoparticle in the non-polar fluid are achieved with using cationic surfactants. The approaches to stabilization of silica nanoparticle suspensions in synthetic oils presented here can also be used to stabilize silica coated core/shell multifunctional nanoparticles, which exhibit great potential for future nanotechnologies. The effects of nanoparticle and surfactant concentrations on viscosity, thermal conductivity and total heat absorption of these nanofluids are studied in a wide temperature range. The experimental data are used to estimate the heat transfer efficiency for both turbulent and laminar flow regimes and to guide the optimization of the nanofluid composition for a better heat transfer performance.

4:30 PM

### (ICACC-S10-009-2012) Using Science to Improve Upon Nature: Why Engineered Thermal Transfer and Thermal Management Media Out Perform Natural Materials

T. Szymanski\*, Saint-Gobain NorPro, USA

Several industrial processes that require a ceramic media either to transfer or manage thermal energy have been recently developed. Natural materials such as gravel and silica sand are typical choices because they are relatively common, easy to obtain and inexpensive. Despite these attributes it is often not the best option for either thermal transfer or thermal management. By comparison, engineered ceramic media can be designed to optimize specific properties such as attrition, density, particle size, sphericity and operating temperature range which can greatly improve process performance. This paper will present some typical uses for ceramic heat transfer and thermal management media. It will also compare and contrast the physical, chemical and thermal management properties of engineered various ceramic media with natural materials such as gravel and sand.

## S11: Nanomaterials for Sensing Applications: From Fundamentals to Device Integration

### Sensing Devices II

Room: Oceanview

Session Chair: Francisco Hernandez-Ramirez, Catalonia Institute for Energy Research

1:30 PM

### (ICACC-S11-009-2012) Sensors and Catalysts in Automotive Exhaust Gas Aftertreatment - an Overview on recent developments and research trends (Invited)

R. Moos\*, Bayreuth Engine Research Center (BERC), Germany

Steadily increasing emission standards for both passenger cars and heavy duty vehicles combined with the need for fuel efficiency lead to novel powertrain concepts like the leanly operated gasoline direct injection engine, or to novel exhaust gas aftertreatment concepts like NO<sub>x</sub> storage catalysts, ammonia SCR NO<sub>x</sub> reduction, or even to a combination of both. Also, soot filters are in series production. In order to control the novel powertrain and/or exhaust gas aftertreatment systems and to monitor on-board the proper operation of these

systems (on-board diagnosis, OBD), novel exhaust gas sensors are required or would at least be very helpful. This presentation gives an overview on the technology and the status of catalysts and sensors for automotive exhaust gas aftertreatment systems. Additionally, a very novel concept is presented. Here, the catalyst itself works as a sensing device that gives directly information on its status. It will be shown that this allows to detect the oxygen loading degree of TWC very clearly, the ammonia loading of SCR catalysts, and the soot loading of DPF. As a conclusion, these novel methods may provide a future alternative for low emission-aiming engine control as well as for on-board diagnosis (OBD) of low emission vehicles with novel exhaust gas aftertreatment systems.

2:00 PM

### (ICACC-S11-010-2012) Improvement of NO<sub>2</sub>-Sensing with Cr-Doped TiO<sub>2</sub>-Nanotubular Sensor Electrodes

B. Saruhan-Brings\*, Y. Gönüllü, German Aerospace Center, Germany

High-temperature processes involving combustion in airplanes, power plants, vehicles and industrial settlements are among the main reasons for pollution. NO<sub>x</sub> is one of the greenhouse pollutants and produced during combustion processes, independent of the fuel quality. Gas sensors are extensively used for the precise determination of the quantity and chemistry of emission for the control of combustion processes. Pure titania is used widely for CO and H<sub>2</sub>-sensing. It behaves as p- or n-type semiconductor, by introducing a dopant into TiO<sub>2</sub> lattice or by phase change. Cr-doping of titania is reported to be effective for NO<sub>2</sub>-sensing. Moreover, it is known that the use of one-dimensional structures yields more than 2-fold increase in sensing efficiency. This has been proven for H<sub>2</sub>-sensing by other works. The present work reports the synthesis of Cr-doped aligned nano-tubular TiO<sub>2</sub>-layers by template-free anodisation in F<sup>-</sup> ions containing ethylene glycol-based electrolyte. The doping with chromium was carried out by wet-chemistry method. On heat-treatment at temperatures up to 700°C, the titania films were converted to rutile. The sensor performance of the nano-tubular TiO<sub>2</sub> sensors were investigated at temperatures up to 500°C for NO<sub>2</sub> concentrations varying from 10 to 50 ppm and CO concentrations from 25 to 75 ppm. Cr-doped nanotubular TiO<sub>2</sub> sensors were highly NO<sub>2</sub>-selective even at a temperature of 500°C.

2:20 PM

### (ICACC-S11-011-2012) Effect of Ion-Implantation on the Binding Energy, Electronic and Chemical States in ZnO nanorods

I. J. Low\*, Curtin University, Australia; A. Djuricic, University of Hong Kong, Hong Kong; M. Ionescu, Australian Nuclear Science & Technology Organisation, Australia

Zinc oxide has great potential for a variety of practical applications such as piezoelectric transducers, optical waveguides, UV-light emitters, varistors, phosphors, chemical and gas sensors. Its wide bandgap (3.37 eV) makes ZnO a promising material for photonic applications in the UV or blue spectral range, while the high exciton-binding energy (60 meV) allows efficient excitonic emission even at room temperature. In addition, ZnO doped with transition metals shows great promise for spintronic applications. However, modified ZnO with narrower band gap can be developed so that they are active under visible light irradiation. Ion-implantation has now emerged as an alternative but effective method to improve the separation of the photo-generated electron-hole pairs or to extend the wavelength range of the ZnO photo-responses into the visible region. In this paper, we describe the use of synchrotron x-ray photoelectron spectroscopy to investigate the effect of ion-implantation (In & Sb) on the binding energy, chemical and electronic states in ZnO nanorods. Depth-profiling of phase composition at the near surface ion-implanted ZnO will be evaluated using ion-beam analysis, Rutherford Back-Scattering and grazing-incidence synchrotron radiation diffraction.



2:40 PM

**(ICACC-S11-012-2012) SWAP: a wireless and power-autonomous new generation sensor node**

J. Llosa, X. Vilajosana, I. Vilajosana\*, WorldSensing, S.L.N.E., Spain; J. Prades, Universitat de Barcelona, Spain

Considerable research efforts have been recently directed towards low profile, low power, energy efficient and self-sustainable sensor networks aiming to harvest ambient energy from vibrations, as well as solar and thermal energy. SWAP offers a new generation sensor node based on the state of the art microelectronic components. SWAP combines the energy-efficient paradigm of wireless sensor networks with the self-sustainable capabilities of harvesting systems. SWAP provides a novel sensor board consisting of i) a high efficiency RF transceiver, ii) a low power, high performance micro controller, iii) an energy accumulator and iv) modular harvesting systems. Achieving a good tradeoff between computational power and power consumption is the main challenge. The increased performance of the new processors combined with strategies to reduce power consumption such as hardware support for time sync, designing very efficient power regulation stages, reducing operation voltage and optimizing battery drain offers outstanding computing capabilities keeping power consumption small and computational performance high. Finally, different harvesting modules will be adapted to the new sensor platform in order to offer a completely autonomous solution for new class of sensing apps, for instance, Thus dealing with environmental monitoring or urban sensor networks under the framework of the smart cities trends.

## **S12: Materials for Extreme Environments: Ultrahigh Temperature Ceramics (UHTCs) and Nanolaminated Ternary Carbides and Nitrides (MAX Phases)**

### **Design of New Compositions/Composites with Fascinating Properties**

Room: Coquina Salon F

Session Chairs: Michel Barsoum, Drexel University; Laura Silvestroni, CNR-ISTEC

1:30 PM

**(ICACC-S12-037-2012) Mechanical Properties of ZrB<sub>2</sub> Ceramics: Performance Improvements (Invited)**

Y. Kagawa\*, The University of Tokyo, Japan; S. Guo, National Institute for Materials Science, Japan

Mechanical properties of ZrB<sub>2</sub> material with addition of SiC, ZrSi<sub>2</sub>, MoSi<sub>2</sub> etc. have been studied. Especially, the effects of the shape and size of the additive particles, grain size on strength and fracture toughness are examined experimentally. The results show possibility of improving both the properties, however, the toughness is still lower and needs improvement; in addition to prevent catastrophic failure is important for practical ultra-high temperature applications. The measured fracture toughness is discussed in terms of available toughening mechanisms. To prevent catastrophic failure of ZrB<sub>2</sub>, continuous SiC fiber is incorporated in to ZrB<sub>2</sub> matrix. Failure behavior of the SiC fiber-ZrB<sub>2</sub> matrix composites is examined and the result shows improvement of the catastrophic failure, the improvement of initial cracking stress is not significant due to thermal stress caused by the mismatch of thermal expansion coefficient between the fiber and matrix. Discussions will be made the way to improve strength, toughness and failure behavior of the continuous SiC fiber-ZrB<sub>2</sub> matrix composites.

1:50 PM

**(ICACC-S12-038-2012) Processing of ZrB<sub>2</sub>-SiC Matrix/SiC Fiber Composites by Means of Polymer Impregnation and Pyrolysis**

B. J. Lai\*, J. Watts, G. Hilmas, W. G. Fahrenholtz, Missouri University of Science &amp; Technology, USA

Ceramic matrix composites (CMCs) based on a zirconium diboride (ZrB<sub>2</sub>) – silicon carbide (SiC) matrix reinforced with SiC fibers were

prepared utilizing a novel combination of processing methods. Specifically, tape casting along with polymeric precursor impregnation and pyrolysis (PIP) were investigated. A standard colloidal processing technique was used for preparation of ZrB<sub>2</sub>-based tape casting slurries, which contained various sintering additives to allow for densification at temperatures in the range of 1400 to 1650°C. Previous studies have made use of SiC precursors to form SiC-based matrices with repeated PIP infiltrations to improve matrix densities and permit control of fine grain size to enhance mechanical behavior. This study focused on fabrication of fiber-reinforced ceramic matrix composites processed with an allylhydridopolycarbosilane polymeric SiC precursor while minimizing successive infiltrations. Specimens were prepared by lamination of alternatively stacked tape cast ZrB<sub>2</sub> layers and slurry-infiltrated SiC fiber preforms; specimens then underwent a number of PIP cycles prior to the final densification temperature. Mechanical performance was evaluated by flexural testing to determine strength, modulus, and work of fracture. Microstructural analysis was also conducted to determine fiber-matrix interaction.

2:10 PM

**(ICACC-S12-039-2012) Mechanical Properties and Characterization of a Heat Treated ZrB<sub>2</sub>-SiC Composite**

E. W. Neuman\*, G. Hilmas, W. Fahrenholtz, Missouri University of S &amp; T, USA

Mechanical properties of hot pressed, heat treated zirconium diboride – silicon carbide (ZrB<sub>2</sub>-SiC) composites were tested at room and elevated temperatures. ZrB<sub>2</sub>-SiC composites with 30vol% SiC as a dispersed particulate phase were hot pressed to full density at 1950°C under an applied pressure of 32MPa in a flowing argon atmosphere. The hot pressed billets were machined to ASTM standard test bars with the tensile surface polished to 1µm. The test bars were heat treated at temperatures in the 1300 to 1600°C range for times up to 100 hours in an argon atmosphere. Four-point bend strengths were measured for the as processed and heat treated bars from room temperature to 1600°C, in air. A 40% increase in retained strength at 1600°C was demonstrated for samples heat treated at 1500°C for 10 hours compared to the as processed material. No additional discrete phases were identified using X-ray diffraction and energy dispersive spectroscopy. Amorphous grain boundary films and triple points containing increased oxygen and carbon content were identified in both the as processed and heat treated samples. Residual strain was measured in the ZrB<sub>2</sub> and SiC grains, and stacking fault density measured for the SiC grains.

2:30 PM

**(ICACC-S12-040-2012) Polyureasilazane Based SiC/ZrB<sub>2</sub>-SiC Fiber Reinforced Ceramic Composites**

J. Nicholas\*, V. Menta, K. Chandrashekhara, J. Watts, B. Lai, G. Hilmas, W. Fahrenholtz, Missouri University of Science and Technology, USA

Monolithic ceramic materials have been commonly used in ultra-high temperature applications. However, these materials are brittle and fail catastrophically. Continuous fiber reinforced ceramic composites (CFCCs) offer substantial improvements in damage tolerance over monolithic ceramic materials. In the present work, SiC fiber reinforced ZrB<sub>2</sub>-SiC composites have been fabricated using polymer infiltration and pyrolysis (PIP) process. Polyureasilazane (PURS), a low cost polymer derived ceramic (PDC) precursor was used for the SiC portion of the ceramic matrix. PDCs are a new class of materials that behave like polymers at low temperatures and transform into ceramic materials upon heating to high temperatures. The use of PDCs allowed for composite processing via a low cost vacuum bagging approach. Plain weave Nicalon SiC fibers were used as the reinforcing phase. The PURS resin system was loaded with different amounts of ZrB<sub>2</sub> to achieve the ultra-high temperature requirements. The challenges involved with manufacturing are addressed and presented in the paper. The microstructures of the panels were investigated by scanning electron microscopy (SEM). Mechanical tests were conducted to evaluate the performance of the composites. Results show

that low cost PURS ceramics are promising materials for ultra-high temperature applications.

**2:50 PM**

### (ICACC-S12-041-2012) Synthesis of Nano-Hafnium Diboride Powder using a Modified Spark Plasma Sintering Method

S. Lee\*, KIMS, Republic of Korea; H. Wang, Zhengzhou Univ., China; H. Kim, KIMS, Republic of Korea

Nano-hafnium diboride powder was synthesized by boro/carborthermal reduction process of HfO<sub>2</sub> using a spark plasma sintering (SPS) apparatus. The synthesis was performed at 1400 - 1500°C under vacuum. The as synthesized HfB<sub>2</sub> agglomerates were 1 - 2 micrometer in size, but they were composed with small primary particles. After milling for 2 hours using spex mill, the agglomerates were easily pulverized into nano-HfB<sub>2</sub> particles having average size of about 100 nm. The size of starting materials played an important role to produce the nano-boride powder. In addition, the grain growth of HfB<sub>2</sub> could be effectively suppressed by using a modified SPS method due to the fast heating rate. The synthesized boride powder had low oxygen content (0.66 wt %).

**3:10 PM**

### (ICACC-S12-042-2012) In situ synthesis mechanism and characterization of ultra-high temperature ceramics

A. Goodarzi\*, Amirkabir University of Tech., Islamic Republic of Iran; H. Taylor, Imperial College London, United Kingdom

The synthesis route, microstructure and properties of ZrB<sub>2</sub>-ZrC-SiC composites prepared from a mixture of Zr-B<sub>4</sub>C-Si powders by in situ reactive synthesis were investigated. The reactive path and synthesized mechanism of ZrB<sub>2</sub>-ZrC-SiC composite were studied through series of pressure-less heat treatments ranging from 800 °C to 1700 °C in argon. The in situ ZrB<sub>2</sub>-ZrC-SiC composites were fabricated under different synthesis processing. The one with 88.4% relative density performed poorly in mechanical properties due to the occurring of self-propagating high-temperature synthesis (SHS). The fully dense ZrB<sub>2</sub>-ZrC-SiC composite was obtained under the optimized synthesis processing without SHS reactions. Its Vickers hardness, flexural strength and fracture toughness were 20.22±0.56 GPa, 526±9 MPa and 6.70±0.20MPa<sup>1/2</sup>, respectively. This work reported in situ synthesis mechanism, microstructure and mechanical properties of ZrB<sub>2</sub>-ZrC-SiC composite synthesized with the mixture of Zr, B<sub>4</sub>C and Si powders. The reaction of Zr-B<sub>4</sub>C-Si powders commenced at 800°C and non-stoichiometric ZrC<sub>1-X</sub> formed preferentially, followed by the solution of B elements in Zr particles and then transformed to ZrB<sub>2</sub> later around 900°C.

## Fundamental Understanding and Novel Processing Methods

Room: Coquina Salon F

Session Chairs: Takuya Aoki, Japan Aerospace Exploration Agency; John Lawson, NASA Ames Research Center

**3:30 PM**

### (ICACC-S12-043-2012) Hardness measurements above 1723 K (Invited)

L. J. Vandeperre\*, J. Wang, E. Feilden-Irving, F. Giuliani, Imperial College London, United Kingdom

Ceramic materials are often used because of their high melting points, which suggests suitability for high temperature use. A key example are ultra high temperature ceramics, which are being investigated for use at very high temperatures (>2273 K), where the number of materials that can be considered is very limited. Despite the fact that these materials are considered for use at these extreme temperatures, measurements of the mechanical properties at the relevant temperatures are limited. Since indentation testing can give an indication of yield strength and creep resistance, the aim of this work is to determine the temperature dependence of the hardness of ZrB<sub>2</sub> and

to link this to the deformation mechanisms. Therefore, a method is being developed for making hardness measurements up to 2273 K. To calibrate the methodology, measurements of the high temperature hardness of aluminium oxide will be contrasted with literature data in the range where such data is available. This is followed by measurements of the high temperature hardness of zirconium diboride. These results will be contrasted with predictions of the variation in properties with temperature made by modelling the hardness results obtained at moderate temperatures.

**3:50 PM**

### (ICACC-S12-044-2012) Investigation of Room Temperature Dislocation Mobility in metal diborides (ZrB<sub>2</sub>) using Nano Indentation and Confinement Studies

G. Subhash\*, D. Ghosh, University of Florida, USA

Unlike structural ceramics that exhibit brittle behavior, transitional metal diborides (ZrB<sub>2</sub> and HfB<sub>2</sub>) which are potential candidates for ultra high temperature applications, exhibit ductile deformation features and high electrical conductivity similar to metals. To further investigate this behavior, we have conducted nano- and micro-indentations and noted extensive slip-line patterns akin to those observed in metals. TEM analysis revealed multiple sets of dislocations and dominance of pyramidal slip. Nano indentation experiments on individual grains before and after macroindentation-induced deformation revealed that these slip regions are harder than the virgin material. The dislocation plasticity and hardening behaviors are argued on the basis of its chemical bonding and non-localized dislocation core structure.

**4:10 PM**

### (ICACC-S12-045-2012) Powder Processing Effects on the Rapid Low-Temperature Densification of ZrB<sub>2</sub>-SiC Ultra-High Temperature Ceramic(UHTC) Composites Using Spark Plasma Sintering

L. S. Walker\*, W. R. Pinc, E. L. Corral, The University of Arizona, USA

Reducing densification temperatures required for processing UHTCs is critical to enable forming of large parts for aerospace applications. New technologies are enabling significant temperature reductions, however densification mechanics are not well understood. Investigating the powder processing effects on a ZrB<sub>2</sub>-25 vol.% SiC ceramic composite densified using spark plasma sintering (SPS) allows for identification of densification mechanisms and enables a reduction in sintering temperature to a minimum of 1650°C. Attrition milling (AM) and ball milling (BM) were investigated as processing methods to produce a fine and coarse powder densified using SPS with or without a tube furnace pre-heat treatment. Ceramics formed from AM and BM powders contain 1.66 Wt.% oxygen contamination, primarily ZrO<sub>2</sub> and SiO<sub>2</sub>, and 0.35 Wt.% oxygen contamination as SiO<sub>2</sub>, respectively. Heat treatment before SPS slightly reduces oxygen contamination, but has significant impacts on the densification mechanisms. Without heat treatment, powder coarsening dominates the initial sintering process in the SPS inhibiting densification until ~1350 °C. With heat treatment, sintering and densification is enabled at low temperature, ~1100 °C. A time-temperature-density plot illustrates a shift in densification mechanism from sintering to pressure forging.

**4:30 PM**

### (ICACC-S12-046-2012) Processing and Thermal Properties of ZrB<sub>2</sub> with Varying Boron Isotope Ratios

J. M. Lonergan\*, B. Fahrenholtz, G. Hilmas, Missouri Science & Technology, USA

Jason Lonergan, Bill Fahrenholtz, & Greg Hilmas Department of Materials Science & Engineering Missouri University of Science & Technology, Rolla, MO 65409, USA jmlr53@mst.edu Abstract The effects of varying the boron isotope concentrations on the thermal properties of ZrB<sub>2</sub> were studied. Reactive hot pressing of ZrH<sub>2</sub> and isotopically pure 10B and 11B powders was used to synthesize nominally

phase-pure ZrB<sub>2</sub>. Samples ranging from 100% Zr10B<sub>2</sub> to 100% Zr11B<sub>2</sub> were synthesized and tested. Microstructure and composition of both processed powders and dense billets were determined using scanning electron microscopy and x-ray diffraction analysis. Thermal conductivity was calculated from the temperature dependent values of heat capacity, thermal diffusivity, and density for temperatures ranging from 250°C to 2000°C. Enrichment of ZrB<sub>2</sub> with the lighter 10B isotope should increase the thermal conductivities by reducing the average mass of the boron sub-lattice and subsequently increasing the frequency of lattice vibrations. This talk will detail the procedures and steps required for high purity processing of fine powders, the sintering conditions required for full densification, and the results and implications that the different boron isotope ratios have on thermal properties of ZrB<sub>2</sub>.

4:50 PM

**(ICACC-S12-047-2012) Investigations on the Mechanism of Zirconium Carbide Formation via Carbothermal Reduction of Yttria Stabilized Zirconia**

A. Sondhi\*, University of North Texas, USA; C. Morandi, Pennsylvania State University, USA; R. F. Reidy, T. W. Scharf, University of North Texas, USA

Zirconium carbide is an important ultra high temperature ceramic (UHTC) due to its refractory properties. ZrC is commonly synthesized via carbothermal reduction of zirconia above 1657°C.  $ZrO_2 + 3C \rightarrow ZrC + 2CO$  Prior research indicates that carbon monoxide (CO) is the responsible species for carburizing zirconia to form zirconium carbide. A number of thermodynamic and kinetic issues are not well understood, including the role of CO as a carburizing species and its partial pressure influence on the reaction. These issues are critical to control the extent of ZrC conversion. Investigations were done by making two mixed phase pellets using 3 mol% yttria-stabilized zirconia (YSZ) and graphite. Both had an upper half made of YSZ. The lower half of one sample consisted of finely mixed YSZ and graphite powder whereas the other was pure graphite. These were heat treated in a high vacuum graphite furnace at 1800°C for 30 minutes under flowing helium. XRD analysis revealed higher ZrC conversion for the YSZ pellet face in direct contact with pure graphite. This contradicts previous work as one would assume higher ZrC yield for YSZ pellet in direct contact with YSZ/graphite mix as they would react and produce more CO. These fundamental results also imply that carbothermal reduction is more dependent on a solid state carburization than a gaseous reaction with CO.

5:10 PM

**(ICACC-S12-048-2012) Processing Thin, Homogeneous and Flexible Tapes of ZrB<sub>2</sub> and ZrB<sub>2</sub>-SiC Using a Solvent-Based Tape Casting Approach**

D. Pham\*, W. R. Pinc, L. S. Walker, E. L. Corral, University of Arizona, USA

An organic solvent-based formula for tape casting is used to form thin, homogeneous and flexible tapes of ZrB<sub>2</sub> and ZrB<sub>2</sub>+25 vol% SiC for potential use as thin layers for thermal protection system materials in advanced aerospace vehicles. Ball-milled (BM) powder is compared to attrition-milled (AM) powder to resolve lower oxygen contents in the powder and organic solvents are used to minimize oxygen contamination. ZrB<sub>2</sub> tape casting slurry compositions contain, in weight percent, 3.8% binder, 6.2% plasticizers, and 63.8% ZrB<sub>2</sub> powder; ZrB<sub>2</sub>-SiC is made of 3.6% binder, 6% plasticizers, and 61% ZrB<sub>2</sub>-SiC. Sedimentation experiments on BM ZrB<sub>2</sub> and as-received SiC provide a range of dispersant concentrations that allow high density powder compacts and lower viscosity measurements than AM slurries. SEM micrographs of crack-free and flexible tapes show continuous and homogeneous particle distribution. ZrB<sub>2</sub> and ZrB<sub>2</sub>-SiC tapes averaged tape thicknesses of 340 μm and 320 μm, respectively. Thermal gravimetric analysis (TGA) performed on both systems determined an optimal lamination procedure temperature of 200°C and a binder burnout schedule temperature of 500°C. Preliminary multilayer studies show promising results in producing discrete layers in

ZrB<sub>2</sub> and ZrB<sub>2</sub>-SiC laminates with average layer thicknesses of 160 μm.

5:30 PM

**(ICACC-S12-049-2012) Application of the Horizontal Dip-Spin Casting (HDSC) Process to Ultra-High Temperature Ceramic Composites Fabricated with Aligned Reinforcing Phases**

M. Acosta, J. P. Youngblood, R. W. Trice, V. L. Wiesner\*, Purdue University, USA

The horizontal dip-spin casting (HDSC) process is a novel fabrication method designed to obtain ceramic bodies with curvature and aligned reinforcing phases. A-16SG alumina and carbon whiskers were initially used as a model system to develop and optimize the associated process parameters. Aqueous alumina gels contained up to 20 vol. % C-whiskers. Yield pseudoplastic suspensions with polymer compositions between 2.6 and 5.1 vol. % polymer carrier had the best rheological properties, and specimens with a high degree of alignment in the microstructure were fabricated. HDSC was characterized mainly via parallel plate rheometry, stereology and flexural strength. The main parameters to consider were ceramic powder type, dispersant and polymer carrier (concentration and average molecular weight), reinforcing phase content, degree of microstructural alignment and sintering conditions. Currently, the process has been adapted to ZrB<sub>2</sub>/SiC UHTCCs. Aqueous ceramic suspension gels containing ~50 vol. % ZrB<sub>2</sub> have been fabricated using low molecular weight PVP and PEO as polymer carriers. These gels have the rheological behavior needed to cast specimens via HDSC. Further characterization work will be performed to adapt this novel process to ZrB<sub>2</sub>/SiC UHTCCs.

5:50 PM

**(ICACC-S12-050-2012) HfC and HfB<sub>2</sub> Powders and Coatings via Sol-Gel Processing**

S. Venugopal\*, A. Paul, J. Binner, B. Vaidyanathan, Loughborough university, United Kingdom; P. Brown, A. Heaton, DSTL, United Kingdom

Developing advanced materials for wing leading edge and propulsion components that can withstand up to 3000°C and offer superior thermal shock resistance is a must to bring these vehicles into reality. The current C-SiC based materials are not capable of withstanding such high temperatures, hence UHTC-based composites, particularly those utilising HfC and HfB<sub>2</sub> are being investigated. HfC and HfB<sub>2</sub> nano crystalline powders have been synthesized via sol-gel based routes. TGA and high temperature XRD have been employed to study the calcination of precursors and crystallisation of the UHTC powder. The HfC powders formed had an average particle size of ~50 nm whilst the HfB<sub>2</sub> powders had average particle sizes of ~25 nm. The precursor gels were also used to coat carbon fibre preforms. The continuity of the coatings on the C fibre preform was characterized using transmission and scanning electron microscopes. Mini composites were prepared using the coated fibre tows to measure the strength and the results were compared to those of uncoated and heat treated fibres. An automated dip coater has also been used to control the thickness of the coating in an attempt to make them crack free. Thicknesses of as little as 0.7 μm can now be achieved.

**S13: Advanced Ceramics and Composites for Nuclear Applications**

**Advanced Non-oxide Ceramics: Fabrication, Characterization, and Radiation Damage Tolerance**

Room: Coquina Salon E

Session Chair: Theodore Besmann, Oak Ridge National Laboratory

1:30 PM

**(ICACC-S13-010-2012) Characterization of Failure Behavior of Silicon Carbide Composites by Acoustic Emission (Invited)**

T. Nozawa\*, K. Ozawa, H. Tanigawa, Japan Atomic Energy Agency, Japan

A silicon carbide fiber reinforced silicon carbide (SiC/SiC) composite is a promising candidate material for various nuclear applications

such as a fusion blanket. Due to the inherent brittle-like failure, identifying failure scenario with consideration of reliability and reproducibility of composite's characteristics is undoubtedly important to develop design codes specialized for composites. This study aims to identify failure behavior of SiC/SiC composites by varied material types, architectures and test modes. For this purpose, acoustic emission (AE) was applied to detect composites' failure. Tensile and compressive tests were conducted for three types of SiC/SiC composites: a unidirectional nano-infiltration transient-eutectic-phase sintered (NITE) composite, a plain-weave (P/W) NITE composite and a P/W chemical vapor infiltration (CVI) composite. Various loading angles were applied to discuss an anisotropic issue. AE results distinguished damage accumulation processes in axial and off-axial loading cases. Specifically, test results indicated a clear difference of damage density between tensile and compressive tests. Furthermore, superior damage tolerance of NITE composites was demonstrated compared with CVI composites. This study will also classify the characteristic failure modes by separately discussing localized variations of power within a time series by wavelet analysis.

**2:00 PM**

### **(ICACC-S13-011-2012) Application of X-ray Tomography to Nuclear Ceramics**

L. Snead\*, J. Hunn, A. Kercher, E. Sphect, ornl, USA

With significant improvement in both beam brightness and detector resolution, the technique of x-ray tomography is making the transition from dedicated beamlines to more routine laboratory use. The purpose of this talk is to describe the application of x-ray tomography to irradiated nuclear ceramics carried out in radiological facilities at the Oak Ridge National Laboratory. Specifically, this technique has been used to characterize the intrinsic and irradiation-altered porosity structure in nuclear graphite. Reconstruction of such features can show not only how the porosity evolves under irradiation, but how matrix features such as coke-particle can reorient under applied stress. Other example applications include the layered structures in high-temperature gas cooled reactor fuels (TRISO fuels.) In that case the nominal micron resolution of the instrument utilized identifies features such as soot inclusions and metallic impurity sites. In summary, the future application and expected technique improvements in terms of finer resolution, improved contrast, and the ability to visualize very highly radioactive samples.

**2:20 PM**

### **(ICACC-S13-012-2012) Microstructural Analysis of Nuclear-Grade Graphite Materials**

K. Takizawa\*, T. Fukuda, A. Kondo, Tokai Carbon Co., LTD., Japan; Y. Katoh, G. E. Jellison, Oak Ridge National Laboratory, USA

Graphite materials under nuclear services undergo very significant irradiation effect phenomena including dimensional instability and modifications in various thermo-physical and mechanical properties. Because these changes are resulting from the irradiation-induced structural changes in graphite in nano-, micro- and meso-scopic scales, it is essential to adequately characterize the materials' structures before and after neutron irradiation and correlate the structural changes with the evolving macroscopic properties. Objective of this work is to characterize the as-fabricated microstructures of fine-grained nuclear graphite manufactured by Tokai Carbon Co., Ltd. The microstructure of graphite consists of filler cokes, binder and pores(cracks). The characteristic microstructures of the fine-grained isotropic graphite were determined by focusing on the attributes of these elements. Specifically, the sizes, shape factors, and the crystallographic anisotropy were evaluated so that these information may be correlated with the thermophysical properties, macroscopic anisotropy, fracture properties, and the irradiation effects. In future work, these materials will be examined for various properties and microstructural changes following the neutron irradiation in High Flux Isotope Reactor, Oak Ridge National Laboratory. This paper intro-

duces the initial results of microstructural evaluation for the pre-irradiated materials.

**2:40 PM**

### **(ICACC-S13-013-2012) Effect of Neutron Irradiation on Bonded Fiber Silicon Carbide Composite**

Y. Katoh\*, K. Ozawa, S. Kondo, Oak Ridge National Lab, USA; Y. Kawaharada, S. Higuchi, Toshiba Corporation, Japan

Silicon carbide-based ceramic composites are promising structural materials for use in high radiation environments including commercial nuclear reactor core. Bonded fiber silicon carbide composite made to near-stoichiometric compositions is particularly attractive for fuel cladding application because of its ability to withstand high mechanical loading and to make into thin walled tubular components with structural homogeneity and tightness against gaseous fission products. This paper will report the physical, mechanical, and thermal properties of near-stoichiometric bonded fiber silicon carbide composite after neutron irradiation to more than 5 displacement per atom at 593K in High Flux Isotope Reactor, Oak Ridge National Laboratory.

**3:20 PM**

### **(ICACC-S13-014-2012) Preparation of isotropic graphite with mesocarbon microbeads and their carbonization mechanism (Invited)**

F. Kang\*, K. Shen, Z. Huang, Tsinghua University, China; J. Yang, University of Shanghai for Science and Technology, China; W. Shen, Tsinghua University, China

A possible way of isotropic graphite preparation is to use mesocarbon microbeads (MCMBs) as the raw material. It has been realized that the pre-oxidation control is an essential step that affects the pyrolysis behavior, sintering mechanism, and the final mechanical properties. In this study, the influences of particle size and pre-oxidation of commercially available MCMBs (China Steel Chemical Corporation) on final product were discussed. Green artifacts with a size of  $\phi 70 \times 70$  mm were prepared by CIP at 200 MPa then studied for carbonization process. TG-mass spectrometry shows that H<sub>2</sub>, CH<sub>4</sub>, CO<sub>2</sub> and H<sub>2</sub>O are the common gaseous products, however, at 400-600 °C, lightly oxidized MCMBs (M-LO) may generate lightweight hydrocarbon component, which was confirmed by TG-IR spectroscopy. Microstructure evolution recorded by in-situ scanning electron microscopy shows the reason for remarkable difference between the physical properties of M-LO and lightly oxidized MCMBs (M-HO). After graphitization, two types of graphite artifacts can be obtained successfully. One has flexural strength of 61.6 MPa and isotropic ratio of 1.06, the other has 34.2 MPa and 1.00. Preparation of artifacts of 200 and 300 mm in diameter was attempted. We think it is possible to prepare isotropic graphite with large size (i.e.  $\phi 300$  mm) by using MCMBs, on the condition that the pre-oxidation control and the heating program can be optimized.

**3:50 PM**

### **(ICACC-S13-015-2012) Study of the ceramic matrix composites densification by film boiling process**

A. M. Serrre\*, F. Audubert, CEA, France; S. Bonnamy, CNRS, France; B. Joëlle, D. Patrick, CEA, France

The Film boiling technique is used to densify ceramic matrices. Its particularities reside in the high thermal gradient (hundreds of degrees per millimetres) and the high precursor concentration which lead to a densification zone moving quickly through the part to densify. The required equipment is called Kalamazoo. The fibrous structure to densify is heated at high temperature in a bath of liquid precursor which becomes gaseous in contact with the hot surfaces. The vapors are then decomposed and infiltrated into the porosities: the part is densified from the hottest zone (inside the fibres) to the cold-

est zone (toward outer the fibres), avoiding the plug of the pore, contrary to CVI. The main parameters (temperature, pressure, precursor, vapour flux) have an influence on both the microstructure of the material and the working of the process (densification rate, material yield, energy efficiency). The study is achieved on laboratory scale equipment: different matrices are developed from many precursors. Carbon and SiC matrices have been manufactured 50 to 100 times faster than by CVI and the results are promising. Other experiments will be done to elaborate different phases such as TiC, HfC and ZrC, which will be chemically and physically characterized. High densification rates, good materials characteristics (mechanical, structural) and reproducibility are the main advantages of this process.

#### 4:10 PM

##### (ICACC-S13-016-2012) Microstructural Development in Cubic Silicon Carbide and SiC/SiC Composites During Neutron Irradiation

P. Dou\*, Y. Katoh, L. Snead, Oak Ridge National Laboratory, USA

Silicon carbide ceramics and composites are promising materials for high temperature nuclear services due to the outstanding mechanical, physical, and chemical stability up to very high temperatures in a high radiation environment. For fusion energy applications of these materials, especially for the proposed use in the near-first wall portions of the breeding blankets, the potential influences of neutron irradiation on various properties are the critical issues. The silicon carbide materials examined are high purity polycrystalline and monocrystalline 3C-SiC produced by chemical vapor deposition. Neutron irradiation was performed in High Flux Isotope Reactor, achieving up to 7 dpa in an inert gas environment. Hi-Nicalon Type-S fiber reinforced chemical-vapor-infiltration (CVI) SiC matrix composites were applied to neutron irradiation. The irradiation doses was up to 70 dpa. We will report the microstructural development, as examined by high resolution transmission electron microscopy, STEM-EELS and diffraction contrast techniques including weak beam electron microscopy, in high purity silicon carbide samples during neutron irradiation. We will also report the irradiation-induced microstructural and chemical changes of SiC and pyrolytic carbon (PyC) as a combined form of the F/M interface.

#### 4:30 PM

##### (ICACC-S13-017-2012) Recision of Silicon Carbide in Steam under Nuclear Plant LOCA conditions up to 1400 °C

G. Markham\*, H. Feinroth, R. Hall, Ceramic Tubular Products, USA

Abstract – Ceramic Tubular Products is developing a multilayered silicon carbide tube for use as fuel cladding in commercial nuclear reactors. In this project, we exposed a number of alpha and beta phase SiC monolith specimens to the type of steam conditions that would exist in a commercial water reactor during a design basis LOCA (Loss of Coolant Accident). We also exposed specimens at 1400 °C, which is 200 °C above the conditions allowed by regulations for a design basis LOCA, and for times up to 8 hours, substantially exceeding the times allowed under current regulatory criteria for licensing of zircaloy clad fuel. The measured recision, and calculated hydrogen gas released during this exposure was compared with that calculated for zircaloy cladding under the same conditions. For example, for a 4 hour exposure test at 1400 °C, the measured recision (loss of clad wall thickness) for SiC, adjusted for actual 17 x 17 LWR fuel clad dimensions, was 0.18%, as compared with 42.1% recision calculated for zircaloy. The data thus demonstrates that use of this cladding in commercial LWRs instead of zircaloy will substantially increase the safety margin of LWRs when subject to Loss of Coolant accidents such as recently occurred at Fukushima. This work was sponsored by the US Department of Energy under Small Business Innovative Research Grant DE-SC0004225.

#### 4:50 PM

##### (ICACC-S13-018-2012) Influence of interphase properties and fiber/matrix coupling on the mechanical behaviour of SiC/SiC composites

E. Buet\*, C. Sauder, S. Poissonnet, R. Gadiou, C. Vix-Guterl, CEA Saclay, France

SiC/SiC composites reinforced with near stoichiometric SiC ceramic fibers (Hi-Nicalon S and SA3 Tyranno fibers) are attractive materials to be used as structural materials in fission reactors. The mechanical properties of these materials strongly depend on the interphase properties and interfaces phenomenas. Right now, pyrocarbon deposited by CVI is the reference materials to be used as interphase in SiC/SiC composites. The mechanical behaviour of CVI SiC/SiC composites reinforced with Hi-Nicalon S or SA3 Tyranno fibers were investigated on minicomposites (unidirectional composite reinforced single tows) test specimen. Tensile tests and push-out tests were used in order to determine the interfacial shear strength. It is found that interfacial shear strength of SiC/SiC composites reinforced by SA3 Tyranno fibers is ten times higher than that of Hi-Nicalon S reinforced composites. The characterization of the SiC fibers and the carbon interphase indicates that the surface properties of the fibers and the pyrocarbon texture (anisotropy/isotropy) could be responsible for this mechanical behaviour difference. Surface treatments were carried out to modify fibers surface roughness and to modulate the fiber / matrix coupling in order to improve the mechanical properties of composites reinforced by SA3 fibers.

#### 5:10 PM

##### (ICACC-S13-019-2012) A New ASTM C28 Test for the Uniaxial Tensile Properties of Carbon-Carbon and SiC-SiC Composite Tubes

S. T. Gonczy\*, Gateway Materials Technology, USA; M. G. Jenkins, California State University, Fresno, USA

The U.S. Department of Energy (US-DOE) is developing the Very High Temperature Reactor (VHTR) as the next-generation nuclear power technology. The VHTR design is a helium-cooled, graphite-moderated, thermal neutron spectrum reactor with a gas outlet temperatures >800°C and off-normal core temperatures >1200°C, well beyond the capability of current metal alloys. Ceramic matrix composites (CMC—carbon-carbon and silicon carbide-silicon carbide) are being developed for the control rod tubes in the reactor. Mechanical properties from CMC flat plates cannot be reliably used for the design of tubes with their 3-D and braided cylinder architectures. Direct tensile strength tests of CMC tubes are needed for accurate design data. A joint US-DOE/ASTM C28 project has developed a new standard test method for the uniaxial tensile properties of ceramic composite tubes at ambient temperatures. This new standard test method is applicable to 1-D, 2-D, and 3-D ceramic composite tubes with diameters up to 150 mm and wall thicknesses up to 25 mm. The test method addresses the following experimental issues — test specimen geometries and preparation, different gripping methods, test equipment, interferences (material, specimen, bending stresses, test conditions, etc), testing modes and procedures, data collection, calculation, reporting requirements, and precision/bias.

#### 5:30 PM

##### (ICACC-S13-020-2012) High Temperature Oxidation of SiC in Steam-Hydrogen Environments

T. Cheng\*, J. R. Keiser, M. P. Brady, B. A. Pint, K. Terrani, Oak Ridge National Laboratory, USA

Mitigation of nuclear reactor core damage under accident scenarios can be achieved by a combination of optimal safety systems and accident tolerant fuels. This is especially the case under conditions that extent beyond the design basis accident scenarios. An outstanding accident tolerant fuel candidate is the fully ceramic microencapsulated fuel (FCM) that consists of TRISO fuel particles embedded in a SiC matrix. SiC has also been proposed to comprise the nuclear fuel

cladding, replacing Zircaloy in the conventional oxide fuel design. SiC forms a thin protective silica layer in dry oxidizing environments. However the recession rate is greatly increased by the presence of water vapor, due to the formation of volatile hydroxide species. The purpose of this work is to compare the performance of monolithic and composite SiC to Zircaloy and stainless steel cladding candidates in steam and steam-H<sub>2</sub> environments at 800°-1200°C and 1-20 bar. At the highest temperature, many of the ~1mm thick metallic candidates are consumed by exposures from 2-24h. The reaction layer thickness on SiC as a function of temperature, time, pressure and environment will be presented.

**5:50 PM**

**(ICACC-S13-021-2012) Measurement of Interfacial Mechanical Properties of SiC Fiber Reinforced SiC Composites with Micro-pillar Mini Samples**

C. Shih\*, Y. Katoh, G. Vasudevamurthy, P. Dou, Oak Ridge National Laboratory, USA; T. Nozawa, Japan Atomic Energy Agency, Japan; H. Bei, Oak Ridge National Laboratory, USA

SiC fiber reinforced SiC composites are promising candidate materials for fusion applications. The mechanical properties of these composites are strongly affected by the fiber/matrix interface. Therefore, the determination of interface properties is important for designing purposes. Moreover, understanding the changes of interfacial properties with respect to neutron fluences is of great interest. These interfacial properties are often determined by single fiber push-out tests. The drawback of this test is the Poisson effect associated with it, which can greatly increase the frictional stress and make the determined interface properties questionable. In this current study, a new test method is proposed and evaluated; where micron sized, pillar shaped SiC samples, containing a fiber/matrix interface, were prepared from a SiC fiber reinforced SiC matrix composites, using a focused ion beam system. The pillar shaped samples were then tested using the nano-indentation technique. This new test method employs a simple geometry and eliminates the Poisson effect. Samples with different interface orientations were prepared and tested. The interfacial debond shear strength and the interfacial friction coefficient are determined and their values are compared with other test methods. The validity of the new test method is evaluated.

## Global Young Investigators Forum

### Frontiers in Ceramic Energy Generation and Storage

Room: Coquina Salon G

Session Chairs: Karra Raveendran Girish Karthik, Nanyang Technological University; Lucky Sikhwihulu, CSIR

**1:30 PM**

**(ICACC-GYIF-021-2012) Efficient dye sensitized solar cell using developed transparent conductive films (Invited)**

D. Sahu\*, University of the Witwatersrand, South Africa

Multilayer transparent conductive oxide thin films are grown using the simultaneous RF and dc sputtering method for deposition of ZnO and Ag layers in case of ZnO/Ag/ZnO (ZAZ) film and e-beam evaporation method in case of Al-doped ZnO (AZO) /Ag/AZO (AAA) film. These developed films are applied to dye sensitized solar cells (DSSC). The electrical and optical properties of the multilayers were studied using four-point probe and UV-Visible spectrophotometer. Mesoporous TiO<sub>2</sub> electrodes for DSSC were coated on multilayer ZAZ and AAA by a spin coating and low temperature sintering method. A ZnO covered TiO<sub>2</sub> (denoted as ZnO/TiO<sub>2</sub>) film was also prepared by incorporating small quantity of ZnO in a TiO<sub>2</sub> matrix by chemical vapor deposition method. The properties of the film and DSSC are compared with well known transparent metal oxides ITO and FTO. These DSSC on the ZAZ and AAA coating yielded an overall cell efficiency of 4.91 and 5.45 % at one sun light intensity. The dye

sensitization process with the low cost mercurochrome is sensitive in this case of ZnO based multilayer.

**1:50 PM**

**(ICACC-GYIF-022-2012) Electrospinning as a Versatile Method for Production of Ceramic and Composite Nanofibers (Invited)**

M. Büyükyazi, A. Lepcha, S. Mathur, R. von Hagen\*, University of Cologne, Germany

Electrospinning is a bottom-up approach for the preparation of nanoscopic ceramic and composite fibers, that has gained rising popularity during the last decade due to its simplicity and flexibility in terms of nanomaterials device integration. The process is crossing borders between chemistry, physics and material science, as it is based on the spinning in electrical fields and the achieved fiber properties (e.g., morphology, architecture, phase-purity) are influenced by the precursor chemistry as well as the experimental setup and post treatment of the material. Therefore the talk is focusing on the nanofiber production with a control over architecture and phase composition by refinement of the involved precursor chemistry as well as the used experimental setup. Furthermore the relationship between the morphological and phase properties of the fibers and the resulting material performance in the device could be carved out. As the presented results were mainly produced in collaborative projects between different workgroups from different scientific backgrounds (chemists, physicists, material scientists), where the involved researchers are not always speaking the same scientific language, special attention will be addressed on the successful organization of such collaborative projects.

**2:10 PM**

**(ICACC-GYIF-023-2012) Design and characterization of inorganic/organic nanohybrid materials for solar cell applications (Invited)**

S. Makuta\*, A. Azarifar, Y. Tachibana, Royal Melbourne Institute of Technology (RMIT University), Australia

Hybridization of inorganic semiconductor nanoparticles and organic conductive polymers has recently received significant interests as one of the most advantageous combinations for photo-electronic devices such as photovoltaics. Such developments are able to provide not only versatile opportunities in designing nanostructures, but also novel functions at the inorganic/organic interface. In addition, compared with the conventional vacuum deposition methods, the low manufacturing cost is expected for the devices based on the hybrid nanomaterials. However, the efficiency of the hybrid solar cells remains low, fundamentally limiting their commercialization. In order to achieve high device performance, understanding the interfacial electron transfer reactions is essential, and the elucidation of the mechanisms will facilitate the interfacial structural design. In this presentation, the factors controlling electron transfer kinetics at the hybrid interface and the device performance will be addressed. This work was financially supported by JST PRESTO program, Japan. The Venture Business Laboratory, Osaka University is also acknowledged for the financial support.

**2:30 PM**

**(ICACC-GYIF-024-2012) Synthesis and characterization of down-converting nanoparticles/PMMA nanocomposites for improving photovoltaic silicon solar cell efficiency**

M. Dai Pre\*, A. Martucci, Università di Padova, Italy

Down conversion property was achieved by ZnS, CdS and ZnO nanoparticles, doped with manganese. A stable and narrowly distributed dispersion of nanoparticles have been obtained via chemical precipitation without using any surfactant. The surface of the particles has been functionalized with a suitable ligand to get a homogeneous dispersion into the polymethylmetacrylate (PMMA) matrix. A

thorough morphological and optical characterization is proposed. The aim is to produce plastic materials doped with down-converting nanoparticles for modification of the solar spectrum in order to enhance the efficiency of solar cells. So the most important properties of those nanocomposites are high transmittance (above 85%) in the visible range and down conversion from 300-500 nm to 600-900 nm. Transparent luminescent nanocomposite powder were obtained mixing directly PMMA and the nanoparticles while the nanocomposites have been obtained by injection molding.

### 2:50 PM

#### (ICACC-GYIF-025-2012) Glass ceramic electrolytes for protecting Li-anodes in Lithium ion/air batteries: Fabrication and characterization

N. Gupta\*, R. Yazami, M. Srinivasan, Nanyang Technological University, Singapore

Future generation of environmentally sustainable power source requires thermodynamically stable, safe, cost-effective and leak-proof electrolytes. There are intense research efforts to develop new formulation of solid electrolyte materials, which are more stable with respect to common electrode materials. Among various electrolytes, the phosphate-based solid glass ceramic electrolytes have great application potential in protecting lithium anodes during the cycling of the battery by decreasing the internal/interfacial resistance. In this work, we report effect of boron nitride substitution on the interfacial stability of Lithium aluminum germanium titanium phosphate (LAGTP) and characterized their properties as solid electrolytes for rechargeable lithium ion/air battery. An important factor for high efficiency of these electrolytes is their high room temperature lithium ion conductivity  $\sim 10^{-3}$ - $10^{-4}$  S/cm. This work focuses on the production of glass and glass-ceramics by melting and quenching. Crystallization was achieved by heat treatment at various temperatures to enhance nucleation and growth mechanism. Cubical crystal structure is confirmed by SEI images for the samples sintered at and above 850°C. The NASICON type crystal structure is confirmed by XRD techniques. The crystalline phase depends greatly on the glass composition and the heat treatment.

### Frontiers in Ceramic Characterization and Catalytical Properties

Room: Coquina Salon G

Session Chairs: Diptiranjana Sahu, University of the Witwatersrand; Robin von Hagen, University of Cologne

### 3:30 PM

#### (ICACC-GYIF-026-2012) Electrical characterization of individual metal-oxide nanowires using AC impedance spectroscopy

K. Karthik\*, K. B. Jinesh, Y. Huang, S. G. Mhaisalkar, Nanyang Technological University, Singapore

Fundamental electrical characterization of individual nanowires is a critical step in understanding the nanowire based device behaviour. With growing applications of metal-oxide nanowires, newer techniques need to be explored to elucidate their device dependent properties. Impedance spectroscopy is a direct technique to explain the interactions of electron with its surrounding lattices, grain boundaries. Impedance spectroscopy is performed on individual nanowire devices fabricated using electron beam induced deposition (EBID) in a focused ion beam system (FIB). Due to high sensitivity of the measurement, EBID was chosen for fabrication and measurements were performed in probe station under vacuum environment, minimizing every possibility of stray capacitance from contacts. The mobility of the majority charge carriers in the nanowire was extracted using modified space charge limited current (SCLC) analysis for the nanowire geometry. The trapping kinetics of the charge carriers and their interaction to the perturbation applied through AC is analyzed in terms of impedance and capacitances. The analysis of the capacitance and phase information obtained from presents us with the dis-

tribution of traps and other defects like grain boundaries. The interpretation of the impedance and capacitance spectra provides us with key parameters and serves as direct measurements for trap kinetics.

### 3:50 PM

#### (ICACC-GYIF-027-2012) Computational and Experimental studies on doped NaTaO<sub>3</sub> photocatalysts

P. Kanhere\*, Nanyang Technological University, Singapore; J. Zheng, Institute of High Performance Computing, Singapore; Z. Chen, Nanyang Technological University, Singapore

Photocatalysis has gained significant attention in the area of environmental cleaning and clean energy generation. NaTaO<sub>3</sub> is a highly efficient photocatalyst for water splitting reaction under UV radiation. In this study, doped NaTaO<sub>3</sub> systems were explored by DFT based electronic structure calculations to narrow the band gaps to visible region. Selected compounds i.e. Bi doped NaTaO<sub>3</sub> and La-Fe co-doped NaTaO<sub>3</sub> were synthesized by solid state method and characterized by various techniques like by X-ray diffraction, Rietveld refinement, electron microscopy, X-ray photoelectron spectroscopy, diffused reflectance spectroscopy, surface area measurements etc. Experimental investigations confirmed that Bismuth doping in NaTaO<sub>3</sub> causes visible light absorption and the band gaps of this system can be tuned by location of Bi ions in the lattice by employing appropriate synthesis conditions. Equal occupancy of Bi ions at Na and Ta sites gave rise to maximum to visible light absorption (E<sub>g</sub> = 2.64 eV) up to 7.5% Bi doping. These samples showed photocatalytic hydrogen evolution as well as degradation of Methylene Blue under visible radiation. Additionally, La-Fe co-doped NaTaO<sub>3</sub> powders with unique surface structure and visible light response were also synthesized for up to 10% doping concentration. The present study shows that modified NaTaO<sub>3</sub> materials have promise to develop photocatalysts working under solar radiation.

### 4:10 PM

#### (ICACC-GYIF-028-2012) Hierarchically ordering of hybrid ceramic catalysts

M. Adam\*, M. Wilhelm, G. Grathwohl, University of Bremen, Germany

The aim of this work was the preparation of platinum containing surface-rich hybrid ceramic foam catalysts. The hybrid ceramic foams were prepared by using platinum containing polysiloxanes as precursor materials and polystyrene beads as template. The conversion to a hybrid ceramic was performed at 500 and 600°C under nitrogen. For the preparation polystyrene beads of 0.5-1.5 mm size were placed in a mold and were then infiltrated with the polysiloxanes. During pyrolysis the polystyrene was almost completely decomposed leading to open-cell foams with different cell window sizes. The cell size was corresponding to size of the templates used and due to the pyrolysis the struts of the foams are micro porous leading to specific surface areas of 300-600 m<sup>2</sup>/g. The platinum was finely dispersed as platinum particles of 2-10 nm and its accessibility for gases was proved using the CO oxidation as model reaction. In this work hybrid ceramic foams with a hierarchically ordered pore structure were generated by a template method and pyrolytic conversion of the polysiloxane precursor at moderate temperatures. Due to the template size and processing parameters the macrostructure could be adjusted. Moreover high specific surface areas were realized and their catalytic activity was verified, making these foams to promising catalysts.

### 4:30 PM

#### (ICACC-GYIF-029-2012) Effects of Synthesis Conditions and Thermal Treatment of Nanostructured Materials on Textural Properties

L. Sikhvivilu\*, S. Sinha Ray, National Centre for Nano-Structured Materials, South Africa

Nanotechnology and nanoscience are underpinned by nanomaterials. Nanomaterials field is the common thread between materials science and nanotechnology. It studies materials with morphological

features on the nanoscale and especially those that have special properties stemming from their nanoscale dimensions. Semiconducting nanomaterials are attractive because their physical properties are different from those of the bulk due to the quantum-size effect. Also, they provide opportunities to study the effect of spatial confinement and problems related to surfaces or interfaces, which is important for chemistry. Recently, one-dimensional (1D) nanomaterials such as nanowires, nanobelts, nanorods, and nanotubes have become the focus of intensive research owing to their potential applications in electronic, optoelectronic, electrochemical, electromechanical, catalysis, and other fields. Nanomaterials are essentially comprised of nanoparticles or nanocrystals made of metals, semiconductors, or oxides and are of particular interest for their mechanical, electrical, magnetic, optical, chemical and other properties. Nanoparticles have been used as quantum dots and as chemical catalysts. This study seeks to address the influence of hydrothermal synthesis conditions and thermal treatment of nanostructured materials on crystallographic and textural properties.

**4:50 PM**

**(ICACC-GYIF-030-2012) Properties of organic semiconductor-metal oxide nanowire composite transistors**

S. Cheng\*, N. Mathews, L. H. Wong, S. G. Mhaisalkar, Nanyang Technological University, Singapore

Transistors fabricated from solution processable organic semiconductors have reached impressive performance, yet suffers from drawbacks like unipolar charge transport behavior. Poly(3-hexylthiophene) (P3HT) represent a class of conjugated polymers that is widely used as the hole-transporting material in organic field-effect transistors (OFETs). Ambipolar transistors which combine P3HT with n-type metal oxide nanowire networks are introduced in this work. Highly oriented tin oxide (SnO<sub>2</sub>) nanowire network (nanonets) were firstly fabricated through contact printing approach. These nanowire networks are studied at submillimeter scales for their utilization as the active material in n-type thin film transistors. The SnO<sub>2</sub> nanowire network transistors show excellent device characteristics and possess electron mobilities of ~7.5 cm<sup>2</sup> V<sup>-1</sup> s<sup>-1</sup> and on/off ratios between 106 and 108 with channel lengths ranging from 75 to 175 μm. For further optimization, the morphology of the organic semiconducting was improved by thermal annealing. Light illumination on the devices enabled the electron-hole pair generation at the nanowire-polymer interface which increased the current and carrier mobility. This study provided the basic idea of nanowire network ambipolar transistors and the interaction between metal-oxide nanowires and organic polymers.

**5:10 PM**

**(ICACC-GYIF-031-2012) XAFS study of mixed metal oxide Cu<sub>0.6</sub>Co<sub>1.2</sub>Mn<sub>1.2</sub>O<sub>x</sub> with spinel structure (Invited)**

A. Fedorova\*, D. Frolov, I. Morozov, Moscow State University, Russian Federation; Y. Zubavichus, Kurchatov Institute National Research Centre, Russian Federation

3d-Metal oxides with spinel structure are well-known catalysts for hydrocarbons and CO oxidation. Their catalytic activity is in strong correlation with their composition and cation distribution. It is difficult to reveal the cationic distributions by usual methods, such as X-ray diffraction, so the XAFS methods (EXAFS and XANES) were used. The mixed 3d-metal oxides CuCo<sub>2</sub>Mn<sub>2</sub>O<sub>x</sub> were prepared both individual and SiO<sub>2</sub>-supported. Both samples have cubic structure (Fd-3m group), cell parameter a was 8.274 Å for individual oxide and 8.24 Å for supported. The TPR study shows, that x is close to 4 in both cases. Comparison of XANES spectra with reference spectra showed that all Cu is in Cu<sup>2+</sup> state. It was deduced from EXAFS spectra fit with parameterized single-scattering ab initio simulated EXAFS data that Mn presents only in octahedral positions, Co equally occupies tetrahedral and octahedral positions and Cu occupies mostly tetrahedral positions. Oxidation states for Co were assigned in accordance with their environment for the reason of highest possible

stabilization energy for octahedral Co<sup>3+</sup> (t<sub>2g</sub><sup>6</sup>e<sub>g</sub><sup>0</sup>). Mn oxidation states were calculated from formula by use of electroneutrality principle In conclusion, the final formula of cation distribution for both samples was [Cu<sup>2+</sup><sub>0.4</sub>Co<sup>2+</sup><sub>0.6</sub>]<sub>tetr</sub>[Cu<sup>2+</sup><sub>0.2</sub>Co<sup>3+</sup><sub>0.6</sub>Mn<sup>3+</sup><sub>1.0</sub>Mn<sup>4+</sup><sub>0.2</sub>]<sub>oct</sub>O<sub>4</sub>.

**5:30 PM**

**(ICACC-GYIF-032-2012) Enhanced charge separation for high efficiency photocatalytic hydrogen production**

S. Shen\*, Xi'an Jiaotong University, China

Photocatalytic water splitting using solar energy has been studied as a potential method of hydrogen production [1]. If we look at the basic mechanism and processes of photocatalytic water splitting, photoinduced charges in the photocatalyst should be separated efficiently in order to avoid bulk/surface electron/hole recombination, for improved performance of photocatalytic water splitting. Hence, any approach beneficial to the charge separation and transport should be taken into account. This work describes the primary approaches for efficient photogenerated charge separation in photocatalytic water splitting, with a focus on the recent progress of our own research. Briefly, modification of crystal structure and morphology, semiconductor combination and cocatalyst loading have been generally adopted to enhance charge separation, opening new potential for the development of high-efficiency photocatalysts for water splitting to produce hydrogen. References [1] X Chen, S Shen, L Guo, S. S. Mao. Chem. Rev. 2010, 110, 6503-6570.

## FS1: Geopolymers, Inorganic Polymers, Hybrid Organic-Inorganic Polymer Materials

### Chemistry, Processing and Microstructure

Room: Coquina Salon A

Session Chairs: Hubert Rahier, Vrije Universiteit Brussel; John Provis, University of Melbourne

**1:30 PM**

**(ICACC-FS1-001-2012) Geopolymers and other alkali-activated binders – Design, characterization and optimization of performance and durability (Invited)**

J. L. Provis\*, S. Bernal, R. San Nicolas, L. Gordon, University of Melbourne, Australia; P. Duxson, Zeobond Pty Ltd., Australia; J. van Deventer, University of Melbourne, Australia

There are a large number of widely differing materials which have fallen under the general umbrella of 'geopolymer' or 'alkali-activated binder' over the past decades. This presentation will be based around a discussion of recent advances in the design and characterization of alkali-activated binders for enhanced resistance to potentially damaging environments, with particular regard to chemical attack either in aqueous media or by carbonation. The role of gel chemistry, pore structure and permeability in controlling various different modes of degradation will be explored, and the advances which have been made in the design of geopolymer binders for optimized microstructure and nanostructure for given environments will be presented. Manipulation of the alkaline activator concentration and modulus, the total water/binder ratio and the calcium content of the binder are seen to provide the most desirable avenues towards optimization of durability. The role of the interfacial transition zone in influencing the properties of mortars and concretes, as opposed to small paste specimens, is also a point of difference between alkali-activated and Portland cement binders.

**2:00 PM**

**(ICACC-FS1-002-2012) On the Effects of Water Content and Si/Al on the Structure and Properties of Geopolymers (Invited)**

M. Radovic\*, M. Lizcano, Texas A&M University, USA

The effects of H<sub>2</sub>O/(SiO<sub>2</sub> + Al<sub>2</sub>O<sub>3</sub>) and SiO<sub>2</sub>/Al<sub>2</sub>O<sub>3</sub> ratios on the density, open porosity, microstructure and the thermal and mechanical properties in K and Na activated geopolymers (GPs) were investi-



gated. All GPs samples were prepared using high purity metakaolin. XRD, NMR as well as alcohol immersion technique were used to characterize the structure of process GPs. In addition, thermal behavior and mechanical properties of processed GPs were characterized by TGA, TMA, TCA and compressive testing. It was found that the amount of water used to process GPs is the governing factor affecting their porosity while SiO<sub>2</sub>/Al<sub>2</sub>O<sub>3</sub> molar ratio plays secondary role. The K- and Na-activated samples have similar amounts of residual water after aging for 21 days at ambient conditions, regardless of the initial water content and SiO<sub>2</sub>/Al<sub>2</sub>O<sub>3</sub> ratios. Results of thermal and mechanical characterization indicate that the dominant factor controlling thermal conductivity of GPs is H<sub>2</sub>O/(SiO<sub>2</sub> + Al<sub>2</sub>O<sub>3</sub>) ratio used in processing and to a lesser degree, the type of activation ion. However, compressive strengths are strongly affected by H<sub>2</sub>O/(SiO<sub>2</sub> + Al<sub>2</sub>O<sub>3</sub>) ratio, only at higher water ratio. At low H<sub>2</sub>O/(SiO<sub>2</sub> + Al<sub>2</sub>O<sub>3</sub>) ratios, SiO<sub>2</sub>/Al<sub>2</sub>O<sub>3</sub> ratio also plays an important role, i.e. compressive strength of GPs increases significantly with increasing Si content.

### 2:30 PM

#### (ICACC-FS1-003-2012) Dissolution rate of silica in solution required to form geopolymer binder (Invited)

S. Rossignol\*, CEC-GEMH -ENSCI, France; A. Autef, CEC-GEMH -ENSCI, France; E. Joussein, GRESE, France; G. Gagnier, IMERYS, France

Geopolymers are materials synthesized by alkaline activation of aluminosilicate at room temperature. Aluminosilicates were obtained from industrial wastes, calcined clays, natural minerals or mixtures of two or more of these materials. Two solutions exist to activate the chemical reaction: the first one based on the use of water glass solutions and the second one making in situ alkaline silicate solution by dissolution of silica in an alkaline medium. The aim of this work is to determine the silicon rate needed in the typical formulation of a geopolymer binder. Then, this study is focused on two types of silica source: amorphous silica and crystallized silica. The use of current geomaterial like sand aims at reducing again the production costs of final materials. Geopolymers were prepared from a mixture containing alkaline silicate solution and metakaolin. The alkaline silicate solution was obtained by dissolution of KOH pellets in water. Several compositions containing 100% of amorphous silica to 100% of sand were attacked by alkaline solution. Finally, the metakaolin was added to the alkaline mixture leading to the gel formation. After characterization of synthesized material, geopolymers working are investigated. Moreover, the influence of the silica used was also performed in term of dissolution by FTIR and thermal analysis. The first results show the interest to use both types of silica.

### 3:20 PM

#### (ICACC-FS1-004-2012) Advanced Characterization of Geopolymer Pore Architecture Using Gas Adsorption

K. Cychosz\*, Quantachrome Inc., USA; T. Metroke, Universal Technology Corporation, USA; M. Thommes, Quantachrome Inc., USA; M. Henley, Air Force Research Laboratory, USA

Geopolymer synthesis results in the formation of a mesoporous gel product. Gas adsorption is the most popular method to obtain surface area, pore size distribution, and porosity information from porous solids. Recently, significant progress was achieved in understanding of the adsorption and phase behavior in ordered micro- and mesoporous materials with simple pore geometries. This led to major advances in structural characterization by physical adsorption, particularly due to development and availability of theoretical approaches based on advanced statistical mechanics such as non-local density functional theory (NLDFT). However, questions remain concerning the structural characterization of more-complex porous systems, such as geopolymers, which exhibit interesting pore condensation and hysteresis behavior. A combination of phenomena such as delayed pore condensation, pore blocking/percolation, and cavitation-induced evaporation have been observed, which is reflected in characteristic types of adsorption hysteresis. Adsorption hysteresis introduces considerable complication into pore size analysis by physical

adsorption but, if interpreted correctly, provides important information about the pore structure/network. We will discuss the application of state-of-the-art physical adsorption methods for comprehensive characterization of the pore structure of geopolymers.

### 3:40 PM

#### (ICACC-FS1-005-2012) Porosity Characteristics of Geopolymers: Influence of Synthesis Conditions

T. Metroke\*, Universal Technology Corporation, USA; M. Thommes, K. Cychosz, Quantachrome Inc., USA; M. Henley, Air Force Research Laboratory, USA

Nitrogen adsorption was used to characterize the porosity of geopolymers as a function of synthesis conditions including reactivity of the source material (metakaolin or fly ash), alkalinity, and curing conditions (23–90°C). In general, geopolymer synthesis results in formation of a mesoporous gel product independent of source material. Alkalinity used during synthesis influenced porosity of the gel product, which was predominately nonporous at low alkalinity and mesoporous at higher alkalinity. Comparison of non-local density functional theory (NLDFT) pore size distribution curves derived from adsorption and desorption nitrogen isotherms revealed that fly-ash-based geopolymers exhibited a larger fraction of blocked pores than analogous materials prepared from metakaolin, which correlates with the higher compressive strengths observed for fly ash-based materials. Increasing cure temperature and time resulted in a reduction in surface area and cumulative pore volume of geopolymers that we attribute to promotion of thermally induced silicate–aluminates or silicate–silicate condensation. The results of this study show that the porosity of the mesoporous geopolymer gel product, including pore architecture, surface area, cumulative pore volume, and pore size distribution are influenced by the reactivity of the source material, alkalinity and curing conditions used during synthesis.

### 4:00 PM

#### (ICACC-FS1-006-2012) Lime-potassium carbonate as an alkali activator for untreated kaolinite (Invited)

H. Rahier\*, M. Esayfan, Vrije Universiteit Brussel, Belgium; H. Khoury, University Jordan, Jordan; T. Tysmans, J. Wastiels, Vrije Universiteit Brussel, Belgium

An alternative alkali activator is studied. Kaolinite can chemically react with alkaline solutions such as NaOH or KOH solutions. The use of these solutions is however not without safety risks if the material is intended to be used by workers in the field. Ca(OH)<sub>2</sub> combined with K<sub>2</sub>CO<sub>3</sub> (or Na<sub>2</sub>CO<sub>3</sub>) is found to be an alternative activator. Besides solving the problem of working with an alkaline solution, an advantage of this system is that all the reactive components can be mixed in the dry state and only water needs to be added to start the reactions, as what is done for ordinary Portland cement. In this study first the reaction between Ca(OH)<sub>2</sub> and K<sub>2</sub>CO<sub>3</sub> in aqueous solution is studied since information on this reaction is scarce in literature. Next to KOH a double salt is formed, containing Ca and K. This implies that using this alkali activator, a larger amount of K will be needed to reach the same reactivity as when pure KOH is used. The reactions are pretty slow (timescale of days at room temperature). Some preliminary results of the materials made with this activator combined with kaolinite will be shown. A compressive strength of over 30MPa can be obtained for dried specimen, but the strength drops by a factor 3 in wet conditions. This alkali activator is promising and further work will be done to optimize the properties of the obtained materials.

### 4:30 PM

#### (ICACC-FS1-007-2012) Geopolymerization technology for manufacture of cold setting building materials (Invited)

B. D. Nayak, S. D. Muduli, D. S. Rao, B. Mishra\*, CSIR-IMMT, India

Geopolymerization technology is a non-fired process and has been developed to treat industrial wastes like fly ash, red mud, blast furnace slag and beneficiated tailings to make value added product.

Durable and high strength building bricks, blocks, concrete, tiles, etc., can be manufactured. The geopolymers can be produced by mixing aluminosilicates as reactive materials with calcium, magnesium, and iron bearing constituents under alkaline condition to form hydrous structures of rock forming silicate minerals at atmospheric temperature. Under a strongly alkaline condition aluminosilicate type reactive materials rapidly dissolve to form free SiO<sub>4</sub> and AlO<sub>4</sub> tetrahedral units. With the progress of reaction, the weakly bridged water is gradually displaced and the SiO<sub>4</sub> and AlO<sub>4</sub> tetrahedral units link alternatively to yield polymeric precursors by sharing oxygen atoms between two tetrahedral units, and thereby form monolithic geopolymers. Here we discuss research results pertaining to development of a sustainable green technology based on geopolymerization for effective utilisation of industrial solid wastes to manufacture cementation and other building materials.

**5:00 PM**

**(ICACC-FS1-008-2012) PVA-fibre reinforced fly-ash based geopolymer composites (Invited)**

K. Krnel\*, N. Petkovic, T. Kosmac, Jozef Stefan Institute, Slovenia

Inorganic polymer concretes, or 'geopolymers,' have emerged as novel engineering materials with the potential to form a substantial element of an environmentally sustainable construction and building products industry. These materials are formed by an alkali activation of natural or synthetic aluminosilicates or industrial aluminosilicate waste materials such as coal ash and blast furnace slag, and, have a very small Greenhouse footprint when compared to traditional concretes. Since these materials are still brittle, for the production of building elements the product will require fibre reinforcement. Much to a surprise, only small amount of research work was done on the properties of fibre reinforced geopolymers, and is mostly focused on carbon and basalt fibres. The aim of this work is to develop an inorganically bonded fibre-reinforced composite that will be suitable for the production of a new generation of building elements preferably using industrial by products such as fly-ash. A concept of using the recycled fibre-cement composite materials as the fillers and fibre source for the production of fibre reinforced geopolymers will also be shown.

**Friday, January 27, 2012**

## **S1: Mechanical Behavior and Performance of Ceramics & Composites**

### **Tribological Applications**

Room: Coquina Salon D

Session Chair: Maria De La Cinta Lorenzo-Martin, Argonne National Laboratory

**8:30 AM**

**(ICACC-S1-077-2012) Tribological Behaviour of Ceramics Laminates Containing Residual Stresses (Invited)**

G. de Portu\*, ISTECC-CNR, Italy

The performances of wear-resistant materials are mainly related to the properties of thin surface layers. Since the removal of material in engineering ceramics under sliding conditions is generally caused by the propagation of surface cracks resulting from tensile stresses in the wake of rubbing contact, an increase in apparent surface toughness should lead to an improvement in wear resistance. The presence of compressive residual stresses on the surface of a component, can lead to an improvement of toughness. The production of laminated structures designed to induce compressive residual stresses at the surface by combining the different thermo-physical characteristics (i.e. thermal expansion and shrinkage on sintering) of the different materials used can be an effective way for achieving the goal. Tape casting technique was used to prepare symmetrical hybrid laminated structures. The values of residual stresses in the different layers were determined by piezo-spectroscopic technique using the fluorescence of alumina.

Both sliding and abrasive wear were studied. It was observed that, within a defined range of experimental conditions, the presence of compressive surface stresses, generated by symmetrical lamination of Al<sub>2</sub>O<sub>3</sub> and Al<sub>2</sub>O<sub>3</sub>-ZrO<sub>2</sub> layers, can improve both the sliding and abrasive wear resistance of alumina.

**9:00 AM**

**(ICACC-S1-079-2012) Use of ceramic sliding systems in a prototype gasoline pump with operating pressures of up to 80 MPa**

C. Pfister\*, H. Kubach, U. Spicher, Karlsruhe Institute of Technology, Germany

The fuel consumption of modern combustion engines can be significantly reduced through the use of gasoline direct injection (GDI). As the time for mixture preparation in GDI engines is very short, the fuel has to be injected at high pressure into the combustion chamber. Modern injection systems provide an injection pressure of up to 20 MPa, whereas investigations performed at the Karlsruhe Institute of Technology have shown strong potential for reduced pollutant emissions by increasing the pressure to 80 MPa. However, the low lubricity of gasoline causes severe friction and wear in the high-pressure pump at fuel pressures above 20 MPa. The use of ceramic components in the sliding systems should help to overcome this limitation. A 3-piston radial pump based on ceramic sliding systems that delivers fuel at up to 80 MPa has been designed at Karlsruhe Institute of Technology. The prototype is based on the knowledge accumulated during former investigations performed on a single-piston pump. It is fitted with pressure and temperature sensors in each cylinder and a torque sensor on the driveshaft in order to measure its efficiency with various material combinations in its sliding systems. The results show that the use of silicon carbide or sialon enable operation at injection pressures of up to 80 MPa with very good mechanical efficiency and low wear.

**9:20 AM**

**(ICACC-S1-078-2012) Real time performance of carbide based cermets versus hardened/alloy steels for cutting tool applications**

A. Ozer, Y. K. Tur, Gebze Institute of Technology, Turkey; W. M. Kriven\*, University of Illinois at Urbana-Champaign, USA

Real time cutting performances of Cr<sub>3</sub>C<sub>2</sub>-NiCr cermet inserts with/without reinforcements and hardened steel cutting inserts were investigated by means of edge sensitivity of inserts, wear-debris formation, effect of reinforcements on wear characteristics against low carbon steel and brass counterfaces. Scanning electron microscopy (SEM) was employed to characterize the wear surfaces and tracks. Energy dispersive spectroscopy was also applied to approve oxide formation. To obtain the most reliable composition among the studied structures, the overall mechanical property comparison was studied.

**9:40 AM**

**(ICACC-S1-080-2012) Grain Size Dependence of Nanoindentation and Nanoscratch Behavior in Polycrystalline Alumina Fabricated by Spark Plasma Sintering**

L. Huang\*, W. Yao, Y. Xiong, A. K. Mukherjee, J. M. Schoenung, UC Davis, USA

Recently, the mechanical properties of ceramic materials with reduced grain sizes have received more attention, especially materials with ultrafine grain sizes. The fraction of grain boundaries dramatically increases with the reduction in grain size, which can cause changes in mechanical properties compared with conventional counterparts with coarser grains. In an effort to systematically study the grain size dependence of the mechanical properties from nanoindentation and nanoscratch tests in alumina ceramics, the spark plasma sintering technique has been applied to fabricate dense alumina ceramics with average grain sizes ranging from 290 nm to 1.3 microns. The data generated in the nanoindentation and nanoscratch processes have been compared in detail by utilizing optical microscopy, scanning electron microscopy (SEM) and atomic force microscopy (AFM). Results show that grain refinement to the ultrafine

grain size regime in alumina ceramics can improve both the mechanical properties and plastic deformation capability at the nano- and micro-scale.

#### 10:00 AM

##### (ICACC-S1-081-2012) The fretting wear response of TiC and Ti(C,N) cermets prepared with a ductile Ni<sub>3</sub>Al binder

S. Buchholz, Z. N. Farhat, G. J. Kipouros, K. P. Plucknett\*, Dalhousie University, Canada

The fretting wear behaviour of titanium carbide (TiC) and titanium carbonitride (Ti(C,N)) based ceramic-metal composites, (or cermets) using a ductile nickel aluminide (Ni<sub>3</sub>Al) binder, has been assessed. Three Ti(C,N) compositions have been studied (TiC<sub>0.7</sub>N<sub>0.3</sub>, TiC<sub>0.5</sub>N<sub>0.5</sub> and TiC<sub>0.3</sub>N<sub>0.7</sub>), along with pure TiC, using Ni<sub>3</sub>Al contents from 20 to 40 vol.%. The cermets were densified using a simple vacuum melt-infiltration technique, and invariably retained grain sizes of ~2 μm. Fretting wear was measured using the 'ball-on-disc' testing geometry, with a tungsten carbide/cobalt ball, and loads between 20 to 80 N. A comparison of the wear behaviour for varying loads, applied times, and the general trends between differing materials will be outlined. The influence of microstructural flaws, such as voids, on the wear response will also be briefly discussed.

#### 10:20 AM

##### (ICACC-S1-082-2012) Development of Nickel Coated Carbon Fiber Reinforced Stellite Alloy Based Composites

A. Khoddamzadeh\*, R. Liu, Carleton University, Canada; M. Liang, University of Ottawa, Canada

This paper reports the design and development of a group of nickel-coated carbon fiber reinforced Stellite 25 composites. The focus of this research is on obviating the problems related to the carbides in Stellite alloys due to the presence of carbon. The attempt is made to incorporate carbon fiber into a low-carbon Stellite alloy so that the amount of carbides can be minimized while the alloy still has equivalent wear resistance to wear-resistant Stellite alloys. Stellite 25 was selected as the matrix because of its very low carbon content (0.1 wt%) and thereby relatively carbide free microstructure. The nickel coating is intended to eliminate any chance of carbide formation due to the possible reaction between carbon fibers and alloying additions in the matrix. The metal matrix composite specimens are produced using the hot isostatic pressing (HIP) and sintering techniques. The density, tribomechanical and corrosion properties of the composites are characterized. The results show that the developed composites exhibit better corrosion resistance than medium carbon Stellite alloys. The addition of carbon fibers into Stellite 25 lowers its tensile properties, while improves its tribological properties. The wear resistance of the composites is better than that of medium-carbon Stellite alloys and comparable with that of high-carbon Stellite alloys.

#### Characterization

Room: Coquina Salon D

Session Chairs: Maria De La Cinta Lorenzo-Martin, Argonne National Laboratory; Goffredo de Portu, ISTECCNR

#### 10:40 AM

##### (ICACC-S1-083-2012) Torsion tests on joined SiC

M. Ferraris\*, A. Ventrella, M. Salvo, M. Avalle, Politecnico di Torino, Italy

Results of an experimental investigation on epoxy-joined SiC tested in torsion will be presented. Torsion tests are proposed in ASTM F734-95 (2006) and ASTM F1362-09, but none of them is directly applicable to joined ceramics; these two ASTM standards have been adapted to joined SiC, by preparing butt-joined cylinders, tubes, and hourglass-shaped samples. Silicon carbide samples have been joined by an epoxy adhesive (AV119), which is a model brittle joining material chosen to obtain several joined samples in a reasonable time. Advan-

tages and disadvantages of each configuration are discussed and compared. Torsion test seems to be one of the most appropriate test for the determination of the shear strength of joined ceramics.

#### 11:00 AM

##### (ICACC-S1-084-2012) Investigation of Compression Strengths of SiC(0001) and ZrC(001) Micropillars

S. Kiani\*, J. Yang, S. Kodambaka, UCLA, USA

Ultra-high temperature ceramics (UHTC) possess excellent high temperature oxidation resistance and chemical stability of monolithic ceramics with the added toughness and light weight and hence are of great importance for the construction of space vehicles and hypersonic flights. Further improvement in their thermochemical and thermomechanical properties is desirable for the development of next generation spacecrafts. Recent studies have indicated that nanostructured bulk composites can exhibit significantly improved properties. Design of new materials and/or structures that can advantage of nanoscale phenomena, however, requires a thorough understanding of the fundamental processes influencing the chemical and mechanical properties. Therefore, as a first step, we focused on the effect of size on the mechanical properties of UHTCs. To this purpose, we chose single-crystalline SiC and ZrC and studied the compression strength of one-dimensional pillars. Using focused ion beam milling, cylindrical pillars were fabricated on SiC(0001) and ZrC(001) substrates. The pillars were then subjected to compression in a MTS Nanoindenter XP system. Interestingly, we found that the strengths of both the SiC and ZrC pillars increased with decreasing diameter and are higher than their bulk counterparts. These results provide new insights into the deformation mechanisms of monolithic refractory carbides.

#### 11:20 AM

##### (ICACC-S1-085-2012) Micromechanical properties of aligned and continuous multi-walled carbon nanotube/aluminoborosilicate glass composites

G. Otieno\*, A. Koos, F. Dillon, N. Yahya, N. Grobert, R. I. Todd, University of Oxford, United Kingdom

Previous attempts to produce carbon nanotube (CNT) ceramic composites have resulted in poorly dispersed, unaligned and non-continuous CNTs in the composites with modest improvements in properties. This presentation reports the production of dense aluminoborosilicate (ABS) glass matrix composites containing aligned and continuous multiwalled carbon nanotubes (MWCNT) of up to 5mm in length. This was achieved by infiltrating CVD grown MWCNT preforms using a precursor sol and hot pressing. Fracture surfaces showed apparent MWCNT pullout lengths of ~ 1 micron, which is an order of magnitude greater than in randomly orientated CNT/ABS composites. This was thought to be due to the alignment of the MWCNTs. Microcantilever bend tests on beams of length approximately 20 microns showed limited "graceful failure" with bend strengths of 1.8 to 2.8 GPa, elastic modulus of 45 to 62GPa and fracture toughness (KIC) of 1.6 to 1.7 MPa/m<sup>1/2</sup>. Although the mechanical properties represent improvements compared with the unreinforced matrix (e.g. a factor of 2 in toughness), analysis indicates that interlayer sliding of the MWCNTs and the observed "sword in sheath" failure mechanism of the MWCNTs prevent the maximum potential performance from being achieved.

#### 11:40 AM

##### (ICACC-S1-086-2012) Quantification of Grinding-Induced Phase Changes in Y-TZP

M. Strasberg\*, A. A. Barrett, K. J. Anusavice, J. J. Mecholsky, J. C. Nino, University of Florida, USA

Zirconia-based dental prostheses undergo various grinding steps and heat treatments in preparation for final cementation in patients. These steps may ultimately induce a tetragonal-to-monoclinic phase

transformation that is not fully recoverable by current annealing heat treatment (regeneration) protocols, thereby yielding a prosthesis with a lower resistance to fracture than anticipated. Post-sintered grinding simulation was performed by automated wet polishing using varying applied loads (10-40 N) and three sizes of diamond grinding particles (15  $\mu\text{m}$ , 45  $\mu\text{m}$ , 70  $\mu\text{m}$ ) on PS e.max ZirCAD (Ivoclar Vivadent, Schaan, Liechtenstein), a polycrystalline yttria-stabilized zirconium oxide containing less than 1% alumina by weight. These idealized conditions are less aggressive than what is used in practice. Grazing incidence x-ray diffraction reveals a presence of monoclinic phase on the ground zirconia surface, which increases with an increase in particle size of the grinding media and the applied load. The amount of transformation is determined as a function of depth. Regeneration recovers most of the change to the tetragonal phase. However, current industry protocol does not require regeneration under the grinding conditions imposed. The effects of grinding and regeneration on the mechanical properties are discussed.

**12:00 PM**

### **(ICACC-S1-087-2012) Study on the stiffness of comeld composites joints**

H. Zhang\*, W. Wen, H. Cui, Nanjing University of Aeronautics and Astronautics, China

It is well known that the joint is one of the weakness points. Comeld is a novel technology which can be applied in connecting composites and metals. However, there are no papers or reports about the study on its mechanical properties. As the directions of the fiber and the distributions of the matrix are changed during comeld process, the mechanical properties of comeld composites joints vary from the un-comeld composites. In this paper, the geometry features of the typical microstructure of comeld composites joints are studied. Then a stiffness prediction model is developed and used to predict the stiffness of the comeld composite joints.

## **S2: Advanced Ceramic Coatings for Structural, Environmental, and Functional Applications**

### **Advanced Processing and Protective Coating Systems for Extreme Environments**

Room: Ponce de Leon

Session Chairs: Houzheng Wu, Loughborough University; Byung-Koog Jang, National Institute for Materials Science

**8:20 AM**

### **(ICACC-S2-039-2012) Growing Integration Layer [GIL] Method: Direct Fabrication of Compositionally, Structurally and Functionally Graded Ceramic Films and/or Coatings from Mother Materials in Solution (Invited)**

M. Yoshimura\*, National Cheng Kung University, Taiwan; N. Matsushita, Tokyo Institute of Technology, Japan

In the fabrication of graded [Compositionally, Structurally and Functionally] ceramic materials and/or ceramic/metal, to overcome weak interfacial bonding and poor adhesion of ceramic layers, we propose a novel concept and technology of the formation "Growing Integration Layer" [GIL] between ceramics and metallic materials. Those GIL(s) can be prepared via integration of ceramic film formation from a component of the metallic materials by chemical and/or electrochemical reactions in a solution at low temperature of RT-200 C. They have particular features: 1) Widely diffused interface(s), 2) Continuously graded layers grown from the bulk (substrate), 3) Low temperature process, etc. BaTiO<sub>3</sub> or SrTiO<sub>3</sub>/TiO<sub>x</sub> GIL films on Ti plates formed by hydrothermal-electrochemical method showed good adhesion. CaTiO<sub>3</sub>/Al<sub>2</sub>O<sub>3</sub>/Ti<sub>2</sub>Al GIL films on TiAl exhibited excellent

adhesion and anti-oxidation performances. The GIL strategy is effective for many metallic alloys and bulk metallic glasses because they generally contain active component(s). On a Ti-base Bulk Metallic Glass, we could succeed to prepare bioactive titanate nano-mesh layer by hydrothermal-electrochemical techniques at 90-120 C [2]. The GIL methods are applicable for various functional and structural ceramics layers.

**9:00 AM**

### **(ICACC-S2-040-2012) Acoustic field assisted drying of electrophoretically deposited green bodies for ceramic coatings**

C. Ji, H. Wu\*, Loughborough University, United Kingdom

Ceramic green bodies with a thickness from tens microns to a few millimeters can be manufactured through electrophoretic deposition on various substrates to produce ceramic coating after heat treatment. Whilst the merits in economic and technical sides are obvious for this manufacturing process, drying of as-deposited preforms is often problematic in controlling possible cracking likely induced by the in-plane tensile introduced by shrinking during the evaporation of solvent from the preforms. It was found that for a given range of particle size and substrate, there existed a critical thickness that above it, cracking started; underneath it, no cracking appeared during drying. With the assistance of acoustic field, generated by an ultrasonic generator, the aforesaid cracking was significantly mitigated and the critical thickness was notably raised. In this paper, the effect of particle sizes on the critical thickness was quantified under chosen depositing and drying conditions with and without acoustic field. The green bodies were characterized to examine the impact of acoustic field, and its frequency on the packing of the particles. Possible mechanisms on the development of drying cracking and the role of acoustic field in mitigating this phenomena were discussed.

**9:20 AM**

### **(ICACC-S2-041-2012) Failure Mechanism and Reliability of Pt-Pt/Rh Temperature Sensor in Extreme Environments**

E. Allain, Watlow R&D, USA; H. Lin\*, Watlow Sensor Division, USA

Pt-Pt/Rh thermocouple (TC) has long been used in high temperature processing environments for providing feedback signal for temperature control. Recently the thermocouple is used extensively by solar energy industry for controlling polycrystalline Si ingot growth furnaces. The environment of Si growth furnaces is characterized by significant Si vapor pressure while a complex atmosphere containing Mg, Al, Si, K... etc, is present inside the Al<sub>2</sub>O<sub>3</sub> protection tube where the TC resides. The high temperature (> 1500 C) and corrosive environment often lead to premature TC failure that jeopardizes the quality of Si ingot. Typical failure mode includes gradual drift of output signal or totally open circuit. Close examination of failed TC wire reveals: 1. Evidences of grain growth; 2. Presence of significant amount of Si on the failed TC wires; 3. Deposits of spherical and acicular phases as Si-Mg-O and Si-Al-O respectively and layer structured compounds (Si-Mg-Pt-O and Si-Al-Pt-O) on TC wires; 4. Necking of TC wires at broken ends. A Si corrosion mechanism was proposed and similar TC failure and corrosion phenomena were recreated in lab environment by reacting Si vapor and TC at high temperatures in Ar atmosphere. Based on this work, design strategy to improve service life of TC including protective coating was implemented and preliminary accelerated life cycle tests indicate promising results.

**10:00 AM**

### **(ICACC-S2-042-2012) Improvement in corrosion resistance of reaction bonded Si<sub>3</sub>N<sub>4</sub>-SiC ceramics to molten aluminum alloy using oxide coatings**

M. Wada\*, K. Kashiwagi, S. Kitaoka, Japan Fine Ceramics Center, Japan

Reaction bonded Si<sub>3</sub>N<sub>4</sub>-SiC refractory ceramics (SNC) is lightweight, and shows excellent thermal resistance and chemical durability in molten Al alloys. SNC is therefore being applied to tools and jigs for Al casting processes. However, when SNC is used as the container

material for the molten alloy transfer, cyclic contact with molten Al alloy results in strong adhesion of the slag to the SNC surface. In this study, an oxide-based multi-layer coating was developed for SNC for improving corrosion resistance of SNC in a molten Al alloy. The coating material consisted of SNC substrate / amorphous  $\text{SiO}_2$  /  $\alpha\text{-Al}_2\text{O}_3$  /  $\text{MgAl}_2\text{O}_4$ . The  $\text{SiO}_2$  layer was formed by pre-oxidization of SNC as a binding layer of sol-gel coating layers. The  $\text{Al}_2\text{O}_3$  layer was formed by sol-gel deposition as a diffusion barrier against cations derived from the molten alloy. The  $\text{MgAl}_2\text{O}_4$  layer that possesses excellent corrosion resistance to the molten Al alloy was deposited by sol-gel technique as a topcoat layer. The corrosion behavior of the multi-layered specimen against the molten Al alloy was investigated by static immersion tests at 993 K. It was found that the introduction of the  $\text{Al}_2\text{O}_3$  interlayer contributes to improving the corrosion resistance of the coated samples, and the alloy ingot could be easily separated from the contact surface of the multi-layered specimen after the immersion test.

10:20 AM

**(ICACC-S2-043-2012) Characterization of sealing treatments on the behavior of aluminium phosphate sealed plasma – sprayed alumina coatings operating in extreme environment**

A. Joly\*, P. Brun, J. Lacombe, Commissariat à l'énergie atomique, France; G. Tricot, Université des Sciences et Technologies de Lille, France; A. Denoirjean, Centre Européen de la Céramique, France; S. Rossignol, Centre Européen de la Céramique, France

Alumina coating deposited by thermal spraying, provides an insulating barrier power. The analysis of past experience shows that the impregnation of an aluminum phosphate deposit is a workaround for the failure of the ceramic seal. This process optimizes the properties of the plasma coating of alumina and seals open and / or interconnected porosities produced during the thermal spraying. The resistance of this coating is tested on samples in order to observe their behaviour in aggressive conditions. This study focuses on the structural characterization of alumino-phosphates materials obtained by the thermal process of a mono-aluminum phosphate solution (MALP). The training protocol is characterized by the molar ratio of phosphorus / aluminum and depends on the heating rate, temperature and isothermal duration. These parameters may result into different kind of compounds. Initially, a study on the MALP solution was conducted to determine the effects of the training protocol parameters. In a second step, a study was conducted on samples of alumina projected plasma and impregnated with a MALP solution. In order to qualify and quantify the physical and chemical properties of these deposits, thermal and electrical test benches are used as well as technical characterization of  $^{31}\text{P}/^{27}\text{Al}$  nuclear magnetic resonance.

10:40 AM

**(ICACC-S2-044-2012) Electrochemical and morphological study on nanoceramic based conversion coating on CRS: The effect of solution pH**

H. Eivaz Mohammadloo\*, A. Sarabi, Amirkabir university of technology, Islamic Republic of Iran; A. Sabbagh Alvani, Color and Polymer Research Center, Amirkabir University of Technology, Islamic Republic of Iran; R. Salimi, H. Sameie, Amirkabir university of technology, Islamic Republic of Iran

The effect of solution pH on anti-corrosion and morphological properties of nanoceramic based conversion coating was investigated. Experimental: Cold rolled steel (CRS) sheets were chosen to investigate conversion coating properties. The pH of all treatment solutions was adjusted by addition of Parco® Neutralizer 700. 4% vol of Bonderite NT-1 used for each treatment solutions. Results and Discussion: Results obtained from polarization curves, reveal that sample treated in pH=4.5 has lowest corrosion current density ( $I_{\text{corr}}=6.158 \mu\text{A}/\text{cm}^2$ ) following by pH=3.5 ( $I_{\text{corr}}=6.556 \mu\text{A}/\text{cm}^2$ ) and pH=5.5 ( $I_{\text{corr}}=6.884 \mu\text{A}/\text{cm}^2$ ). The EIS results are presented in Fig 2.a – c. sample that treated in pH=4.5 is more effective compared to pH=3.5 and pH=5.5. Fig 3.a – c shows FE-SEM micrographs of samples

treated in different solution pH. With increasing pH from 3.5 to 5.5 the surface morphology changed and samples treated in solution pH of 4.5 and 5.5 have similar morphological structure. SEM micrographs clearly show existence of a precipitated layer on the surface for pH=4.5 and 5.5. This layer can increase anti-corrosion performance. Conclusion: According to DC polarization and EIS data, sample treated in pH=4.5 had best anti-corrosion performance and FE-SEM micrographs showed existence of a precipitated layer on the surface that can increase anti-corrosion performance.

## S3: 9th International Symposium on Solid Oxide Fuel Cells (SOFC): Materials, Science and Technology

### Novel Processing Approaches for Cell and Stack

#### Materials

Room: Coquina Salon H

Session Chair: Amit Shyam, Oak Ridge National Laboratory

8:00 AM

**(ICACC-S3-034-2012) Fabrication of Cathode Layer by Non-contact Printing Process**

K. Kikuta\*, N. Yashiro, S. Ayabe, Nagoya University, Japan

Non-contact printing process was applied for the preparation of cathode layer on GDC/Ni-GDC bi-layer. In order to control the composition and the microstructure of the cathode layer, several kinds of ceramic slurries were prepared from LSCF and GDC powders. In the present work, preparation of ceramic slurries was studied by changing the conditions. SEM observation revealed that large difference in grain size between LSCF and GDC leads to the inhomogeneous microstructure due to the large force by collision, leading to poor cell performance. This inhomogeneous structure was improved by adjusting the size distribution of these powders. It is also required to obtain adequate porous microstructure by the addition of pore former such as carbon black. Non-contact print process can be used for making a thin layer even on the curved substrate without a screen. A thick layer more than 20 microns was prepared on a tubular cell by the dispenser print which is useful for the viscous slurries.

8:20 AM

**(ICACC-S3-035-2012) Current Developments in Solid Oxide Fuel Cell Development at Forschungszentrum Juelich**

R. Steinberger-Wilckens, L. Blum, H. Buchkremer, L. Haart, J. Malzbender\*, M. Pap, Forschungszentrum Juelich, Germany

The SOFC group at FZJ has assembled and tested more than 400 SOFC stacks to date, rated between 100 W and 15 kW. The research topics cover materials and thin layer deposition, stack design, manufacturing of cells and stacks, mechanical and electrochemical characterisation, up to system design and demonstration. The use of improved steels, coatings and cathodes has resulted in reduced degradation rates around 10 mV (~1%) per 1000 hours at 700°C and 500 mA/sqcm over tested stack lifetimes of over 35 000 hours. However, the target of development is directed at even further lowered degradation for commercial operation in stationary applications. A stack with improved protective coating reached an operating time of 20 000 hours with an average degradation of approx. 5 mV (0.5%) per 1000 hours running at 800°C and 500 mA/sqcm. The follow-up, operating at 700°C is showing similarly promising behaviour. If the latter results were extrapolated to the end-of-life, this stack would be able to fulfill 80 000 hours of continuous operation. Not having proven this result experimentally, though, this still remains speculation. Further work concerns the thermo-mechanics of lightweight stacks and stacks for stationary applications, the further reduction of operating temperature by applying thin layers, and the proof-of-concept for a high-performance, robust stack of 2 kW rating.

8:40 AM

### (ICACC-S3-036-2012) Enhanced Ionic Conductivity of CeO<sub>2</sub>-YSZ Nanocomposite Electrolyte

A. Gupta\*, S. Sharma, S. Omar, K. Balani, Indian Institute of Technology Kanpur, India

In an effort to develop novel electrolyte materials, the present work explores oxide-ion conduction behaviour through the interface of CeO<sub>2</sub>-YSZ grains. The CeO<sub>2</sub>-YSZ nano-composites have been synthesized and tested at intermediate temperatures. Polycrystalline samples of 8 mol. % YSZ with different CeO<sub>2</sub> content (5 mol. % and 10 mol.%) were fabricated using conventional sintering and spark plasma sintering (SPS). The particle size for both the starting powders is in the sub-nano range. The samples synthesized using SPS technique with lower sintering parameters (1200 C, 5 min holding time) exhibited comparatively lower density than that of conventionally sintered samples (1450 C, 4 h holding time). Relative theoretical density for all samples was above 96%. Phase and microstructural analysis indicated the formation of CeO<sub>2</sub>-YSZ solid-solution when fabricated using conventional sintering, while CeO<sub>2</sub> forms nano-composite with 8YSZ when synthesized via SPS. The ionic conductivity measurement was performed using AC impedance spectroscopy in air from 300 to 700°C. We will discuss the conductivity behavior of the nano-composites of CeO<sub>2</sub>-8YSZ and compare the result with the solid-solution of similar compositions.

9:00 AM

### (ICACC-S3-037-2012) Synthesis and Calorimetric Studies of La<sub>9.33+x</sub>(Si/GeO<sub>4</sub>)<sub>6</sub>O<sub>2+3x/2</sub>: Fast Oxide Ion Conductors

S. Hosseini\*, A. Navrotsky, University of California, Davis, USA

Lanthanum silicate/germanate oxyapatite materials, La<sub>9.33+x</sub>(Si/GeO<sub>4</sub>)<sub>6</sub>O<sub>2+3x/2</sub>, are attracting interest as a new family of fast oxide-ion conductors with potential use in solid oxide fuel cells (SOFCs), oxygen sensors and, ceramic membranes. The most attractive feature of these materials is their high conductivity at a relatively low temperature compared to conventional oxide ion conductors. Their complex structure brings a new conduction mechanism, interstitial oxide ion conduction, which makes them exciting candidates for solid electrolyte research. Recent studies have reported that the non-stoichiometric compositions with cation vacancies or oxygen excess show higher conductivity than the stoichiometric system. In this study, lanthanum silicate and lanthanum germanate materials, La<sub>9.33+x</sub>(SiO<sub>4</sub>)<sub>6</sub>O<sub>2+3x/2</sub> and La<sub>9.33+x</sub>(GeO<sub>4</sub>)<sub>6</sub>O<sub>2+3x/2</sub> (0 ≤ x ≤ 0.67), have been synthesized by solid state reaction method. To study the thermodynamic stability of these materials, energetic studies have been done by high temperature oxide melt solution calorimetry using molten 2PbO-B<sub>2</sub>O<sub>3</sub> solvent at 1078 K.

9:20 AM

### (ICACC-S3-038-2012) Sr Doped LaPO<sub>4</sub> Monazite for Proton Conductivity

J. P. Angle\*, M. Ng, P. Morgan, M. L. Mecartney, UC Irvine, USA

LaPO<sub>4</sub>, monazite is a promising electrolyte material for intermediate temperature proton conducting fuel cells and for humidity sensing. Studies have shown that proton conduction improves with increasing strontium content but higher doping levels can result in Sr rich second phase(s) formation. In this study, a unique synthesis route was utilized via low temperature direct precipitation of monoclinic monazite (viz. not rhabdophane) doped with 0, 5, 10 and 15% strontium. Using this low temperature synthesis, higher doping concentrations of Sr are achieved by allowing in-situ protons to remain within the monazite structure and preventing Sr segregation as a second phase(s). Dense compacts of La(1-x)Sr<sub>x</sub>PO<sub>4</sub>-x(OH)<sub>x</sub> (x = 0, 0.05, 0.1, 0.15) were successfully formed by sintering at low temperatures in a proton rich environment. X-ray diffraction (XRD) and chemical analysis by energy dispersive x-ray spectroscopy (EDS) defined the Sr solubility limit in LaPO<sub>4</sub>. Results from electrochemical impedance

spectroscopy (EIS), done in environments with varying proton concentrations will be used to show the effect Sr-doping has on the proton conductivity.

### Cell Component, Cell Design and Reliability

Room: Coquina Salon H

Session Chairs: Nguyen Minh, Consultant; Jeffrey Stevenson, PNNL

10:00 AM

### (ICACC-S3-039-2012) Processing of CGO electrolyte layers with a thickness of ~1 μm: thin film wet coating methods and PVD

T. Van Gestel\*, F. Han, H. Moon, S. Uhlenbruck, H. Buchkremer, Forschungszentrum Jülich, Germany

In this paper, two thin film processing methods are evaluated that can deliver thin CGO electrolyte layers. These include wet coating of nanoparticles (e.g. spin-coating, dip-coating) and physical vapour deposition (PVD). Previously, impressive results have already been achieved at our institute with these methods, including the preparation of 5 x 5 cm<sup>2</sup> cells composed of our regular Ni/8YSZ anode substrate, a 1 μm thick 8YSZ electrolyte layer and a LSCF cathode, which show a power output > 1 W/cm<sup>2</sup> at 650°C. Further lowering the operation temperature to the range 400–600°C requires the use of even thinner 8YSZ electrolytes or an alternative electrolyte material, e.g. CGO. In this contribution, the development of 1 μm thick CGO layers is described. Results from He leakage tests of such layers, made by a wet coating process and a sintering at 1400°C, confirmed the feasibility of our method (leak rate: 10<sup>-4</sup> mbar.l.s<sup>-1</sup>.cm<sup>-2</sup> range). Currently, research is directed towards a reduction of the firing temperature and the alternative of using PVD is investigated. In this paper, the different preparation routes of the CGO electrolyte layers are reported. In addition, the preparation of our first low temperature 5 x 5 cm<sup>2</sup> cells is shown and their morphology is illustrated. Finally, the performance in standard SOFC tests at 400–600°C is shown and compared with results from 8YSZ layers.

10:20 AM

### (ICACC-S3-040-2012) Low temperature proton conduction in nanocrystalline ceria

G. Gregori\*, M. Shirpour, R. Merkle, J. Maier, Max Planck Institute for Solid State Research, Germany

Electrochemical impedance spectroscopy measurements were performed on both microcrystalline and nanocrystalline ceria (undoped as well as 6 at.% gadolinium-doped) in dry and wet atmosphere. Below 200–250°C, both nanocrystalline samples (with density equal to 93% of the theoretical value) exhibit an enhanced total conductivity under wet conditions, which decreases with increasing temperature. Then, after having reached a minimum, the conductivities increase with temperature according to the water-free situation. Such findings, together with direct current measurements indicate that the nanocrystalline samples exhibit protonic conductivity at low temperatures. Remarkably, the total conductivity values below 200°C are very similar for both nanocrystalline compositions considered here, indicating that the role of the dopant is negligible with respect to the protonic conduction mechanism. In addition, the hydration behavior obtained from thermo-gravimetric analysis (performed in the same wet conditions of the EIS measurements) reveals a strong water uptake below 200°C, exactly in the same temperature range of the increased protonic conductivity. In light of these results, the role of both the grain boundaries and the residual mesosized porosity with regard to the protonic conductivity of nanocrystalline ceria is discussed.

10:40 AM

### (ICACC-S3-041-2012) Mixed conducting praseodymium cerium gadolinium oxide (PCGO) nano-composite cathode for ITSOFC applications

R. Chockalingam\*, A. Ganguli, S. Basu, Indian Institute of Technology, India

A mixed ionic and electronic conducting (MIEC) cathode based on ceria co doped with praseodymium and gadolinium oxide (PCGO) at various proportions was synthesized through wet chemical co precip-

itation method. Phase analysis of the prepared samples was performed using X-ray diffraction and microstructures of the sintered samples determined by Scanning Electron Microscopy (SEM). The XRD results show the formation of a single fluorite phase which appears to be stable up to 900 °C. A pO<sub>2</sub> dependent ionic conductivity was observed at high pO<sub>2</sub> in the PCGO composite at low temperature regions, due to the oxidation of Pr<sup>3+</sup> to Pr<sup>4+</sup>. The results of impedance measurements indicate that the Area Specific Resistance (ASR) values increases with increasing Pr content. The ASR value of PCGO is found to be significantly lower than that of conventional LSCF. The ASR value of LSCF is found to be 6.3687Ω-cm<sup>2</sup> at 550°C whereas the Ce<sub>0.80</sub>Pr<sub>0.15</sub>Gd<sub>0.05</sub>O<sub>2-δ</sub> sample shows a value 0.299 Ω-cm<sup>2</sup> at the same temperature. Praseodymium cerium gadolinium nano-composite was found to be a promising material for the application of intermediate temperature solid oxide fuel cell air electrodes.

11:00 AM

**(ICACC-S3-042-2012) High Protonic Conductivity in LaBaGaO<sub>4</sub>**

K. Huang\*, X. Zhao, N. Xu, University of South Carolina, USA

Ceramic oxide proton conductors with high conductivity are widely recognized as the promising solid electrolytes for low/intermediate solid oxide electrochemical cells. Conventional proton conductors based on BaCeO<sub>3</sub> and BaZrO<sub>3</sub> of perovskite structure have shown high protonic conductivity at T<600°C and good chemical stability with appropriate doping on the B-site. In this study, we report that LaBaGaO<sub>4</sub> of perovskite-related intergrowth structure also exhibits high protonic conductivity over a wide range of partial pressure of H<sub>2</sub>O. In particular, an order of magnitude enhancement in conductivity has been observed by increasing PH<sub>2</sub>O from 0.2% to 56%. The mechanism of proton conduction is also discussed with solid state chemistry defect model and verified by the lowered ionic conductivity in D<sub>2</sub>O.

11:20 AM

**(ICACC-S3-043-2012) Portable 100W Power Generator based on Efficient Planar SOFC Technology**

A. Poenicke\*, S. Reuber, M. Schneider, M. Stelter, A. Michaelis, Fraunhofer Institute for Ceramic Technologies and Systems IKTS, Germany

Portable power generators for camping and leisure applications require start-up times of around 30 minutes and need to achieve a life time of 3000h including 300 cycles. Preferably they operate on available fuels and have a compact and lightweight system design. Eneramic®, a portable solid oxide fuel cell (SOFC) system in the 100 Watt class will be presented. The system runs on LPG or on bio-ethanol. Due to its good thermal packaging, the system achieves gross efficiencies of 33% and a net efficiency up to 24% with off-the-shelf BoP components, which is at the forefront among those devices. With the developed prototype life time targets have been reached in stationary operation mode. The main challenges for such SOFC applications are transient operation modes and rapid start up cycles. Usually tubular cells are applied as they sustain higher temperature gradients than planar cells. However, with the planar eneramic® system heating rates of 16K/min have already been realized at system level. In a close-to-system environment higher gradients at stack level are currently being tested and the results will be discussed. Besides SOFC start-up characteristics at lower stack temperatures and the arising effects on life-time are demonstrated. The presented work will show that a highly efficient power generator with short start-up time can be build with planar SOFC technology.

11:40 AM

**(ICACC-S3-044-2012) Nano-crystalline 8-mol% Scandia Stabilized Zirconia: Synthesis, Characterization and Its Chemical Compatibility with SOFC Cathode Material**

S. Koley\*, A. K. Sahu, A. Laik, S. J. Patwe, N. S. Achary, Bhabha Atomic Research Centre, India

8-mol% scandia stabilized zirconia has been recognized as a good candidate electrolyte material for solid oxide fuel cell (SOFC), owing

to its high ionic conductivity. One of the essential requirements of the electrolyte material is it should be chemically compatible with cathode material over the long-term use at high temperature. In the present work this aspect has been addressed. Nano-crystalline, cubic phase, sinter-active 8-SSZ powder was synthesized by reverse strike co-precipitation technique. The ultra-fine powder was characterized for phase evolution, green microstructure and sinterability using different available techniques. Dense, sintered pellets were characterized using impedance spectroscopy. To study the chemical compatibility between 8-SSZ and LSM, green compacts made of equi-molar mixture of 8-SSZ and LSM powder (synthesized in-house) were sintered at 1400C for 3 hours followed by annealing at 1000C for 1000 hours in air. Both XRD patterns and electron probe microanalysis (EPMA) of the annealed samples did not indicate formation of any insulating phase(s). However, sample sintered at 1600C for 1 hour showed formation of La<sub>2</sub>Zr<sub>2</sub>O<sub>7</sub> phase. These experiments showed that both synthesized 8-SSZ and LSM powder are mutually compatible for long-term use till the maximum processing temperature is restricted up to 1400C.

12:00 PM

**(ICACC-S3-045-2012) Development of improved tubular metal supported solid oxide fuel cells resistant to high fuel utilization**

L. Otaegui\*, L. Rodriguez-Martinez, A. Arregi, A. Laresgoiti, I. Villarreal, Ikerlan, Spain

Tubular metal supported SOFC technology has successfully been developed over the past years with the aim at small domestic CHP and portable systems. First generation of cells have been successfully tested up to 2000 hours under current loading and more than 450 thermal cycles at low humidification conditions (3% H<sub>2</sub>O/H<sub>2</sub>). However, good resistance against oxidation due to high fuel utilization was not succeed. A special effort has been devoted to determine the reason for the catastrophic degradation observed during operation at high fuel utilization conditions. Tests performed in metal support, diffusion barrier layer and anode structured samples under high humidification atmospheres (50% H<sub>2</sub>O/H<sub>2</sub>) have demonstrated that modifications in the diffusion barrier layer, improve significantly the resistance to oxidation of the metallic support, achieving more than 500 hours with almost no degradation. Furthermore, a second generation of cells that can operate at high fuel utilization conditions for more than 1000 hours have been successfully demonstrated.

## S5: Next Generation Bioceramics

### Medical and Dental Applications of Bioceramics I

Room: Coquina Salon C

Session Chairs: Jay Hanan, Oklahoma State University; Paulo Coelho, New York University

8:00 AM

**(ICACC-S5-036-2012) Evaluating Flaws in Ceramic Dental Crowns Using Microfocus X-ray Computed Tomography (Invited)**

Y. Zhang, J. C. Hanan\*, Oklahoma State University, USA

Size and distribution of flaws are important factors that will affect fatigue and fracture of ceramic dental crowns. In some cases, a crown would fail unexpectedly due to flaws. Reliability and longevity of all ceramic crowns have always been a concern. Knowing flaw size and distribution will be a significant advantage for predicting performance and can help control the quality of the crowns—reducing the failure rate in clinical practice. Microfocus X-ray computed tomography (μCT) can be a powerful tool to evaluate flaws. It is nondestructive and can successfully visualize and measure internal structure with almost no material preparation. μCT is efficient and convenient, particularly when considering 3D evaluation, and outperforms conventional optical microscopes and Scanning Electron Microscopes (SEM). In this study, μCT was used to characterize flaws in three crowns made at different cooling rates to help determine the best

manufacturing process. Results shows that there are flaws as big as 220  $\mu\text{m}$  existing in porcelain. A faster cooling rate corresponds to more flaws, but not necessarily big flaws. The crown with the slowest cooling rate had fewer flaws. The corresponding critical fracture stress was predicted based on the biggest flaw.

**8:30 AM**

**(ICACC-S5-037-2012) Slow crack growth velocities (v-K curves) of dental bioceramics**

H. N. Yoshimura\*, Federal University of ABC, Brazil; C. C. Gonzaga, Positivo University, Brazil; W. G. Miranda, P. F. Cesar, University of São Paulo, Brazil

Slow or subcritical crack growth (SCG) phenomenon is one of the paramount factors that determine the lifetime of ceramic dental restorations because of the humid oral environment. In this study the SCG behaviors of five dental bioceramics were evaluated with the aim to plot the crack growth velocity versus stress intensity factor (v-K) curves. Disc-shaped samples of two sintered porcelains, two heat-pressed glass-ceramics, and a glass-infiltrated composite were prepared and tested in artificial saliva at 37°C using a biaxial flexure jig. The SCG parameters were evaluated by the dynamic fatigue method using five constant stress rates and an inert condition. Among the tested materials, the lithium disilicate glass-ceramic presented the highest susceptibility for strength degradation by SCG while the glass infiltrated alumina composite the lowest. The v-K curves showed that the SCG susceptibility affects significantly the crack growth velocity and the differences in velocities can achieve more than six fold among the different bioceramics.

**8:50 AM**

**(ICACC-S5-038-2012) Validating FEM of Ceramic Dental Restorations**

P. Coelho\*, New York University, USA; J. C. Hanan, Oklahoma State University, USA; H. Bale, University of California, Berkeley, USA; Y. Zhang, Oklahoma State University, USA; N. Silva, New York University, USA; V. Thompson, New York University College of Dentistry, USA

This study evaluated the level of detail needed for predicting thermal residual stresses in zirconia supported all-ceramic crowns. A CAD-based crown comprising a 0.5 mm core and a porcelain veneer of a 5-cusp first lower molar configuration was designed and fabricated. The crown fabrication was scanned using micro-CT. A solid tetrahedral mesh was constructed from the surface model geometry. The model was cooled from 900 °C for predicting stresses. Residual stresses of the crown resulting from coefficient of thermal expansion mismatch were modeled. Higher magnitude stresses of up to 400 MPa were observed in irregular cusped zones of the crown. Tensile residual stresses were observed at the core interface region for both CAD-based and real geometry-based models. Conversely, the porcelain veneer layer of both models showed compressive fields at regions close to the core interface and the average maximum principal stresses were comparable. The CAD based model had some advantages for efficient calculation. However, it missed some intricacies of the geometry, which lead to significant local deviation. Simulations on geometries incorporating more details assisted in understanding the impact residual stresses have on crack initiation and propagation, and aided in predicting mechanical performance of new designs.

**9:10 AM**

**(ICACC-S5-039-2012) Fracture Surface Analysis of Multilayer Ceramic – Polymer Composites**

P. A. Robinson\*, C. A. Wilson, J. J. Mecholsky, University of Florida, USA

Multilayer laminates of hydroxyapatite (HA) and polysulfone (PSu) biaxial disks show an increase in apparent fracture toughness over HA alone. The fracture surfaces were analyzed using quantitative fractography, fractal analysis and Raman spectroscopy to determine mechanisms of failure. The fractal dimensional increment ( $D^*$ ) measured for the ceramic lamina agrees with data reported for brittle ceramics.

Surface analysis was performed on the polymer lamina. Contributions of the polymer phase towards improving the toughness and strength of these laminates will be discussed, including the interfacial bonding between the polymer layers and the porous ceramic.

**Medical and Dental Applications of Bioceramics II**

Room: Coquina Salon C

Session Chairs: Laura Wortmann, University of Cologne; Janet Krevolin, Bio2 Technologies

**9:50 AM**

**(ICACC-S5-040-2012) Fabrication of Monophasic HAp Discs from Tricalcium Phosphate by Hydrothermal Treatment in Ammonia Solution**

N. Ahmad\*, M. Nakagawa, M. L. Munar, Kyushu University, Japan; S. Matsuya, Fukuoka Dental College, Japan; K. Ishikawa, Kyushu University, Japan

Hydroxyapatite (HAp) can be formed by the phase transformation in hydrothermal process based on dissolution-precipitation reaction. Interlocking of the precipitated crystals during dissolution-precipitation reaction is an important factor which governs the mechanical strength of the precipitated HAp crystals. Alpha tricalcium phosphate ( $\alpha$ -TCP) is known to transform to HAp in hydrothermal treatment. However,  $\alpha$ -TCP that has high reactivity in aqueous solution causes rapid dissolution-precipitation and inhibits interlocking of the crystals. Beta tricalcium phosphate ( $\beta$ -TCP) has the same chemical composition as  $\alpha$ -TCP, but has lower reactivity, may be used to fabricate HAp of higher mechanical strength.  $\alpha$ -TCP and  $\beta$ -TCP discs were treated hydrothermally at 200°C ammonia ( $\text{NH}_3$ ) solution for various durations. X-ray diffraction (XRD) analysis showed that both  $\alpha$ -TCP and  $\beta$ -TCP transformed into HAp. The reaction rate of transformation into HAp from  $\beta$ -TCP was slower than from  $\alpha$ -TCP. Crystallinity of HAp transformed from  $\beta$ -TCP disc was found to be higher than that of HAp transformed from  $\alpha$ -TCP disc. Diametral tensile strength (DTS) of HAp disc transformed from  $\beta$ -TCP showed higher value than that of HAp disc transformed from  $\alpha$ -TCP. We concluded that slower reaction rate was one of the key factors for the fabrication of HAp disc with higher mechanical strength.

**10:10 AM**

**(ICACC-S5-041-2012) Role of ultrasonic irradiation and drying on the physical properties of nanohydroxyapatite**

E. K. Giriya\*, G. Kumar, Periyar University, India; A. Thamizhavel, Tata Institute of Fundamental Research, India; Y. Yokogawa, Osaka City University, Japan; S. Kalkura, Anna University, India

Hydroxyapatite (HA) resembles natural bone mineral in its major composition and is widely applied for various biomedical applications in different forms. Wet chemical precipitation is an economic and simple route to synthesize of HA. But the thermal stability and other related properties of synthesized HA depends on various factors. In this study, we investigate the effect of ultrasonic irradiation and freeze drying on wet chemical precipitation of HA and its characteristics. The comparison of conventional hot air drying with that of freeze drying showed that the later method is found to offer HA with reduced particle size, low crystallinity and less agglomeration. The HA obtained from this method showed a significant increase in crystallinity, high densification, more homogeneously aligned grains, high thermal stability and enhanced mechanical properties on sintering. Thus HA with better physical properties can be achieved by the incorporation of ultrasonication during the synthesis and freeze drying instead of conventional drying.

**10:30 AM**

**(ICACC-S5-042-2012) Resorption rate and strength degradation of a novel bioactive scaffold**

J. Krevolin\*, J. Liu, V. Valant, Bio2 Technologies, USA

Highly porous scaffolds fabricated with fibers drawn from a resorbable (bioactive) glass were immersed in agitated Simulated Body



Fluid to evaluate the effects on the resorption rate and strength degradation when fabricated using different fiber diameters. The scaffolds were manufactured by sintering bioactive glass fibers to create a cross linked microstructure with an interconnected pore network and load bearing capabilities. The bioactive sodium-calcium-silicate composition forms a hydroxyapatite layer on the surface which allows bone tissue to bind directly to the surface. The samples were analyzed by the change in mass and compressive strength, the change in pH of the SBF, and by imaging with Scanning Electron Microscopy and Energy-Dispersive X-ray spectroscopy to detect the presence of hydroxyapatite formation and scaffold resorption. The larger diameter fibers saw increased mass resorption when normalized for the surface area, but the ionic surface concentrations of phosphate and calcium relative to silicon were much higher for smaller fiber diameters. By weight, the resorption rates were found to be much more sensitive to the bulk porosity than to fiber diameter. In vivo data shows bone ingrowth and direct bone bonding in two weeks for the smallest and most surface active fiber size used. This study supports the use of smaller fibers and the use of Bioglass in a bioactive, resorbable scaffold.

10:50 AM

**(ICACC-S5-043-2012) Nano grain sized silica-zirconia glass ceramics for dental applications**

W. Xia, C. Persson, E. Unosson, M. Andersson, J. Engstrand, H. Engqvist\*, Uppsala University, Engineering Sciences, Applied Materials Science, Sweden

The purpose of the study is to develop a high strength glass ceramic material for dental crown applications based on a sol-gel manufacturing method. The strategy to significantly increase strength of glass ceramics is to tailor the composition and manufacturing process of sol-gel silica-zirconia materials, and thereby introduce phase-transformation-toughened glass ceramic as dental material. Sols were prepared using tetraethyl orthosilicate and zirconium propoxide, with a calculated final composition of 30 wt% zirconia in the samples. Sols were put into Teflon molds and left for aging and drying until almost dry gels were formed. After that a crack-free material was ready for heat treatment; drying at 100 and 150 °C, and sintering at 1000 or 1100 °C. The achieved monoliths were examined in terms of microstructure, phase composition, mechanical toughness and translucency. Via the sol-gel method, a material with nano-grain size zirconia particles in a silica matrix could be formed. Instead the drying time was more than one week and several of the xerogels showed cracks. With a proper sol-gel method, dense and translucent materials were achieved with a toughness of above 4 MPa√m. In conclusion, the sol-gel method shows some promise to be used as a manufacturing method of translucent high strength glass ceramics for dental applications.

11:10 AM

**(ICACC-S5-044-2012) Surface properties of nano-structured TiO2 for dental implants design**

S. Issa\*, IICMPE-MCMC, CNRS UMR 7182, 2-8, rue Henri Dunant, 94320 THIAIS, France; P. Cenedese, C. Azavedo, P. Dubot, Universite Paris 7, France

The objective of our study is to characterize the adsorption of small organic molecules on nano-structured Ti surfaces and to characterize them by using different spectroscopies, such as X-photoelectron spectroscopy (XPS), infrared (IR) spectroscopy and scanning electron microscope (SEM), which may define the ideal surface properties for better biological results of dental implants. Methods: TiO<sub>2</sub> nanotubes arrays were fabricated by anodic oxidation of titanium samples in a fluoride-based solution at a constant potential. We have studied the adsorption of sodium phosphate, aspartic acid and Amoxicilline. The molecular deposition was carried out by two methods; the first one was electro-deposition and the other was simply immersing the samples in the solution and then rinsing. Results obtained from infrared spectroscopy showed that the molecular adsorption by nano-structured titanium is realizable in both methods and infrared spec-

troscopy allows to highlight differences in the mechanism of adsorption between early and late filing of deposit. Similarly, different levels of adsorption can be observed according to the potential of working electrode and the molecules themselves. X-photoelectron spectroscopy confirmed the previous results. Conclusion: Molecular adsorption by titanium nanotubes arrays is realizable depending on many factors such as the conditions of deposition, nanotubes size and the studied molecules.

**S12: Materials for Extreme Environments: Ultrahigh Temperature Ceramics (UHTCs) and Nanolaminated Ternary Carbides and Nitrides (MAX Phases)**

**Methods for Improving Mechanical, Oxidation and Thermal Shock Resistance**

Room: Coquina Salon F

Session Chairs: Per Eklund, Linköping University; Sea-Hoon Lee, KIMS

8:00 AM

**(ICACC-S12-051-2012) Anisotropy in the electronic structure of Cr<sub>2</sub>GeC probed by x-ray emission spectroscopy in comparison to ab initio calculations (Invited)**

M. Magnuson\*, Linköping University, Sweden; M. Mattesini, Instituto de Geociencias (CSIC-UCM), Spain; M. Bugnet, V. Mauchamp, T. Cabioch, Université de Poitiers, France, Université de Poitiers, France

The anisotropy in the electronic structure of the inherently nanolaminated phase Cr<sub>2</sub>GeC has been investigated using bulk-sensitive and element selective x-ray fluorescence spectroscopy. We use Cr<sub>2</sub>GeC(0001) thin films epitaxially grown on MgO(111) substrates with elemental-target sputtering. Angle-resolved precision measurements reveal differences between the in-plane and out-of-plane bonding at the (0001) interfaces of Cr<sub>2</sub>GeC. The Cr L, C K and Ge M<sub>1</sub>, M<sub>2,3</sub> emission spectra are compared with first-principles density-functional theory including core-to-valence dipole transition matrix elements. Strongly hybridized spectral shapes are detected for phonon-active Ge embedded in Cr<sub>2</sub>GeC. The anisotropy of the electronic structure and chemical bonding is discussed in relation to the various hybridization regions and macroscopic properties such as conductivity, elasticity, Hall effect, and thermopower. The latter two are particularly interesting, as preliminary results indicate negative Hall coefficient and positive Seebeck coefficient for this material.

8:20 AM

**(ICACC-S12-052-2012) Microstructural evolution during oxidation and its effect on strength of ultra-high temperature ceramics (UHTCs)**

E. Zapata-Solvas\*, D. D. Jayaseelan, Imperial College London, United Kingdom; P. Brown, DSTL, United Kingdom; W. E. Lee, Imperial College London, United Kingdom

ZrB<sub>2</sub> and HfB<sub>2</sub> based ultra-high temperature ceramics (UHTCs) are promising materials for future hypersonic vehicle leading edge applications. Currently, the strength degradation after oxidation at high temperatures limits UHTCs lifetimes making the understanding of this behaviour an important area of research. Fully-dense monolithic ZrB<sub>2</sub> and HfB<sub>2</sub>, 20 vol.% SiC-reinforced with ZrB<sub>2</sub> (ZS20) and HfB<sub>2</sub> (HS20) with and without 2 wt.% La<sub>2</sub>O<sub>3</sub> (ZS20La, HS20La) and HfB<sub>2</sub> with 2 wt.% La<sub>2</sub>O<sub>3</sub> (HfLa) were fabricated by spark plasma sintering (SPS). Room temperature flexural strengths of these materials were measured after oxidation at different temperatures ranging from 1200 °C to 1600 °C for different holding times from 0 to 32h. For example, the flexural strength of monolithic ZrB<sub>2</sub> was 450 MPa but after 0h oxidation at 1300 °C it was 570 MPa and further reduced to 390 MPa after 1h at 1300 °C and to 120 MPa after 8h at 1300 °C. Oxidation resistance was estimated in terms of oxide layer thickness, i.e., the higher the density of the oxide scale, the higher the oxidation

resistance and lower the strength retention after oxidation for the same scale oxide layer thickness. Strength reduction and microstructural evolution during oxidation are analysed in terms of the oxidation kinetics.

**8:40 AM**

**(ICACC-S12-053-2012) Micromechanics Modeling of Oxidation Effects on Mechanical Behavior of ZrB<sub>2</sub> at High Temperature**

J. Wei\*, L. R. Dharani, Missouri University of Science and Technology, USA; G. E. Hilmas, Missouri University of Science and Technology, USA; W. G. Fahrenholtz, Missouri University of Science and Technology, USA

ZrB<sub>2</sub> oxidation in air at high temperature (1273 – 2073 K) results in two new products, porous solid ZrO<sub>2</sub> and liquid B<sub>2</sub>O<sub>3</sub>. The material and geometry changes from the original ZrB<sub>2</sub> affect the heat transfer and the mechanical response after the oxidation. This study relates to a micromechanics based finite element modeling of oxidation effects on heat transfer and mechanical behavior of ZrB<sub>2</sub> at high temperature. Cylindrical representative volume unit is treated as 2D axisymmetric model (pseudo-3D). Two steps were used in the transient heat transfer analyses to calculate the temperature distribution: 5 minutes representing local heat up of a space vehicle reentry atmosphere and 30 minutes representing a cool-down event after landing. The resulting temperature distributions were applied to the subsequent thermal stress analysis to calculate the stress distribution. Adaptive remeshing technique is employed in both heat transfer and thermal stress analysis to improve accuracy. A “global-local modeling” technique is used combining finite element with infinite element for thermal stress analysis. All thermal and mechanical properties are temperature dependent. Temperature, thermal and residual stress distributions are presented and heat flux and thermal stress concentrations occur at the pore corner.

**9:00 AM**

**(ICACC-S12-054-2012) New Energy Applications for Ultra-Thin, Durable, Dense Zirconia Membranes**

V. Venkateswaran, J. Olenick\*, K. Olenick, ENrG Inc., USA

Historically, zirconia membranes have been used mainly for applications such as solid oxide fuel cells and O<sub>2</sub> sensors, making use of the ionic property of partially stabilized zirconia at elevated temperatures. Higher yttria content zirconia equates to higher O<sub>2</sub> ionic conductivity and therefore better power performance, but these materials are inherently weak. 3mol% yttria-stabilized zirconia (3YSZ) is preferred for its strength. In 2010, ENrG Inc. commercialized thin (40μ thick), flexible, 3YSZ-based ceramic foils that are gas-tight (dense), strong, flexible, thermal shock tolerant and chemically inert for SOFC. Alternative purposes were not envisioned but are becoming evident as other inherent properties of the membrane are tested in new energy markets where ionic conductivity is not required. The uses include extreme temperature sensors, solar substrates, thin IR windows, flexible electronics and superconductor substrates. These harsh environment applications may tap into additional properties such as translucency, low thermal mass, chemical resistance, IR optical transmission, ability to bend and enhanced properties via coatings. A porous version of this membrane is being tested for biomedical applications. The development and cross-market opportunities will enable cost reductions of these thin zirconia membranes. In this paper ENrG will present results of this year-long investigation.

**9:20 AM**

**(ICACC-S12-055-2012) The Melt Infiltrated C/ZrC Composite by Using a Zr-Si Alloy**

L. Zou\*, S. Prikhodko, University of California, Los Angeles, USA; T. Stewart, Ultramet, USA; J. M. Yang, University of California, Los Angeles, USA

Ultrahigh temperature materials (UHTMs) have been identified as one of the critical enabling technologies for hypersonic flight, atmospheric re-entry and rocket. Among all the potential refractory materials, continuous carbon fiber reinforced ZrC composite is one of the most promising materials for ultrahigh temperature structural applications. The oxidation resistance of ZrC is comparable to hafnium

carbide. However, the density of ZrC (6.73 g/cm<sup>3</sup>) is much lower than that of the HfC (12.2 g/cm<sup>3</sup>). The reactive melt infiltration process with a Zr-Si alloy was successfully used to fabricate C/ZrC composites. The matrix phases, composition, and microstructural features of the composite were studied by using XRD, SEM/EDS, and TEM/EDS, respectively. The fundamental processing/microstructure relationship for C/ZrC composites will be presented.

**Fundamental Understanding of the Structure-Property Relationships**

Room: Coquina Salon F

Session Chairs: Thierry Cabioch, University of Poitiers; Luke Walker, The University of Arizona

**10:00 AM**

**(ICACC-S12-056-2012) Rapid Single-Step Synthesis of Ultrahigh Temperature Ceramic Hafnium, Tantalum, and Zirconium Diborides by Sol-Gel Processing for Carbon-Carbon Reverse Infiltrated Ceramic Matrix Composites**

L. S. Walker\*, V. R. Marotto, E. L. Corral, The University of Arizona, USA

Carbon-carbon (C-C) composites meet the structural requirements for hot surface materials in hypersonic and reentry vehicles however they lack necessary oxidation resistance for use at extreme temperatures. Ultrahigh temperature ceramics (UHTC) integrated into these composites can provide oxidation resistance if infiltrated through the porous C-C composite in the form of stable liquid precursors that are in situ heat-treated into ceramic particles. HfB<sub>2</sub>, ZrB<sub>2</sub> and TaB<sub>2</sub> precursors are synthesized using a rapid single-step ultrasonic mixing process resulting in stable precipitate free sols that can be pressure infiltrated into C-C composites, forming a reverse infiltrated ceramic matrix composite. Characterization of the liquid sol precursors and UHTCs synthesized externally or within the C-C composites will be presented in addition to the effect of coating cycles on the C-C composite microstructure. Oxidation testing of C-C composites by TGA and oxy-acetylene ablation torch allows optimization of the coating process and an investigation of the oxidation mechanisms taking place within the UHTC/C-C composites at high temperature.

**10:20 AM**

**(ICACC-S12-057-2012) Phase Stability of Al<sub>3</sub>BC<sub>3</sub> under High Temperature and Pressure: An in situ Raman Analysis**

H. Xiang\*, J. Wang, Institute of Metal Research, China; Y. Zhou, Aerospace Research Institute of Materials and Processing Technology, China

In situ Raman spectra of Al<sub>3</sub>BC<sub>3</sub> were measured at different temperatures and pressures. The experiments showed that there are no abrupt changes in the spectra of Al<sub>3</sub>BC<sub>3</sub> up to 1000°C and 27 GPa, by which indicates excellent structural stability of Al<sub>3</sub>BC<sub>3</sub> throughout the studied conditions. Experimental Raman peaks were completely assigned to the corresponding phonon modes by first-principles calculation. In addition, an abnormal softening of E<sub>1g</sub> (567cm<sup>-1</sup>) mode is observed after the pressure is higher than 27 GPa, which may originate from change of the coordination number and bonding between Al and C atoms along the basal plane. Correlating the atomic motions to the peak shifts and broadenings, the phonon anharmonicity of involving modes is discussed. The results also highlighted that in situ Raman observation is a sensitive and illustrative method to investigate the structure and phase stability of complex ceramics.

**10:40 AM**

**(ICACC-S12-058-2012) Effect of Boron on the Thermodynamic Stability of Amorphous Polymer-Derived Si-(B)-C-N Ceramics**

A. Tavakoli\*, University of California at Davis, USA; J. A. Golczewski, Max Planck Institute for Intelligent Systems (Former Max Planck Institute for Metals Research), Germany; J. Bill, University of Stuttgart, Germany; A. Navrotsky, University of California at Davis, USA

The reason for the higher thermal persistence of amorphous polymer derived Si-B-C-N ceramics (T~1700-2000°C) compared to Si-C-N

ones ( $T \sim 1500^\circ\text{C}$ ) has been a matter of debate for more than a decade. Despite recent experimental results which indicate a major kinetic effect of boron on the thermal persistence of the ceramics, no experimental investigation of the thermodynamic stability of the materials has been reported. In this work, we present measured energetics of a series of amorphous ceramics with a constant Si:C:N molar ratio and various boron contents (0-8.3 at.%) using high temperature oxidative drop-solution calorimetry. Through measurement of the drop-solution enthalpies in molten sodium molybdate at  $800^\circ\text{C}$ , the formation enthalpies of the amorphous ceramics from crystalline components (SiC, BN,  $\text{Si}_3\text{N}_4$ , C) at  $25^\circ\text{C}$  were calculated to be between  $-2.3$  and  $-25.2$  kJ/g-at. The results point to the thermodynamic stability of the amorphous ceramics relative to the crystalline phases, but such stabilization diminishes with increasing boron content. In contrast, higher boron content increases the  $\text{Si}_3\text{N}_4$  crystallization temperature, despite less favorable energetics. Thus the so called "High Temperature Stability" of Si-B-C-N ceramics appears to be controlled purely by the kinetics rather than to be determined by thermodynamic stability.

#### 11:00 AM

##### (ICACC-S12-059-2012) A Comparative Study of Kinetics of Decomposition in MAX Phases at Elevated Temperature

I. J. Low\*, Curtin University, Australia; W. Pang, Tatung University, Taiwan

The susceptibility of 211, 312 and 413 MAX phases to thermal dissociation at  $1300$ - $1800^\circ\text{C}$  in high vacuum has been studied using in-situ neutron diffraction. Above  $1400^\circ\text{C}$ , all MAX phases decomposed to binary carbide (e.g. TiCx) or binary nitride (e.g. TiNx), primarily through the sublimation of A-elements such as Al or Si, which results in a porous surface layer of MXx being formed. Positive activation energies were determined for the decomposition of MAX phases except for  $\text{Ti}_3\text{AlC}_2$  where negative activation energy of  $71.9$  kJ mol<sup>-1</sup> was obtained due to formation of fine pores on TiCx. The kinetics of isothermal phase decomposition at  $1550^\circ\text{C}$  was modelled using a modified Avrami equation. An Avrami exponent (n) of  $< 1.0$  was determined, indicative of the highly restricted diffusion of Al or Si between the channels of M<sub>6</sub>X octohedra. The role of microstructures on the characteristics and kinetics of phase decomposition is discussed.

#### 11:20 AM

##### (ICACC-S12-060-2012) Insights into high temperature oxidation of Al<sub>2</sub>O<sub>3</sub>-forming Ti<sub>3</sub>AlC<sub>2</sub>

Y. Zhou\*, X. H. Wang, F. Z. Li, Aerospace Research Institute of Materials & Processing Technology, China; J. X. Chen, Institute of Metal Research, Chinese Academy of Sciences, China

$\text{Ti}_3\text{AlC}_2$  is one of the most light-weight and oxidation resistant layered ternary carbides belong to the MAX phases. Due to its superior properties such as low density, electrical and thermal conductivities, oxidation resistance and good machinability than its binary counterpart,  $\text{Ti}_3\text{AlC}_2$  holds promise in diverse potential applications including high temperature structural component. Hence, extensive investigations focusing on the oxidation and corrosion behaviors of  $\text{Ti}_3\text{AlC}_2$  have been carried out. However, in-depth studies of the diffusion process in the scales formed on  $\text{Ti}_3\text{AlC}_2$  are lacking. In this work, quantitative knowledge of the diffusion process in the scales has been established through systemically studying the oxidation behavior of  $\text{Ti}_3\text{AlC}_2$  at  $1000$ - $1250^\circ\text{C}$  in a dry atmosphere (20 vol% O<sub>2</sub> in Ar flow). It is demonstrated that a protective Al<sub>2</sub>O<sub>3</sub> scale was formed, the oxidation rate followed a sub-parabolic rate law, and Al-depletion zone was absent. The scale resulted from selective oxidation of Al that migrated from  $\text{Ti}_3\text{AlC}_2$  according to  $\text{Ti}_3\text{AlC}_2 + 3/2y \text{O}_2 = \text{Ti}_3\text{Al}_{1-y}\text{C}_2 + 1/2y \text{Al}_2\text{O}_3$ , leaving Al vacancy in the substrate. Outward diffusion of oxygen via grain boundary of the Al<sub>2</sub>O<sub>3</sub> scale was rate-limiting step. As the Al<sub>2</sub>O<sub>3</sub> grains grew larger with time, the scale growth rate became sub-parabolic. The Al diffused in a fast manner, accounting for the absence of Al-depletion zone.

## S13: Advanced Ceramics and Composites for Nuclear Applications

### Ceramics and Glass for Waste Immobilization

Room: Coquina Salon E

Session Chair: Josef Matyas, Pacific Northwest National Lab

#### 8:00 AM

##### (ICACC-S13-022-2012) Characterisation of nuclear metal wastes in magnesium silicate hydrate cement

L. J. Vandepierre\*, T. Zhang, C. R. Cheeseman, Imperial College London, United Kingdom

A novel low pH magnesium silicate hydrate cement system for encapsulating nuclear industry wastes have been developed using blends of MgO, silica fume (SF), MgCO<sub>3</sub> and sand. Aluminium, Magnox swarf and AGR fuel cladding supplied by the National Nuclear Laboratory (NNL) were encapsulated in this system and also in a BFS/PC control system used in nuclear industry. The interaction of the optimised mortar with the metal strips has been investigated, both in terms of rate of continued corrosion as well as the phases that form by reaction of the binder with different metal strips. Magnox swarf was better bound into the BFS/PC system than MgO:SF:MgCO<sub>3</sub>:sand system whereas Al 1050 and the AGR fuel cladding metal strips were bound better into the MgO:SF:MgCO<sub>3</sub>:sand samples than into the BFS/PC reference mortar. For the aluminium and the steel no H<sub>2</sub> emission was recorded when encapsulated in the new binder, which is substantially better than what can be achieved with the reference system. For magnox swarf the hydrogen development was limited and similar in both binder systems. Hence, the newly developed binder could potentially encapsulate mixtures of reactive metals better than the existing solution.

#### 8:20 AM

##### (ICACC-S13-023-2012) Progress in the Development of Crystalline Ceramic Waste Forms for an Advanced Nuclear Fuel Cycle

K. S. Brinkman\*, K. Fox, Savannah River National Laboratory (SRNL), USA; M. Tang, Los Alamos National Laboratory (LANL), USA

An objective of the U.S. Department of Energy's Fuel Cycle Research and Development program is to identify transformational waste management solutions for a closed nuclear fuel cycle. Crystalline materials with potentially enhanced thermodynamic stability as compared to glass wastefoms are currently being developed and evaluated for the encapsulation of species for repository disposal. Titanate, alumina and calcium based oxides were added to cesium and lanthanide streams with transition metal additions (CS/LN/TM) in order to target crystalline phase assemblages of perovskite, pyrochlore, hollandite, powellite. Waste form processing involved a melting and solidification approach as well as conventional ceramic press and sinter methods. Conclusions to date include i) identification of crystalline phase assemblage in ceramics by XRD and SEM/EDS as a function of composition, waste loading, and processing conditions ii) comparison of composition dependent dissolution (product consistency PCT) tests for crystalline ceramics normalized to surface area and post-processing chemical composition and iii) radiation stability as determined by ambient temperature exposure to 5 MeV alpha, 2 MeV proton and electron irradiation in high resolution TEM and corresponding structural analysis before/after exposure.

#### 8:40 AM

##### (ICACC-S13-024-2012) The effect of temperature on densification behavior of silica aerogels

J. Matyas\*, G. Fryxell, M. Robinson, Pacific Northwest National Lab, USA

Silver functionalized silica aerogel developed at PNNL shows great promise in effective removal and immobilization of gaseous radioiodine that is released during reprocessing of spent nuclear fuel. The iodine-loaded aerogel can be consolidated to form a dense and durable waste form with little loss of I<sub>2</sub> at temperatures above

900°C. To determine the optimum densification conditions, the sintering behavior of silica aerogel granules during isothermal heat treatments at temperatures from 900 to 1400°C and times from 2.5 to 90 min was investigated by BET and helium pycnometry. The raw granules had a surface area (SA) 1114 m<sup>2</sup>/g, pore volume (PV) 7.4 cm<sup>3</sup>/g, average pore size (PS) 18.6 nm, and skeletal density (SD) 1.7 g/cm<sup>3</sup>. This low SD, compared to the bulk density of amorphous silica (~ 2.2 g/cm<sup>3</sup>), was due to the presence of the closed pores and the complex nature of the micropore structure. Five minute heat-treatments at 900, 1050 and 1200°C resulted in decrease of SA (945, 482, and 68 m<sup>2</sup>/g) and PV (6.6, 2.3, and 0.2 cm<sup>3</sup>/g) with SD ranging from 2.2 to 2.3 g/cm<sup>3</sup>. Prolonged heat-treatments at 900°C resulted in small changes in SA, PV, and PS. Foaming that occurred at temperatures above 1200°C caused the SD of granules to be less than that of the raw granules. We have determined the optimum densification temperature for iodine-loaded aerogel to be between 1050 and 1200°C where rapid densification was observed.

### 9:00 AM

#### (ICACC-S13-025-2012) A Model Waste Form of <sup>90</sup>Sr in SrTiO<sub>3</sub>

W. Jiang\*, L. Kovarik, M. Bowden, Z. Zhu, B. Arey, Pacific Northwest National Laboratory, USA

A high percentage of <sup>90</sup>Sr radionuclide is contained in the nuclear waste stream from reprocessing of spent fuels. Strontium titanate (SrTiO<sub>3</sub> or STO) is used in this study as a model material to simulate a waste form for <sup>90</sup>Sr disposal. Sequential implantation of <sup>16</sup>O<sup>+</sup> and <sup>90</sup>Zr<sup>+</sup> ions was performed at 550 K to minimize the charge imbalance and to avoid full amorphization of STO. Various experimental methods have been employed to characterize the implanted sample, including time-of-flight secondary-ion mass spectroscopy, multiaxial ion-channeling analysis, high-resolution transmission electron microscopy, and micro-beam x-ray diffraction. The results show that the implanted Zr does not diffuse noticeably during the ion implantation or thermal annealing up to 1423 K, indicating formation of strong chemical bonds of the implanted Zr in the structure. A defect concentration was generated and nearly all the implanted Zr was not located at the original lattice site. A high density of dislocations exists in the damage layer, where there are also Zr-containing microstructures. The implanted Zr is found to locate at every other Sr site at low Zr concentrations. At higher concentrations, zirconia precipitates are formed. A minor phase with a tetragonal structure was observed. It survived thermal annealing at temperatures up to 1423 K. Discussion about the results and a general assessment of the model waste form will be also provided in this presentation.

### 9:20 AM

#### (ICACC-S13-026-2012) Incorporation of High TiO<sub>2</sub> Concentrations in Nuclear Waste Glass

K. M. Fox\*, F. C. Johnson, T. B. Edwards, Savannah River National Laboratory, USA

Modular Salt Processing (MSP) is planned to disposition radioactive salt solution in the Savannah River Site Tank Farm. MSP will remove Cs-137 from salt solution using Crystalline Silicotitanate (CST) resin via small column ion exchange (SCIX). The salt solution will be struck with Mono Sodium Titanate (MST) to remove actinides prior to being processed in the SCIX. The Cs-137 laden CST resin, MST, and insoluble salt solids will be added to the high level sludge vitrified at the Defense Waste Processing Facility. These additional streams have the potential to impact the processing constraints of the borosilicate glass waste form. In particular, the titanium concentration limit must be increased and higher concentrations of niobium and zirconium must be incorporated. This paper will present the results of experimental investigations into solubility of these components, as well as impacts to process control models. Of particular focus is the prediction of liquidus temperature.

## Joining and Coating

Room: Coquina Salon E

Session Chair: Josef Matyas, Pacific Northwest National Lab

### 10:00 AM

#### (ICACC-S13-029-2012) Glass-ceramics as joining materials for nuclear applications

M. Ferraris\*, V. Casalegno, S. Han, S. Rizzo, M. Salvo, A. Ventrella, Politecnico di Torino, Italy

Joining of SiC/SiC composites for nuclear applications can be of interest for both future thermo-nuclear fusion reactors and new generation fission reactors components. In both cases, the main issues are the extreme thermo-mechanical loads on the joined components, the not completely known service conditions and requirements, their resistance to high temperatures, to neutron irradiation and to harsh chemical environment. Three silica and non silica based glass-ceramic have been used to join SiC and SiC/SiC by a pressure-less joining technique. The mechanical characterization of the joints will be discussed in terms of bending and torsion tests, in particular for the latter, on joined miniaturized hour-glass shaped specimens, designed to fit irradiation capsules. Bending strength has been measured on glass-ceramic joined SiC/SiC before and after neutron irradiation at the High Flux Reactor in Petten, within the EU project EXTREMAT: preliminary results showed almost the same bending strength before and after irradiation at 600 °C. Finally, the behaviour of glass-ceramics as joining materials for SiC/SiC will be shown before and after fast neutron irradiation: results showed the same glass ceramic structure and phases before and after irradiation at 600 °C.

### 10:20 AM

#### (ICACC-S13-028-2012) Joining of SiC Monolithic Components for Nuclear Applications

H. E. Khalifa\*, C. P. Deck, O. Gutierrez, C. A. Back, General Atomics, USA

General Atomics is developing a high temperature gas-cooled fast spectrum reactor called the Energy Multiplier Module (EM<sup>2</sup>). The high fluence, high operating temperature and long lifetime of this reactor design necessitate the use of SiC-SiC composite cladding. Implementation of SiC-SiC composites to EM<sup>2</sup>, or other nuclear reactors hinges upon not only the successful development of SiC-SiC composite, but also a reliable means to join SiC components to make more complex geometries. While composite development has continued to advance, similar progress in nuclear grade joining of SiC-SiC components has been elusive. Too often joining agents rely on multi-phase braze alloys, fillers, and sintering aids that invariably lead to failure from differential thermal and neutron induced dimensional change. A critical criterion in GA's investigation of nuclear grade joining is a reliance on low activation joint materials that behave similarly under reactor operating conditions to the SiC-SiC composite they are joining. Mechanical tests were performed on sintered SiC monolith, CVD SiC monolith, and SiC-SiC composites to assess the role of surface finish and geometry on shear and flexural joint strength. Data on joint strength and permeability will be examined as a function of temperature and discussed with reference to the conditions under which the joints were prepared. This work supported by General Atomics internal funding.

### 10:40 AM

#### (ICACC-S13-027-2012) Joining Silicon Carbide for Nuclear and Fusion Energy Applications

Y. Katoh\*, Oak Ridge National Lab, USA; M. Ferraris, Politecnico di Torino, Italy; T. Hinoki, Kyoto University, Japan; C. H. Henager, Pacific Northwest National Lab, USA

Based on the recent development of highly radiation-resistant silicon carbide-based ceramic matrix composites, applications of these materials to various nuclear and fusion energy systems are presently proposed and being researched. However, development of joining

for these materials for use in the harsh radiation environment remains as a significant challenge. Moreover, additional requirements such as gas impermeability and water corrosion resistance have to be considered for use in the specific application environments. In the recent collaborative project among the U.S. Fusion Materials Program, Politecnico di Torino, and Kyoto University, development and evaluation of joining technologies for silicon carbide ceramics and composites for use in fusion and nuclear reactors were attempted. This paper will discuss the recent progress including 1) identifying promising joining techniques for radiation services, 2) development of small specimen test technique adequate to evaluate the shear strength of ceramic joints, 3) baseline characterization of the joint mechanical properties, and 4) progress in neutron irradiation program.

## Global Young Investigators Forum

### Frontiers in Hybrid Materials and Composites

Room: Coquina Salon G

Session Chairs: Lisa Brueckmann, University of Cologne; Mohammad Imteyaz Ahmad, Iowa State University

**8:00 AM**

#### (ICACC-GYIF-033-2012) Dielectric and Ferroelectric Studies of SBN-PVDF Composites

S. N. Kumar\*, P. Kumar, National Institute of Technology, India

Ferroelectric ceramic and polymer composites are widely studied as they combine the most important features of the both the phases and their properties can be easily tailored as required in various applications. Composites of ferroelectric polymer, polyvinylidene fluoride (PVDF) and perovskite type ferroelectric ceramics are well studied. Composites of tungsten bronze type ferroelectric ceramics and PVDF are less studied. In this work, composites of polyvinylidene fluoride and strontium barium niobate ( $\text{Sr}_x\text{Ba}_{1-x}\text{Nb}_2\text{O}_6$  with  $x=0.53$ ) with 10, 20 and 30 volume % ceramic content have been prepared by hot uniaxial press. Thick films with 0-3 connectivity have been obtained. Structural, morphological, dielectric, ferroelectric and piezoelectric properties have been studied.

**8:20 AM**

#### (ICACC-GYIF-034-2012) Microstructure, oxidation resistance and mechanical properties of fiber bonded silicon carbide ceramics

M. Vera\*, J. Ramirez-Rico, J. Martinez Fernandez, Universidad de Sevilla - CSIC, Spain; M. Singh, NASA Glenn Research Center, USA

Advanced SiC-based ceramics and fiber reinforced composites are enabling materials for a wide variety of high-temperature and extreme environment applications because of their excellent thermo-mechanical properties and thermal stability. The microstructure, oxidation behavior, and mechanical properties of sintered SiC fiber bonded ceramics (SA Tyrannohex) was studied. The material is composed by SiC-fibers in two orientations, with polygonal cross sections and cores having higher carbon content than their surroundings. A thin layer composed of C exists between the fibers. The microstructure of the fibers, as observed with TEM, consists of SiC grains of ~200 nm in diameter, with a considerable amount of free pyrolytic carbon at triple points which is homogeneously distributed in the fiber. XRD shows that the material is highly crystalline and composed mostly of  $\beta$ -SiC with small amounts of  $\alpha$ -SiC. Microstructural stability has been studied after exposure in vacuum to temperatures ranging 1400-2000C. TGA experiments were performed to study the oxidation resistance of the material at temperatures ranging from 800-1400C. The effect of thermal treatments on the mechanical properties of the material was evaluated.

**8:40 AM**

#### (ICACC-GYIF-035-2012) Mechanical Properties of Topologically Interlocked Ceramic-Based Structures with Various Degrees of Porosity

A. Molotnikov, Monash University, Australia; T. Krause\*, M. Carlesso, J. Rente, K. Rezwani, University of Bremen, Germany; D. Koch, German Aerospace Center, Germany; Y. Estrin, Monash University, Australia

A pathway to improving the toughness and bending flexibility of ceramics by using segmented, rather than monolithic, structures based on topological interlocking of the building blocks is presented. Topologically interlocking blocks with matching concavo-convex surfaces were produced by freeze gelation of ceramic suspensions in specially formed moulds. Varying the suspension and adding styropor particles, various degrees of porosity were achieved. Blocks were assembled to a plate-like structure that was tested under point loading with different levels of lateral pre-stress, thus varying the bending stiffness of the structure and the friction forces between the interlocked blocks. For comparison, monolithic plates were tested. It was shown that segmentation of a ceramic plate into topologically interlocked blocks can significantly enhance its bending compliance. FEM calculations were also conducted to simulate deformation behaviour of the assemblies tested. The effect of porosity, particularly in the critical regions of the blocks, on the compliance and the load bearing capacity of the assemblies will be discussed.

**9:00 AM**

#### (ICACC-GYIF-036-2012) Graphitic carbon obtained from pyrolysis of natural precursors

A. Gutierrez-Pardo\*, J. Ramirez-Rico, J. Martinez Fernandez, Universidad de Sevilla - CSIC, Spain

Porous Graphitic carbons can be obtained through pyrolysis of natural cellulosic precursors by a prior treatment of the precursor with a catalyst, resulting in a porous structure that mimics the microstructure of the precursor materials used. A material that combines the properties of pyrolysis-derived carbon, such as high surface area, open and interconnected porosity and high pore volume, with the properties of graphite, such as high electrical and thermal conductivity and a low coefficient of thermal expansion, are obtained. These properties make it an interesting for thermal applications, electrocatalysis or energy storage materials by electrochemical processes. In this work, samples of beech wood and medium density boards are treated with a saturated solution of nickel nitrate and we study the impact of these treatments and the influence of the maximum temperature used during the pyrolysis process (from 600 to 1600 C) on the carbon structures, evaluating the differences with the carbon obtained by traditional pyrolysis, without catalytic treatment. We characterize the material obtained by scanning electron microscopy, X-ray diffraction, thermogravimetric analysis and physisorption. The observed differences are shown and discussed.

**9:20 AM**

#### (ICACC-GYIF-037-2012) Mechanical property of CNT-dispersed $\text{Si}_3\text{N}_4$ ceramics

S. Yoshio\*, M. Matuoka, J. Tatami, T. Wakihara, K. Komeya, T. Meguro, Yokohama National University, Japan

We succeeded in the fabrication of electrically conductive CNT-dispersed  $\text{Si}_3\text{N}_4$  ceramics. However the reaction between  $\text{Si}_3\text{N}_4$  and CNTs degraded strength of the  $\text{Si}_3\text{N}_4$  ceramics. In this study, we improved the strength of the CNT-dispersed  $\text{Si}_3\text{N}_4$  ceramics by using sintering aids for lower temperature densification. The sintering aids used in this study were  $\text{Y}_2\text{O}_3$ ,  $\text{Al}_2\text{O}_3$ , AlN,  $\text{TiO}_2$  and  $\text{HfO}_2$ . The strength of the sintered body was higher compared with our previous study. The density of the CNT-dispersed  $\text{Si}_3\text{N}_4$  ceramics was also improved by using the sintering aids because the gas was not formed due to inhibition of the reaction between CNTs and  $\text{Si}_3\text{N}_4$ . It was shown that the higher strength of the CNT-dispersed  $\text{Si}_3\text{N}_4$  ceramics resulted from

higher density. We also uniformly dispersed CNTs by bead milling process which is well-known as an effective technique to disperse nanoparticles using fine grinding media (<1 mm). The strength of the CNT-dispersed  $\text{Si}_3\text{N}_4$  ceramics was as high as that without CNTs because there were no agglomerations of CNTs which should be the fracture origin.

### Frontiers in Precursor and Ceramic Chemistry

Room: Coquina Salon G

Session Chairs: Yakup Goenuellue, German Aerospace Center; Sara Yoshio, Yokohama National University

**10:00 AM**

#### (ICACC-GYIF-038-2012) New and well analysed route to obtain water soluble gold, gold/silver or gold/copper Nanoparticles by hydrolysing $[\text{Au}(\text{CF}_3)_2]$ -species (Invited)

D. Zopes\*, W. Tyrre, S. Mathur, University of Cologne, Germany

Monodisperse Au-NP's were obtained by microwave assisted hydrolysis of  $[\text{NMe}_4][\text{Au}(\text{CF}_3)_2]$ . The new well characterised (NMR, Crystal Structure) precursor can be used as an easy prepare-able and alternative source for  $\text{HAuCl}_4$ . Additionally the tetra-methyl-ammonium cation was exchanged for Ag(+I) and Cu(+I) by salt metathesis, leading to a single precursor yielding alloyed nanoparticles (Ag/Au, Cu/Au) by the same hydrolysis reactions. Particles were investigated by TEM, UV/Vis and XRD/EDX. The whole decomposition mechanism was explored using NMR- and UV/Vis spectroscopy. Size (10-60 nm) and stability of the naked particles could be adjusted by changing the precursor concentration (0.2 mM – 4.0 mM) and by addition of PEG as a stabilising agent.

**10:20 AM**

#### (ICACC-GYIF-039-2012) Thermal barrier coatings on fluorine treated $\gamma$ -TiAl alloys

N. Niessen\*, R. Braun, Deutsches Zentrum für Luft- und Raumfahrt e.V. (DLR), Germany; S. Friedle, M. Schütze, DECHEMA e.V., Germany

Gamma titanium aluminides are considered as promising candidates for high temperature applications in automotive and aero engines. However, the oxidation resistance of  $\gamma$ -TiAl alloys decreases rapidly at temperatures above 800°C. In the present work, thermal barrier coating (TBC) systems were deposited on the alloy Ti-45Al-8Nb, consisting of a zirconia top layer and a novel thin bond coat. The surfaces of  $\gamma$ -TiAl specimens were treated with fluorine by means of gas and liquid phase treatments as well as plasma immersion ion implantation to increase the oxidation resistance utilising the halogen effect. Subsequently, TBCs were deposited by electron-beam physical vapor deposition (EB-PVD) at substrate temperatures of 900 and 1000°C. Post-oxidation analyses of the coating systems were carried out using scanning electron microscopy and energy dispersive X-ray spectroscopy. EB-PVD yttria partially stabilized zirconia coatings were successfully deposited on fluorine treated  $\gamma$ -TiAl samples at 1000°C. At this substrate temperature, previous TBCs failed by severe spallation during deposition due to the poor oxidation behavior of the bond coats used. The best performance under thermal cycling conditions was found for the TBC deposited on gas phase fluorine treated samples at 1000°C, related to the excellent oxidation resistance of the fluorinated surfaces and a pronounced columnar morphology of the zirconia top layer.

**10:40 AM**

#### (ICACC-GYIF-041-2012) New Air-Stable and Volatile Heteroarylalkenolate palladium(II) and platinum (II) Complexes (Invited)

L. Brückmann\*, W. Tyrre, S. Mathur, University of Cologne, Germany

Noble metal coatings and clusters are finding increasing applications due to their useful optical and catalytic properties. The major limiting factor in the chemical synthesis of palladium and platinum structures is the lack of adequate precursors that would produce high pu-

riety materials under mild processing conditions. The main aim of this work was to synthesize new Pd(II) and Pt(II) compounds with physico-chemical properties promising for CVD applications. The precursor synthesis was performed using a  $\beta$ kalenol containing a heteroaryl substituent, which exhibited chemical characteristics comparable to  $\beta$ -diketones. The chelating ability of the  $\text{Ar}(\text{N})\text{CHC}(\text{CF}_3)\text{OH}$  backbone and the stability of the resulting six-membered ring offer an interesting option to limit the oligomerisation of metal derivatives. The introduction of different alkyl groups with or without fluorine revealed the influence of ligand periphery and associated electronic periphery on the volatility of the complexes. The compounds were characterized by elemental analyses, mass spectrometry and in solution by  $^1\text{H}$ ,  $^{13}\text{C}$  and  $^{19}\text{F}$  NMR spectroscopy. In addition, solid state structures of were determined using single-crystal X-ray diffraction analyses which showed the expected square planar spatial arrangement at the palladium and platinum atoms with the heteroaryl ring nitrogens situated mutually in trans position.

**11:00 AM**

#### (ICACC-GYIF-042-2012) Synthesis of metaloxides via hydrothermal and microwave technique

T. Lehnen\*, S. Mathur, University of Cologne, Germany

Nanostructured ternary semiconducting metal oxides receive much attention in recent times owing to their unique properties rendering them suitable for a wide range of applications. Zinc stannate or zinc tin oxide (ZTO), an inverse spinel structured  $\text{AB}_2\text{O}_4$  compound (space group  $\text{Fd}\bar{3}m$ ), is known for its high electron mobility, high-electrical conductivity and its interesting optical properties. Therefore,  $\text{Zn}_2\text{SnO}_4$  seems to be a promising material for anodes in lithium ion batteries, transparent conducting oxides, photocatalytic materials, and as photoelectrodes in DSSCs. Nanosized  $\text{Zn}_2\text{SnO}_4$  (ZTO) particles were successfully synthesized by a simple microwave process in water using NaOH as mineralizer. The products were characterized by X-ray diffractions (XRD), scanning electron microscopy (SEM) and transmission electron microscopy (TEM). The results indicate that the synthesis conditions, such as alkaline concentration, reaction temperature, solvent composition and the duration of the synthesis had an important influence on the composition and crystallinity of the product. Printed structures fabricated from the as-synthesized ZTO nano particles showed typical semiconduction I-V behaviors and gas sensing properties.

**11:20 AM**

#### (ICACC-GYIF-043-2012) Single crystal growth of $\text{ZrMo}_2\text{O}_8$ (Invited)

M. Ahmad\*, M. Akinc, Iowa State University, USA

$\text{AM}_2\text{O}_8$  compound has received a lot of attention due to their unusual negative coefficient of thermal expansion (NCTE) over a wide range of temperature.  $\text{ZrW}_2\text{O}_8$  exhibits isotropic NCTE over a wide range from -269-777 °C, however, it is metastable in this temperature range and therefore decomposes to  $\text{ZrO}_2$  and  $\text{WO}_3$  on heating above 777 °C.  $\text{ZrMo}_2\text{O}_8$  is another compound which is stable at room temperature. However, the room temperature stable phase of this compound is monoclinic. In order to utilize the unusual NCTE of these compounds in actual application, it is important to characterize their intrinsic physical chemical and mechanic properties. Growing single crystals of reasonable sizes would be the first step in that direction. The volatility of oxides of W and Mo coupled with limited temperature range of their stability with liquid phase makes the single crystal growth of these compounds a formidable challenge. Here we report the growth of  $\text{ZrMo}_2\text{O}_8$  single crystals for the first time. We utilized  $\text{LiMo}_2\text{O}_4$  as a flux while the growth was carried out in a horizontal tubular furnace using a platinum boat. The synthesized nicely faceted crystals were up to 4 mm in size. Laue and single crystal X-ray diffraction confirmed the monoclinic crystal structure having a space group  $\text{C12/C1}$  and single crystallographic domain within the crys-

tals. This research work is partly funded by Office of Naval Research, Arlington, VA under the grant no. 0053098440000

## FS1: Geopolymers, Inorganic Polymers, Hybrid Organic-Inorganic Polymer Materials

### Fiber-reinforced Geopolymer Composites

Room: Coquina Salon A

Session Chair: Tomaz Kosmac, Josef Stefan Institute

#### 8:00 AM

#### (ICACC-FS1-009-2012) Fibre-Matrix Interactions in Geopolymer Matrix Composites

M. Welter\*, K. MacKenzie, Victoria University of Wellington, New Zealand

Geopolymers are a type of generally amorphous aluminosilicate binder that hardens at low temperature to form a solid ceramic-like material with moderate strength and good temperature stability up to ~1000°C. The incorporation of fibres into the matrix can significantly increase the strength of the matrix and induce non-catastrophic failure. The combination of PMC-like processing with CMC-like properties makes geopolymer matrix composites a cost-effective, light-weight alternative to other composite materials for mid-range temperature applications. Although geopolymer matrices remain largely amorphous upon heating, they can be transformed into crystalline ceramics at higher temperatures. Fibre-matrix interactions between several types of inorganic fibres and a simple geopolymer model matrix were investigated by SEM. The effect of the bonding behaviour of the different fibres and the matrix on the flexural strength will be analysed. Also the influence of heat treatment on the fibre-matrix bond and the flexural strength of the composite will be discussed.

#### 8:20 AM

#### (ICACC-FS1-010-2012) Properties of Basalt Fiber Reinforced Geopolymer Composites

G. P. Kutyla\*, S. Musil, W. M. Kriven, University of Illinois at Urbana-Champaign, USA

The properties, microstructure, and processing of potassium and cesium-based geopolymer ( $M_2O \cdot Al_2O_3 \cdot 4SiO_2 \cdot 11H_2O$ , where  $M = K, Cs$ ) composites made with basalt chopped fibers of various lengths have been systematically studied. Geopolymers were manufactured at ambient temperature and cured in a humidity controlled, constant temperature oven at 50°C. The effects of varying weight percents of fibers, length of chopped fibers, processing methods and heat treatments were examined by comparing the strengths of each sample with the corresponding pure geopolymer.

#### 8:40 AM

#### (ICACC-FS1-011-2012) High Temperature 4-Pt Flexural Strength of Chopped Fiber Reinforced Geopolymer Composites (Invited)

T. P. Dietz, W. M. Kriven\*, University of Illinois at Urbana-Champaign, USA

High temperature, castable materials are desired for numerous applications. Presented is an experimental investigation of geopolymers to be used up to 1500 C to satisfy this need. Geopolymers were synthesized with a composition based on the activation of metakaolin with an alkali hydroxide solution containing cesium plus refractory fibers for reinforcement. The reinforcements were chopped graphite fibers and subsequently, high alumina content (95%) fibers from Saffil® with a melting temperature of >2000 C. The flexural strength of the samples were determined at room temperature in a 4-point bend configuration for samples that were cast and fired at temperatures up to 1500C, as well as samples that were tested at their respective firing temperatures. The data was analyzed according to Weibull statistics. Generally the strength of heated samples improved over unheated samples and the strength of both heated and unheated samples was on par with that of unheated high strength concrete. The reinforce-

ment also protected the samples from cracking during dehydration and from disintegration when wet.

#### 9:10 AM

#### (ICACC-FS1-012-2012) Microwave Processing of Chopped Silicon Carbide Reinforced Geopolymers (Invited)

M. L. Fall\*, S. M. Allan, Ceralink Inc., USA; W. M. Kriven, University of Illinois at Urbana Champaign, USA; H. S. Shulman, Ceralink Inc., USA

An investigation into the effects of thermal treatments of geopolymers using microwave and Microwave Assist Technology (microwave plus electric radiant heat) was conducted. Microwave heating has been demonstrated to be a feasible method for rapidly converting geopolymers to ceramics for densification. A previous study showed that geopolymers heat very well with microwave energy at high temperatures, but heat slowly at room temperature. The use of chopped silicon carbide fibers provides mechanical reinforcement to the geopolymer, as well as a source of microwave absorption in the geopolymer at low temperatures. Microwave heating experiments were conducted between 800 and 1200 °C. Results will be presented on the effect of microwave process conditions on cracking, ceramic conversion, and microstructure of the sintered geopolymers.

### Bioapplications, Inorganic-organic Hybrids, and Phosphate-based Inorganic Polymers

Room: Coquina Salon A

Session Chair: Waltraud Kriven, University of Illinois at Urbana-Champaign

#### 10:00 AM

#### (ICACC-FS1-013-2012) Metakaolin Nanosilver as Biocide Agent in Geopolymer (Invited)

J. S. Moya\*, B. Cabal, J. Sanz, ICMM-CSIC, Spain

Metakaolin is an aluminosilicate mineral product which is produced in quantities of several million tons per year worldwide and used in applications including supplementary cementitious materials in concretes, an intermediate phase in ceramic processing, as a paint extender, and as a geopolymer precursor. Meanwhile, geopolymers are also being considered for a variety of applications including low CO<sub>2</sub> producing cements, fiber-reinforced composites, refractories, and as precursors to ceramic formation. Sanz et al. studied the kaolinite-mullite transformation by magic-angle spinning nuclear magnetic resonance (MAS-NMR) and determined the presence of Al in tetra- and penta-coordination in metakaolinite. Given the importance of metakaolin in several industry sectors, and also taking into account the possible large spectrum of applications, incorporating silver nanoparticles could provide an additional biocide functionality. In this regard, further studies of their structural evolution, are required because of the presence of silver nanoparticles. For this purpose, this work is mainly focused on the evaluation of the effect of the presence of silver nanoparticles on kaolin/metakaolin structures and on their biocide activity.

#### 10:30 AM

#### (ICACC-FS1-014-2012) Organic-Aluminosilicate Interface Interactions (Invited)

B. E. Glad\*, W. M. Kriven, University of Illinois at Urbana-Champaign, USA

Structure-property relationships of organic-aluminosilicate solids and interfaces are evaluated. Surface energies, condensation conditions and organic material length scales are found to be as important as aluminosilicate composition in determining the resulting microstructure. Large microstructural and nanostructural changes in the aluminosilicate occur in the vicinity of organic materials, allowing for property modification and control through relatively small amounts of additives. It is found that the creation of an interface and separate organic phase is a sufficient but not necessary condition for property modification. Such structures can self-assemble through typical polycondensation methods. Resulting synthesized products

have been characterized through such means as electron microscopy, nitrogen porosimetry, mercury intrusion porosimetry, pycnometry, mechanical testing and X-ray diffraction.

**11:00 AM**

**(ICACC-FS1-015-2012) Ligational Aspects of the Mesogenic Schiff-base, N,N'-di-(4'-octadecyloxybenzoate) salicylidene diaminoethane with Some Rare Earth Metal Ions**

S. Kumari\*, T. R. Rao, A. K. Singh, Banaras Hindu University, India

A novel mesogenic Schiff-base, N,N'-di-(4'-octadecyloxybenzoate) salicylidene diaminoethane (H<sub>2</sub>L<sub>4</sub>) with smectic-F(SmG) and smectic-F(SmF) mesophases, was synthesized and its structure studied by elemental analyses and mass, NMR & IR spectra. The bi-dentate bonding of the Schiff-base in the mesogenic (nematic) LaIII complex, as implied on the basis of IR & NMR spectral data. As per the spectral studies of the complex, the Zwitterionic-species of the ligand, coordinates to the LnIII ion through two phenolate oxygens, rendering the overall geometry around LnIII to distorted Square Anti-prism polyhedron.

**11:20 AM**

**(ICACC-FS1-016-2012) CeramicAsh: a new ultra low cost chemically bonded ceramic material**

H. A. Colorado\*, J. Yang, UCLA, USA

CeramicAsh is a new concept of green materials fabricated mainly from Fly ash, reacting with an acidic liquid such as phosphoric acid

formulations. These materials, depending on the ratio of the constituents, can vary from a glazy dense to a micro or nano porous ultra low density structure. Microstructure was characterized using a Scanning Electron Microscope and X-ray diffraction. Density measurement and compression tests were conducted for samples with different compositions. Results show CeramicAsh is an ultra light ceramics with high compressive strength and resistant to high temperatures. They are promising materials for thermal, structural and hazardous waste stabilization applications.

**11:40 AM**

**(ICACC-FS1-017-2012) Chemically bonded phosphate ceramics for stabilizations of high-sodium containing waste streams**

H. A. Colorado\*, R. Ganga, D. Singh, Argonne National Laboratory, USA

Chemically bonded phosphate ceramics (CBPC) to stabilize high sodium containing waste streams were fabricated and tested in this work. CBPC based waste forms were prepared by mixing the sodium-based simulant, with magnesium oxide (MgO) and Class C fly ash as filler. A mechanical mixer was used for mixing all the components. Different compositions and samples sizes were fabricated. Microstructure was identified with X-ray diffraction and electron microscopy. Water immersion, density, compressive strength and curing curves were evaluated. Surrogates of radioactive species such as technetium and iodine were also used in this work. American Nuclear Society's ANS 16.1 test was conducted on the waste forms to determine the diffusion of the radionuclide surrogates. Results from this presentation will demonstrate the applicability of CBPC in the stabilization of high sodium containing waste streams.



# Author Index

\* Denotes Presenter

## A

Abdelmalak, M. . . . .114  
 Abdollahi, S. . . . .33  
 Abdulkadhim, A. . . . .78  
 Abotula, S. . . . .78  
 Abu-Lebdeh, Y.\* . . . .29  
 Acchar, W. . . . .104  
 Achary, N.S. . . . .161  
 Acosta, M. . . . .149  
 Adam, M. . . . .26  
 Adam, M.\* . . . .153  
 Adschiri, T. . . . .112  
 Aggarwal, I. . . . .38  
 Aghajanian, M. . . . .11, 52, 56  
 Aghajanian, M.\* . . . .53  
 Ahearn, D. . . . .37  
 Ahlberg, N.\* . . . .102  
 Ahmad, M.\* . . . .168  
 Ahmad, N.\* . . . .162  
 Ahmad, W. . . . .122  
 Ahmed, Y.Y. . . . .102  
 Ahn, J.\* . . . .41  
 Ahrens, M. . . . .36  
 Aindow, M. . . . .122  
 Ajayi, O.\* . . . .81  
 Ajayi, O.O. . . . .139  
 Ajitdoss, L. . . . .105  
 Ajitdoss, L.C. . . . .142  
 Akatsu, T. . . . .137  
 Akbas, M.A.\* . . . .54  
 Akedo, J. . . . .32, 49  
 Akinc, M. . . . .168  
 Alam, K.\* . . . .144  
 Alberga, M.A. . . . .50  
 Alexander, S.\* . . . .22  
 Allahkarami, M. . . . .124  
 Allain, E. . . . .158  
 Allan, S. . . . .80  
 Allan, S.M. . . . .169  
 Allan, S.M.\* . . . .37, 42  
 Allemand, A.\* . . . .77  
 Allen, J. . . . .79  
 Allen, J.\* . . . .60  
 Alling, B. . . . .131  
 Almer, J. . . . .66  
 Alpas, A. . . . .29  
 Al-Sharab, J.F. . . . .118  
 Amani, M.\* . . . .45  
 Amarume, S.\* . . . .62  
 Amine, K. . . . .80  
 Amit, D. . . . .106  
 An, B. . . . .25  
 An, R. . . . .107  
 Ananthanarayanan, K. . . . .7  
 Andersen, H. . . . .13  
 Andersen, H.F. . . . .125  
 Anderson, C.E. . . . .5  
 Anderson, C.E.\* . . . .6  
 Anderson, H. . . . .119  
 Anderson, H.\* . . . .84  
 Anderson, T.J. . . . .125  
 Anderson, M. . . . .163  
 Andreu, T. . . . .101, 113  
 Andrew, J.S.\* . . . .75, 110  
 Andzelm, J. . . . .30  
 Aneziris, C. . . . .130  
 Aneziris, C.G. . . . .20, 25, 66  
 Aneziris, C.G.\* . . . .10  
 Angelkort, J. . . . .65, 119  
 Angelkort, J.\* . . . .65

Angle, J.P. . . . .133  
 Angle, J.P.\* . . . .4, 160  
 Antoun, T.H.\* . . . .4  
 Anusavice, K.J. . . . .157  
 Aoki, T. . . . .51  
 Aoki, T.\* . . . .131  
 Aonuma, S. . . . .137  
 Apelian, D. . . . .72  
 Apostolov, Z.\* . . . .65  
 Apostolov, Z.D. . . . .64, 65, 119  
 Appel, L. . . . .108  
 Aravind, P. . . . .11, 27  
 Arbiol, J. . . . .101  
 Arey, B. . . . .166  
 Arregi, A. . . . .161  
 Arregui, A.\* . . . .88  
 Arroub, K. . . . .134  
 Arslan, O. . . . .108  
 Artilia, I. . . . .143  
 Aryal, S. . . . .15  
 Asami, H. . . . .62  
 Ashok Kumar, S. . . . .115  
 Asthana, R. . . . .137  
 Asthana, R.\* . . . .145  
 Au, M. . . . .28  
 Audubert, F. . . . .150  
 Autfef, A. . . . .155  
 Autio, R. . . . .135  
 Avalue, M. . . . .157  
 Ayabe, S. . . . .159  
 Ayre, M. . . . .4, 85  
 Azais, T. . . . .70, 123, 124, 134  
 Azarifar, A. . . . .7, 152  
 Azavedo, C. . . . .163  
 Azzaz, M. . . . .106

## B

Babonneau, F. . . . .42, 123, 134  
 Babonneau, F.\* . . . .70, 124  
 Babu, N. . . . .133  
 Babynina, A.\* . . . .116  
 Bache, M.R. . . . .66, 136  
 Back, C.A. . . . .166  
 Backhaus-Ricoult, M.\* . . . .27  
 Badot, J. . . . .28  
 Bae, M. . . . .48  
 Baehz, C. . . . .13  
 Baek, S. . . . .59  
 Baeurer, M. . . . .29  
 Baidak, V. . . . .106  
 Baik, K. . . . .63  
 Baik, K.\* . . . .31  
 Balani, K. . . . .160  
 Balasubramanian, K. . . . .101  
 Balasubramanian, M. . . . .28  
 Balasubramanian, S. . . . .57  
 Balat-Pichelin, M. . . . .113  
 Balaya, P.\* . . . .7  
 Bale, H. . . . .162  
 Bales, A. . . . .119  
 Ban, C. . . . .12  
 Banera, U. . . . .13  
 Baney, R. . . . .133  
 Bao, L. . . . .45, 110  
 Baral, J. . . . .82  
 Baranova, I. . . . .37  
 Baratto, C. . . . .100  
 Barborini, E.\* . . . .39  
 Barnett, S.A. . . . .121  
 Barré, O. . . . .137

Barreca, D.\* . . . .35  
 Barrett, A.A. . . . .157  
 Barsan, N. . . . .99  
 Barsoum, M. . . . .66, 114, 131  
 Barsoum, M.\* . . . .131  
 Barsoum, M.W. . . . .98  
 Basu, S. . . . .78, 98, 104, 114, 160  
 Batfalsky, P. . . . .89  
 Batyrev, I.G.\* . . . .30  
 Baumann, S. . . . .71  
 Bauschlicher, C.W. . . . .15, 97  
 Bay, I. . . . .141  
 Bayya, S. . . . .38  
 Bazarjani, M. . . . .72  
 Bea, M.\* . . . .111  
 Bécares, J. . . . .113  
 Beck, R. . . . .120  
 Becker, T. . . . .99  
 Beer, S. . . . .34  
 Begley, M.R. . . . .42  
 Bei, H. . . . .152  
 Beissel, S.R.\* . . . .6  
 Beitsprecher, T. . . . .80  
 Ben Amara, M. . . . .12  
 Benitez, R. . . . .98  
 Benkstein, K.D.\* . . . .128  
 Bentley, J. . . . .122  
 Beresnev, V. . . . .106  
 Beresnev, V.M. . . . .40, 128  
 Beretta, D. . . . .105  
 Bergheul, S. . . . .106  
 Bermejo, R.\* . . . .137  
 Bernal, S. . . . .154  
 Bernardo, E.\* . . . .11, 95, 124  
 Bertoldi, M. . . . .88  
 Besmann, T.M.\* . . . .132  
 Bhakhri, V.\* . . . .89  
 Bhandavat, R.\* . . . .13, 40, 126  
 Bhatt, R. . . . .119  
 Bhattacharya, R. . . . .68  
 Bhattacharya, S.\* . . . .29  
 Bi, Y. . . . .46  
 Bianchini, R. . . . .70  
 Bigger, R. . . . .6  
 Bill, J. . . . .164  
 Bilyk, S. . . . .6  
 Bin, W. . . . .36  
 Bindi, M. . . . .142  
 Bindi, M.\* . . . .105  
 Binner, J. . . . .77, 90, 109, 149  
 Birch, R. . . . .56  
 Birnie, D.P.\* . . . .80  
 Blair, R. . . . .112  
 Blum, L. . . . .159  
 Blum, Y. . . . .27  
 Blum, Y.\* . . . .11  
 Bo, L. . . . .36  
 Boakye, E.E. . . . .120  
 Boakye, E.E.\* . . . .36  
 Boccaccini, A.\* . . . .2  
 Boccaccini, A.R. . . . .118, 135  
 Boccaccini, A.R.\* . . . .76, 143  
 Bodiford, N. . . . .60  
 Bohlender, C. . . . .92  
 Böhlke, T.\* . . . .47  
 Boivin, D. . . . .67  
 Boltalin, A. . . . .116  
 Bonewald, L. . . . .144  
 Bonhomme, C. . . . .70, 124, 144  
 Bonhomme, C.\* . . . .90  
 Bonifacio, C. . . . .20

# Author Index

Bonnamy, S. ....	150
Bonnett, J.F. ....	87
Bonneville, J. ....	115
Bordia, R.K. ....	120
Boss, M.A. ....	33
Bossi, F. ....	86
Bossmann, H. ....	87
Bottiglieri, S.* ....	55
Bouffloux, R. ....	36
Bourke, P. ....	21
Bowden, M. ....	166
Boyd, S. ....	82
Brabec, C.J. ....	10
Bradley, R. ....	60
Bradt, R.* ....	37
Brady, M.P. ....	151
Braga, A. ....	7, 33
Braginsky, M.* ....	48
Bram, M. ....	59
Brandell, D. ....	12
Brandon, N.P. ....	60
Braue, W. ....	67
Bräuer, B. ....	83
Braun, R. ....	168
Breede, F.* ....	136
Brennan, R.E. ....	57
Brennan, R.E.* ....	69
Brennfleck, K. ....	10
Brewer, D. ....	43, 111
Brinch-Larsen, M.* ....	103
Brindley, W. ....	86
Brinkman, K.S.* ....	165
Brisebourg, M.Q.* ....	102, 120
Britton, D.T. ....	125
Brodie, J. ....	122
Brougham, D.F. ....	92
Brouillet, F.* ....	142
Brow, R.K. ....	142
Brown, D. ....	66
Brown, P. ....	56, 70, 76, 77, 90, 149, 163
Brown, R. ....	144
Bruce, R.L. ....	83
Brückmann, L.* ....	168
Brueckmann, L.* ....	108
Brun, P. ....	159
Bruno, G.* ....	44
Buchholz, S. ....	157
Buchkremer, H. ....	59, 71, 159, 160
Buck, Z. ....	131
Buet, E.* ....	151
Bugnet, M. ....	77, 78, 163
Bunch, J.* ....	122
Burdinski, D.* ....	92
Burghard, M. ....	101
Burnage, S. ....	90
Butler, B. ....	57
Büyükyazi, M. ....	13, 152
Byler, D.D. ....	133
Byrappa, K. ....	134
Byun, C. ....	63
<b>C</b>	
Cabal, B. ....	169
Cabana, J. ....	79
Cabe, F. ....	80
Cabe, F.J. ....	42
Cabioch, T. ....	163
Cabioch, T. ....	78, 131
Cabioch, T.* ....	77, 113
Cahyanto, A.* ....	143
Caldato, R. ....	27
Call, A.* ....	121
Calomino, A. ....	3, 43
Campostrini, P. ....	27
Cao, L. ....	7, 75
Capelli, S. ....	86
Carberry, J.* ....	34
Carbone, R. ....	39
Carlesso, M. ....	167
Carlier, D.* ....	12
Carolan, M.F. ....	2
Cartas, A. ....	133
Caruso, R. ....	7
Casalegno, V. ....	166
Casals Guillen, O.* ....	99
Casarin, M.* ....	121
Case, E.D.* ....	76
Castanho, S. ....	104
Cater, J.D. ....	122
Cavanagh, A. ....	12
Ceh, M. ....	128
Cempura, G. ....	139
Cenedese, P. ....	163
Cernuschi, F.* ....	86
Cerruti, M.G.* ....	33
Cesar, P.F. ....	162
Chaka, A.* ....	29
Chan, M.M. ....	4, 133
Chandrashekhara, K. ....	147
Chaput, L. ....	114
Charpentier, L. ....	113
Chaussende, D.* ....	78
Chazeau, L. ....	91
Cheeseman, C.R. ....	165
Chellah, N. ....	67
Chen, B. ....	124
Chen, C. ....	21
Chen, D. ....	7
Chen, F. ....	122
Chen, G. ....	79, 82
Chen, H.* ....	145
Chen, J.C.* ....	2
Chen, J.X. ....	165
Chen, M. ....	145
Chen, N. ....	28
Chen, W. ....	90
Chen, X.* ....	15
Chen, Y. ....	7, 46, 122
Chen, Y.* ....	8, 140
Chen, Z. ....	28, 80, 153
Chenal, J. ....	91
Cheng, L. ....	120
Cheng, L.* ....	79
Cheng, S.* ....	154
Cheng, T.* ....	151
Cheng, Y.* ....	7, 95
Chevalier, J.* ....	91
Chhillar, P. ....	54
Chichkov, B.N. ....	82
Ching, W. ....	47
Ching, W.* ....	15, 60
Chinje Melo, U.F. ....	116
Chlubny, L.* ....	98
Chlup, Z. ....	137
Cho, H. ....	48
Cho, H.* ....	16
Cho, J. ....	52
Cho, K. ....	52
Cho, Y. ....	52, 117
Chockalingam, R.* ....	104, 160
Chocron, S. ....	6
Chocron, S.* ....	5
Choi, B. ....	104
Choi, H. ....	17, 23
Choi, J. ....	87, 141
Choi, J.* ....	49, 88
Choi, S.* ....	85
Choi, S.R. ....	4
Choi, W.* ....	32
Choi, Y.* ....	117
Chollon, G. ....	42, 61, 95
Chou, M. ....	88
Chou, Y.* ....	87, 141
Choudhary, S. ....	109
Christian, J. ....	143
Chun, D. ....	52, 53
Chun, S.* ....	102
Chung, J. ....	88, 104, 105
Cicoira, E.* ....	101
Cingarapu, S.* ....	39
Cinibulk, M.K. ....	36, 145
Cirera, A. ....	113
Ciupinski, L. ....	145
Clark, B.M. ....	50
Clarke, D.R. ....	68
Clausen, B. ....	66
Clegg, W.J.* ....	97
Clyne, B. ....	43, 64
Clyne, T.W. ....	21, 36, 67
Coddington, B.P. ....	137
Coelho, C. ....	124
Coelho, P.* ....	162
Colligon, J. ....	98
Colombo, P. ....	11, 95, 124
Colombo, P.* ....	2, 27
Colorado, H.A.* ....	170
Comini, E. ....	100
Comini, E.* ....	71
Compton, B.G. ....	42, 57
Compton, B.G.* ....	5
Concina, I. ....	7, 33
Corral, E. ....	42
Corral, E.L. ....	53, 77, 96, 97, 114, 130, 148, 149, 164
Corral, E.L.* ....	22, 41
Cosandey, F. ....	56
Costa, C.A. ....	51
Couegnat, G. ....	61
Couegnat, G.* ....	48
Coury, J. ....	27
Cozzika, T. ....	77
Croguennec, L. ....	12
Cui, B. ....	76
Cui, H. ....	37, 158
Cuisinier, M.* ....	28
Cupid, D.M. ....	47
Curran, D.J.* ....	140
Curran, J. ....	43, 64
Curtin, W.A. ....	36
Cychosz, K. ....	155
Cychosz, K.* ....	155
Cypris, J. ....	11
<b>D</b>	
Da Costa, J. ....	15
Dahlqvist, M.* ....	131
Dahotre, N.* ....	92
Dai Pre, M.* ....	152
Dainoviec, J. ....	3
Dancer, C. ....	47
Dancer, C.J.* ....	21, 56
Dannemann, K.A. ....	5
Danzer, R. ....	137
Daphalapurkar, N.* ....	5
Dargad, J.S.* ....	103
Dass, S. ....	109
Dattoli, E.N. ....	128
Datye, A. ....	42, 54, 109

David, L. ....	13	Duxson, P. ....	154	Feliu, N. ....	92
David, P. ....	77	Dyer, T.S.* ....	138	Fellows, J.R. ....	84
Daw, M.S. ....	15, 97			Fenske, G. ....	81, 139
Day, D. ....	144	<b>E</b>		Ferdinandy, M. ....	139
De Genua, F.* ....	85	Eakins, E. ....	76	Ferko, G.J. ....	38
De La Prida, V. ....	64	Eda, T. ....	26	Ferraris, M. ....	142, 166
De la Torre Garcia, R. ....	121	Edmonds, I.M. ....	66, 136	Ferraris, M.* ....	18, 157, 166
de Leeuw, N. ....	144	Edstrom, K.* ....	12	Ferroni, M. ....	71
de Portu, G.* ....	156	Edwards, D. ....	139	Fey, T. ....	11
Deck, C.P. ....	166	Edwards, D.J. ....	121	Fidler, B. ....	141
Dehnen, S. ....	125	Edwards, T.B. ....	166	Finoli, A. ....	94
Deliormanli, A.M.* ....	105	Efremov, A.M. ....	44	Fischer, M. ....	27
Delmas, C. ....	12	Eichler, J.* ....	116	Fischer, T. ....	39, 108, 129
Delplancke, M. ....	116	Eivaz Mohammadloo, H.* ....	159	Fischer, T.* ....	71, 135
DeLucca, V.* ....	70	Eklund, P. ....	98, 113	Fisher, C.* ....	30
Demas, N. ....	81, 139	Eklund, P.* ....	78	Fiz, R.* ....	108
Demir-Cakan, R. ....	79	El Khakani, M. ....	82	Foghmoes, S.P. ....	95
Demyanenko, A. ....	106	El_sheikh, S.M.* ....	102	Folliet, N. ....	70
Deniz, Y. ....	103	Elangovan, S. ....	141	Fontcuberta-Morrall, A.* ....	40
Denoirjean, A. ....	159	Elangovan, S.* ....	141	Fornalczyk, G. ....	108
Desinan, S. ....	82	El-Gamel, N. ....	134	Foti, R.A. ....	57
Deutsch, S.* ....	118	Eljarrat, A. ....	93	Fouad, O.A. ....	102
Dey, G. ....	100	Ellingson, W. ....	70	Foucaud, S. ....	68
Dhara, S.* ....	59, 143	Emmel, M. ....	10	Fountzoulas, C.G. ....	57, 69
Dharani, L.R. ....	164	Endo, S. ....	48, 62	Fountzoulas, C.G.* ....	6, 56
Dhineshbabu, N.R. ....	24	Endo, T. ....	31	Fox, E.E. ....	37
Dias, P.M. ....	124	Engel, T.* ....	3	Fox, E.E.* ....	44
Diau, E.W.* ....	83	Engqvist, H.* ....	163	Fox, E.K. ....	92
Diaz, R. ....	66	Engstrand, J. ....	163	Fox, K. ....	165
Diaz, R.J. ....	129	Epifani, M.* ....	50	Fox, K.M.* ....	166
Dickinson, A. ....	44	Erdemir, A.* ....	80	Frandsen, H.L. ....	103
Diefendorf, R.J.* ....	8	Erode Natarajan, A. ....	4	Franks, L.P. ....	70
Dietz, T.P. ....	169	Eryilmaz, O.L. ....	80	Franks, L.P.* ....	58
Dillon, A.C.* ....	12	Esayfan, M. ....	155	Fredrick, D. ....	42
Dillon, F. ....	157	Espinoza Santos, C.J.* ....	58	Frenzel, V. ....	136
Ding, Y. ....	41	Esposito, V. ....	95	Freund, H. ....	75
Djurisic, A. ....	146	Esquenazi, G. ....	37	Friedle, S. ....	168
Dobrosz, P. ....	98	Esquerre, M. ....	87	Friess, M. ....	136
Doeff, M. ....	79	Estrade, S.* ....	93	Frodelius, J. ....	98
Doerwald, D. ....	82	Estrin, Y. ....	167	Frolov, D. ....	154
Dogan, F. ....	121	European ....	1, 18, 34	Frolov, D.* ....	116
Dominko, R.* ....	79	Evans, G. ....	11	Frot, T.J. ....	83
Domnich, V. ....	89	Evans, L. ....	3	Fryxell, G. ....	165
Dong, S.* ....	41			Fu, Q. ....	128
Dong, Y.* ....	4	<b>F</b>		Fujihara, T. ....	48
Donthu, S. ....	128	Faber, K. ....	10, 145	Fujii, T. ....	37
Doriot, S. ....	77	Fabrega, C. ....	101	Fujiki, T. ....	33, 134
Dou, P. ....	152	Fadeel, B. ....	92, 135	Fujishima, S. ....	32
Dou, P.* ....	151	Faglia, G. ....	7, 33, 71, 100	Fujishiro, Y. ....	122
Doubina, N. ....	82	Fahrenholtz, B. ....	148	Fujita, K. ....	131
Downs, J.* ....	112	Fahrenholtz, W. ....	147	Fukuda, K. ....	54
Dragan, M.* ....	105	Fahrenholtz, W.G. ....	56, 97, 130, 132, 147, 164	Fukuda, T. ....	150
Dravid, V. ....	128	Fair, G. ....	36	Fukunaga, K.* ....	127
Dréan, V. ....	61	Falco, S. ....	21, 56	Fukushima, M. ....	10, 27
Drechsler, K. ....	36, 136	Falco, S.* ....	47	Fukushima, T. ....	31
Drummond, K. ....	144	Fall, M.* ....	80	Fung, K.* ....	46, 59
Du, J. ....	92	Fall, M.L. ....	37, 42	Furushima, R. ....	25, 119
Du, J.* ....	30	Fall, M.L.* ....	169		
Duan, W. ....	106	Fan, J. ....	139	<b>G</b>	
Duan, X. ....	27, 117	Fanchini, G.* ....	83	Gaberscek, M. ....	79
Dubois, G.* ....	83	Fantozzi, G. ....	84, 85	Gabr, M.H.* ....	37
Dubois, S. ....	78	Farbos, B. ....	15	Gad, A.* ....	108
Dubois, S.* ....	115, 131	Farhat, Z.N. ....	54, 157	Gadiou, R. ....	151
Dubot, P. ....	163	Farrokhzad, M.A. ....	139	Gadow, R. ....	118, 127
Dubrunfaut, O. ....	28	Faucett, D. ....	85	Gadow, R.* ....	17, 92
Dudczig, S. ....	20	Faucett, D.C.* ....	4	Gajjela, S.R. ....	7
Dudney, N. ....	72	Fayon, F. ....	144	Galstyan, V. ....	7, 33
Dudney, N.J. ....	79	Fedorova, A. ....	116	Galtsyan, E. ....	46
Dukhin, A. ....	27	Fedorova, A.* ....	154	Gamble, E.A. ....	5
Dunleavy, C. ....	43, 64	Feilden-Irving, E. ....	56, 148	Gamble, E.A.* ....	57
Dunleavy, C.S. ....	21	Feinroth, H. ....	151	Gandhi, A.K. ....	11
Dunn, J.S.* ....	61			Ganga, R. ....	170
Dupré, N. ....	28				



Honma, T.\* ..... 16  
 Hoppe, A. .... 76, 143  
 Hoppe, A.\* ..... 135  
 Hornak, P. .... 139  
 Horner, S.E. .... 52  
 Hosenfeldt, T. .... 80  
 Hosenfeldt, T.\* ..... 81  
 Hosseini, S.\* ..... 160  
 Hotta, M. .... 73, 74  
 Howe, J. .... 79  
 Hsu, C. .... 94  
 Hu, C. .... 130  
 Hu, G. .... 5, 59  
 Hu, G.\* ..... 5, 21  
 Hu, H. .... 138  
 Hu, J. .... 41  
 Hu, L. .... 114  
 Hu, L.\* ..... 98  
 Huang, F. .... 7  
 Huang, H. .... 95  
 Huang, J.\* ..... 42  
 Huang, K.\* ..... 161  
 Huang, L.\* ..... 20, 156  
 Huang, S.\* ..... 90  
 Huang, X. .... 19, 140  
 Huang, Y. .... 153  
 Huang, Z. .... 115, 150  
 Huelser, T.P. .... 23  
 Hug, G. .... 114  
 Huger, M. .... 68  
 Hultman, L. .... 98, 163  
 Humphrey, C. .... 97  
 Hung, C. .... 8  
 Hunn, J. .... 150  
 Hunt, M. .... 38  
 Hurst, J. .... 54  
 Hurst, J.B.\* ..... 8  
 Hwang, C. .... 91  
 Hwang, H. .... 104  
 Hwang, T. .... 48, 49, 63  
 Hwang, T.\* ..... 17  
 Hwang, Y.\* ..... 52  
 Hyuga, H. .... 59, 73

I

Idrobo, J.C. .... 30, 103  
 Ikuhara, Y. .... 30, 127  
 Ilyashenko, M. .... 106  
 Ilyashenko, M.V. .... 128  
 Imbrie, P. .... 66  
 Imshennik, V. .... 115  
 Inata, Y.\* ..... 111  
 Inayat, A. .... 75  
 Ingram, B. .... 122  
 Innocentini, M. .... 27  
 Inoue, K. .... 111  
 Inoue, R.\* ..... 53  
 Ionescu, M. .... 64, 146  
 Iqbal, N. .... 55  
 Iqbal, N.\* ..... 55  
 Ishida, Y. .... 131  
 Ishihara, T.\* ..... 121  
 Ishikawa, K. .... 75, 143, 144, 162  
 Ishikawa, T.\* ..... 9  
 Islam, M. .... 94  
 Issa, S.\* ..... 163  
 Itakura, Y. .... 96  
 Ito, Y. .... 44  
 Ivanov, V. .... 116  
 Ivanova, M. .... 71  
 Iwamoto, Y. .... 26, 44, 58, 59, 96, 111  
 Iwamoto, Y.\* ..... 26

Iwano, Y. .... 46  
 Iwata, T. .... 96  
 Izquierdo, R. .... 82  
 Izutsu, Y. .... 74

J

Jacobs, R. .... 82  
 Jaervi, T.T.\* ..... 125  
 James, B. .... 70  
 James, B.\* ..... 21  
 Jang, B. .... 68  
 Jang, B.\* ..... 102  
 Jankovic, S. .... 126  
 Janssen, R. .... 26, 111  
 Jansson, K. .... 45, 50, 125  
 Jansson, U.\* ..... 40  
 Jansz, M. .... 66  
 Jaouen, M. .... 77, 78  
 Jarligo, M.\* ..... 86  
 Jarmon, D. .... 53, 111  
 Jayaseelan, D.D. .... 76, 163  
 Jee, S.\* ..... 28, 115  
 Jefferson, G. .... 70  
 Jellison, G.E. .... 150  
 Jemmal, R. .... 76  
 Jenkins, M.G. .... 151  
 Jensen, J. .... 78  
 Jeon, H. .... 16  
 Jeon, H.\* ..... 17  
 Jeon, K. .... 98  
 Jeong, D.\* ..... 32, 62  
 Jeong, S. .... 62  
 Jeong, Y. .... 62, 64  
 Jessen, T.L. .... 57  
 Ji, C. .... 158  
 Ji, M. .... 104  
 Jia, D. .... 117  
 Jia, D.\* ..... 27, 117  
 Jianbao, H.\* ..... 36  
 Jiang, J. .... 8, 55  
 Jiang, W. .... 16, 48, 62, 140  
 Jiang, W.\* ..... 166  
 Jiang, Y.\* ..... 30  
 Jimenez, J.A. .... 106  
 Jimenez, J.A.\* ..... 110  
 Jimenez-Diaz, R. .... 100  
 Jin, T. .... 122  
 Jinesh, K.B. .... 153  
 Jing, D. .... 51, 107  
 Jinshan, Y. .... 36  
 Jo, G. .... 16  
 Joachim, K.\* ..... 34  
 Joëlle, B. .... 150  
 Johansson, M. .... 23  
 Johnson, F.C. .... 166  
 Johnson, J.\* ..... 91  
 Johnson, M.\* ..... 145  
 Johnston, J. .... 119  
 Johnston, R.E.\* ..... 66, 136  
 Jokiniemi, J. .... 23  
 Joly, A.\* ..... 159  
 Jones, T. .... 84  
 Jones, Z.A. .... 119  
 Jones, Z.A.\* ..... 65  
 Jordan, E.\* ..... 86  
 Joulain, A. .... 98, 115  
 Joulia, A.\* ..... 68  
 Joussein, E. .... 155  
 Ju, Y. .... 121  
 Jung, D. .... 16, 17, 63, 81  
 Jung, J.\* ..... 30  
 Jung, S. .... 117

Jung, S.\* ..... 144  
 Jung, Y. .... 12  
 Jurgaitis, P. .... 54

K

Kagawa, Y. .... 4, 53, 86, 102, 137, 145  
 Kagawa, Y.\* ..... 9, 147  
 Kaib, T. .... 125  
 Kaib-Haddadpour, S. .... 125  
 Kaiser, A.\* ..... 25  
 Kaiser, A.F.\* ..... 95  
 Kakisawa, H. .... 4, 53, 86, 102  
 Kakisawa, H.\* ..... 145  
 Kakitsuji, A. .... 31  
 Kalita, H. .... 133  
 Kalkura, S. .... 162  
 Kang, C. .... 62  
 Kang, C.\* ..... 81  
 Kang, E. .... 49  
 Kang, E.\* ..... 150  
 Kang, H. .... 52  
 Kang, H.\* ..... 52  
 Kang, M. .... 52  
 Kanhere, P.\* ..... 153  
 Kania, M.J. .... 132  
 Kanno, R. .... 28  
 Kano, F. .... 132  
 Karaman, I. .... 98, 114  
 Karan, N. .... 28  
 Karandikar, P.\* ..... 11, 56  
 Karis, O.\* ..... 50  
 Karpf, J. .... 106, 109  
 Karra Raveendran, G.\* ..... 93  
 Karthik, K.\* ..... 153  
 Kashalikar, U. .... 57  
 Kashiwagi, K. .... 158  
 Kasica, R. .... 139  
 Katcoff, C.Z.\* ..... 5  
 Katoh, Y. .... 132, 150, 151, 152  
 Katoh, Y.\* ..... 150, 166  
 Katou, J. .... 110  
 Kaur, H. .... 96  
 Kaverin, M. .... 106  
 Kaverin, M.V. .... 40  
 Kaverina, A.S. .... 115, 128  
 Kawaharada, Y. .... 132, 150  
 Kawai, A. .... 26  
 Kayhan, S. .... 103  
 Kazemzadeh Dehdashti, M.\* ..... 132  
 Kazin, A.\* ..... 115  
 Keane, M.\* ..... 141  
 Keane, P.F. .... 65  
 Kear, B.H. .... 118  
 Kehr, D. .... 10  
 Keiser, J.R. .... 151  
 Keller, K.A. .... 36  
 Kelley, C. .... 86  
 Kelly, J.P. .... 50  
 Kemmler, J.\* ..... 99  
 Kercher, A. .... 150  
 Kern, F. .... 118, 127  
 Kern, K.\* ..... 101  
 Kesseli, J.\* ..... 2  
 Key, T.\* ..... 120  
 Khalifa, H.E.\* ..... 166  
 Khan, M. .... 55  
 Khan, T.I. .... 139  
 Khatri, N. .... 46  
 Khoddamzadeh, A.\* ..... 157  
 Khoury, H. .... 155  
 Kiani, S.\* ..... 157  
 Kiessling, E. .... 92

# Author Index

- Kikuta, K.\* .....159  
Kilczewski, S.\* .....58  
Kilczweski, S. ....38  
Killinger, A. ....17, 92  
Kim, B. ....49  
Kim, C.\* .....142  
Kim, E. ....17, 48  
Kim, E.\* .....40  
Kim, G. ....16, 17, 48  
Kim, G.\* .....48  
Kim, H. ....16, 17, 25, 48, 62, 68, 102, 105, 111, 148  
Kim, H.\* .....48, 49, 63  
Kim, I. ....81  
Kim, J. ....16, 23, 63, 117  
Kim, J.\* .....59  
Kim, K. ....63, 111  
Kim, M. ....40  
Kim, S. ....40, 41, 102, 111  
Kim, S.\* .....17, 49, 63, 68  
Kim, T. ....104  
Kim, T.\* .....105  
Kim, W. ....38  
Kim, Y. ....41, 52, 53  
Kim, Y.\* .....48, 62  
King, D.\* .....56  
King, N.L. ....5  
Kipouros, G.J. ....54, 157  
Kirihara, S. ....95, 134  
Kirihara, S.\* .....96  
Kirkham, M. ....142  
Kiser, J. ....3  
Kishimoto, H. ....33, 134  
Kita, H. ....51, 73, 74, 127  
Kita, K.\* .....74  
Kitaoka, S. ....158  
Kitazawa, R.\* .....86  
Klatt, E. ....136  
Kleczeck, M. ....97  
Kleebe, H. ....38  
Klemm, H. ....35  
Klemm, H.\* .....119  
Klimov, E. ....18  
Klimov, M. ....112  
Kneser, U. ....135  
Knessler, U. ....76  
Knox, V. ....8  
Kobayashi, R. ....110  
Koch, D. ....76, 135, 136, 167  
Koch, D.\* .....84  
Kochupurackal, J. ....71, 93  
Kodambaka, S. ....157  
Kogo, Y. ....51  
Kolesnikov, D.A. ....40, 128  
Koley, S.\* .....161  
Kolmakov, A.\* .....129  
Komada, N. ....111  
Komarov, E.F. ....40  
Komeya, K. ....19, 95, 127, 167  
Komori, N.\* .....95  
Konarski, P. ....40  
Kondo, A. ....150  
Kondo, N. ....59, 74, 127  
Kondo, N.\* .....73  
Kondo, S. ....150  
Kondou, N. ....51  
Konstantinova, E. ....116  
Koos, A. ....157  
Koratkar, N. ....22, 41  
Korde, N.S. ....103  
Koroleva, A. ....82  
Kosec, M.\* .....100  
Koslowska, M.\* .....122  
Kosmac, T. ....128, 156  
Kothalkar, A.\* .....114  
Kotovshikov, Y. ....116  
Kotzott, D. ....97  
Kouchmeshky, B. ....14, 60, 61  
Kovarik, L. ....166  
Kr, G. ....71  
Krause, T.\* .....135, 167  
Krell, A.\* .....69  
Krenkel, W. ....73, 136  
Krenkel, W.\* .....9, 18  
Krevolin, J.\* .....162  
Kriegesmann, J. ....26, 111  
Kriven, W. ....58  
Kriven, W.M. ....65, 119, 169  
Kriven, W.M.\* .....64, 90, 156, 169  
Krnel, K.\* .....128, 156  
Krogstad, J.A.\* .....68  
Kroll, P.\* .....13, 14, 60, 61, 138  
Kronawitter, C.X. ....8  
Kropf, J. ....122  
Krug, T. ....82  
Ku, S. ....16  
Kubach, H. ....156  
Kuebler, J. ....130, 140  
Kuhn, A.\* .....13  
Kuhn, W. ....126  
Kulik, I. ....106  
Kulkarni, A. ....43  
Kumar, A.\* .....54, 106  
Kumar, B. ....52, 133  
Kumar, B.\* .....100  
Kumar, G. ....162  
Kumar, K.\* .....52  
Kumar, P. ....106, 109, 167  
Kumar, P.\* .....109  
Kumar, R.S.\* .....3  
Kumar, S.N.\* .....167  
Kumari, S.\* .....170  
Kumazawa, T. ....73  
Kundu, A.\* .....38  
Kupp, E.R.\* .....140  
Kurkina, T. ....101  
Kurtz, G. ....84  
Kurzydowski, K.J. ....145  
Kusnezoff, M.\* .....87  
Kutyla, G.P.\* .....169  
Kuwabara, A. ....30  
Kwack, W. ....16  
Kwack, W.\* .....62  
Kwak, K. ....68  
Kwon, S. ....16, 62  
Kwon, S.\* .....16  
Kylyshkanov, M.K. ....115
- L**
- Lacombe, J. ....159  
Ladisch, S. ....135  
Ladner, J. ....37  
Ladouceur, A. ....142  
Ladouceur, Z. ....142  
Lahde, A.\* .....18  
Lähde, A.\* .....23  
Lahesmaa, R. ....135  
Lai, B. ....147  
Lai, B.J.\* .....147  
Laik, A. ....161  
Lake, J. ....86  
Lam, Y. ....83  
Lam, Y.\* .....83  
Lamberson, L.E.\* .....22  
Lamon, J. ....85  
Lamon, J.L.\* .....35, 84, 136  
Lanagan, M.\* .....45  
Lance, M.J. ....44  
Landfried, R. ....118  
Landfried, R.\* .....127  
Lane, N.\* .....114  
Lang, K. ....20  
Langhof, N. ....73  
Langlais, F. ....95  
Lara-Curzio, E. ....142  
Laresgoiti, A. ....161  
Larimer, C. ....94  
Larsen, D. ....141  
LaSalvia, J.C. ....61, 89  
Lasalvia, J.C. ....56  
LaSalvia, J.C.\* .....90  
Lashgari, K. ....50  
Laskowsky, A. ....10  
Lau, S.H.\* .....60, 66, 144  
Laurencin, D.\* .....144  
Laurent, G. ....123, 134  
Lauridsen, E.M. ....29  
Lavigne, O. ....67  
Lawrence, A.\* .....90  
Lawson, J.W. ....144  
Lawson, J.W.\* .....15, 97  
Le Cras, F. ....12  
Le Flem, M.\* .....77  
Le Petitcorps, Y. ....77  
Leavy, B.\* .....57  
Lecomte, G. ....137  
Lecomte-Nana, G.\* .....137  
Lee, B. ....117  
Lee, C. ....17, 42  
Lee, D.\* .....63  
Lee, H. ....17, 81, 140  
Lee, H.\* .....16  
Lee, K.\* .....64  
Lee, M. ....16, 48, 111  
Lee, S. ....12, 28, 62, 63, 68, 115  
Lee, S.\* .....25, 111, 148  
Lee, W. ....62, 123  
Lee, W.E. ....118, 163  
Lee, W.E.\* .....76  
Lehmann, J. ....136  
Lehnen, T.\* .....168  
Lehto, V. ....23  
Leidolph, L.\* .....23  
Lemoungna, P.N. ....116  
Lenz, F. ....9  
Leone, P. ....142  
Lepcha, A. ....13, 152  
Lepple, M. ....68  
Leskela, M.\* .....35  
Lestriez, B.\* .....28  
Leuckerth, H. ....97  
Levandovskiy, A.N. ....44  
Levasseur, S. ....28  
Levi, C.G. ....68  
Lewinsohn, C.\* .....119  
Lewinsohn, C.A. ....84  
Leyssale, J. ....15, 42, 61  
Li, D. ....15  
Li, D.\* .....12  
Li, F.Z. ....165  
Li, H. ....128  
Li, H.\* .....120  
Li, K. ....128  
Li, L. ....83  
Li, M. ....12  
Li, N. ....122  
Li, Q.\* .....75  
Li, S. ....107  
Li, W. ....108

Li, X.*	45, 123	Macleod, S.G.	89	Mayrhofer, L.	125
Li, Y.	15, 30, 107	Mädler, L.	99	Mazerat, S.	42
Li, Y.*	107, 138	Magbitang, T.	83	McAlpine, K.*	106
Liang, B.	122	Maglica, A.	128	McCarty, E.	139
Liang, M.	157	Magner, M.J.	58	McCauley, J.	21, 57, 69
Liang, S.	95	Magness, L.S.	57	McCauley, J.*	37
Liang, Y.	110	Magnuson, M.*	163	McClellan, K.J.	133
Liaptsis, D.	22, 66	Mahaffey, P.	114	McCloskey, B.D.*	78
LiHao, G.	133	Mahapatra, M.K.*	122	McClurg, D.	142
Lim, H.	52	Maheshwari, A.*	4	McCormick, A.	53
Lima, M.M.	138	Maier, J.	50, 103, 160	McDeavitt, S.M.	132
Limarga, A.M.*	68	Maillet, E.	84	McDonald, A.G.	142
Lin, C.	28	Maillet, E.*	85	McElwee-White, L.*	125
Lin, H.	46, 54	Maiorano, D.*	89	McGilvray, T.	72
Lin, H.*	19, 158	Majewski, M.	86	McKenna, E.	133
Lin, S.*	46	Majkic, G.	46	McKinley, W.*	109
Lin, Y.	50	Major, F.	18	Mecartney, M.L.	4, 133, 160
Lingfeng, H.	62	Makhmudov, N.	106	Mechnich, P.*	67
Lipkin, D.M.	68	Makhmudov, N.A.	40, 128	Mecholsky, J.J.	157, 162
Lis, J.	98	Makuta, S.	7	Mecholsky, Jr., J.J.	19
Little, J.	70	Makuta, S.*	152	Medvedovski, E.*	25
Liu, J.	8, 162	Malanga, M.	74	Meerkamm, H.	80
Liu, J.*	42	Malony, R.	79	Meguro, T.	19, 95, 127, 167
Liu, R.	157	Malshe, A.*	140	Meille, S.	91
Liu, W.	120	Malzbender, J.	20, 51, 66	Melandri, C.	130
Liu, X.	77	Malzbender, J.*	20, 89, 159	Memarian, N.	7
Lizcano, M.	154	Mandal, M.	100, 133	Men, D.A.*	133
Llosa, J.	113, 147	Maniprasad, P.	94	Mendes, C.E.	139
Lockwood, G.	13, 14	Manivasakan, P.	24	Menezes, R.	94
Lockwood, G.K.*	43	Mansfield, E.	126	Meng, Y.S.	72
Lofaj, F.*	139	Manzanares, M.	101, 113	Menta, V.	147
Lofaro, M.	83	Manzat, A.	17	Menzler, N.	59
Lofland, S.	131	Mao, S.*	34	Mercatelli, L.	113
Lomov, I.	4	Mao, S.S.	8	Mercurio, S.	56
Lonergan, J.M.*	148	Maqsood, A.	55	Merkel, G.	27
Longo, E.	1	Marianna, P.	91	Merkle, R.	160
López Conesa, L.	93	Maric, R.	105	Messing, G.L.	140
López, N.	112, 129	Marichal, C.	98	Metroke, T.	116, 155
Lopez, S.	75	Markham, G.*	151	Metroke, T.*	155
Lorenzo Martin, M.*	139	Markovska, I.G.*	59	Mettenboerger, A.	82
Lorenzo-Martin, C.	81	Marotto, V.	41	Mettenboerger, A.*	62, 107
Lorenzoni, L.	86	Marotto, V.R.	22, 164	Meulenberg, W.	71
Lorrmann, H.	13	Marotto, V.R.*	53	Meyer, T.	44
Low, I.J.*	64, 146, 165	Marshall, A.*	112	Mhaisalkar, S.	71
Lowry, D.R.	65, 119	Marshall, D.*	1	Mhaisalkar, S.G.	23, 93, 153, 154
Lu, G.	107	Marston, L.	36	Michael, J.	56
Lu, G.*	8	Martin, C.	136	Michaelis, A.	35, 119, 161
Lu, H.	42	Martin, E.	48	Michaelis, A.*	1
Lu, J.*	80	Martin, J.	28	Michalski, A.	145
Lu, K.*	108, 110, 122, 124	Martínez de Marigorta, M.	113	Miettinen, M.	23
Lu, P.	12	Martinez Fernandez, J.	167	Miklos, R.	38
Lu, Z.	121	Martinez-Fernandez, J.*	35	Miles, G.	90
Ludford, N.P.	22	Martucci, A.	152	Miljkovic, M.	110
Ludwig, W.	29	Marx, N.	12	Miller, A.	70
Lugovy, M.	130	Maslova, O.	116	Miller, D.	83
Lund Frandsen, H.	140	Mastrobattisto, D.	54	Miller, M.E.	43
Lundberg, P.*	6	Mathews, N.	23, 71, 93, 154	Miller, P.R.	82
Luo, J.	30	Mathur, S.13, 34, 39, 62, 71, 82, 92, 107, 108, 113, 129, 134, 135, 152, 168		Miller, S.	70
Luo, J.*	30	Matsui, T.*	31	Miller, S.*	10
Lupascu, D.C.	43, 53	Matsukata, M.*	26	Miller, S.L.*	56, 89
Luscombe, C.*	82	Matsumoto, T.*	102	Miller-Oana, M.*	77
		Matsumura, S.	65	Milobar, D.	141
		Matsuoka, M.*	127	Miranda, W.G.	162
		Matsushita, N.	158	Mirelman, L.K.*	43, 64
		Matsuya, S.	75, 162	Mishra, B.*	155
		Mattesini, M.	163	Mishra, B.K.*	108
		Matthews, S.	11	Misra, A.	15
		Matuoka, M.	167	Misture, S.	141
		Matyas, J.*	165	Misture, S.*	8
		Mauchamp, V.	77, 78, 163	Misture, S.T.	43
		Maximov, Y.	115	Mitic, V.*	110, 126
		May, M.	122	Mitsuhashi, M.	16
				Mitsuhashi, M.*	62

M

Ma, D.*	82
Ma, J.	22
Ma, L.	51
Ma, Y.*	13, 14
Mabuchi, H.	31
Mack, D.E.	86
MacKean, C.	122
MacKenzie, K.	169
Mackovic, M.	118

# Author Index

Miyajima, K. ....	26	Nagib Afifi, N.* .....	93	Ohtaki, M.* .....	46
Miyata, K.* .....	112	Naik, R. ....	53	Ohtani, A.* .....	4
Miyazaki, H.* .....	74	Naji, I. ....	136	Ojard, G.* .....	53, 111
Mizuno, M. ....	131	Nakagawa, M. ....	144, 162	Ojha, A. ....	94
Mntungwa, M.N. ....	72	Nakagawa, N.* .....	137	Okasinski, J. ....	66
Mo, Y. ....	60	Nakai, S. ....	123	Oki, H. ....	30
Modena, S. ....	88	Nakamata, C. ....	85	Okita, Y. ....	85
Mogilevsky, P. ....	36	Nakayama, T. ....	16, 31, 49, 62, 81	Okojie, R. ....	3
Mohanty, S. ....	59, 143	Nakayama, T.* .....	48	Okubo, K. ....	37
Möller, K. ....	13, 125	Namratha, K.* .....	134	Okunishi, E. ....	103
Molotnikov, A. ....	167	Nanda, J. ....	79	Olenick, J. ....	87
Monereo, O. ....	113	Narayan Rath, S. ....	76	Olenick, J.* .....	164
Monnet, I. ....	77	Narayan, J.* .....	34	Olenick, K. ....	87, 164
Monroe, C.W.* .....	79	Narayan, R.* .....	82	Oliveira, J.S. ....	138
Monteverde, F. ....	76	Nash, J. ....	2	Olson, R.A.* .....	10
Montgomery, C.B. ....	128	Nassif, N. ....	123, 134	Omar, S. ....	160
Moon, G. ....	117	Navrotsky, A. ....	160, 164	Orlovskaya, N. ....	112, 114, 140
Moon, H. ....	160	Nawrocki, M.J. ....	39	Orlovskaya, N.* .....	130
Moon, K. ....	16, 62, 63	Nayak, B.B. ....	108	Ortega, F.S.* .....	11
Moon, K.* .....	63, 81	Nayak, B.D. ....	155	Ortigoza Villalba, G. ....	142
Moon, M. ....	16, 17	Nayak, P. ....	42	Osaka, A. ....	143
Moos, R.* .....	146	Naylor, M.O.* .....	141	Osaka, A.* .....	123
Morandi, C. ....	149	Nechache, R. ....	82, 83	Ostrikov, K.* .....	125
Morante, J. ....	100, 113, 128, 129	Nechache, R.* .....	100	Otaegui, L.* .....	161
Morante, J.* .....	113, 129	Nedin, J. ....	110	Otieno, G.* .....	157
Morante, J.R. ....	34, 112, 129	Nejo, A.A. ....	72	Ouisse, T. ....	78
Morante, J.R.* .....	101	Nejo, O.A. ....	72	Ouyang, L.* .....	14
Moravek, M.R. ....	39, 146	Nelson, A.T. ....	133	Ouyang, S. ....	51
Morcrette, M. ....	79	Nelson, G.M.* .....	142	Ovsianikov, A. ....	82
Moreno, M. ....	27	Nettleship, I.* .....	94	Oxford, G. ....	29
Morgan, D. ....	14	Neubert, M. ....	130	Ozawa, K. ....	149, 150
Morgan, G. ....	44	Neuman, E.W.* .....	147	Ozer, A. ....	90, 156
Morgan, P. ....	160	Neutzler, J. ....	140	Özkan, S. ....	45, 71
Mori, A.* .....	58	Newman, B. ....	74	Ozturk, A. ....	27
Mori, S. ....	73	Ng, M. ....	160		
Moriwake, H. ....	30	Ni, C. ....	46, 59	<b>P</b>	
Morozov, I. ....	116, 154	Nicholas, J.* .....	147	Packard, C.E. ....	118
Morrissey, A.* .....	109	Nicholls, A.E. ....	5	Pailler, R. ....	9, 42
Morrissey, T.G.* .....	37	Nie, X. ....	90	Paital, S.R. ....	92
Morscher, G. ....	54	Nie, X.* .....	138	Pakkanen, T.T. ....	23
Morscher, G.* .....	3	Niessen, N.* .....	168	Palaez-Perez, H. ....	66
Moseler, M. ....	125	Niihara, K. ....	16, 31, 48, 62, 81	Pan, M. ....	118
Mossaddad, M. ....	66	Ning, C.* .....	106	Pan, M. ....	118
Motz, G.* .....	120	Nino, J.C. ....	157	Pang, W. ....	165
Moya, J.S.* .....	169	Nishihara, N. ....	26	Pap, M. ....	159
Muduli, S.D. ....	155	Nishimura, T. ....	130	Papageorgopoulos, D. ....	87
Mueller, G.* .....	34	Nishimura, Y. ....	54	Parcianello, G. ....	11, 95
Mujahid, M. ....	55	Nishimura, Y.* .....	51	Park, C.* .....	63
Mukherjee, A.K. ....	20, 42, 156	Nita, K.* .....	85	Park, D. ....	32
Mukherjee, S. ....	87	Niu, H. ....	15	Park, J. ....	16, 49, 59, 63, 104
Müller, G. ....	129	Noh, B. ....	59	Park, J.* .....	17, 104
Müller, R. ....	129	Noh, D. ....	31	Park, Y. ....	23, 137
Mumm, D.R. ....	133	Nony, C. ....	137	Parra, A. ....	101
Munar, G.M.* .....	75	Noritake, K. ....	95	Parthasarathy, T. ....	36
Munar, M.L. ....	75, 162	Novak, M.D.* .....	3	Parthasarathy, T.A. ....	145
Munnik, F. ....	78	Novochikhin, S. ....	115	Passlick, C. ....	91
Murakami, H. ....	102	Nozawa, T. ....	152	Pastewka, L. ....	125
Murakawa, H. ....	127	Nozawa, T.* .....	149	Patel, M. ....	79
Murtagh, M.* .....	74	Nychka, J.A. ....	142	Patel, M.K. ....	133
Musayev, Y. ....	80			Patel, P. ....	37
Music, D. ....	78	<b>O</b>		Patel, P.J. ....	6
Musil, S. ....	169	O'Brien, J.R. ....	109	Patel, S. ....	61
Myung, J. ....	81	Oberg, E.K.* .....	21	Patelli, A. ....	98
<b>N</b>		Ogasawara, T. ....	51, 131	Pathak, A. ....	100, 133
Na, B. ....	81	Oh, C. ....	49	Patrick, D. ....	150
Na, S. ....	16, 17, 111	Oh, M. ....	40	Patwe, S.J. ....	161
Nabielek, H. ....	88	Oh, Y. ....	68, 102	Paul, A. ....	149
Nabielek, H.* .....	132	Ohashi, K. ....	32	Paul, A.* .....	77
Nadeem, D.* .....	91	Ohiwa, T. ....	143	Paunovic, V. ....	110, 126
Nag, N. ....	57	Ohji, T. ....	127	Pavia, F.* .....	36
Nagai, H. ....	32	Ohji, T.* .....	10	Pavlacka, R. ....	38, 58
		Ohnishi, M. ....	19	Pavlacka, R.* .....	58
				Pavlovic, V. ....	126



Pecanac, G. . . . .20  
 Peiró, F. . . . .93  
 Peltsman, M. . . . .25  
 Pemberton, S.R.\* . . . .36  
 Peng, S. . . . .107  
 Pennycook, S.J. . . . .103  
 Pérez-Flores, J. . . . .13  
 Perrot, G. . . . .61  
 Persson, C. . . . .163  
 Peters, J. . . . .60  
 Peterson, D.\* . . . .87  
 Peterson, I.\* . . . .27  
 Petkovic, N. . . . .156  
 Petrinic, N. . . . .21, 47, 56  
 Petrovsky, V. . . . .121  
 Pfister, C.\* . . . .156  
 Pham, D.\* . . . .130, 149  
 Phan, M. . . . .101  
 Philips, N.R.\* . . . .42  
 Piat, R.\* . . . .47  
 Picard, M. . . . .84  
 Pilati, S. . . . .95  
 Pinc, W.\* . . . .42, 96, 97  
 Pinc, W.R. . . . .77, 114, 130, 148, 149  
 Pinkas, J.\* . . . .2  
 Pint, B.A. . . . .151  
 Piraux, L. . . . .78, 131  
 Plucknett, K.P. . . . .54  
 Plucknett, K.P.\* . . . .11, 157  
 Poenicke, A.\* . . . .161  
 Pogrebniak, A.D.\* . . . .40, 106, 115, 128  
 Pohl, A. . . . .50, 125  
 Poissonnet, S. . . . .151  
 Pokhrel, S. . . . .99  
 Ponzoni, A. . . . .71  
 Ponzoni, A.\* . . . .100  
 Popovici, D.\* . . . .32  
 Portune, A.\* . . . .57  
 Post, E.\* . . . .141  
 Prabhakar, R.\* . . . .71  
 Prades, J. . . . .34, 113, 128, 129, 147  
 Prades, J.\* . . . .100, 113, 129  
 Prades, J.D. . . . .112, 129  
 Pramana, S. . . . .71  
 Prasad, A.S. . . . .95  
 Presley, K.F. . . . .120  
 Presser, V. . . . .66  
 Prevost, E. . . . .53  
 Price, M.\* . . . .69  
 Prieto, A.\* . . . .13  
 Prikhodko, S. . . . .164  
 Proctor, J. . . . .89  
 Provis, J.L.\* . . . .154  
 Prusakov, V. . . . .115  
 Pruyne, T.\* . . . .25  
 Przybyła, C.P. . . . .48  
 Purenovic, J. . . . .110, 126  
 Purushothaman, S. . . . .83  
 Puvvada, N. . . . .100  
 Puvvada, N.\* . . . .133  
 Puyoo, G. . . . .42  
 Pyzik, A.J.\* . . . .74

Q

Qin, Y. . . . .80  
 Qinggang, L. . . . .36  
 Qu, C. . . . .139  
 Quiazon, R. . . . .138  
 Quinn, G. . . . .54  
 Quinn, G.\* . . . .20, 143  
 Quinn, J. . . . .20, 143

R

R'Mili, M. . . . .35, 84, 85  
 Radovic, M. . . . .98, 114  
 Radovic, M.\* . . . .78, 98, 154  
 Raeis Hosseini, N.\* . . . .88  
 Rafaniello, W. . . . .89  
 Rafiee, M.A. . . . .22, 41  
 Raghavan, S.\* . . . .66  
 Rahaman, M.N. . . . .105  
 Rahaman, M.N.\* . . . .124  
 Rahier, H.\* . . . .116, 155  
 Rai, A.K.\* . . . .68  
 Raj, R. . . . .112  
 Rajasekhar, P.V.S.R. . . . .72  
 Rajendran, V.\* . . . .24  
 Rajesh, S. . . . .134  
 Rajput, S. . . . .100  
 Ramalingam, S.\* . . . .118  
 Ramasamy, S.\* . . . .54  
 Ramaseshan, R. . . . .62  
 Ramesh, K. . . . .5, 21  
 Ramesh, K.T. . . . .5, 22  
 Ramesh, K.T.\* . . . .21  
 Rameshbabu, A. . . . .59  
 Ramirez, F.H. . . . .129  
 Ramirez, F.H. . . . .112  
 Ramirez, M.A. . . . .1  
 Ramirez-Hernandez, F. . . . .34  
 Ramirez-Rico, J. . . . .167  
 Ramirez-Rico, J. . . . .35  
 Ramsburg, K. . . . .124  
 Rangasamy, E. . . . .79  
 Rank, S.\* . . . .99  
 Rankin, J. . . . .126  
 Rao, D.S. . . . .155  
 Rao, T.R. . . . .170  
 Rasmussen, S. . . . .140  
 Rauta, P.R. . . . .24  
 Ravishankar Rai, V. . . . .134  
 Rebillat, F. . . . .102, 120  
 Rebled, J.M. . . . .93  
 Rech, S. . . . .98  
 Recnik, A. . . . .128  
 Régo, S.A. . . . .139  
 Reidy, R.F. . . . .149  
 Reilly-Shapiro, N. . . . .42  
 Reimanis, I. . . . .38  
 Reimanis, I.E. . . . .109, 118  
 Reinhart, W. . . . .22  
 Reinisch, G. . . . .61  
 Reiterer, M. . . . .75  
 Ren, Y. . . . .80  
 Ren, Y.\* . . . .28  
 Renard, E. . . . .68  
 Renfro, M. . . . .86  
 Renström, R. . . . .6  
 Rente, J. . . . .167  
 Renz, R. . . . .18  
 Restrepo, D. . . . .112  
 Reuber, S. . . . .161  
 Revaprasadu, N.\* . . . .72  
 Rey, C. . . . .142  
 Reynaud, P. . . . .84, 85  
 Reza, C. . . . .101  
 Rezwani, K. . . . .124, 167  
 Rheinheimer, W. . . . .29  
 Riahi, A. . . . .29  
 Ricchiuto, M. . . . .61  
 Rice, B.M. . . . .30  
 Richardson, T. . . . .79  
 Riedel, R. . . . .72  
 Rielly, C. . . . .109

Riikonen, J. . . . .23  
 Riley, L. . . . .12  
 Rio, C. . . . .67  
 Riu, D. . . . .52  
 Riu, D.\* . . . .49  
 Rizzo, S. . . . .166  
 Roa, J. . . . .98  
 Roberson, C.\* . . . .22  
 Robinson, M. . . . .70, 165  
 Robinson, P.A.\* . . . .162  
 Rochais, D. . . . .77  
 Rodgers, M. . . . .138  
 Rodriguez, L. . . . .88  
 Rodriguez-Martinez, L. . . . .161  
 Rolandi, M.\* . . . .34  
 Romano-Rodriguez, A. . . . .99  
 Romano-Rodriguez, A. . . . .100  
 Roosen, A. . . . .55  
 Ros, W. . . . .48, 95  
 Rosei, F. . . . .82  
 Rosei, E.\* . . . .124  
 Rosei, R. . . . .82  
 Rosén, J. . . . .131  
 Rosen, J.\* . . . .131  
 Rosinski, M.\* . . . .145  
 Rossignol, S. . . . .68, 159  
 Rossignol, S.\* . . . .155  
 Rouleau, J.\* . . . .75  
 Rountos, V. . . . .10  
 Rubat du Merac, M.\* . . . .38  
 Ruediger, A. . . . .83  
 Ruediger, A.\* . . . .101  
 Ruggles-Wrenn, M.\* . . . .84  
 Rulis, P. . . . .60  
 Rulis, P.\* . . . .47  
 Rumyantseva, M. . . . .39, 115, 116  
 Ryan, S. . . . .88  
 Ryu, J. . . . .32

S

Sabbagh Alvani, A. . . . .159  
 Sabolsky, E.M. . . . .88  
 Sabolsky, K. . . . .88  
 Sadovskaya, E. . . . .116  
 Sadowski, B. . . . .38  
 Sagar, S. . . . .55  
 Sagar, S.\* . . . .55, 115  
 Saha, R.\* . . . .139  
 Sahu, A.K. . . . .161  
 Sahu, D.\* . . . .39, 152  
 Saito, N.\* . . . .54  
 Saito, T. . . . .127  
 Sakamoto, J. . . . .79  
 Sakka, Y. . . . .130  
 Salamone, S.\* . . . .52  
 Salem, J. . . . .54  
 Salim, T. . . . .83  
 Salimi, R. . . . .159  
 Salminen-Mankonen, H. . . . .135  
 Salvo, M. . . . .142, 157, 166  
 Sambandam, S. . . . .46  
 Sameie, H. . . . .159  
 Sammes, N. . . . .88  
 San Nicolas, R. . . . .154  
 Sanghera, J. . . . .38  
 Sanguinetti Ferreira, R.A. . . . .138, 139  
 Sani, E. . . . .113  
 Sans, J. . . . .113  
 Santarelli, M. . . . .142  
 Santhosh, U. . . . .53  
 Santra, S.\* . . . .94  
 Sanz, J. . . . .13, 169

# Author Index

Sarabi, A. ....	159	Shanholtz, E. ....	69	Skiera, E.* .....	20
Sarikaya, A.* .....	121	Shanholtz, E.R. ....	90	Skierab, E. ....	66
Sarin, P. ....	64, 65	Shanholtz, E.R.* .....	89	Sleightholme, A. ....	79
Sarin, P.* .....	65, 119	Shao, F.* .....	112, 129	Slusark, D.* .....	58
Saruhan Brings, B. ....	99	Shaoming, D. ....	36	Smeacetto, F. ....	105
Saruhan, B.* .....	71	Sharma, L.K. ....	96	Smeacetto, F.* .....	142
Saruhan-Brings, B.* .....	45, 146	Sharma, N.* .....	96	Smith, C. ....	3, 38
Sastri, S. ....	57	Sharma, P. ....	109	Smith, C.* .....	3
Satapathy, S.* .....	5	Sharma, S. ....	160	Smith, C.E. ....	145
Sato, A. ....	31	Sharma, V. ....	109	Smith, M.E. ....	144
Sato, Y. ....	62	Shearing, P.R. ....	60	Smith, P. ....	70, 90
Satsangi, V.R. ....	109	Shelby, J. ....	141	Snead, L. ....	151
Sauder, C. ....	151	Sheldon, B.W. ....	126, 127	Snead, L.* .....	150
Savino, R. ....	76	Shemet, V. ....	89	Snead, L.L. ....	132
Sberveglieri, G. ....	7, 71, 100	Shen, H. ....	108	Snoha, D. ....	57
Sberveglieri, G.* .....	33	Shen, K. ....	150	Sobrados, I. ....	13
Schaff, F. ....	98, 114	Shen, S. ....	7	Sodano, H.A. ....	50
Schaffoener, S.* .....	25	Shen, S.* .....	8, 154	Soga, K. ....	33, 134
Scharf, T.W. ....	149	Shen, W. ....	150	Søgaard, M. ....	103
Schäuble, R. ....	135	Shi, J. ....	8, 107	Soh, W. ....	31
Scheffler, M. ....	10	Shi, J.* .....	51, 110	Sohn, Y. ....	87
Scheler, S. ....	136	Shi, X. ....	120, 128	Solanki, A. ....	109
Scheler, T. ....	89	Shi, X.* .....	144	Sommer, F.* .....	118
Schierle-Arndt, K.* .....	18	Shih, C.* .....	152	Somov, S.* .....	88
Schlaefer, J. ....	108	Shimoda, K. ....	137	Sondhi, A.* .....	149
Schlier, L. ....	11	Shimoda, K.* .....	132	Song, H. ....	62
Schlördt, T. ....	11, 111	Shin, D. ....	48, 52	Song, R. ....	104
Schmelzer, E. ....	94	Shin, H.* .....	53	Song, Z. ....	12
Schmidt, K.* .....	70	Shin, S. ....	16, 63, 81	Soraru, G.D. ....	11
Schmitt, M.P. ....	68	Shin, T. ....	121	Soraru, G.D.* .....	27
Schneider, J.* .....	78	Shin, Y. ....	16	Sousa, C.R.* .....	104
Schneider, M. ....	161	Shin, Y.* .....	16	Sow, C. ....	71
Schnetter, L. ....	51	Shinavski, R. ....	43	Spacie, C. ....	90
Schoenfeld, K. ....	119	Shinavski, R.* .....	9	Spatz, C.* .....	73
Schoenfeld, K.* .....	35	Shinkle, A.A. ....	79	Spawton, J.F. ....	56
Schoenung, J.M. ....	20, 156	Shinoda, Y.* .....	137	Speyer, R.* .....	89
Schuetz, A. ....	120	Shinozaki, M.* .....	67	Sphect, E. ....	150
Schulz, C. ....	23	Shirahata, J. ....	81	Spicher, U. ....	156
Schulz, E.* .....	80	Shirosaki, Y. ....	123, 143	Spiecker, E. ....	118
Schulz, U. ....	67	Shirpour, M. ....	160	Spriggs, O. ....	52
Schulz, U.* .....	67	Shpak, A.P. ....	40	Squire, T.H. ....	15, 144
Schütze, M. ....	168	Shrivastav, R. ....	109	Srikanth, H.* .....	101
Schwab, A. ....	75	Shrivastava, J. ....	109	Srinivasan, M. ....	153
Schweizer, S. ....	91	Shukla, A. ....	78	Srinivasan, R. ....	115
Schwieger, W.* .....	75	Shulman, H. ....	80	Srivastava, O.N. ....	106, 108
Sciti, D. ....	76, 130	Shulman, H.S. ....	37, 42, 169	Stadelmann, R. ....	130
Sciti, D.* .....	113	Shvedova, A. ....	135	Stadelmann, R.* .....	114
Scriba, M.R.* .....	125	Shyam, A. ....	44	Stafford, R.* .....	44
Seid, K. ....	28	Shyam, A.* .....	142	Stafford, R.J. ....	44
Seifert, H.J.* .....	47	Shyplyenko, A. ....	106	Starr, J. ....	110
Seki, S. ....	7	Sickafus, K.E. ....	133	Steinberger-Wilckens, R. ....	159
Sekimoto, K. ....	26	Sightler, J. ....	140	Steinbrech, R. ....	66
Sekine, K.* .....	73	Sikhwihilu, L.* .....	153	Steinbrech, R.W. ....	20, 51
Selig, J. ....	46	Silva, L. ....	104	Stellacci, F.* .....	32
Selvamanickam, V.* .....	46	Silva, M. ....	58	Stelter, M. ....	161
Semancik, S. ....	128	Silva, N. ....	162	Stern, E. ....	10
Sena, K. ....	127	Silva, R.P.* .....	51	Stevenson, J.W. ....	87, 88, 121, 141
Sendova, M. ....	106, 110	Silvestroni, L. ....	113	Stewart, T. ....	164
Seo, D. ....	102	Silvestroni, L.* .....	76, 130	Stiegler, N. ....	92
Sepka, S.* .....	120	Sinchuk, Y. ....	47	Strasberg, M.* .....	157
Serizawa, H.* .....	127	Singh, A.K. ....	170	Strassburger, E. ....	37, 57, 69
Serre, A.M.* .....	150	Singh, A.K.* .....	126	Strutt, P. ....	105
Sestakova, L. ....	137	Singh, A.P. ....	62, 107, 108	Stucky, S. ....	108
Sevecek, O. ....	137	Singh, A.P.* .....	82	Studer, D.W. ....	2
Sglavo, V. ....	88, 114	Singh, D. ....	39, 81, 146, 170	Su, B. ....	91
Sglavo, V.M. ....	85, 112, 121	Singh, G. ....	13, 40, 126	Su, J.F. ....	138
Shaffer, M.S. ....	118	Singh, J. ....	43	Subhani, T.* .....	118
Shah, M. ....	121	Singh, J.* .....	106, 108	Subhash, G.* .....	39, 55, 133, 148
Shahbazian Yassar, R.* .....	28	Singh, M. ....	35, 73, 137, 145, 167	Suematsu, H. ....	16, 31, 48, 49, 62
Shahid, M. ....	55	Singh, N. ....	109	Suematsu, H.* .....	81
Shahin, D. ....	20	Singh, P. ....	105, 122, 141	Sugawara, J. ....	65
Shamma, M.M.* .....	66	Sinha Ray, S. ....	153	Sullivan, M.H. ....	133
Shang, J.K. ....	75	Sisson, R.D.* .....	72	Sumi, H. ....	122

Sun, C. ....75  
 Sun, C.\* .....23, 93  
 Sun, G.\* .....55  
 Sun, J. ....102  
 Sun, J.\* .....66  
 Sun, S. ....83  
 Sun, Y. ....55  
 Sun, Z. ....117  
 Sundaram, R. ....101  
 Surpi, A. ....98  
 Suryanarayana, C. ....112  
 Suvanto, S. ....23  
 Suzdalev, I. ....115  
 Suzuki, K. ....28, 81  
 Suzuki, K.\* .....31  
 Suzuki, M.\* .....49  
 Suzuki, T. ....16, 31, 51, 54, 62, 81, 131  
 Suzuki, T.\* .....122  
 Swab, J. ....69  
 Swab, J.\* .....38, 57  
 Swab, J.J. ....30, 57, 58  
 Swaminathan, N. ....14  
 Syha, M.\* .....29  
 Synowczynski, J. ....30  
 Szlufarska, I.\* .....14  
 Szwedek, O. ....77  
 Szymanski, T.\* .....146

T

Tachibana, Y. ....152  
 Tachibana, Y.\* .....7, 33  
 Tada, K. ....48  
 Tadachika, N. ....62  
 Takahashi, T. ....78  
 Takeda, H. ....96  
 Takeshita, H. ....33, 134  
 Takeuchi, Y. ....111  
 Takizawa, K.\* .....150  
 Tallman, D.J.\* .....114  
 Tan, G. ....22  
 Tanabe, E. ....27  
 Tanaka, H. ....130  
 Tanaka, S. ....16  
 Tanaka, S.\* .....25, 119  
 Tandon, R.\* .....19, 20, 85  
 Tandon, R.P.\* .....24  
 Tang, M. ....165  
 Tang, W.\* .....107  
 Tang, Y. ....107, 138  
 Tanigawa, H. ....149  
 Tao, T. ....122  
 Tao, X. ....46  
 Tapper, U. ....23  
 Tarascon, J. ....79  
 Tas, A.\* .....123  
 Tasaki, S. ....95, 96  
 Tasaki, S.\* .....134  
 Tashmetov, M. ....106  
 Tatami, J. ....95, 127, 167  
 Tatami, J.\* .....19  
 Tavakoli, A.\* .....164  
 Taylor, D.M. ....2  
 Taylor, H. ....61, 114, 148  
 Tchou-Kien, D. ....68  
 Teja, A.S. ....4  
 Templeton, J.W. ....121  
 Teneze, N. ....77  
 Terao, J. ....7  
 Terauchi, M. ....62  
 Terrani, K. ....151  
 Terrani, K.A. ....132  
 Teyssandier, F. ....102, 120

Teyssandier, F.\* .....9, 42  
 Thamizhavel, A. ....162  
 Thanganathan, U.\* .....41  
 Thilly, L.\* .....98  
 Thomas, E.L.\* .....69  
 Thommes, M. ....155  
 Thommes, M.\* .....27  
 Thompson, D. ....136  
 Thompson, L.T. ....79  
 Thompson, M.\* .....97  
 Thompson, V. ....162  
 Thomsen, E.C. ....87, 141  
 Thornhill, T. ....22  
 Tian, W. ....73  
 Tian, Z. ....117  
 Tielens, F. ....70  
 Tietema, R.\* .....82  
 Tietz, F. ....89  
 Tikare, V.\* .....133  
 Timofeeva, E.V. ....39  
 Timofeeva, E.V.\* .....99, 146  
 Ting, J.\* .....94  
 Tiwari, R.S. ....106, 108  
 Todd, R. ....21, 47  
 Todd, R.I. ....56, 118, 157  
 Todd, R.I.\* .....19  
 Togo, A. ....114  
 Toh, S. ....65  
 Tokariev, O.A.\* .....51  
 Toksoy, F. ....89  
 Tokuhiro, A.\* .....132  
 Tomiyama, S. ....127  
 Tong, H. ....94  
 Torrel, S. ....139  
 Torres-Andon, F.\* .....135  
 Tortorelli, D.A. ....58  
 Tosun, N. ....62, 82, 107  
 Tougas, I.M. ....45  
 Trad, K. ....12  
 Trahey, L. ....28  
 Travitzky, N.\* .....11, 24  
 Treccani, L. ....124  
 Trejo, R. ....142  
 Tremmel, S. ....80  
 Trentin, A. ....98  
 Trice, R.W. ....24, 149  
 Tricot, G. ....159  
 Trofimenko, N. ....87  
 Tromas, C. ....78, 98  
 Truong, V. ....82  
 Tse, S.D. ....118  
 Tsuda, H. ....31  
 Tsuda, H.\* .....32, 73  
 Tsuru, K. ....75, 143, 144  
 Tulenko, J. ....139  
 Tuo, S. ....46  
 Tuomela, S. ....135  
 Tur, Y.K. ....90, 156  
 Turan, D.\* .....103  
 Turan, S.\* .....103  
 Tushtev, K. ....84, 135  
 Tyrra, W. ....39, 108, 168  
 Tysmans, T. ....155  
 Tyurin, Y.N. ....115

U

Uehara, S. ....65  
 Uehara, Y. ....96  
 Uematsu, K. ....25, 119  
 Uetsuki, K. ....123  
 Uglov, V.V. ....40  
 Uhlenbruck, S. ....160

Ukyo, Y.\* .....1  
 Uludag, A. ....103  
 Umeda, T. ....59  
 Unno, H.\* .....65  
 Uno, K.\* .....53  
 Unosson, E. ....163  
 Upadhyay, S.\* .....109  
 Ur-Rehman, N. ....56  
 Usami, H. ....111

V

Vaßen, R. ....86  
 Vadala, M.\* .....43, 53  
 Vaidhyanathan, B. ....77, 90, 109, 149  
 Valanezhad, A. ....144  
 Valant, V. ....162  
 Valdez, M. ....41  
 Valdez, M.A. ....53  
 Valdez, M.A.\* .....114  
 Van Bael, M.K.\* .....19  
 van Benthem, K. ....20  
 Van Boxel, S. ....136  
 Van der Biest, O. ....130  
 van Deventer, J. ....154  
 Van Gestel, T.\* .....59, 71, 160  
 Van Petegem, S. ....98  
 Van Swygenhoven, H. ....98  
 Vance, B. ....54  
 Vandeperre, L. ....118  
 Vandeperre, L.J.\* .....56, 148, 165  
 Vang Hendriksen, P. ....140  
 Vardelle, M. ....68  
 Varechkina, E. ....39  
 Varela, J.\* .....1  
 Varela-Feria, F.M. ....35  
 Varghese, B. ....71  
 Vasiliev, R. ....116  
 Vassen, R. ....86, 89  
 Vasudevamurthy, G. ....152  
 Vasudevan, S.\* .....126, 127  
 Vaughan, B. ....90  
 Veith, G.M.\* .....79  
 Velasco Davalos, I.\* .....83  
 Venkateswaran, V. ....164  
 Ventrella, A. ....157, 166  
 Venugopal, S. ....77  
 Venugopal, S.\* .....149  
 Vera, M.\* .....167  
 Vera-García, C. ....35  
 Verfondern, K. ....132  
 Verma, A. ....105, 141  
 Vetrone, F.\* .....33  
 Vezzù, S.\* .....98  
 Vick, M. ....118  
 Vidal-Setif, M.\* .....67  
 Viggato, V.T. ....58  
 Vignoles, G.L. ....48  
 Vignoles, G.L.\* .....15, 61, 95  
 Vilajosana, I. ....113  
 Vilajosana, I.\* .....147  
 Vilajosana, X. ....147  
 Vilasi, M. ....67  
 Villalobos, G.\* .....38  
 Villarreal, I. ....161  
 Villechaise, P. ....98  
 Vinati, S. ....39  
 Vishnyakov, V.\* .....98  
 Vix-Guterl, C. ....151  
 Vleugels, J. ....130  
 Voggenreiter, H. ....76, 136  
 Vogler, T. ....22  
 Voigt, I. ....1

# Author Index

- Voigt, R. . . . . 9  
Voldrich, W.E. . . . . 87, 141  
Volksen, W. . . . . 83  
Vomiero, A. . . . . 33  
Vomiero, A.\* . . . . 7  
von Hagen, R.\* . . . . 13, 152  
von Niessen, K. . . . . 86  
Vorobiev, O. . . . . 4  
Vorobyeva, N.\* . . . . 116  
Vu, M.\* . . . . 38  
Vuono, D.J. . . . . 37
- W**
- Wada, M.\* . . . . 158  
Waggoner, M. . . . . 53  
Waghmare, U.V. . . . . 109  
Wakai, F. . . . . 137  
Wakihara, T. . . . . 19, 127, 167  
Wakihara, T.\* . . . . 95  
Walden, B. . . . . 126  
Walker, C.H.\* . . . . 139  
Walker, L. . . . . 41, 97  
Walker, L.S. . . . . 22, 42, 53, 77, 96, 114, 130, 149  
Walker, L.S.\* . . . . 148, 164  
Walker, W.J.\* . . . . 73  
Wallen, M. . . . . 27  
Walz, J. . . . . 108  
Wamser, T.\* . . . . 136  
Wang, D. . . . . 82  
Wang, D.\* . . . . 12  
Wang, F. . . . . 72  
Wang, H. . . . . 19, 46, 95, 145, 148  
Wang, J. . . . . 15, 27, 148, 164  
Wang, J.\* . . . . 14  
Wang, K. . . . . 95, 120  
Wang, M.\* . . . . 91, 94, 123  
Wang, S. . . . . 27  
Wang, X.\* . . . . 139  
Wang, X.H. . . . . 165  
Wang, Y.\* . . . . 72, 86, 120, 123, 134  
Wang, Z. . . . . 28, 41  
Warren, C. . . . . 27  
Wartzack, S. . . . . 80  
Wastiels, J. . . . . 155  
Watanabe, H. . . . . 26  
Watkins, M. . . . . 53  
Watkins, T. . . . . 44  
Watkins, T.R.\* . . . . 44  
Wattiaux, A. . . . . 12  
Watts, J. . . . . 147  
Watts, J.\* . . . . 130  
Weber, O.\* . . . . 24, 73  
Weber, S.\* . . . . 76  
Weclas, M. . . . . 11  
Wei, D. . . . . 125  
Wei, J.\* . . . . 164  
Wei, R. . . . . 139  
Weimar, U. . . . . 99  
Weingarten, N.S. . . . . 30  
Weiss, R.\* . . . . 10  
Welch, C. . . . . 60  
Wells, J.\* . . . . 69  
Welter, M.\* . . . . 169  
Wen, W. . . . . 37, 158  
Wereszczak, A.A. . . . . 37, 44  
Westbrook, J. . . . . 44  
Westin, G.\* . . . . 45, 50, 125  
Weygand, D. . . . . 29  
White, B.\* . . . . 87  
White, J.T. . . . . 109  
White, S. . . . . 120  
Wicks, G.\* . . . . 1
- Wiegandt, K. . . . . 26  
Wiesner, V.L.\* . . . . 24, 149  
Wiggers, H.\* . . . . 23  
Wiley, C.S. . . . . 89  
Wilhelm, M. . . . . 153  
Wilhelm, M.\* . . . . 26  
Williams, C. . . . . 21  
Williams, T. . . . . 95  
Wilson, C.A. . . . . 162  
Wilson, M.A. . . . . 84  
Wing, Z. . . . . 96, 97  
Wippler, J. . . . . 47  
Withers, P.J. . . . . 60, 136  
Witz, G.\* . . . . 87  
Woerner, C.\* . . . . 20  
Woiton, M.\* . . . . 10  
Wolf, T. . . . . 2  
Wolfe, D.E. . . . . 68  
Wolfenstine, J.\* . . . . 79  
Wong, L.H. . . . . 23, 93, 154  
Wong, S. . . . . 56  
Wortmann, L.\* . . . . 108, 134  
Wright, J. . . . . 38, 85  
Wright, J.C. . . . . 58  
Wright, J.C.\* . . . . 57  
Wright, J.M. . . . . 4  
Wright, K.J. . . . . 44  
Wu, B. . . . . 41  
Wu, H. . . . . 21  
Wu, H.\* . . . . 158  
Wu, K. . . . . 54, 106, 109  
Wu, K.H. . . . . 42  
Wu, N. . . . . 82  
Wu, P.\* . . . . 107  
Wu, Y.\* . . . . 56  
Wynick, G. . . . . 139
- X**
- Xia, G.G. . . . . 87  
Xia, W. . . . . 163  
Xiang, H. . . . . 14  
Xiang, H.\* . . . . 164  
Xiang, Y. . . . . 92  
Xiangyu, Z. . . . . 36  
Xiao, L. . . . . 108, 135  
Xiao, L.\* . . . . 92  
Xiao, P. . . . . 86  
Xie, Z.\* . . . . 112  
Xiong, Y. . . . . 156  
Xu, B. . . . . 60  
Xu, C.\* . . . . 88  
Xu, N. . . . . 161  
Xu, T. . . . . 12  
Xue, X.\* . . . . 122
- Y**
- Yadava, Y.P.\* . . . . 138, 139  
Yahya, N. . . . . 157  
Yahya, N.A.\* . . . . 118  
Yakuschenko, I.V. . . . . 128  
Yakushchenko, I.V. . . . . 115  
Yakyschenko, I.V. . . . . 40  
Yam, F.W. . . . . 64  
Yamada, T. . . . . 131  
Yamagata, T. . . . . 112  
Yamaguchi, T. . . . . 122  
Yamano, T. . . . . 33, 134  
Yamaoka, S. . . . . 86  
Yamazoe, M. . . . . 145  
Yan, L. . . . . 122  
Yan, W.\* . . . . 107
- Yang, F. . . . . 86  
Yang, G. . . . . 107  
Yang, J. . . . . 150, 157, 170  
Yang, J.M. . . . . 164  
Yang, L. . . . . 107  
Yang, Q. . . . . 107, 138  
Yang, X. . . . . 91  
Yang, Z. . . . . 27, 117  
Yao, D.\* . . . . 128  
Yao, W. . . . . 42, 156  
Yao, X. . . . . 120, 128  
Yao, Y. . . . . 46  
Yashiro, N. . . . . 159  
Yazami, R. . . . . 153  
Ye, D. . . . . 117  
Ye, J. . . . . 51  
Yedra, L. . . . . 93  
Yeomans, J. . . . . 70, 90  
Yim, T.\* . . . . 31  
Yin, F. . . . . 41  
Yin, J. . . . . 107  
Yizhong, H. . . . . 93  
Yokogawa, Y. . . . . 162  
Yoon, D. . . . . 102  
Yoon, H. . . . . 88, 104  
Yoon, J.\* . . . . 104  
Yoon, M.\* . . . . 104  
Yoon, Y. . . . . 28, 115  
Yoshimura, H.N.\* . . . . 162  
Yoshimura, M.\* . . . . 91, 158  
Yoshio, S. . . . . 127  
Yoshio, S.\* . . . . 167  
Yoshizawa, Y. . . . . 10  
Youngblood, J.P. . . . . 24, 149  
Yu, W. . . . . 131  
Yuan, J.\* . . . . 22  
Yuan, M. . . . . 82  
Yufu, L. . . . . 119  
Yurdakul, H. . . . . 103
- Z**
- Zagar, K.\* . . . . 128  
Zang, J. . . . . 45  
Zapata-Solvas, E.\* . . . . 163  
Zappa, D. . . . . 71  
Zaremba, S. . . . . 36  
Zaretski, A. . . . . 42, 109  
Zeiser, T. . . . . 75  
Zeng, D. . . . . 72  
Zhai, H. . . . . 115  
Zhang, C. . . . . 107  
Zhang, G.\* . . . . 126, 130  
Zhang, H.\* . . . . 37, 158  
Zhang, K. . . . . 19  
Zhang, L. . . . . 79, 138  
Zhang, L.\* . . . . 107  
Zhang, P.\* . . . . 117  
Zhang, T. . . . . 165  
Zhang, X. . . . . 7, 41  
Zhang, Y. . . . . 120, 161, 162  
Zhang, Y.\* . . . . 15, 109  
Zhao, F. . . . . 141  
Zhao, H. . . . . 82  
Zhao, X. . . . . 161  
Zheng, J. . . . . 153  
Zheng, M. . . . . 14  
Zhidan, R.\* . . . . 119  
Zhihui, H. . . . . 36  
Zhing, J. . . . . 95  
Zhou, H. . . . . 41  
Zhou, L.\* . . . . 87  
Zhou, Y. . . . . 14, 15, 27, 59, 117, 164

Zhou, Y.*	.165
Zhou, Z.*	.50
Zhu, D.	.68, 102, 119
Zhu, Y.	.72
Zhu, Z.	.166
Ziebarth, R.	.74
Zimmermann, J.*	.44
Zok, F.*	.3
Zok, F.W.	.3, 5, 57
Zondlo, J.W.	.88
Zopes, D.*	.168
Zou, J.	.104, 130
Zou, J.*	.104
Zou, L.*	.164
Zubavichus, Y.	.154